

UNIVERSITY OF KWAZULU-NATAL



**DESIGN, SYNTHESIS AND PHARMACOLOGICAL
EVALUATION OF NOVEL FUSED PYRIMIDINE
ANALOGUES AS ANTICANCER AGENTS**

By

SRINIVASULU CHERUKUPALLI M. Sc

215081586

2018

**DESIGN, SYNTHESIS AND PHARMACOLOGICAL
EVALUATION OF NOVEL FUSED PYRIMIDINE
ANALOGUES AS ANTICANCER AGENTS**

SRINIVASULU CHERUKUPALLI M. Sc

215081586

2018

A thesis submitted to the School of Health Science, Discipline of Pharmaceutical science, Department of Pharmaceutical Chemistry, University of KwaZulu-Natal, Westville, for the degree of Doctor of Philosophy.

This thesis has been prepared according to **Format 4** (Thesis by publications) as outlined in the guidelines of College of Health Sciences, University of KwaZulu-Natal. The chapters consist of an overall introduction, chapters in discrete research papers and a final discussion. Two chapters have been published and the remaining chapters have been submitted in peer-reviewed internationally accepted journals.

As the candidate's supervisor, I have approved this thesis for examination/submission.

Supervisor: Dr. R. Karpoormath

Signed:  _____

Date: 11/April/2018

ABSTRACT

Cancer is a multifaceted disease considered as the most serious health burden all over the world. Due to existing of limited anticancer drugs and detrimental side effects, the anticancer research has been challenging. An investigation on identifying novel potential drugs is highly required to treat this serious abnormal cell growth. Advanced potential anticancer drug entrants are crucially required to combat the drawbacks linked with current drugs or line of therapies. Extensive investigations are being carried out on synthetic manipulations of heterocyclic aromatic compounds (purines) for developing efficient and potent anticancer drugs. Besides, these manipulations also offer effective leads for further optimization. Therefore, this project is an effort in detecting a novel and potent anticancer leads based on bioisostere of purines called pyrazolopyrimidines.

In this research project we have performed an comprehensive literature survey of structural isomers of pyrazolopyrimidines (pyrazolo[1,5-*a*]pyrimidine and pyrazolo[4,3-*d*]pyrimidine) for their synthetic approaches and biological activities with special emphasis on structure-activity relationship (SAR) studies. These SAR studies prompted us to implement the observed studies on one of the structural isomer of pyrazolopyrimidine called pyrazolo[3,4-*d*]pyrimidine. And further, we have synthesized some novel series of pyrazolo[3,4-*d*]pyrimidine derivatives with various substituents at C-4 and C-6 positions of the scaffold. A total 71 compounds comprising of phenethyl and pentane hybrids (**7-43**, Chapter 4), benzoyl hybrids (**5a-5h**, **6a-6d** and **7a-7c**, Chapter 5) and lastly phenylcarbamoyl acetamide hybrids (**9a-9s**, Chapter 6) have been synthesized by molecular hybridization approach as outlined in schemes of respective chapters. The completion of reaction and the purity of novel synthesized compounds were confirmed by chromatographic analysis. All the newly synthesized compounds displayed acceptable analysis for their anticipated structures, which were established based on physicochemical and spectral data (IR, ¹H NMR, ¹³C NMR and HRMS).

All synthesized compounds were primarily evaluated for their *in vitro* anticancer activities at Laboratory of Growth Regulators, Centre of the Region Hana for Biotechnological and Agricultural Research, Palacky University & Institute of Experimental Botany ASCR, Slechtitelu 27, 78371 Olomouc, Czech Republic.

From the systematic analysis of anticancer activity, results obtained following key observations were made.

- i. Structural isomers of fused pyrimidines have been looked upon for molecular changes in emerging drug like candidates. Pyrazolopyrimidine is a bioisostere of purines has acquired considerable importance due to its diverse, facile and general synthetic methodologies with great medicinal importance. Several analogs of this scaffold have emerged as a promising leads in the design of some novel pharmacologically active compounds with enhanced

metabolic, pharmacokinetic and pharmacological profiles, representing that there is plenty scope for considering pyrazolopyrimidine as a structural framework for evolving effective leads.

- ii. Chapter 4: From the 37 novel phenethyl and alkyl pentane pyrazolo[3,4-*d*]pyrimidine derivatives synthesized and evaluated for CDK2/Cyclin E, Abl kinase inhibitory activity and anti-proliferative activity against K-562 (chronic myelogenous leukemia) and MCF-7 (breast adenocarcinoma) cell lines. From the tested results, compounds **11** (CDK: IC₅₀ = 5.1 μM; Abl: >12.5 μM), **8** (CDK: IC₅₀ = 7.8 μM; Abl: >25 μM) and **36** (CDK: IC₅₀ = 8.8 μM; Abl: >25 μM) exhibited significant inhibitory activity. Further from this series, most of the synthesized compounds indicated prominent anti-proliferative effects with IC₅₀ value ranging from 19.2 μM to 27.4 μM. Incorporation of monosubstituted phenyl groups at C-4 of the pyrazolo[3,4-*d*]pyrimidine nucleus had favored for most prominent anticancer activity.
- iii. Chapter 5: Among the 15 novel benzoyl hybrids synthesized and evaluated, compounds **5a** and **6c** displayed (CDK2: IC₅₀ = 8.8 μM, 6.8 μM) commendable inhibitory activity and notable anti-proliferative activity ranging from 18.9 μM to 89.3 μM). Presence of heteroatom containing bicyclic moieties at C-4 of the nucleus enhanced both inhibitory and anti-proliferative activity.
- iv. Chapter 6: Of the 19 novel phenylcarbamoyl acetamide hybrids synthesized and tested, compounds **9a**, **9c**, **9g**, **9m** and **9p** showed moderate enzymatic inhibitory activity with an IC₅₀ value >12.5 μM against both CDK2 and Abl kinases while, remaining compounds of this series could not generate IC₅₀ values due to solubility limit (IC₅₀ = >25 μM to >100 μM).

DECLARATION 1: PLAGIARISM

I, **Srinivasulu Cherukupalli**, declare that

- i. The research reported in this dissertation, except where otherwise indicated, is my original work.
- ii. This dissertation has not been submitted for any degree or examination at any other university.
- iii. This dissertation does not contain other persons' data, pictures, graphs or other information, unless specifically acknowledged as being sourced from other persons.
- iv. This dissertation does not contain other persons' writing, unless specifically acknowledged as being sourced from other researchers. Where other written sources have been quoted, then:
 - a. their words have been re-written but the general information attributed to them has been referenced;
 - b. Where their exact words have been used, their writing has been placed inside quotation marks, and referenced.
- v. Where I have reproduced a publication of which I am an author, co-author or editor, I have indicated in detail which part of the publication was actually written by myself alone and have fully referenced such publications.
- vi. This dissertation does not contain text, graphics or tables copied and pasted from the Internet, unless specifically acknowledged, and the source being detailed in the dissertation and in the References sections.

Signed:  _____

Date: 11-04-2018 _____

DECLARATION 2: PUBLICATIONS

DETAILS OF CONTRIBUTION TO PUBLICATIONS that form part and/or include research presented in this thesis (include publications in preparation, submitted, *in press* and published and give details of the contributions of each author to the experimental work and writing of each publication).

Publications

1. S. Cherukupalli, R. Karpoornath, B. Chandrasekaran, G. A. Hampannavar, N. Thapliyal, V. N. Palakollu, An insight on synthetic and medicinal aspects of pyrazolo[1,5-*a*]pyrimidine scaffold, *European Journal of Medicinal Chemistry*, **2017**, 126, 298-352, <https://doi.org/10.1016/j.ejmech.2016.11.019>.

Contributions: I did the literature review and wrote the entire manuscript under the supervision of Dr. Rajshekhar Karpoornath. Rest all the co-authors assisted me in improvisation, writing up and summarizing the literature review (conclusion).

2. S. Cherukupalli, G. A. Hampannavar, C. Sampath, B. Chandrasekaran, N. Sayyad, F. Kayamba, R. R. Aleti, R. Karpoornath, An appraisal on synthetic and pharmaceutical perspectives of pyrazolo[4,3-*d*]pyrimidine scaffold. *Bioorganic and Medicinal Chemistry*, **2017**, <https://doi.org/10.1016/j.bmc.2017.10.012>.

Contributions: I did the literature review and wrote the entire manuscript under the supervision of Dr. Rajshekhar Karpoornath. Rest all the co-authors assisted me in improvisation, writing up and summarizing the literature review (conclusion).

3. S. Cherukupalli, B. Chandrasekaran, N. Sayyad, R. R. Aleti, S. R. Merugu, R. Karpoornath, Synthesis, anticancer evaluation, and molecular docking studies of some novel 4,6-disubstituted pyrazolo[3,4-*d*]pyrimidines as potential cyclin dependent kinase 2 (CDK2) inhibitors. *Bioorganic Chemistry*, **2018**, <https://doi.org/10.1016/j.bioorg.2018.02.030>.

Contributions: I generated the rationale and did all the experimental and characterization as well as writing up of manuscript under the guidance of Dr. Rajshekhar Karpoornath (Supervisor). The co-authors assisted me in writing up of results and discussion and designing of the target molecules.

4. S. Cherukupalli, B. Chandrasekaran, N. Sayyad, R. R. Aleti, S. R. Merugu, R. Karpoornath, Synthesis of 4,6-disubstituted pyrazolo[3,4-*d*]pyrimidine analogues: molecular docking, anticancer evaluation as potential cyclin dependent kinase 2 (CDK2) inhibitors. *Submitted to Chemical Biology and Drug Design (CBDD)*.

Contributions: I generated the rationale and did all the experimental and characterization as well as writing up of manuscript under the guidance of Dr. Rajshekhar Karpoornath

(Supervisor). The co-authors assisted me in writing up of results and discussion and designing of the target molecules.

Conference contributions

1. **Oral presentation:** Synthesis and anticancer evaluation of some novel 4,6-disubstituted pyrazolo[3,4-*d*] pyrimidines as potential cyclin dependent kinase 2 (CDK2) inhibitors. College of Health Sciences Research Symposium, held at Nelson R Mandela School of Medicine Campus, Durban, South Africa, from 5th to 6th October **2017**.

Other publications

1. B. Chandrasekaran, R. Muthusamy, T. L. Chuin, K. P. Samukelisiwe, S. Cherukupalli, G. A. Hampannavar, N. Sayyad, E. S. Soliman, R. Karpoormath, Ligand and structure based in silico studies to identify kinesin spindle protein (KSP) inhibitors as potential anticancer agents, *Journal of Biomolecular Structure and Dynamics*, **2017**, <http://dx.doi.org/10.1080/07391102.2017.1396255>.
2. V. N. Palakollu, N. Thapliyal, T. Chiwunze, R. Karpoormath, S. Karunanidhi, **S. Cherukupalli**, Electrochemically reduced graphene oxide/Poly-Glycine composite modified electrode for sensitive determination of L-dopa, *Material Science and Engineering: C*, **2017**, 77, 394-404.
3. N. Thapliyal, T. Chiwunze, R. Karpoormath, **S. Cherukupalli**, Fabrication of gold nanourchins based electrochemical sensor for nanomolar determination of primaquine, *Material Science and Engineering: C*, **2017**, 74, 27-35.
4. N. Thapliyal, T. Chiwunze, R. Karpoormath, **S. Cherukupalli**, Research progress in electroanalytical techniques for determination of antimalarial drugs in pharmaceutical and biological samples, *RSC Advances*, **2016**, 6, 57580-57602.

Signed: _____



Date: 11-04-2018

Dedicated

To

*My Mother, a strong and gentle soul, who have raised me to be the
person I am today*

*My Father for his unconditional care, unceasing support and
Encouragement*

My Sisters for their solace and love all the way of my life

*My brother-in-law for his gentleness and affection without whom
none of my success would be possible*

ACKNOWLEDGEMENT

I bow to almighty and my parents, to whom I owe the successful completion of my thesis. I would also like to express my deepest gratitude and heartfelt thanks to all those who helped me directly or indirectly in the completion of my research work.

I am deeply indebted to my supervisor Dr. Rajshekhar Karpoormath, for his valuable guidance, patience and stimulating suggestions in all the times of research and writing of this thesis. Your kindness, enthusiasm, and faith in me energized me all throughout. Thank you, Dr. for your generosity and commitment to excellence.

Special thanks to Prof. Neil Koorbanally, School of Chemistry, my previous supervisor for his cooperation and assistance in joining and carrying out my doctoral studies.

I honestly thank Prof. Vladimir Krystof, Laboratory of Growth Regulators, Centre of the Region Hana for Biotechnological and Agricultural Research, Palacky University & Institute of Experimental Botany ASCR, Slechtitelu, Olomouc, Czech Republic for his cooperation and assistance in carrying out anticancer screening studies.

Special thanks to Dr. Balakumar Chandrasekaran, Girish. A. Hampannavar for their precious scientific contributions all throughout the research. I am beholden for your constant encouragement and moral support in tough times.

I would like to thank the technical staff Mr. Dilip Jagjivan, School of Physics and Chemistry and Ms. Caryl Janse van Rensburg, Mass Spectrometry Laboratory, School of Chemistry, UKZN Pietermaritzburg for their assistance in spectroscopic experiments.

My special thanks to all the past and present group members of Synthetic and Medicinal Chemistry Research Group, for their support and contributions. The blissful days spent with you all will be cherished forever.

My humble gratitude to University of KwaZulu-Natal, South Africa, for granting approval for my research proposal and providing all the necessary facilities to carrying it out successfully. My sincere thanks and appreciations for all the supporting staff at Discipline of Pharmaceutical Sciences College of Health Sciences.

I am also thankful to my teachers at Sri Venkateswara University, Tirupati helping me to keep my spirits high in my profession.

Words aren't enough to express how lucky I'm to have Subbareddy as my dearest brother-in-law, for his gentleness, love and financial support all throughout the academics. I'm blessed to have you. I am beholden for your constant encouragement and moral support in tough times. I feel short of words to thank you.

I owe deep honor and love to my Parents Shri. Venkata SubbaReddy and Smt. Seethamma, for my existence and I am indebted to you both for inculcating in me the dedication and discipline to do

whatever I undertake well. Thank you both for pushing me to reach for the stars there by raising my spirits to achieve the same, which could never be accomplished without the support of this wonderful family. I have to specially mention my deep gratitude and love to my sisters Lakshmi and Malleswari for being with me all the times with their constant encouragement and co-operation. I have to mention special thanks and love to Supriya Reddy, whose lovable words always brightens up my day. Cheers, warm blessings and love to my nephews Sumanth Reddy, Shashank Reddy, and niece Pranavi.

Finally, I would like to take the opportunity to thank all my relatives and teachers. I ask for forgiveness for any inadvertent exclusions.

LIST OF ABBREVIATIONS

<i>A. alternate</i>	:	<i>Alternaria alternate</i>
<i>A. flavus</i>	:	<i>Aspergillus flavus</i>
<i>A. niger</i>	:	<i>Aspergillus niger</i>
<i>A. terreus</i>	:	<i>Aspergillus terreus</i>
ARB	:	Non-peptide angiotensin II receptor antagonists
<i>B. fabae</i>	:	<i>Botrytis fabae</i>
<i>B. subtilis</i>	:	<i>Bacillus subtilis</i>
<i>B. thuringiensis</i>	:	<i>Bacillus thuringiensis</i>
<i>B. cereus</i>	:	<i>Bacillus cereus</i>
BMP	:	Bone morphogenetic protein
B-Raf	:	Rapidly accelerated fibrosarcoma
BZR	:	Benzodiazepine receptor
<i>C. albicans</i>	:	<i>Candida albicans</i>
cAMP	:	Cyclic Adenosine Monophosphate
CB ₂	:	Cannabinoid receptor type-2
CBZR	:	Central benzodiazepine receptor
CCR1	:	C-C chemokine receptor type-1
CDK	:	Cyclin-dependent kinase
CHK	:	Checkpoint kinase
CK2	:	Casein kinase-2
CNS	:	Central nervous system
COX	:	Cyclooxygenase
CRF	:	Corticotropin-releasing factor
CRK	:	Cdc2-related kinase
c-Src	:	Proto-oncogene tyrosine-protein kinase Src
CYC6	:	Cyclin 6
DNA	:	Deoxyribonucleic acid
DPP-IV	:	Dipeptidyl peptidase-4
<i>E. coli</i>	:	<i>Escherichia coli</i>
EAC	:	Ehrlich ascites carcinoma
EC ₅₀	:	Half maximal effective concentration

ECMA	:	Endothelial cell mitogenesis assay
ED ₅₀	:	Median effective dose
ER	:	Estrogen receptor
ERK	:	Extracellular signal-regulated kinase
<i>F. oxysporum</i>	:	<i>Fusarium oxysporum</i>
<i>G. candidum</i>	:	<i>Geotrichum candidum</i>
GABA _A	:	Gamma-aminobutyric acid
GI ₅₀	:	Half maximal growth inhibition
GSK-3 β	:	Glycogen synthase kinase 3 beta
hA	:	Human adenosine
HCV	:	Hepatitis C virus
HIV	:	Human immunodeficiency virus
HLM	:	Human liver microsome
HMG-CoA	:	3-hydroxy-3-methylglutaryl-coenzyme-A
HSV-1	:	Herpes simplex virus type-1
5-HT ₆ R	:	5-hydroxytryptamine subtype 6 receptor
IC ₅₀	:	Half maximal inhibitory concentration
IRAK-4	:	Interleukin-1 receptor associated kinase-4
JNK-1	:	c-Jun N-terminal kinase-1
<i>K. pneumonia</i>	:	<i>Klebsiella pneumonia</i>
KDR	:	Kinase insert domain receptor
K_i	:	Inhibition constant
kNN-MFA	:	k-nearest neighbor molecular field analysis
Lck	:	Lymphocyte-specific protein tyrosine kinase
MAPKAP K-2	:	Mitogen-activated protein kinase-activated protein kinase-2
MIC	:	Minimum inhibitory concentration
MLC	:	Minimum lethal concentration
MMP-13	:	Matrix metalloproteinase-13
mTOR	:	Mammalian target of rapamycin
NPY1R	:	Neuropeptide Y receptor type-1
OMF	:	Mass of fabric
<i>P. aeruginosa</i>	:	<i>Pseudomonas aeruginosa</i>
PAH	:	Pulmonary arterial hypertension
<i>P. chrysogenum</i>	:	<i>Penicillium chrysogenum</i>

PBZR	:	Peripheral benzodiazepine receptor
PDE	:	Phosphodiesterase
PDK1	:	Pyruvate dehydrogenase lipoamide kinase isozyme-1
PET	:	Positron emission tomography
Pim	:	Proviral integrations of moloney
PKB	:	Protein kinase B
RNA	:	Ribonucleic acid
ROCK-II	:	Rho associated coiled-coil containing protein kinase-2
RSV	:	Human respiratory syncytial virus
<i>S. racemosum</i>	:	<i>Syncephalastrum racemosum</i>
<i>S. aureus</i>	:	<i>Staphylococcus aureus</i>
<i>S. marcescens</i>	:	<i>Serratia marcescens</i>
SI	:	Selectivity index
<i>T. cruzi</i>	:	<i>Trypanosoma cruzi</i>
Thym	:	Thymus
TSPO	:	Translocator protein
TTK	:	Threonine tyrosine kinase
VEGFR-2	:	Vascular endothelial growth factor receptor-2

TABLE OF CONTENTS

Abstract	ii
Declaration 1: Plagiarism	iv
Declaration 2: Publications	v
Dedication	vii
Acknowledgement	viii
List of abbreviations	x
Table of contents	xiii
List of figures	xvii
List of tables	xxiii

Chapter 1:

1 General introduction	1
1.1 Background	1
1.2 Types of cancer	1
1.3 Causes of cancer	3
1.3.1 Tobacco	3
1.3.2 Physical inactivity/obesity	4
1.3.3 Infectious agents	5
1.3.4 Radiation	6
1.3.5 Heredity	6
1.3.6 Hormones	7
1.3.7 Physical/environmental agents	7
1.4 Types of cancer treatments	7
1.4.1 Surgery	8
1.4.2 Chemotherapy	8
1.4.3 Radiation therapy	8
1.4.4 Targeted therapy	9
1.4.5 Immunotherapy	9
1.4.6 Hormonal therapy	9
1.5 Cyclin dependent kinase inhibitors (CDKs)	9
1.6 Marketed drugs containing pyrimidine/fused pyrimidine scaffold	12

2	Rationale of our research	17
3	Objectives of the present research work	19

Chapter 2:

1	Introduction	26
2	Synthetic approaches for pyrazolo[1,5- <i>a</i>]pyrimidine scaffold	28
3	Pharmacology	34
3.1	Anti-cancer agents.....	35
3.1.1	Anti-proliferatives	35
3.1.2	CDK inhibitors	40
3.1.3	c-Src, lck and chk inhibitors	45
3.1.4	B-raf kinase inhibitors	49
3.1.5	Pim kinase inhibitors	52
3.1.6	KDR kinase inhibitors	55
3.2	Central nervous system (CNS) agents	58
3.2.1	Benzodiazepine receptor modulators	58
3.2.2	5-HT ₆ receptor antagonists	62
3.3	Anti-infectious agents	64
3.4	Anti-inflammatory agents	75
3.5	CRF-1 receptor antagonists	82
3.6	Radiopharmaceuticals	85
3.7	Organic dyes	87
3.8	Miscellaneous agents	89
3.9	Patents covering pyrazolo[1,5- <i>a</i>]pyrimidine nucleus and their target activity	96
4	Conclusion	99
5	Conflicts of interest	99
6	Acknowledgements	99

Chapter 3:

1	Introduction	116
2	Synthetic methodologies for pyrazolo[4,3- <i>d</i>]pyrimidine scaffold	117
3	Biological activities	133
3.1	Anti-cancer agents	133
3.2	Anti-infectious agents	139
3.3	CNS agents	144

3.3.1	Phosphodiesterase-5 inhibitor activity	144
3.3.2	Adenosine receptor antagonists activity	150
3.4	Cytokinin activity	156
3.5	Miscellaneous agents	158
3.6	Patents covering pyrazolo[4,3-d]pyrimidine scaffold with diverse biological activities.....	160
4	Conclusion	162
5	Conflicts of interest	163
6	Acknowledgements	163

Chapter 4:

1	Introduction	171
2	Results and discussion	173
2.1	Chemistry	173
2.2	<i>In vitro</i> evaluation for CDK2 and Abl kinase inhibitors	176
2.3	Anti-proliferative activity against K-562 and MCF-7 cell lines	178
2.4	Structure-activity relationship (SAR) studies	178
2.5	Molecular docking study	179
3	Conclusion	181
4	Experimental section	182
5	Biological activity	192
5.1	CDK2 and Abl kinase inhibition assays.....	192
5.2	Anti-proliferation evaluation for K-562 and MCF-7 cell lines	193
6	Molecular docking simulation	193
6.1	Protein preparation	193
6.2	Grid file generation	194
6.3	Ligand preparation	194
6.4	Docking simulation	194
6.5	Binding mode analysis	194

Chapter 5:

1	Introduction	201
2	Results and discussion	204
2.1	Chemistry	204
2.2	<i>In vitro</i> evaluation for CDK2 and Abl kinase inhibitors	207
2.3	Anti-proliferative activity against K-562 and MCF-7 cell lines	208

2.4	Structure-activity relationship (SAR) studies	209
2.5	Molecular docking study	209
3	Conclusion	211
4	Experimental section	212
5	Biological activity protocol	218
5.1	CDK2 and Abl kinase inhibition assays	218
5.2	Anti-proliferation (K-562 and MCF-7) activity assays	218
6	Molecular docking simulation	219
6.1	Protein preparation	219
6.2	Grid file generation	219
6.3	Ligand preparation	219
6.4	Docking simulation	220
6.5	Binding mode analysis	220
 Chapter 6:		
1	Introduction	226
2	Results and discussion	228
2.1	Chemistry	229
2.2	<i>In vitro</i> evaluation for anti-cancer (CDK2 & Abl) and anti-proliferative (K-562 and MCF-7) activity	231
3	Conclusion	232
4	Experimental section	233
5	Biological activity protocol	238
5.1	CDK2 and Abl kinase inhibition assays	238
5.2	Anti-proliferative activity for K-562 and MCF-7 cell lines	239
 Chapter 7:		
1	Summary and conclusion	242
2	Future work	245
 APPENDIX – I (Supplementary information- chapter 4)		
		246
 APPENDIX – II (Supplementary information- chapter 5)		
		314
 APPENDIX – III (Supplementary information- chapter 6)		
		345

LIST OF FIGURES

Chapter 1:

Figure 1: Estimated number of new cancer cases by area	2
Figure 2: Cancer Incidence and mortality by region	2
Figure 3: a) top 10 most common cancers; b) causes of cancer death	3
Figure 4. International Variation in Lung Cancer Incidence Rates, 2012	4
Figure 5. Association of body fat with increased risks of a number of cancers	5

Chapter 2:

Figure 1: The General structure of pyrazolo[1,5- <i>a</i>]pyrimidine.....	26
Figure 2: Marketed drugs containing pyrazolo[1,5- <i>a</i>]pyrimidine nucleus.....	28
Figure 3: Synthetic approaches for pyrazolo[1,5- <i>a</i>]pyrimidines.....	30
Figure 3: (continued). Synthetic approaches for pyrazolo[1,5- <i>a</i>]pyrimidines.....	31
Figure 3: (continued). Synthetic approaches for pyrazolo[1,5- <i>a</i>]pyrimidines.....	33
Figure 3: (continued). Synthetic approaches for pyrazolo[1,5- <i>a</i>]pyrimidines.....	34
Figure 4: SAR of p21 chemoselective pyrazolo[1,5- <i>a</i>]pyrimidin-7-yl-phenyl amides and the anti-proliferative activity of the representative compound 1	35
Figure 5: SAR of amino alkoxy moiety containing pyrazolo[1,5- <i>a</i>]pyrimidines and anti-tumor activities of the representative compound 2.....	36
Figure 6: SAR and anti-proliferative activity of pyrazolo[1,5- <i>a</i>]pyrimidine derivatives.....	37
Figure 7: Pyrazolo[1,5- <i>a</i>]pyrimidin-7-ylphenyl amides and their effect on colon cell lines.....	37
Figure 8: Anti-tumor activity of <i>N</i> -(4-chlorophenyl)-2-(methylthio)-5-(naphthalene-2-yl) pyrazolo[1,5- <i>a</i>]pyrimidine-3-carboxamide.....	38
Figure 9: SAR and anti-tumor properties of thiazolo[3,2- <i>a</i>]benzimidazole linked pyrazolo[1,5- <i>a</i>]pyrimidines.....	39
Figure 10: SAR of pyrazolo[1,5- <i>a</i>]pyrimidine-3-carbonitriles as anti-tumor agents.....	39
Figure 11: SAR of pyrazolo[1,5- <i>a</i>]pyrimidine derivative as anti-tumor agent.....	40
Figure 12: SAR of pyrazolo[1,5- <i>a</i>]pyrimidines as CDK2 inhibitors.....	41
Figure 13: SAR studies and pharmacokinetic properties of pyrazolo[1,5- <i>a</i>]pyrimidine derivatives as orally available CDK2 inhibitors.....	42
Figure 14: SAR studies of (2 <i>S</i> ,3 <i>S</i>)-3-((7-(benzylamino)-3-isopropylpyrazolo[1,5- <i>a</i>]pyrimidine-5-yl)amino)butane-1,2,4-triol as CDK inhibitors.....	42
Figure 15: SAR and effect of 2-aminobenzothiazole linked pyrimidines on human cancer cell lines.....	43

Figure 16: SAR of pyrazolo[1,5- <i>a</i>]pyrimidine type CDK2 inhibitors.....	45
Figure 17: SAR and pharmacological activities of compound 26 as CDK9 inhibitor.....	45
Figure 18: SAR and pharmacokinetic properties of (7-((<i>S</i>)-1-benzyl-2-hydroxyethylamino)-5-cyclopropyl-2-(3,5-dimethoxyphenylamino)pyrazolo[1,5- <i>a</i>]pyrimidine-3-carboxamide.....	47
Figure 19: SAR and selectivity values of Isobutyl(4-(7-amino-3-(3-(piperzin-1-yl)pyrazolo[1,5- <i>a</i>]pyrimidin-6-yl)phenyl)carbamate.....	47
Figure 20: SAR and molecular interactions of 3-methyl- <i>N</i> -(3-(1-methyl-1 <i>H</i> -pyrazol-4-yl)-5-(piperidin-3-yl)pyrazolo[1,5- <i>a</i>]pyrimidin-7-yl)isothiazol-5-amine.....	48
Figure 21: SAR studies of 5-(3-aminocyclohexyl)-6-bromo-3-(1-methyl-1 <i>H</i> -pyrazol-4-yl)pyrazolo[1,5- <i>a</i>]pyrimidin-7-amine derivatives.....	49
Figure 22: SAR study of pyrazolo[1,5- <i>a</i>]pyrimidine-3-carboxylates as potent B-Raf kinase inhibitors.....	50
Figure 23: SAR and B-Raf kinase activity of 3-substituted <i>N</i> -(3-(pyrazolo[1,5- <i>a</i>]pyrimidin-7-yl)phenyl)-3-(trifluoromethyl)benzamides.....	50
Figure 24: B-Raf kinase activity and SAR studies of disubstituted pyrazolo[1,5- <i>a</i>]pyrimidines.....	51
Figure 25: SAR and B-Raf kinase activity of lead compound consisting pyrazolo[1,5- <i>a</i>]pyrimidine.....	52
Figure 26: Pin-pam inhibitory activities and SAR of <i>N</i> -(5-(2-fluorophenyl)-1 <i>H</i> -pyrrolo[2,3- <i>b</i>]pyridin-3-yl)-5-(((3-fluoropiperidin-4-yl)methyl)amino)pyrazolo[1,5- <i>a</i>]pyrimidine-3-carboxamide.....	53
Figure 27: SAR, Pim and kinase activity of 3,5-disubstituted pyrazolo[1,5- <i>a</i>]pyrimidine.....	54
Figure 28: SAR and pim activities of disubstituted pyrazolo[1,5- <i>a</i>]pyrimidine derivatives.....	55
Figure 29: SAR and KDR kinase and KDR selectivity values of 3,6-diaryl pyrazolo[1,5- <i>a</i>]pyrimidines.....	56
Figure 30: KDR kinase and ECMA activities.....	57
Figure 31: Structural activity studies, KDR and UE results of 7-aminopyrazolo[1,5- <i>a</i>]pyrimidines.....	58
Figure 32: SAR and activity values of thienyl and methoxyphenyl substituted pyrazolo[1,5- <i>a</i>]pyrimidines.....	59
Figure 33: SAR and PBBR, CBZR studies of <i>N,N</i> -diethyl-(2-aryl)pyrazolo[1,5- <i>a</i>]pyrimidin-3-yl acetamides.....	60
Figure 34: SAR and activity data of 3-aryl-6-(3-thienyl)pyrazolo[1,5- <i>a</i>]pyrimidin-7-ones against recombinant BZR.....	60
Figure 35: SAR and activity studies of 2-phenyl pyrazolo[1,5- <i>a</i>]pyrimidin-3-yl acetamides.....	61
Figure 36: Recombinant BZR affinity values of <i>N,N</i> -dimethyl-2-(5-methyl-2-(<i>p</i> -tolyl)pyrazolo[1,5- <i>a</i>]pyrimidin-3-yl)acetamide.....	61
Figure 37: TSPO and CBZR binding and selectivity studies of pyrazolo[1,5- <i>a</i>]pyrimidines.....	62
Figure 38: SAR and 5-HT ₆ receptor studies of pyrazolo[1,5- <i>a</i>]pyrimidines.....	63
Figure 39: SAR, 5-HT ₆ R activity profiles of substituted 5, <i>N</i> ² -dimethyl-3-phenylsulfonyl-pyrazolo[1,5- <i>a</i>]pyrimidine-2-amine.....	64

Figure 40: SAR of multi substituted pyrazolo[1,5- <i>a</i>]pyrimidines as antitrichomonal agents.....	64
Figure 41: SAR and antitrypanosomal activity studies of compound 83.....	65
Figure 42: SAR of 7-alkylamino substituted pyrazolo[1,5- <i>a</i>]pyrimidines antifungal compounds.....	66
Figure 43: SAR and active antibacterial pyrazolo[1,5- <i>a</i>]pyrimidines.....	67
Figure 44: Structures and results of the antimicrobial (inhibition zone) potency of pyrazolo[1,5- <i>a</i>]pyrimidines.....	67
Figure 45: SAR and antiviral properties of active compounds.....	68
Figure 46: Structures and MIC values of pyrazolo[1,5- <i>a</i>]pyrimidines against different bacterial and fungal strains.....	69
Figure 47: SAR and antimicrobial results of pyrazolo[1,5- <i>a</i>]pyrimidines.....	70
Figure 48: Structures and antimicrobial results of pyrazolo[1,5- <i>a</i>]pyrimidines.....	71
Figure 49: SAR, antibacterial activity of pyrazolo[1,5- <i>a</i>]pyrimidines.....	71
Figure 50: SAR and antimicrobial studies of pyrazolo[1,5- <i>a</i>]pyrimidines.....	73
Figure 51: SAR and activity data of active compounds.....	73
Figure 52a: SAR and biological studies of a lead compound.....	74
Figure 52b: Pharmacokinetic properties of potent derivative 116.....	75
Figure 53: 3,5-cyclic-AMP phosphodiesterase inhibitory abilities of active compounds.....	75
Figure 54: SAR and 3',5'-phosphate phosphodiesterase inhibitor studies of substituted pyrazolo[1,5- <i>a</i>]pyrimidines.....	76
Figure 55: SAR and anti-inflammatory properties of 2-phenylpyrazolo[1,5- <i>a</i>]pyrimidin-7-ones.....	77
Figure 56: SAR and the data of potent molecule.....	77
Figure 57: Pharmacological evaluation results of active compounds.....	78
Figure 58: Selectivity and potency of compound 128 towards MMP-13.....	79
Figure 59: SAR, MAPKAP-K2 kinase and CDK2 selectivity values of 5,6,7-trisubstituted pyrimidines.....	80
Figure 60: SAR and IRAK4 inhibitory, pharmacokinetic activities of pyrazolo[1,5- <i>a</i>]pyrimidine-3-carboxamide derivatives.....	81
Figure 61: SAR and PDE4 inhibitory studies.....	82
Figure 62: CRF binding affinity studies of pyrazolo[1,5- <i>a</i>]pyrimidine derivative.....	82
Figure 63: SAR and single dose pharmacokinetic data of pyrazolo[1,5- <i>a</i>]pyrimidines.....	83
Figure 64: SAR and CRF ₁ affinity studies of pyrazolo[1,5- <i>a</i>]pyrimidines.....	84
Figure 65: CRF ₁ and antagonist studies of pyrazolo[1,5- <i>a</i>]pyrimidines.....	85
Figure 66: Structure and bio-distribution of ^{99m} TcN-MAG-ABCPP in mice bearing S 180 tumor (% ID/g).....	86
Figure 67: Structure and bio-distribution in mice bearing S180 for [¹⁸ F]1 expressed as % injected dose per gram.....	87

Figure 68: Organic dye properties of synthesized compounds.....	87
Figure 69: Dye properties of bis-sulphatoethylsulphone and bis-monochlorotriazine containing pyrazolo[1,5- <i>a</i>]pyrimidines.....	88
Figure 70: Dye properties of the representative compound.....	89
Figure 71: SAR and the binding affinity of active compounds towards angiotensin II receptors.....	90
Figure 72: SAR, pharmacological and selected pharmacokinetic data of active compounds.....	90
Figure 73: SAR, binding affinity and selected pharmacokinetic data of potent inhibitors.....	92
Figure 74: Estrogen receptor ligands bearing pyrazolo[1,5- <i>a</i>]pyrimidine scaffold.....	92
Figure 75: Cytotoxicity studies of pyrazolo[1,5- <i>a</i>]pyrimidines with reference drug doxorubicin.....	93
Figure 76: SAR and cytotoxic properties of highly active compounds consisting pyrazolo[1,5- <i>a</i>]pyrimidine scaffold.....	94
Figure 77: SAR and BMP4 cell line properties of 3,6-difunctionalized pyrazolo[1,5- <i>a</i>]pyrimidines.....	95
Figure 78: SAR and cannabinoid receptor studies of 7-oxopyrazolo[1,5- <i>a</i>]pyrimidine-6-carboxamides.....	95
Figure 79: SAR and TTK activity studies.....	96
Figure 80: Biological activities of pyrazolo[1,5- <i>a</i>]pyrimidines.....	97
Figure 81: Summary of structural modifications to influence the activity.....	98

Chapter 3:

Figure 1: General structures of purine (a) and pyrazolo[4,3- <i>d</i>]pyrimidine (b)	117
Figure 2: Marketed drug Sildenafil containing pyrazolo[4,3- <i>d</i>]pyrimidine scaffold	117
Figure 3: Possible reaction centres of pyrazolo[4,3- <i>d</i>]pyrimidine scaffold	118
Figure 4: Synthetic methodologies for pyrazolo[4,3- <i>d</i>]pyrimidine scaffold	120
Figure 4: (<i>Continued</i>). Synthetic strategies for pyrazolo[4,3- <i>d</i>]pyrimidines	121
Figure 4: (<i>Continued</i>). Synthetic strategies for pyrazolo[4,3- <i>d</i>]pyrimidines	123
Figure 4: (<i>Continued</i>). Synthetic strategies for pyrazolo[4,3- <i>d</i>]pyrimidines	124
Figure 4: (<i>Continued</i>). Synthetic strategies for pyrazolo[4,3- <i>d</i>]pyrimidines	126
Figure 4: (<i>Continued</i>). Synthetic strategies for pyrazolo[4,3- <i>d</i>]pyrimidines	127
Figure 4: (<i>Continued</i>). Synthetic strategies for pyrazolo[4,3- <i>d</i>]pyrimidines	129
Figure 4: (<i>Continued</i>). Synthetic strategies for pyrazolo[4,3- <i>d</i>]pyrimidines	130
Figure 4: (<i>Continued</i>). Synthetic strategies for pyrazolo[4,3- <i>d</i>]pyrimidines	132
Figure 4: (<i>Continued</i>). Synthetic strategies for pyrazolo[4,3- <i>d</i>]pyrimidines	133
Figure 5: SAR and anticancer properties of 2-(((3-isopropyl-1 <i>H</i> -pyrazolo[4,3- <i>d</i>]pyrimidin-7-yl)amino)methyl)phenol	134

Figure 6: Figure 6. SAR and antiproliferative activity of compound 2 on various cancer cell lines...	135
Figure 7: Anticancer activity on various cancer cell lines and kinase selectivity profile for compound 3.....	136
Figure 8: CDK kinase activity of lead compounds consisting trisubstituted pyrazolo[4,3- <i>d</i>]pyrimidine scaffold.....	136
Figure 9: SAR and anti-proliferative activity of compound 6 on various human cancer cell lines.....	137
Figure 10: Anticancer activity and SAR studies of 3,5,7-trisubstituted pyrazolo[4,3- <i>d</i>]pyrimidines..	138
Figure 11: SAR study of 3-isopropyl-7-[4-(2-pyridyl)benzyl]amino-1(2) <i>H</i> -pyrazolo[4,3- <i>d</i>]pyrimidines as potent CDK inhibitors.....	139
Figure 12: Structures and anti-viral activity of 1- β -D-ribofuranosyl-3-methyl-6-substituted-7 <i>H</i> -pyrazolo[4,3- <i>d</i>]pyrimidin-7-ones against HSV-1.....	140
Figure 13: Anti-viral activity of 5-amino-1-methyl-3- β -D-ribofuranosyl-pyrazolo[4,3- <i>d</i>]pyrimidin-7(6 <i>H</i>)-one.....	141
Figure 14: Anti-microbial values of 3-(4-bromophenyl)-1,6-dihydro-7 <i>H</i> -pyrazolo[4,3- <i>d</i>]pyrimidin-7-one against different bacterial and fungal strains.....	142
Figure 15: Antimicrobial and anti-cancer properties of 6-amino-3-(4-chlorophenyl)-5-methyl-1,6-dihydro-7 <i>H</i> -pyrazolo[4,3- <i>d</i>]pyrimidin-7-one derivatives.....	144
Figure 16: SAR and phosphodiesterase inhibitory abilities of active compounds.....	145
Figure 17: SAR and pharmacokinetic properties of piperazine linked pyrazolo[4,3- <i>d</i>]pyrimidines as potent phosphodiesterase inhibitors.....	147
Figure 18: 3D-QSAR studies of 1-(2-ethoxyethyl)-1 <i>H</i> -pyrazolo[4,3- <i>d</i>]pyrimidines as PDE5 inhibitors.....	148
Figure 19: Structures, biological results of active compounds as potent PDE5 inhibitors.....	150
Figure 20: SAR and adenosine receptor antagonist activity of 1,3-dialkyl pyrazolo[4,3- <i>d</i>]pyrimidin-7-ones.....	151
Figure 21: SAR and human A ₃ adenosine receptor antagonist activity of 2-(4-methoxyphenyl)-5-methyl-2,6-dihydro-7 <i>H</i> -pyrazolo[4,3- <i>d</i>]pyrimidin-7-one.....	151
Figure 22: Structures, binding results of 7-amino-2-phenylpyrazolo[4,3- <i>d</i>]pyrimidines as A ₃ adenosine receptor antagonists.....	152
Figure 23: SAR and A ₁ and A _{2A} adenosine receptor activity of pyrazolo[4,3- <i>d</i>]pyrimidines.....	153
Figure 24: SAR and human A ₃ adenosine receptor activity of lead compounds consisting pyrazolo[4,3- <i>d</i>]pyrimidine.....	154
Figure 25: Structures and biological activity of 7-aminopyrazolo[4,3- <i>d</i>]pyrimidines as human A ₁ and A _{2A} adenosine receptors.....	156
Figure 26: Structures of lead compounds with potent cytokinin activity.....	156
Figure 27: SAR of 7-substituted 3-methylpyrazolo[4,3- <i>d</i>]pyrimidines as cytokinin antagonists in tobacco bioassay.....	157
Figure 28: Cytokinin activity of pyrazolo[4,3- <i>d</i>]pyrimidines on various tobacco cells.....	158
Figure 29: SAR, structures and CRF-1 binding affinity studies of lead compounds.....	159

Figure 30: Anti-leishmanial activity and SAR studies of 3,7-disubstituted pyrazolo[4,3-*d*]pyrimidines.....160

Figure 31: Summary of structural amendments to influence the biological activity.....162

Chapter 4:

Figure 1. Structures of active drugs containing fused pyrimidine172

Figure 2. Literature reported derivatives containing pyrazolo[3,4-*d*]pyrimidine scaffold and their anticancer activities along with the designed molecules. A: (K_{i50} against Src, AblT315I = 0.056, 0.01 μ M); B: (IC_{50} against CDK9 = 17 nM); C: (IC_{50} against CDK2 = 0.5 μ M); D: (K_{i50} against Abl = 80 nM); E: (K_{i50} against cSrc, Abl = 0.21 \pm 0.02, 0.15 \pm 0.02 μ M); F: (IC_{50} against Src = 1.2 \pm 0.4 μ M)173

Figure 3. SAR study of 4,6-disubstituted pyrazolo[3,4-*d*]pyrimidines as potent anticancer agents179

Figure 4: Reported pose (wire-frame model) and Docked pose (thick tube model) into the active site showing similar interactions (docking validation)180

Figure 5. Molecular interactions of a) active compound 11 b) moderately active compound 27 c) less active compound 30 into the binding site of CDK2/cyclin E protein. Nonpolar hydrogens were hidden for clarity and yellow dashed line indicate H bond181

Chapter 5:

Figure 1. Structures of the CDK2 inhibitors in clinical trials203

Figure 2. Literature reported derivatives containing pyrazolo[3,4-*d*]pyrimidine scaffold and their anticancer activities. Compound A: (K_{i50} against Src, AblT315I = 0.056, 0.01 μ M); B: (IC_{50} against CDK2 =0.020 μ M); C: (IC_{50} against CDK2 = 0.5 μ M); D: (K_{i50} against Abl = 80 nM); E: (K_{i50} against cSrc, Abl = 0.21 \pm 0.02, 0.15 \pm 0.02 μ M); F: (IC_{50} against Src = 1.2 \pm 0.4 μ M).....204

Figure 3. SAR study around pyrazolo[3,4-*d*]pyrimidine scaffold towards potent activity209

Figure 4. Reported pose (wire-frame model) and Docked pose (thick tube model) into the active-site showing similar interactions (docking validation)210

Figure 5. Molecular interactions of a) **14c** (most active compd) b) **15c** (less active compd) in the binding site of CDK2. Nonpolar hydrogens were hidden for clarity and yellow dashed line indicate H bond. The cyano and green coloured dashed lines indicate π - π interactions and π -cation interactions, respectively211

Chapter 6:

Figure 1. Structures of the CDK2 inhibitors in clinical trials227

Figure 2. Literature reported derivatives containing pyrazolo[3,4-*d*]pyrimidine scaffold and their anticancer activities along with the designed molecules. A: (K_{i50} against Src, AblT315I = 0.056, 0.01 μ M); B: (IC_{50} against CDK9 = 17 nM); C: (IC_{50} against mTOR = 13 nM); D: (IC_{50} against mTOR = 9 nM); E: (K_{i50} against cSrc, Abl = 25, 41 nM); F: (IC_{50} against Src = 1.2 \pm 0.4 μ M).....228

LIST OF TABLES

Chapter 1

Table 1: Different types of cancers caused by virus, bacteria and parasites	6
Table 2. Pyrimidine/fused pyrimidine containing marketed drugs as anticancer agents	12
Table 3. Structures of CDK drugs under clinical trials	17

Chapter 2

Table 1: Pyrazolo[1,5- <i>a</i>]pyrimidine nucleus containing patents having numerous biological activities	97
--	----

Chapter 3

Table 1: Pyrazolo[4,3- <i>d</i>]pyrimidine nucleus containing patents having numerous biological activities	161
--	-----

Chapter 4

Table 1: Anticancer evaluation of novel 4,6-disubstituted pyrazolo[3,4- <i>d</i>]pyrimidine derivatives...	178
---	-----

Chapter 5

Table 1: Anticancer evaluation of novel 4,6-disubstituted pyrazolo[3,4- <i>d</i>]pyrimidine derivatives...	208
---	-----

Chapter 6

Table 1: Anticancer evaluation of novel mono substituted pyrazolo[3,4- <i>d</i>]pyrimidines against CDK2/Abl kinases and K-562/MCF-7 cell lines.....	232
---	-----

Note: Referencing styles of individual chapters are as per guidelines of communicated journals.

CHAPTER 1

1 GENERAL INTRODUCTION

1.1 Background

Cancer is a generic term for a complex disease characterized by uncontrolled growth of the abnormal cells beyond their usual margins that can then enter contiguous parts of the body and/or spread to other organs. Other common terms used are malignant tumors and neoplasms. Cancer can affect almost any part of the body and has many anatomic and molecular subtypes, each one requiring particular management approaches. Cancer has an impending mortality and morbidity rate with a staggering 14.1 million people worldwide. The rise in the frequency of confirmed cancer cases remains a challenge, especially in South Africa, which ranks as one of the highest statistics in comparison to other countries that have been stricken by this devastating disease. In 2012, the World Health Organization (WHO) estimated that out of 14.1 million individuals affected with cancer, 8.8 million people (approximately 22,000 cancer deaths a day) have succumbed to this disease. By 2030, new cancer cases are expected to grow to 21.7 million with a staggering 13 million deaths as a result of the rapid growth and aging of the population unless preventative measures are put into place.¹ Some important lifestyle factors known to increase the cancer risk is the consumption of alcohol, poor diet, smoking, reproductive alterations and physical inactivity in developing nations. It is important to take note that the actual Fig.s for estimated cancer cases will be considerably larger.² Therefore, it is for this reason that cancer is considered as a serious public health burden worldwide as illustrated in **Fig. 1 & 2**.

1.2 Types of cancer

Cancer is a multifaceted disease, which commences when healthy cells change and grow out of control, resulting in the formation of a mass called a tumor. A tumor can be cancerous or benign. A cancerous tumor is malignant, meaning it can grow and spread to other parts of the body. A benign tumor describes a tumor that can grow but does not spread. There are almost 100 types of cancers existing in human body and these are titled according to organs or tissues in which they form. The worldwide cancer statistics from cancer research UK, the top five most commonly diagnosed cancers are the lung, breast, colorectal, prostate and stomach cancers (**Fig.3a**) accounting for more than half of total cancer deaths (**Fig. 3b**).³ Over the last 40 years, the common cancer profiles have slightly changed with lung, liver, stomach and bowel cancers accounting for most deaths.⁴

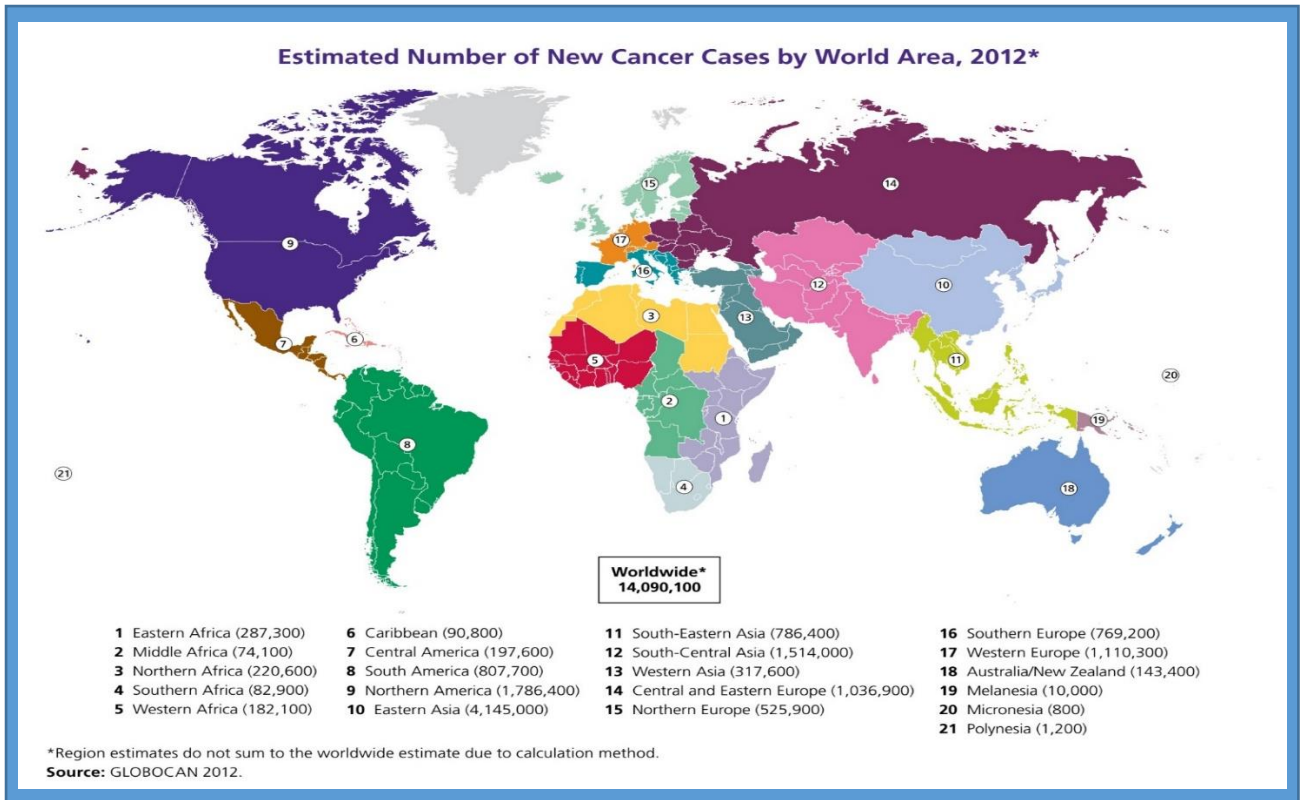


Fig. 1. Estimated number of new cancer cases by area.¹

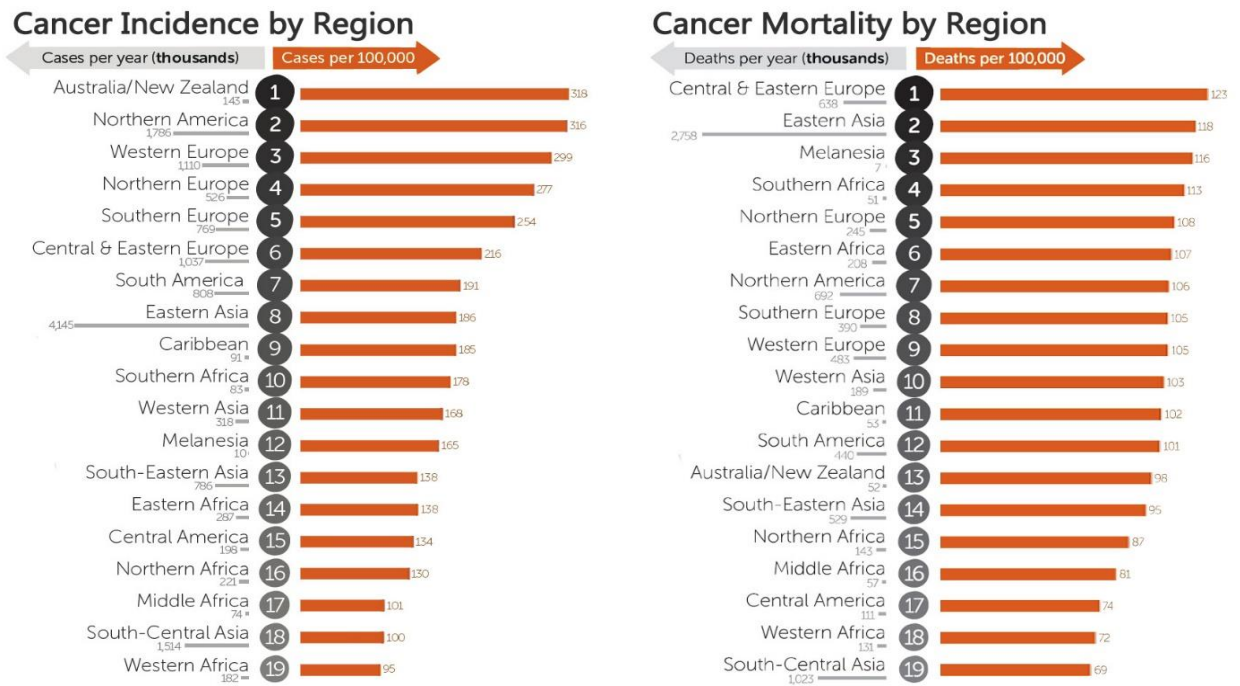


Fig. 2. Cancer Incidence and mortality by region.^{3,4}

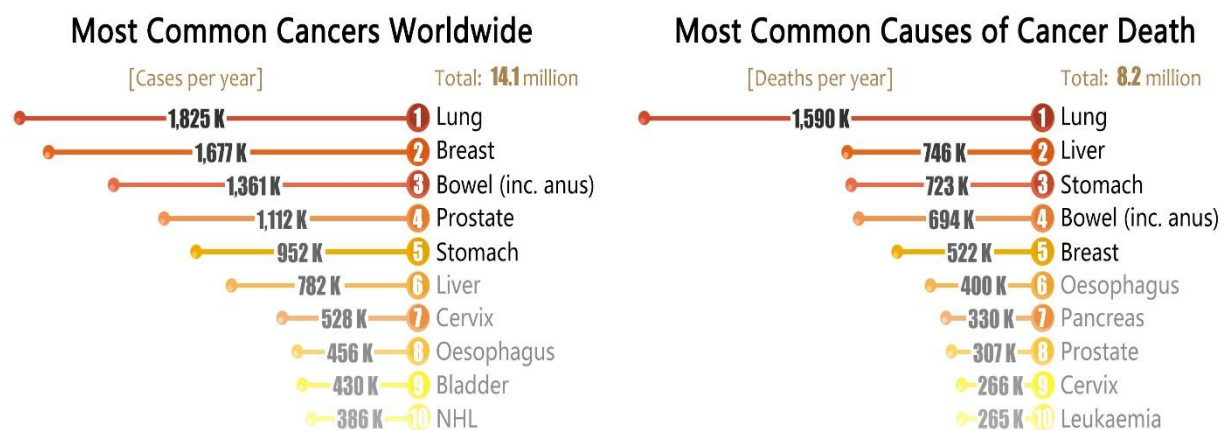


Fig. 3. a) top 10 most common cancers; b) causes of cancer death.^{3,4}

1.3 Causes of cancer

Most cancers are associated with environmental, lifestyle as well as economical and behavioral factors.⁵ Some of the common factors that contribute to cancer death include infections (15-20%), tobacco (25-30%), obesity/diet/physical inactivity (30-35%), radiation (up to 10%), heredity (3-10%), hormones and physical/environmental agents.⁶ General signs and symptoms associated with cancer are prolonged cough, lump in the affected area, baffling weight loss, abnormal bleeding and change in bowel movements.

1.3.1 Tobacco

In 2008, WHO named *Nicotiana* as the global single greatest preventable cause of death.⁷ Tobacco is a product obtained from the dried leaves of tobacco plant and mostly consumed in the form of cigarettes, cigars, pipe tobacco and other tobacco containing chewable products. Tobacco contains an alkaloid called nicotine, which is stimulant responsible for the addictive nature and affects many organs such as the heart, liver and lungs. Its use is associated with many forms of cancers resulting in 80% of lung cancer,⁸ which could be attributed to approximately fifty known carcinogens such as nitrosamines and polycyclic aromatic hydrocarbons.⁹

Moreover, smoking non-tobacco containing electronic cigarettes is more harmful as it generates the chemical formaldehyde. Lung cancer is one of the most often detected cancer and the leading cause of the cancer related deaths worldwide. Globally, 1.8 million new cases have been reported in 2012, accounting for 13% total cancer detection and an estimated 1.6 million (1.1 million in men and 491,200 deaths in women).² In some nations, it has been shown to be the leading cause of death for women as opposed to breast cancer. **Fig. 4** unveils the prevalence of lung cancer worldwide.¹

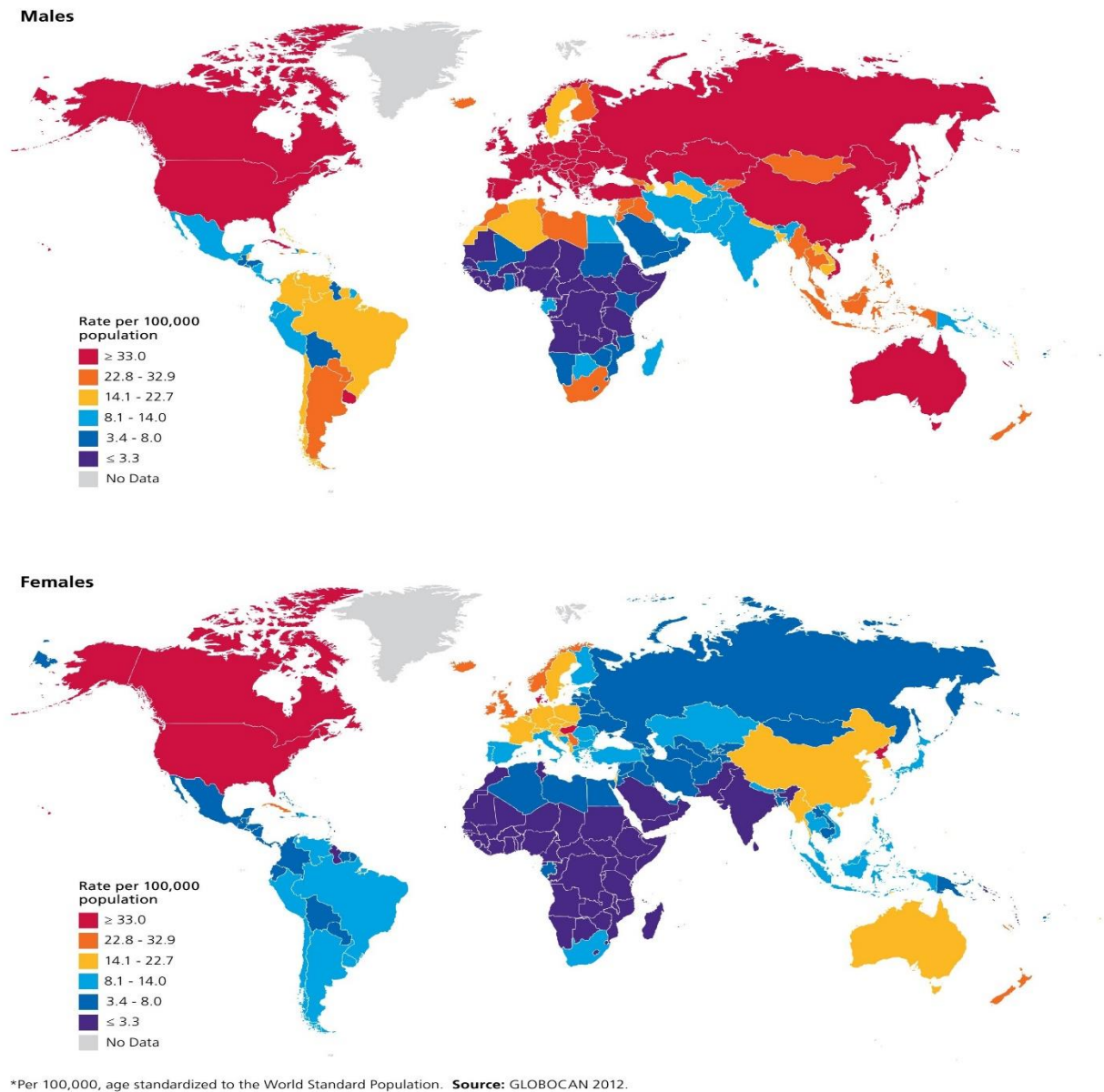


Fig. 4. International Variation in Lung Cancer Incidence Rates, 2012.¹

1.3.2 Physical inactivity/obesity

Human life has been associated with several physical activities including exercising, performing household chores, working, and leisure-time activities such as hiking, walking, to name but a few. Physical activity is crucial for the human body to maintain an equilibrium between the number of calories consumed and the number of calories utilized. Using less calories than one consumes leads to obesity, in which a person has an unhealthy body fat, developed when the energy intake from food and drink exceeds energy outlay from physical activity and other metabolic processes. Obesity is a risk factor for cancer, as well as other chronic diseases such as type 2 diabetes and cardiovascular disease.⁶ Obese people often have chronic low-level inflammation, which can cause DNA damage that can lead

to cancer overtime. Overweight and obese people in comparison to normal-weight people are more likely to have conditions or disorders that are connected to or that cause chronic local inflammation and those are risk factors for certain cancers.¹⁰ Globally, 30-35% cancer deaths have been attributed to poor diet/obesity/physical inactivity. Data obtained from the National Health and Nutrition Examination Survey (NHANES) revealed that in 2011–2014, almost 70% of U.S. adults age 20 years or older were overweight and more than one-third (36.5%) were obese.¹¹ An increase in body weight has been linked to several different types of cancers. (**Fig. 5**) with an estimated 14-20% cancer deaths been reported.¹²

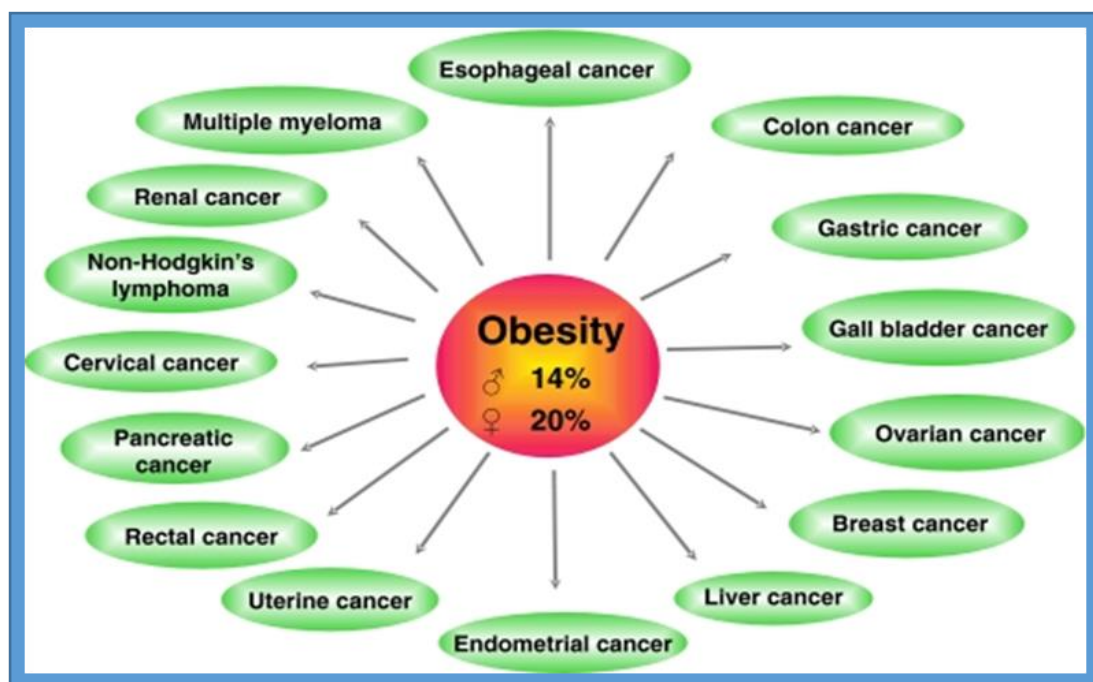


Fig. 5. Association of body fat with increased risks of a number of cancers.

1.3.3 Infectious agents

Several infectious agents such as viruses, parasites and bacteria can cause cancer or may increase the risk factor that forms cancer. In addition, some viruses can interrupt signaling that are typically responsible for cell growth and proliferation in both prokaryotes and eukaryotes. Therefore, some infections are known to weaken the immune system and the human body becomes more susceptible to these cancer causing agents. Generally, viruses that are associated with an augmented risk of cancer can be passed on from one person to another through blood and other body fluid transfusions, unprotected sex as well as the sharing of needles. Globally an estimated 16.1% of cancer cases are attributable to infectious agents,¹³ especially for cervical cancers, liver cancers (80%) and other cancers (15-20%).¹⁴ This global percentage varies from one regions to the other with as high as 32.7% in Africa to 3.3% in New Zealand and Australia.¹⁵ A virus that could be responsible for causing cancer is called oncovirus

and is the most significant risk factor for several cancer growth in the humans.¹⁶ The table below briefly gives the various cancers causing viruses, bacteria's and parasites.

Virus/bacteria/parasite	Name	Type of cancer
Virus	Hepatitis B	Liver cancer
	Hepatitis C	Liver cancer ¹⁵
	Human papilloma	Cervical, nose, throat, anus, larynx and esophagus cancer ¹⁶
	Epstein-barr	Nasopharyngeal, burkitt lymphoma and hodgkins lymphoma cancer
	Human herpesvirus 8	Kaposi sarcoma and B-cell lymphoma cancer ¹⁷
	Human T cell lymphotropic	Adult T cell leukemia cancer ¹⁸
	Merkel cell polyoma	Merkel cell carcinoma ¹⁹
Bacteria	<i>Helicobacter pylori</i>	Gastric cancer ²⁰
	<i>Chlamydothila pneumoniae</i>	Lung cancer ²¹
Parasite	<i>Schistosoma haematobium</i>	Bladder cancer
	<i>Schistosoma japonicum</i>	Colorectal cancer ²²

Table 1. Different types of known cancer causing viruses, bacteria's and parasites.

1.3.4 Radiation

The radiation of certain wavelengths/frequencies such as ionizing radiation has sufficient energy to damage DNA and cause cancer. Globally up to 10% of critical cancers are due to radiations, which compromises of both ionizing and non-ionizing radiation whereas most of the non-melanoma skin cancers is caused by non-ionizing ultraviolet radiation.⁶ Radiation can cause cancer in any part of the human body, and at any age. Radiation influenced solid tumors generally takes 10-15 years to become clinically visible and radiation induced leukemias characteristically takes 2-10 years.²³ The sources of radiation include radon, x-rays, gamma rays, medical imaging, alpha particles, neutrons, beta particles. In addition, various medical techniques, such as positron emission tomography (PET) scans, chest x-rays, computed tomography (CT) scans and radiation therapy can also cause cell damage that can lead to cancer. However, the advantages from these medical techniques are very high while the risk posed is trivial.

1.3.5 Heredity

A genetic defect is usually passed from parents to their offspring, either by sexual or asexual reproduction and the progeny cells or organisms obtain the genetic information from their parents. Majority of cancers are non-hereditary whereas hereditary cancers are mainly caused by an inherited genetic defect. Globally an estimated 0.3% of people are carriers of a genetic mutation that has a great effect on cancer risk and cause around 3-10% of all cancers. In addition, a set of medical signs include inherited mutations in BRCA1 (breast cancer susceptibility gene 1) and BRCA2 (breast cancer susceptibility gene 2) which is responsible for more than 75% risk for breast cancer, ovarian cancer²⁴ and hereditary nonpolyposis colorectal cancer, which is existing in about 3% of persons diagnosed with colorectal cancer.²⁵

1.3.6 Hormones

Hormone is a chemical messenger that is secreted into the blood to communicate between organs and tissues for physiological regulation, behavioral actions including digestion, tissue function, metabolism, sleep, respiration, lactation, sensory perception, stress, growth and development, reproduction, excretion, movement, and mood.²⁶ Apart from those listed, some hormones play a major role in the development of cancer by encouraging cell proliferation. Hormones are important in sex-related cancers include breast, prostate, testis, endometrium, ovary, as well as bone and thyroid cancer. One such example is estrogen a female sex hormone, known as a human carcinogen. Even though these sex hormones have crucial physiological roles in both females and males as well as linked with an increased risk of certain cancers. For example, taking combined menopausal hormone therapy (estrogen & progesterone) can increase a woman's risk of breast cancer. Menopausal hormone therapy with estrogen alone results in an increased risk of endometrial cancer. In addition, person on hormone replacement therapy would have increasingly high levels of hormones, thus a greater risk of developing cancer. On the other hand, a person who does exercise more than average will have a lower level of hormones and consequently a reduced risk of cancer.²⁷

1.3.7 Physical/environmental agents

Apart from chemical agents, there are certain matter/substances which on prolonged exposure could physically induce cancer and are called physical cancer agents. For instance, continued exposure to asbestos leads to membrane cancer. Similarly, other natural and synthetic asbestos-like fibers such as glass wool, wollastonite, rock wool and attapulgite are also known to cause cancer. In addition, non-fibrous materials such as powdered metallic nickel and cobalt, crystalline silica can also induce cancer.²⁸

1.4 Types of cancer treatments

Total removal of cancerous tissue without causing harm to the rest of the healthy tissue is an ideal goal of treatment. There are several types of cancer treatments and the choice of treatment depends on

location, type, grade of tumor and the phase of the disease. Most of the cancers can be treated mainly using chemotherapy, hormonal therapy, surgery, radiation therapy, immunotherapy as well as targeted therapy.

1.4.1 Surgery

Cancer surgery is used to prevent, diagnose, and treat cancer. It is the oldest type (Ancient Egypt) of cancer treatment and normally works best for solid tumors existing in specific areas. The main objective of the surgery can be removal of only the tumor or whole organ. Each cancer type has specific cancer operations such as whipple surgery for pancreatic cancer, mastectomy for breast cancer, prostatectomy for prostate cancer and lung surgery for non-small cell lung cancer.²⁹ In addition, surgery is often essential for cancer staging (determining the extent of the disease and whether it has metastasized to regional lymph nodes) and to control bowel obstruction or spinal cord compression.³⁰

1.4.2 Chemotherapy

Chemotherapy (frequently abbreviated to CTX or chemo or CTx) is a type of cancer treatment with one or more drugs (chemotherapeutic agents) that can kill cancer cells. Combination chemotherapy is a combination of two or more cancer drugs is usually used for the efficient treatment of cancer. Chemotherapy may be specified with a curative intent (combinations of drugs), or it may aim to prolong life or to diminish symptoms (palliative chemotherapy). Traditional chemotherapeutic agents are cytotoxic as they have been seen to interfere with rapid cell division and affect the normal healthy cells as well, but cancer cells may vary broadly in their susceptibility to these agents. Chemotherapeutic drugs in a number of ways can cause interference of cell division and these include duplication of DNA and separation of just formed chromosomes. Majority of leukemia and lymphoma cancers could be treated by chemotherapy and on the other hand, chemotherapy and combination chemotherapy have the potential to damage healthy tissues or organs, particularly those tissues have a great replacement rate. However, these cells have the capability to repair themselves after chemotherapy.

1.4.3 Radiation therapy

Radiation therapy is the use of ionization radiation to kill cancer cells. This therapy can be administrated internally through brachytherapy or externally through external beam radiotherapy. Radiation therapy can kill almost every type of solid tumors, including cancers of the cervix, breast, prostate, lung, liver, brain, pancreas, uterus, larynx, skin, stomach, or soft tissue sarcomas. In addition, it is also useful in the treatment of leukemia and lymphoma. Radiation therapy harms or eliminates cells in the area being treated (target tissue) by harming their genetic material, thus making it difficult for these cells to continue to grow and divide. Although radiation harms both cancer cells and normal cells, most normal

cells can improve from the effects of radiation and function properly. The main target of radiation therapy is to damage as many cancer cells as possible, while limiting harm to nearby healthy tissue.

1.4.4 Targeted therapy

Targeted therapy since 1990s, plays a significant role in the effective treatment of some specific cancers. In general, the target therapy utilizes small molecules as inhibitors of enzymatic domains on mutated or overexpressed target enzymes. One such example of targeted chemotherapy are the tyrosine kinase inhibitors such as imatinib and gefitinib. Monoclonal antibody therapy is another target therapy in which the therapeutic agent is antibody, which exactly binds to a protein on the surface of the cancer cells. Prominent examples are anti-HER2/neu antibody called trastuzumab used in the treatment of breast cancer, and anti-CD20 antibody called rituximab employed in the treatment of a variety of B-cell malignancies. Further, photodynamic therapy (PDT) is another strategy for treatment of basal cell carcinoma or lung cancer comprising a tissue oxygen, light and a photosensitizer. Photodynamic therapy can also be involved in eliminating traces of malignant tissue and later the surgical removal of huge tumors.³¹

1.4.5 Immunotherapy

Immunotherapy refers to a set of various therapeutic approaches aimed to induce the patient's own immunity to fight the tumor. Recent approaches for producing an immune response against tumors include intravesical Bacillus Calmette-Guerin (BCG) immunotherapy for bladder cancer, and use of interferons and other cytokines to induce an immune response in renal cell carcinoma and melanoma patients. Vaccines to produce particular immune responses are the topic of intensive research for many tumors, especially malignant melanoma and renal cell carcinoma. Sipuleucel-T is a vaccine-like strategy for prostate cancer in which dendritic cells from the patient are loaded with prostatic acid phosphatase peptides to induce a specific immune response against prostate-derived cells.

1.4.6 Hormonal therapy

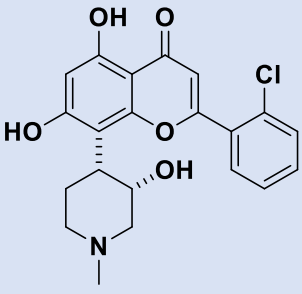
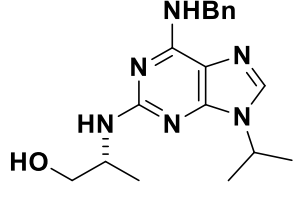
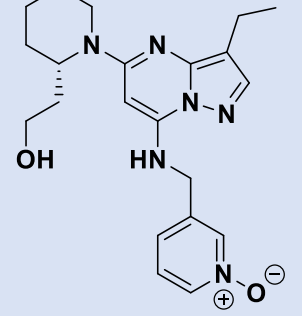
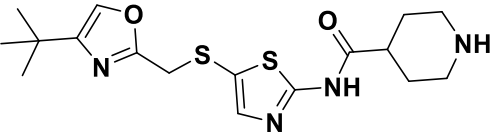
The development of some cancers can be inhibited by providing or blocking some hormones. General examples of hormone-sensitive tumors include certain types of prostate and breast cancers. Eliminating or blocking testosterone or estrogen is often a significant additional treatment. In certain cancers, administration of hormone agonists, such as progestogens may be therapeutically beneficial.

1.5 Cyclin-dependent kinase (CDK) inhibitors

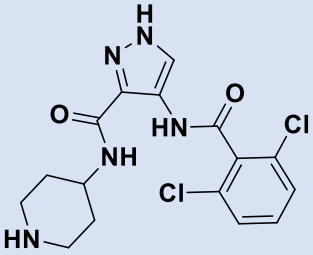
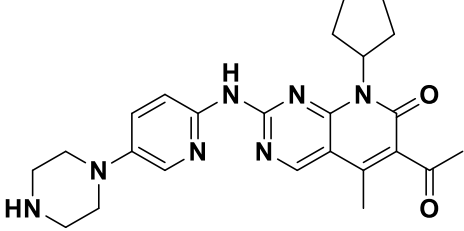
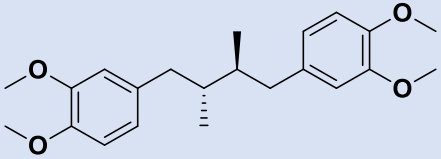
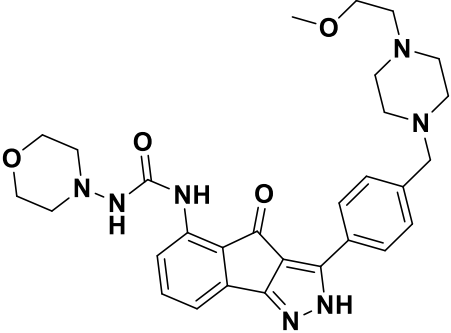
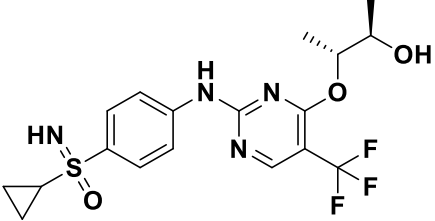
Cyclin-dependent kinases (CDKs) are a family of serine/threonine or mammalian heterodimeric enzymes comprising more than 13 members. These kinases are connected with regulation of cell-cycle progression by phosphorylating proteins in cell division. Dysregulation of the cell cycle control is a

Chapter 1

common cause of various human cancers and is normally associated with aberrant activation of cyclin-dependent kinases.^{32,33} CDK1 and CDK2 kinases play significant role in cell division, contribute to the phosphorylation and inactivation of the retinoblastoma (Rb) tumor suppressor protein, which is produced throughout late G1, S and G2-M phases.³⁴⁻³⁶ Other members of this family such as CDK7, CDK8 and CDK9 etc. contribute to the regulation of RNA polymerase II and the control of cellular transcription.^{37,38} Consequently, inhibition of CDKs represents an attractive therapeutic strategy in oncology. The structures of these CDK molecules are quite varied and they are generally constituted or derived from various heterocyclic families such as purines, pyrimidines, indoles, pyrazoles, thiazoles, or derived from natural products such as flavones or staurosporine. Several compounds from these families such as roscovitine, dinaciclib, palbociclib etc. are existing under clinical evaluation. **Table 2** indicates clinical drugs with their respective structures, administration mode and clinical trial stage.

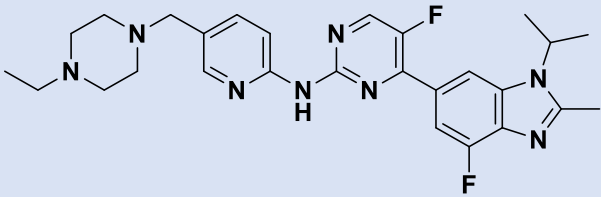
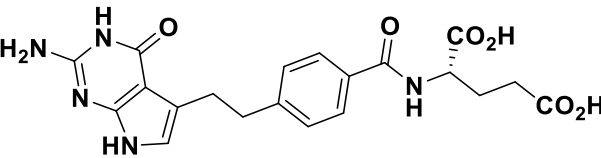
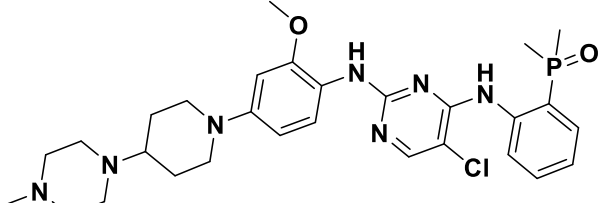
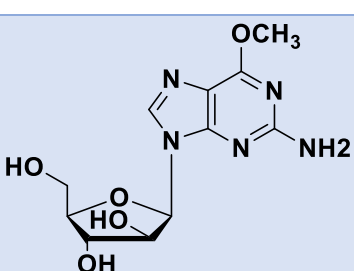
Drug	Structure	Administration Mode	Clinical Trial Stage
Flavopiridol		Intravenous	II
Roscovitine		Oral	II
Dinaciclib		Intravenous	III
SNS032		Intravenous	I

Chapter 1

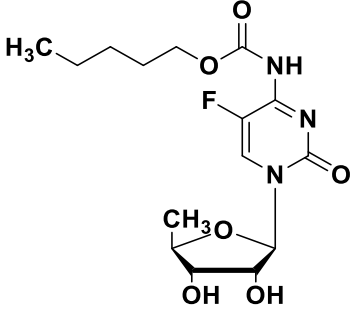
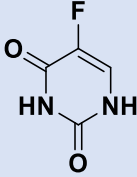
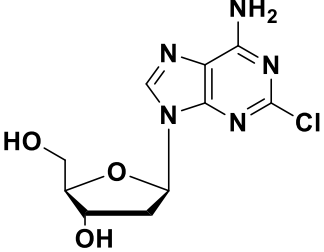
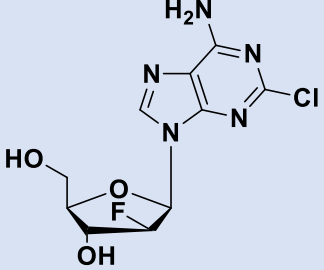
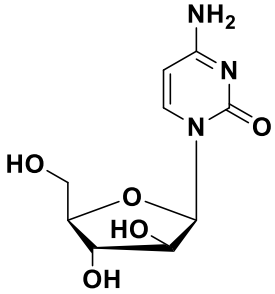
<p style="text-align: center;">AT7519</p>		<p style="text-align: center;">Intravenous</p>	<p style="text-align: center;">I/II</p>
<p style="text-align: center;">Palbociclib or PD0332991</p>		<p style="text-align: center;">Oral</p>	<p style="text-align: center;">III</p>
<p style="text-align: center;">EM-1421</p>		<p style="text-align: center;">Intravenous</p>	<p style="text-align: center;">I/II</p>
<p style="text-align: center;">RGB-286638</p>		<p style="text-align: center;">Intravenous</p>	<p style="text-align: center;">I</p>
<p style="text-align: center;">P276-00</p>		<p style="text-align: center;">Intravenous</p>	<p style="text-align: center;">II</p>
<p style="text-align: center;">BAY-1000394</p>		<p style="text-align: center;">Oral</p>	<p style="text-align: center;">I</p>

Chapter 1

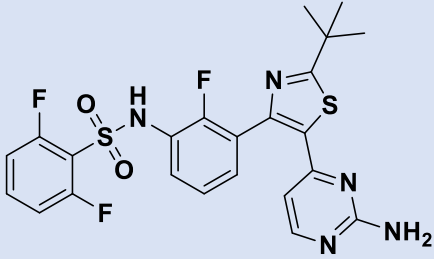
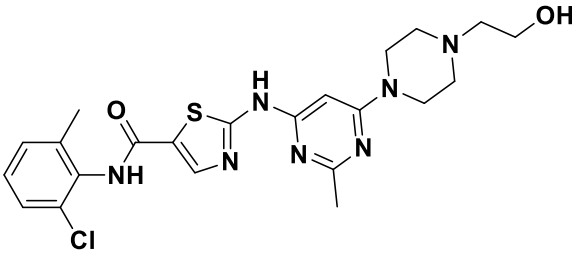
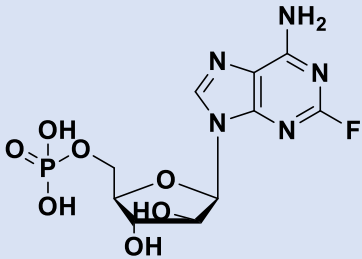
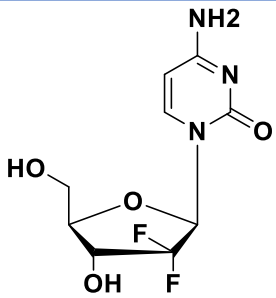
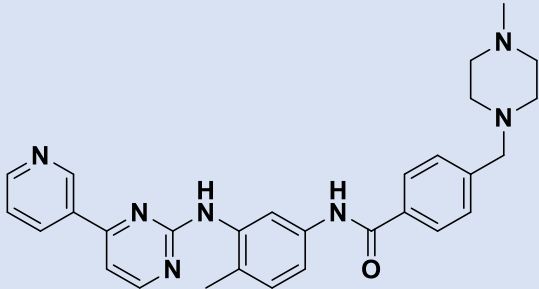
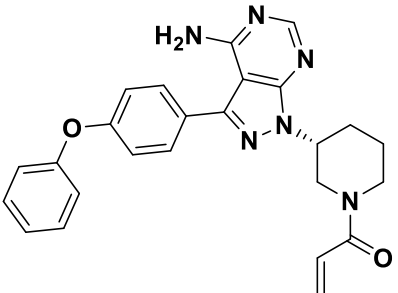
Pyrazolopyrimidines are the fused heterocyclic ring systems, which structurally resemble purines have prompted medicinal investigations to evaluate their potential therapeutic significance. Several anticancer drugs with pyrimidine/fused pyrimidine scaffold such as abemaciclib, afatinib, copanlisib, brigatinib, nelarabine, capecitabine to name but a few exist in the market and are illustrated in **Table 3**.

Drug	Structure	Target
Abemaciclib		Advanced/metastatic breast cancers.
Afatinib		Pleural mesothelioma and non-small cell lung cancer.
Copanlisib		Non-Hodgkin lymphoma and chronic lymphocytic leukemia.
Brigatinib		Anaplastic lymphoma.
Nelarabine		Acute lymphoblastic leukemia and T-cell lymphoblastic lymphoma.

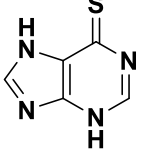
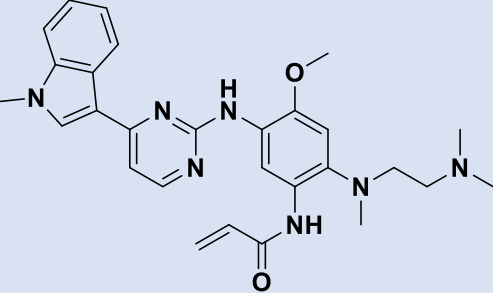
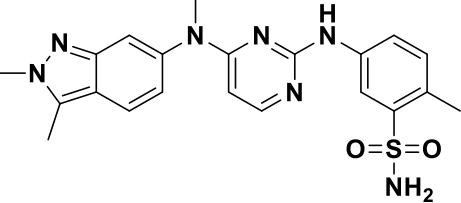
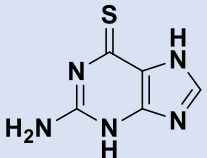
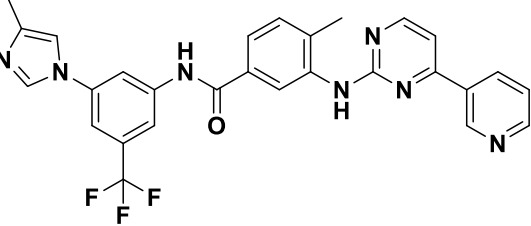
Chapter 1

<p>Capecitabine</p>		<p>Breast cancer, gastric and colorectal cancer.</p>
<p>Fluorouracil</p>		<p>Colon cancer, esophageal cancer, pancreatic cancer, breast cancer, cervical cancer.</p>
<p>Cladribine</p>		<p>Hairy cell leukemia B-cell chronic lymphocytic leukemia.</p>
<p>Clofarabine</p>		<p>Acute lymphoblastic leukemia.</p>
<p>Cytarabine</p>		<p>Acute myeloid leukemia, acute lymphocytic leukemia, chronic myelogenous leukemia, and non-Hodgkin's lymphoma.</p>

Chapter 1

<p>Dabrafenib</p>		<p>Non small-cell lung cancer.</p>
<p>Dasatinib</p>		<p>Chronic myelogenous leukemia, acute lymphoblastic leukemia.</p>
<p>Fludarabine</p>		<p>Leukemia and lymphoma.</p>
<p>Gemcitabine</p>		<p>Breast cancer, ovarian cancer, non-small cell lung cancer, pancreatic cancer.</p>
<p>Imatinib</p>		<p>Chronic myelogenous leukemia and acute lymphocytic leukemia.</p>
<p>Ibrutinib</p>		<p>Mantle cell lymphoma, chronic lymphocytic leukemia, and Waldenström's macroglobulinemia.</p>

Chapter 1

<p>Ribociclib</p>		<p>Breast cancer</p>
<p>Mercaptopurine</p>		<p>Acute lymphocytic leukemia, chronic myeloid leukemia Crohn's disease.</p>
<p>Osimertinib</p>		<p>Non-small-cell lung cancer.</p>
<p>Pazopanib</p>		<p>Renal cell carcinoma and soft tissue sarcoma.</p>
<p>Tioguanine</p>		<p>Acute myeloid leukemia (AML), acute lymphocytic leukemia.</p>
<p>Nilotinib</p>		<p>Chronic myelogenous leukemia.</p>
<p>Trifluridine</p>		<p>Colorectal cancer</p>

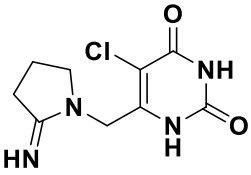
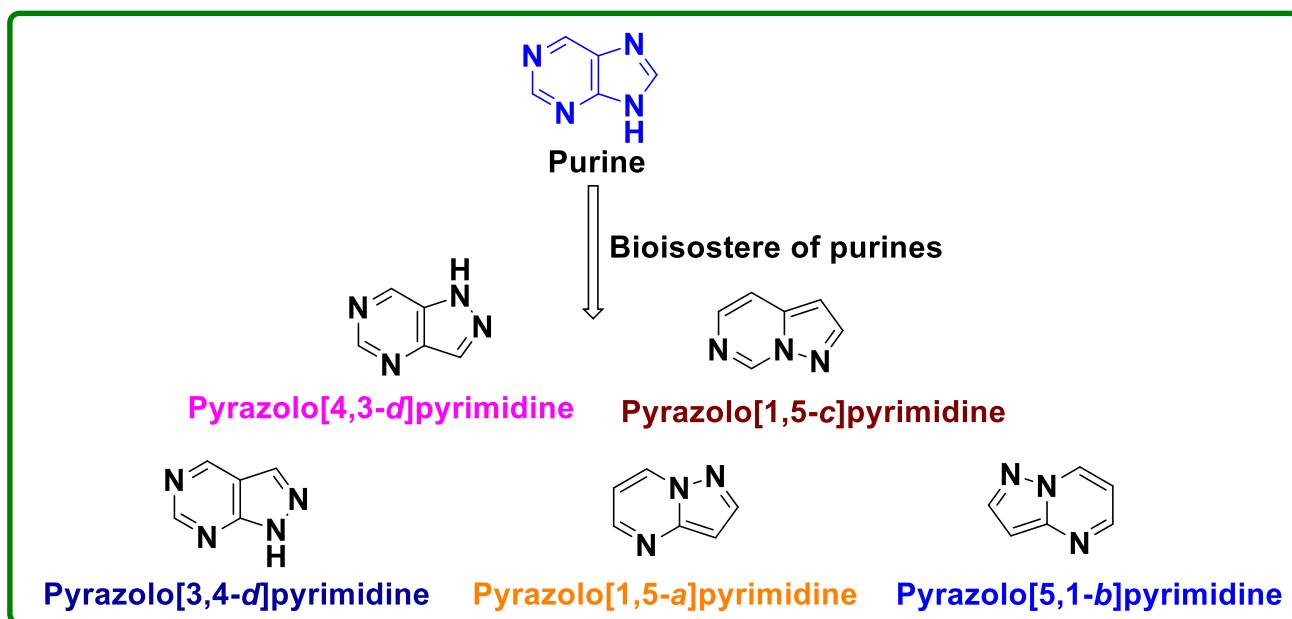
tipiracil		Colorectal cancer
Ceritinib		Metastatic non-small cell lung cancer.

Table 3. Pyrimidine/fused pyrimidine containing marketed drugs as anticancer agents

2 RATIONALE OF OUR RESEARCH

From our literature review, it was noted that countries like Africa, Northern America, Eastern Asia, Central, Eastern Europe, and Australia/New Zealand carry a massive burden of cancer making it a multifaceted disease affecting every region of the world. Clinicians handling the cancer cases, frequently encounter significant challenges such as lack of clinical experience, adverse events, lack of patients adherence, inadequate availability diagnostics or second line drugs, thus augmenting the risk of drug resistance. Therefore, after considering all the above mentioned facts, a robust and diverse drug discovery and development approach needs to be implemented to fill the pipeline with potential leads as well as developing new drug molecules against the new cancer targets. One should also look for extensive exploitation of chemical space and optimize lead hits for effective cancer drugs for future. Scaffolds such as nitrogen containing heterocyclic compounds have been widely known to display anticancer activity. One such scaffold is “Purine” which has been widely used as a building block for developing various anticancer drugs. Bioisosteric replacement of purines has resulted in several potential anticancer drugs like roscovitine, dinaciclib, nelarabine, cladribine, etc. Similarly, abemaciclib, brigatinib, capecitabine, etc, are examples of some of the significant anticancer drugs derived from pyrimidine scaffold³⁹. Thus, bioisosteric replacement is an important tool/technique in developing potential anticancer drugs. Pyrazolo[3,4-*d*]pyrimidine is one such scaffold that could be used as an bioisostere in developing new potential anticancer drugs. Hence, in an effort to identify new leads, a pyrazolo[3,4-*d*] pyrimidine scaffold was exploited.



Structural isomers of pyrazolopyrimidine

Fusion of pyrazole with the pyrimidine ring results in the formation of a bicyclic system known as “pyrazolopyrimidine”. Approximately five different structural isomers of this bicyclic system are known, such as pyrazolo[1,5-*a*]pyrimidine, pyrazolo[4,3-*d*]pyrimidine, pyrazolo[3,4-*d*]pyrimidine, pyrazolo[5,1-*b*]pyrimidine, and pyrazolo[1,5-*c*]pyrimidine. These isomers vary by the position of nitrogen, degree of saturation or unsaturation, or the number of nitrogen’s in the pyrazole nucleus.

Form our extensive literature survey, it was noted that pyrazolo[3,4-*d*]pyrimidine is a versatile and pharmacologically significant scaffold. Pyrazolo[3,4-*d*]pyrimidine is also known for its diverse of biological activities namely anticancer, anti-inflammatory, antibacterial, antiviral and antifungal properties to name but a few. However, there were only few research articles on pyrazolo[3,4-*d*]pyrimidines as specific CDK2 inhibitors. Thus we envisaged to further exploit pyrazolo[3,4-*d*]pyrimidine as potential CDK2 inhibitors. We aimed to design and synthesize a library of novel pyrazolo[3,4-*d*]pyrimidine as potential anticancer agents keeping in mind the active site of CDK2 enzyme as well as the core structural features highly active ligands against kinases family. The paragraphs below outlines our work plan in brief.

- Our comprehensive literature search revealed that there were no comprehensive reviews published on structural isomers of pyrazolopyrimidines such as pyrazolo[1,5-*a*]pyrimidine and pyrazolo[4,3-*d*]pyrimidine. Hence we envisioned to write a review on synthetic and medicinal aspects of pyrazolo[1,5-*a*]pyrimidine and pyrazolo[4,3-*d*]pyrimidine with special emphasis on structure-activity relationship studies.

- Phenethyl and pentane groups are essential moieties in drug discovery. The derivatives from these moieties are well known to possess varied range of activities such as anti-inflammatory, anticancer, anti-HIV, antibacterial, and anti-inflammatory. However, there were no reports on phenethyl/pentane containing pyrazolo[3,4-*d*]pyrimidines as anticancer agents. Therefore, we attempted to synthesize pyrazolo[3,4-*d*]pyrimidine analogs incorporating phenethyl/pentane groups as potential anticancer agents.
- Ring systems such as furan, benzofuran and thiophene are pharmacologically active five and six membered heterocycles, which contain oxygen and sulphur heteroatoms. These vital core structures have been extensively investigated for numerous biological properties namely anticancer, antitubercular, anti-inflammatory, antimicrobial, antiviral and anticonvulsant. In this chapter we attempted to synthesize a number of substituted benzoate derivatives as potential CDK2 inhibitors by incorporating different acid chlorides at the C-4 position of the pyrazolo[3,4-*d*]pyrimidine scaffold while keeping phenethyl/pentane groups at C-6 of the scaffold.
- Phenylcarbamoyl acetamide is a well-known six membered heterocycle, which contains urea functional group. This vital core structure has been known to exhibit a significant range of biological activities namely, anticancer, anti-inflammatory, antibacterial, antifungal, antiviral, antidiabetic, anti-atherosclerosis, and antimycobacterial. Therefore, in this chapter we anticipated to synthesize phenylcarbamoyl acetamide derivatives of pyrazolo[3,4-*d*]pyrimidine as potential anticancer agents.

3 OBJECTIVES OF THE PRESENT RESEARCH WORK

Cancer is affecting humans at an alarming rate. New drugs with an ability to overcome the drawbacks of existing anticancer chemotherapy are of high priority. The field of medicinal chemistry is contributing implicitly to the process of drug discovery and development. Synthesis of novel chemical entities, modification of existing scaffolds, combining two or more bioactive molecules (hybridization), replacing groups with bioisosteres, and optimization of natural compounds to identify promising leads are some of the interesting themes in the field of medicinal chemistry. Heterocyclic scaffolds having one or more hetero atoms have become crucial in drug discovery, which is evident from the fact that more than 95% of the marketed drugs are built on heterocyclic scaffolds.

Based on the abovementioned, the aims and objectives of the present research work are:

Chapter 1

1. To carry out a comprehensive literature review/assessment for identification of new chemical entities as anticancer activity (Identification of a research gap and defining the scope of proposed work).
2. To synthesize a novel series of pyrazolo[3,4-*d*]pyrimidine by incorporating certain structural features/groups that could lead to hit molecules as CDK2 inhibitors:
 - a. Phenethyl/pentane/hexane derivatives.
 - b. Furan, thiophene and benzofuran etc. derivatives
 - c. Phenylcarbamoyl acetamide derivatives.
3. To purify the synthesized compounds by chromatographic techniques namely column (flash) chromatography.
4. To establish the structures of synthesized compounds by physicochemical and spectral analysis (IR, ¹H NMR, ¹³C NMR and High-resolution mass spectrometry).
5. To carry out the preliminary biological evaluation of the synthesized compounds for their anticancer activity.
6. Molecular docking studies to determine the binding affinity of these molecules against CDK2 active site.
7. To generate a valid SAR based on the data obtained from the CDK2 inhibitory activity, molecular docking studies and the chemical structures of the inhibitors.
8. Based on this research to develop a future strategy to improve/optimize the lead molecules as potential CDK2 inhibitors.

The subsequent chapters unveils the extensive literature review on pyrazolo[1,5-*a*]pyrimidine, pyrazolo[4,3-*d*]pyrimidine scaffolds with emphasis on novel synthetic routes, pharmacological activity and SAR.

References

1. Cancer Facts and Fig.s, *Am. Can. Soc.* 2016.
2. L. A. Torre, F. Bray, R. L. Siegel, J. Ferlay, J. Lortet-Tieulent, A. Jemal. *CA Cancer J. Clin.* 2015, 65, 87-108.
3. Worldwide Cancer Incidence, International Agency for Research on Cancer of WHO and Cancer Research UK, 2012.
4. Worldwide Cancer Mortality, International Agency for Research on Cancer of WHO and Cancer Research UK, 2012.
5. Cancer-Signs and symptoms, *NHS Choices.* 2014.
6. P. Anand, A. B. Kunnumakkara, A. B. Kunnumakara, C. Sundaram, K. B. Harikumar, S. T. Tharakan, O. S. Lai, B. Sung, B. B. Aggarwal, *Pharm. Res.* 2008, 25, 2097-2116.
7. WHO Report on the global tobacco epidemic, 2008.
8. H. K. Biesalski, B. B. D. Mesquita, A. Chesson, F. Chytil, R. Grimble, R. J. Hermus, J. Kohrle, R. Lotan, K. Norpoth, U. Pastorino, D. Thurnham, *CA Cancer J. Clin.* 1998, 48, 167-176.
9. H. Kuper, H. O. Adami, P. Boffetta, *J. Intern. Med.* 2002, 251, 455-66.
10. M. F. Gregor, G. S. Hotamisligil, *Annu. Rev. Immunol.* 2011, 29, 415-445
11. National Center for Health Statistics (US), 2015.
12. L. H. Kushi, T. Byers, C. Doyle, E. V. Bandera, M. McCullough, A. McTiernan, T. Gansler, K. S. Andrews, M. J. Thun, *CA Cancer J. Clin.* 2006, 56, 254-281.
13. C. de Martel, J. Ferlay, S. Franceschi, J. Vignat, F. Bray, D. Forman, M. Plummer, *Lancet Oncol.* 2012, 13, 607-615.
14. P. D. Paoli, A. Carbone, *Int. J. Cancer.* 2013, 133, 1517-1529.
15. M. W. Sung, S. N. Thung, *Holland-Frei Cancer Medicine*, 6th edition. 2003.
16. C. M. McLachlin, C. P. Crum, *Holland-Frei Cancer Medicine*, 5th edition. 2000.
17. J. I. Cohen, *Holland-Frei Cancer Medicine*, 5th edition. 2000.
18. K. Takatsuki, *Retrovirology.* 2005, 2, 16-19.
19. H. Feng, M. Shuda, Y. Chang, P. S. Moore, *Science.* 2008, 319, 1096-1100.
20. C. Wang, Y. Yuan, R. H. Hunt, *Am. J. Gastroenterol.* 2007, 102, 1789-98.
21. A. J. Littman, L. A. Jackson, T. L. Vaughan, *Cancer Epidemiol. Biomarkers Prev.* 2004, 14, 773-778.
22. M. Piero, *Holland-Frei Cancer Medicine*, 5th edition. 2000.
23. J. B. Little, *Holland-Frei Cancer Medicine*, 5th edition. 2000.
24. D. H. Roukos, *Expert Rev. Anticancer Ther.* 2009, 9, 389-392.

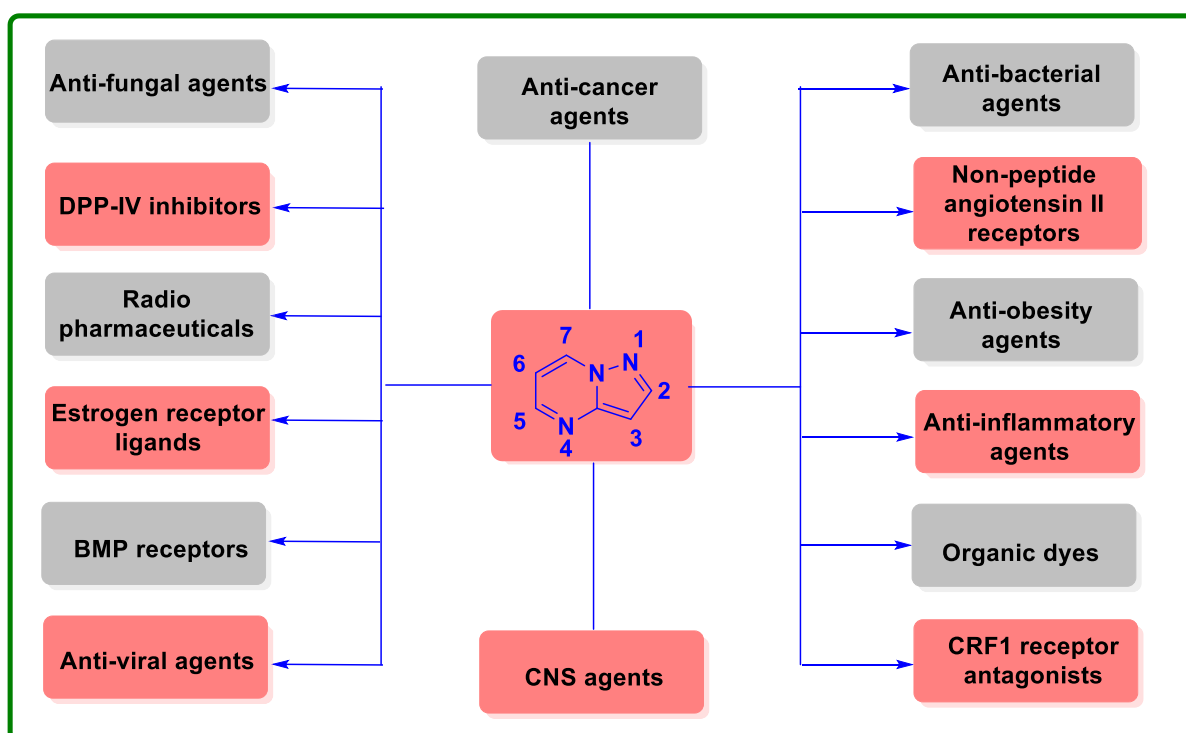
25. D. Cunningham, W. Atkin, H. J. Lenz, H. T. Lynch, B. Minsky, B. Nordlinger, N. Starling, *Lancet*. 2010, 375, 1030-1047.
26. M. A. Rowlands, D. Gunnell, R. Harris, L. J. Vatten, J. M. Holly, R. M. Martin, *Int. J. Cancer*. 2009, 124, 2416-2419.
27. B. E. Henderson, L. Bernstein, R. K. Ross, *Holland-Frei Cancer Medicine*, 5th edition. 2000.
28. C. Maltoni, F. Minardi, J. F. Holland, *Holland-Frei Cancer Medicine*, 5th edition. 2000.
29. S. Subotic, S. F. Wyler, A. Bachmann, *Eur. Urol. Suppl.* 2012, 11, 60-65.
30. J. S. D. Mieog, J. A. van der Hage, C. J. H. van de Velde, *Br. J. Surg.* 2007, 94 1189-1200.
31. D. E. J. G. J. Dolmans, D. Fukumura R. K. Jain, *Nat. Rev. Cancer*. 2003, 3, 380-387.
32. C. J. Sherrm, *Cancer Res.* 2000, 60, 3689-3695.
33. J. R. Nevins, *Hum. Mol. Genet.* 2001, 10, 699-703.
34. T. Hunter, J. Pines, *Cell*, 1994, 79, 573-582.
35. M. E. Ewen, *Cancer Metastasis Rev.* 1994, 13, 45-66.
36. M. E. Ewen, *Results Probl. Cell Differ.* 1998, 22, 149-179.
37. D. B. Bregman, R. G. Pestell, V. J. Kidd, *Front Biosci.* 2000, 5, 244-257.
38. T. J. Oelgeschlager, *Cell Physiol.* 2002, 190, 160-169.
39. G. Mariaule, P. Belmont, *Molecules*, 2014, 19, 14366-14382.

CHAPTER 2

An insight on synthetic and medicinal aspects of pyrazolo[1,5-*a*]pyrimidine scaffold

Department of Pharmaceutical Chemistry, College of Health Sciences, University of KwaZulu-Natal, Durban 4000, South Africa

Graphical Abstract





Contents lists available at ScienceDirect

European Journal of Medicinal Chemistry

journal homepage: <http://www.elsevier.com/locate/ejmech>



Review article

An insight on synthetic and medicinal aspects of pyrazolo[1,5-*a*]pyrimidine scaffold



Srinivasulu Cherukupalli, Rajshekhar Karpoormath*, Balakumar Chandrasekaran, Girish. A. Hampannavar, Neeta Thapliyal, Venkata Narayana Palakollu

Department of Pharmaceutical Chemistry, College of Health Sciences, University of KwaZulu-Natal, Durban 4000, South Africa

ARTICLE INFO

Article history:

Received 17 August 2016
Received in revised form
19 October 2016
Accepted 8 November 2016
Available online 10 November 2016

Keywords:

Pyrazolo[1,5-*a*]pyrimidine
Anti-cancer agents
Anti-infectious agents
CNS agents
Anti-inflammatory agents
Radiopharmaceuticals

ABSTRACT

Pyrazolo[1,5-*a*]pyrimidine scaffold is one of the privileged hetrocycles in drug discovery. Its application as a buliding block for developing drug-like candidates has displayed broad range of medicinal properties such as anticancer, CNS agents, anti-infectious, anti-inflammatory, CRF₁ antagonists and radio diagnostics. The structure-activity relationship (SAR) studies have acquired greater attention amid medicinal chemists, and many of the lead compounds were derived for various disease targets. However, there is plenty of room for the medicinal chemists to further exploit this privileged scaffold in developing potential drug candidates. The present review briefly outlines relevant synthetic strategies employed for pyrazolo[1,5-*a*]pyrimidine derivatives. It also extensively reveals significant biological properties along with SAR studies. To the best of our understanding current review is the first attempt made towards the compilation of significant advances made on pyrazolo[1,5-*a*]pyrimidines reported since 1980s.

© 2016 Elsevier Masson SAS. All rights reserved.

Abstract:

Pyrazolo[1,5-*a*]pyrimidine scaffold is one of the privileged heterocycles in drug discovery. Its application as a building block for developing drug-like candidates has displayed broad range of medicinal properties such as anticancer, CNS agents, anti-infectious, anti-inflammatory, CRF₁ antagonists and radio diagnostics. The structure-activity relationship (SAR) studies have acquired greater attention amid medicinal chemists, and many of the lead compounds were derived for various disease targets. However, there is plenty of room for the medicinal chemists to further exploit this privileged scaffold in developing potential drug candidates. The present review briefly outlines relevant synthetic strategies employed for pyrazolo[1,5-*a*]pyrimidine derivatives. It also extensively reveals significant biological properties along with SAR studies. To the best of our understanding current review is the first attempt made towards the compilation of significant advances made on pyrazolo[1,5-*a*]pyrimidines reported since 1980s.

Keywords: Pyrazolo[1,5-*a*]pyrimidine, Anti-cancer agents, Anti-infectious agents, CNS agents, Anti-inflammatory agents, Radiopharmaceuticals.

1 Introduction

Heterocycles hold a key point in organic and medicinal chemistry as they act as a bridge between life sciences and biochemical investigations. A significant amount of contemporary investigation is being currently pursued on these compounds world wide. Aza-heterocycles are essential scaffolds for generating wide range of chemical libraries/drug-like candidates for their applications to obtain desired therapeutic/pharmacological activity. Among all the aza-heterocycles, pyrazolo pyrimidine is one such essential drug-like nucleus bearing enormous biological applicability [1]. From historic point of view, pyrazolo pyrimidines were first described as adenosine receptor antagonists [2]. Numerous isomeric forms of pyrazolo pyrimidine namely pyrazolo[5,1-*b*]pyrimidines, pyrazolo[5,1-*a*]pyrimidines, pyrazolo[4,3-*d*]pyrimidines, pyrazolo[1,5-*c*]pyrimidines and pyrazolo[3,4-*d*]pyrimidines are known [3]. Among all, pyrazolo[1,5-*a*]pyrimidine is a rigid bicyclic heterocycle core (**Fig. 1**) and has emerged a vital building block for medicinal compounds. The synthesis is accomplished by condensing 3 or 5-amino pyrazoles with sodium salts of formyl ketones [4], 1,3-diketones [5,6], enamines [7–9], acetoacetanilides [10], β -ketoesters [11], enamino-nitriles [12], β -ketoaldehydes [13], 3-oxo-2-phenylpropanenitrile [14], dehydroacetic acid [15], malononitriles [16] and β,γ -unsaturated- γ -alkoxy- α -keto esters [17].

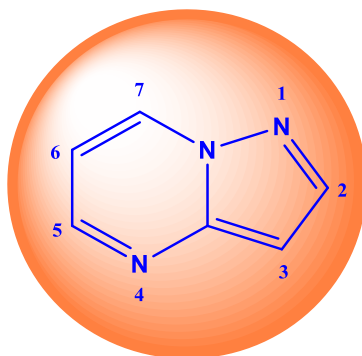
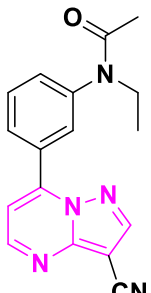
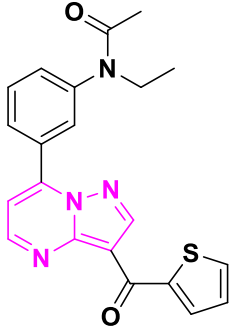
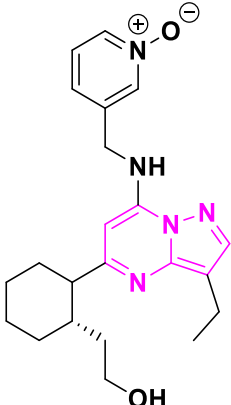
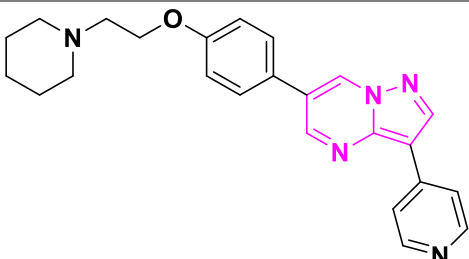


Fig. 1. The General structure of pyrazolo[1,5-*a*]pyrimidine.

These numerous synthetic pathways have prompted medicinal scientists to discover several new drugs consisting of pyrazolo[1,5-*a*]pyrimidines as a core moiety. These are also known to be purine analogues with diverse biological applications as antimetabolites in purine bio-chemical interactions, antischistosomal, antitrypanosomal and sedative [18], anxiolytic [19], AMP phosphodiesterase inhibitors [20], benzodiazepine receptor ligands [21], HMG-CoA reductase inhibitors [22], KDR kinase inhibitors [23], COX-1, COX-2 selective inhibitors [24], HCV inhibitors [25], PET tumor imaging agents [26], serotonin 5-HT₆ receptor antagonists [27], kinase inhibitors [28], HIV reverse transcriptase inhibitors [29], CCR1 antagonists [30], antimalarial and antifungal activities [31]. Several marketed drugs with pyrazolo[1,5-*a*]pyrimidine nucleus such as zaleplon, indiplon [32], dinaciclilb [33], dorsomorphin [34], ocinaplon [1], anagliptin [35], lorediplon and pyrazophos [36] are illustrated in **Fig.**

Chapter 2

2 with their respective structures and the approved activities. Inspired by these observations, in this review we summarize and represent the latest progress on synthetic strategies and medicinal properties of pyrazolo[1,5-*a*]pyrimidine derivatives, along with special emphasis on SAR of aforementioned derivatives.

Name of the Drug	Structure	Approved activity
Zaleplon		Insomnia
Indiplon		Hypnotic and sedative
Dinaciclib		Melanoma, chronic lymphocytic leukemia, pancreatic cancer
Dorsomorphin		Bone and cartilage

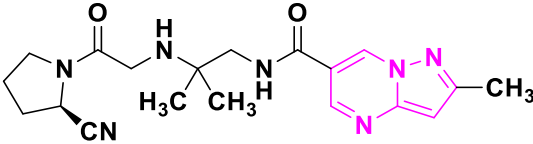
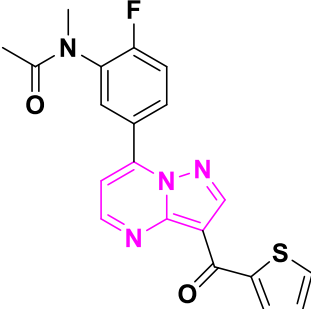
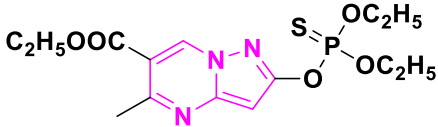
Ocinaplon		Anxiolytic, sedative and amnestic
Anagliptin		Type 2 diabetes mellitus
Lorediplon		Insomnia
Pyrazophos		Fungicide and insecticide

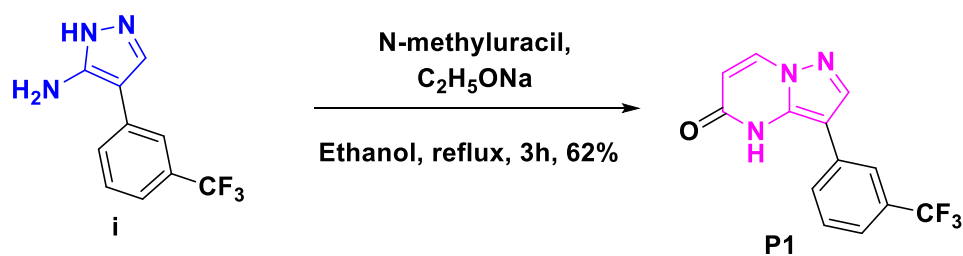
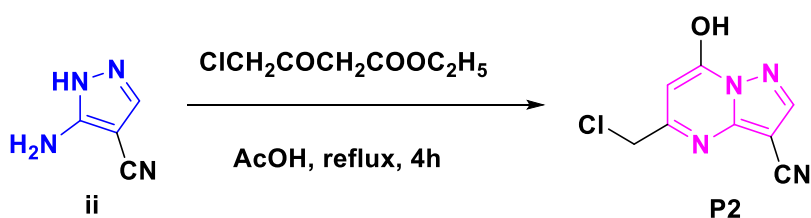
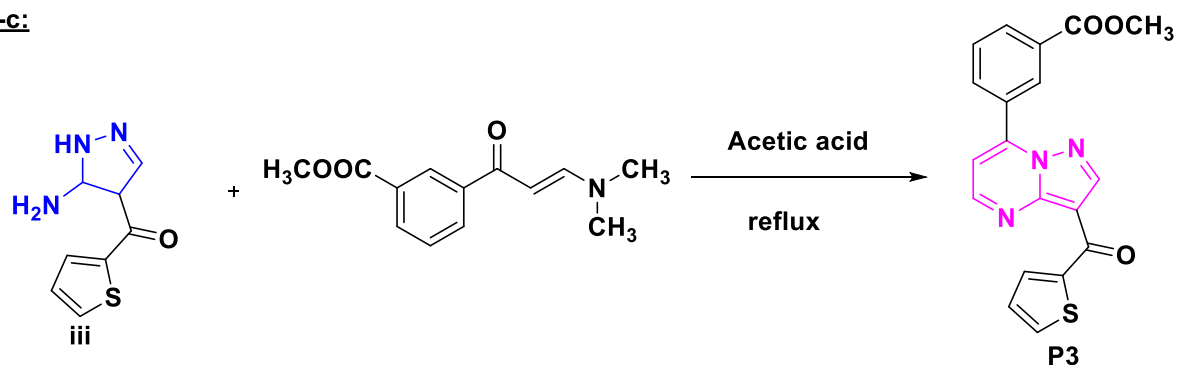
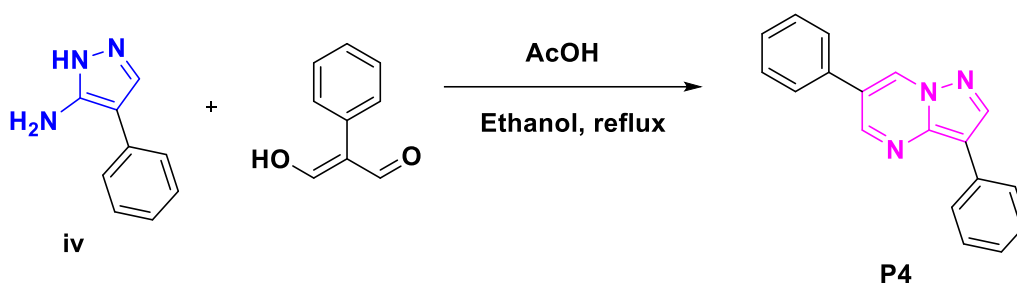
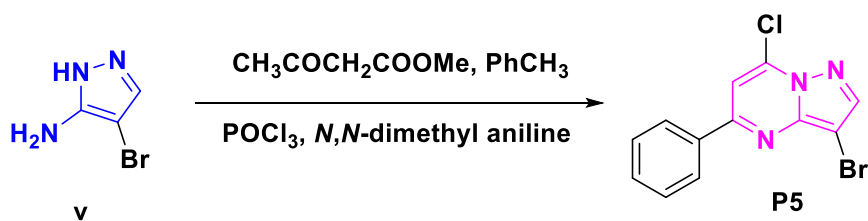
Fig. 2. Marketed drugs containing pyrazolo[1,5-*a*]pyrimidine nucleus.

2 Synthetic approaches for pyrazolo[1,5-*a*]pyrimidine scaffold

Synthesis of fused pyrimidine compounds was first reported in mid-1950's [2]. Since then thousands of derivatives have been synthesized by applying numerous synthetic strategies and analysed for their pharmacological properties. The various strategies for synthesis of pyrazolo[1,5-*a*]pyrimidines have been presented in Fig. 3.

One of the most common reagent, i.e. substituted 1*H*-pyrazole-5-amine (**i-xviii**), was used to obtain the target pyrazolo[1,5-*a*]pyrimidines (**P1-P18**) through numerous synthetic routes. Xu et al. prepared the desired product **P1** by cyclization of **i** with *N*-methyluracil in the presence of sodium ethoxide as a Michael acceptor in ethanol (route-a) [37]. Li and co-workers synthesized **P2** by allowing the reaction between **ii** and ethyl 4-chloroacetoacetate in acetone under refluxed conditions (route-b) [38]. Wang et al. reacted 5-amino-1*H*-pyrazol-4-yl thiophen-2-yl methanone (**iii**) with methyl (*E*)-3-(3-

(dimethylamino)acryloyl)benzoate to afford pyrazolo[1,5-*a*]pyrimidine scaffold **P3** under reflux conditions in acetone (route-c) [7]. Fraley et al. have accomplished the desired product **P4** by treating 4-phenyl-1*H*-pyrazol-5-amine (**iv**) with 3-hydroxy-2-phenylacrylaldehyde in acidic condition (route-d) [39]. Paruch et al. reported one pot synthesis of **P5** by reacting **v** with methyl-3-oxobutanoate, phosphorus oxychloride and *N,N*-dimethylaniline under inert conditions (route-e) [40]. Gommermann and co-workers carried out the cyclization reaction of 4-(4-(4-methylpiperazin-1-yl)phenyl)-1*H*-pyrazol-5-amine (**vi**) with 3-(dimethylamino)-2-(4-nitrophenyl)acrylonitrile to achieve **P6** under acidic conditions (1.25 M HCl in ethanol) in acetone (route-f) [41]. Frey and co-workers established cyclocondensation reaction between 3-amino-4-bromo pyrazole (**vii**) with 3-oxo-2-phenyl propanenitrile to get target compound **P7** (route-g) [12]. Selleri et al. obtained **P8** via treating **viii** with ethyl-3-hydroxy-2-(thiophen-3-yl)acrylate (route-h) [42]. Labroli and co-workers introduced cyclization reaction of 3-amino pyrazole (**ix**) with *tert*-butyl 3-(3-methoxy-3-oxopropanoyl)piperidine-1-carboxylate to afford **P9** (route-i) [43]. Engers et al. reported condensation reaction of 1*H*-pyrazole-5-amine (**x**) with 2-(4-methoxyphenyl)malonaldehyde to achieve product **P10** under microwave irradiation conditions (route-j) [44].

Route-a:**Route-b:****Route-c:****Route-d:****Route-e:****Fig. 3.** Synthetic approaches for pyrazolo[1,5-*a*]pyrimidines.

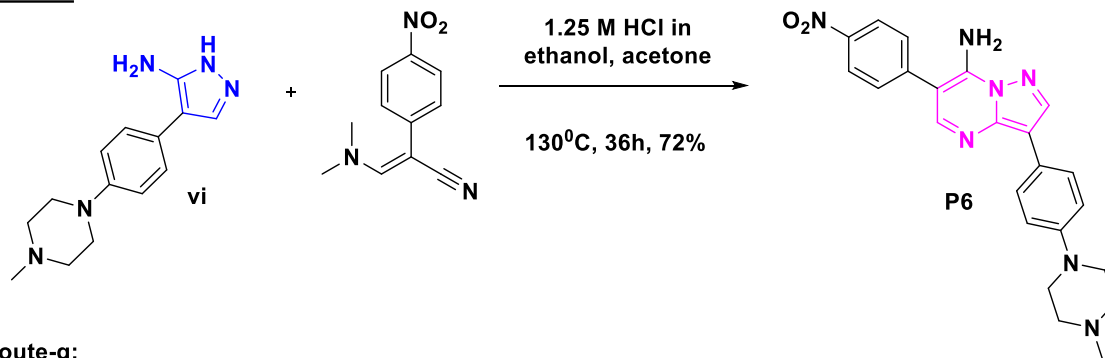
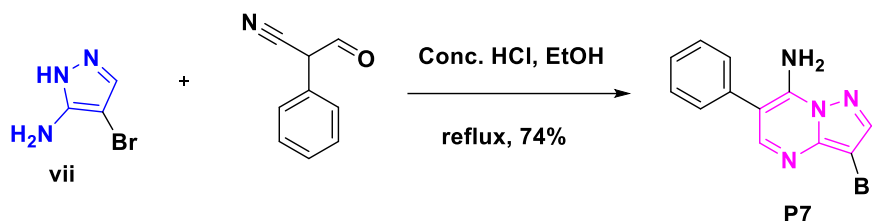
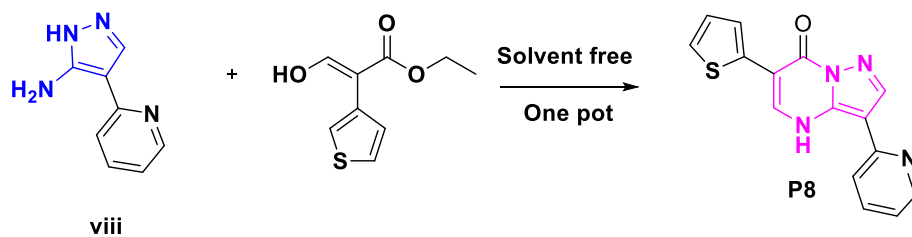
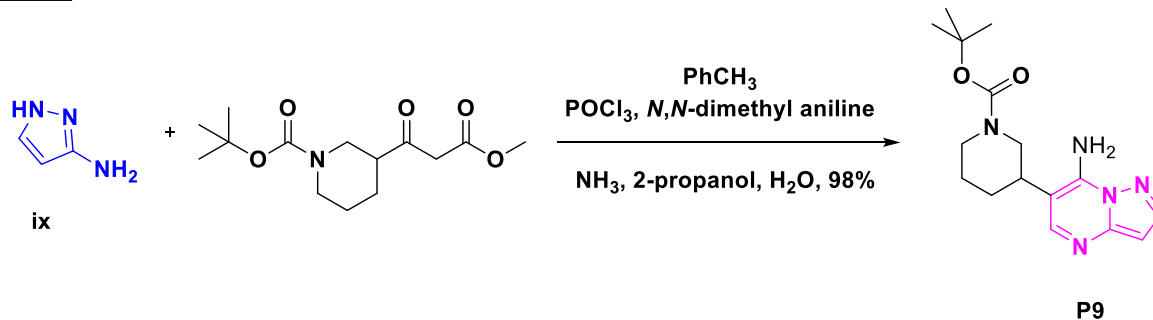
Route-f:**Route-g:****Route-h:****Route-i:**

Fig. 3 (continued). Synthetic approaches for pyrazolo[1,5-*a*]pyrimidines.

Dwyer et al. acquired the final compound **P11** by the condensation reaction of 3-aminopyrazole (**xi**) with 1,3-dimethyluracil (route-k) [45]. Enany et al. attempted the reaction between **xii** and malanonitrile to produce **P12** in presence of organic base like triethylamine (route-l) [46]. Kosugi and co-workers acquired **P13** by treating **xiii** with 2-substituted malonic acid diester in the presence of sodium ethoxide in ethanol under reflux conditions (route-m) [47]. Campton et al. reported the reaction of **xiv** with 1,1,3,3-tetramethoxypropane to attain the desired product **P14** (route-n) [48]. Selleri and co-workers attempted condensation reaction between 2-(5-amino-3-(*p*-tolyl)-1*H*-pyrazol-4-yl)acetic acid (**xv**) and 4,4-dimethoxy-2-butanone to attain **P15** in ethanol (route-o) [19]. Ivachtchenko et al. blended *N*³-

methyl-4-(phenylsulfonyl)-4*H*-pyraole-3,5-diamine (**xvi**) and 3-aminobut-2-enenitrile in acetic acid to give **P16** (route-p) [49]. Patnaik and co-workers reported condensation of ethyl 5-amino-1*H*-pyrazole-4-carboxylate (**xvii**) with pentane-2,4-dione in the presence of aqueous NaOH and CH₃OH in acetic acid yielding **P17** (route-q) [50]. Tabrizi et al. offered synthesis of **P18** employing cyclization of **xviii** with diethyl ethoxymethylenemalonate (route-r) [51].

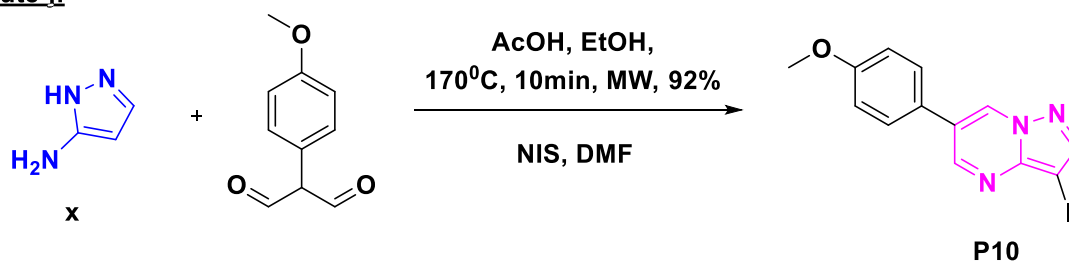
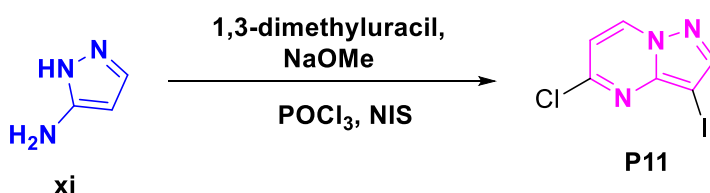
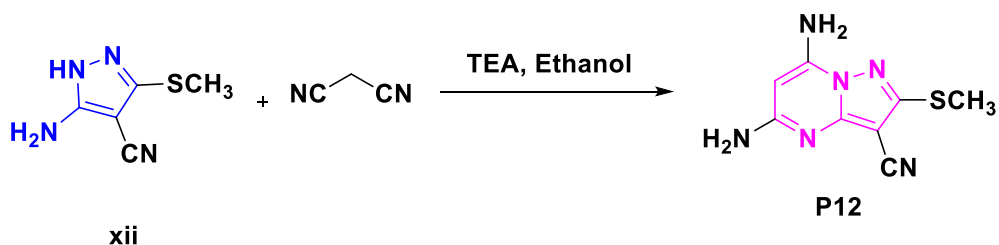
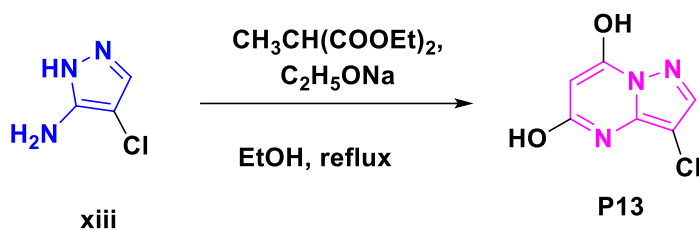
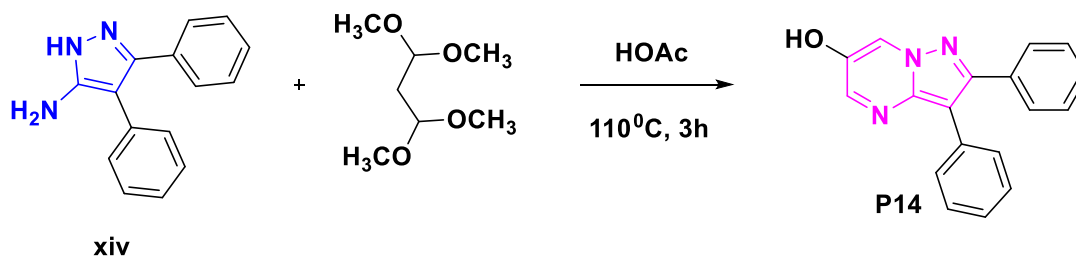
Route-j:**Route-k:****Route-l:****Route-m:****Route-n:**

Fig. 3 (continued). Synthetic approaches for pyrazolo[1,5-*a*]pyrimidines.

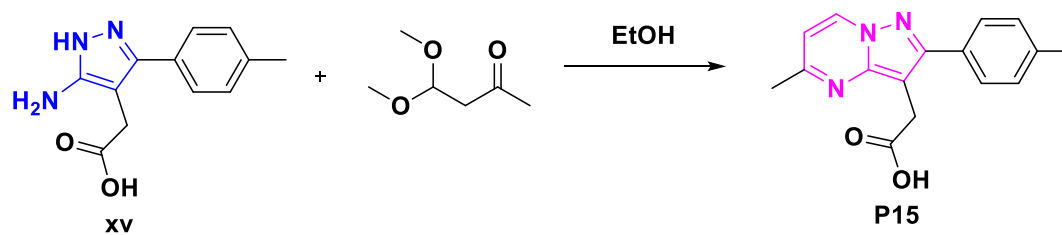
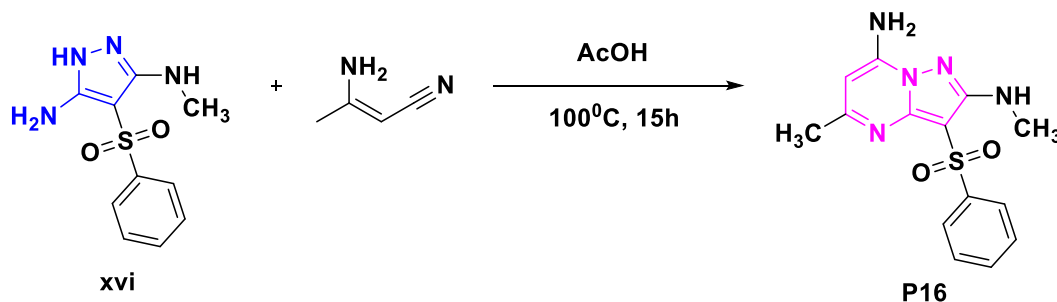
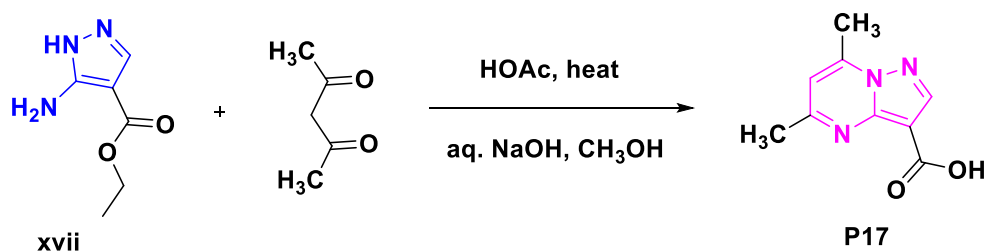
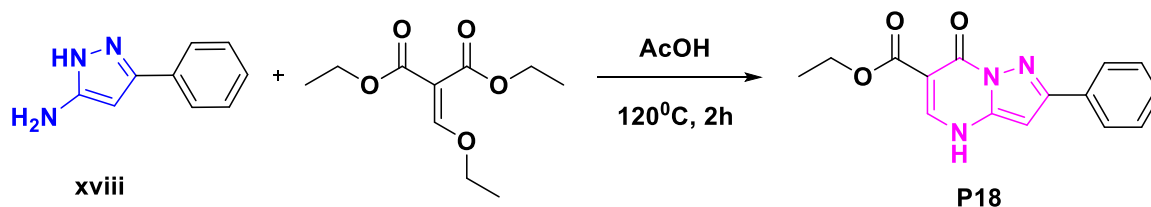
Route-o:**Route-p:****Route-q:****Route-r:**

Fig. 3 (continued). Synthetic approaches for pyrazolo[1,5-*a*]pyrimidines.

3 Pharmacology

During the course of literature study on pyrazolo pyrimidines such as pyrazolo[1,5-*a*]pyrimidines, pyrazolo[4,3-*d*]pyrimidines, pyrazolo[3,4-*d*]pyrimidines and pyrazolo[5,1-*b*]pyrimidines, it has been identified that pyrazolo[1,5-*a*]pyrimidines emerged as a promising lead agents against several ailments namely cancer, malaria, fungal infections, inflammation and etc. The following discussions illustrate the pharmacological applications of pyrazolo[1,5-*a*]pyrimidines against various biological properties.

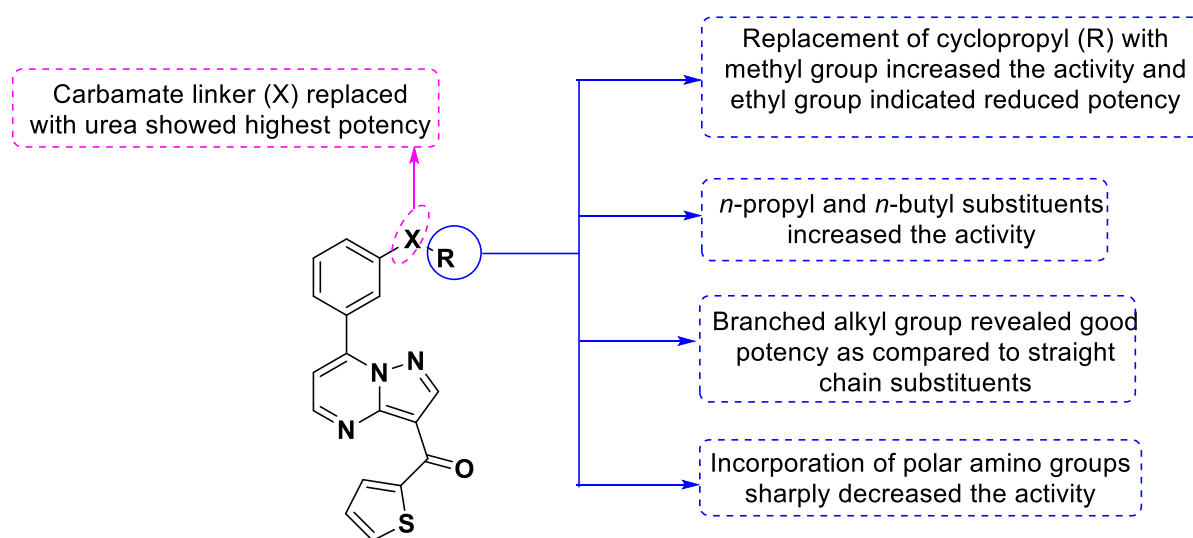
It is quite evident that variations in functionalities on this scaffold brings about diverse biological activities.

3.1 Anti-cancer agents

3.1.1 Anti-proliferatives

Cell proliferation is the process resulting in a progression of cell number and is a balance between cell divisions and cell death. Deregulation in cell proliferation or suppression of cell death is a hallmark cause of varied clinical consequences including several forms of cancers. These cancer cells may abstain the normal regulatory control of cell division, thus failing to undergo appropriate cell death resulting into tumorigenic state [52]. Drugs or chemical entities that selectively kill these aberrant cells have emerged as promising antiproliferative agents in cancer drug discovery [53].

In 2005, Gopalsamy et al. reported a series of pyrazolo[1,5-*a*]pyrimidin-7-yl phenyl amides as p21 chemoselective compounds for anti-proliferative activity. A p21 protein is a downstream effector of p53 gene, a major regulator of the DNA damage thus inhibiting cyclin dependent kinases (CDK) activity arresting the progression of cell cycle. The pharmacological evaluation was performed against HCT116 and 80S14 cell lines. Among the tested series, compound **1** exhibited potential activity and SAR study revealed the significance of R group as shown in **Fig. 4** [54].



C. No	X	R ¹	HCT116	80S14	Ratio
			IC ₅₀ (μM)	IC ₅₀ (μM)	
1	NHCONH	<i>i</i> -propyl	2.7	0.089	30

Fig. 4. SAR of p21 chemoselective pyrazolo[1,5-*a*]pyrimidin-7-yl-phenyl amides and the anti-proliferative activity of the representative compound **1**.

Chapter 2

In 2006, Li and co-workers introduced a series of 3-cyano-5,7-disubstituted pyrazolo[1,5-*a*]pyrimidine derivatives and evaluated them for anti-tumor activity. Among the series, derivative **2** presented excellent anti-tumor activity against human liver (Bel-7402) and human fibro sarcoma (HT-1080) cancer cell lines. SAR studies revealed that compound with bis(trifluoromethyl)aniline at C-7 and piperdinyl at C-5 position enhanced anti-tumor activity as compared to other groups as displayed in **Fig. 5** [38].

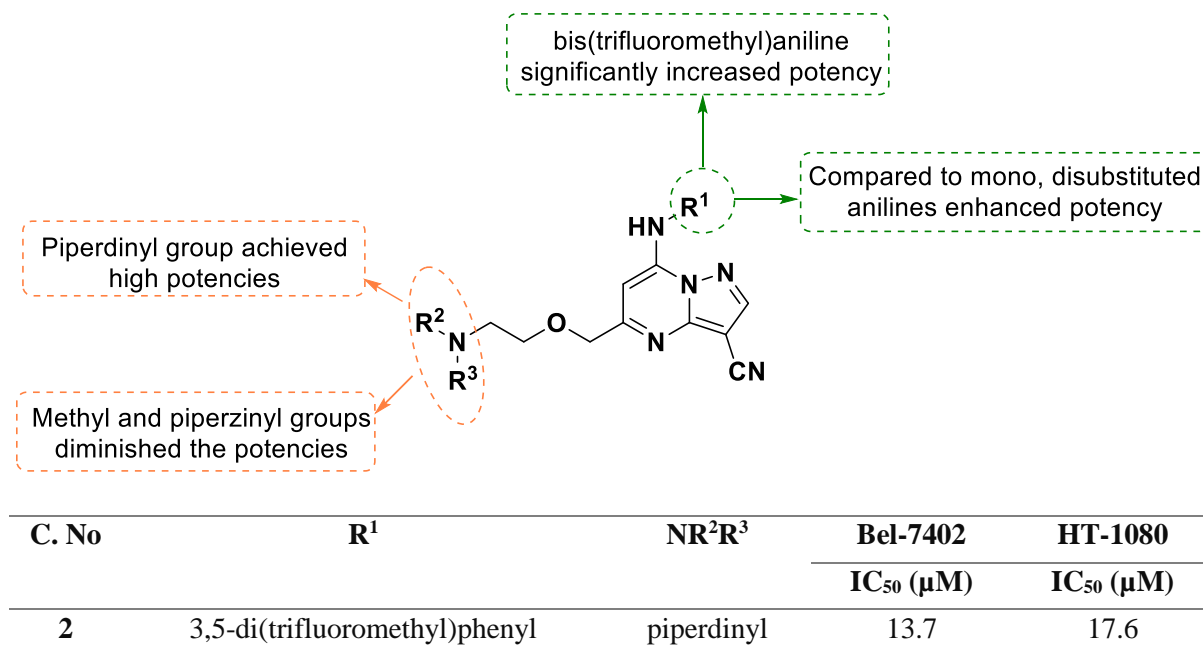
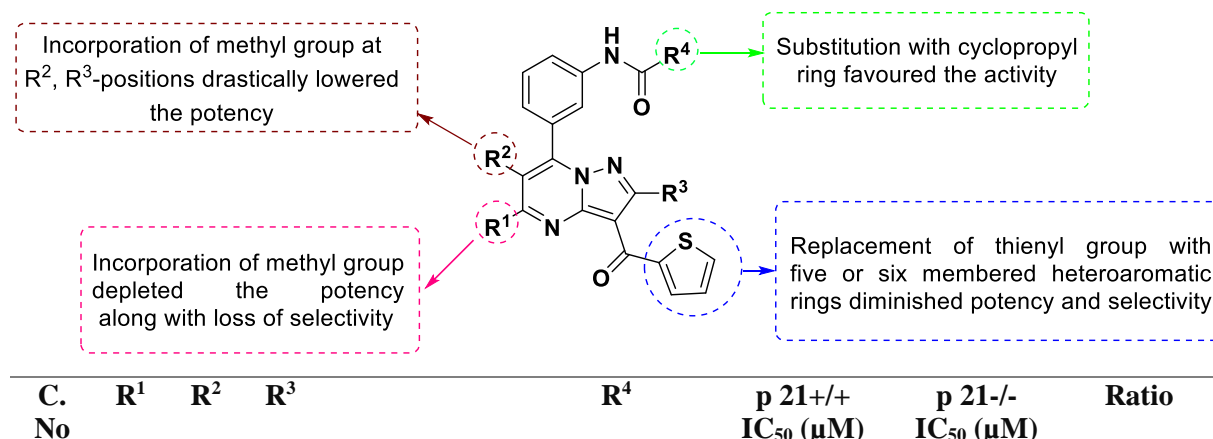


Fig. 5. SAR of amino alkoxy moiety containing pyrazolo[1,5-*a*]pyrimidines and anti-tumor activities of the representative compound **2**.

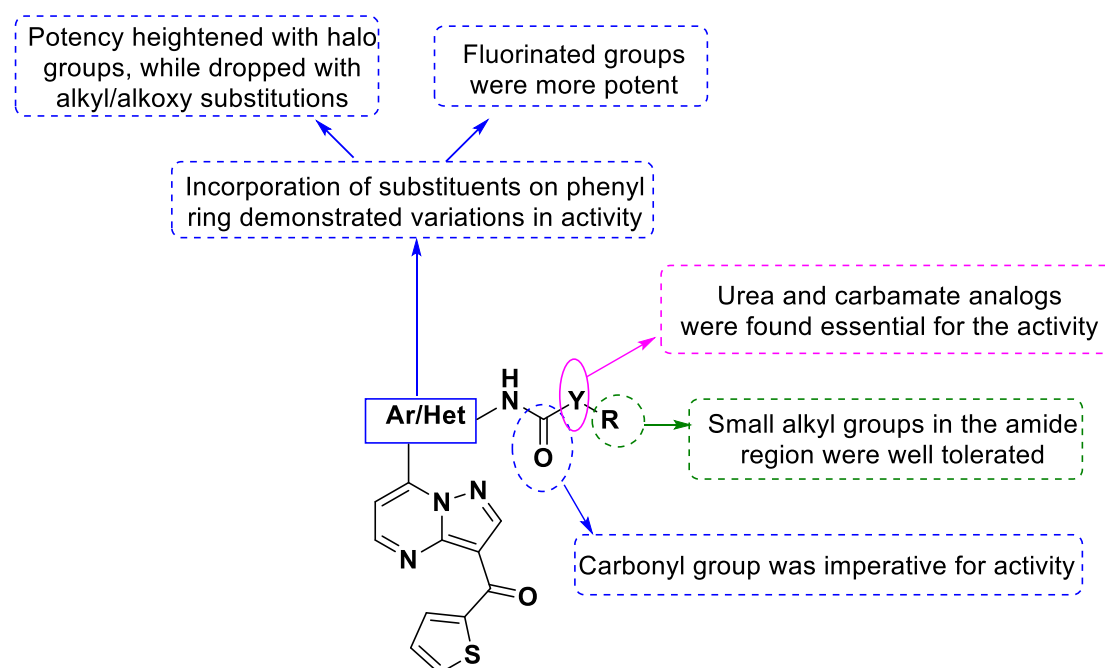
In 2007, Powell et al. discovered *N*-(3-(3-(thiophene-2-carbonyl)pyrazolo[1,5-*a*]pyrimidin-7-yl)phenyl)cyclopropane carboxamide derivatives as anti-proliferative agents. SAR studies indicated that methyl group at position 2 (R³) and 6 (R²) was responsible for lower activity as shown in **Fig. 6**. Among the tested series, compound **3** exhibited promising activity against HCT116 (p21+/+) and 80S14 (p21-/-) cell lines [55].



3	H	H	H	cyclopropyl	11	0.45	23
---	---	---	---	-------------	----	------	----

Fig. 6. SAR and anti-proliferative activity of pyrazolo[1,5-*a*]pyrimidine derivatives.

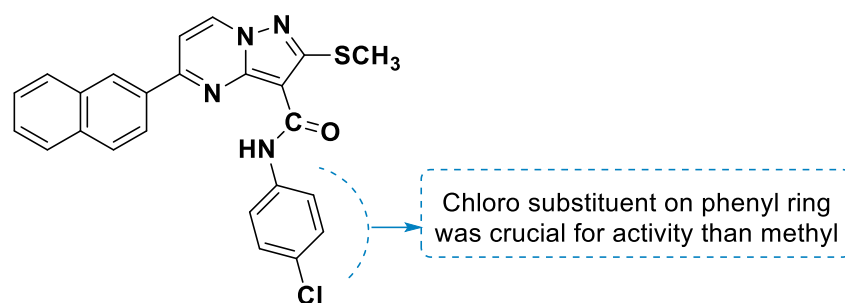
In 2009, Wang et al. derivatized a series of pyrazolo[1,5-*a*]pyrimidin-7-ylphenyl amides and evaluated them as anti-proliferative agents. SAR was carried out to correlate the importance of numerous substituents with the observed activity. From the series, compound **4** exhibited excellent potency against six colon cell lines (**Fig. 7**), namely HCT116 (p21+/+), 80S14 (p21-/-), LoVo, SW620, DLD1 and HT-29 [7].



C. No	Ar/Het	R	Y	p 21+/+	p 21-/-	LoVo	SW620	DLD1	HT-29	Ratio
				IC ₅₀ (μM)						
4	1,3-Ph- 4-F	<i>i</i> -Pr	O	2.3	0.035	0.012	0.015	0.015	0.015	65

Fig. 7. pyrazolo[1,5-*a*]pyrimidin-7-ylphenyl amides and their effect on colon cell lines.

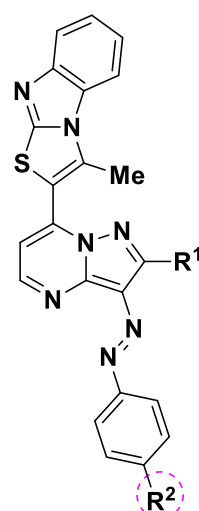
In 2009, Ahmed et al. reported synthesis of novel compound **5** [*N*-(4-chlorophenyl)-2-(methylthio)-5-(naphthalene-2-yl)pyrazolo[1,5-*a*]pyrimidine-3-carboxamide] by reacting sodium salt of 3-hydroxy-1-(2-naphthyl)prop-2-en-1-one with substituted 3-aminopyrazole as anti-tumor agent. The pharmacological evaluation was carried out at different concentrations against four cell lines, namely HCT116 (colon carcinoma), HepG2 (liver carcinoma cell line), Hela (cervix carcinoma cell line) and MCF7 (breast carcinoma). Results revealed that compound **5** exhibited effective toxicity against HCT116 and Hela cell lines as shown in **Fig. 8** [56].



C. No	HepG2	MCF7	HCT116	Hela
	IC ₅₀ (µg/mL)	IC ₅₀ (µg/mL)	IC ₅₀ (µg/mL)	IC ₅₀ (µg/mL)
5	1.88	0.47	0.54	0.40

Fig. 8. Anti-tumor activity of *N*-(4-chlorophenyl)-2-(methylthio)-5-(naphthalene-2-yl) pyrazolo[1,5-*a*]pyrimidine-3-carboxamide.

In 2010, Abdel-Aziz et al. described a facile synthesis of thiazolo[3,2-*a*]benzimidazole linked pyrazolo[1,5-*a*]pyrimidines and performed *in vitro* anti-tumor activity against CaCo-2 (colon cancer cell line) and cytotoxicity against BHK (fibroblast cell line). SAR studies revealed the role of different functional groups and their effect on anti-tumor activity and cytotoxicity, which is presented in **Fig. 9**. All the compounds exhibited good activity. However, compound **6** showed potential activity for both the cell lines CaCo-2 and BHK [57].



Fluoro group favoured the anti-tumor activity compared to chloro and methyl substitutions

C. No	R ¹	R ²	CaCo-2 IC ₅₀ (µg/mL)	BHK IC ₅₀ (µg/mL)
6	NH ₂	F	0.5	2.3

Fig. 9. SAR and anti-tumor properties of thiazolo[3,2-*a*]benzimidazole linked pyrazolo[1,5-*a*]pyrimidines.

In 2011, El-Enany et al. described the synthesis of new pyrazolo[1,5-*a*]pyrimidine-3-carbonitriles with 7-substituted amino groups along with anti-tumor activity. Compound **7** [7-cyclohexylamino-2-methylthio-5-phenylpyrazolo[1,5-*a*]pyrimidine-3-carbonitrile] of this series displayed high potency against HCT116 cell line. SAR study revealed that the presence of functional groups at C-7 was essential for anti-tumor activity (**Fig. 10**) [46].

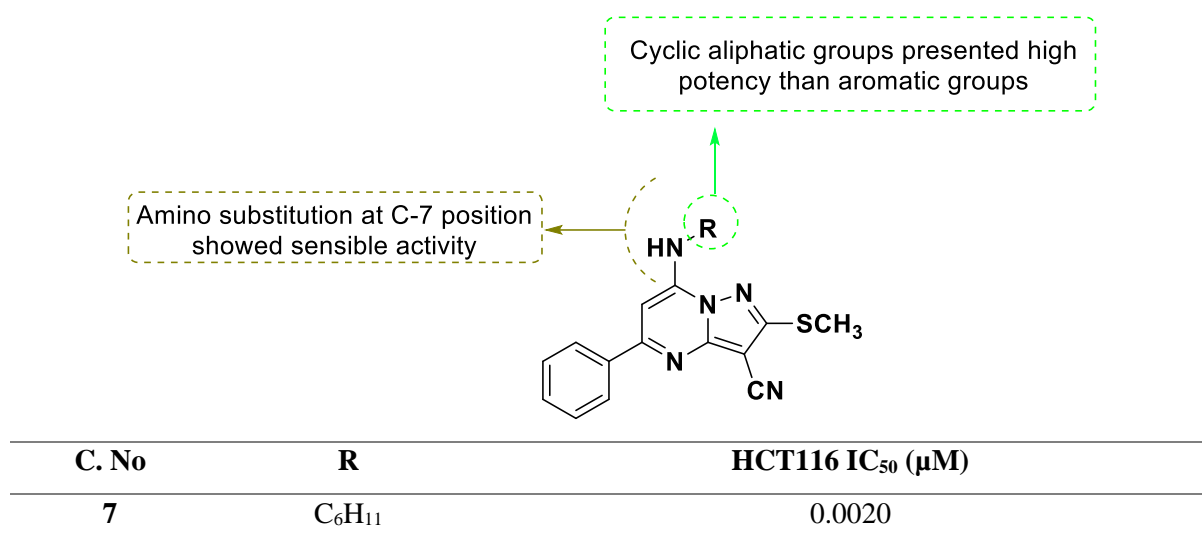
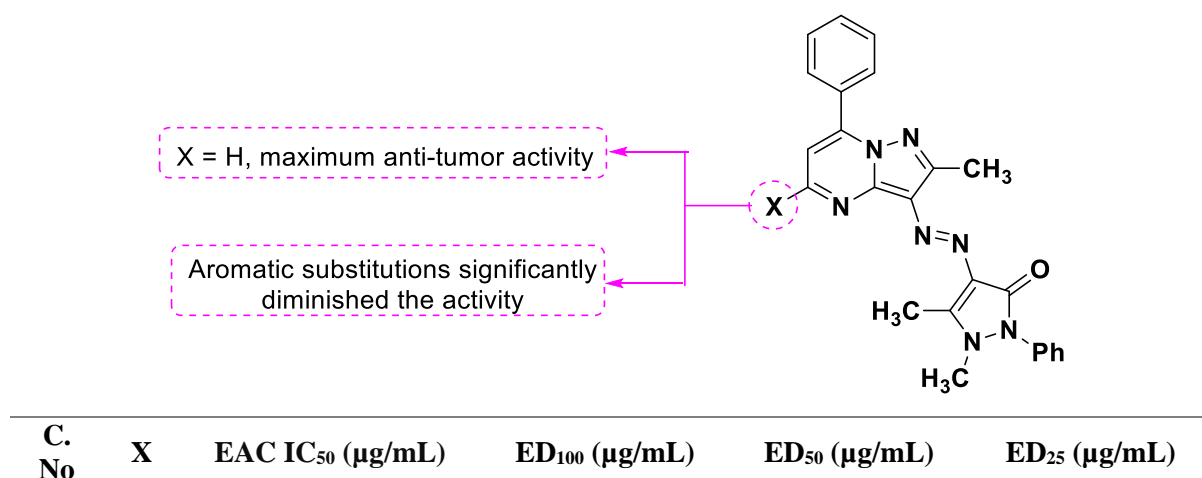


Fig. 10. SAR of pyrazolo[1,5-*a*]pyrimidine-3-carbonitriles as anti-tumor agents.

In 2012, Metwally et al. synthesized novel substituted pyrazolo[1,5-*a*]pyrimidine compounds and evaluated them for their anti-tumor and antioxidative properties. SAR study presented the significance of substituents for favourable activity. However, outcome of this work concluded that compound **8** [(*E*)-1,5-dimethyl-4-((2-methyl-7-phenylpyrazolo[1,5-*a*]pyrimidin-3-yl)diazenyl)-2-phenyl-1,2-dihydro-3*H*-pyrazol-3-one] showed promising potency against ehrlich ascites carcinoma cells (EAC) at different effective doses (ED) (**Fig. 11**) [58].



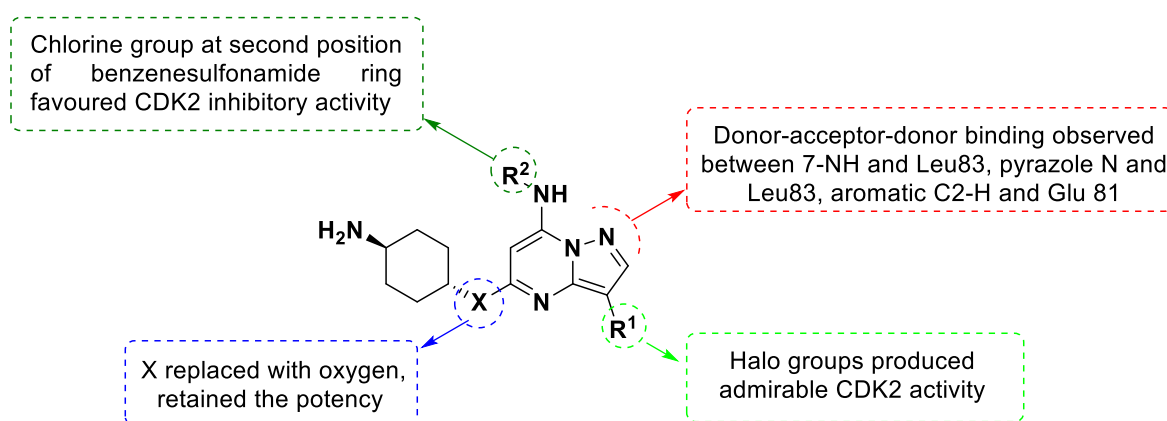
8	H	3.13	99.8	87.1	70.2
---	---	------	------	------	------

Fig. 11. SAR of pyrazolo[1,5-*a*]pyrimidine derivative as anti-tumor agent.

3.1.2 CDK Inhibitors

Cyclin-dependent kinases (CDKs) are a group of serine/threonine or mammalian heterodimeric kinase enzymes that are associated with regulation of cell-cycle progression by phosphorylating proteins involved in cell division. Regulatory subunits of these enzymes play a crucial role in controlling cell cycle, cell division and transcription mechanism in eukaryotes and hence regulate DNA replication process. Any disruptions in routine activity or deregulations result in numerous tumors, thus making the critical target for anticancer therapy. CDK inhibitors oversee the regulation of CDKs, and hence control cell cycle progression [59,60].

In 2005, Williamson et al. attempted structure-guided synthesis of pyrazolo[1,5-*a*]pyrimidines as CDK2 inhibitors. Among the synthesized series, compounds **9-11** exhibited potent activity against tested enzymes CDK2 and GSK-3 β . GI₅₀ was also determined on a cancer cell line HCT 116. A close SAR observation (**Fig. 12**) revealed the effect of substituents [61].



C. No	X	R ¹	R ²	CDK2	GSK-3 β	HCT 116
				IC ₅₀ (μ M)	IC ₅₀ (μ M)	GI ₅₀ (μ M)
9	NH	Br		0.002	8.7	0.34

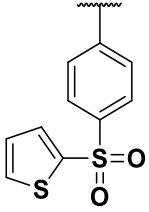
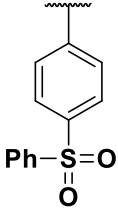
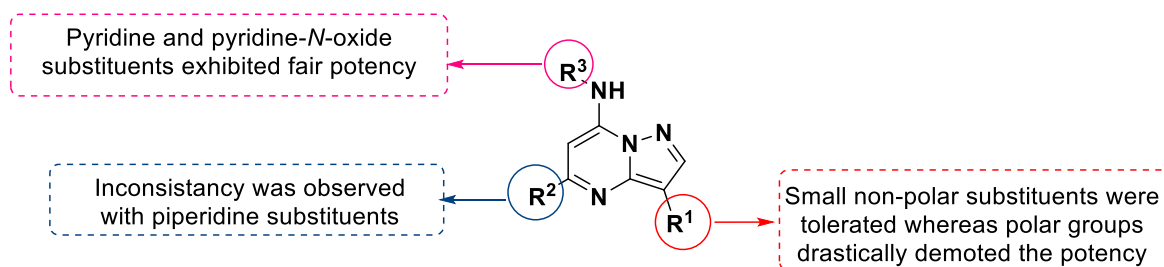
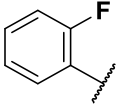
10	NH	Cl		0.011	4.0	0.12
11	NH	Br		0.016	5.3	0.08

Fig. 12. SAR of pyrazolo[1,5-*a*]pyrimidines as CDK2 inhibitors.

In 2007, Paruch and co-workers prepared pyrazolo[1,5-*a*]pyrimidine derivatives as orally available CDK2 inhibitors from suitable acetonitrile and β -keto esters. Among the synthesised molecules, compound **12** exhibited excellent potency against CDK2/cyclin A, GSK-3 β and Thym. Further screening against a panel of around 50 kinases (e.g. JNK 1, PKB, PDK1, ROCK-II) and 17 tumor cell lines was performed. The outcome of this work concluded that compound **12** was orally active and exhibited efficacy in A2780 mouse tumor xenograft model. SAR study depicting various substituents is elaborated in **Fig. 13** [40].

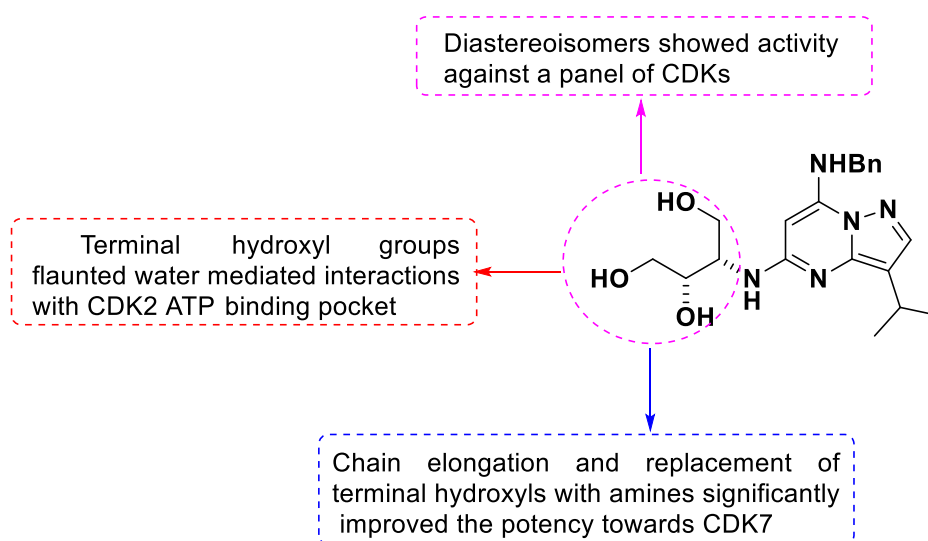


C. No	R ¹	R ²	R ³	CDK2/CyclinA	GSK-3 β	Thym
				IC ₅₀ (μ M)	IC ₅₀ (μ M)	IC ₅₀ (μ M)
12	Br		CH ₂ -3Pyr-O	0.013	0.13	0.21
Animal model	Dose, mpk ^δ vehicle		AUC (μ M h)	C _{max} (μ M)	T _{max} (h)	
Mouse	40 20 % HPBCD ^φ		17.9	6.81	2.0	

mpk^δ: milligrams per kilograms; HPBCD^φ: Hydroxy propyl-beta-cyclodextrin

Fig. 13. SAR studies and pharmacokinetic properties of pyrazolo[1,5-*a*]pyrimidine derivatives as orally available CDK2 inhibitors.

In 2010, Heathcote et al. reported synthesis and biological evaluation of compound **13** [(2*S*,3*S*)-3-((7-(benzylamino)-3-isopropylpyrazolo[1,5-*a*]pyrimidine-5-yl)amino)butane-1,2,4-triol] as effective inhibitor for CDK1, 2, 5 and 9 kinases. The cell line studies of this compound showed potent activity against various CDKs, namely CDK9, CDK2, CDK5, CDK1 and CDK7. This cell based study also displayed inhibition of phosphorylation of CDK substrate. The pharmacokinetic studies concluded that **13** is a potent and novel CDK inhibitor with a potential for oral delivery in cancer patients. SAR studies identified the significant role of side chain, hydroxyl group along with terminal amine group as depicted in **Fig. 14** [62].

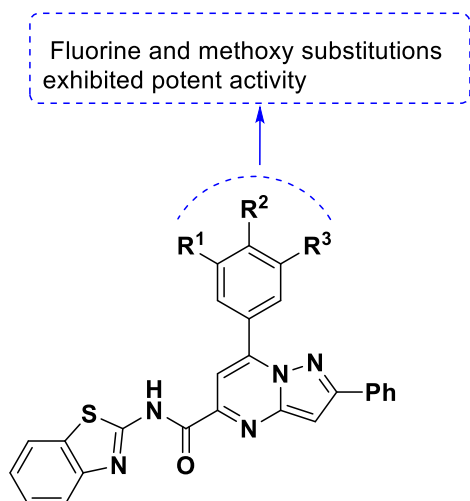


C. No	Kinase	IC ₅₀ (μM) (SD)
13	CDK1	0.033 (0.01)
	CDK2	0.003 (0.001)
	CDK4	20 (1.3)
	CDK5	0.03 (0.006)
	CDK6	35.5 (1.3)
	CDK7	0.25 (0.04)
	CDK9	0.09 (0.01)

Fig. 14. SAR studies of (2*S*,3*S*)-3-((7-(benzylamino)-3-isopropylpyrazolo[1,5-*a*]pyrimidine-5-yl)amino)butane-1,2,4-triol as CDK inhibitors.

In 2013, Kamal et al. introduced a series of 2-aminobenzothiazole linked pyrazolo[1,5-*a*]pyrimidines and determined their anticancer activities against five cell lines A549, DU-145, ACHN, MCF-7 and Hela. From series, compounds **14** and **15** displayed promising activity with IC₅₀ values ranging from

2.01 to 7.07 and 1.94 to 3.46 μM respectively. Further, highly active compounds were screened on A549 cell line to know the molecular events involved in G_2/M cell cycle and the expression of CDKs. Results suggested that the most active compound arrested G_2/M cell cycle and reduced the expression level of CDKs. **Fig. 15** illustrates a brief SAR study depicting the effect of various substituents on the cancer activity [63].

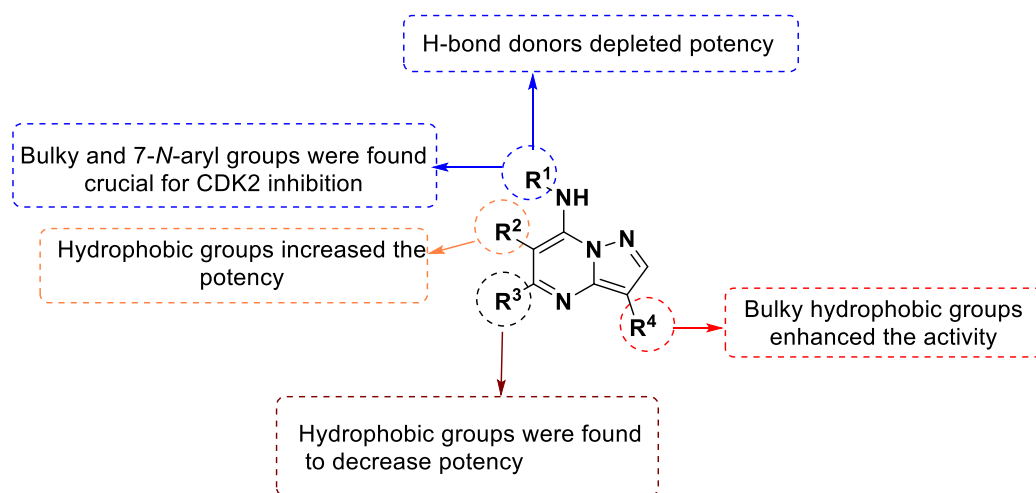


C. No	R ¹	R ²	R ³	A549	DU-145	MCF-7	ACHN	Hela
				IC ₅₀ (μM)				
14	OCH ₃	OCH ₃	OCH ₃	2.01	3.16	2.88	4.36	7.07
15	H	F	H	1.94	2.08	2.29	3.46	2.63

Fig. 15. SAR and effect of 2-aminobenzothiazole linked pyrimidines on human cancer cell lines.

In 2013, Li et al. selected pyrazolo[1,5-*a*]pyrimidine type cyclin A/CDK2 inhibitors and carried out an inclusive *in silico* investigation by three dimensional quantitative structure-activity relationship (3D-QSAR), MD simulations and docking experiments. The results of CoMSIA (SEE = 0.347, $Q^2 = 0.516$, $R_{\text{pre}}^2 = 0.914$, $R_{\text{ncv}}^2 = 0.912$, $R_{\text{m}}^2 = 0.843$, SEP = 0.812) with ten constituents (**16-25**) by steric, hydrophobic and H-bond donor showed internal and external predictive capacity. SAR studies were developed to determine the role of different substituents on the activity as depicted in **Fig. 16** [33].

Chapter 2



C. No	R ¹	R ²	R ³	R ⁴	pIC ₅₀ (M)
16	H	H		H	5.11
17	H	H			6.19
18		H			4.51
19	H	Et			6.48
20	H	3-pyridyl			5.82
21	H	Br			5.55
22		H	Ph	<i>c</i> -Pr	7.15
23		H	Ph	S(CH ₂) ₂ NHAc	8.70

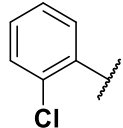
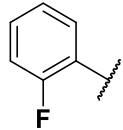
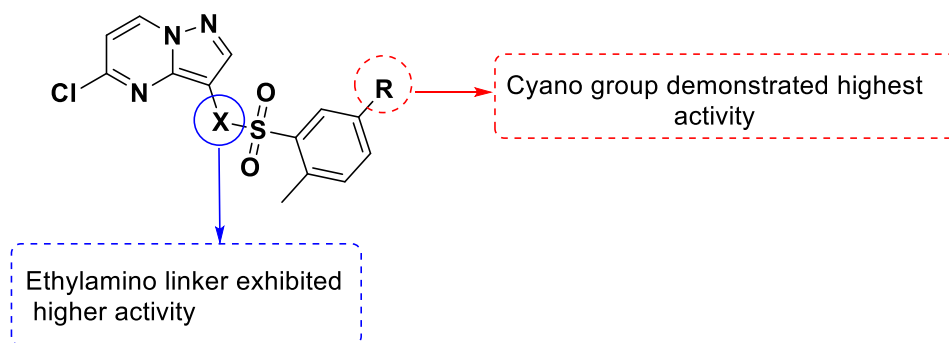
24	Pr	H		Br	6.79
25	CH ₂ -3Pyr-O	H		Br	7.89

Fig. 16. SAR of pyrazolo[1,5-*a*]pyrimidine type CDK2 inhibitors.

In 2015, Phillipson et al. reported pyrazolo[1,5-*a*]pyrimidine derivatives as effective CDK9 inhibitors. Among all the synthesized molecules, compound **26** [*N*-(2-(5-chloropyrazolo[1,5-*a*]pyrimidin-3-yl)ethyl)-5-cyano-*N*,2-dimethylbenzenesulfonamide] showed significant potency against CDK9, CDK7, P13K α and FLT3 enzymes. SAR observations suggest the importance of functionalities as illustrated in **Fig. 17** [64]



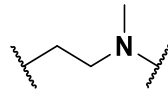
C. No	R	X	IC ₅₀ (nM)				
			CDK9	CDK7	P13K α	FLT3	MV4:11
26	CN		203	>10,000	>10,000	219	0.177

Fig. 17. SAR and pharmacological activities of compound **26** as CDK9 inhibitor.

3.1.3 *c-Src, lck and chk inhibitors*

Src family kinase (SFKs) is a non-receptor tyrosine kinase that plays a crucial role in tumor growth [65]. SFKs consists nine family members that share alike structural and functional features. Their over-expressed or elevated levels is known to be linked to cancer progression by mediating or promoting signal pathways of oncogenesis [66].

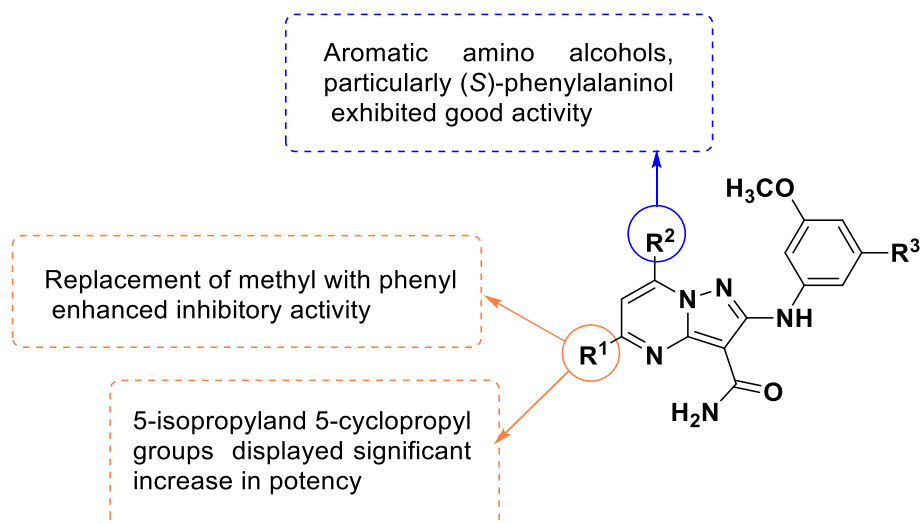
Lymphocyte-specific protein tyrosine kinase (Lck), a member of the Src-family is a key activator enzyme playing role in signal transductions essential in T-cell differentiation and proliferation.

Chapter 2

Functions of T-cell are widely implicated in malignancies and autoimmune diseases. Lck inhibitors necessarily inhibit T-cell activation and are therefore widely used in T-cell mediated responses including cell proliferation and auto immune responses [67,68].

Serine/threonine checkpoint kinases (CHKs) are intracellular kinases that regulate checkpoints in cellular growth cycles [69]. CHKs specifically control both the G2/M and intra-S checkpoints and hence play a key role in cell-cycle progression [70].

In 2008, Makaiyama et al. reported synthesis of pyrazolo[1,5-*a*]pyrimidines as c-Src kinase inhibitors to decrease I_{Kr} channel blockade. Among all, compound **27** [7-((*S*)-1-benzyl-2-hydroxyethylamino)-5-cyclopropyl-2-(3,5-dimethoxyphenylaminopyrazolo[1,5-*a*]pyrimidine-3-carboxamide)] surfaced as the most potent structure having good activity with less I_{Kr} channel blockade and excellent *in vivo* efficacy in middle cerebral artery (MCA) in rat. SAR study (**Fig. 18**) revealed the effect of incorporating different substituents on pyrazolo[1,5-*a*]pyrimidine scaffold for c-Src kinase activity [71].

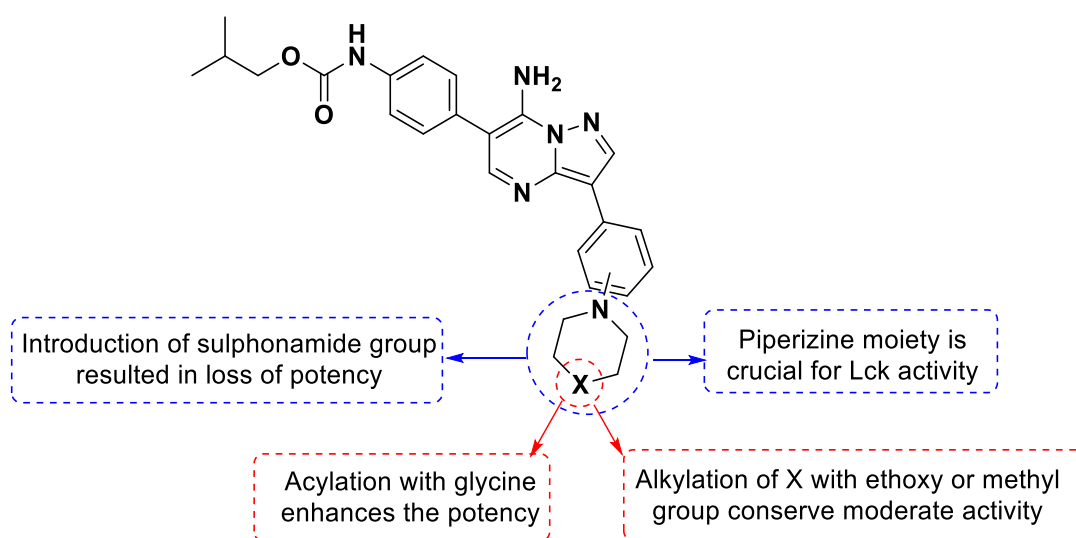


C. No	R ¹	R ²	R ³	c-Src IC ₅₀ (μM)	ELISA		I_{Kr} % inhibition
					% inhibition at 1 μM	IC ₅₀ (μM)	
27			OCH ₃	0.003	100	0.1	23.4
Animal Model	AUC (μg h/mL)		CI (mL/min/kg)		t_{1/2} (min)		V_{ss} (L/kg)

Rat	1.99	25	22	0.53
------------	------	----	----	------

Fig. 18. SAR and pharmacokinetic properties of (7-((*S*)-1-benzyl-2-hydroxyethylamino)-5-cyclopropyl-2-(3,5-dimethoxyphenylamino)pyrazolo[1,5-*a*]pyrimidine-3-carboxamide.

In 2010, Gommermann and co-workers reported the design and synthesis of pyrazolo[1,5-*a*]pyrimidine compounds as orally active inhibitors of Lck. A SAR study towards an effective Lck activity and also for selectivity against Hck, cSrc and KDR is shown in **Fig. 19**. Among the series of compounds, **28** [Isobutyl (4-(7-amino-3-(3-(piperzin-1-yl)pyrazolo[1,5-*a*]pyrimidin-6-yl)phenyl)carbamate)] was optimized as active Lck inhibitor which also indicated excellent selectivity against Hck, cSrc and KDR [41].



C. No	X	Lck lance*	cSrc lance	Hck lance	KDR
		IC ₅₀ (nM)	IC ₅₀ (nM)	IC ₅₀ (nM)	IC ₅₀ (nM)
28	NH, <i>meta</i>	7	642	310	2100

*Lance is a trademark for assay kits by PerkinElmer, Inc.

Fig. 19. SAR and selectivity values of Isobutyl(4-(7-amino-3-(3-(piperzin-1-yl)pyrazolo[1,5-*a*]pyrimidin-6-yl)phenyl)carbamate.

In 2011, Dwyer et al. reported the synthesis of a series of pyrazolo[1,5-*a*]pyrimidine compounds as CHK1 and CDK2 inhibitors. Compound **29** [3-methyl-*N*-(3-(1-methyl-1*H*-pyrazol-4-yl)-5-(piperidin-3-yl)pyrazolo[1,5-*a*]pyrimidin-7-yl)isothiazol-5-amine] emerged as the most active against CHK1 enzyme and also displayed selectivity against CDK2 enzyme. Single X-ray crystal structure of compound **29** bound to CHK1 protein was determined. Molecular docking studies of **29** presented significant interactions between pyrazolo[1,5-*a*]pyrimidine scaffold and CHK1 active site. Further, from SAR studies it was observed that substitution at C-7 was crucial for activity as shown in **Fig. 20** [11].

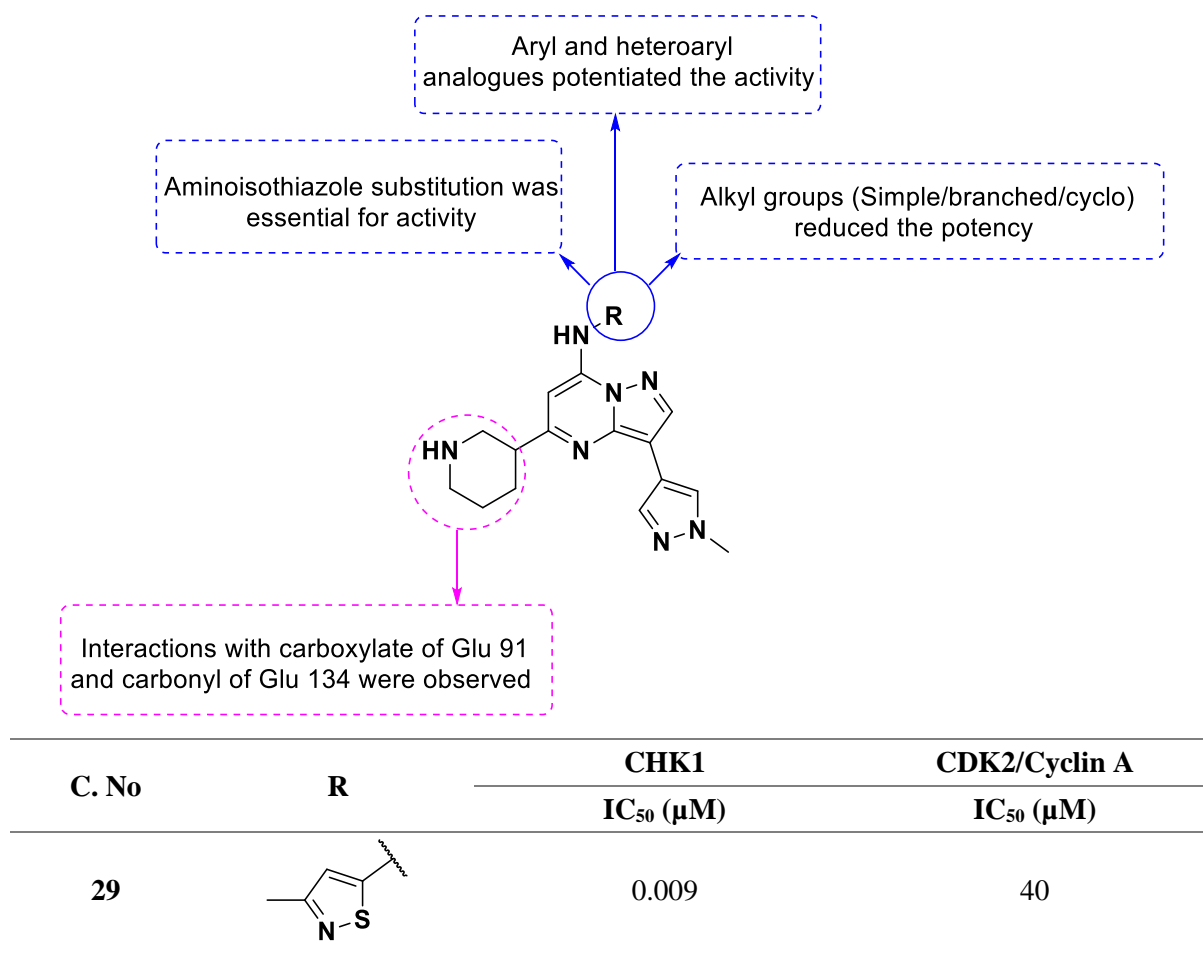
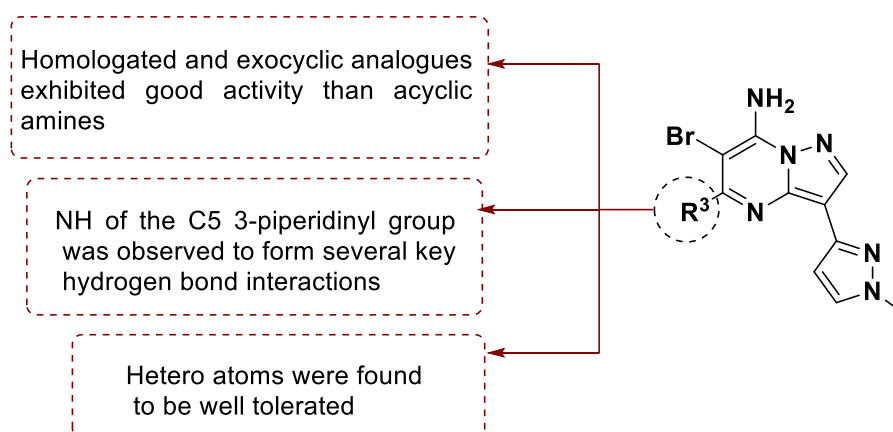


Fig. 20. SAR and molecular interactions of 3-methyl-*N*-(3-(1-methyl-1*H*-pyrazol-4-yl)-5-(piperidin-3-yl)pyrazolo[1,5-*a*]pyrimidin-7-yl)isothiazol-5-amine.

In 2011, Labroli et al. reported the preparation and pharmacological properties of novel pyrazolo[1,5-*a*]pyrimidines as CHK1 inhibitors. Compounds **30-32** from this series were highly potent against CHK1 and CDK2. X-ray crystallographic studies of potent compound **31**, revealed that the -NH₂ group at C-7 displayed strong hydrogen bonding interactions with the water molecule at the CHK1 enzyme active site. The SAR study is elaborated in **Fig. 21** [43].



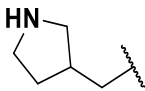
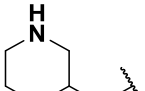
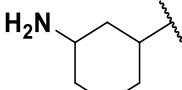
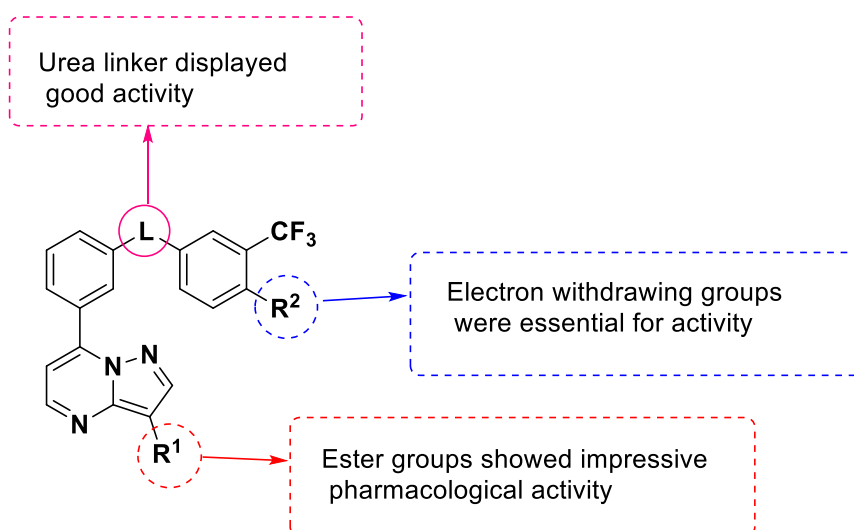
C. No	R ³	CHK1	CDK2/Cyclin A
		IC ₅₀ (μM)	IC ₅₀ (μM)
30		0.007	0.84
31		0.007	2.4
32		0.005	0.44

Fig. 21. SAR studies of 5-(3-aminocyclohexyl)-6-bromo-3-(1-methyl-1*H*-pyrazol-4-yl)pyrazolo[1,5-*a*]pyrimidin-7-amines derivatives.

3.1.4 B-Raf kinase inhibitors

Rapidly accelerated fibrosarcoma (Raf) kinase is a class of serine/threonine protein kinases and a key component in growth and survival of the cell. It is also known to be an important constituent of Raf-MEK-ERK signalling pathway. B-Raf kinase is active in several human cancers and has therefore been a potential target for inhibition in cancer therapeutics [72-74].

In 2009, Gopalsamy and co-workers reported the synthesis of a series of novel pyrazolo[1,5-*a*]pyrimidine-3-carboxylates and evaluated these compounds as B-Raf kinase inhibitors. In this series, compounds **33-35** exhibited potent activity. A brief SAR study of this series is presented in **Fig. 22** [75].

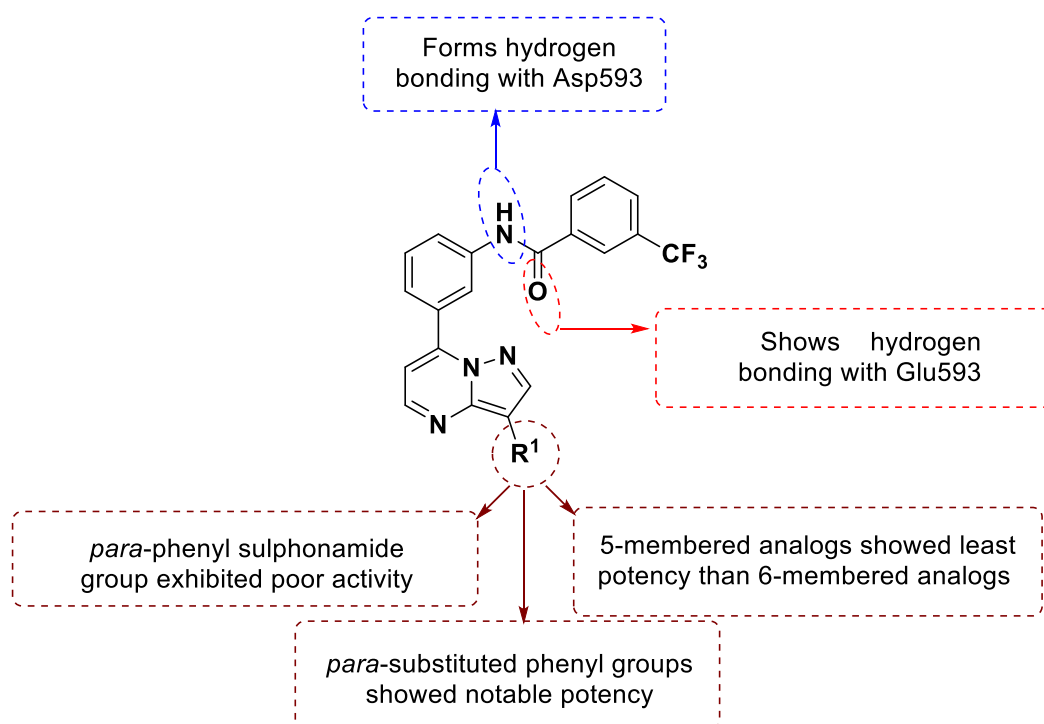


C. No	R ¹	R ²	Linker (L)	B-Raf kinase
				IC ₅₀ (μM)

33	CONHCH ₂ CH ₂ N(C ₂ H ₅) ₂	Cl	NH-CO-NH	0.17
34	CONH(CH ₂) ₃ OCH ₃	Cl	NH-CO-NH	0.27
35	CONHCH ₂ CH ₂ - <i>N</i> -morpholinyl	Cl	NH-CO-NH	0.16

Fig. 22. SAR study of pyrazolo[1,5-*a*]pyrimidine-3-carboxylates as potent B-Raf kinase inhibitors.

In 2009, Berger et al. reported synthesis of novel 3-substituted pyrazolo[1,5-*a*]pyrimidin-7-yl)phenyl)-3-(trifluoromethyl)benzamides as active B-Raf kinase inhibitors. Potent B-Raf kinase activity was observed for the compounds **36-38** from this series. Compounds were also tested against WM 266-4 and HT29 cell lines and the results are shown in Fig. 23. From SAR studies, it was noted that higher potency was exhibited for compounds with basic amine residue at C-3 position (**Fig. 23**) [76].

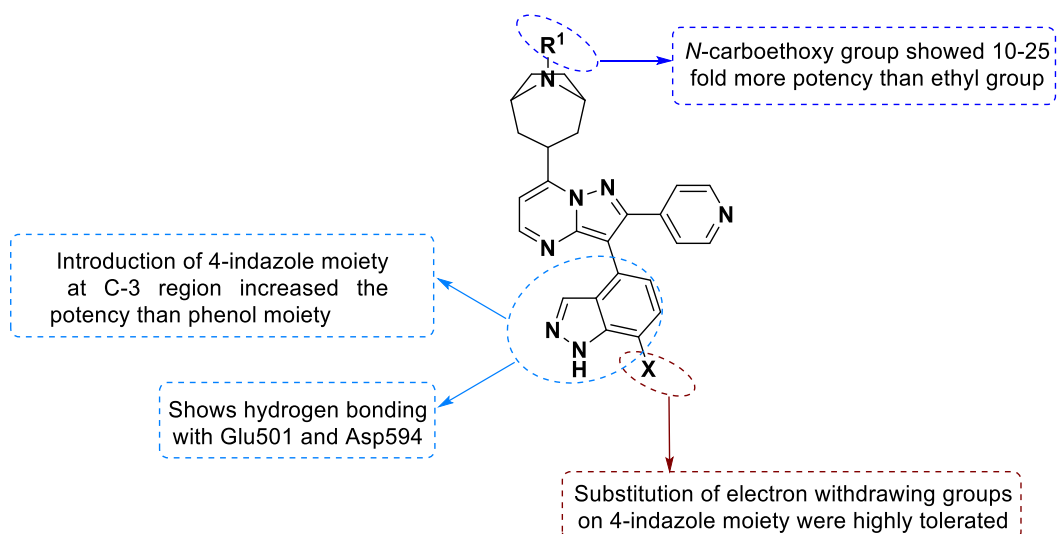


C. No	R ¹	B-Raf	HT29	WM 266-4
		IC ₅₀ (μM)	IC ₅₀ (μM)	IC ₅₀ (μM)
36	4-Ph-CH ₂ -N(CH ₃) ₂	0.024	0.78	0.92
37	3-Pyridinyl-6-NHCH ₂ CH ₂ N(CH ₃) ₂	0.030	0.46	0.92
38	3-Pyridinyl-6-N-methylpiperazine	0.044	0.31	0.74

Fig. 23. SAR and B-Raf kinase activity of 3-substituted *N*-(3-(pyrazolo[1,5-*a*]pyrimidin-7-yl)phenyl)-3-(trifluoromethyl)benzamides.

In 2009, Grandi and co-workers reported the synthesis of 3,7-disubstituted pyrazolo[1,5-*a*]pyrimidines and evaluated them as B-Raf kinase inhibitors. SAR study revealed that the compounds with tropanes

at C-7, indazole at C-3 positions were well tolerated as depicted in **Fig. 24**. From the synthesized compounds, **39-41** exhibited good activity against B-Raf, A375 and WM266-4 cell lines [77].



C. No	X	R ¹	B-Raf	A375	WM266-4
			IC ₅₀ (μM)	IC ₅₀ (μM)	IC ₅₀ (μM)
39	H	COOC ₂ H ₅	0.002	0.38	0.30
40	Cl	COOC ₂ H ₅	0.0004	0.58	0.28
41	F	COOC ₂ H ₅	0.0004	0.62	0.30

Fig. 24. B-Raf kinase activity and SAR studies of disubstituted pyrazolo[1,5-*a*]pyrimidines.

Wang et al. in 2009 reported a series of novel pyrazolo[1,5-*a*]pyrimidines and as B-Raf type-1 kinase inhibitors. Compound **42** [3-(7-(2-chloro-4-((1*S*,4*S*)-5-methyl-2,5-diazabicyclo[2.2.1]heptan-2-yl)phenyl)-2-(pyridin-4-yl)pyrazolo[1,5-*a*]pyrimidin-3-yl)phenol] was highly selective and potent against B-Raf kinase as well as significantly effective against A 375 cell line. **Fig. 25** briefly describes the SAR studies for this series [78].

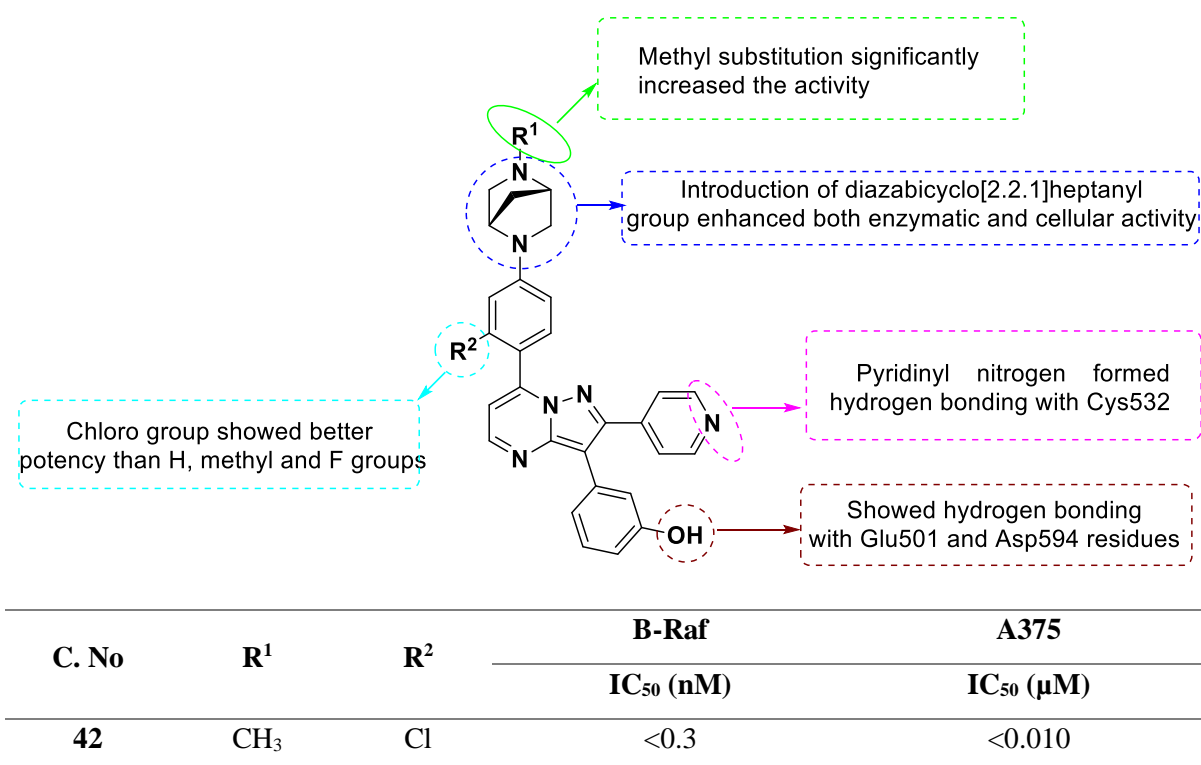
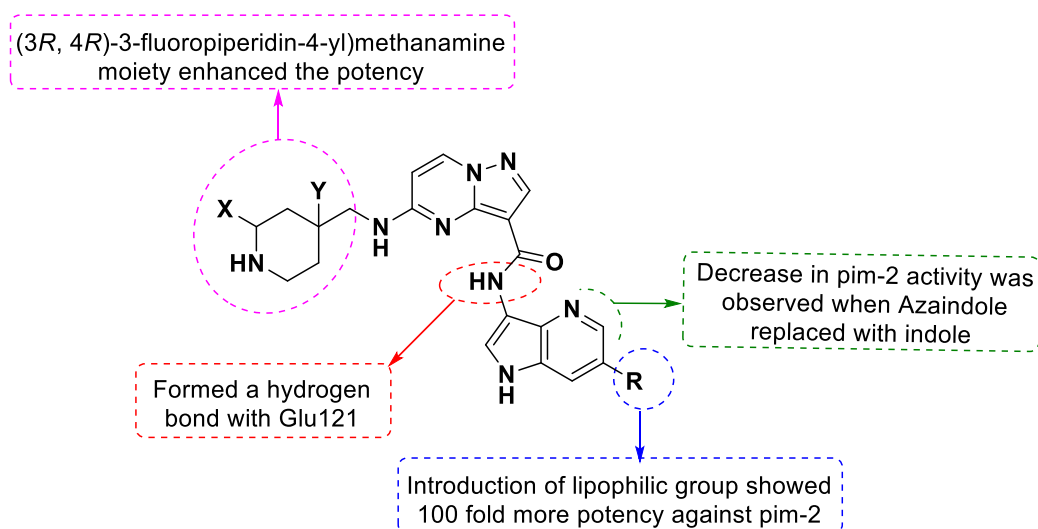


Fig. 25. SAR and B-Raf kinase activity of lead compound consisting pyrazolo[1,5-*a*]pyrimidine.

3.1.5 Pim kinase inhibitors

The PIM family of serine/threonine kinases are highly homologous (60-70%) in their kinase domains. They are mainly comprised of three members, Pim-1, Pim-2, and Pim-3 that regulate numerous signalling pathways essential in tumor development and progression. Overexpression of these kinases results in several forms of cancers namely pancreatic, prostate, bladder, haematological and many others. PIM inhibitors reduced the survival, progression and migration of these tumor cells thus proving to be effective in cancer treatment [79].

In 2013, Wang and co-workers reported structure and property based pyrazolo[1,5-*a*]pyrimidines as pan-pim inhibitors. For this series, SAR studies and lead optimization techniques identified a potent compound **43** [*N*-(5-(2-fluorophenyl)-1*H*-pyrrolo[2,3-*b*]pyridin-3-yl)-5-(((3-fluoropiperidin-4-yl)methyl)amino)pyrazolo[1,5-*a*]pyrimidine-3-carboxamide] (**Fig. 26**). Along with pan-pim activity, **43** also exhibited good potency (IC₅₀ of 1.9 μM) against multiple myeloma cell line (MM1s) [80].



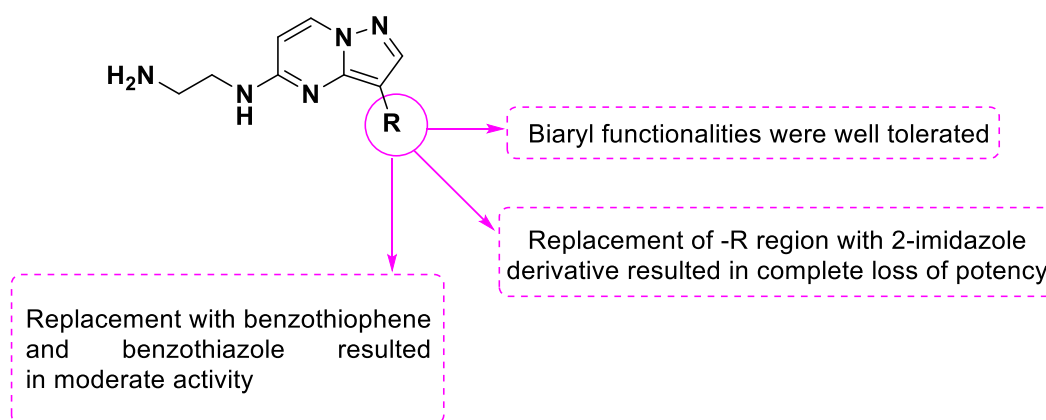
C. No	X	Y	R	^ψ SC	K _i (nM)			[‡] c.pKa
					Pim-1	Pim-2	Pim-3	
43	F	H	2-F-Ph	Trans	0.003	0.032	0.009	8.3

^ψSC: relative stereochemistry amid X- and -NHCH₂- functional groups.

[‡]c.pKa: Calculated pKa of piperidine nitrogen using MoKa 1.1.0 through the proprietary roche model.

Fig. 26. Pin-pam inhibitory activities and SAR of *N*-(5-(2-fluorophenyl)-1*H*-pyrrolo[2,3-*b*]pyridin-3-yl)-5-(((3-fluoropiperidin-4-yl)methyl)amino)pyrazolo[1,5-*a*]pyrimidine-3-carboxamide.

Dwyer et al. in 2013 reported the synthesis of C-3, C-5 di-substituted pyrazolo[1,5-*a*]pyrimidines as pim inhibitors. Among this series, compound **44** [*N*1-(3-(3-(5-methyl-1,3,4-oxadiazol-2-yl)phenyl)pyrazolo[1,5-*a*]pyrimidin-5-yl)ethane-1,2-diamine] exhibited potent inhibitory activity against pim-1 and pim-2 as well as indicated moderate selectivity against CDK2, pim-3, CK2, CHK1, P13K and mTOR kinases. It was observed from SAR studies that appropriate substitution at C-3 position influenced the activity. **Fig. 27** concisely presents the SAR studies and various kinase enzyme activities for the potent compound **44** [45].



C. No	R	Pim-1	Pim-2
-------	---	-------	-------

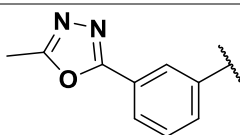
		IC ₅₀ (nM)	IC ₅₀ (nM)
44		1.3	7.3
	Kinase	IC₅₀ (nM)	
	CDK2	580	
	Pim-3	1.8	
	CK2	950	
	CHK1	7100	
	mTor	>3000	
	P1K	>3000	

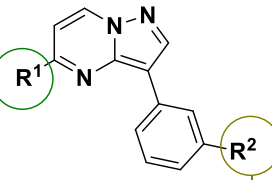
Fig. 27. SAR, Pim and kinase activity of 3,5-disubstituted pyrazolo[1,5-*a*]pyrimidine.

Xu and co-workers in 2015 reported synthesis of disubstituted pyrazolo[1,5-*a*]pyrimidine derivatives and evaluated their pharmacological properties as potent pim-1 and Flt-3 kinase inhibitors. Compounds **45-49** in this series unveiled good inhibition. Further, it was revealed that compound **49** also exhibited strong inhibition of BAD phosphorylation at 1 μ M concentration. A brief SAR study has been represented in **Fig. 28** [37].

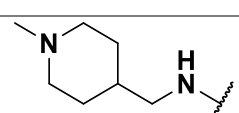
Introduction of *trans*-4-aminocyclohexanol enhanced potency by 100 folds

Substitutions with -OH group exhibited greater potency than ketone, ether and sulfone functionalities

Amino substituent displayed most potent pim-1 inhibition



Electron withdrawing groups namely -Cl, trifluoro indicated a major role in pim-kinase activity

C. No	R ¹	R ²	Pim-1	Pim-2	Flt-3
			IC ₅₀ (nM)	IC ₅₀ (nM)	IC ₅₀ (nM)
45		OCF ₃	45	1491	ND

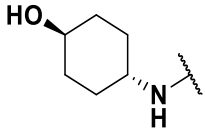
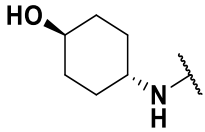
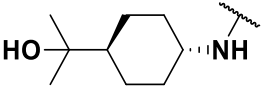
46		CF ₃	25	282	157
47		OCF ₃	27	269	53
48		CF ₃	17	525	271
49		Cl	23	228	125

Fig. 28. SAR and pim activities of disubstituted pyrazolo[1,5-*a*]pyrimidine derivatives.

3.1.6 KDR kinase inhibitors

The kinase insert domain-containing receptor (KDR), also referred to as VEGFR-2, is one of the vital mediators of vascular endothelial growth factor (VEGF) functions in endothelial cells, and a key regulator of angiogenesis and subsequent progression of the tumor. Thus making it a potential and valid target for anticancer drug discovery [81].

In 2002, Fraley et al. synthesized 3,6-diaryl pyrazolo[1,5-*a*]pyrimidines by the condensation reaction between 2-arylmalondialdehydes and 3-amino-4-aryl pyrazoles and evaluated their activity as KDR kinase inhibitors. SAR studies suggested that substituents at C-6 and C-3 positions are essential for potency and are presented in **Fig. 29**. Among the series, compounds **50-53** showed moderate to good activity against KDR kinase and these compounds were also further screened against highly homologous receptor tyrosine kinases (PDGFR β , FLT-4, FGFR-1 and FLT-1) and SRC kinase [39].

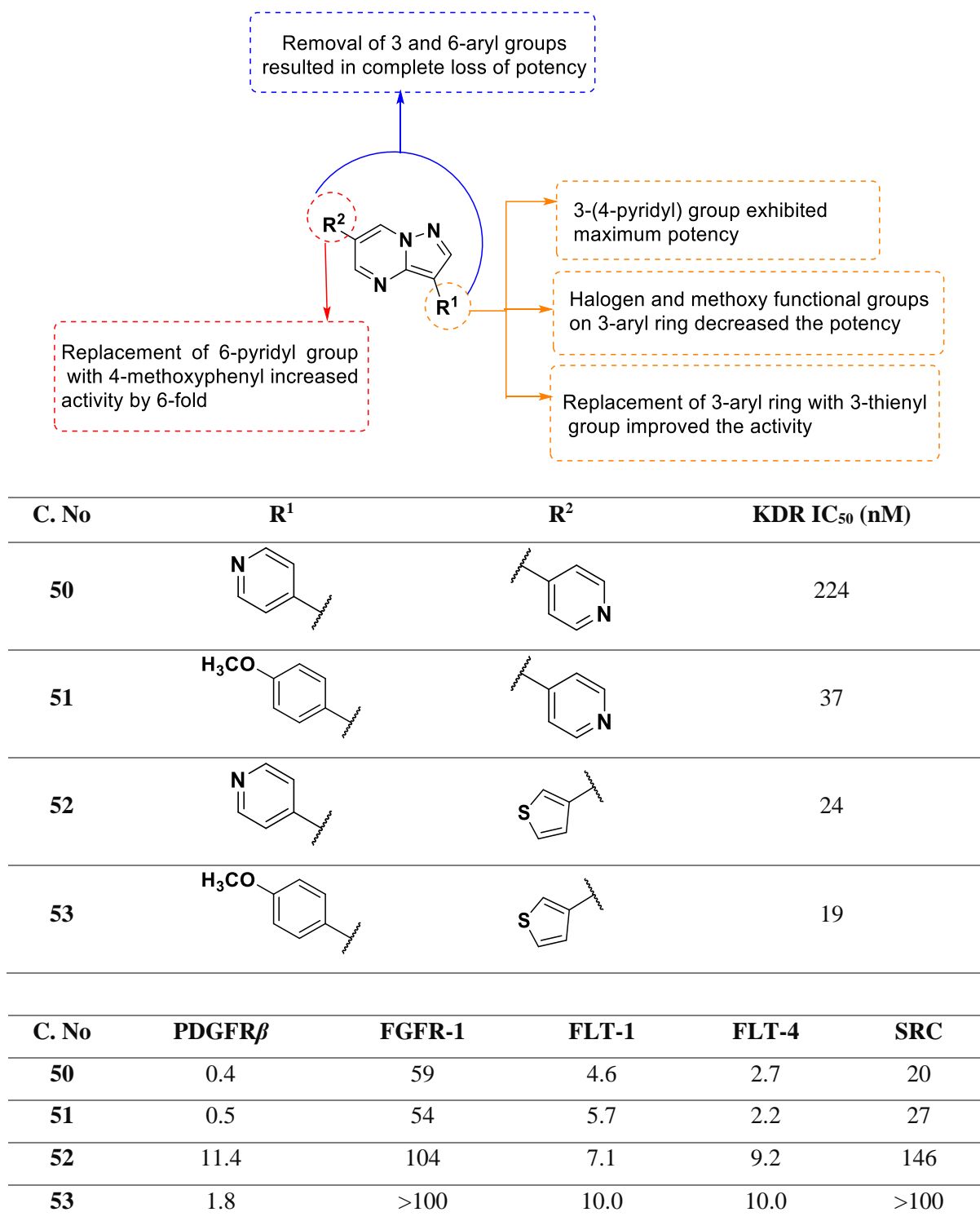


Fig. 29. SAR and KDR kinase and KDR selectivity values of 3,6-diaryl pyrazolo[1,5-*a*]pyrimidines.

The same research group in order to improve the solubility and biological property, reported a novel series of pyrazolo[1,5-*a*]pyrimidines as KDR kinase inhibitors. From the reported series, compounds **54-56** exhibited promising potency against KDR kinase, thus inferring the importance of physical

properties in improving the activity. SAR study reveals the importance of structural modifications at C-6 of pyrazolo[1,5-*a*]pyrimidine core to afford greater kinase activity as depicted in **Fig. 30** [20].

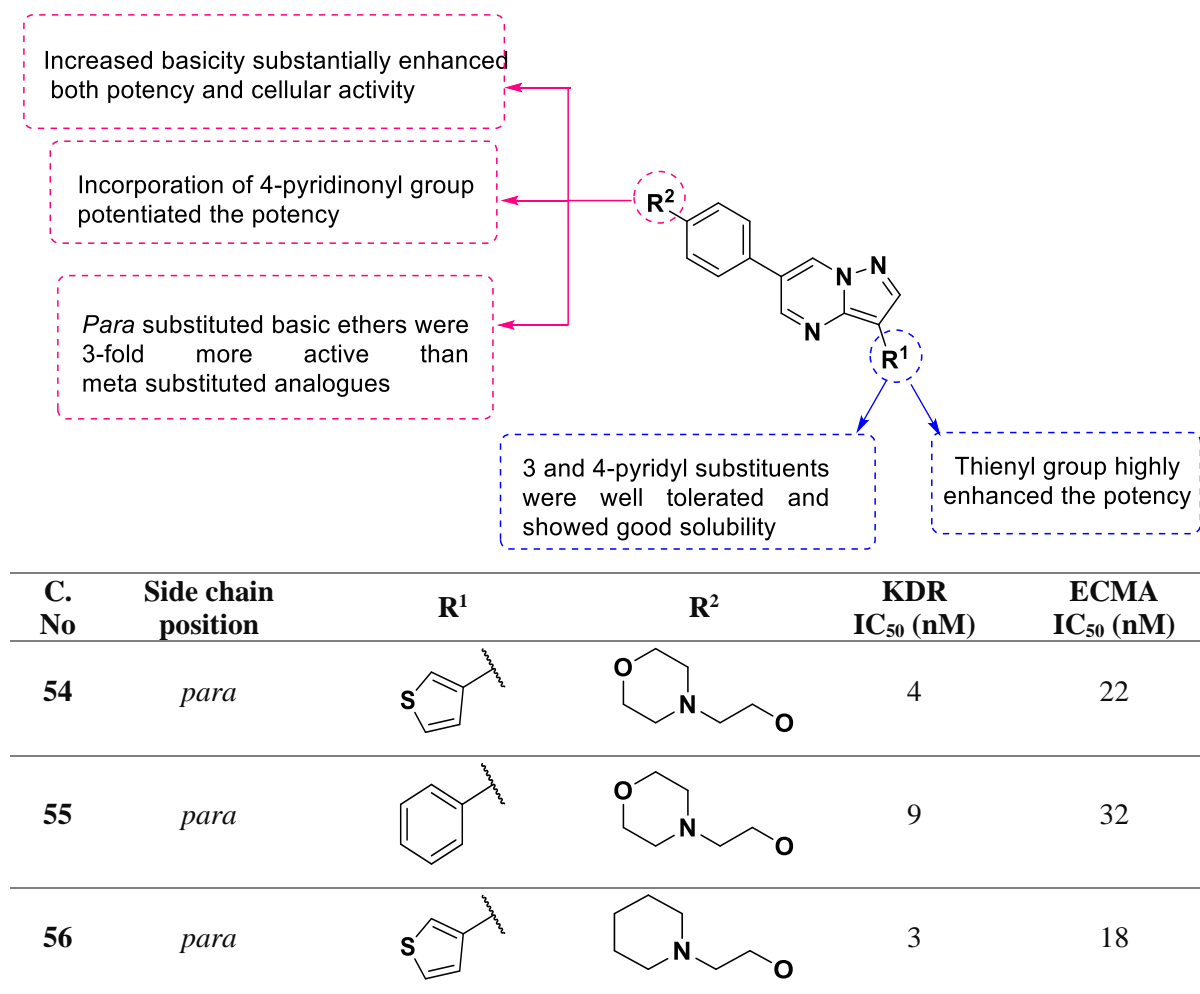


Fig. 30. KDR kinase and ECMA activities.

In 2008, Frey et al. reported the synthesis of 7-aminopyrazolo[1,5-*a*]pyrimidines as KDR inhibitors. SAR study revealed that incorporation of *N,N*-diaryl urea moiety at C-6 region and *N*-methyl pyrazole at C-3 region enhanced the kinase and cellular activity as shown in **Fig. 31**. It was noted that compound **57** exhibited greater KDR kinase and cellular activity. The compounds were also found to have good pharmacokinetic profiles and efficacy in estradiol-induced murine uterine edema (UE) assay [12].

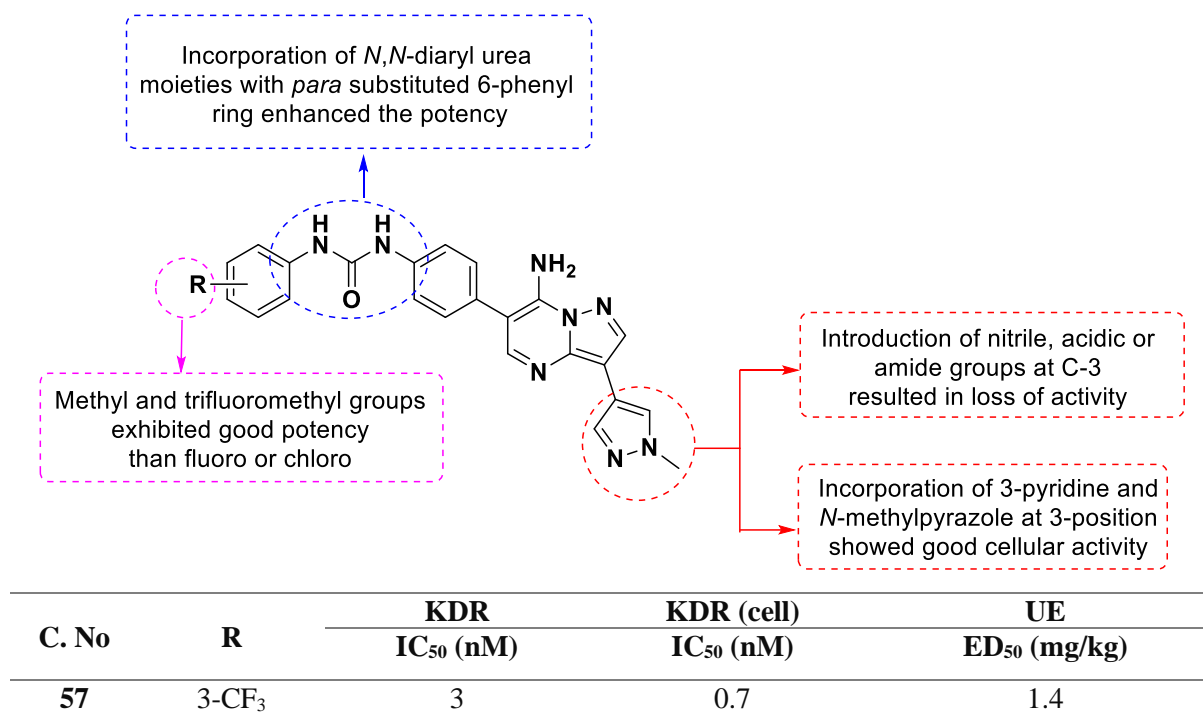


Fig. 31. Structural activity studies, KDR and UE results of 7-aminopyrazolo[1,5-*a*]pyrimidines.

3.2 Central nervous system (CNS) agents

3.2.1 Benzodiazepine receptor modulators

Benzodiazepines are a class of drugs affecting the central nervous system. They have been commonly prescribed as medications mainly as anxiolytics, hypnotics, sedatives and as anticonvulsants. The pharmacological response is believed to be mediated by the benzodiazepine receptors (BZR) in the brain [82]. This receptor is known to be a supramolecular complex consisting of the binding site for benzodiazepine, the recognition sites for GABA, and the GABA-dependent chloride channel, thus bringing about two types of pharmacological profile namely benzodiazepine agonists (anxiolytic, anticonvulsant and sedative), and inverse agonists (cause anxiety and convulsions) [83].

In 1999, Selleri et al. synthesized thienyl and methoxyphenyl substituted pyrazolo[1,5-*a*]pyrimidines and evaluated their biological activity against BZR. Within the series, compounds **58** [3-(4-methoxyphenyl)-6-(thiophen-3-yl)pyrazolo[1,5-*a*]pyrimidin-7(4*H*)-one] and **59** [3,6-di(thiophen-3-yl)pyrazolo[1,5-*a*]pyrimidin-7(4*H*)-one] were reported as highly active compounds. SAR study is briefed in **Fig. 32** [84].

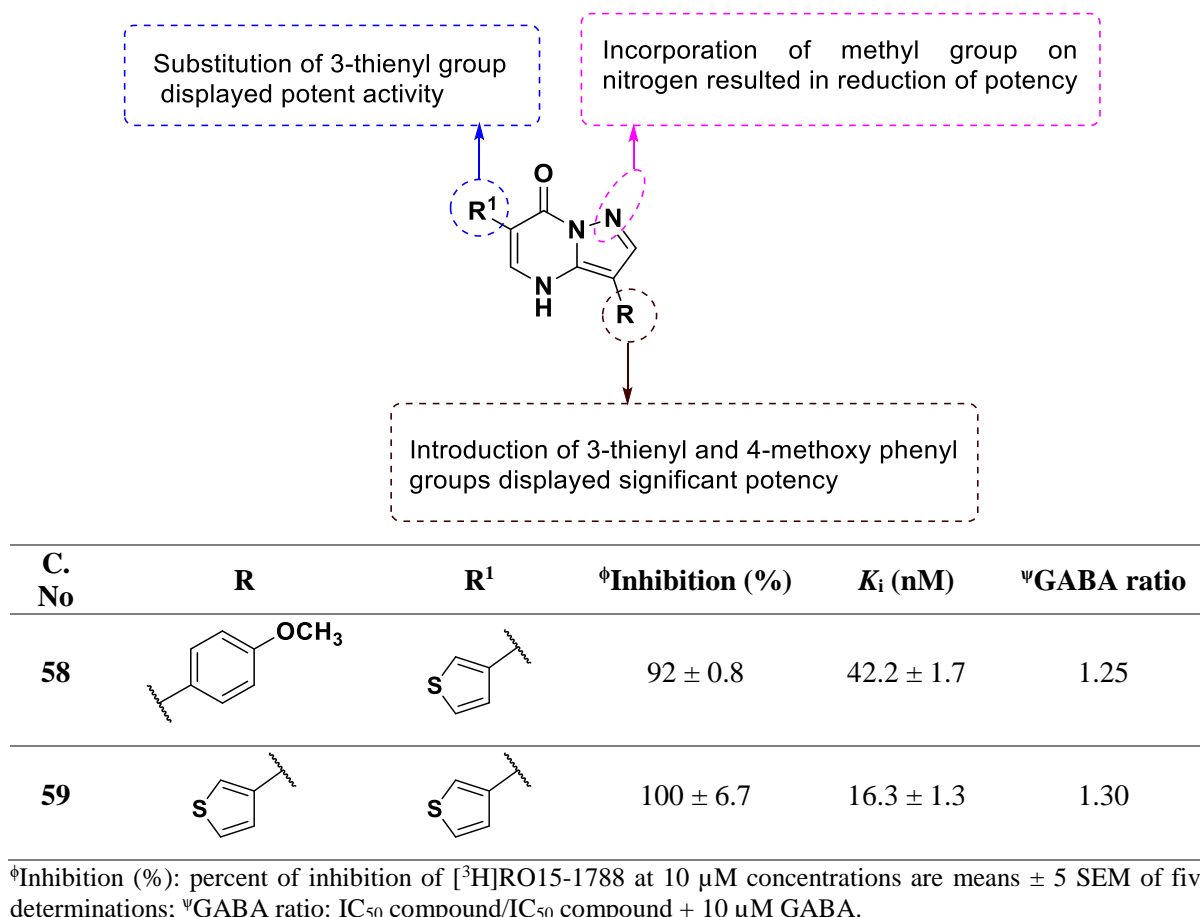
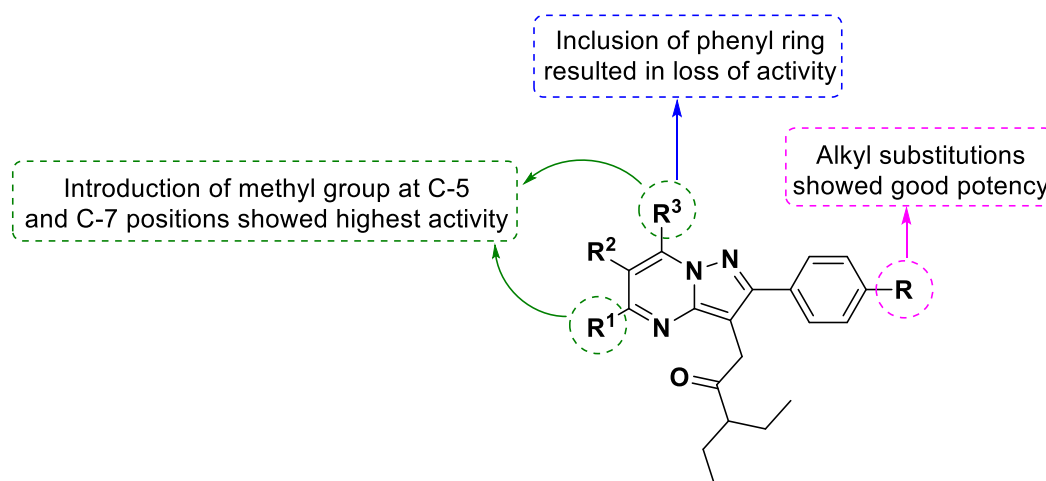


Fig. 32. SAR and activity values of thienyl and methoxyphenyl substituted pyrazolo[1,5-*a*]pyrimidines.

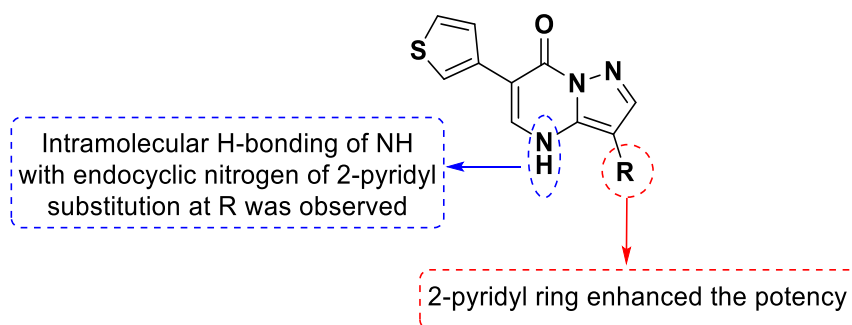
The same research group in 2001, reported the synthesis of 2-aryl pyrazolo[1,5-*a*]pyrimidine-3-yl acetamides as potent peripheral and central BZR ligands (PBZR & CBZR). Binding assays were performed for PBZR ([³H]PK 11195 and [³H]Ro 5-4864) and CBZR ([³H]Ro 15-1788) using radio ligands. SAR studies concluded with a key factor that was anticipated to enhance the cellular activity for both CBZR and PBZR ligands as shown in **Fig. 33**. Among the series, compounds **60-64** were found to be more selective and potent inhibitors [21].



C. No	R ¹	R ²	R ³	R	K _i (nM) PBZR		K _i (nM) CBZR
					[³ H]PK 11195	[³ H]Ro 5-4864	
60	CH ₃	H	CH ₃	Cl	2.4 ± 0.2	1.4 ± 0.2	>10.00
61	CH ₃	H	CH ₃	CH ₃	0.8 ± 0.1	1.7 ± 0.2	>10.00
62	CH ₃	H	CH ₃	OCH ₃	4.7 ± 0.4	3.1 ± 0.2	>10.00
63	CH ₃	H	Ph	Cl	2.4 ± 0.2	2.5 ± 0.2	>10.00
64	Ph	H	CH ₃	Cl	3.4 ± 0.2	2.7 ± 0.2	>10.00

Fig. 33. SAR and PBBR, CBZR studies of *N,N*-diethyl-(2-arylpyrazolo[1,5-*a*]pyrimidin-3-yl)acetamides.

In 2003, Selleri et al. reported the synthesis of 3-aryl-6-(3-thienyl)pyrazolo[1,5-*a*]pyrimidin-7-ones and *in vitro* biological evaluation on Bz/GABA_A and recombinant BZR_s ($\alpha 1235\beta 2/3\gamma 2$). Compound **65** [3-(pyridin-2-yl)-6-(thiophen-3-yl)pyrazolo[1,5-*a*]pyrimidin-7(4*H*)-one] was found to be the most active in comparison to the standard drugs (diazepam, zolpidem) and a brief SAR study has been depicted in **Fig. 34**. [42].

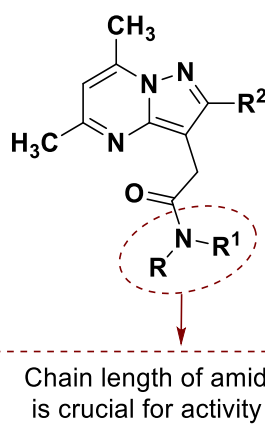


C. No	R	Inhibition (%)	K _i (nM)	*GR	$\alpha 1$	$\alpha 2$	$\alpha 3$	$\alpha 5$
65	2-pyridyl	98 ± 1	3.9 ± 0.5	1.10	7.0 ± 0.8	927 ± 83	ND	740 ± 51
Diazepam		NR	10	1.5	14	20	15	11
Zolpidem		NR	NR	NR	26.7	156	383	>10000

ND: Not determined; NR: Not reported; *GR: GABA ratio.

Fig. 34. SAR and activity data of 3-aryl-6-(3-thienyl)pyrazolo[1,5-*a*]pyrimidin-7-ones against recombinant BZR_s.

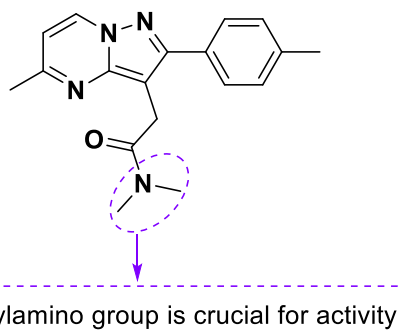
In 2005, the same research group reported the synthesis and biological properties of 2-phenyl pyrazolo[1,5-*a*]pyrimidin-3-yl acetamides as peripheral benzodiazepine receptor (PBZR) ligands. SAR study is briefed in **Fig. 35**. Among the discovered series, ligands **66-68** showed prominent affinity for both PBZR and central benzodiazepine receptors (CBZR) [85].



C. No	R	R ¹	R ²	PBR K _i (nM)	CBR K _i (nM)
66	C ₂ H ₅	C ₂ H ₅	4-CH ₃ -Ph	0.8	>10.00
67	<i>n-but</i>	<i>n-but</i>	Ph	4.5	10.00
68	C ₂ H ₅	Ph	Ph	0.8	10.00

Fig. 35. SAR and activity studies of 2-phenyl pyrazolo[1,5-*a*]pyrimidin-3-yl acetamides.

The same research group (in 2005) reported the synthesis of compound **69** [*N,N*-dimethyl-2-(5-methyl-2-(*p*-tolyl)pyrazolo[1,5-*a*]pyrimidin-3-yl)acetamide] as selective GABA_A α1 receptor antagonist. *In vitro* studies were performed in comparison with the standard drugs, namely zolpidem and diazepam, on bovine brain homogenate along with recombinant BZR_s (αβ2/3γ2, x = 123&5). The results emphasise the binding affinities only for α1 as illustrated in **Fig. 36** [19].



C. No	K _i (nM)			
	α 1	α 2	α 3	α 5
69	31 ± 4	>10000	>10000	>10000
Zolpidem	26.7	156	383	>10000
Diazepam	14	20	15	11

Fig. 36. Recombinant BZR_s affinity values of *N,N*-dimethyl-2-(5-methyl-2-(*p*-tolyl)pyrazolo[1,5-*a*]pyrimidin-3-yl)acetamide.

In 2010, Reynolds et al. discovered the synthesis of pyrazolo[1,5-*a*]pyrimidine acetamides bearing phenyl alkyl ether functional groups and evaluated them as translocator protein (TSPO) and CBZR ligands. All the synthesized compounds **70-75** exhibited good affinity for TSPO with broad selectivity over CBZR as well as CNS transporters and receptors, as illustrated in **Fig. 37** [86].

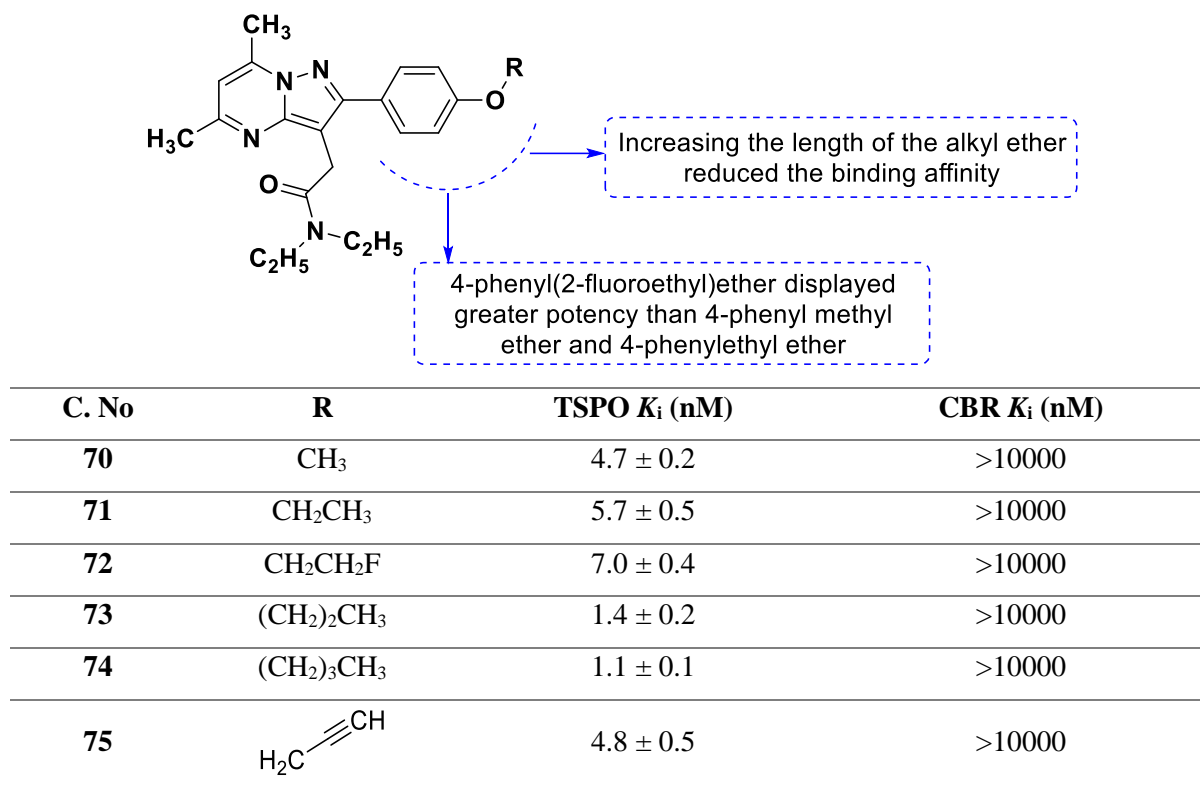


Fig. 37. TSPO and CBZR binding and selectivity studies of pyrazolo[1,5-*a*]pyrimidines.

3.2.2 5-HT₆ receptor antagonists

5-Hydroxytryptamine subtype 6 receptor (5-HT₆R) is a recently discovered serotonin receptor (a typical G protein-coupled receptor) and a promising target for cognitive disorders like Alzheimer's, schizophrenia, anxiety and obesity [87,88].

In 2010, Ivachtchenko et al. reported the synthesis of (3-phenylsulfonylcycloalkano[*e* and *d*]pyrazolo[1,5-*a*]pyrimidin-2-yl)amines as serotonin 5-HT₆ receptors. Among the series, compounds **76** and **77** exhibited the maximum affinity against 5-HT₆ receptor. A brief SAR study has been depicted in **Fig. 38** [27].

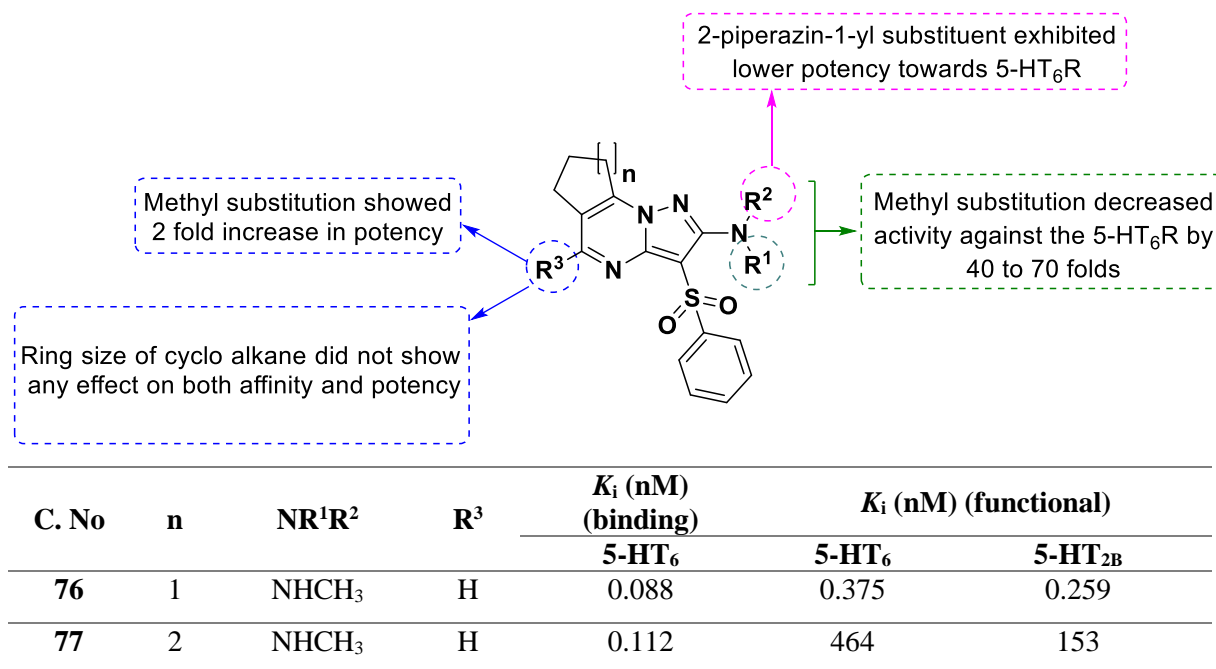
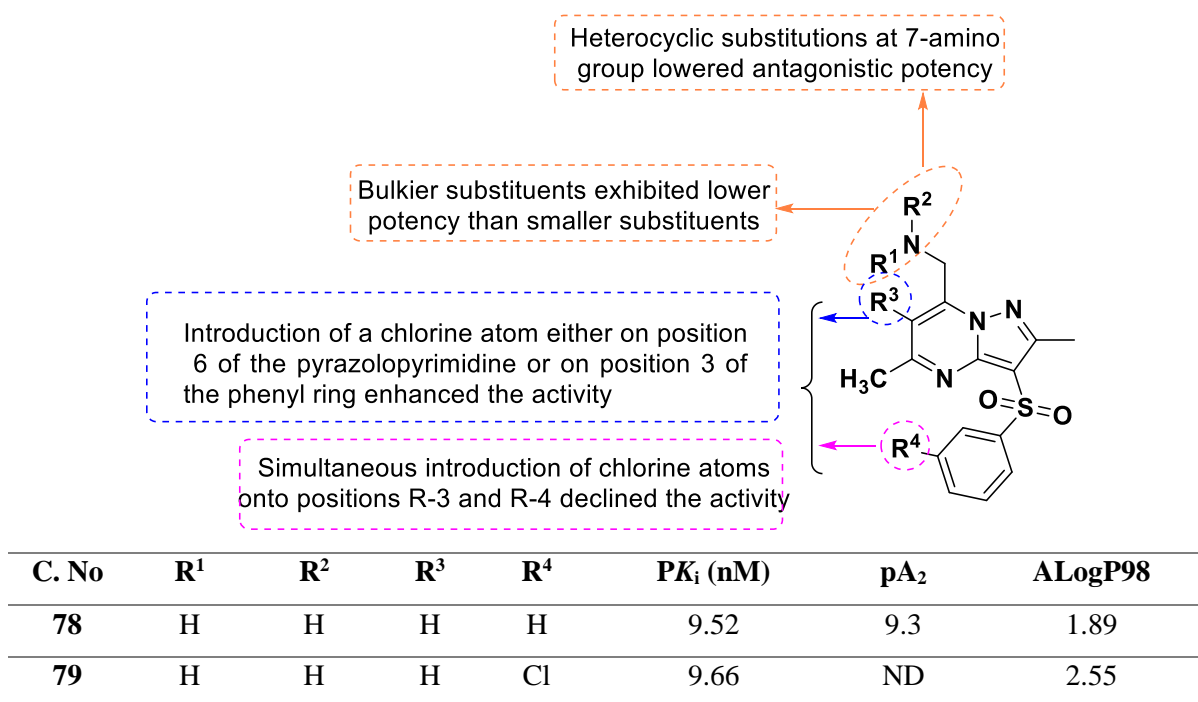


Fig. 38. SAR and 5-HT₆ receptor studies of pyrazolo[1,5-*a*]pyrimidines.

The same research group (in 2011) reported the synthesis and SAR studies of substituted 5, *N*²-dimethyl-3-phenylsulfonyl-pyrazolo[1,5-*a*]pyrimidine-2-amines and evaluated them as 5-HT₆ receptor ligands. SAR studies reveal that the formation of intermolecular hydrogen bond between 2-methylamino and 3-sulfo group highly enhanced the potency and selectivity to block serotonin responses in HEK-293 cells. Among the series, compounds **78-81** were found to be more potent inhibitors of 5-HT₆ receptors and the activity values are represented in **Fig. 39** [49].



80	H	H	Cl	H	9.85	ND	2.55
81	CH ₃	CH ₃	H	H	9.46	ND	2.80

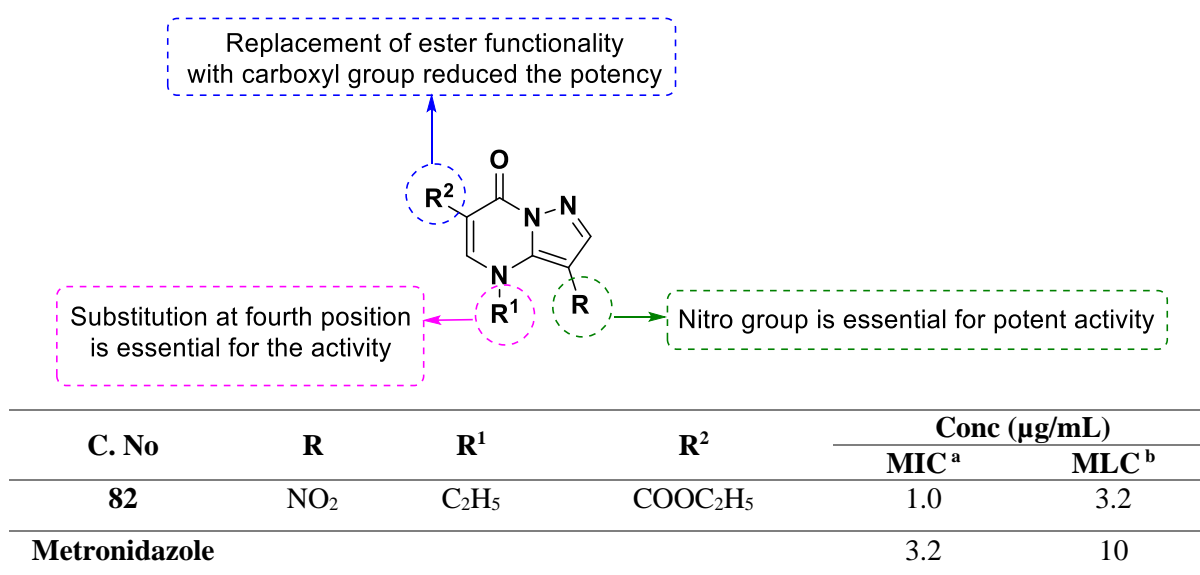
ND: Not determined.

Fig. 39. SAR, 5-HT₆R activity profiles of substituted 5,N²-dimethyl-3-phenylsulfonyl-pyrazolo[1,5-*a*]pyrimidine-2-amines.

3.3 Anti-infectious agents

Infectious diseases are major threat to human kind from pre-historic era. In recent decades, the emergence of drug-resistance microbial infections has generated serious life-threatening health issues and are responsible for highest mortality [89]. Various analogs of pyrazolo[1,5-*a*]pyrimidines scaffold have been reported possess effective antimicrobial activity as mentioned in the succeeding sections.

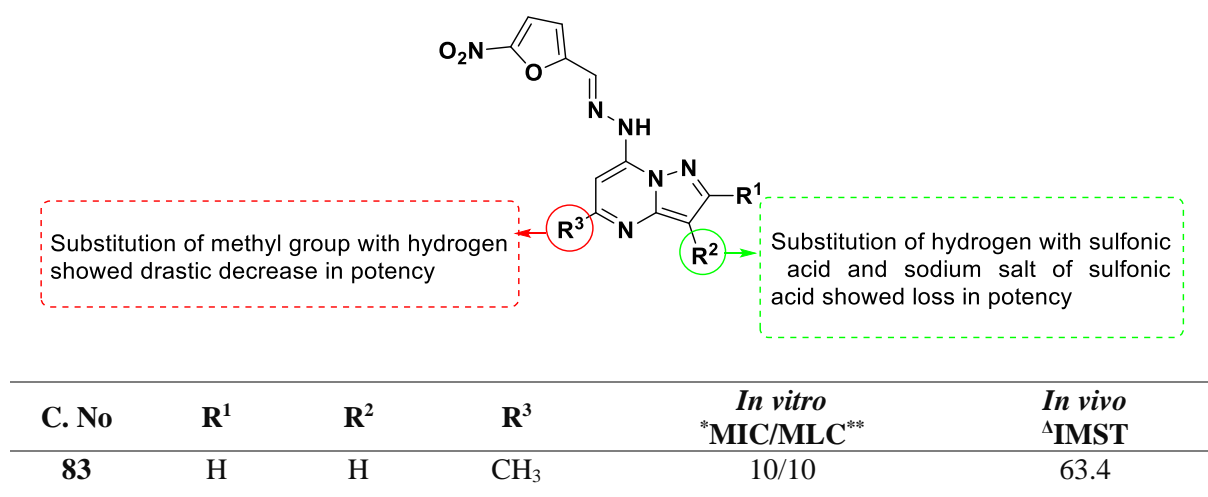
In 1975, Senga et al. discovered the synthesis of pyrazolo[1,5-*a*]pyrimidines as antitrichomonal agents. In this series, compound **82** [6-carbethoxy-4-ethyl-3-nitropyrazolo[1,5-*a*]pyrimidin-7-one] demonstrated potent antitrichomonal activity than the standard drug metronidazole. From the SAR, it was deduced that 3-nitro, 6-carbethoxy and 4-ethyl groups are essential for activity. The structure of potent compound has been described in **Fig. 40** including its inhibitory potency [90].



MIC^a: Minimum inhibitory concentration; MLC^b: Minimum lethal concentration.

Fig. 40. SAR of multi substituted pyrazolo[1,5-*a*]pyrimidines as antitrichomonal agents.

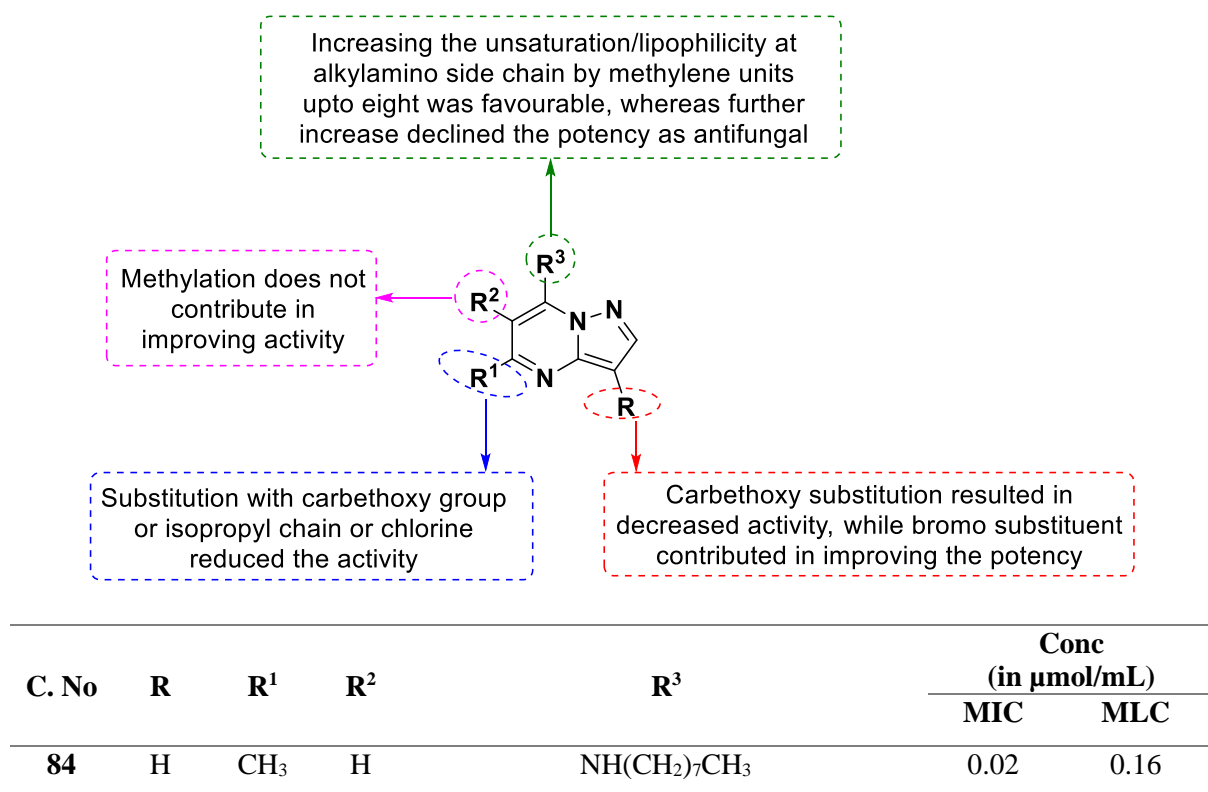
In 1976, Novinson and co-workers reported the synthesis of hydrazine containing pyrazolo[1,5-*a*]pyrimidine derivatives and evaluated them for *in vitro* antitrypanosomal activity. Further, the authors have screened the title compounds for *in vitro* and *in vivo* activities against *Trypanosoma cruzi*. Among all the synthesized molecules, compound **83** showed significant activity. A brief SAR study on the scaffold is presented in **Fig. 41** [91].



*MIC: Minimum inhibitory concentration; MLC**: Minimum lethal concentration expressed in $\mu\text{g/mL}$; ^ΔIMST: Increase in mean survival time was expressed as present increase beyond survival time of control mice 100 mg/kg twice daily by gavage.

Fig. 41. SAR and antitrypanosomal activity studies of compound **83**.

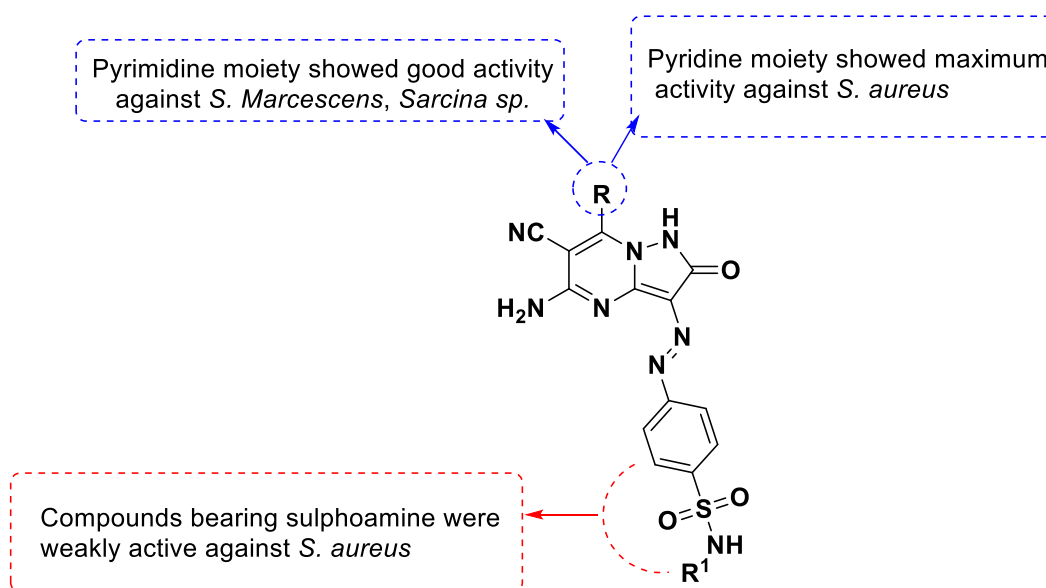
In 1977, Novinson et al. synthesized 7-alkylamino substituted pyrazolo[1,5-*a*]pyrimidines and *in vitro* antifungal activity against *Trichophyton mentagrophytes* was performed. Out of 22 tested derivatives, compounds **84** and **85** revealed potent fungicidal activity (*in vitro*). It was also observed that compound **85** was one fold more potent than **84**. However, their topical applications on unabraded and abraded guinea pig skin (*in vivo*) generated skin irritation. Preliminary SAR and structures of active compounds are presented in **Fig. 42** [92].



85	Br	CH ₃	H	NH(CH ₂) ₈ CH=CH(CH ₂) ₇ CH ₃	0.01	0.02
----	----	-----------------	---	--	------	------

Fig. 42. SAR of 7-alkylamino substituted pyrazolo[1,5-*a*]pyrimidines as antifungal compounds.

El-Gaby and co-workers in 2000 carried out the synthesis and antibacterial evaluation of pyrazolo[1,5-*a*]pyrimidines bearing sulfonamido moieties. Of the screened compounds, four derivatives (**86-89**) exhibited potent activity against gram negative than gram positive bacterial strains in comparison to the standard drug streptomycin. The preliminary SAR study suggested arylamino substitutions on basic nucleus contributed maximum inhibition against gram negative bacterial strains, whereas unsubstitution on sulphonamido moiety generated weak inhibition. The antibacterial screening results for the active compounds are presented in **Fig. 43** [93].



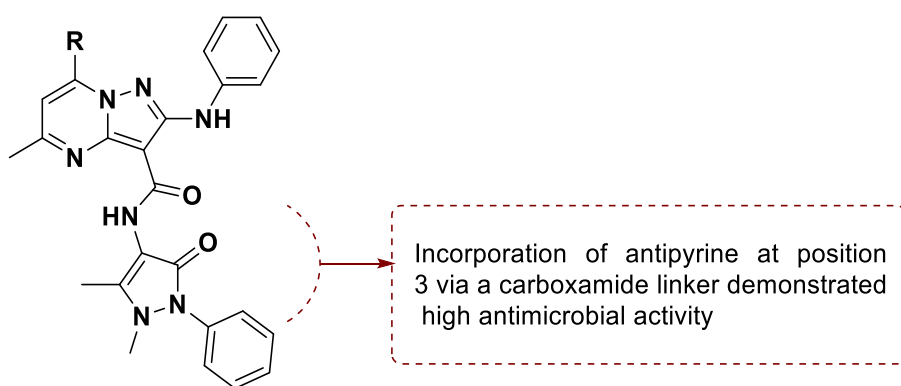
C. No	R	R ¹	Gram positive			Gram negative	
			<i>Staphylococcus aureus</i>	<i>Bacillus subtilis</i>	<i>Sarcina sp.</i>	<i>Escherichia coli</i>	<i>Serratia marcescens</i>
86	2-Pyrimidinyl	NH-C ₆ H ₄ -O-CH ₃ - <i>p</i>	++	+	+++	+++	+++
87	2-(4-Methyl pyrimidinyl)	NH-C ₆ H ₄ -O-CH ₃ - <i>p</i>	++	+	+++	++	+++
88	H	C ₆ H ₄ -O-CH ₃ - <i>o</i>	+	+++	++	++	++
89	2-Pyridinyl	C ₆ H ₄ -O-	+++	+++	++	++	++

CH ₃ - <i>o</i>					
Streptomycin	++++	++++	++++	++++	++++

+: moderately sensitive giving a zone of inhibition 9–11 mm; ++: sensitive giving a zone of inhibition 12–14 mm; +++: very sensitive giving a zone of inhibition 15–18 mm.

Fig. 43. SAR and active antibacterial pyrazolo[1,5-*a*]pyrimidines.

In 2008, Bondock et al. synthesized new heterocyclic analogs including pyrazolo[1,5-*a*]pyrimidines containing antipyrine moiety and evaluated for antimicrobial potency against bacterial and fungal strains along with reference drugs like ampicillin, chloramphenicol and fluconazole. Compounds **90** and **91** exhibit higher antimicrobial properties than the evaluated reference drugs. The SAR of the same is shown in Fig. 44 [94].



C. No	R	Zone inhibition (in mm)			
		Gram positive bacteria	Gram negative bacteria	Fungi	
		<i>B. thuringiensis</i>	<i>K. pneumoniae</i>	<i>B. fabae</i>	<i>F. oxysporum</i>
90	CH ₃	21	28	24	25
91	OH	20	24	27	25
Ampicillin		18	19	17	15
Chloramphenicol		23	20	16	15
Fluconazole		NA	NA	22	16

NA: No activity.

Fig. 44. Structures and results of the antimicrobial (inhibition zone) potency of pyrazolo[1,5-*a*]pyrimidines.

Popovici-Muller et al. (2009) reported a novel series of pyrazolo[1,5-*a*]pyrimidines as Hepatitis-C Virus (HCV) RNA polymerase inhibitors. Authors synthesized three different analogues by modifying different functional groups/moieties at C-3 (carboxylic acid group), C-7 (cyclohexyl group) and C-6 (aromatic substituents) positions. Authors evaluated all the synthesized compounds for HCV RNA

polymerase inhibition. Of the evaluated compounds (**92-95**), **95** was discovered as potent HCV RNA polymerase inhibitor. **Fig. 45** illustrates a brief SAR study and active compounds of the series [95].

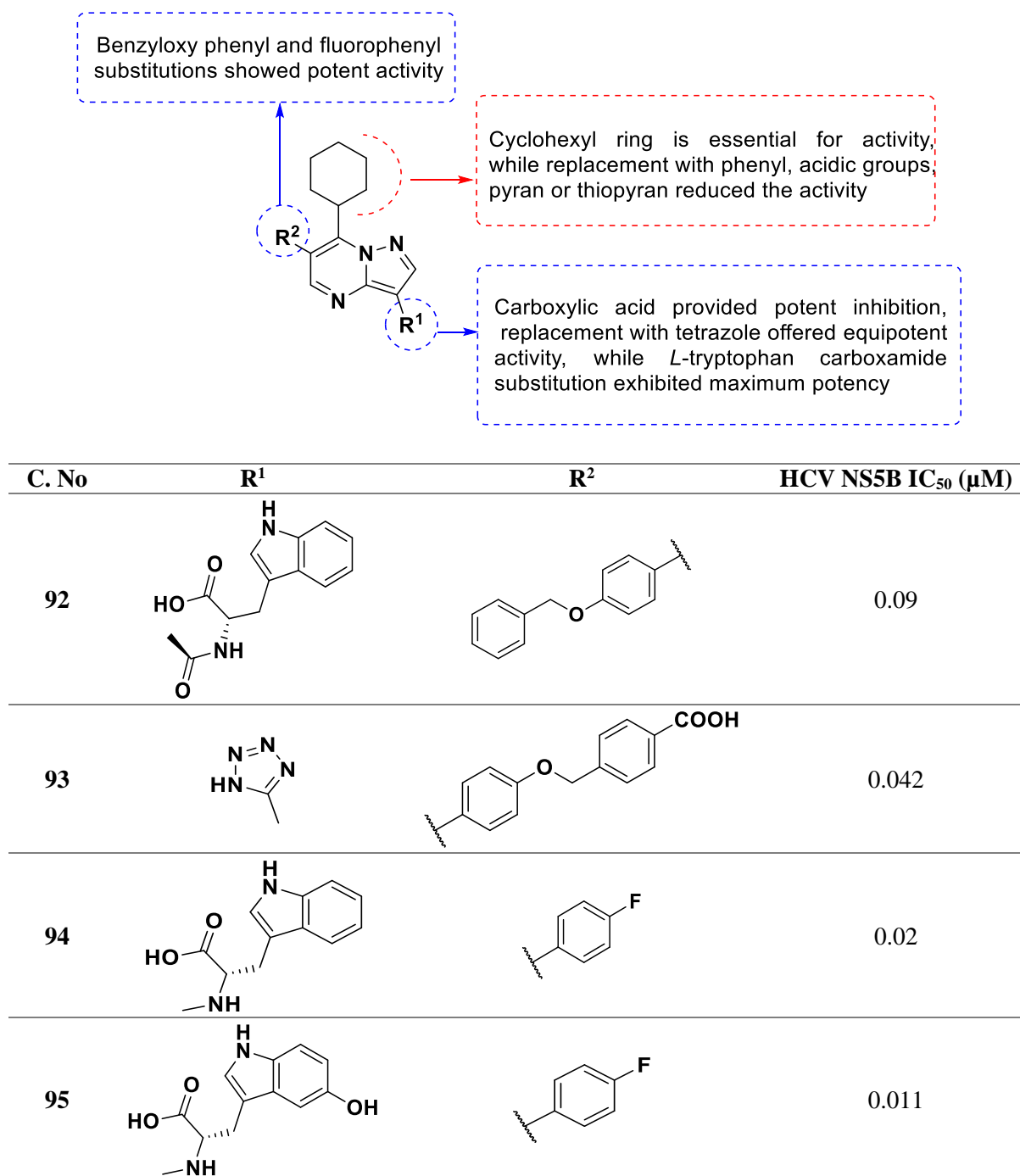


Fig. 45. SAR and antiviral properties of active compounds.

In 2010, Abdelhamid et al. carried out the synthesis and antimicrobial activity of some fused pyrimidine compounds including pyrazolo[1,5-*a*]pyrimidines bearing thiazole moiety. From the eight synthesized pyrazolo[1,5-*a*]pyrimidines, only four compounds (**96-99**) were evaluated for their biological activity. Moderate activity was observed as compared to the standard drugs (**Fig. 46**) [96].

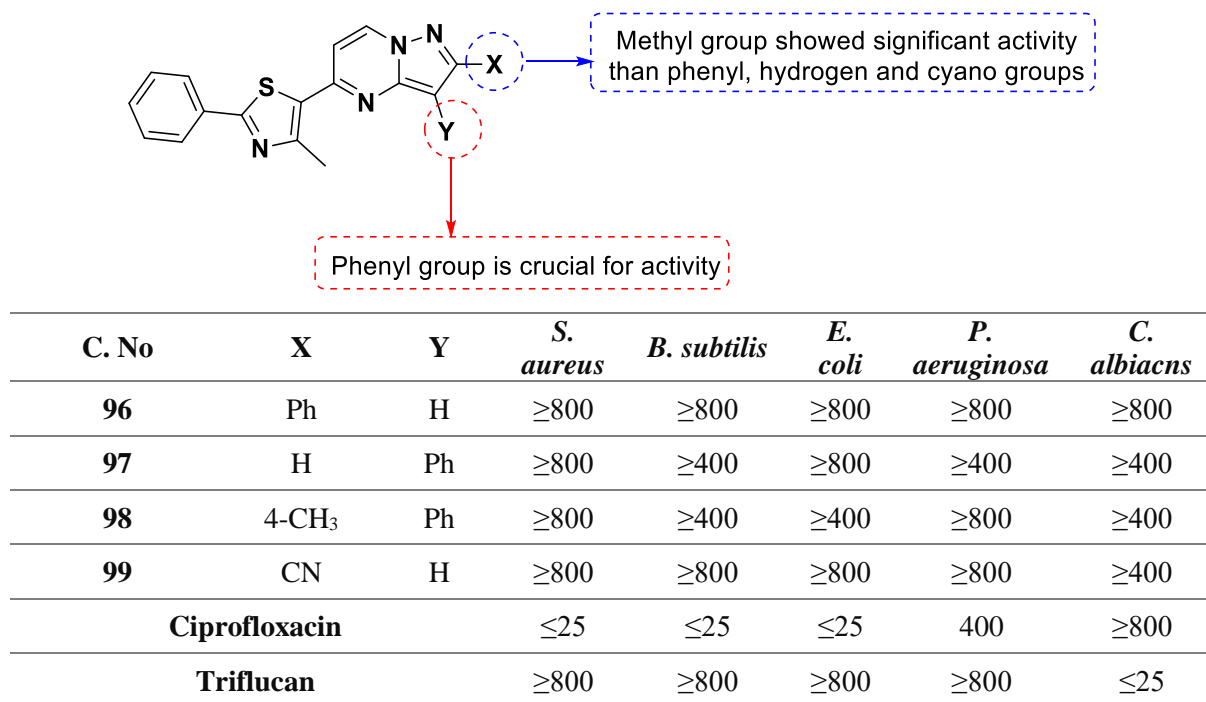
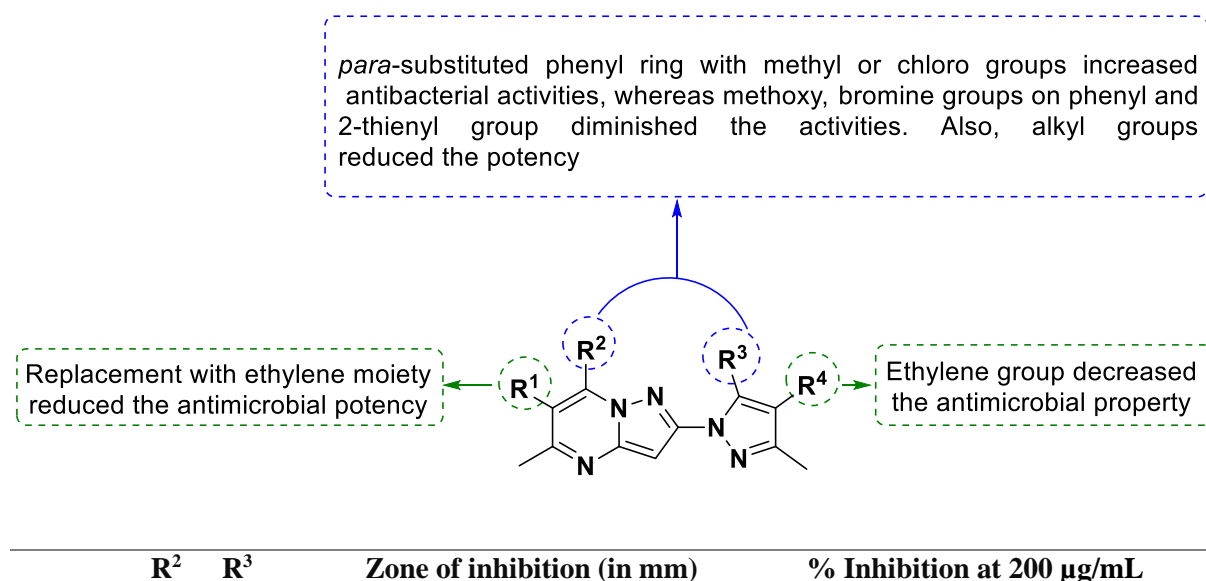


Fig. 46. Structures and MIC values of pyrazolo[1,5-*a*]pyrimidines against different bacterial and fungal strains.

In 2011, Aggarwal et al. synthesized pyrazol-1-ylpyrazolo[1,5-*a*]pyrimidines regioselectively. All the synthesized molecules were tested for antimicrobial properties against two gram positive and gram negative bacterial strains along with four phytopathogenic fungi. Among the screened molecules, compound **100** and **101** exhibited maximum antibacterial potency on par with standard drugs, gentamycin and linezolid. Compound **102** displayed potent antifungal activity (200 mg/mL) than the standard drugs gentamycin, linezolid and mancozeb. SAR study on this series has been presented in **Fig. 47** [97].

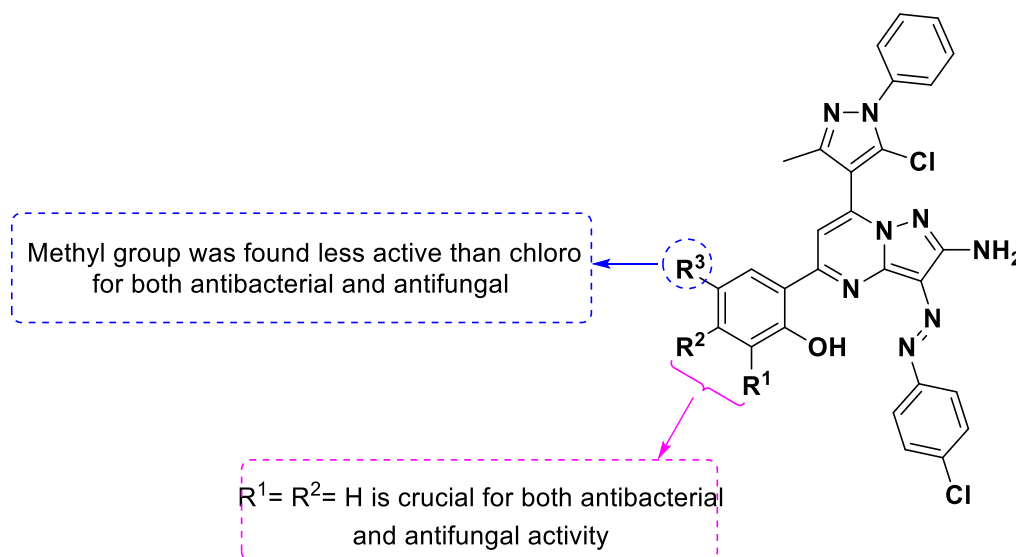


C. No	R ¹	R ⁴	Gram negative bacteria		Gram positive bacteria		<i>A. terreus</i>	<i>A. alternata</i>	<i>F. oxysporum</i>	<i>Helminthosporium</i> sp.	
			<i>E. coli</i>	<i>P. aeruginosa</i>	<i>S. aureus</i>	<i>B. cereus</i>					
100	H	4-CH ₃ -C ₆ H ₄ -	H	10.5	8	8	8.5	ND	ND	ND	ND
101	H	4-Cl-C ₆ H ₄ -	H	13	10	9	13	12.5	0	16.3	36.6
102	H	CH ₃ CH ₃	H	7	7	7	7	73.2	73.1	71.9	79.2
Gentamycin				24	12	14	14	ND	ND	ND	ND
Linezolid				12	8.5	18	10	ND	ND	ND	ND
Mancozeb				ND	ND	ND	ND	76.40	65.90	81.11	70.00

ND: Not determined.

Fig. 47. SAR and antimicrobial results of pyrazolo[1,5-*a*]pyrimidines.

In the same year, Shaikh et al. reported an eco-friendly green synthesis and *in vitro* antimicrobial screening studies for pyrazolo[1,5-*a*]pyrimidine compounds. Of the evaluated compounds, **103-105** exhibited maximum inhibition against *E. coli*, while **106** and its analog **107** showed good activity against *A. niger*. The structures of the active compounds with screening results and SAR studies are disclosed in **Fig. 48** [98].



C. No	R ₁	R ₂	R ₃	Zone of inhibition (in mm)							
				Bacterial strains				Fungal strains			
				<i>E. coli</i>	<i>B. subtilis</i>	<i>S. aureus</i>	<i>S. typhi</i>	<i>A. niger</i>	<i>A. flavus</i>	<i>C. albicans</i>	<i>P. chrysogenum</i>
103	H	H	Cl	18	12	15	15	20	NA	11	13
104	I	H	Cl	17	15	18	16	26	21	19	17

105	Br	CH ₃	Cl	19	NA	10	30	14	17	15	16
106	Cl	H	Cl	26	16	NA	24	18	21	17	24
107	H	CH ₃	Cl	16	18	14	NA	16	10	20	19

NA: No activity.

Fig. 48. Structures and antimicrobial results of pyrazolo[1,5-*a*]pyrimidines.

In 2013, Al-Adiwish et al. synthesized derivatives of pyrazolo[1,5-*a*]pyrimidine, pyrazolo[5,1-*c*][1,2,4]triazine and evaluated for their antibacterial and cytotoxicity properties. Further, these compounds were screened against a panel of two gram positive and three gram negative bacterial strains. The prepared compounds exhibited moderate to low antibacterial activity than the standard drugs (chloramphenicol and streptomycin). All the compounds were demonstrated to be non-cytotoxic to Vero cells. **Fig. 49** illustrates the SAR, highly active structures (**108-110**) and MIC values of evaluated compounds [99].

Presence of piperidine group increased antibacterial activity than pyrrolidine and morpholine groups

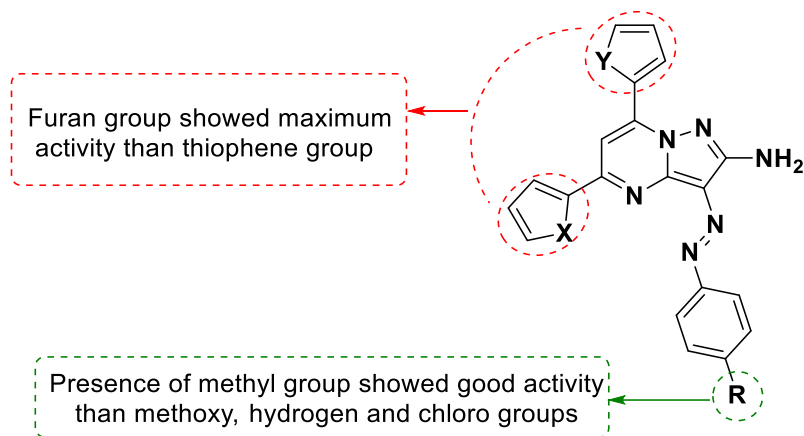
C. No	R	R ¹	R ²	R ³	Gram positive bacteria		Gram negative bacteria		
					Zone of inhibition (in mm)		Zone of inhibition (in mm)		
					<i>B. subtilis</i>	<i>S. aureus</i>	<i>E. coli</i>	<i>P. aeruginosa</i>	<i>S. marcescens</i>
108	NH ₂	CN	SCH ₃		10 ± 0.57	11 ± 0.57	10 ± 0.55	7 ± 1.15	7 ± 1.00
109	CH ₃	H	OH		10 ± 0.58	12 ± 0.58	11 ± 0.58	7 ± 0.00	7 ± 1.15
110	CH ₃	H	CH ₃		9 ± 0.58	9 ± 0.55	10 ± 0.57	7 ± 0.57	6 ± 0.00
Chloramphenicol					25 ± 0.28	25 ± 0.28	NT	NT	NT
Streptomycin					NT	NT	13 ± 0.58	14 ± 0.57	20 ± 0.57

NT: Not tested.

Fig. 49. SAR, antibacterial activity of pyrazolo[1,5-*a*]pyrimidines.

Chapter 2

In the same year, Ishak et al. reported the synthesis and antimicrobial screening of pyrazolo[1,5-*a*]pyrimidine derivatives. Of the thirteen derivatives synthesized, six compounds were evaluated for both antibacterial and antifungal activities. Among the screened derivatives, compounds **111-113** showed potent activity comparable to that of standard drugs. **Fig. 50** represents the structures, zone of inhibition (values) of active compounds and reference drugs along with SAR studies [31].

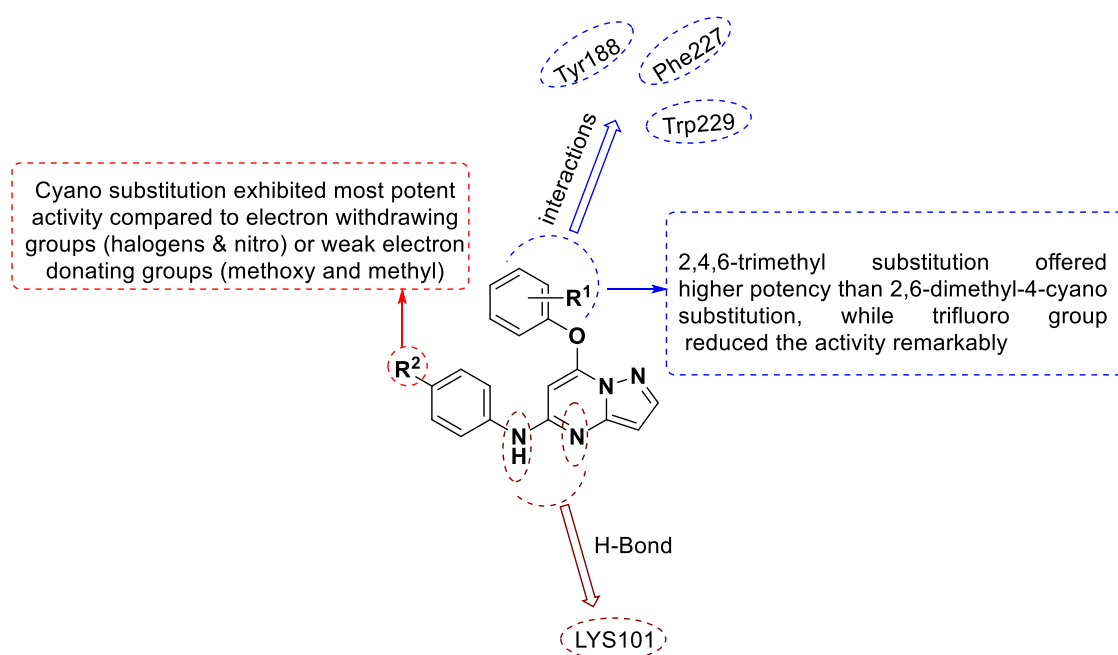


C. No	R	X	Y	Zone of inhibition (in mm)							
				Bacterial strains				Fungal strains			
				<i>S. aureus</i>	<i>B. subtilis</i>	<i>P. aeruginosa</i>	<i>E. coli</i>	<i>A. fumigatus</i>	<i>G. candidum</i>	<i>C. albicans</i>	<i>S. racemosum</i>
111	H	S	S	15.3 ± 0.03	17.9 ± 0.09	9.3 ± 0.05	14.9 ± 0.07	15.2 ± 0.08	11.3 ± 0.05	10 ± 0.04	8.2 ± 0.06
112	H	O	O	16.7 ± 0.05	15.7 ± 0.3	NA	15.2 ± 0.2	14.2 ± 0.09	15.3 ± 0.3	NA	10.2 ± 0.06
113	CH ₃	O	O	22.2 ± 0.09	23.3 ± 0.2	18.5 ± 0.08	21.9 ± 0.1	21.8 ± 0.2	19.5 ± 0.08	18.1 ± 0.3	14.8 ± 0.09
Pencillin G				30.1 ± 0.06	31.6 ± 0.05	28.3 ± 0.08	33.1 ± 0.09	ND	ND	ND	ND
Streptomycin				28.1 ± 0.07	29.7 ± 0.06	25.2 ± 0.09	29.7 ± 0.09	ND	ND	ND	ND
Itraconazole				ND	ND	ND	ND	27.4 ± 0.05	24.2 ± 0.09	25.2 ± 0.07	23.9 ± 0.04
Clotrimazole				ND	ND	ND	ND	26.3 ± 0.08	23.2 ± 0.03	20.8 ± 0.02	21.4 ± 0.05

NA: No activity; ND: Not determined.

Fig. 50. SAR and antimicrobial studies of pyrazolo[1,5-*a*]pyrimidines.

Recently in 2014, Tian et al. reported the synthesis and medicinal properties of new pyrazolo[1,5-*a*]pyrimidines as HIV-1 non-nucleoside reverse transcriptase inhibitors (NNRTIs). Within the evaluated derivatives, compound **114** was found to be the most potent inhibitor with an EC₅₀ of 0.07 μM against wild-type HIV-1 with high selectivity index (SI, 3999). Moreover, **114** was determined as an effective NNRTI than the standard drugs (nevirapine and delavirdine). Authors also performed HIV-1 RT inhibitory assay for compound **114**, which showed an IC₅₀ of 2.26 μM. The SAR and anti-HIV evaluation results of active compound are given in **Fig. 51** [29].



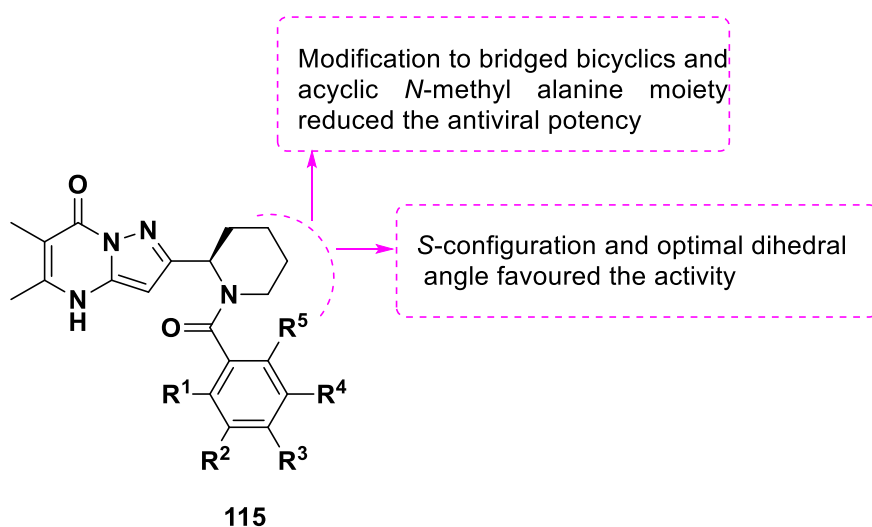
C. No	R ¹	R ²	EC ₅₀ (μM)			SI		RT inhibition (μM)
			HIV-1 IIB	HIV-2 ROD	CC ₅₀ (μM)	HIV-1 IIB	HIV-2 ROD	
114	2,4,6-Trimethyl	4-CN	0.07 ± 0.01	>276	276 ± 53.7	3999	<1	2.26
	Nevirapine		0.07 ± 0.06	NA	>14.99	>89	NA	ND
	Delavirdine		0.16 ± 0.15	NA	>43.81	>277	NA	ND

ND: Not determined; NA: No activity.

Fig. 51. SAR and activity data of active compounds.

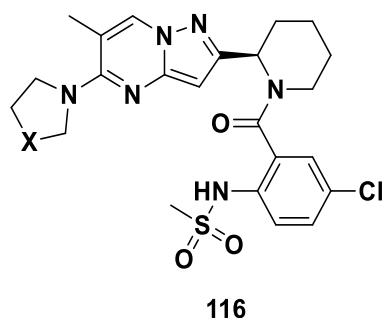
Recently (2015) Mackman et al. discovered new pyrazolo[1,5-*a*]pyrimidine derivatives as orally bio-available respiratory syncytial virus (RSV) fusion inhibitor through hit-to-lead optimization campaign. Authors conducted phenotypic screen using HEp-2 cells infected with RSV A2 virus on a library of ~4,00,000 molecules and identified compound **115** as a lead antiviral molecule (EC₅₀ = 65 nM) for

optimization. Further, X-ray crystallography of **115** confirmed the *S*-configuration in which 2-heteroaryl functional group on piperidine ring positioned into an axial alignment with a dihedral angle of 95°. The pharmacokinetic study of **115** indicated the poor passive permeability and oral bioavailability as depicted in **Fig. 52a**. Hence, pyrazolo[1,5-*a*]pyrimidin-2-yl C-5 *N*-linked pyrrolidine and azetidine analogues were developed to obtain a potent compound with enhanced permeability or efflux properties. Among the evaluated derivatives, compound **116** displayed higher potency with favourable properties as illustrated in **Fig. 52b**. Apart from pharmacokinetic studies, authors also investigated *in vivo* preclinical (cotton rat model) and clinical evaluation of **116** that demonstrated antiviral efficacy in a dose-dependent manner [100].



C. No	R ¹	R ²	R ³	R ⁴	R ⁵	RSV EC ₅₀ (nM)	log D	Caco2 AB/BA (× 10 ⁻⁶ cm/s)	% Free human plasma	Fold plasma shift
115	H	NHSO ₂ CH ₃	H	H	H	65	1.3	0.33/2.2	6.5	13

Fig. 52a. SAR and biological studies of a lead compound.



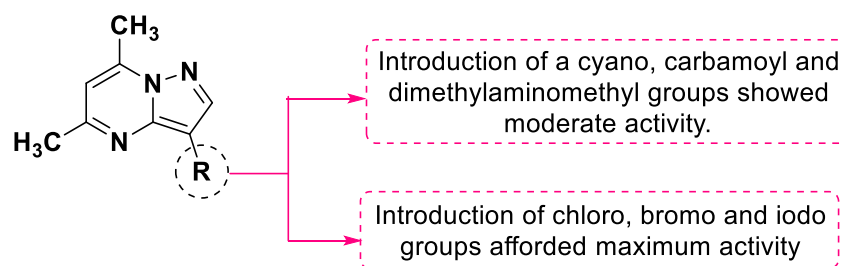
C. No	X	RSV EC ₅₀ (nM)	log D	Caco2 AB/BA (× 10 ⁻⁶ cm/s)	% Free human plasma	MS pred CL human/rat/dog (L/h/kg)	Fold plasma shift	SD rat F %
116	CH-NH ₂ (S)	0.37	2.0	6.4/19	4.4	<0.16/0.26/0.41	22	46

Fig. 52b. Pharmacokinetic properties of potent derivative **116**.

3.4 Anti-inflammatory agents

Inflammation is a beneficial and defensive biological response to tissue damage, infections, toxins or autoimmune injury in order to abolish or limit the blow-out of an injurious agent. The process is a complex phenomenon involving the role of several cellular mediators [101]. Management of inflammatory disorders encompasses usage of drugs or anti-inflammatory agents.

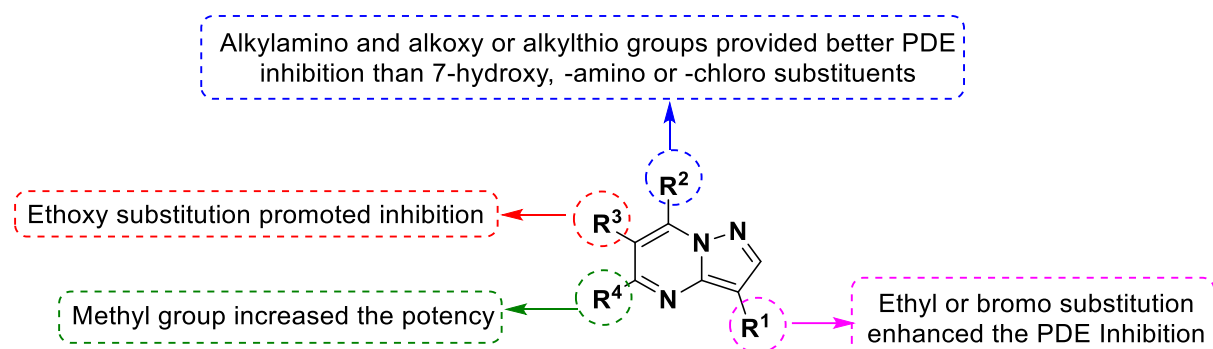
In 1974, Novinson and co-workers reported the synthesis of 3-substituted 5,7-dimethyl pyrazolo[1,5-*a*]pyrimidines and evaluated them against 3,5-cyclic-AMP phosphodiesterase enzyme. Out of the 15 synthesized molecules, compounds **117-120** having halogen (-Br, Cl, I) and acetyl groups at C-3 position were found to be more potent in inhibiting phosphodiesterase enzyme as illustrated in **Fig. 53** [23].



C. No	R	High K_m PDE IC_{50} (nM)		Low K_m PDE IC_{50} (nM)	
		Rabbit kidney	Rabbit lung	Beef heart	Rabbit lung
117	Br	2.20	2.40	1.7	0.7
118	Cl	1.33	3.11	1.7	2.2
119	I	1.23	3.55	1.5	3.5
120	COCH ₃	0.57	1.5	0.4	1.0

Fig. 53. 3,5-cyclic-AMP phosphodiesterase inhibitory abilities of active compounds.

In 1982, Springer et al. synthesized pyrazolo[1,5-*a*]pyrimidines and their related analogs for adenosine cyclic 3',5'-phosphate phosphodiesterase (PDE) inhibition. Of the tested derivatives, **121** and **122** were determined to be potent inhibitors. In the case of ADP-induced platelet aggregation inhibitory studies, **123** was identified as a potent compound. A brief SAR of this series and the activity data of most active compounds is illustrated in **Fig. 54** [102].

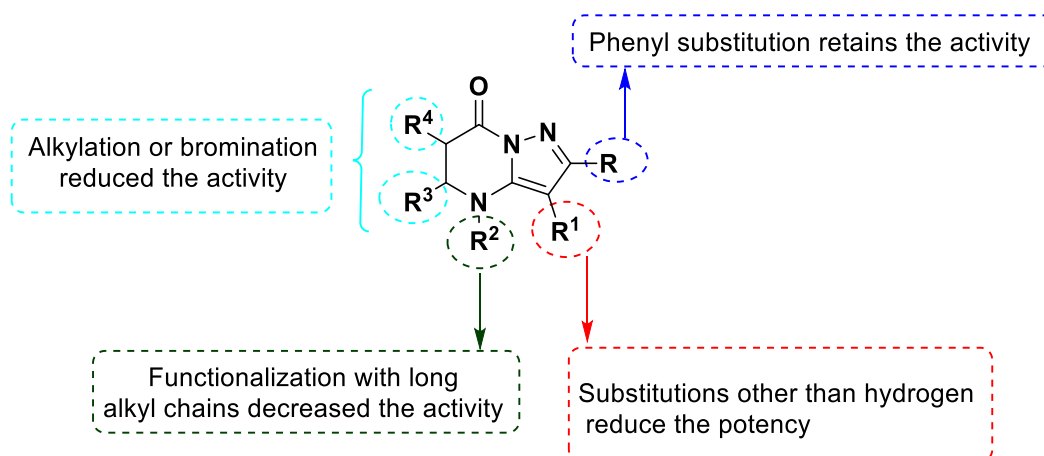


C. No	R ¹	R ²	R ³	R ⁴	PDE Inhibition			Inhibition of ADP-induced platelet Aggregation	
					Lung	Kidney	Heart	Conc.	Inhibition
121	Br	OH	COOC ₂ H ₅	H	0.5	1.0	NA	50	34
122	H	NHCH ₂ CH ₂ OH	H	CH ₃	0.5	NA	3.7	NA	NA
123	Br	NH ₂	COOC ₂ H ₅	H	NA	NA	NA	25	67

NA: No activity.

Fig. 54. SAR and 3',5'-phosphate phosphodiesterase inhibitor studies of substituted pyrazolo[1,5-*a*]pyrimidines.

In 1983, Auzzi et al. synthesized 2-phenylpyrazolo[1,5-*a*]pyrimidin-7-ones and explored their antipyretic and anti-inflammatory properties. While deriving a relationship between chemical structure and anti-inflammatory potential, authors further synthesized some more derivatives with modifications of an elongated side chain at the C-4 position. Among the tested derivatives, compound **124** [4-ethyl-5,6-dihydro-2-phenylpyrazolo[1,5-*a*]pyrimidine-7-one] exhibited potent anti-inflammatory and moderate antiulcer activity. **Fig. 55** illustrates a brief SAR and activity profile of compound **124** [103].

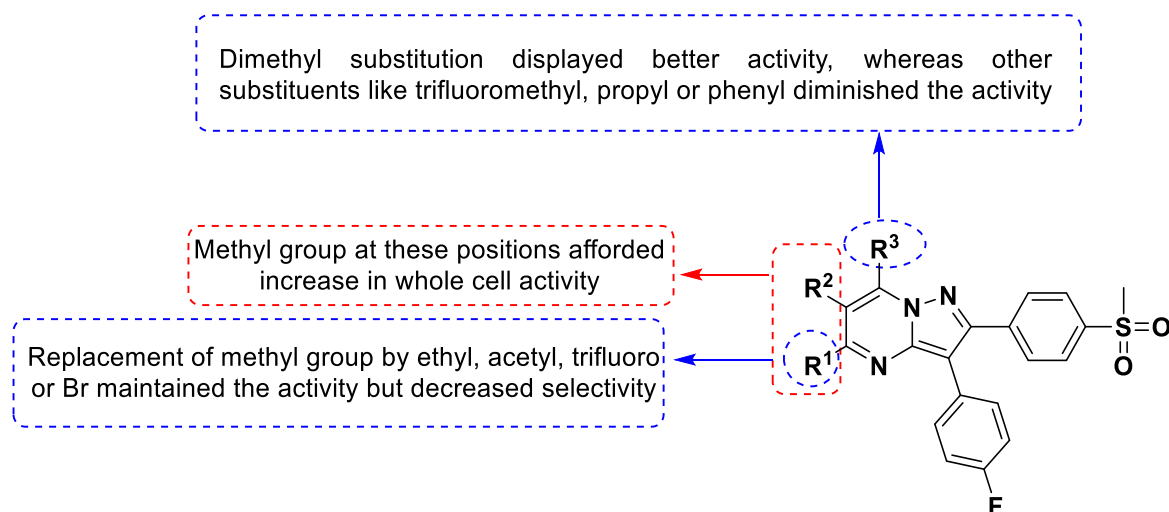


R	R ¹	R ²	R ³	R ⁴	Anti-inflammatory activity
---	----------------	----------------	----------------	----------------	----------------------------

C. No						Dose (mg)	% reduction of edema, 3 h	ED ₅₀ mg/kg
						10	54.1 ± 4.9	
124	Ph	H	C ₂ H ₅	H	H	25	69.8 ± 4.1	7.3 (2.4-22.1)
						100	90.1 ± 2.6	

Fig. 55. SAR and anti-inflammatory properties of 2-phenylpyrazolo[1,5-*a*]pyrimidin-7-ones.

In 2001, Almansa et al. reported the synthesis and anti-inflammatory evaluation of a series of bicyclic pyrazolo[1,5-*a*]pyrimidines. Authors performed *in vitro* COX-1 and COX-2 enzyme inhibition assay and *in vivo* (carrageenan-induced paw edema, air-pouch model) studies. From this series, compound **125** exhibited potent and selective COX-2 inhibition. The SAR and pharmacological data of the potent molecule **125** are presented in **Fig. 56** [24].

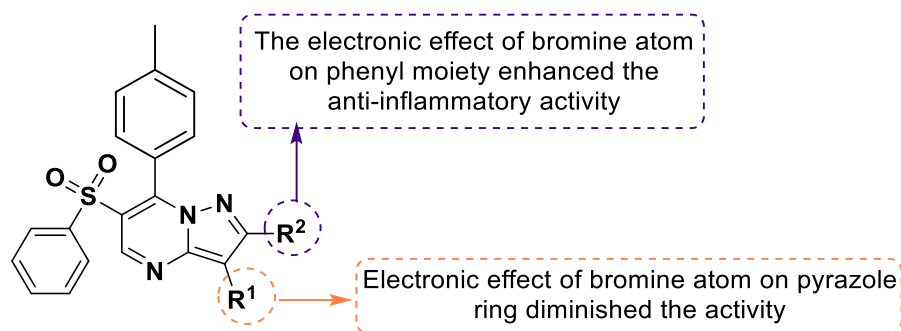


C. No	R ¹	R ²	R ³	% Inh HWB		IC ₅₀ Whole Cell	
				COX-1	COX-2	COX-1	COX-2
				10 (μM)	10 (μM)	(μM)	(μM)
125	H	CH ₃	CH ₃	47.5	96.4	>10	0.012

Fig. 56. SAR and the data of potent molecule.

In 2008, Shaaban et al. synthesized pyrazolo[1,5-*a*]pyrimidines, pyrimido[1,2-*a*]benzimidazole and triazolo[1,5-*a*]pyrimidine ring systems and evaluated all the synthesized compounds for the analgesic and anti-inflammatory properties. Compounds **126** [2-(4-bromophenyl)-6-(phenylsulphonyl)-7-(4-methylphenyl)-pyrazolo[1,5-*a*]pyrimidine] and **127** [3-bromo-2-phenyl-6-(phenylsulphonyl)-7-(4-methylphenyl)-pyrazolo[1,5-*a*]pyrimidine] were reported as potent anti-inflammatory as well as analgesic agents. SAR study demonstrated that the other scaffolds exhibited lower activity as compared to pyrazolo[1,5-*a*]pyrimidine system. Among the series, bromine substituent on pyrazole moiety **127**

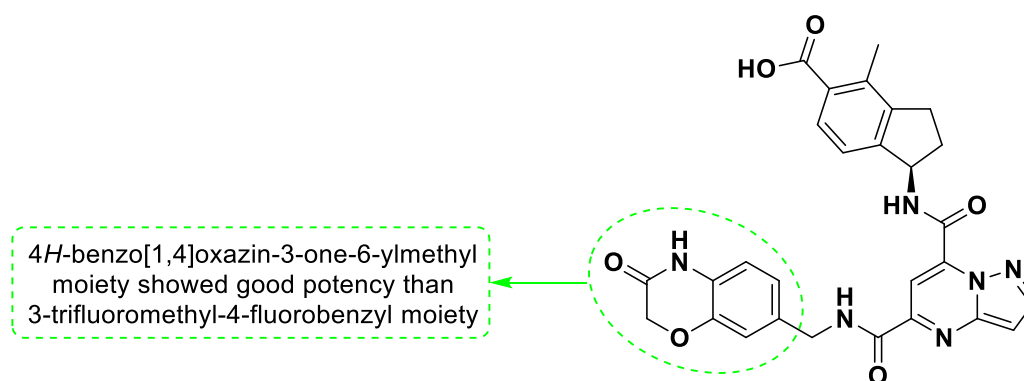
enhanced the analgesic effect. In compound **126**, the electronic influence of bromine on aryl ring over pyrazole exhibited higher anti-inflammatory activity. The pharmacological evaluation results and SAR of active compounds are given in **Fig. 57** [104].



C. No	R ¹	R ²	Anti-inflammatory profile						Analgesic profile		
			% edema inhibition						Number of writhing		
			1h	2h	3h	4h	5h	6h	30 min	% Change	Potency
126	H	4-Br-C ₆ H ₄	74.1	72.6	69.2	26.6	31.7	54.3	29.5 ± 1.4	65.2	0.76
127	Br	Ph	65.5	61.0	54.8	12.5	0	6.6	12.2 ± 1.1	85.6	0.99

Fig. 57. Pharmacological evaluation results of active compounds.

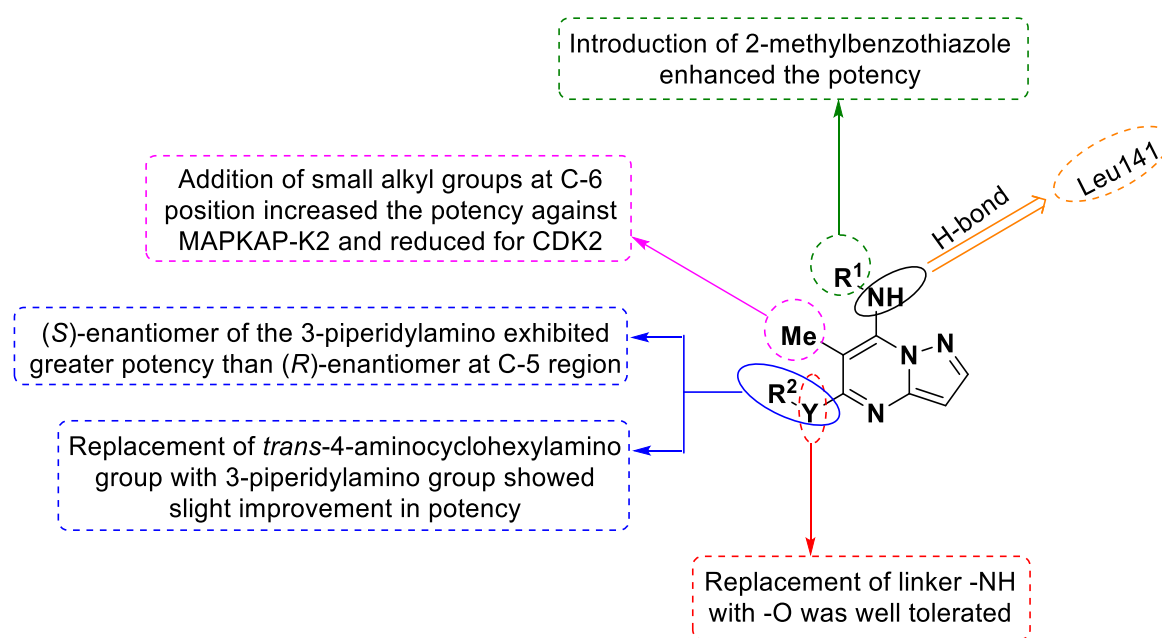
In 2012, Gege et al. discovered non-Zn chelating, selective matrix metalloproteinase 13 (MMP-13) inhibitors for the cure of osteoarthritis. Of the synthesized molecules, compound **128** was considered as intra-articular disease modifying osteoarthritic drug (IA-DMOAD). Further, it had a favourable pharmacokinetic profile which minimized the total exposure. Insignificant levels of the constituent were noticed in the plasma resulting 1 mg/kg (IV route) or 0.5 mg/kg (IA route) administration to rats. Moreover, derivative **128** exhibited good *ex vivo* and *in vitro* efficacy, effectively blocking collagen degradation in a dose-dependent manner with an IC₅₀ of 20 nM as depicted in **Fig. 58**. This study concluded that **128** possess long permanency in joints, penetrates cartilage efficiently with no measurable systemic exposure and has significant efficacy [105].



C. No	IC ₅₀ (nM) vs. catalytic domain										
	MMP -1	MMP -2	MM P-3	MMP -7	MM P-8	MMP -9	MM P-12	MM P-13	MMP -14	TAC E	Agg 1
12	>2000	>2000	8200	>2000	3200	>2000	655	0.03	>2000	>2000	240
8	0	0	8200	0	3200	0	655	0.03	0	0	0

Fig. 58. Selectivity and potency of compound **128** towards MMP-13.

In 2012, Kosugi et al. reported the synthesis of 5,6,7-trisubstituted pyrazolo[1,5-*a*]pyrimidines and evaluated their biological properties as mitogen-activated protein kinase-activated protein kinase-2 (MAPKAP K-2) inhibitors. SAR studies were performed to optimize highly potent and selective analogues and revealed that substitution at C-6 position was necessary to enhance the activity as depicted in **Fig. 59**. All the synthesized derivatives exhibited good activity and compounds **129-131** were most potent [47].

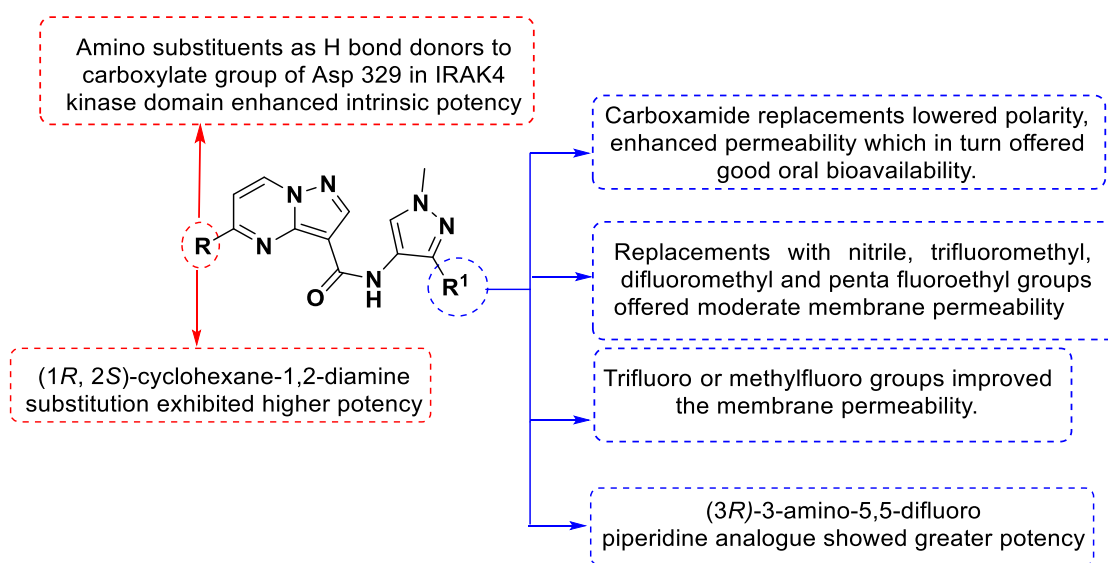


C. No	R ¹	Y-R ²	MAPKAP-K2	CDK2	Selectivity CDK2/ MAPKAP-K2
			IC ₅₀ (μM)	IC ₅₀ (μM)	
129			0.054	25	463
130			0.057	21	368

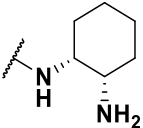
131			0.076	27	355
-----	--	--	-------	----	-----

Fig. 59. SAR, MAPKAP-K2 kinase and CDK2 selectivity values of 5,6,7-trisubstituted pyrimidines.

Recently (2015), Lim et al. developed a methodology for the synthesis of 5-amino-*N*-(1*H*-pyrazol-4-yl)pyrazolo[1,5-*a*]pyrimidine-3-carboxamides as Interleukin-1 receptor associated kinase 4 (IRAK4) inhibitors. Initially, authors identified compound **132** as a lead molecule through high-throughput screening (HTS) campaign. Encouraging results of compound **132** with an IC₅₀ value of 110 nM and high ligand binding efficiency (LBE) of 0.44 encouraged the authors to further explore the pyrazolo[1,5-*a*]pyrimidine scaffold as inhibitors to IRAK4, which is a remarkable target for many inflammatory diseases. A library of pyrazolopyrimidines bearing amine substitutions at the 5-position of the ring followed by carboxamide replacement and finally diamino substitutions at the 5th position to obtain potent inhibitor **133** was generated. Robust PK/PD response in the R848-induced rat model was reported for compound **134**. Molecular modelling guided SAR studies and pharmacological evaluation including cell potencies, kinase selectivities, and pharmacokinetic profiles are given in **Fig. 60** [106].



C. No	R	R ¹	IRAK4 IC ₅₀ (nM)	cLogD	Polar surface area (Å ²)	Cell permeability (Papp)
132	H	CONH ₂	110	1.7	127	17
133		-CHF ₂	< 0.5	-2.8	ND	30

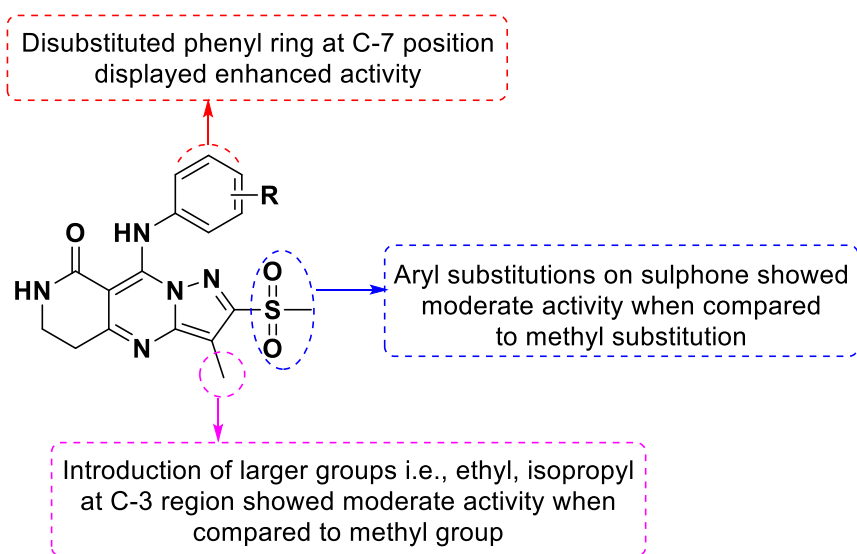
134		- CONH ₂	0.3	-4.3	152	2
-----	---	------------------------	-----	------	-----	---

ND: Not determined.

C. No	hPBMC IC ₅₀ (nM)	rWB IC ₅₀ (nM)	No. of kinases tested	% of kinases	rat Cl _p (mL min ⁻¹ kg ⁻¹)	rat %F
133	12	81	101	> 95	46	42
134	31	300	264	99	56	0

Fig. 60. SAR and IRAK4 inhibitory, pharmacokinetic activities of pyrazolo[1,5-*a*]pyrimidine-3-carboxamide derivatives.

In 2016, Roux and co-workers reported novel substituted pyrazolo[1,5-*a*]pyrimidines and evaluated them as potent phosphodiesterase-4 (PDE4) inhibitors. These tested molecules showed moderate to high activity against PDE4. Among all, compounds **135** and **136** revealed 200 fold improvement in both activity and cellular potency. SAR was performed to optimize the potent molecules as PDE-4 inhibitors and is illustrated in **Fig. 61** [107].



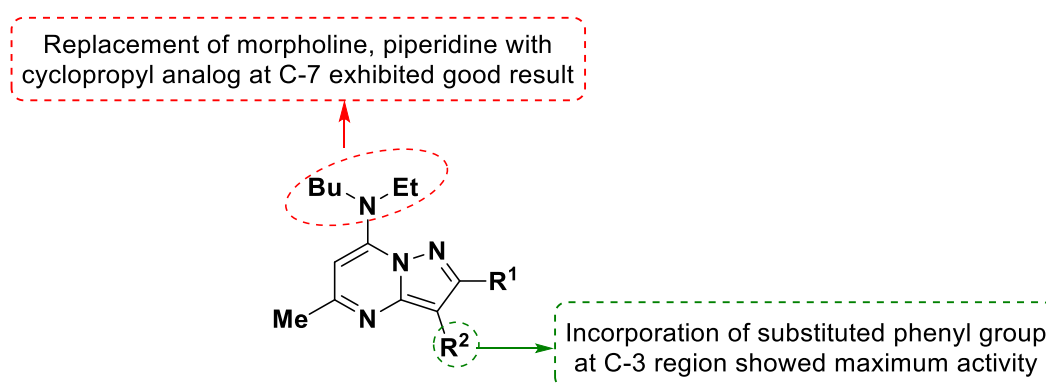
C. No	R	PDE4B1 IC ₅₀ (nM)
135	3-OCH ₃	0.1
136	3,5-Cl	0.03

Fig. 61. SAR and PDE4 inhibitory studies.

3.5 CRF-1 receptor antagonists

Corticotropin-releasing factor (CRF) is a 41-amino-acid neuropeptide produced in the paraventricular nucleus of the hypothalamus and released in response to stress and pain [108]. CRF binds to CRF receptors in the anterior pituitary, resulting in release of adrenocorticotrophic hormone (ACTH) [109,110].

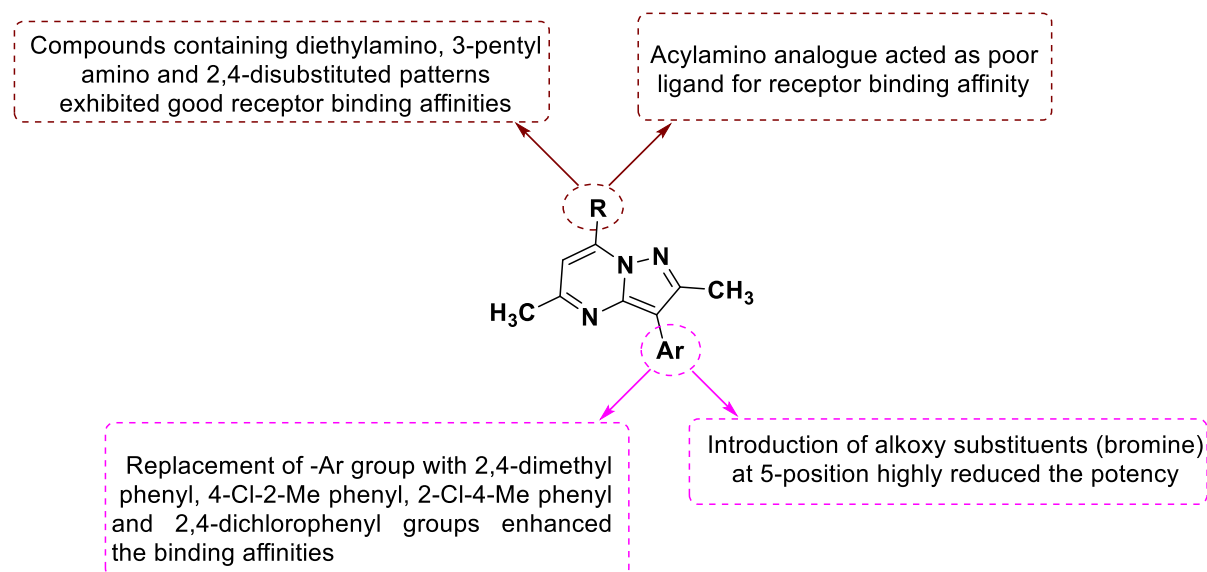
In 1998, Wustrow et al. reported the synthesis, X-ray crystallography studies and evaluation of pyrazolo[1,5-*a*]pyrimidines for their binding affinity towards human CRF-1 receptor. SAR and X-ray crystallographic studies revealed the extension of the 3-phenyl ring and alkyl group on 7-position of the amino substituent are essential for CRF binding affinity as illustrated in **Fig. 62**. Among the series, compound **137** was identified as essential CRF inhibitor with high affinity [111].



C. No	R	R ¹	R ²	CRF ₁ Binding (K _i nM)
137	Ethyl	Butyl	2,4-Dichlorophenyl	5

Fig. 62. CRF binding affinity studies of pyrazolo[1,5-*a*]pyrimidine derivative.

In 2000, Gilligan et al. discovered a series of novel pyrazolo[1,5-*a*]pyrimidines as corticotropin-releasing factor (hCRF₁) antagonists. In this series, compounds **138-140** demonstrated good hCRF₁ activity. Results of their work concluded that compound **140** showed good anxiety efficacy in the dog (0.3 mg/kg). The results of key intravenous (iv) pharmacokinetic parameters ($t_{1/2}$, CL and $V_{d,ss}$) and a brief SAR study are depicted in **Fig. 63** [112].



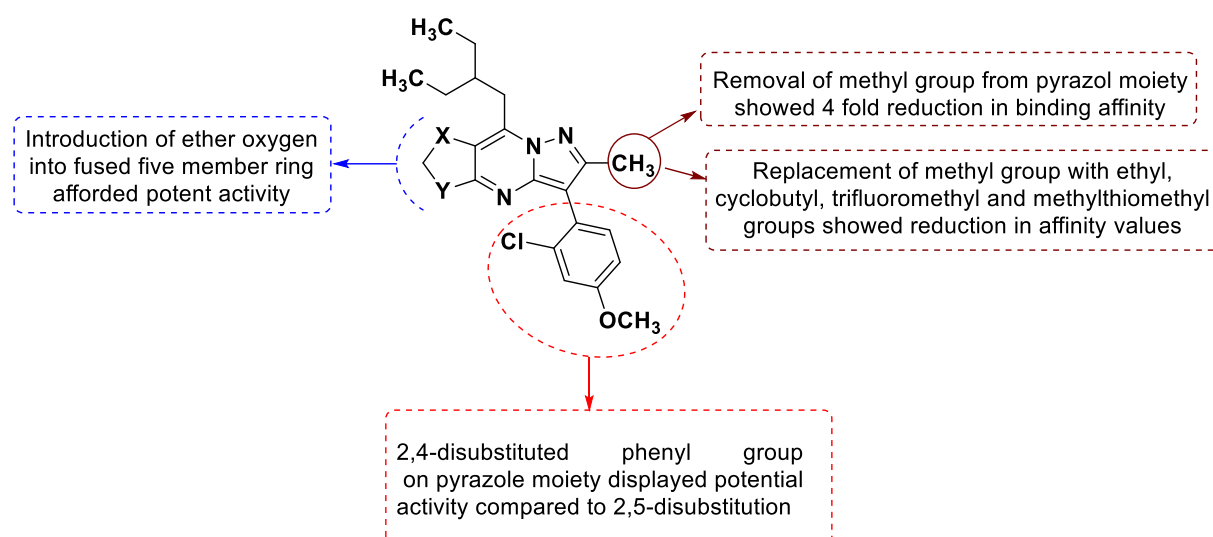
C. No	R	Ar	Mean hCRF ₁ K _i (nM)
138	NH-3-pentyl	2-CH ₃ -4-ClPh	1.7 ± 0.9
139	NH-3-pentyl	2-Cl-4-CH ₃ Ph	1.5 ± 1.0
140	NH-3-pentyl	2-Me-4-CH ₃ OPh	1.0 ± 0.2

Parameter	iv (intravenous)	po (peroral)
<i>t</i> _{1/2} (h)	46.4 ± 7.6	45.1 ± 10.2
CL (L/h/kg)	049 ± 0.08	NA
V _{d,ss} (L/kg)	23.0 ± 4.2	NA

NA: No activity

Fig. 63. SAR and single dose pharmacokinetic data of pyrazolo[1,5-*a*]pyrimidines.

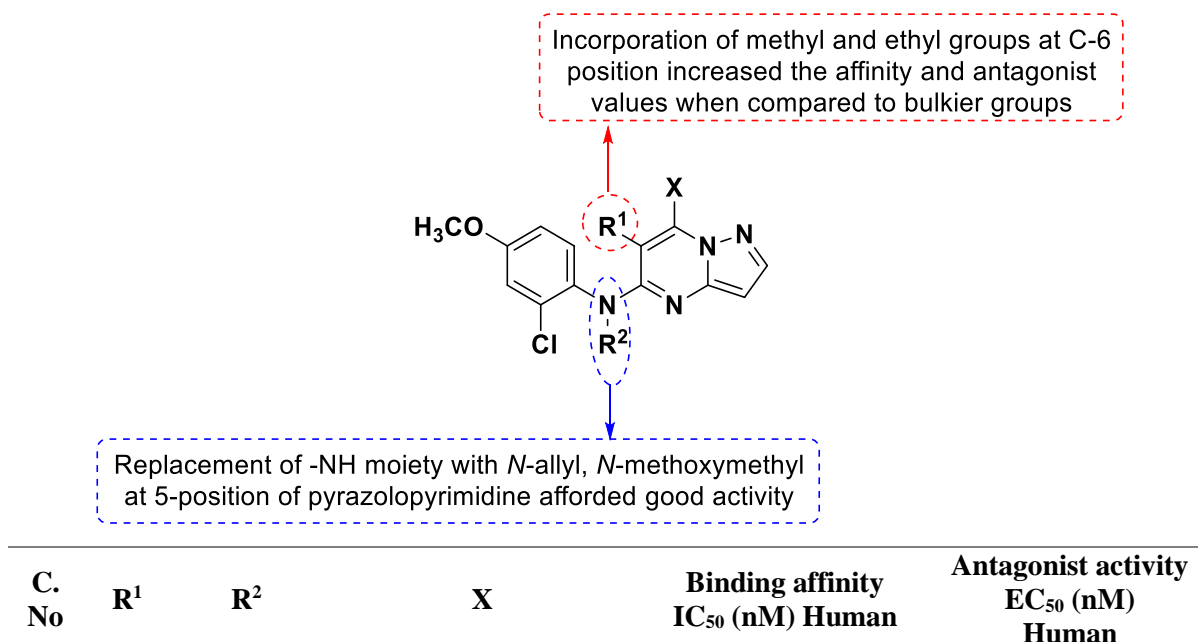
In 2011, Saito and co-workers discovered 6,7-dihydro-5*H*-cyclopenta[*d*]pyrazolo[1,5-*a*]pyrimidines as novel CRF₁ antagonists. SAR studies revealed the role of different functional groups on the moiety, which is presented in **Fig. 64**. Among the synthesized compounds, **141-143** exhibited both binding affinities and potent antagonist activity. Later, pharmacokinetic studies were carried out in a rat model and it was concluded that compound **141** was orally effective CRF₁ antagonist [30].



C. No	X	Y	Binding affinity IC ₅₀ (nM)	Antagonist activity EC ₅₀ (nM)
			Human	Human
141	H	H	4	40
142	O	H	7	4
143	H	O	84	8

Fig. 64. SAR and CRF₁ affinity studies of pyrazolo[1,5-*a*]pyrimidines.

In the same year, the same research group reported the synthesis of pyrazolo[1,5-*a*]pyrimidines and triazolo[1,5-*a*]pyrimidines as novel CRF₁ receptor antagonists. SAR studies revealed that the significant activity was afforded by changing substitutions at C-5 and C-7 positions as depicted in **Fig. 65**. Among the series, compounds **144-147** showed potent results for binding affinity and antagonist activity [113].



C. No	R ¹	R ²	X	Binding affinity IC ₅₀ (nM) Human	Antagonist activity EC ₅₀ (nM) Human
-------	----------------	----------------	---	--	---

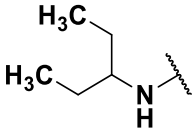
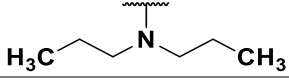
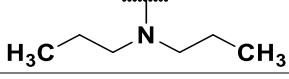
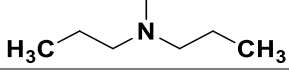
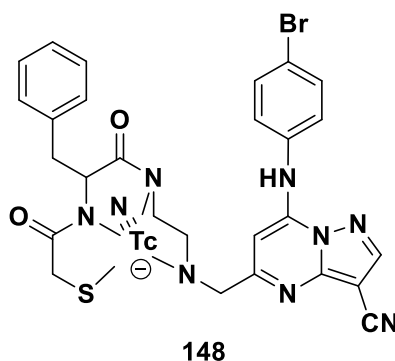
144	CH ₃	H		7.4	7.4
145	CH ₃	H		8	4
146	C ₂ H ₅	H		4.2	8.6
147	H	CH ₂ OCH ₃		15	4.4

Fig. 65. CRF₁ binding affinity and antagonist studies of pyrazolo[1,5-*a*]pyrimidines.

3.6 Radiopharmaceuticals

In 2010, Ding et al. reported the synthesis and medicinal valuation of pyrazolo[1,5-*a*] pyrimidines as imaging agents for tumors. Initially, authors synthesized 5-((2-aminoethylamino)methyl)-7-(4-bromoanilino)-3-cyanopyrazolo[1,5-*a*]pyrimidine (ABCPP) and conjugated the compound with *N*-mercaptoacetyl glycine (MAG), MAF (*N*-mercaptoacetyl-phenylalanine) and *N*-mercaptoacetylvaline (MAA). All the conjugates were radiolabelled with isotope [^{99m}TcN]²⁺ and studied for their bio-distribution towards tumor-bearing mice. Of the evaluated complexes, *N*-mercaptoacetyl glycine tagged compound exhibited maximum favorable tumor/muscle ratios, tumor/blood ratios reaching 2.97 and 1.51 at thirty minute post-injection. Structure and bio-distribution results are presented in **Fig. 66** for the favourable complex ^{99m}TcN-MAG-ABCPP (**148**) [114].



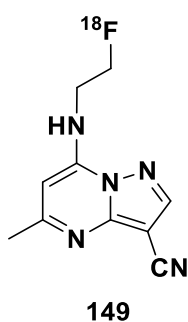
C. No	Tissue	5 min	30 min	60 min	120 min
148	Heart	0.93 ± 0.11	0.32 ± 0.06	0.35 ± 0.02	0.37 ± 0.08
	Blood	2.38 ± 0.17	0.77 ± 0.01	0.46 ± 0.04	0.38 ± 0.01
	Spleen	19.90 ± 1.70	14.38 ± 1.64	8.16 ± 0.10	8.32 ± 1.05
	Stomach	0.69 ± 0.12	0.54 ± 0.11	0.32 ± 0.04	0.09 ± 0.02
	Kidney	11.08 ± 1.13	5.06 ± 1.16	3.58 ± 0.21	3.35 ± 0.29

Liver	23.32 ± 1.32	23.88 ± 2.83	14.67 ± 0.87	12.84 ± 0.91
Muscle	0.72 ± 0.05	0.39 ± 0.08	0.34 ± 0.07	0.22 ± 0.03
Small Intestine	8.82 ± 1.29	3.42 ± 0.42	0.64 ± 0.08	0.62 ± 0.15
Large Intestine	1.62 ± 0.20	0.62 ± 0.08	0.68 ± 0.02	0.67 ± 0.06
Tumor	1.23 ± 0.13	1.16 ± 0.14	0.86 ± 0.14	0.45 ± 0.07
Bone	1.25 ± 0.74	0.95 ± 0.27	0.73 ± 0.28	0.86 ± 0.09
Brain	0.13 ± 0.01	0.04 ± 0.004	0.08 ± 0.01	0.07 ± 0.01
Lung	4.53 ± 0.99	2.30 ± 0.60	0.86 ± 0.07	0.73 ± 0.41
*T/B ratio	0.52	1.51	1.84	1.17
§T/M ratio	1.71	2.97	2.49	2.01

§T/M: tumor-to-muscle; *T/B: tumor-to-blood; All data are the mean percentage (n = 3) of the injected dose per gram of tissue, ±: the standard deviation of the mean.

Fig. 66. Structure and bio-distribution of $^{99m}\text{TcN-MAG-ABCPP}$ in mice bearing S 180 tumor (% ID/g).

In 2011, Xu et al. synthesized 7-(2-[^{18}F]fluoroethylamino)-5-methylpyrazolo[1,5-*a*] pyrimidine-3-carbonitrile ([^{18}F]FEMPPC, [^{18}F]1) and evaluated as positron emission tomography (PET) imaging agents for tumor detection. Initially, authors conducted uptake characteristics of [^{18}F]1 against S180 tumor cells and mice bearing S180 tumor followed by *ex vivo* bio distribution studies and concluded higher features for [^{18}F]1 with respect to the total tracer accumulation and preservation in the tumor. *In vitro* and *in vivo* results suggested that [^{18}F]1 (**149**) could be a favorable PET tracer for tumor detection. The structure and bio-distribution results are presented in **Fig. 67** for [^{18}F]1 (**149**) [115].



C. No	Tissue	5 min	15 min	30 min	60 min	120 min
149	Lung	6.61 ± 0.54	3.79 ± 0.93	3.77 ± 0.31	2.78 ± 0.19	2.54 ± 0.96
	Heart	5.53 ± 0.61	3.57 ± 0.65	4.06 ± 0.09	3.46 ± 0.78	2.59 ± 0.18
	Spleen	4.66 ± 0.26	3.42 ± 0.52	3.43 ± 0.39	2.82 ± 0.31	2.15 ± 0.94
	Brain	3.17 ± 0.48	2.70 ± 0.07	2.47 ± 0.24	1.93 ± 0.25	1.79 ± 0.27
	Blood	4.83 ± 0.45	4.65 ± 0.05	4.49 ± 0.31	3.63 ± 0.33	2.95 ± 0.30

Chapter 2

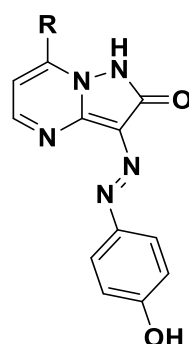
Kidney	7.93 ± 1.27	5.04 ± 0.48	3.28 ± 0.20	2.58 ± 0.16	1.92 ± 0.40
Tumor	1.88 ± 0.63	4.37 ± 0.30	5.51 ± 0.31	2.95 ± 0.36	2.88 ± 0.34
Muscle	3.99 ± 1.05	3.84 ± 0.45	3.05 ± 0.22	2.31 ± 0.48	2.64 ± 0.60
Liver	6.99 ± 1.00	4.02 ± 0.20	3.17 ± 0.16	2.45 ± 0.30	1.84 ± 0.22
T/muscle ratio	0.47	1.14	1.81	1.28	1.09
T/Blood ratio	0.39	0.94	1.23	0.81	0.98
T/brain ratio	0.59	1.62	2.23	1.53	1.61

Fig. 67. Structure and bio-distribution in mice bearing S180 for [^{18}F]1 expressed as % injected dose per gram.

3.7 Organic dyes

Dyes are coloured substances having affinity to the substrate being applied on. They usually possess chromophoric groups and have a conjugated system [116].

Al-Etaibi et al. in 2011 synthesized dyes consisting of pyrazolo[1,5-*a*]pyrimidine moiety and applied those dyes to polyester fibers employing high temperature method using microwave as heating source. Results of the study indicated that the dyed fabrics demonstrated reasonable light fastness and good washing fastness characteristics. Structures of dyes (150-153) and the results are given in **Fig. 68** [117].

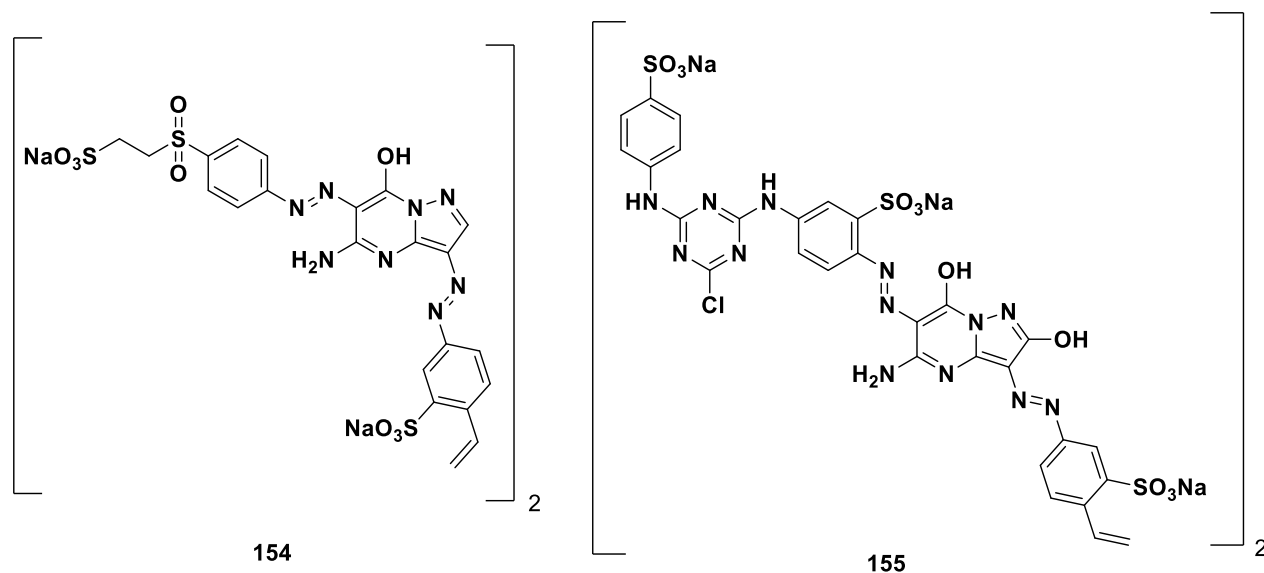


C. No.	R	Wash Fastness			Light fastness
		(4 % o.m.f. dyeing)			
		Ψ Alt	*SC	Δ SW	
150	Ph	5	5	5	2
151	4-Cl-Ph	5	5	5	2
152	-Fur-2-yl	4	5	4	2
153	-Thien-2-yl	4-5	4-5	4-5	2

ISO CO2/CO41; Ψ Alt: alteration; *SC: staining on cotton; Δ SW: staining on wool; o.m.f: mass of fabric.

Fig. 68. Organic dye properties of synthesized compounds.

In 2014, Kamel et al. prepared bifunctional bis-sulphatoethylsulphone (**154**) and bis-monochlorotriazine (**155**) reactive dyes bearing pyrazolo[1,5-*a*]pyrimidine as a basic nucleus. Authors tested the synthesized dyes for their behavior on cotton, wool and silk fabrics. The results of this study indicated maximum fixation values and level of exhaustion for the dyes and the dyed fabrics exhibited nice light fastness, good rubbing, washing and perspiration fastness. The chemical structure of dyes and the study results at 4% shade are depicted in **Fig. 69** [118].



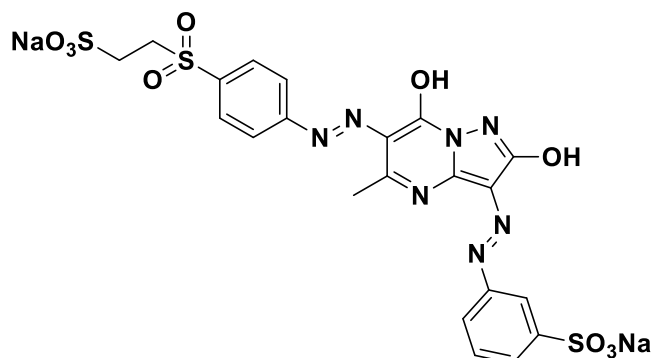
C. No	Dyed samples	K/S	Fastness to rubbing		Wash Fastness			Fastness to perspiration						Light	
			Wet	Dry	ΨAlt	*SC	ΔSW	Alkaline			Acidic				
								Alt	SC	SW	Alt	SC	SW		
154	C	12.5 1	4-5	5	5	4-5	4-5	5	4-5	5	4-5	5	4-5	5	4-5
	W	20.4 5	5	4-5	4-5	5	4-5	5	4-5	5	5	5	5	5	5-6
	S	15.9 5	5	5	5	5	5	4-5	5	5	4-5	5	4-5	4-5	4-5
155	C	14.7 1	5	5	5	5	5	4-5	5	4-5	4-5	5	4-5	4-5	6
	W	26.8 5	4-5	4-5	4-5	4-5	4-5	4-5	4-5	4-5	5	4-5	4-5	4-5	5-6
	S	16.3 5	4-5	4-5	4-5	4-5	4-5	5	4-5	5	5	4-5	5	5	6

ΨAlt: alteration; *SC: staining on cotton; ΔSW: staining on wool; K/S: color strength.

Fig. 69. Dye properties of bis-sulphatoethylsulphone and bis-monochlorotriazine containing pyrazolo[1,5-*a*]pyrimidines.

Moreover, the same research group reported the synthesis of heterocyclic reactive dyes based on disazo pyrazolopyrimidine analogs possessing a sulfatoethylsulfone reactive group and applied to cotton, wool

and silk fabrics. Their research findings evidenced that the dyed fabrics manifested notable light fastness, good rubbing, washing and perspiration fastness. The chemical structure of representative dye **156** and its fastness properties as well as colour yields on the test fabrics are given in **Fig. 70** [119]

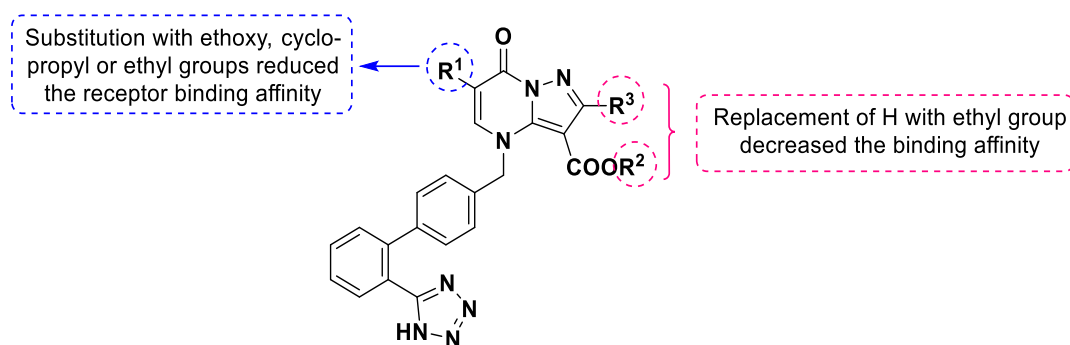


C. No	Shade (%)	Sample dyed	K/S	Fastness to rubbing		Wash fastness		Fastness to perspiration					Light	
				Wet	Dry	Acidic	Alkaline	Alkaline			Acidic			
								Al	S	S	Al	S		S
								t	C	W	t	C	W	
156		C	1.93	4-5	4-5	4-5	5	5	5	4-5	5	4-5	4-5	3-4
	2	W	13.19	4-5	4-5	5	4-5	4-5	4-5	5	4-5	4-5	5	6
		S	4.44	4-5	4-5	5	4-5	5	5	5	5	4-5	5	5-6
		C	4.12	4-5	4-5	5	4-5	5	5	4-5	4-5	4-5	5	2-3
	4	W	18.99	5	5	4-5	5	5	5	4-5	5	4-5	5	5-6
		S	6.35	5	5	5	5	4-5	4-5	5	5	5	4-5	2-3

Fig. 70. Dye properties of the representative compound.

3.8 Miscellaneous agents

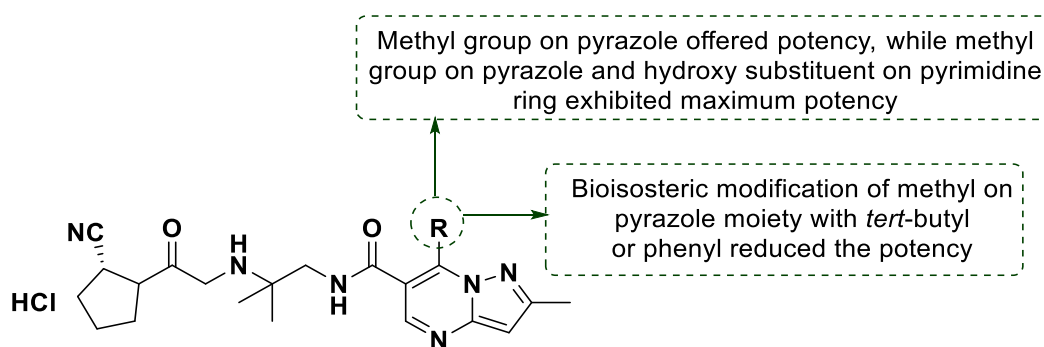
In 1995, Kiyama et al. reported the synthesis and evaluation of pyrazolo[1,5-*a*]pyrimidine derivatives as non-peptide angiotensin II receptor antagonists. Among the evaluated compounds, derivative **157** decreased the mean blood pressure by more than 30 mmHg from the normal at a dose of 1 mg/kg by intravenous administration spontaneously to hypertensive rats. **Fig. 71** illustrates the SAR studies and the structures of active compounds (**158** and **159**) in the angiotensin II receptor binding assay [120].



C. No	R ¹	R ²	R ³	Receptor Assay (K _i nM)	
				Human	Rat
157	<i>n</i> -Propyl	H	H	0.68	2.5
158	<i>n</i> -Pentyl	H	H	0.36	3.4
159	<i>n</i> -Butyl	H	H	0.85	2.5

Fig. 71. SAR and the binding affinity of active compounds towards angiotensin II receptors.

In 2011, Kato et al. discovered a series of pyrazolo[1,5-*a*]pyrimidine derivatives as novel Dipeptidyl peptidase-IV (DPP-IV) inhibitors. Among the series, compounds **159-161** were discovered as potent DPP-IV inhibitors. Pharmacokinetics studies revealed compound **159** exhibited metabolic stability and well balanced elimination. SAR, pharmacological and selected pharmacokinetic data are presented in **Fig. 72** [35].

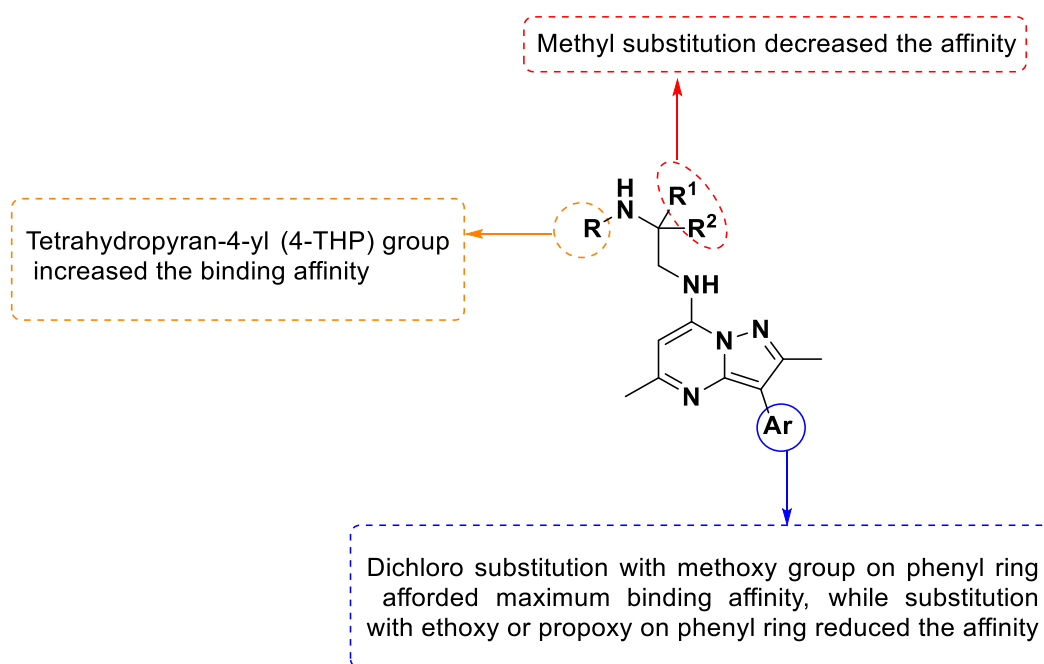


C. No	R	IC ₅₀ (nM)			Serum Protein binding (%) 20 hg/mL			Metabolic activity [CL'int (l/h/kg)]		
		DPP-IV	DPP-8	DPP-9	Rat	Dog	Human	Rat	Dog	Human
159	H	3.8	68	60	77.3	64.8	29.2	1.4	0.1	0.3
160	CH ₃	13	76	64	22.1	22.5	18.9	NA	NA	NA
161	OH	1.8	58	45	NA	NA	NA	NA	NA	NA

NA: No activity.

Fig. 72. SAR, pharmacological and selected pharmacokinetic data of active compounds.

In the same year (2011), Griffith et al. discovered and synthesized pyrazolo[1,5-*a*]pyrimidine derivatives as neuropeptide Y1 receptor (an anti-obesity drug target) antagonists. Authors prepared thirteen new final compounds and evaluated (*in vitro*) using human Y1R radioligand binding assay. Within the series, compound **162** was discovered as a potent antagonist with the binding affinity value of 1 nM with comparatively active compound **163**. Further, compound **162** inhibited NPY-induced rises in blood pressure (BP) and food intake after intravenous and intracerebroventricular administration in an animal model. In feeding behavioural studies of **162**, modest inhibitions of food intake were reported in several lean rodent models. SAR, binding affinity and selected pharmacokinetic data are demonstrated in **Fig. 73** [121].

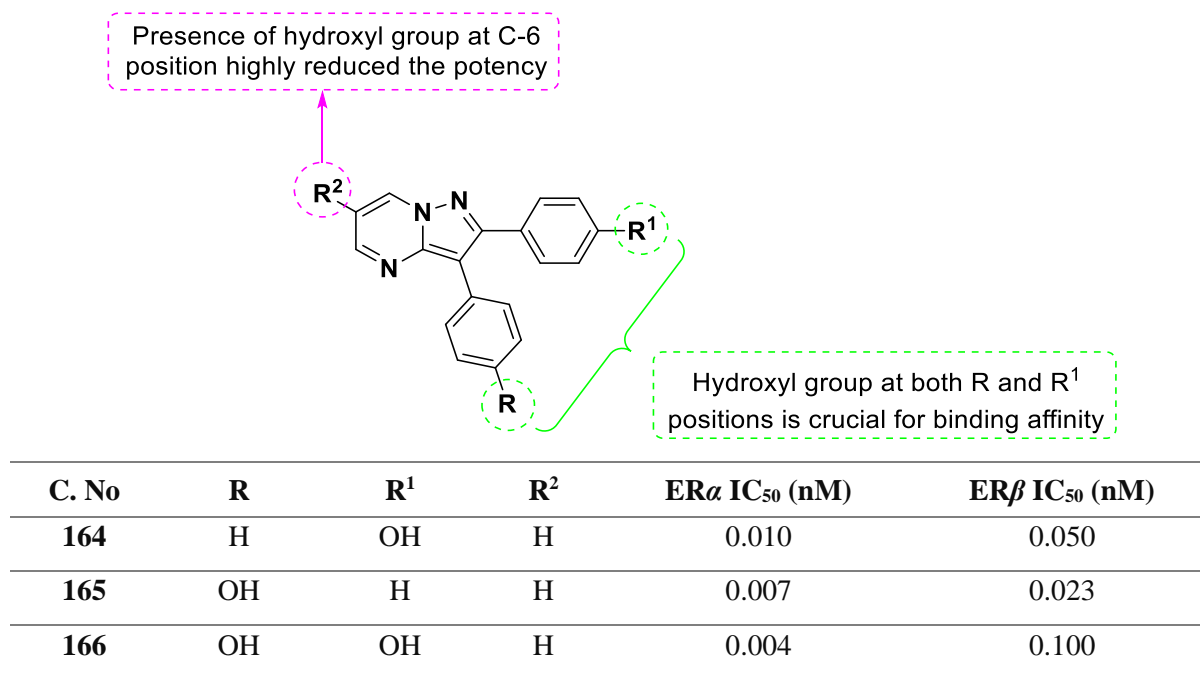


C. No	Ar	R ¹ , R ²	R	<i>cE</i> log <i>D</i>	^v <i>K</i> _i (nM)	Rat Clp (mL/min/kg)	Rat fu,p	Rat Clp, u (mL/min/kg)	NPY pressor response (% inh at 3 mg/kg iv)
162	2,6-Cl-4-CH ₃ O-Ph	H,H	tetrahydropyran-4-yl	2.6	1	45	0.059	763	92
163	2,6-Cl-4-C ₂ H ₅ O-Ph	H,H	tetrahydropyran-4-yl	2.8	3	28	0.029	996	47

^v*K*_i: Human Y1R radioligand binding assay; Rat Clp: Rat plasma clearance; Rat fu,p: Rat functional potency; Rat Clp, u: Rat plasma clearance, unbound clearance; iv: intra venous.

Fig. 73. SAR, binding affinity and selected pharmacokinetic data of potent inhibitors.

In 2004, Campton and co-workers discovered and optimized the pyrazolo[1,5-*a*]pyrimidines as estrogen receptor (ER) ligands. Among those, compounds **164-166** exhibited promising binding affinities for ER α and ER β . The optimized SAR studies revealed that incorporation of –OH group on the structure resulted in low affinity values at C-6 as shown in **Fig. 74**, which indicated that ligand core was attached to the ER in a reverse mode and served as isostere of the A-ring of estradiol [48].

**Fig. 74.** Estrogen receptor ligands bearing pyrazolo[1,5-*a*]pyrimidine scaffold.

In 2015, Hassan and co-workers synthesized pyrazolo[1,5-*a*]pyrimidine derivatives by reacting 5-amino-*N*-aryl-1*H*-pyrazoles with acetylacetone and 2-(4-methoxybenzylidene)-malononitrile. All the synthesized compounds were tested against Ehrlich ascites carcinoma (EAC) cell line for their *in vitro* cytotoxic activity. Among those, compounds **167** and **168** displayed potential activity when compared to doxorubicin as a reference drug. A brief SAR study has been presented in **Fig. 75** [32].

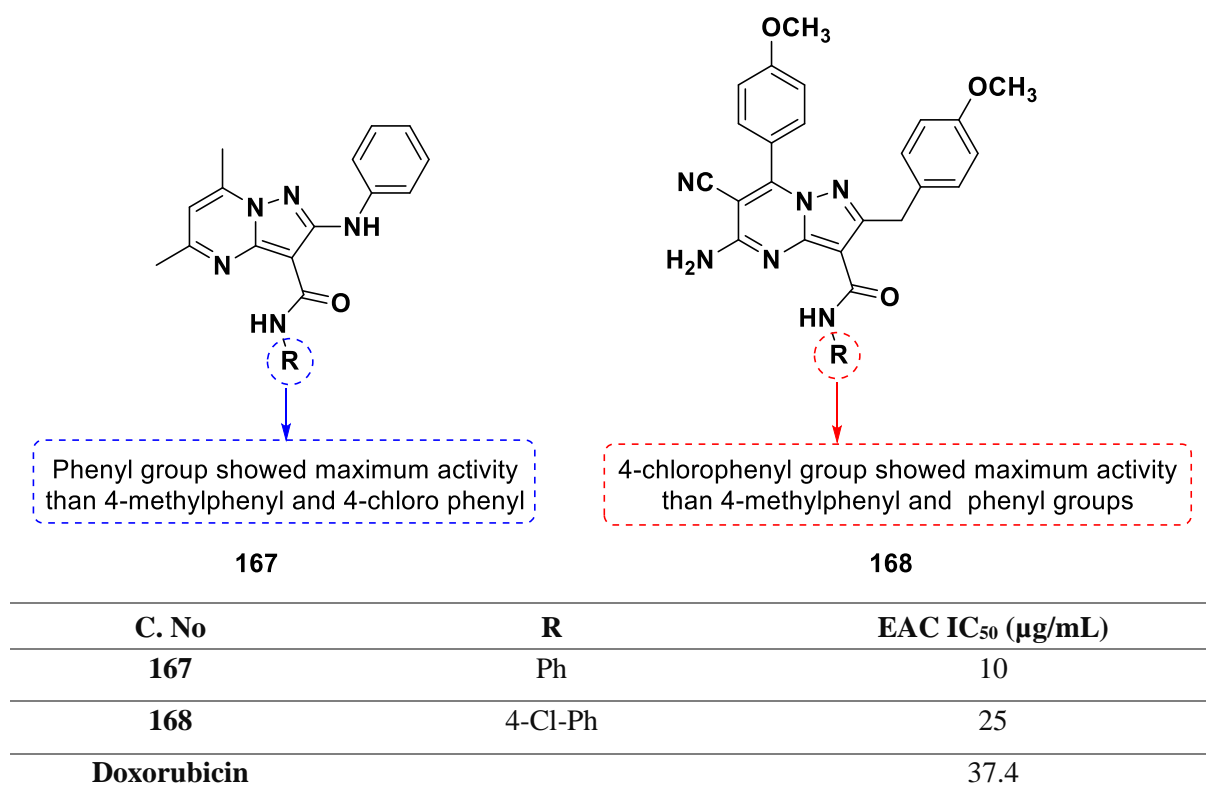
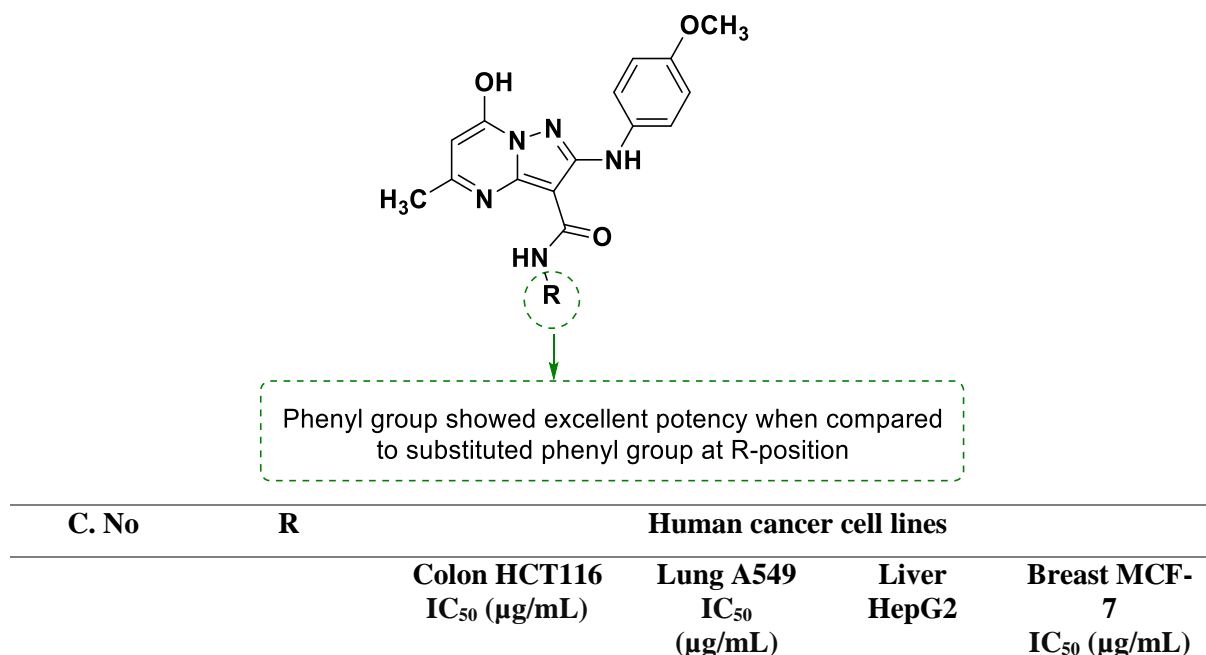


Fig. 75. Cytotoxicity studies of pyrazolo[1,5-*a*]pyrimidines with reference drug doxorubicin.

In 2015, the same above mentioned authors (Hassan and co-workers) reported the synthesis and *in vitro* cytotoxic activities of 7-hydroxy-5-methyl-*N*-(aryl)pyrazolo[1,5-*a*] pyrimidines. All the synthesized compounds were tested against four human cancer cell lines (lung A549, liver HepG, colon HCT116 and breast MCF-7). Within the series, compounds **169** and **170** showed significant cytotoxic activities when compared to reference drug doxorubicin. SAR studies have been represented in **Fig. 76** [122].

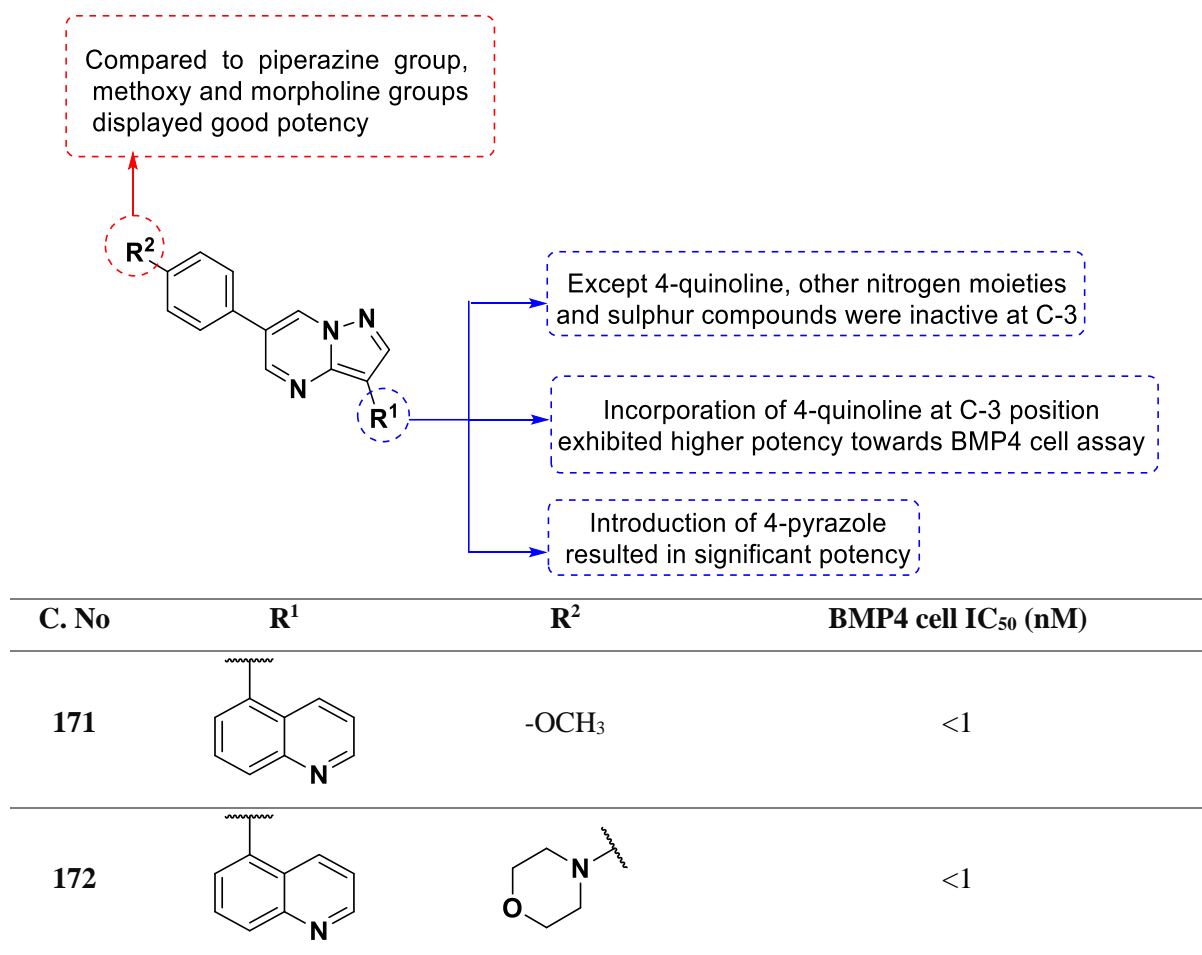


			IC ₅₀ (µg/mL)		
169	Ph	NA	5.00 ± 0.50	4.00 ± 0.44	4.60 ± 0.55
170	4-Cl-C ₆ H ₄	NA	5.45 ± 0.62	6.10 ± 0.62	4.20 ± 0.60
Doxorubicin			6.30 ± 0.60	5.10 ± 0.50	4.20 ± 0.46
				4.20 ± 0.46	4.70 ± 0.55

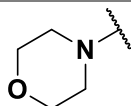
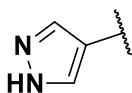
NA: No activity.

Fig. 76. SAR and cytotoxic properties of highly active compounds consisting pyrazolo[1,5-*a*]pyrimidine scaffold.

Engers and co-workers reported the synthesis and pharmacological evaluation of 3,6-disubstituted pyrazolo[1,5-*a*]pyrimidine derivatives as bone morphogenetic protein (BMP) receptors. SAR studies were carried out to determine the active functional groups at C-6, C-3 positions in order to enhance the potency and also carried out comparative studies with known drugs such as dorsomorphin, LDN-193189 and DMH-1 as represented in **Fig. 77**. Among the series, compounds **171-173** exhibited equipotent activity against BMP receptors (BMP4 cell IC₅₀ = <1 nM) [44].



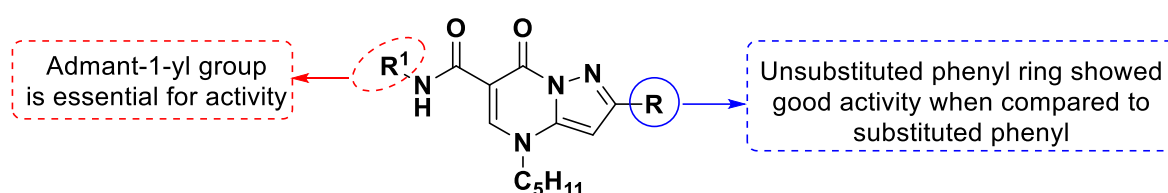
173



<1

Fig. 77. SAR and BMP4 cell line properties of 3,6-difunctionalized pyrazolo[1,5-*a*]pyrimidines.

In 2013, Tabrizi and co-workers reported the synthesis of 7-oxopyrazolo[1,5-*a*]pyrimidine-6-carboxamides and evaluated their pharmacological activity as effective and selective cannabinoid receptor inverse agonists. SAR studies were performed to find out the effective functional groups at C-6 and C-2 positions to achieve potent cannabinoid receptor type-2 (CB₂) receptors. Among the series, compounds **174-177** displayed potent and selective CB₂ receptor affinities as depicted in **Fig. 78** [51].



C. No	R	R ¹	K _i (nM)				
			⁴ rCB ₁	[*] rCB ₂	^ψ hCB ₁	[§] hCB ₂	^φ SI
174	Ph	Adamant-1-yl	> 10000 (40%)	2.74 ± 0.28	>10000 (40%)	2.56 ± 0.22	>3906
175	2-CH ₃ - Ph	Adamant-1-yl	> 10000 (30%)	3.21 ± 0.30	>10000 (22%)	2.86 ± 0.25	>3496
176	4-Cl-Ph	Adamant-1-yl	> 10000 (10%)	4.21 ± 0.42	>10000 (13%)	3.88 ± 0.31	>2577
177	Furan-2- yl	Adamant-1-yl	> 10000 (40%)	5.14 ± 0.42	>10000 (34%)	4.92 ± 0.43	>2032

Here ⁴rCB₁: rat brain for CB₁ receptors; ^{*}rCB₂: rat spleen for CB₂ receptors; ^ψhCB₁: human CB₁ CHO membrane; [§]hCB₂: human CB₂ CHO membrane; ^φSI: selectivity.

Fig. 78. SAR and cannabinoid receptor studies of 7-oxopyrazolo[1,5-*a*]pyrimidine-6-carboxamides.

In 2016, Liu et al. reported the discovery of pyrazolo[1,5-*a*]pyrimidines as threonine tyrosine kinase (TTK) inhibitors. All synthesized molecules were screened against various cancer cell lines. Compound **178** indicated potent activities against all tested cancer cell lines. SAR studies concluded that assimilation of polar, basic and solubilizing groups in the hydrophobic and solvent accessible areas modulated physiochemical assets while maintaining potency, as illustrated in **Fig. 79** [123].

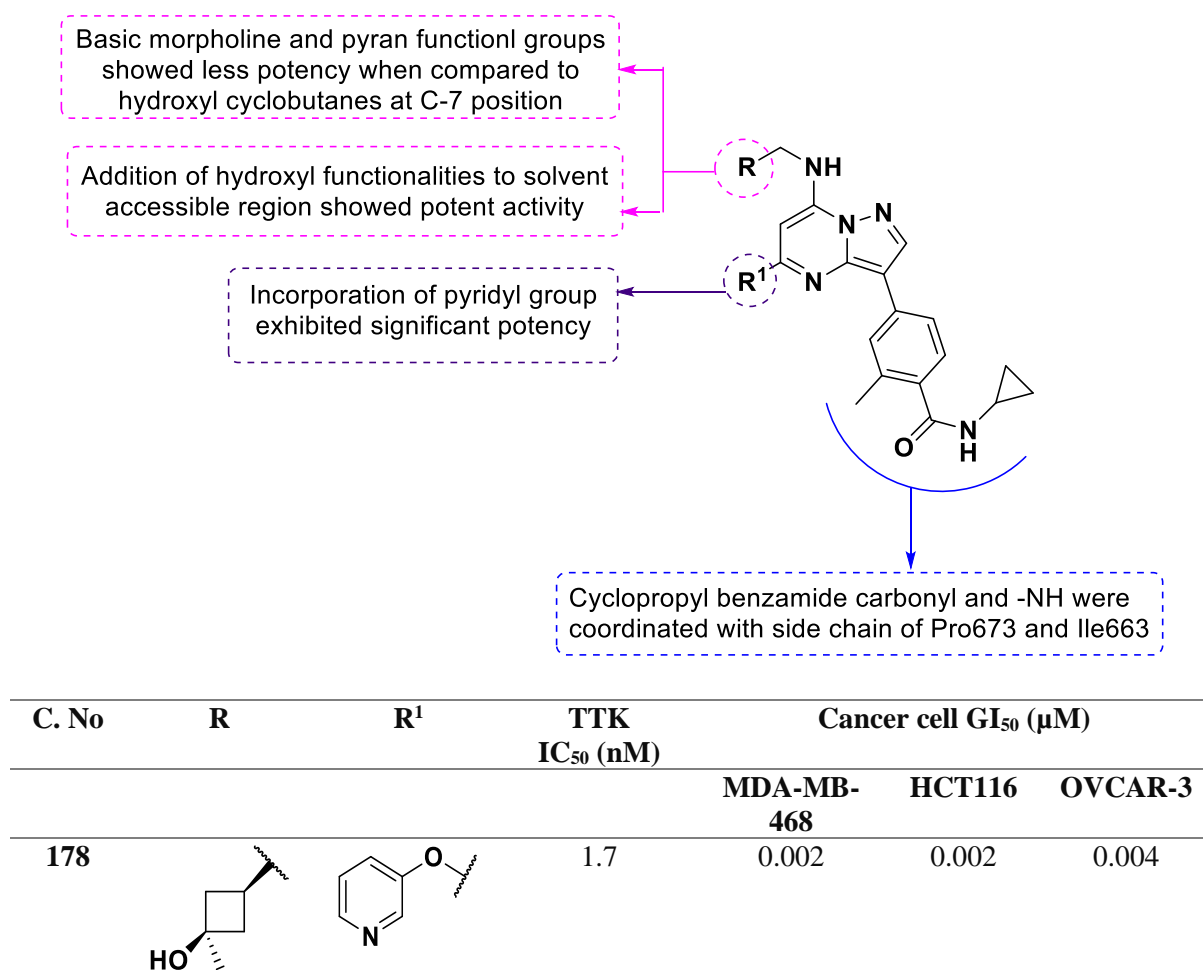


Fig. 79. SAR and TTK activity studies.

3.9 Patents covering pyrazolo[1,5-*a*]pyrimidine nucleus and their target activity

Medicinal importance of pyrazolo[1,5-*a*]pyrimidine scaffold is further evidenced based on numerous patents registered from 1980 to recent past. Various research groups that patented this scaffold for different therapeutic segments are concisely presented in **Table-1**.

Research group	Patent number	Target activity	Year
Dusza	US4626538	Anxiolytic, antiepileptic, sedative-hypnotic agents [9]	1986
Nugent	US005397774A	Anti-inflammatory[124]	1995
Inoue	US005688949A	Anti-inflammatory [125]	1997
Inoue	US005843951A	Analgesic [126]	1998
Levin	US20070219183A1	Cancer [127]	2007
Chen	WO2008036579A1	CRF ₁ receptor antagonists [128]	2008
Andrews	WO2011029027A1	mTOR inhibitors [129]	2011

Zhao	WO2012027239A1	mTOR inhibitors [130]	2012
Marugan	WO2012078855A1	Glucocerebrosidase activators [131]	2012
Bearss	US8710057B2	Protein kinase inhibitors [132]	2014
Ahmad	WO2014089379A9	ATR kinase inhibitors [133]	2014

Table-1. Pyrazolo[1,5-*a*]pyrimidine nucleus containing patents having numerous biological activities.

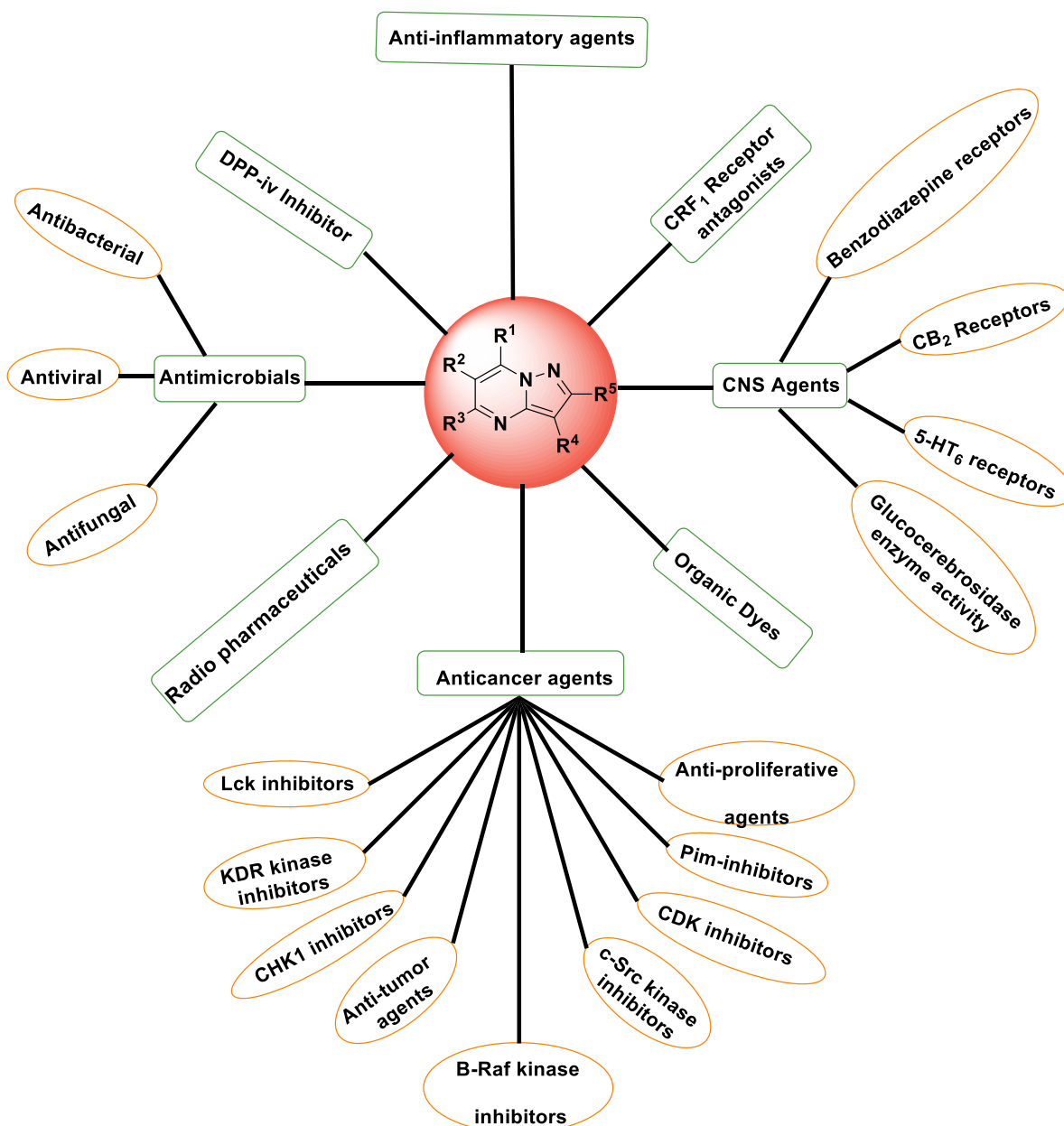


Fig. 80. Biological activities of pyrazolo[1,5-*a*]pyrimidines.

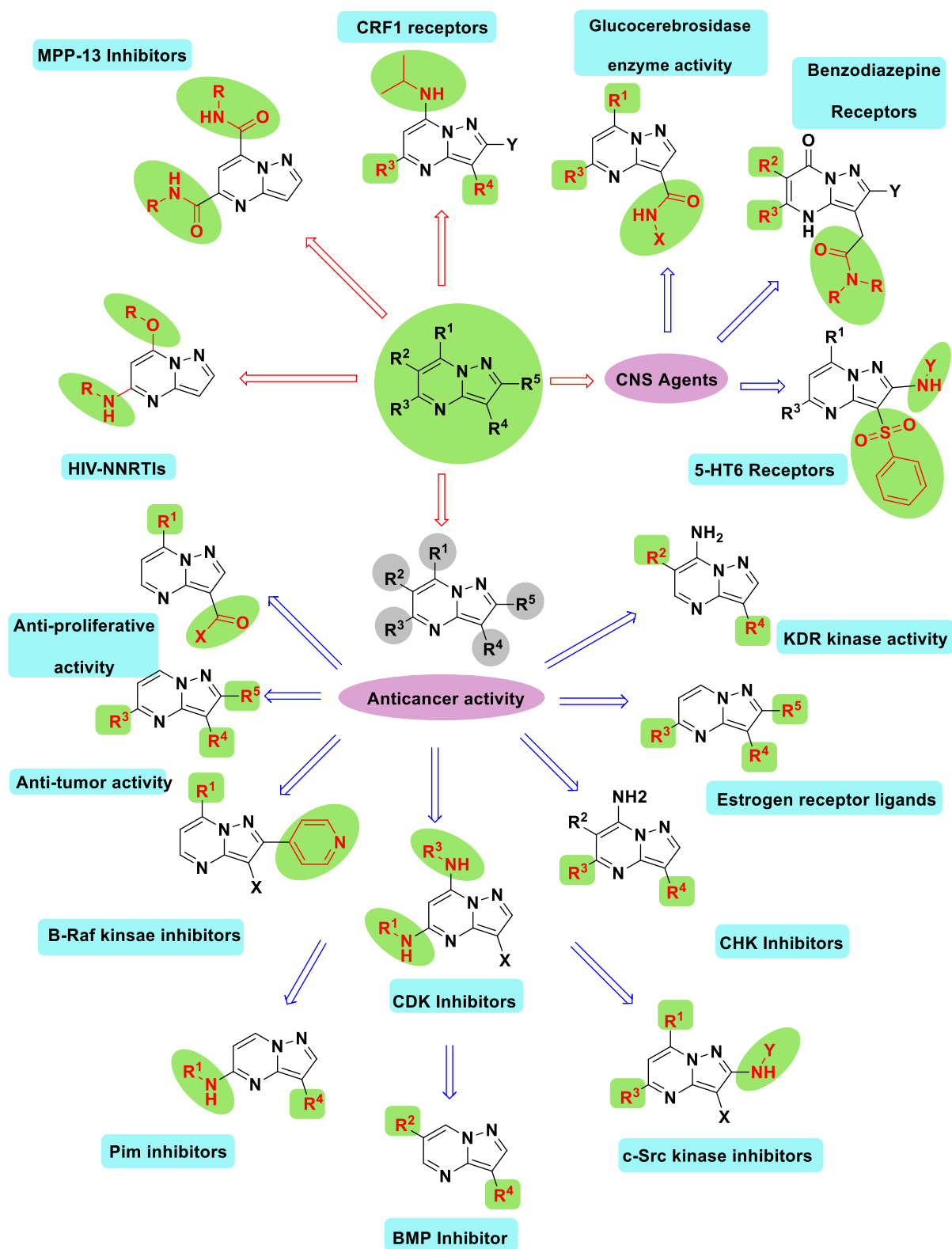


Fig. 81. Summary of structural modifications to influence the activity.

4 Conclusion

Literature survey indicated pyrazolo[1,5-*a*]pyrimidine as a privileged scaffold in medicinal chemistry with diverse pharmacological activities. In this review, we initially discussed various strategies employed for the syntheses of substituted pyrazolo[1,5-*a*]pyrimidines through multi-component reactions (MCRs), conventional heating and/or microwave-assisted organic reactions (MAORs). Moreover, these synthetic protocols offer pharmaceutical chemists to generate a library of pyrazolo[1,5-*a*]pyrimidines for high throughput screening (HTS) analysis. Clinically administered drugs such as zaleplon, indiplon, ocinaplon, dinaciclib, dosomorphin, anagliptin, pyrazophos and lorediplon bearing pyrazolo[1,5-*a*]pyrimidine nucleus have been effectively used till date for therapy of numerous ailments. Medicinal attributes of pyrazolo[1,5-*a*]pyrimidines have been extensively studied for different biological activities such as anticancer, antimicrobials, CNS depressant and other applications such as organic dyes, and in radiopharmaceuticals, as illustrated in **Fig. 80**. Recently, several therapeutic applications and patents on this scaffold have been emerged and much more is yet to be explored. A number of researchers and scientists analyzed SAR of pyrazolo[1,5-*a*]pyrimidines and deduced the bioactive structures in a quantitative manner (QSAR). The C-3 position of pyrazolo[1,5-*a*]pyrimidines accomplished favourable CNS activity, whereas modifications at C-2, C-3, C-5, C-6 and C-7 positions attributed towards different anticancer targets. Further, change in substitution patterns on C-5 and C-7 positions imparted higher affinity towards HIV-NNRTIs and CRF₁ receptors. Overall structural diversifications and their effects on biological activities are presented in **Fig. 81**. A wide range of pharmaceutical properties displayed by this privileged scaffold will definitely serve the purpose for developing effective potent chemotherapeutics. This review aims to provide an extensive information to the scientific community to design novel, target selective, optimized and varied pyrazolo[1,5-*a*]pyrimidine analogs for the treatment of multifactorial diseases.

5 Conflicts of Interest

Authors hereby declare that there are no financial/commercial conflicts of interest.

6 Acknowledgement

The authors are thankful to the College of Health Sciences, University of KwaZulu-Natal, Durban, South Africa for the facilities and financial support.

References

- [1] M. Drev, U. Groselj, S. Mevec, E. Pusavec, J. Strekelj, A. Golobic, G. Dahmann, B. Stanovnik, J. Svete, Regioselective synthesis of 1- and 4-substituted 7-oxopyrazolo[1,5-*a*]pyrimidine-3-carboxamides, *Tetrahedron*. 70 (2014) 8267–8279. doi:10.1016/j.tet.2014.09.020.
- [2] J.D. Davidson, P. Feigelson, The inhibition of adenosine deaminase by 8-azaguanine *in vitro*, *J. Biol. Chem.* 223 (1956) 65–73. <http://www.ncbi.nlm.nih.gov/pubmed/13376577> (accessed June 15, 2016).
- [3] M. Chauhan, R. Kumar, Medicinal attributes of pyrazolo[3,4-*d*]pyrimidines: A review, *Bioorg. Med. Chem.* 21 (2013) 5657–5668. doi:10.1016/j.bmc.2013.07.027.
- [4] A.M. Hussein, Synthesis of some new purine-related compounds: Regioselective one-pot synthesis of new tetrazolo[1,5-*a*]pyrimidine, pyrazolo[1,5-*a*]pyrimidine and pyrimido[1,6-*a*]pyrimidine derivatives, *J. Saudi Chem. Soc.* 14 (2010) 61–68. doi:10.1016/j.jscs.2009.12.010.
- [5] Y.C. Wu, H.J. Li, L. Liu, D. Wang, H.Z. Yang, Y.J. Chen, Efficient construction of pyrazolo[1,5-*a*]pyrimidine scaffold and its exploration as a new heterocyclic fluorescent platform, *J. Fluoresc.* 18 (2008) 357–363. doi:10.1007/s10895-007-0275-0.
- [6] K.U. Sadek, R.A. Mekheimer, T.M. Mohamed, M.S. Moustafa, M.H. Elnagdi, Regioselectivity in the multicomponent reaction of 5-aminopyrazoles, cyclic 1,3-diketones and dimethylformamide dimethylacetal under controlled microwave heating, *Beilstein J. Org. Chem.* 8 (2012) 18–24. doi:10.3762/bjoc.8.3.
- [7] Y.D. Wang, E. Honores, B. Wu, S. Johnson, D. Powell, M. Miranda, J. P. McGinnis, C. Discifani, S. K. Rabindran, W. Cheng, G. Krishnamurthy, Synthesis, SAR study and biological evaluation of novel pyrazolo[1,5-*a*]pyrimidin-7-yl phenyl amides as anti-proliferative agents, *Bioorg. Med. Chem.* 17 (2009) 2091–2100. doi:10.1016/j.bmc.2008.12.046.
- [8] P.G. Baraldi, F. Fruttarolo, M.A. Tabrizi, R. Romagnoli, D. Preti, E. Ongini, H. El-Kashef, M.D. Carrion, P.A. Borea, Synthesis of a new series of pyrazolo[1,5-*a*]pyrimidines structurally related to zaleplon, *J. Heterocycl. Chem.* 44 (2007) 355–361. doi:10.1002/chin.200731131.
- [9] J.P. Dusza, A.S. Tomcufcik, J.D. Albright, [7-(3-disubstituted amino)phenyl]pyrazolo[1,5-*a*]pyrimidines, US4626538, 1986.
- [10] T.M.A. Elmaati, F.M.A. El-Taweel, Routes to Pyrazolo[3,4-*e*][1,4]thiazepine, Pyrazolo[1,5-*a*]pyrimidine and pyrazole derivatives, *J. Chinese Chem. Soc.* 50 (2003) 413–418. doi:10.1002/jccs.200300063.
- [11] M.P. Dwyer, K. Paruch, M. Labroli, C. Alvarez, K.M. Keertikar, C. Poker, R. Rossman, T.O. Fischmann, J.S. Duca, V. Madison, D. Parry, N. Davis, W. Seghezzi, D. Wiswell, T.J. Guzi, Discovery of pyrazolo[1,5-*a*]pyrimidine-based CHK1 inhibitors: A template-based approach—Part 1, *Bioorg. Med. Chem. Lett.* 21 (2011) 467–470. doi:10.1016/j.bmcl.2010.10.113.

- [12] R.R. Frey, M.L. Curtin, D.H. Albert, K.B. Glaser, L.J. Pease, N.B. Soni, J.J. Bouska, D. Reuter, K.D. Stewart, P. Marcotte, G. Bukofzer, J. Li, S.K. Davidsen, M.R. Michaelides, 7-Aminopyrazolo[1,5-*a*]pyrimidines as potent multitargeted receptor tyrosine kinase inhibitors, *J. Med. Chem.* 51 (2008) 3777–3787. doi:10.1021/jm701397k.
- [13] I. Kim, J.H. Song, C.M. Park, J.W. Jeong, H.R. Kim, J.R. Ha, Z. No, Y. Hyun, Y.S. Cho, N.S. Kang, D.J. Jeon, Design, synthesis, and evaluation of 2-aryl-7-(3',4'-dialkoxyphenyl)-pyrazolo[1,5-*a*]pyrimidines as novel PDE-4 inhibitors, *Bioorg. Med. Chem. Lett.* 20 (2010) 922–926. doi:10.1016/j.bmcl.2009.12.070.
- [14] E. Alcalde, J.D. Mendoza, J. Elguero, J. Marino, Garcia-Marquina, C. Almera, Elude de la réaction du β -aminocrotonitrile et du α -formyl phénylacétonitrile avec l'hydrazine: Synthèse d'amino-7 pyrazolo[1,5-*a*]pyrimidines, *J. Heterocycl. Chem.* 11 (1974) 423–429. doi:10.1002/jhet.5570110330.
- [15] R. Aggarwal, C. Rani, R. Kumar, G. Garg, J. Sharma, Synthesis of new bi (pyrazolo[1 ,5-*a*] pyrimidinyl)-7-one derivatives from dehydroacetic acid and its analogues as antibacterial agents, (2014) 120–134. doi:DOI: <http://dx.doi.org/10.3998/ark.5550190.p008.089>.
- [16] H.A. Elfahham, F.M. Abdel-Galil, Y.R. Ibraheim, M.H. Elnagdi, Activated nitriles in heterocyclic synthesis. A novel synthesis of pyrazolo[1,5-*a*]pyrimidines and pyrano[2,3-*c*]pyrazoles, *J. Heterocycl. Chem.* 20 (1983) 667–670. doi:10.1002/jhet.5570200331.
- [17] O.O. Stepaniuk, V.O. Matviienko, I.S. Kondratov, I. V. Vitruk, A.O. Tolmachev, Synthesis of new pyrazolo[1,5-*a*]pyrimidines by reaction of β,γ -unsaturated γ -alkoxy- α -keto esters with *N*-unsubstituted 5-aminopyrazoles, *Synth.* 45 (2013) 925–930. doi:10.1055/s-0032-1318329.
- [18] T. Novinson, B. Bhooshan, T. Okabe, G.R. Revankar, R.K. Robins, K. Senga, H.R. Wilson, Novel heterocyclic nitrofurfural hydrazones. *In vivo* antitrypanosomal activity, *J. Med. Chem.* 19 (1976) 512–516. doi:10.1021/jm00226a013.
- [19] S. Selleri, F. Bruni, C. Costagli, A. Costanzo, G. Guerrini, G. Ciciani, P. Gratteri, F. Besnard, B. Costa, M. Montali, C. Martini, J. Fohlin, G.D. Siena, P.M. Aiello, A novel selective GABAA α 1 receptor agonist displaying sedative and anxiolytic-like properties in rodents, *J. Med. Chem.* 48 (2005) 6756–6760. doi:10.1021/jm058002n.
- [20] M.E. Fraley, R.S. Rubino, W.F. Hoffman, S.R. Hambaugh, K.L. Arrington, R.W. Hungate, M.T. Bilodeau, A.J. Tebben, R.Z. Rutledge, R.L. Kendall, R.C. Mcfall, W.R. Huckle, K.E. Coll, K.A. Thomas, Optimization of a pyrazolo[1,5-*a*]pyrimidine class of KDR kinase inhibitors: Improvements in physical properties enhance cellular activity and pharmacokinetics, *Bioorg. Med. Chem. Lett.* 12 (2002) 3537–3541. doi:10.1016/S0960-894X(02)00525-5.
- [21] S. Selleri, F. Bruni, C. Costagli, A. Costanzo, G. Guerrini, G. Ciciani, B. Costa, C. Martini, 2-Arylpyrazolo[1,5-*a*]pyrimidin-3-yl acetamides . New potent and selective peripheral benzodiazepine receptor ligands, *Bioorg. Med. Chem.* 9 (2001) 2661–2671. doi:10.1016/S0968-

- 0896(01)00192-4.
- [22] M. Suzuki, H. Iwasaki, Y. Fujikawa, M. Sakashita, M. Kitahara, R. Sakoda, Synthesis and biological evaluations of condensed pyridine and condensed pyrimidine-based HMG-CoA reductase inhibitors, *Bioorg. Med. Chem. Lett.* 11 (2001) 1285–1288. doi:10.1016/S0960-894X(01)00203-7.
- [23] T. Novinson, R. Hanson, M.K. Dimmitt, L.N. Simon, R.K. Robins, D.E. O'Brien, 3-Substituted 5,7-dimethylpyrazolo[1,5-*a*]pyrimidines, 3',5'-cyclic AMP phosphodiesterase inhibitors, *J. Med. Chem.* 17 (1974) 645–648. doi:10.1021/jm00252a016.
- [24] C. Almansa, A.F. De Arriba, F.L. Cavalcanti, L.A. Gómez, A. Miralles, M. Merlos, J. Garcia-Rafanell, J. Forn, Synthesis and SAR of a new series of COX-2-selective inhibitors: Pyrazolo[1,5-*a*]pyrimidines, *J. Med. Chem.* 44 (2001) 350–361. doi:10.1021/jm0009383.
- [25] J.Y. Hwang, M.P. Windisch, S. Jo, K. Kim, S. Kong, H.C. Kim, S. Kim, H. Kim, M. E. Lee, Y. Kim, J. Choi, D. Park, E. Park, J. Kwon, J. Nam, S. Ahn, J. Cechetto, J. Kim, M. Liuzzi, Z. No, J. Lee, Discovery and characterization of a novel 7-aminopyrazolo[1,5-*a*]pyrimidine analog as a potent hepatitis C virus inhibitor, *Bioorg. Med. Chem. Lett.* 22 (2012) 7297–7301. doi:10.1016/j.bmcl.2012.10.123.
- [26] J. Xu, H. Liu, G. Li, Y. He, R. Ding, X. Wang, M. Feng, S. Zhang, Y. Chen, S. Li, M. Zhao, Y. Li, C. Qi, Synthesis and biological evaluation of 7-(2-chlorophenylamino)-5-((2-[18F]fluoroethoxy)methyl)pyrazolo[1,5-*a*]pyrimidine-3-carbonitrile as PET tumor imaging agent, *Z. Naturforsch. B. Chem. Sci.* 67 (2012) 827–834. doi:10.5560/ZNB.2012-0047.
- [27] A.V. Ivachtchenko, D.E. Dmitriev, E.S. Golovina, M.G. Kadieva, A.G. Koryakova, V.M. Kysil, O.D. Mitkin, I.M. Okun, S.E. Tkachenko, A.A. Vorobiev, (3-Phenylsulfonylcycloalkano[*e* and *d*]pyrazolo[1,5-*a*]pyrimidin-2-yl)amines: Potent and selective antagonists of the serotonin 5-HT₆ receptor, *J. Med. Chem.* 53 (2010) 5186–5196. doi:10.1021/jm100350r.
- [28] E.J. Hanan, A.V. Abbema, K. Barrett, W.S. Blair, J. Blaney, C. Chang, C. Eigenbrot, S. Flynn, P. Gibbons, C.A. Hurley, J.R. Kenny, J. Kulagowski, L. Lee, S.R. Magnuson, C. Morris, J. Murray, R.M. Pastor, T. Rawson, M. Siu, M. Ultsch, A. Zhou, D. Sampath, J.P. Lyssikatos, Discovery of potent and selective pyrazolopyrimidine Janus kinase 2 inhibitors, *J. Med. Chem.* 55 (2012) 10090–10107. doi:10.1021/jm3012239.
- [29] Y. Tian, D. Du, D. Rai, L. Wang, H. Liu, P. Zhan, E.D. Clercq, C. Pannecouque, X. Liu, Fused heterocyclic compounds bearing bridgehead nitrogen as potent HIV-1 NNRTIs. Part 1: Design, synthesis and biological evaluation of novel 5,7-disubstituted pyrazolo[1,5-*a*]pyrimidine derivatives, *Bioorg. Med. Chem.* 22 (2014) 2052–2059. doi:10.1016/j.bmc.2014.02.029.
- [30] T. Saito, T. Obitsu, T. Kondo, T. Matsui, Y. Nagao, K. Kusumi, N. Matsumura, S. Ueno, A. Kishi, S. Katsumata, Y. Kagamiishi, H. Nakai, M. Toda, 6,7-Dihydro-5*H*-cyclopenta[*d*]pyrazolo[1,5-*a*]pyrimidines and their derivatives as novel corticotropin-releasing

- factor 1 receptor antagonists, *Bioorg. Med. Chem.* 19 (2011) 5432–5445. doi:10.1016/j.bmc.2011.07.055.
- [31] C.Y. Ishak, N. H. Metwally, H. I. Wahbi, *In vitro* antimicrobial and antifungal activity of pyrimidine and pyrazolo[1,5-*a*]pyrimidine, *Int. J. Pharm. Phytopharm. Res.* 2 (2013) 407–411. <https://pmindexing.com/journals/index.php/IJPPR/article/view/66> (accessed June 15, 2016).
- [32] A.S. Hassan, T.S. Hafez, S.A. Osman, Synthesis, characterization and cytotoxicity of some new 5-aminopyrazole and pyrazolo[1,5-*a*]pyrimidine derivatives, *Sci. Pharm.* 83 (2015) 27–39. doi:10.3797/scipharm.1409-14.
- [33] Y. Li, W. Gao, F. Li, J. Wang, J. Zhang, Y. Yang, S. Zhang, L. Yang, An *in silico* exploration of the interaction mechanism of pyrazolo[1,5-*a*]pyrimidine type CDK2 inhibitors, *Mol. Biosyst.* 9 (2013) 2266–2281. doi:10.1039/C3MB70186G.
- [34] P.B. Yu, C.C. Hong, C. Sachidanandan, J.L. Babitt, D.Y. Deng, S.A. Hoyng, H.Y. Lin, K.D. Bloch, R.T. Peterson, Dorsomorphin inhibits BMP signals required for embryogenesis and iron metabolism, *Nat Chem Biol.* 4 (2008) 33–41. doi:10.1038/nchembio.2007.54.
- [35] N. Kato, M. Oka, T. Murase, M. Yoshida, M. Sakairi, S. Yamashita, Y. Yasuda, A. Yoshikawa, Y. Hayashi, M. Makino, M. Takeda, Y. Mirenska, T. Kakigami, Discovery and pharmacological characterization of *N*-[2-({2-[(2*S*)-2-cyanopyrrolidin-1-yl]-2-oxoethyl}amino)-2-methylpropyl]-2-methylpyrazolo[1,5-*a*]pyrimidine-6-carboxamide hydrochloride (anagliptin hydrochloride salt) as a potent and selective DPP-IV inhibitor, *Bioorg. Med. Chem.* 19 (2011) 7221–7227. doi:10.1016/j.bmc.2011.09.043.
- [36] P. Kaswan, K. Pericherla, D. Purohit, A. Kumar, Synthesis of 5,7-diarylpyrazolo[1,5-*a*]pyrimidines via KOH mediated tandem reaction of 1*H*-pyrazol-3-amines and chalcones, *Tetrahedron Lett.* 56 (2015) 549–553. doi:10.1016/j.tetlet.2014.11.121.
- [37] Y. Xu, B.G. Brenning, S.G. Kultgen, J.M. Foulks, A. Cli, S. Lai, A. Chan, S. Merx, M.V. McCullar, S.B. Kanner, K. Ho, Synthesis and biological evaluation of pyrazolo[1,5-*a*]pyrimidine compounds as potent and selective Pim-1 inhibitors, *ACS Med. Chem. Lett.* 6 (2015) 63–67. doi:10.1021/ml500300c.
- [38] J. Li, Y.F. Zhao, X.L. Zhao, X.Y. Yuan, P. Gong, Synthesis and anti-tumor activities of novel pyrazolo[1,5-*a*]pyrimidines, *Arch. Pharm. (Weinheim).* 339 (2006) 593–597. doi:10.1002/ardp.200600098.
- [39] M.E. Fraley, W.F. Hoffman, R.S. Rubino, R.W. Hungate, A.J. Tebben, R.Z. Rutledge, R.C. McFall, W.R. Huckle, R.L. Kendall, K.E. Coll, K.A. Thomas, Synthesis and initial SAR studies of 3,6-disubstituted pyrazolo[1,5-*a*]pyrimidines : A new class of KDR kinase inhibitors, *Bioorg. Med. Chem. Lett.* 12 (2002) 2767–2770. doi:10.1016/S0960-894X(02)00525-5.
- [40] K. Paruch, M.P. Dwyer, C. Alvarez, C. Brown, T.Y. Chan, R.J. Doll, K. Keertikar, C. Knutson, B. McKittrick, J. Rivera, R. Rossman, G. Tucker, T.O. Fischmann, A. Hruza, V. Madison, A.A.

- Nomeir, Y. Wang, E. Lees, D. Parry, N. Sgambellone, W. Seghezzi, L. Schultz, F. Shanahan, D. Wiswell, X. Xu, Q. Zhou, R.A. James, V.M. Paradkar, H. Park, L.R. Rokosz, T.M. Stauffer, T.J. Guzi, pyrazolo[1,5-*a*]pyrimidines as orally available inhibitors of cyclin-dependent kinase 2, *Bioorg. Med. Chem. Lett.* 17 (2007) 6220–6223. doi:10.1016/j.bmcl.2007.09.017.
- [41] N. Gommermann, P. Buehlmayer, A.V. Matt, W. Breitenstein, K. Masuya, B. Pirard, P. Furet, S.W. Cowan-Jacob, G. Weckbecker, New pyrazolo[1,5-*a*]pyrimidines as orally active inhibitors of Lck, *Bioorg. Med. Chem. Lett.* 20 (2010) 3628–3631. doi:10.1016/j.bmcl.2010.04.112.
- [42] S. Selleri, F. Bruni, C. Costagli, A. Costanzo, G. Guerrini, G. Ciciani, P. Gratterer, C. Bonaccini, P.M. Aiello, F. Besnard, S. Renard, B. Costa, C. Martini, Synthesis and benzodiazepine receptor affinity of pyrazolo[1,5-*a*]pyrimidine derivatives. 3. new 6-(3-thienyl) series as $\alpha 1$ selective ligands, *J. Med. Chem.* 46 (2003) 310–313. doi:10.1021/jm020999w.
- [43] M. Labroli, K. Paruch, M.P. Dwyer, C. Alvarez, K. Keertikar, C. Poker, R. Rossman, J.S. Duca, T.O. Fischmann, V. Madison, D. Parry, N. Davis, W. Seghezzi, D. Wiswell, T.J. Guzi, Discovery of pyrazolo[1,5-*a*]pyrimidine-based CHK1 inhibitors: A template-based approach—Part 2, *Bioorg. Med. Chem. Lett.* 21 (2011) 471–474. doi:10.1016/j.bmcl.2010.10.114.
- [44] D.W. Engers, A.Y. Frist, C.W. Lindsley, C.C. Hong, C.R. Hopkins, Synthesis and structure-activity relationships of a novel and selective bone morphogenetic protein receptor (BMP) inhibitor derived from the pyrazolo[1,5-*a*]pyrimidine scaffold of Dorsomorphin: The discovery of ML347 as an ALK2 versus ALK3 selective MLPCN, *Bioorg. Med. Chem. Lett.* 23 (2013) 3248–3252. doi:10.1016/j.bmcl.2013.03.113.
- [45] M.P. Dwyer, K. Keertikar, K. Paruch, C. Alvarez, M. Labroli, C. Poker, T.O. Fischmann, R. Mayer-Ezell, R. Bond, Y. Wang, R. Azevedo, T.J. Guzi, Discovery of pyrazolo[1,5-*a*]pyrimidine-based Pim inhibitors: A template-based approach, *Bioorg. Med. Chem. Lett.* 23 (2013) 6178–6182. doi:10.1016/j.bmcl.2013.08.110.
- [46] M.M. El-Enany, M.M. Kamel, O.M. Khalil, H.B. El-Nassan, Synthesis and anti-tumor activity of novel pyrazolo[1,5-*a*]pyrimidine derivatives, *Eur. J. Chem.* 2 (2011) 331–336. doi:10.5155/eurjchem.2.3.331-336.319.
- [47] T. Kosugi, D.R. Mitchell, A. Fujino, M. Imai, M. Kambe, S. Kobayashi, H. Makino, Y. Matsueda, Y. Oue, K. Komatsu, K. Imaizumi, Y. Sakai, S. Sugiura, O. Takenouchi, G. Unoki, Y. Yamakoshi, V. Cunliffe, J. Frearson, R. Gordon, C.J. Harris, H. Kalloo-Hosein, J. Le, G. Patel, D.J. Simpson, B. Sherborne, P.S. Thomas, N. Suzuki, M. Takimoto-Kamimura, K. Ktaoka, Mitogen-activated protein kinase-activated protein kinase 2 (MAPKAP-K2) as an anti-inflammatory target: Discovery and *in vivo* activity of selective pyrazolo[1,5-*a*]pyrimidine inhibitors using a focused library and structure-based optimization approach, *J. Med. Chem.* 55 (2012) 6700–6715. doi:10.1021/jm300411k.
- [48] D.R. Compton, K.E. Carlson, J.A. Katzenellenbogen, Pyrazolo[1,5-*a*]pyrimidines as estrogen

- receptor ligands: Defining the orientation of a novel heterocyclic core, *Bioorg. Med. Chem. Lett.* 14 (2004) 5681–5684. doi:10.1016/j.bmcl.2004.08.046.
- [49] A. V. Ivachtchenko, E.S. Golovina, M.G. Kadieva, V.M. Kysil, O.D. Mitkin, S.E. Tkachenko, I. M. Okun, Synthesis and structure-activity relationship (SAR) of (5,7- disubstituted 3-phenylsulfonyl-pyrazolo[1,5-*a*]pyrimidin-2-yl)-methylamines as potent serotonin 5-HT₆ receptor (5-HT₆R) antagonists, *J. Med. Chem.* 54 (2011) 8161–8173. doi:10.1021/jm201079g.
- [50] S. Patnaik, W. Zheng, J.H. Choi, O. Motabar, N. Southall, W. Westbroek, W.A. Lea, A. Velayati, E. Goldin, E. Sidransky, W. Leister, J.J. Murugan, Discovery, structure-activity relationship, and biological evaluation of noninhibitory small molecule chaperones of glucocerebrosidase, *J. Med. Chem.* 55 (2012) 5734–5748. doi:10.1021/jm300063b.
- [51] M.A. Tabrizi, P.G. Baraldi, G. Saponaro, A.R. Moorman, R. Romagnoli, D. Preti, S. Baraldi, E. Ruggiero, C. Tintori, T. Tuccinardi, F. Vincenzi, P.A. Borea, K. Varani, Discovery of 7-oxopyrazolo[1,5-*a*]pyrimidine-6-carboxamides as potent and selective CB₂ cannabinoid receptor inverse agonists, *J. Med. Chem.* 56 (2013) 4482–4496. doi:10.1021/jm400182t.
- [52] A.G. Paulovich, D.P. Toczyski, L.H. Hartwell, When checkpoints fail, *Cell.* 88 (1997) 315–321. doi:10.1016/S0092-8674(00)81870-X.
- [53] C.J. Torrance, V. Agrawal, B. Vogelstein, K.W. Kinzler, Use of isogenic human cancer cells for high-throughput screening and drug discovery, *Nat. Biotechnol.* 19 (2001) 940–945. doi:10.1038/nbt1001-940.
- [54] A. Gopalsamy, H. Yang, J.W. Ellingboe, H.R. Tsou, N. Zhang, E. Honores, D. Powell, M. Miranda, J.P. McGinnis, S.K. Rabindran, Pyrazolo[1,5-*a*]pyrimidin-7-yl phenyl amides as novel anti-proliferative agents: Parallel synthesis for lead optimization of amide region, *Bioorg. Med. Chem. Lett.* 15 (2005) 1591–1594. doi:10.1016/j.bmcl.2005.01.066.
- [55] D. Powell, A. Gopalsamy, Y.D. Wang, N. Zhang, M. Miranda, J.P. McGinnis, S.K. Rabindran, Pyrazolo[1,5-*a*]pyrimidin-7-yl phenyl amides as novel antiproliferative agents: Exploration of core and headpiece structure-activity relationships, *Bioorg. Med. Chem. Lett.* 17 (2007) 1641–1645. doi:10.1016/j.bmcl.2006.12.116.
- [56] O.M. Ahmed, M.A. Mohamed, R.R. Ahmed, S.A. Ahmed, Synthesis and anti-tumor activities of some new pyridines and pyrazolo[1,5-*a*]pyrimidines, *Eur. J. Med. Chem.* 44 (2009) 3519–3523. doi:10.1016/j.ejmech.2009.03.042.
- [57] H.A. Abdel-Aziz, T.S. Saleh, H.S.A. El-Zahabi, Facile synthesis and *in vitro* anti-tumor activity of some pyrazolo[3,4-*b*]pyridines and pyrazolo[1,5-*a*]pyrimidines linked to a thiazolo[3,2-*a*]benzimidazole moiety, *Arch. Pharm. (Weinheim)*. 343 (2010) 24–30. doi:10.1002/ardp.200900082.
- [58] M.A. Metwally, M.A. Gouda, A.N. Harmal, A.M. Khalil, 3-Iminobutanenitrile as building block for the synthesis of substituted pyrazolo[1,5-*a*]pyrimidines with anti-tumor and antioxidant

- activities, *Int. J. Mod. Org. Chem.* 1 (2012) 96–114.
- [59] D.O. Morgan, Principles of CDK regulation, *Nature*. 374 (1995) 131–4. doi:10.1038/374131a0.
- [60] U. Asghar, A.K. Witkiewicz, N.C. Turner, E.S. Knudsen, The history and future of targeting cyclin-dependent kinases in cancer therapy, *Nat. Rev. Drug Discov.* 14 (2015) 130–146. doi:10.1038/nrd4504.
- [61] D.S. Williamson, M.J. Parratt, J.F. Bower, J.D. Moore, C.M. Richardson, P. Dokurno, A.D. Cansfield, G.L. Francis, R.J. Hebdon, R. Howes, P.S. Jackson, A.M. Lockie, J.B. Murray, C.L. Nunns, J. Powels, A. Robertson, A.E. Surgenor, C.J. Torrance, Structure-guided design of pyrazolo[1,5-*a*]pyrimidines as inhibitors of human cyclin-dependent kinase 2, *Bioorg. Med. Chem. Lett.* 15 (2005) 863–867. doi:10.1016/j.bmcl.2004.12.073.
- [62] D.A. Heathcote, H. Patel, S.H.B. Kroll, P. Hazel, M. Periyasamy, M. Alikian, S.K. Kanneganti, A.S. Jogalekar, B. Scheiper, M. Barbazanges, A. Blum, J. Brackow, A. Siwicka, R.D.M. Pace, M.J. Fuchter, J.P. Snyder, D.C. Liotta, P.S. Freemont, E.O. Aboagye, R.C. Coombes, A.G.M. Barrett, S. Ali, A novel pyrazolo[1,5-*a*]pyrimidine is a potent inhibitor of cyclin-dependent protein kinases 1, 2, and 9, which demonstrates anti-tumor effects in human tumor xenografts following oral administration, *J. Med. Chem.* 53 (2010) 8508–8522. doi:10.1021/jm100732t.
- [63] A. Kamal, J.R. Tamboli, V.L. Nayak, S.F. Adil, M.V.P.S. Vishnuvardhan, S. Ramakrishna, Synthesis of pyrazolo[1,5-*a*]pyrimidine linked aminobenzothiazole conjugates as potential anticancer agents, *Bioorg. Med. Chem. Lett.* 23 (2013) 3208–3215. doi:10.1016/j.bmcl.2013.03.129.
- [64] L.J. Phillipson, D.H. Segal, T.L. Nero, M.W. Parker, S. San, M.D. Silva, M.A. Guthridge, A.H. Wei, C.J. Burns, Discovery and SAR of novel pyrazolo [1,5-*a*] pyrimidines as inhibitors of CDK9, *Bioorg. Med. Chem.* 23 (2015) 6280–6296. doi:10.1016/j.bmc.2015.08.035.
- [65] L.C. Kim, L. Song, E.B. Haura, Src kinases as therapeutic targets for cancer, *Nat. Rev. Clin. Oncol.* 6 (2009) 587–595. doi:10.1038/nrclinonc.2009.129.
- [66] J.M. Summy, G.E. Gallick, Src family kinases in tumor progression and metastasis, *Cancer Metastasis Rev.* 22 (2003) 337–358. doi:10.1023/A:1023772912750.
- [67] A. Weiss, D.R. Littman, Signal transduction by lymphocyte antigen receptors, *Cell*. 76 (1994) 263–274. doi:10.1016/0092-8674(94)90334-4.
- [68] A.C. Chan, D.M. Desai, A. Weiss, The role of protein tyrosine kinases and protein tyrosine phosphatases in T cell antigen receptor signal transduction, *Annu. Rev. Immunol.* 12 (1994) 555–592. doi:10.1146/annurev.iy.12.040194.003011.
- [69] H.C. Reinhardt, M.B. Yaffe, Kinases that control the cell cycle in response to DNA damage: Chk1, Chk2, and MK2, *Curr. Opin. Cell Biol.* 21 (2009) 245–255. doi:10.1016/j.ceb.2009.01.018.
- [70] Y. Dai, S. Grant, New insights into checkpoint kinase 1 in the DNA damage response signaling

- network, *Clin. Cancer Res.* 16 (2010) 376–383. doi:10.1158/1078-0432.CCR-09-1029.
- [71] H. Mukaiyama, T. Nishimura, S. Kobayashi, Y. Komatsu, S. Kikuchi, T. Ozawa, N. Kamada, H. Ohnota, Novel pyrazolo[1,5-*a*]pyrimidines as c-Src kinase inhibitors that reduce I_{K_r} channel blockade, *Bioorg. Med. Chem.* 16 (2008) 909–921. doi:10.1016/j.bmc.2007.10.068.
- [72] K. Moelling, B. Heimann, P. Beimling, U.R. Rapp, T. Sander, Serine- and threonine-specific protein kinase activities of purified gag-mil and gag-raf proteins., *Nature.* 312 (1984) 558–561. doi:10.1038/312558a0.
- [73] A. Zebisch, J. Troppmair, Back to the roots: The remarkable RAF oncogene story, *Cell. Mol. Life Sci.* 63 (2006) 1314–1330. doi:10.1007/s00018-006-6005-y.
- [74] U.R. Rapp, M.D. Goldsborough, G.E. Mark, T.I. Bonner, J. Groffen, F.H. Reynolds, J.R. Stephenson, Structure and biological activity of v-raf, a unique oncogene transduced by a retrovirus (malignant transformation/transduction/molecular cloning), *Biochemistry.* 80 (1983) 4218–4222. doi:10.1073/pnas.80.14.4218.
- [75] A. Gopalsamy, G. Ciszewski, Y. Hu, F. Lee, L. Feldberg, E. Frommer, S. Kim, K. Collins, D. Wojciechowicz, R. Mallon, Identification of pyrazolo[1,5-*a*]pyrimidine-3-carboxylates as B-Raf kinase inhibitors, *Bioorg. Med. Chem. Lett.* 19 (2009) 2735–2738. doi:10.1016/j.bmcl.2009.03.129.
- [76] D.M. Berger, N. Torres, M. Dutia, D. Powell, G. Ciszewski, A. Gopalsamy, J.I. Levin, H. Kim, W. Xu, J. Wilhelm, Y. Hu, K. Collins, L. Feldberg, S. Kim, E. Frommer, D. Wojciechowicz, R. Mallon, Non-hinge-binding pyrazolo[1,5-*a*]pyrimidines as potent B-Raf kinase inhibitors, *Bioorg. Med. Chem. Lett.* 19 (2009) 6519–6523. doi:10.1016/j.bmcl.2009.10.049.
- [77] M.J. Di Grandi, D.M. Berger, D.W. Hopper, C. Zhang, M. Dutia, A.L. Dunnick, N. Torres, J.I. Levin, G. Diamantidis, C.W. Zapf, J.D. Bloom, Y. Hu, D. Powell, D. Wojciechowicz, Novel pyrazolopyrimidines as highly potent B-Raf inhibitors, *Bioorg. Med. Chem. Lett.* 19 (2009) 6957–6961. doi:10.1016/j.bmcl.2009.10.058.
- [78] X. Wang, D.M. Berger, E.J. Salaski, N. Torres, Y. Hu, J.I. Levin, D. Powell, D. Wojciechowicz, K. Collins, E. Frommers, Discovery of highly potent and selective type I B-Raf kinase inhibitors, *Bioorg. Med. Chem. Lett.* 19 (2009) 6571–6574. doi:10.1016/j.bmcl.2009.10.030.
- [79] M.C. Nawijn, A. Alendar, A. Berns, For better or for worse: the role of Pim oncogenes in tumorigenesis, *Nat Rev Cancer.* 11 (2011) 23–34. doi:10.1038/nrc2986.
- [80] X. Wang, S. Magnuson, R. Pastor, E. Fan, H. Hu, V. Tsui, W. Deng, J. Murray, M. Steffek, H. Wallweber, J. Moffat, J. Drummond, G. Chan, E. Harstad, A.J. Ebens, Discovery of novel pyrazolo[1,5-*a*]pyrimidines as potent pan-Pim inhibitors by structure- and property-based drug design, *Bioorg. Med. Chem. Lett.* 23 (2013) 3149–3153. doi:10.1016/j.bmcl.2013.04.020.
- [81] S.J. Boyer, Small molecule inhibitors of KDR (VEGFR-2) kinase: an overview of structure activity relationships, *Curr. Top. Med. Chem.* 2 (2002) 973–1000.

- doi:10.2174/1568026023393273.
- [82] C. Braestrup, R.F. Squires, Specific benzodiazepine receptors in rat brain characterized by high-affinity [³H]diazepam binding, *Proc. Natl. Acad. Sci.* 74 (1977) 3805–3809. doi:10.1073/pnas.74.9.3805.
- [83] M.J. Woods, D.C. Williams, Multiple forms and locations for the peripheral-type benzodiazepine receptor, *Biochem. Pharmacol.* 52 (1996) 1805–1814. doi:10.1016/S0006-2952(96)00558-8.
- [84] S. Selleri, F. Bruni, C. Costagli, A. Costanzo, G. Guerrini, G. Ciciani, B. Costa, C. Martini, Synthesis and BZR affinity of pyrazolo[1,5-*a*]pyrimidine derivatives. Part 1: Study of the structural features for BZR recognition, *Bioorg. Med. Chem.* 7 (1999) 2705–2711. doi:10.1016/S0968-0896(99)00232-1.
- [85] S. Selleri, P. Gratteri, C. Costagli, C. Bonaccini, A. Costanzo, F. Melani, G. Guerrini, G. Ciciani, B. Costa, F. Spinetti, C. Martini, F. Bruni, Insight into 2-phenylpyrazolo[1,5-*a*]pyrimidin-3-yl acetamides as peripheral benzodiazepine receptor ligands: Synthesis, biological evaluation and 3D-QSAR investigation, *Bioorg. Med. Chem.* 13 (2005) 4821–4834. doi:10.1016/j.bmc.2005.05.015.
- [86] A. Reynolds, R. Hanani, D. Hibbs, A. Damont, E.D. Pozzo, S. Selleri, F. Dolle, C. Martini, M. Kassiou, Pyrazolo[1,5-*a*]pyrimidine acetamides: 4-Phenyl alkyl ether derivatives as potent ligands for the 18 kDa translocator protein (TSPO), *Bioorg. Med. Chem. Lett.* 20 (2010) 5799–5802. doi:10.1016/j.bmcl.2010.07.135.
- [87] M.J. Ramírez, 5-HT₆ receptors and alzheimer's disease, *Alzheimers. Res. Ther.* 5 (2013) 15. doi:10.1186/alzrt169.
- [88] D.J. Heal, S.L. Smith, A. Fisas, X. Codony, H. Buschmann, Selective 5-HT₆ receptor ligands: Progress in the development of a novel pharmacological approach to the treatment of obesity and related metabolic disorders, *Pharmacol. Ther.* 117 (2008) 207–231. doi:10.1016/j.pharmthera.2007.08.006.
- [89] P.M. Bales, E.M. Renke, S.L. May, Y. Shen, D.C. Nelson, Purification and characterization of biofilm-associated EPS exopolysaccharides from ESKAPE organisms and other pathogens, *PLoS One.* 8 (2013) e67950. doi:10.1371/journal.pone.0067950.
- [90] K. Senga, T. Novinson, R.H. Springer, R.P. Rao, D.E. O'Brien, R.K. Robins, H.R. Wilson, Synthesis and antitrichomonal activity of certain pyrazolo[1,5-*a*]pyrimidines, *J. Med. Chem.* 18 (1975) 312–314. doi:10.1021/jm00237a021.
- [91] T. Novinson, B. Bhooshan, T. Okabe, G.R. Revankar, R.K. Robins, K. Senga, H.R. Wilson, Novel heterocyclic nitrofurfural hydrazones. *In vivo* antitrypanosomal activity, *J. Med. Chem.* 19 (1976) 512–516. doi:10.1021/jm00226a013.
- [92] T. Novinson, R.K. Robins, T.R. Matthews, Synthesis and antifungal properties of certain 7-

- alkylaminopyrazolo[1,5-*a*]pyrimidines, *J. Med. Chem.* 20 (1977) 296–299. doi:10.1021/jm00212a021.
- [93] M.S.A. El-Gaby, A.A. Atalla, A.M. Gaber, K.A. Abd Al-Wahab, Studies on aminopyrazoles: Antibacterial activity of some novel pyrazolo[1,5-*a*]pyrimidines containing sulfonamido moieties, *Farmaco.* 55 (2000) 596–602. doi:10.1016/S0014-827X(00)00079-3.
- [94] S. Bondock, R. Rabie, H.A. Etman, A.A. Fadda, Synthesis and antimicrobial activity of some new heterocycles incorporating antipyrine moiety, *Eur. J. Med. Chem.* 43 (2008) 2122–2129. doi:10.1016/j.ejmech.2007.12.009.
- [95] J. Popovici-Muller, G.W. Shipps, K.E. Rosner, Y. Deng, T. Wang, P.J. Curran, M. A. Brown, M. A. Siddiqui, A. B. Cooper, J. Duca, M. Cable, V. Girijavallabhan, Pyrazolo[1,5-*a*]pyrimidine-based inhibitors of HCV polymerase, *Bioorg. Med. Chem. Lett.* 19 (2009) 6331–6336. doi:10.1016/j.bmcl.2009.09.087.
- [96] A.O. Abdelhamid, E.K.A. Abdelall, N.A. Abdel-Riheem, S.A. Ahmed, Synthesis and antimicrobial activity of some new 5-Arylazothiazole, pyrazolo[1,5-*a*]pyrimidine, [1,2,4]triazolo[4,3-*a*]pyrimidine, and pyrimido[1,2-*a*]benzimidazole derivatives containing the thiazole moiety, *Phosphorus. Sulfur. Silicon Relat. Elem.* 185 (2010) 709–718. doi:10.1080/10426500902922933.
- [97] R. Aggarwal, G. Sumran, N. Garg, A. Aggarwal, A regioselective synthesis of some new pyrazol-1-ylpyrazolo[1,5-*a*]pyrimidines in aqueous medium and their evaluation as antimicrobial agents, *Eur. J. Med. Chem.* 46 (2011) 3038–3046. doi:10.1016/j.ejmech.2011.04.041.
- [98] B.M. Shaikh, S.G. Konda, S.S. Chobe, G.G. Mandawad, O.S. Yemul, B.S. Dawane, PEG-400: Prompted eco-friendly synthesis of some novel pyrazolo[1,5-*a*]pyrimidine derivatives and their *in vitro* antimicrobial evaluation, *J. Chem. Pharm. Res.* 3 (2011) 435–443.
- [99] W.M. Al-Adiwish, M.I.M. Tahir, A. Siti-Noor-Adnalizawati, S.F. Hashim, N. Ibrahim, W.A. Yaacob, Synthesis, antibacterial activity and cytotoxicity of new fused pyrazolo[1,5-*a*]pyrimidine and pyrazolo[5,1-*c*][1,2,4]triazine derivatives from new 5-aminopyrazoles, *Eur. J. Med. Chem.* 64 (2013) 464–476. doi:10.1016/j.ejmech.2013.04.029.
- [100] R.L. Mackman, M. Sangi, D. Sperandio, J.P. Parrish, E. Eisenberg, M. Perron, H. Hui, L. Jhang, D. Siegel, H. Yang, O. Saunders, C. Booramra, G. Lee, D. Samuel, K. Babaoglu, A. Carey, B.E. Gilbert, P.A. Piedra, R. Strickley, Q. Iwata, J. Hayes, K. Stray, A. Kinkade, D. Theodore, R. Jordan, M. Desai, T. Cihlar, Discovery of an oral respiratory syncytial virus (RSV) fusion inhibitor (GS-5806) and clinical proof of concept in a human RSV challenge study, *J. Med. Chem.* 58 (2015) 1630–1643. doi:10.1021/jm5017768.
- [101] B.S. Thyagarajan, Principles of Medicinal Chemistry, Fourth Edition (Foye, William O; Lemke, Thomas L; Williams, David A.), 1996. doi:10.1021/ed073pA110.2.

- [102] R.H. Springer, M.B. Scholten, D.E. O'Brien, T. Novinson, J.P. Miller, R.K. Robins, Synthesis and enzymic activity of 6-carbethoxy- and 6-ethoxy-3,7-disubstituted pyrazolo[1,5-*a*]pyrimidines and related derivatives as adenosine cyclic 3',5'-phosphate phosphodiesterase inhibitors, *J. Med. Chem.* 25 (1982) 235–242. doi:10.1021/jm00345a009.
- [103] G. Auzzi, F. Bruni, L. Cecchi, A. Costanzo, L.P. Vettori, R. Pirisino, M. Corrias, G. Ignesti, G. Banchelli, L.Raimondi, 2-Phenylpyrazolo[1,5-*a*]pyrimidin-7-ones. A new class of nonsteroidal anti-inflammatory drugs devoid of ulcerogenic activity, *J. Med. Chem.* 26 (1983) 1706–1709. doi:DOI: 10.1021/jm00366a009.
- [104] M.R. Shaaban, T.S. Saleh, A.S. Mayhoub, A. Mansour, A.M. Farag, Synthesis and analgesic/anti-inflammatory evaluation of fused heterocyclic ring systems incorporating phenylsulfonyl moiety, *Bioorg. Med. Chem.* 16 (2008) 6344–6352. doi:10.1016/j.bmc.2008.05.011.
- [105] C. Gege, B. Bao, H. Bluhm, J. Boer, B.M. Gallagher, B. Korniski, T. S. Powers, C. Steeneck, A.G. Taveras, V.M. Baragi, Discovery and evaluation of a non-Zn chelating, selective matrix metalloproteinase 13 (MMP-13) inhibitor for potential intra-articular treatment of osteoarthritis, *J. Med. Chem.* 55 (2012) 709–716. doi:10.1021/jm201152u.
- [106] J. Lim, M.D. Altman, J. Baker, J.D. Brubaker, H. Chen, Y. Chen, T. Fischmann, C. Gibeau, M.A. Kleinschek, E. Leccese, C. Lesburg, J.K.F. Maclean, L.Y. Moy, E.F. Mulrooney, J. Presland, L. Rakhilina, G.F. Smith, D. Steinhuebel, R. Yang, Discovery of 5-Amino-*N*-(1*H*-pyrazol-4-yl)pyrazolo[1,5-*a*]pyrimidine-3-carboxamide inhibitors of IRAK4, *ACS Med. Chem. Lett.* 6 (2015) 150427071124001. doi:10.1021/acsmchemlett.5b00107.
- [107] J. Le Roux, C. Leriche, P. Chamiot-Clerc, J. Feutrill, F. Halley, D. Papin, N. Derimay, C. Mugler, C. Grepin, L. Schio, Preparation and optimization of pyrazolo[1,5-*a*]pyrimidines as new potent PDE4 inhibitors, *Bioorg. Med. Chem. Lett.* 26 (2016) 454–459. doi:10.1016/j.bmcl.2015.11.093.
- [108] C.P. Chang, R. V. Pearse, S. O'Connell, M.G. Rosenfeld, Identification of a seven transmembrane helix receptor for corticotropin-releasing factor and sauvagine in mammalian brain, *Neuron.* 11 (1993) 1187–1195. doi:10.1016/0896-6273(93)90230-O.
- [109] D. Refojo, F. Holsboer, CRH signaling: Molecular specificity for drug targeting in the CNS, *Ann. N. Y. Acad. Sci.* 1179 (2009) 106–119. doi:10.1111/j.1749-6632.2009.04983.x.
- [110] T.L. Bale, Stress sensitivity and the development of affective disorders, *Horm. Behav.* 50 (2006) 529–533. doi:10.1016/j.yhbeh.2006.06.033.
- [111] D.J. Wustrow, T. Capiris, R. Rubin, J.A. Knobelsdorf, H. Akunne, M. Duff Davis, R. MacKenzie, T.A. Pugsley, K.T. Zoski, T.G. Heffner, L.D. Wise, Pyrazolo[1,5-*a*]pyrimidine CRF-1 receptor antagonists, *Bioorg. Med. Chem. Lett.* 8 (1998) 2067–2070. doi:10.1016/S0960-894X(98)00372-2.

- [112] P.J. Gilligan, C. Baldauf, A. Cocuzza, D. Chidester, R. Zaczek, L.W. Fitzgerald, J. McElroy, M.A. Smith, H.S.L. Shen, J.A. Saye, D. Christ, G. Trainor, D.W. Robertson, P. Hartig, The discovery of 4-(3-pentylamino)-2,7-dimethyl-8-(2-methyl-4-methoxyphenyl)-pyrazolo[1,5-*a*]pyrimidine: A corticotropin-releasing factor (hCRF1) antagonist, *Bioorg. Med. Chem.* 8 (2000) 181–189. doi:10.1016/S0968-0896(99)00271-0.
- [113] T. Saito, T. Obitsu, C. Minamoto, T. Sugiura, N. Matsumura, S. Ueno, A. Kishi, S. Katsumata, H. Nakai, M. Toda, Pyrazolo[1,5-*a*]pyrimidines, triazolo[1,5-*a*]pyrimidines and their tricyclic derivatives as corticotropin-releasing factor 1 (CRF1) receptor antagonists, *Bioorg. Med. Chem.* 19 (2011) 5955–5966. doi:10.1016/j.bmc.2011.08.055.
- [114] R. Ding, Y. He, J. Xu, H. Liu, X. Wang, M. Feng, C. Qi, J. Zhang, Synthesis and biological evaluation of pyrazolo[1,5-*a*]pyrimidine-containing ^{99m}Tc Nitrido radiopharmaceuticals as imaging agents for tumors, *Molecules.* 15 (2010) 8723–8733. doi:10.3390/molecules15128723.
- [115] J. Xu, H. Liu, G. Li, Y. He, R. Ding, X. Wang, M. Feng, S. Zhang, Y. Chen, S. Li, M. Zhao, C. Qi, Y. Dang, Synthesis and biological evaluation of novel F-18 labeled pyrazolo[1,5-*a*]pyrimidine derivatives: Potential PET imaging agents for tumor detection, *Bioorg. Med. Chem. Lett.* 21 (2011) 4736–4741. doi:10.1016/j.bmcl.2011.06.072.
- [116] M. V. Supekar, Nithyamol, P. M, D.V.T. Jaya, A. Babu, Analysis of different chemical dyes on fabrics based on their dyeing properties, *Int. J. Dev. Res.* 4 (2014) 1779–1782.
- [117] A.M. Al-Etaibi, N.A. Al-Awadi, M.A. El-Asasery, M.R. Ibrahim, Synthesis of some novel pyrazolo[1,5-*a*]pyrimidine derivatives and their application as disperse dyes, *Molecules.* 16 (2011) 5182–5193. doi:10.3390/molecules16065182.
- [118] M.M. Kamel, Y.A. Youssef, N.F. Ali, S.A. Abd, E. Megiede, Synthesis and application of novel bifunctional pyrazolo[1,5-*a*]pyrimidine reactive dyes, *Int. J. Curr. Microbiol. App. Sci.* 3 (2014) 519–530.
- [119] Y.A. Youssef, M.M. Kamel, M.S. Taher, N.F. Ali, S.A. Abd El Megiede, Synthesis and application of disazo reactive dyes derived from sulfatoethylsulfone pyrazolo[1,5-*a*]pyrimidine derivatives, *J. Saudi Chem. Soc.* 18 (2014) 220–226. doi:10.1016/j.jscs.2011.06.015.
- [120] R. Kiyama, K. Hayashi, M. Hara, M. Fujimoto, T. Kawabata, M. Kawakami, S. Nakajima, T. Fujishita, Synthesis and evaluation of novel pyrazolo[1,5-*a*]pyrimidine derivatives as nonpeptide angiotensin II receptor antagonists, *Chem. Pharm. Bull. (Tokyo).* 43 (1995) 960–965. doi:10.1248/cpb.43.960.
- [121] D.A. Griffith, D.M. Hargrove, T.S. Maurer, C.A. Blum, S.D. Lombaert, J.K. Inthavongsay, L.E. Klade, C.M. Mack, C.R. Rose, M.J. Sanders, Discovery and evaluation of pyrazolo[1,5-*a*]pyrimidines as neuropeptide Y1 receptor antagonists, *Bioorg. Med. Chem. Lett.* 21 (2011) 2641–2645. doi:10.1016/j.bmcl.2010.12.116.
- [122] A.S. Hassan, T.S. Hafez, S. A. M. Osman, M. M. Ali, Synthesis and *in vitro* cytotoxic activity

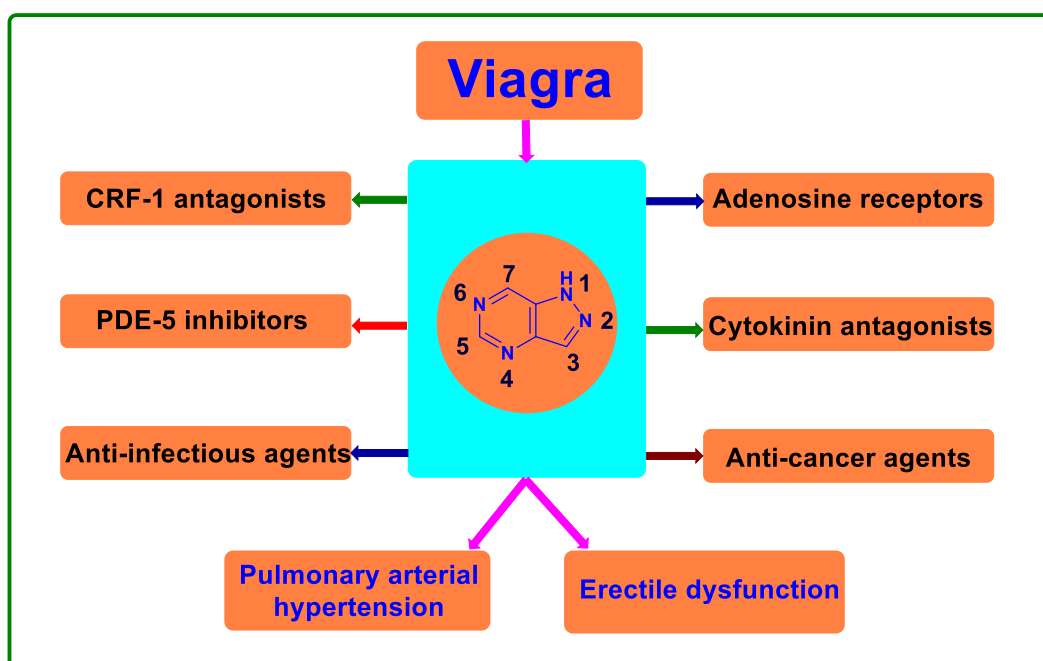
- of novel pyrazolo[1,5-*a*]pyrimidines and related schiff bases, *Turk. J. Chem.* 39 (2015) 1102–1113. doi:10.3906/kim-1504-12.
- [123] Y. Liu, R. Laufer, N.K. Patel, G. Ng, P.B. Sampson, S.W. Li, Y. Lang, M. Feher, R. Brokx, I. Beletskaya, R. Hodgson, O. Plotnikova, D.E. Awrey, W. Qiu, N.Y. Chirgadze, J.M. Mason, X. Wei, D.C. Lin, Y. Che, R. Kiarash, G.C. Fletcher, T.W. Mak, M.R. Bray, H.W. Pauls, Discovery of pyrazolo[1,5-*a*]pyrimidine TTK Inhibitors: CFI-402257 is a Potent, Selective, Bioavailable Anticancer Agent, *ACS Med. Chem. Lett.* 7 (2016) 671–675. doi:10.1021/acsmchemlett.5b00485.
- [124] R.A. Nugent, S.T. Schlachter, pyrazolopyrimidine and pyrimidinyl bisphosphonic esters as anti-inflammatories, US 5397774, 1995.
- [125] M. Inoue, K. Hashimoto, T. Kuwahara, Y. Sugimoto, T. Uesako, T. Funato, pyrazolo[1,5-*a*]pyrimidine derivatives and anti-inflammatory agent containing the same, US5688949, 1997.
- [126] M. Inoue, T. Okamura, Y. Shoji, K. Hashimoto, M. Ohara, T. Yasuda, analgesic composition of pyrazolo[1,5-*a*]pyrimidines, US5843951, 1998.
- [127] J.I. Levin, Z. Li, D. Powell, dihydropyrazolo+8 1,5-*a*+9 pyrimidine and dihydroimidazo+8 1,5-*a*+9 pyrimidine derivatives and methods of use thereof, US20070219183, 2007.
- [128] C. Zhaogen, H.H. Chafiq, J.H. Erik, A.H. Philip, K.M. Jason, T. Takako, T. Lee, thiazole pyrazolopyrimidines as CRF1 receptor antagonists, WO2008036579, 2008.
- [129] S.W. Andrews, K.R. Condroski, L.A. Demeese, J. B. Fell, J. P. Fischer, Y. Lehuero, J. A. Josey, K. Koch, G.F. Miknis, M.E. Rodriguez, G.T. Topalov, E.M. Wallace, R. Xu, substituted pyrazolo[1,5-*a*]pyrimidine compounds as mTOR inhibitors, WO2011029027, 2011.
- [130] L. Zhao, D. Liu, M.A. Siddiqui, novel pyrazolo[1,5-*a*]pyrrolo[3,2-*e*]pyrimidine derivatives as mTOR inhibitors, WO2012027239, 2012.
- [131] J.J. Murugan, N. Southall, E. Goldin, S. Patnaik, E. Sidransky, O. Motabar, W. Westbrook, substituted pyrazolopyrimidines as glucocerebrosidase activators, WO2012078855, 2012.
- [132] D.J. Bearss, L. Xiao-Hui, V. Hariprasad, X. Yong, imidazo[1,2-*b*]pyridazine and pyrazolo[1,5-*a*]pyrimidine derivatives and their use as protein kinase inhibitors, US8710057, 2014.
- [133] N. Ahmed, D. Boyal, J.D. Charrier, C. Davis, R. Davis, S. Durrant, G. Etxebarriaiajardi, J. M. Jimenez, D. Kay, R. Knegt, D. Middleton, M. Odonnell, M. Panesar, F. Pierard, J. Pinder, compounds useful as inhibitors of ATR kinase, WO2014089379, 2014.

CHAPTER 3

An appraisal on synthetic and pharmaceutical perspectives of pyrazolo[4,3-*d*]pyrimidine scaffold

Department of Pharmaceutical Chemistry, College of Health Sciences, University of KwaZulu-Natal, Durban 4000, South Africa

Graphical Abstract





Review article



Download PDF

Export

Srinivasulu Cherukupalli, Girish A. Hampannavar, Sampath Chinnam, Balakumar Chandrasekaran, Nisar Sayyad, Francis Kayamba, Rajeswar Reddy Aleti, Rajshekhar Karpoormath

Show more

<https://doi.org/10.1016/j.bmc.2017.10.012>

[Get rights and content](#)

Highlights

- Pyrazolo[4,3-*d*]pyrimidine: Nitrogen containing bicyclic heterocyclic ring with diverse biological activities.
- Synthetic strategies for variously substituted pyrazolo[4,3-*d*]pyrimidine.
- The numerous pharmacological activities of pyrazolo[4,3-*d*]pyrimidine has been discussed.
- SAR of pyrazolo[4,3-*d*]pyrimidine scaffold for miscellaneous activities has been explained.
- This review will be helpful for medicinal chemists in designing future drugs.

Abstract:

Pyrazolo[4,3-*d*]pyrimidine, a fused heterocycle bearing pyrazole and pyrimidine portions has gained a significant attention in the field of bioorganic and medicinal chemistry. Pyrazolo[4,3-*d*]pyrimidine derivatives have demonstrated numerous pharmacological activities particularly, anti-cancer, anti-infectious, phosphodiesterase inhibitors, adenosine antagonists and cytokinin antagonists etc. This review extensively unveils the synthetic and pharmacological diversity with special emphasis on structural variations around pyrazolo[4,3-*d*]pyrimidine scaffold. This endeavour has thus uncovered the medicinal worthiness of pyrazolo[4,3-*d*]pyrimidine framework. To the best of our knowledge this review is the first compilation on synthetic, medicinal and structure activity relationship (SAR) aspects of pyrazolo[4,3-*d*]pyrimidines since 1956.

Keywords: Pyrazolo[4,3-*d*]pyrimidine, Synthetic strategies, Anti-cancer agents, Anti-infectious agents, PDE-5 inhibitors, Cytokinin antagonists.

1 Introduction

Heterocyclic compounds have been significant part of both organic and medicinal chemistry research. Majority of the commercially available drugs are built on heterocyclic scaffolds and these scaffolds are core part of the drugs responsible for desired pharmacological activity. Over the years, these heterocycles have been synthesized with numerous improved synthetic methods.¹ Further these compounds have also been a valuable source of intermediates in the synthesis of several fused heterocyclic compounds of biological importance.² These fused heterocyclic compounds have major roles in biological processes, and they are present in a wide variety of drugs, antibiotics, vitamins, natural products and many other biomolecules. In addition, nitrogen bearing fused heterocycles have gained a substantial attention and occur in a variety of bioactive natural products, pharmaceuticals, organic materials, dyes and agrochemicals.³ Among these *N*-fused heterocycles, pyrazolopyrimidine is one of the attractive fused heterocyclic moiety owing to its synthesis and immense pharmacological importance. Some of the marketed drugs containing pyrazolopyrimidine core structure are allopurinol,⁴ zaleplon, indiplon,⁵ dinaciclib,⁶ dorsomorphin,⁷ ocinaplon,⁸ anagliptin,⁹ lorediplon and pyrazophos,¹⁰ sildenafil,¹¹ tisopurine.¹² Pyrazolopyrimidines show pharmacological properties such as cyclin-dependent kinase (CDK) inhibitors,^{13,14} anti-proliferative,¹⁵ anti-bacterial,¹⁶ anti-fungal,^{17,18} anti-viral agents,¹⁹ anti-leishmanial.²⁰ Furthermore, pyrazolopyrimidines acts as central nervous system depressants,²¹ COX-1, COX-2 selective inhibitors,²² antitrypanosomal and sedative,²³ serotonin 5-HT₆ receptor antagonists,^{24,25} corticotropin-releasing factor (CRF) 1 receptor antagonists,²⁶ tuberculostatic²⁷ and PET tumor imaging agents.²⁸

Several isomeric forms of pyrazolopyrimidines are well-known such as pyrazolo[1,5-*c*]pyrimidines, pyrazolo[5,1-*b*]pyrimidines, pyrazolo[5,1-*a*]pyrimidines, pyrazolo[4,3-*d*]pyrimidines and pyrazolo[3,4-*d*]pyrimidines.²⁹ Of them, pyrazolo[4,3-*d*]pyrimidine (**Fig. 1**), which is an isostere of purines has acquired considerable importance due to its diverse, facile and general synthetic methodologies with great medicinal importance. In 1958, Robins reported the synthesis of pyrazolo pyrimidines as potential purine antagonists.³⁰ Substituted 1*H*-pyrazole and 1,3-dimethylpyrimidine-2,4-(1*H*,3*H*)-dione are the most common substrates for synthesizing pyrazolo[4,3-*d*]pyrimidine derivatives.

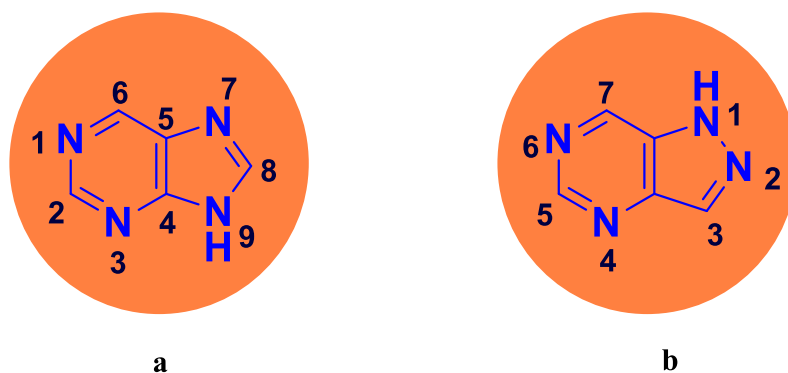


Fig. 1. General structures of purine (a) and pyrazolo[4,3-*d*]pyrimidine (b).

The versatile synthetic approaches for pyrazolo[4,3-*d*]pyrimidine derivatives have gained significant interest of the medicinal chemists due to its wide range of pharmacological applications namely, adenosine receptor antagonists,³¹ cytokinin antagonists,³² corticotrophin-releasing factor receptor antagonists,³³ anti-leishmanial,¹⁹ phosphodiesterase 5 (PDE5) inhibitors,³⁴ anti-viral, anti-fungal,³⁵ diagnostic agents,³⁶ anti-inflammatory,³⁷ agents in male and female sexual dysfunctions³⁸ etc. Marketed drug, Sildenafil is a well-known example of a drug containing pyrazolo[4,3-*d*]pyrimidine scaffold. This drug is marketed with brand names as Viagra® and Revatio®, is the first drug of its kind to be used for the treatment of male erectile dysfunction and pulmonary arterial hypertension (PAH)³⁹ (**Fig. 2**). Pyrazolo[4,3-*d*]pyrimidine scaffold also forms a vital component of naturally occurring nucleoside antibiotics such as formycin A and B.⁴⁰

Recently, our research group reported a review on pyrazolo[1,5-*a*]pyrimidine framework emphasising on methods of synthesis, structure activity correlations with their reported pharmacological activities.⁴¹ In continuation of our interest on pyrazolopyrimidines, the current review reveals various synthetic approaches and medicinal properties of pyrazolo[4,3-*d*]pyrimidine derivatives. To the best of our understanding, this review is the first of its kind with extensive compilation on synthesis, structure-activity relationship (SAR) and medicinal properties of pyrazolo[4,3-*d*]pyrimidine derivatives.

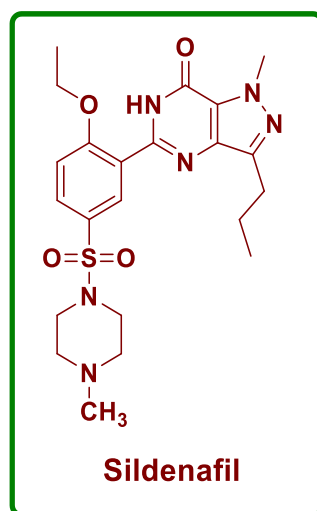


Fig. 2. Marketed drug Sildenafil containing pyrazolo[4,3-*d*]pyrimidine scaffold.

2 Synthetic methodologies for pyrazolo[4,3-*d*]pyrimidine scaffold

Pyrimidine is a six membered 1,3-diazine heterocycle containing two imine nitrogen atoms. These two nitrogens exhibit electron withdrawing tendency on the surrounding atoms thus making pyrimidine ring more resistant towards electrophilic substitution while facilitating nucleophilic attack.⁴² On the other hand, pyrazole a five membered 1,2-diazine heterocycle bearing two nitrogen atoms adjacent to each other and is a structural isomer of imidazole having nitrogen atoms at 1- and 3-position.⁴³ Fusion of pyrazole with the

pyrimidine ring results in the formation of new bicyclic system known as “pyrazolopyrimidine”. There are almost five different structural isomers of this bicyclic system, which exists due to the varying position of nitrogen, degree of saturation or unsaturation, or the number of nitrogens in the pyrazole nucleus.⁴⁴ Among those, pyrazolo[4,3-*d*]pyrimidine scaffold is privileged and medicinally significant as it has multiple reaction centres (Nitrogen at 1, 2, 4 and 6 positions and Carbon at 3, 5 and 7 positions). Their manifestation contributes to the expression of dual or multiple reactive abilities in terms of electrophilic as well as nucleophilic substitution reactions (**Fig. 3**). These properties outlined above, prompted chemists to synthesize pyrazolopyrimidine derivatives for their potential application in medicinal chemistry. From the historic point of view, synthesis of pyrazolo[4,3-*d*]pyrimidines was first reported in 1956,³⁰ since then numerous derivatives have been synthesized by applying various synthetic methodologies and were evaluated for their biological properties. The numerous synthetic strategies of pyrazolo[4,3-*d*]pyrimidines are represented in **Fig. 4**.

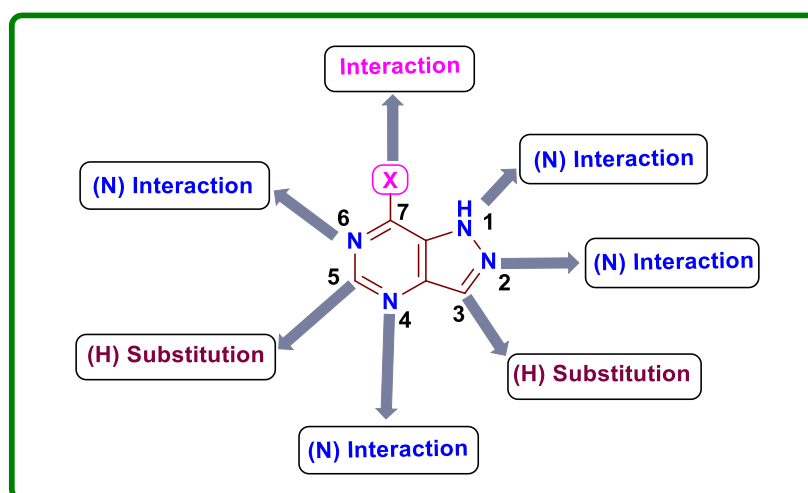
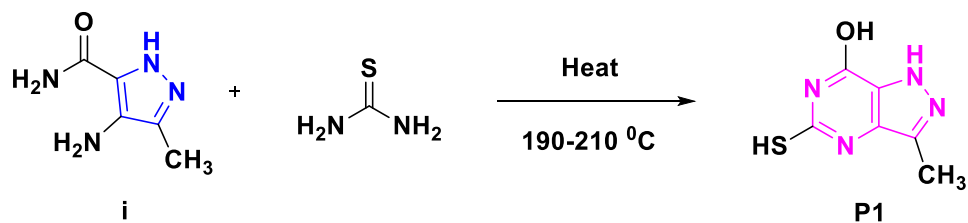


Fig. 3. Possible reaction centres of pyrazolo[4,3-*d*]pyrimidine scaffold.

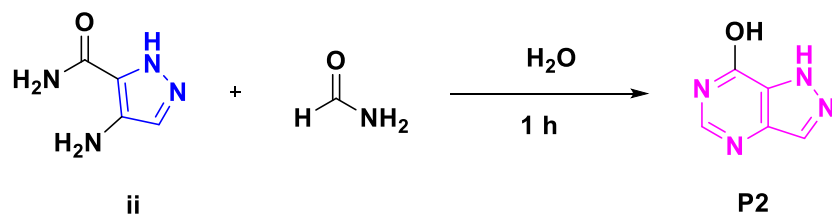
The synthesis of pyrazolo[4,3-*d*]pyrimidine derivatives (**P1-P39**) have been achieved by utilizing several simple substituted 1*H*-pyrazoles (**i-xxxvi**) and substituted 1,3-dimethylpyrimidine-2,4(1*H*,3*H*)-diones (**xxxvii-xxxix**) by employing different synthetic routes. The following discussion divulges in detail about the synthesis of pyrazolo[4,3-*d*]pyrimidines derivatives.

Robins *et al.* accomplished the desired product **P1** by the cyclization of **i** (4-amino-3-methyl-1*H*-pyrazole-5-carboxamide) with thiourea under reflux conditions (scheme-1).⁴⁵ Robins *et al.* treated 4-amino-1*H*-pyrazole-5-carboxamide (**ii**) with formamide under boiling conditions to afford 7-hydroxypyrazolo[4,3-*d*]pyrimidine (**P2**) as a target molecule (scheme-2).⁴⁶ Long and co-workers introduced a fusion reaction by ring annulation of **iii** (4-amino-3-methyl-1*H*-pyrazole-5-carbothioamide) with urea to achieve **P3** (scheme-3).⁴⁷ Acton and co-workers carried out the Curtius rearrangement of **iv** in boiling toluene to achieve pyrazolo[4,3-*d*]pyrimidinedione (**P4**) as a final compound (scheme-4).⁴⁸ Takei *et al.* attempted the reaction

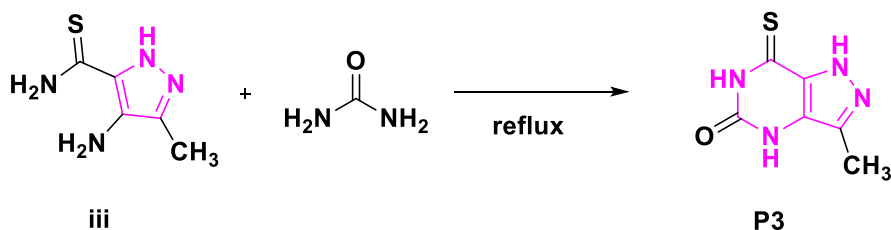
between **v** (ethyl 4-amino-5-oxo-4,5-dihydro-1*H*-pyrazole-3-carboxylate hydrochloride) and formamidine acetate to attain **P5** in presence of triethylamine as a base in 2-ethoxy ethanol (scheme-5).⁴⁹ Wierzchowski and co-workers reported the cyclization reaction of ethyl 4-amino-1-ethyl-3-propyl-1*H*-pyrazole-5-carboxylate (**vi**) with formamide to afford **P6** under reflux conditions (scheme-6).⁵⁰ Lewis *et al.* obtained **P7** via treating methyl (*Z*)-*N*-benzoyl-*N'*-(5-carbamoyl-1*H*-pyrazol-4-yl)carbamimidothioate (**vii**) with a saturated solution of ammonia in dimethylformamide and dilute NaOH solution under reflux conditions (scheme-7).⁵¹ Ochi and co-workers have reported hydrogenation and subsequent cyclization of **viii** (4-nitroso-5-hydroxy-1-phenyl-1*H*-pyrazole-3-carboxylate) with formamide to obtain **P8** under inert conditions at 180-190 °C (scheme-8).⁵²



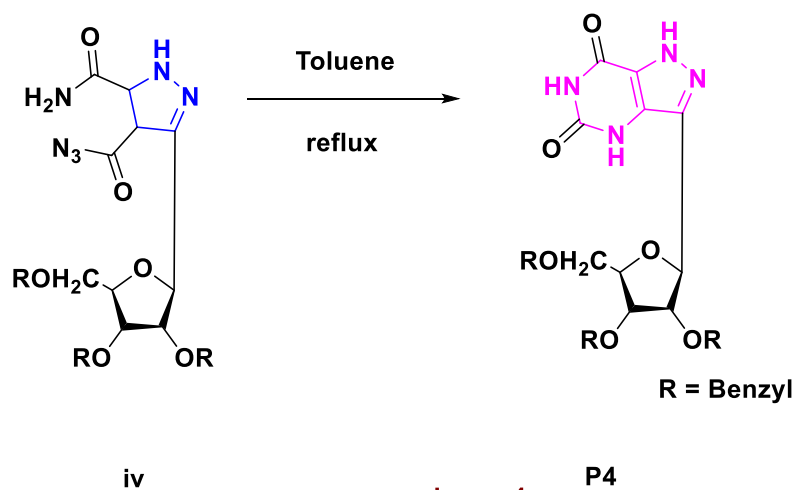
scheme-1



scheme-2

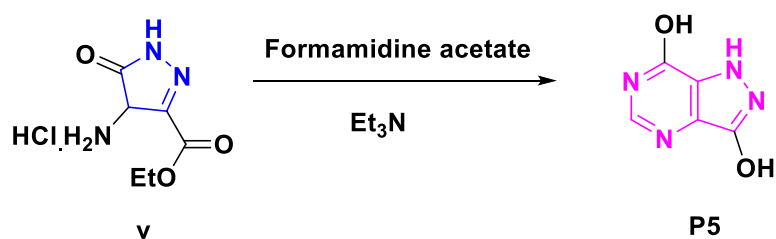


scheme-3

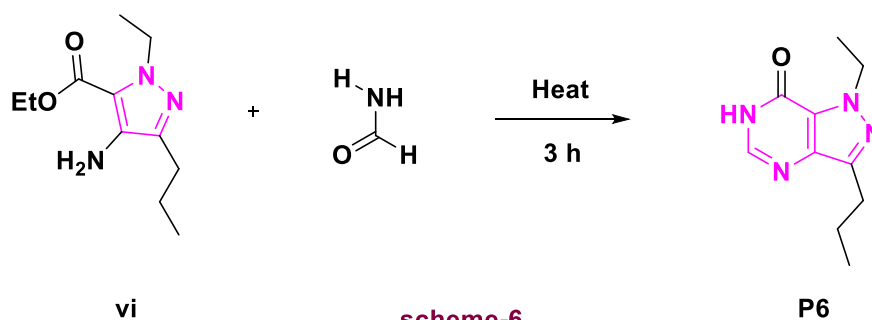


scheme-4

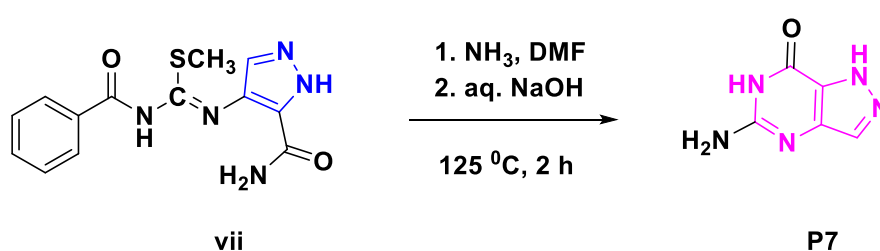
Fig. 4. Synthetic strategies for pyrazolo[4,3-*d*]pyrimidines.



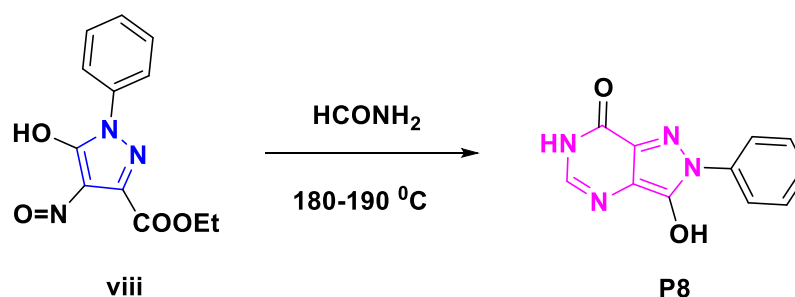
scheme-5



scheme-6



scheme-7



scheme-8

Fig. 4. (Continued). Synthetic strategies for pyrazolo[4,3-*d*]pyrimidines.

Acton *et al.* have obtained the desired product **P9**, by cyclization reaction of **ix** with ammonia (scheme-9).⁵³ Baraldi and co-workers synthesized **P10** by allowing the cyclization reaction between 4-amino-*N*-(4-chlorophenyl)-3-methyl-1*H*-pyrazole-5-carboxamide (**x**) and formamide (scheme-10).¹⁷ Hamilton *et al.* have performed cyclization reaction between 4-amino-1,3-dimethyl-1*H*-pyrazole-5-carboxamide (**xi**) and

4-methylbenzoic acid to obtain **P11** in polyphosphoric acid (scheme-11).³¹ Buchanan and co-workers have attained the desired product **P12** by cyclization of **xii** with ammonia in dimethylformamide (scheme-12).⁵⁴ Haddad *et al.* have successfully carried out the cyclization reaction of methyl 1,3-diphenyl-4-(3-phenylureido)-1*H*-pyrazole-5-carboxylate (**xiii**) with sodium ethoxide in ethanol under reflux conditions to achieve **P13** (scheme-13).⁵⁵ Dale and co-workers have performed cyclization reaction of 4-(2-ethoxybenzamido)-1-methyl-3-propyl-1*H*-pyrazole-5-carboxamide (**xiv**) in presence of sodium hydroxide as a base to afford **P14** (scheme-14).⁵⁶ El-abadelah *et al.* have reported cyclo-condensation reaction between 4-amino-1-methyl-5-propyl-1*H*-pyrazole-3-carboxamide (**xv**) and 2-ethoxybenzoic acid in polyphosphoric acid at 130-140 °C to obtain **P15** (scheme-15).⁵⁷ Yuan and co-workers attempted and achieved the reaction between ethyl 4-amino-5-(2,4-dichlorophenyl)-1-methyl-1*H*-pyrazole-3-carboxylate (**xvi**) and benzyl thioacetimidate hydrobromide in pyridine to afford **P16** (scheme-16).³³

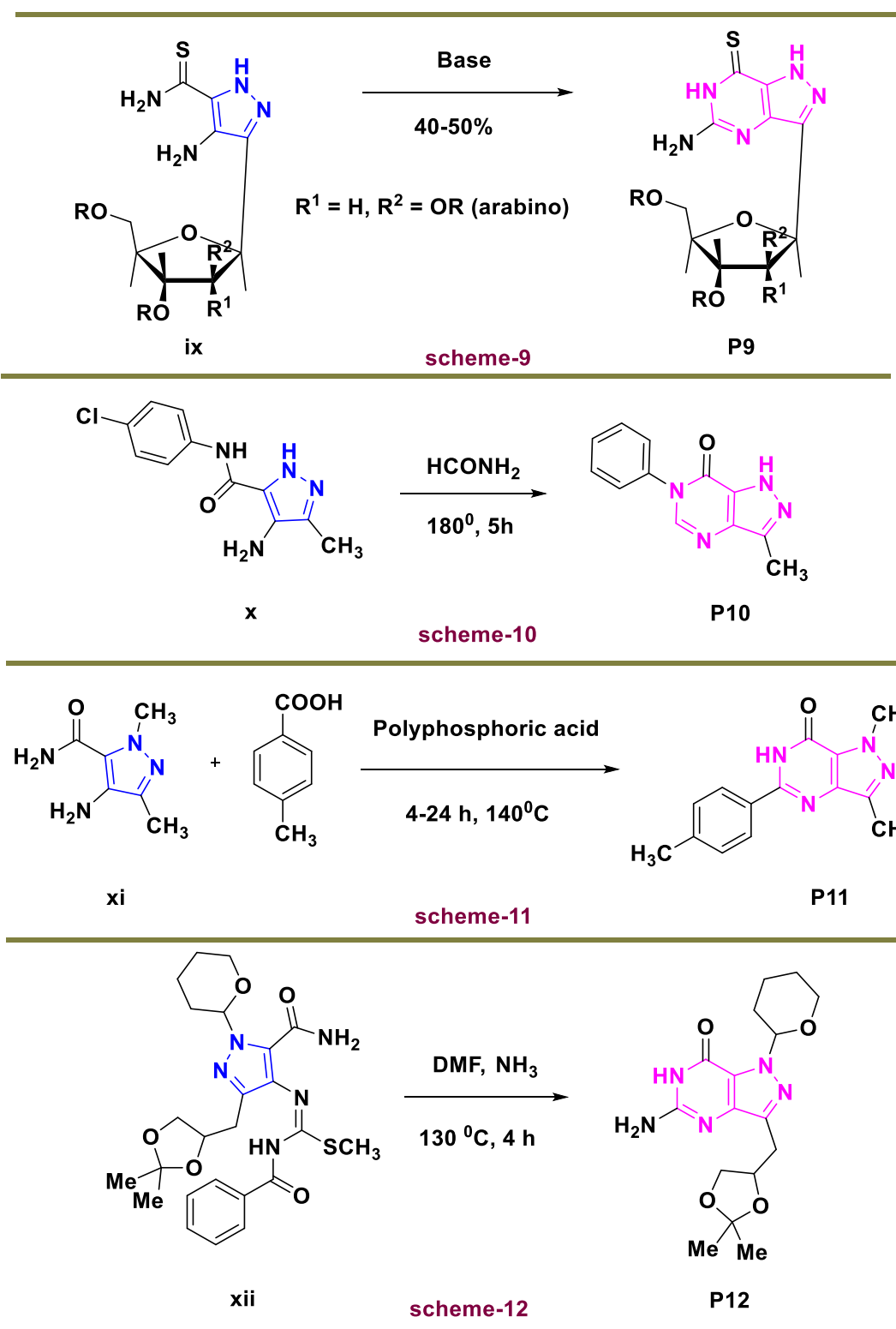


Fig. 4. (Continued). Synthetic strategies for pyrazolo[4,3-*d*]pyrimidines.

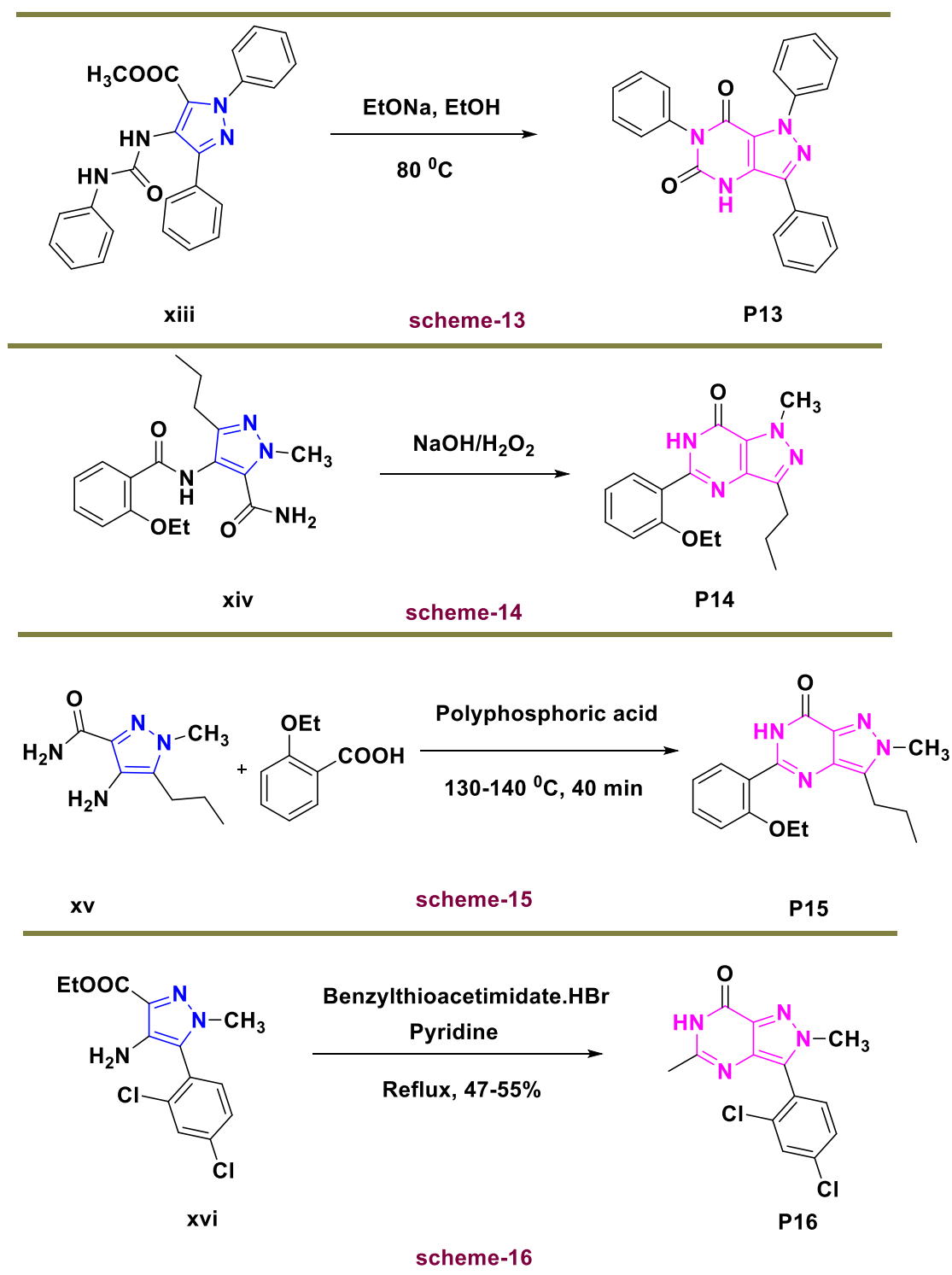


Fig. 4. (Continued). Synthetic strategies for pyrazolo[4,3-*d*]pyrimidines.

Moravcova and co-workers acquired the desired compound **P17** by the cyclization reaction of methyl 4-amino-3-isopropyl-1*H*-pyrazole-5-carboxylate (**xvii**) with formamidine acetate in presence of triethylamine (scheme-17).¹⁴ Reddy *et al.* attempted the reaction between 4-amino-1-methyl-3-propyl-1*H*-pyrazole-5-

carboxamide (**xviii**) and benzaldehyde to attain **P18** in acetic acid containing catalytic amount of *p*-toluene sulfonic acid (scheme-18).⁵⁸ Khan and co-workers obtained **P19** via treating 4-(3-bromobenzamido)-1-methyl-3-propyl-1*H*-pyrazole-5-carboxamide (**xv**) with basic alumina under microwave irradiation conditions (scheme-19).⁵⁹ Krystof *et al.* reported fusion reaction of 4-amino-3-isopropyl-1*H*-pyrazole-5-carboxamide (**xx**) with urea to achieve compound **P20** (scheme-20).⁶⁰ Brady and co-workers acquired **P21** by treating 4-amino-*N*-ethyl-1-methyl-3-phenyl-1*H*-pyrazole-5-carboxamide (**xxi**) with carbonyldiimidazole or other phosgene equivalent reagents (scheme-21).⁶¹ Lenzi *et al.* attempted the cyclization reaction of ethyl 4-amino-1-(4-methoxyphenyl)-1*H*-pyrazole-3-carboxylate (**xxii**) with 1,1,1-triethoxyethane in presence of ammonium acetate to afford **P22** under microwave irradiation conditions (scheme-22).⁶² Tollefson and co-workers carried out the cyclization reaction of 4-amino-3-ethyl-1-(2,2,2-trifluoroethoxy)ethyl)-1*H*-pyrazole-5-carboxamide (**xxiii**) with carbonyldiimidazole to get target molecule **P23** (scheme-23).³⁴ Reddy *et al.* obtained the final compound **P24** by condensation reaction of methyl 4-amino-1-methyl-3-propyl-1*H*-pyrazole-5-carboxylate (**xxiv**) with triethyl orthoformate in presence of aromatic amines (scheme-24).⁶³

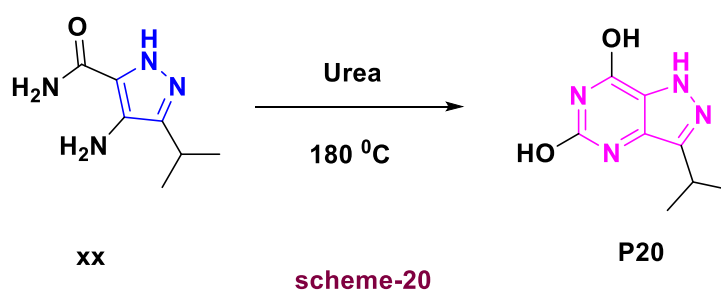
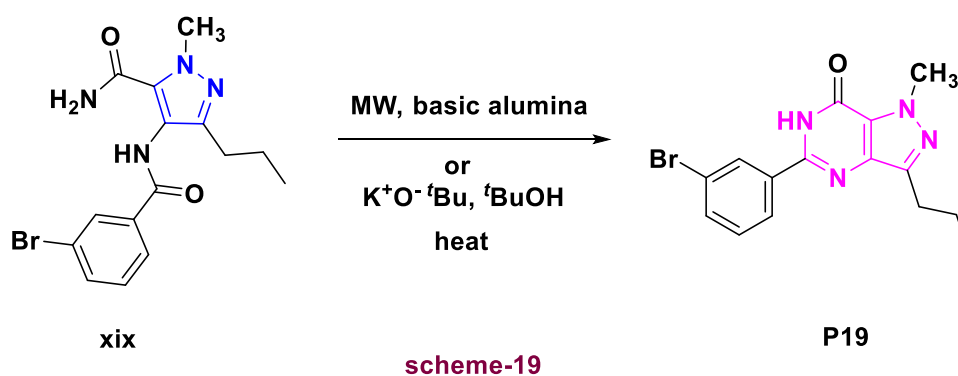
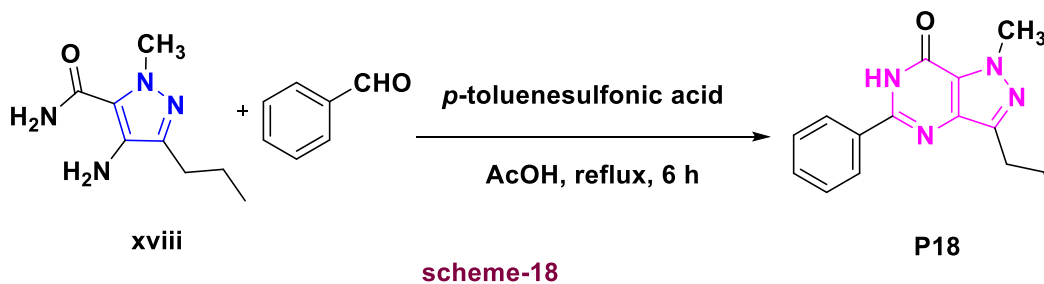
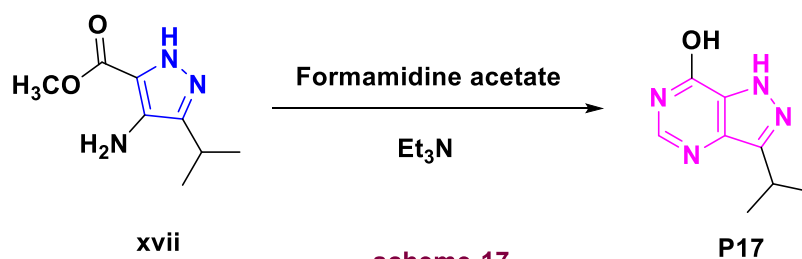


Fig. 4. (Continued). Synthetic strategies for pyrazolo[4,3-*d*]pyrimidines.

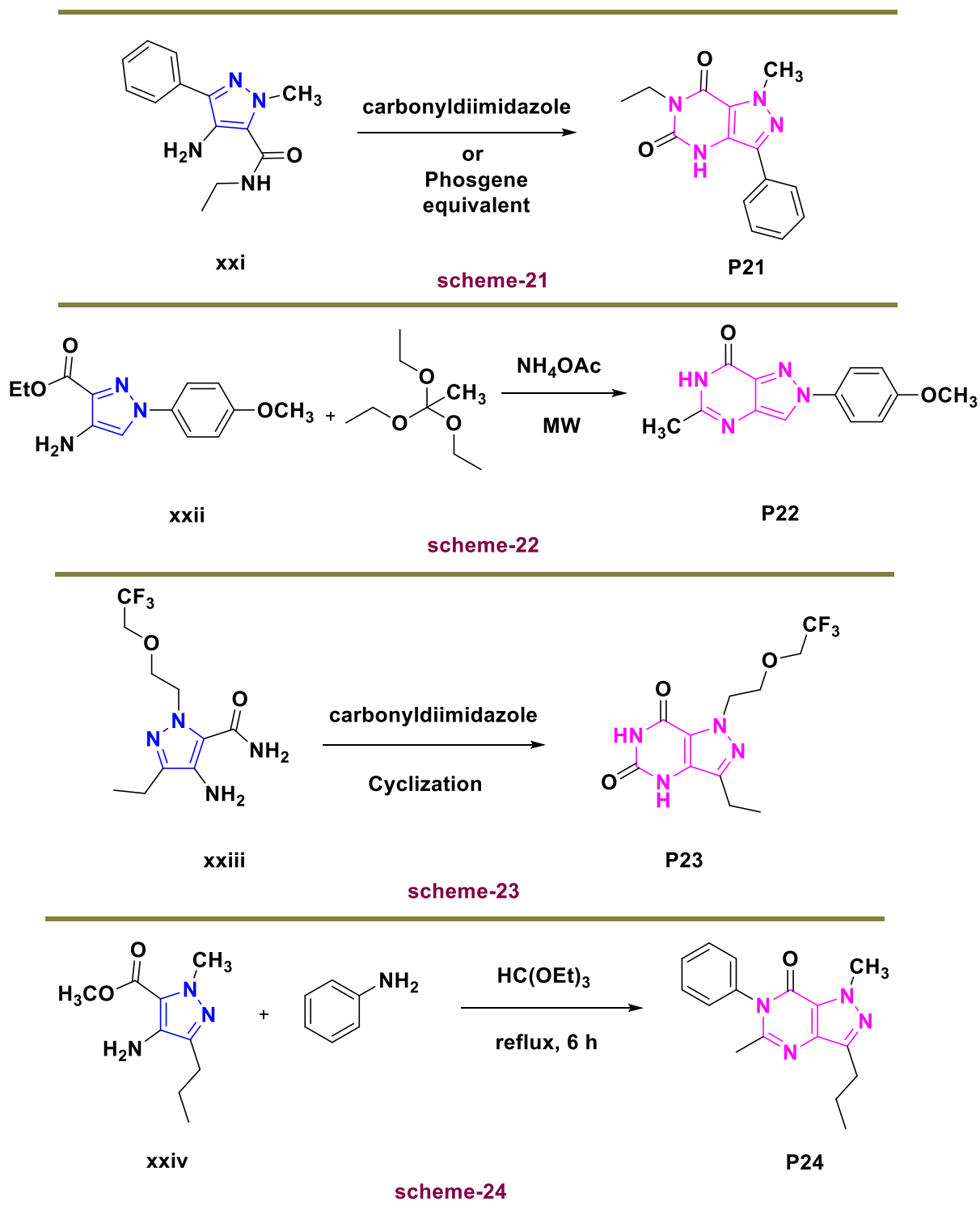
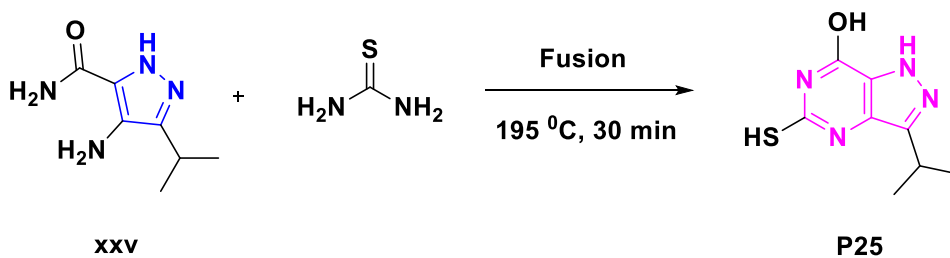


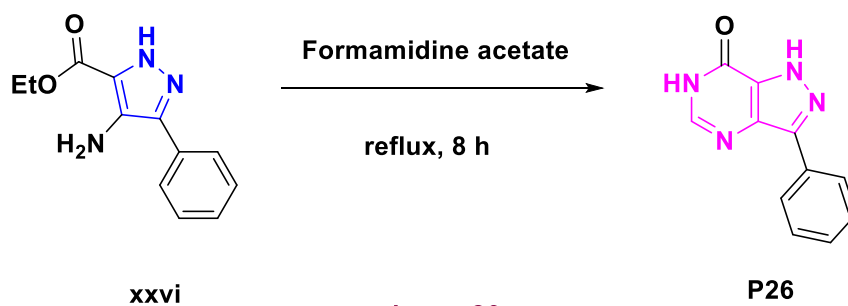
Fig. 4. (Continued). Synthetic strategies for pyrazolo[4,3-*d*]pyrimidines.

Jorda and co-workers established fusion reaction between 4-amino-3-isopropyl-1*H*-pyrazole-5-carboxamide (**xxv**) with thiourea under inert conditions to attain the desired product **P25** (scheme-25).¹³ Geffken *et al.* offered synthesis of desired compound **P26** employing cyclization of ethyl 4-amino-3-phenyl-1*H*-pyrazole-5-carboxylate (**xxvi**) with formamidine acetate under reflux conditions (scheme-26).⁶⁴ Nayak

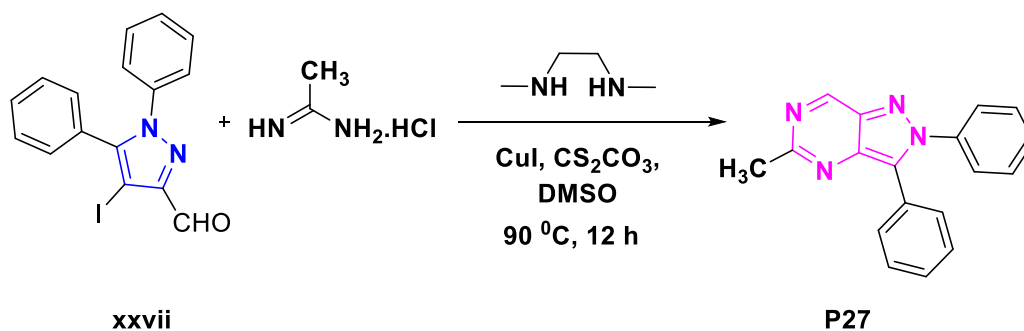
and co-workers blended 4-iodo-1,5-diphenyl-1*H*-pyrazole-3-carbaldehyde (**xxvii**) and acetamidine hydrochloride in presence of catalytic amount of copper iodide and cesium carbonate to achieve **P27** (scheme-27).⁶⁵ Bratenko and co-workers attempted intramolecular cyclization reaction of **xxviii** by treating with potassium hydroxide or potassium *tert*-butoxide in ethanol to afford **P28** (scheme-28).⁶⁶ Squarcialupi *et al.* established one pot synthesis of **P29** by reacting **xxix** (4-amino-1-(4-methoxyphenyl)-1*H*-pyrazole-3-carbonitrile) with triethyl orthobenzoate and ammonium acetate under microwave conditions (scheme-29).⁶⁷ Reddy and co-workers reported the cyclization reaction of 4-amino-1-methyl-3-propyl-1*H*-pyrazole-5-carboxamide (**xxx**) with 2-ethoxybenzaldehyde to afford **P30** in presence of catalytic amount of potassium persulfate in H₂O:DMSO (1:1) under microwave irradiation conditions (scheme-30).⁶⁸ Squarcialupi *et al.* reacted 4-amino-1-phenyl-1*H*-pyrazole-3-carbonitrile (**xxxi**) with ethyl (*E*)-3-(4-methoxyphenyl)acrylimidate hydrochloride to attain **P31** in presence of ammonium acetate under microwave conditions (scheme-31).⁶⁹ Rote and co-workers have carried out the regioselective condensation of 4-amino-1-methyl-3-propyl-1*H*-pyrazole-5-carboxamide (**xxxii**) with benzaldehyde in presence of acetonitrile and slight excess of molecular iodine to afford **P32** (scheme-32).⁷⁰



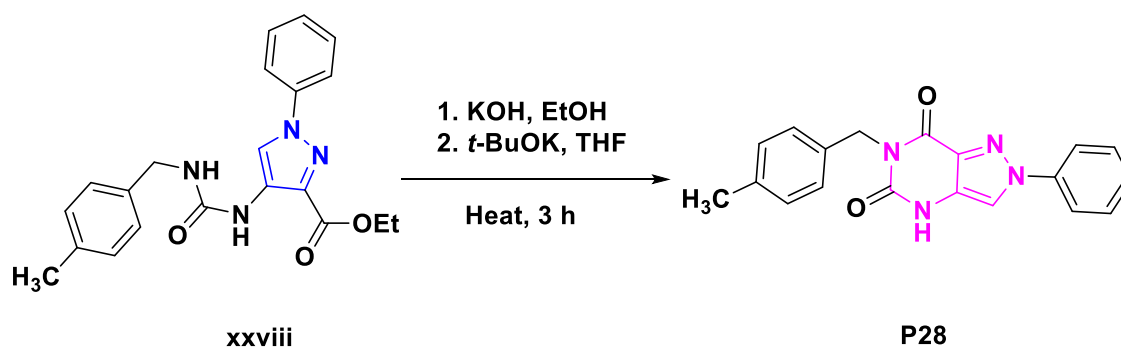
scheme-25



scheme-26

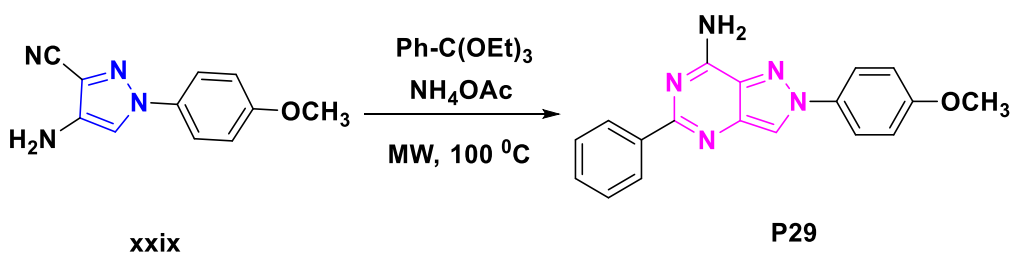


scheme-27

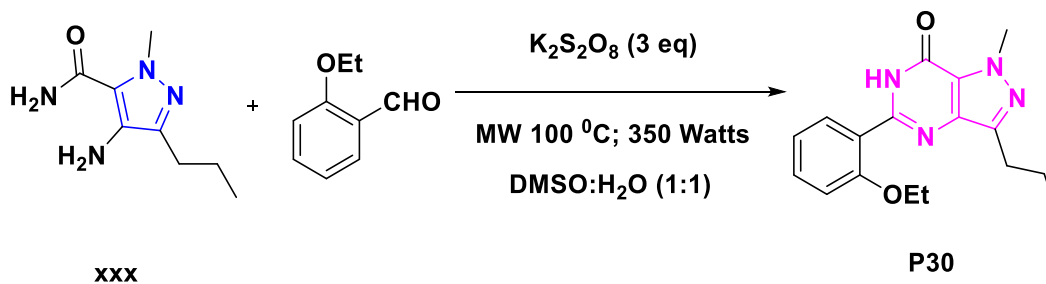


scheme-28

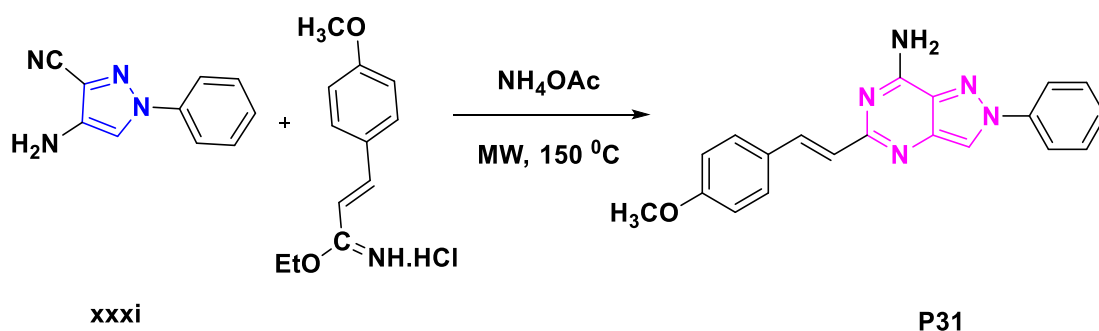
Fig. 4. (Continued). Synthetic strategies for pyrazolo[4,3-d]pyrimidines.



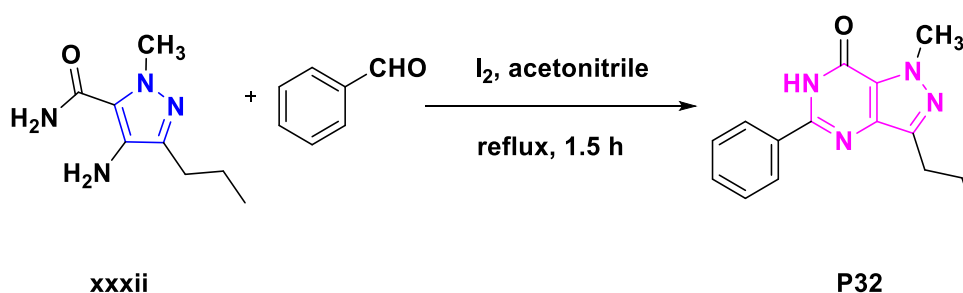
scheme-29



scheme-30



scheme-31



scheme-32

Fig. 4. (Continued). Synthetic strategies for pyrazolo[4,3-d]pyrimidines.

Mohammed and co-workers have treated 4-amino-1-methyl-3-propyl-1*H*-pyrazole-5-carboxamide (**xxxiii**) and 1-(4-nitrophenyl)ethan-1-one to achieve **P33** in presence of catalytic amount of molecular iodine (scheme-33).⁷¹ Hafez *et al.* have obtained **P34** by treating (*E*)-*N*-(5-(2-benzylidenehydrazine-1-carbonyl)-3-(4-chlorophenyl)-1*H*-pyrazol-4-yl)acetamide (**xxxiv**) with sodium ethoxide under reflux conditions (scheme-34).³⁵ Squarcialupi and co-workers have accomplished the target product **P35** by reacting 4-amino-1-(2-hydroxyphenyl)-1*H*-pyrazole-3-carbonitrile (**xxxv**) with ethyl iminoester hydrochloride (scheme-35).⁷² Squarcialupi *et al.* treated methyl 4-amino-1-methyl-1*H*-pyrazole-3-carboxylate (**xxxvi**) with (triethoxymethyl)benzene to get target compound **P36** under microwave irradiation conditions (scheme-36).⁷³ Pepesch and co-workers have treated **xxxvii** with strong alkali (NaOH) to afford the desired molecule **P37** (scheme-37).⁷⁴ Senda *et al.* have accomplished the desired molecule **P38** by reacting 6-(bromomethyl)-1,3-dimethyl-5-nitropyrimidine-2,4(1*H*,3*H*)-dione (**xxxviii**) with methylamine in ethanol under reflux conditions (scheme-38).⁷⁵ Hirota and co-workers introduced cyclization of 1,3-dimethyl-5-nitro-6-((phenylamino)methyl)pyrimidine-2,4(1*H*,3*H*)-dione (**xxxix**) to achieve the desired molecule **P39** (scheme-39).⁷⁶

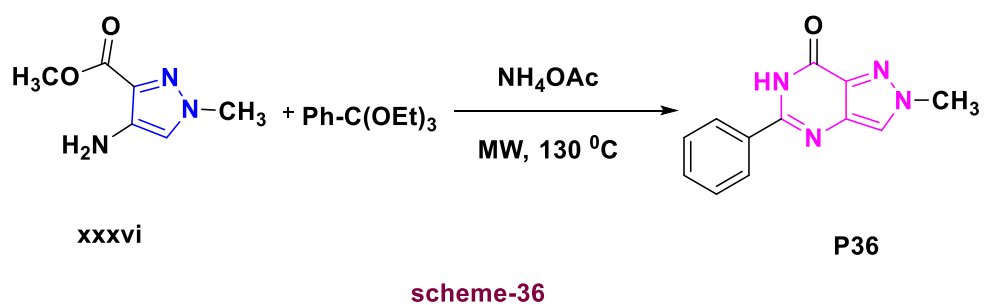
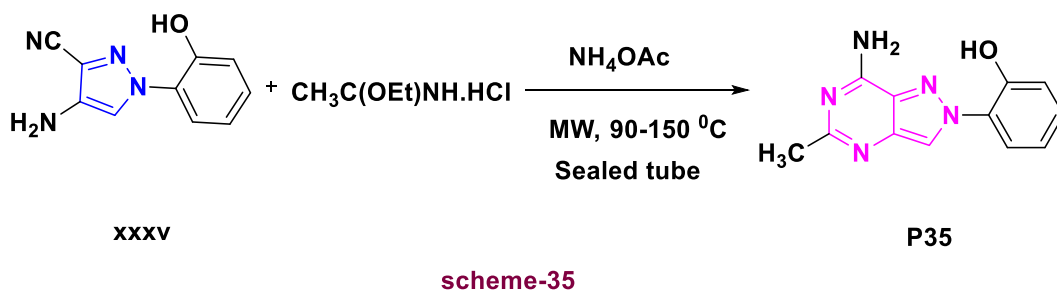
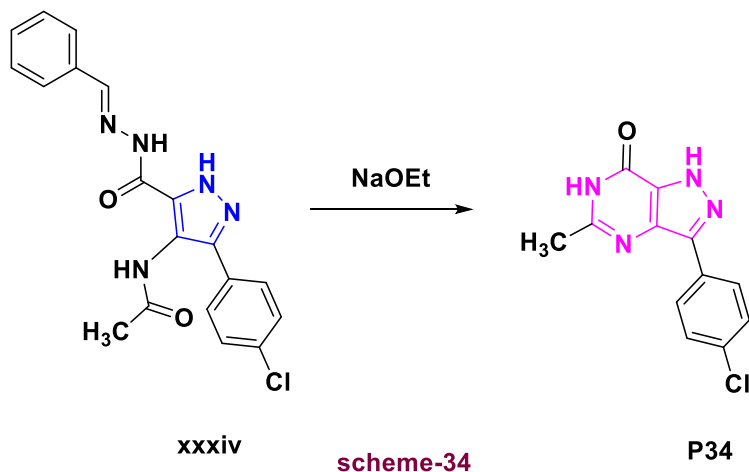
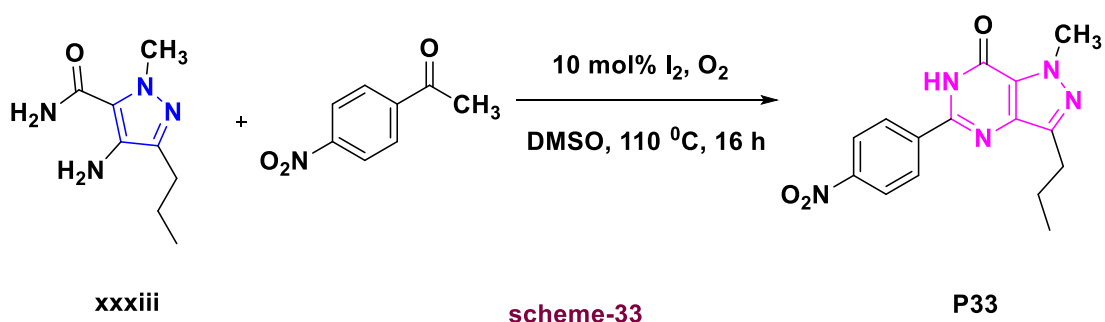


Fig. 4. (Continued). Synthetic strategies for pyrazolo[4,3-*d*]pyrimidines.

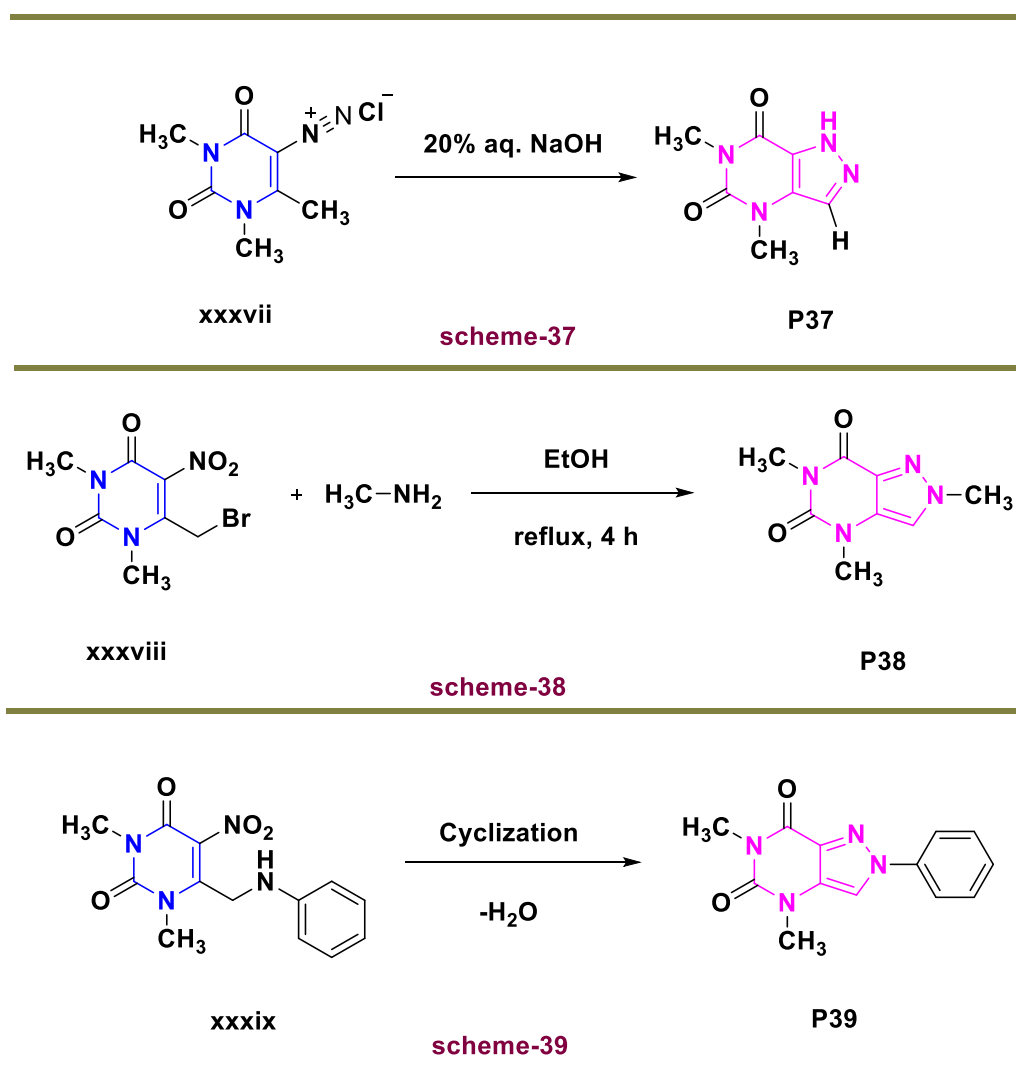


Fig. 4. (Continued). Synthetic strategies for pyrazolo[4,3-*d*]pyrimidines.

3 Biological activities

3.1 Anti-cancer agents

In 2003, Moravcova *et al.* attempted novel synthesis of 3,7-disubstituted pyrazolo[4,3-*d*]pyrimidines and evaluated their anticancer activity against CDK1/Cyclin B kinase and anti-proliferative activity against myeloid leukemia cell line (K-562). All the molecules exhibited good potency against both CDK1/Cyclin B kinase and K-562 cell line. From the series, compound **1** (2-(((3-isopropyl-1*H*-pyrazolo[4,3-*d*]pyrimidin-7-yl)amino)methyl)phenol) showed maximum CDK1 inhibitory activity ($IC_{50} = 0.44 \mu\text{mol}/\text{dm}^3$) as well as K-562 cell line activity ($IC_{50} = 54 \mu\text{mol}/\text{dm}^3$) when compared to reference drug olomoucine (CDK1: $IC_{50} = 7 \mu\text{mol}/\text{dm}^3$; K-562: $IC_{50} = 163 \mu\text{mol}/\text{dm}^3$). SAR studies revealed that the presence of hydroxy benzyl functional group at C-7 was essential for both anticancer and anti-proliferative activity **Fig. 5**.¹⁴

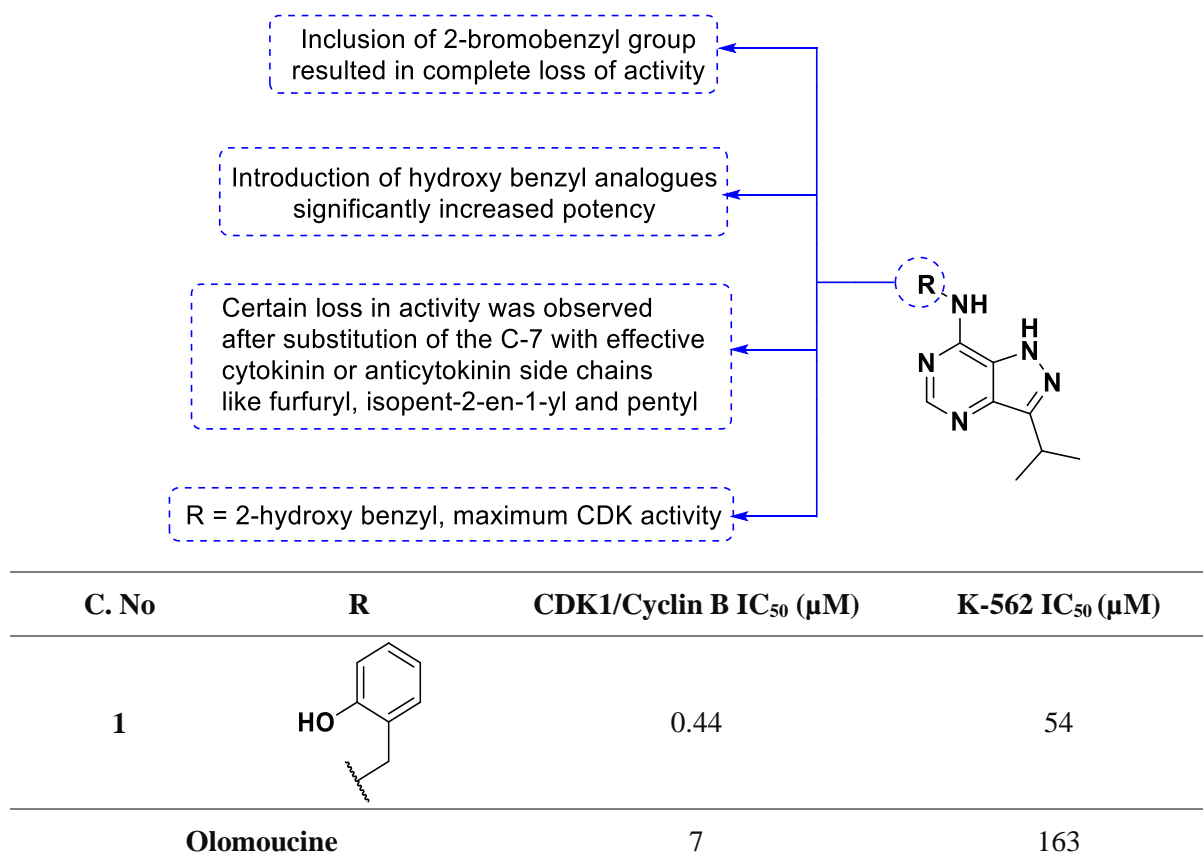
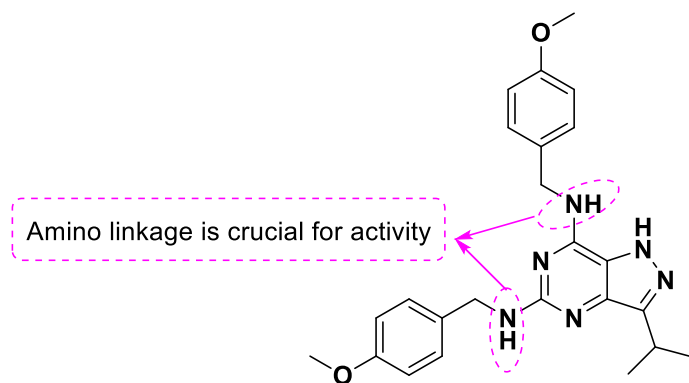


Fig. 5. SAR and anticancer properties of 2-(((3-isopropyl-1*H*-pyrazolo[4,3-*d*]pyrimidin-7-yl)amino)methyl)phenol.

In 2006, Krystof and co-workers synthesized 3-isopropyl-*N*⁵,*N*⁷-bis(4-methoxybenzyl)-1*H*-pyrazolo[4,3-*d*]pyrimidine-5,7-diamine (**2**) as CDK1 inhibitor. Compound **2** was also tested against a panel of human cancer cell lines (A431, A549, BT474, CEM, G361, HBL100, HeLa, K562, MCF7 and many others) for their anti-proliferative activity. Of the tested cell lines, compound **2** showed significant potency against HeLa cell line. From SAR studies, it was revealed that amino linkage at C-5 and C-7 positions have greatly influenced the activity as depicted in **Fig. 6**.⁶⁰



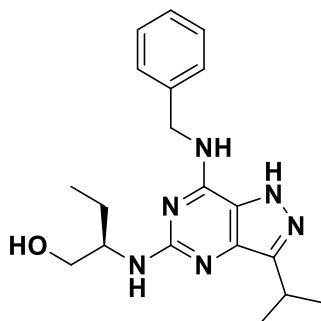
Chapter 3

C. No	CDK1 IC ₅₀ (μM)
2	4.1 ± 1.3

C. No	Cell lines	IC ₅₀ (μM)
2	A431	6.9 ± 0.2
	A549	6.8 ± 0.4
	BT474	6.8 ± 0.2
	CEM	6.3 ± 0.6
	G361	6.7 ± 0.2
	HBL100	6.4 ± 0.1
	HeLa	5.2 ± 0.4
	K562	6.2 ± 0.2
	MCF7	6.4 ± 0.5

Fig. 6. SAR and antiproliferative activity of compound **2** on various cancer cell lines.

In 2011, Jorda and co-workers reported synthesis of (*R*)-2-((7-(benzylamino)-3-isopropyl-1*H*-pyrazolo[4,3-*d*]pyrimidin-5-yl)amino)butan-1-ol (**3**) and determined its anti-proliferative activity against a panel of human cancer cell lines (MCF-7, HCT-116, RPMI-8226, CEM, G-361, A-549, A-431 and others). Further, compound **3** was found to have potent inhibitory activity against several CDKs, namely CDK2, CDK5, CDK7 and CDK9. **Fig. 7** briefly displays the anti-proliferative and CDK activity of compound **3**.¹³

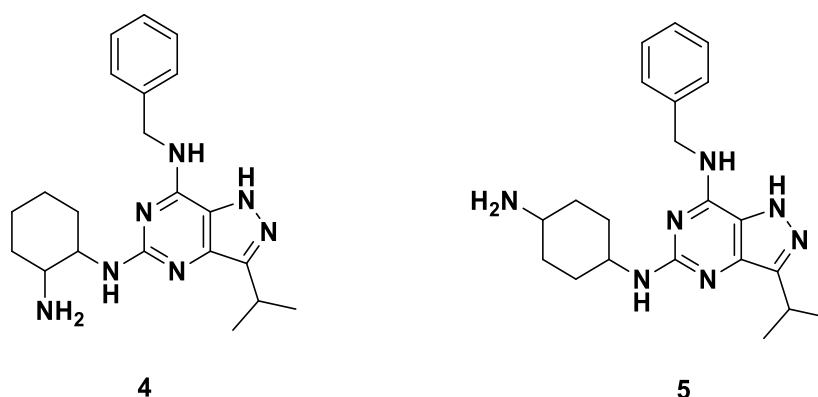


C. No	Human tumor Cell lines	IC ₅₀ (μM)
3	MCF-7	7.5 ± 2.3
	HCT-116	11.0 ± 1.8
	RPMI-8226	3.6 ± 0.3
	CEM	3.8 ± 0.8
	G-361	4.8 ± 1.6
	A-549	7.1 ± 2.1
	A-431	7.7 ± 0.3

C. No	IC ₅₀ (μM)			
	CDK2/Cyclin E	CDK5/P35	CDK7/Cyclin H/MAT1	CDK9/Cyclin T1
3	0.04	0.20	0.16	1.00

Fig. 7. Anticancer activity on various cancer cell lines and kinase selectivity profile for compound **3**.

In 2013, Weitensteiner *et al.* observed potential anti-angiogenic activity of the newly synthesized 3,5,7-trisubstituted pyrazolo[4,3-*d*]pyrimidine derivatives by employing three *in vitro* assays (proliferation, cell migration and tube formation) and substantiated based on *n vivo* chorioallantoic membrane assay. The most active compounds were examined further for their kinase selectivity profile against a panel of 24 different kinases including other isoforms of CDK (**Fig. 8**). From the experimental data, compound **4** and **5** displayed high selectivity towards Cdk2 and Cdk5. Authors also investigated to understand the relationship between the CDK-5 inhibition and anti-angiogenic properties of **4** and **5** by quantifying lamellipodia formation followed by immunocytochemistry analysis. Thus, concluding that these two compounds (**4** and **5**) inhibited angiogenesis (*in vitro*) via CDK5 inhibitory mechanism.⁷⁷



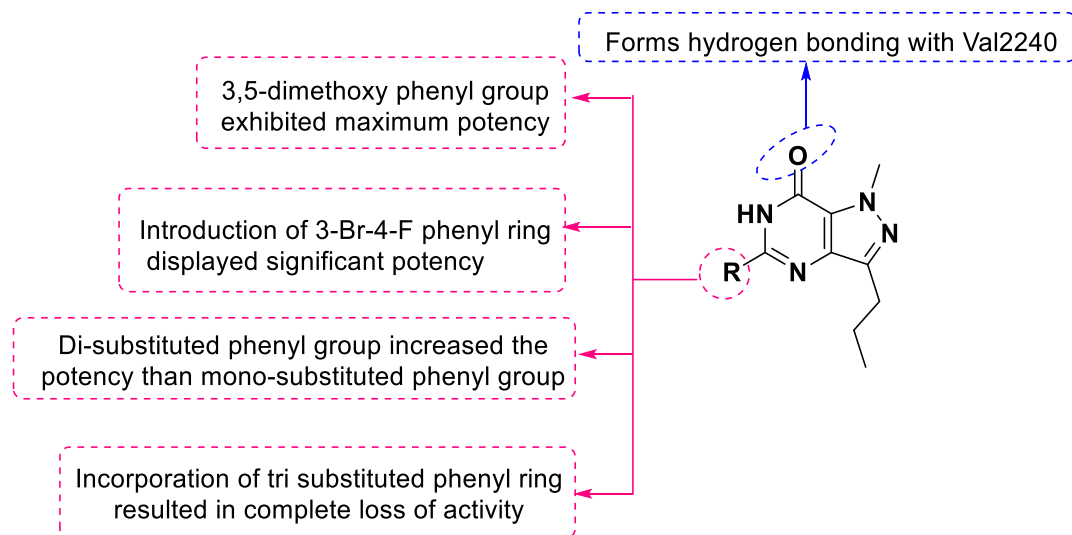
C. No	CDK1 IC ₅₀	CDK2 IC ₅₀	CDK4 IC ₅₀	CDK5 IC ₅₀	CDK6 IC ₅₀	CDK7 IC ₅₀	CDK9 IC ₅₀
4	3.2×10^{-6}	9.9×10^{-7}	1.5×10^{-5}	4.4×10^{-7}	$> 10^{-4}$	$> 10^{-4}$	$> 10^{-6}$
5	5.8×10^{-6}	1.5×10^{-6}	6.6×10^{-6}	1.6×10^{-6}	9.1×10^{-5}	$> 10^{-4}$	1.9×10^{-6}

IC₅₀ values are given in molar.

Fig. 8. CDK kinase activity of lead compounds consisting trisubstituted pyrazolo[4,3-*d*]pyrimidine scaffold.

In 2014, Reddy and co-workers reported a microwave assisted synthesis of 5-substituted-1*H*-pyrazolo[4,3-*d*]pyrimidine-7(6*H*)-one analogs and evaluated their pharmacological activity against various human cancer

cell lines (HeLa, CAKI-1, PC-3, MiaPaca-2 and A-549). From this series, compound **6**, (5-(3,5-dimethoxyphenyl)-1-methyl-3-propyl-1,6-dihydro-7H-pyrazolo[4,3-d]pyrimidin-7-one displayed potent activity against all cancer cell lines. SAR studies revealed that appropriate substitutions at C-5 influenced the potency as shown in **Fig. 9**.⁶⁸



C. No	R	IC ₅₀ (μM)				
		HeLa	CAKI-1	PC-3	Miapaca-2	A-549
6		19	17	37	24	14

Fig. 9. SAR and anti-proliferative activity of compound **6** on various human cancer cell lines.

In 2015, Reznickova *et al.* reported the synthesis of 3,5,7-trisubstituted pyrazolo[4,3-d]pyrimidines and evaluated their CDK inhibitor activity. All the synthesized molecules having isopropyl group at C-3 position showed significant activity. From the series, compounds **7**, **8** and **9** exhibited potent CDK2 inhibitory activity and excellent cytotoxicity against MCF-7 and K-562 human cancer cell lines as represented in **Fig. 10**. From SAR studies, it was concluded that substitutions at C-5 and C-7 positions were necessary for both CDK2 and cancer activities.⁷⁸

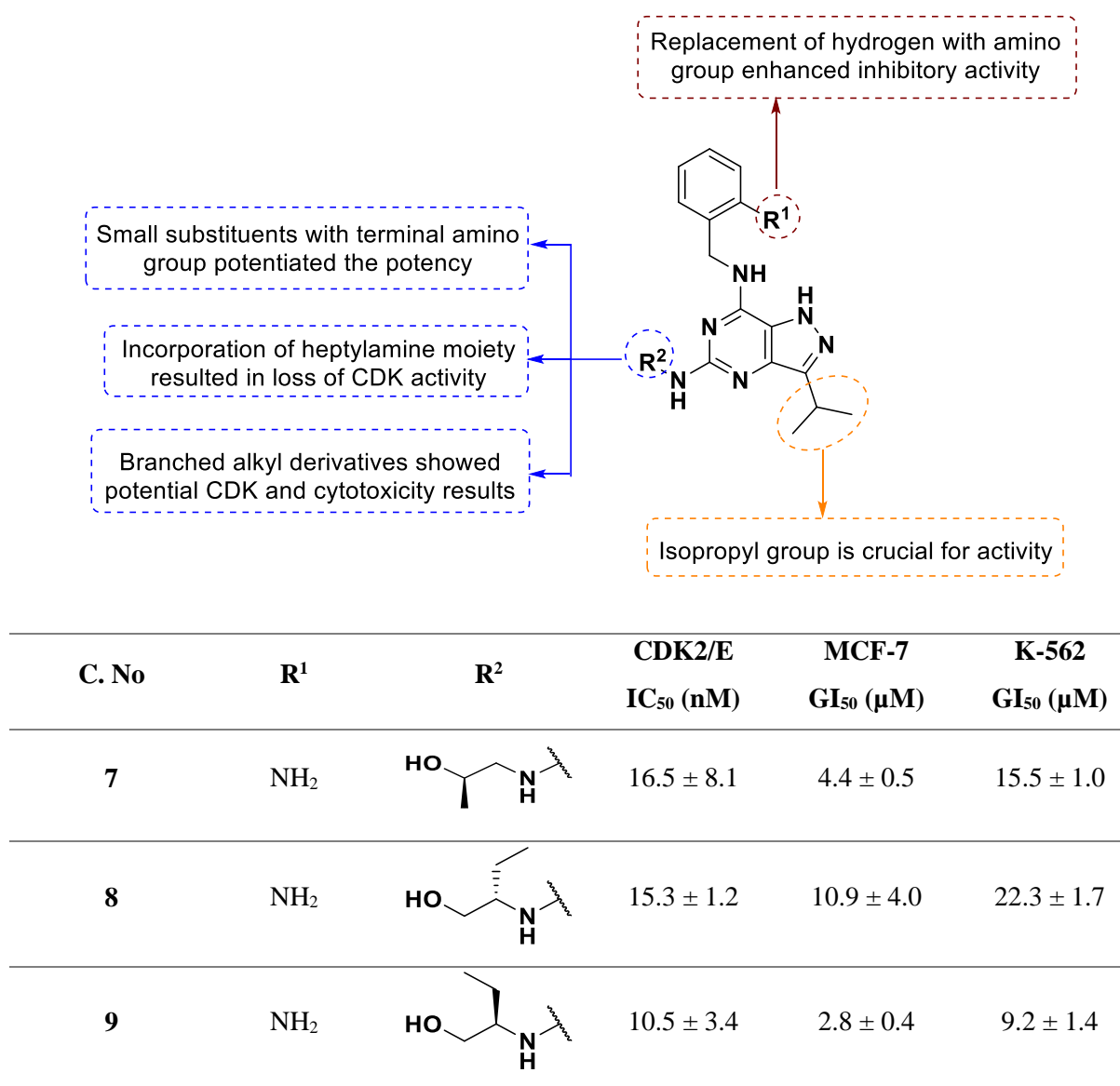
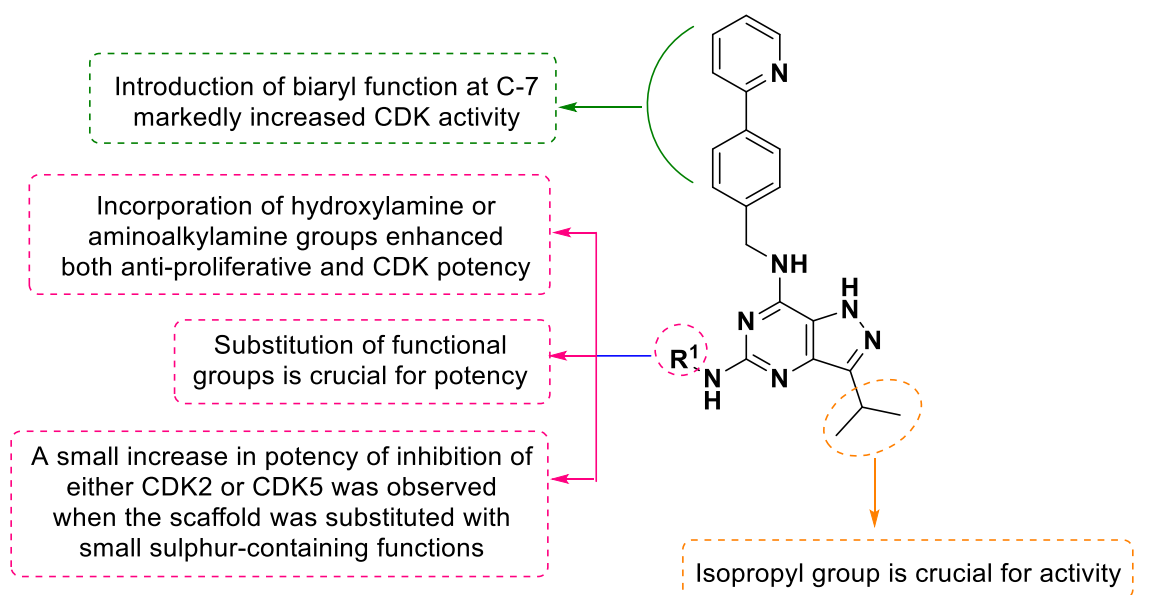


Fig. 10. Anticancer activity and SAR studies of 3,5,7-trisubstituted pyrazolo[4,3-*d*]pyrimidines.

In 2016, Vymetalova and co-workers reported the synthesis of 3-isopropyl-7-[4-(2-pyridyl)benzyl]amino-1(2)*H*-pyrazolo[4,3-*d*]pyrimidines and evaluated for their CDK inhibition activity. SAR study revealed that compounds contained hydroxyalkylamines at C-5 exhibited maximum potency for both CDK2 and CDK5. Compounds were also tested against K-562, MCF-7, G-361 and HCT-116 cell lines and the activity results are shown in **Fig. 11**. From the synthesized series, compounds **10**, **11**, **12** and **13** exhibited significant potency against CDK2 and CDK5 kinases, K-562, MCF-7, G-361 and HCT-116 cell lines. Further highly active compound **10** was screened against a panel of 50 protein kinases revealed its selectivity for CDKs.⁷⁹

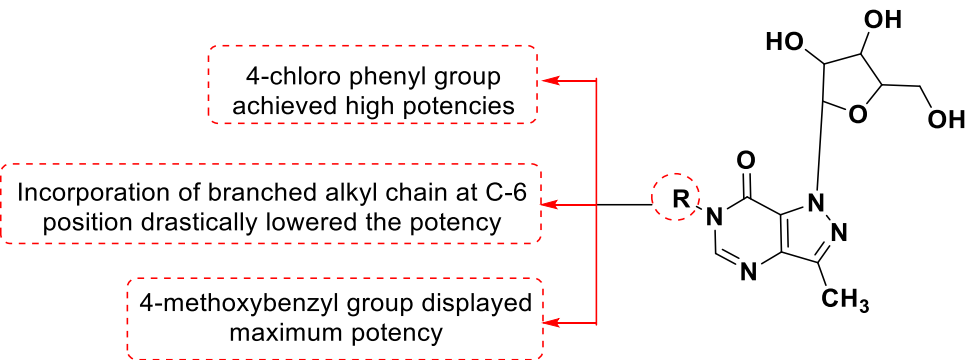


C. No	R ¹	IC ₅₀ (μM)					
		K-562	MCF-7	G-361	HCT-116	CDK2	CDK5
10		0.029	0.024	0.048	0.085	0.009	0.001
11		0.047	0.059	0.072	0.087	0.012	0.021
12		0.110	0.163	0.197	0.270	0.018	0.005
13		0.063	0.062	0.230	0.227	0.018	0.008

Fig. 11. SAR study of 3-isopropyl-7-[4-(2-pyridyl)benzyl]amino-1(2)*H*-pyrazolo[4,3-*d*]pyrimidines as potent CDK inhibitors.

3.2 Anti-infectious agents

In 1984, Baraldi and co-workers reported the synthesis and antiviral activity of 1-β-D-ribofuranosyl-3-methyl-6-substituted-7*H*-pyrazolo[4,3-*d*]pyrimidin-7-ones. From SAR studies, it was noted that significant activity was displayed for compounds with 4-methoxybenzyl and 4-chlorophenyl moieties at C-6 as shown in **Fig. 12**. From the series, compounds **14**, **15** and **16** exhibited moderate activity against herpes simplex virus type-1 (HSV-1) when compared to 5-iodo-2-deoxyuridine (IDU) as reference drug.¹⁷



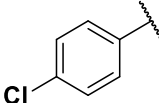
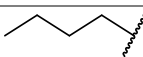
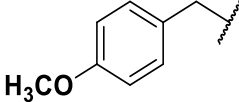
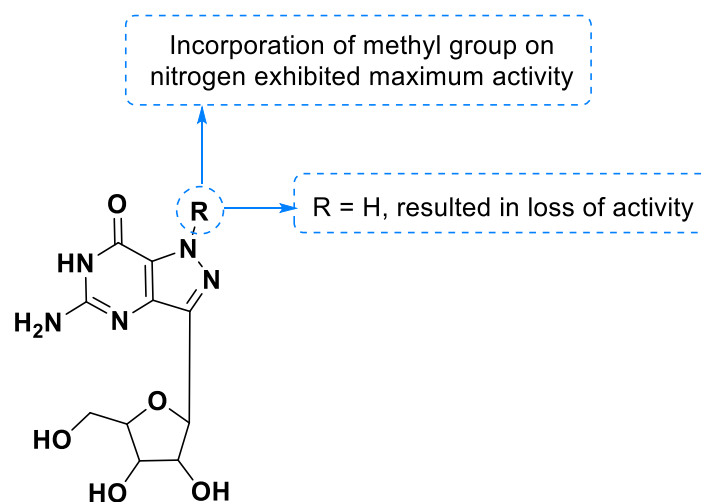
C. No	R	HSV-1 ED ₅₀ (μM)
14		50
15		152
16		49.5
IDU		1.2

Fig. 12. Structures and anti-viral activity of 1-β-D-ribofuranosyl-3-methyl-6-substituted-7H-pyrazolo[4,3-d]pyrimidin-7-ones against HSV-1.

In 1991, Sanghvi *et al.* reported *in vivo* anti-viral activity of pyrazolo[4,3-*d*]pyrimidines and related guanosine analogues prepared from formycin. Three derivatives were prepared and tested for their ability to inhibit certain RNA and DNA viral replication by *in vitro* and semliki forest virus infection by *in vivo* methods. From the synthesized compounds, 5-amino-1-methyl-3-β-D-ribofuranosyl-pyrazolo[4,3-*d*]pyrimidin-7(6*H*)-one (**17**) exhibited favourable protection survivor against a lethal dose of semliki forest virus infection in mice model as compared to the standard drug. A brief SAR study and activity data have been represented in **Fig. 13**.⁸⁰

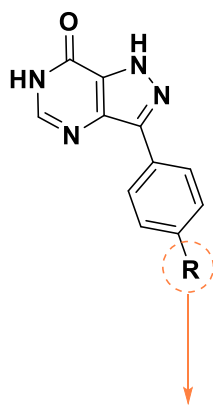


C. No	R	Dose ^a (mg/kg)	Survivors/total (%) ^b	Mean survival time ^c
17	CH ₃	200	7/12 (58)	7 ± 0.8
		100	8/12 (67)	8 ± 0.8
		50	8/12 (67)	6 ± 0.8
		30	6/12 (50)	9.2 ± 2.9
		10	1/12 (8)	9.6 ± 2.4
7-thia-8-oxo-guanosine		100	11/12 (92)	8 ± 0.0

a: Half daily doses were administered intraperitoneally at 24 and 18 hours relative to virus inoculation; b: Statistically significant ($p < 0.025$) determined by the two-tailed fisher exact test; c: Dead mice.

Fig. 13. Anti-viral activity of 5-amino-1-methyl-3-β-D-ribofuranosyl-pyrazolo[4,3-d]pyrimidin-7(6H)-one.

In 2011, Geffken and co-workers reported design and synthesis of pyrazolo[4,3-d]pyrimidin-4-ones and evaluated their pharmacological activity against bacterial and fungal strains. Of the screened compounds, 3-(4-bromophenyl)-1,6-dihydro-7H-pyrazolo[4,3-d]pyrimidin-7-one (**18**) exhibited moderate activity against *C. albicans* and inactive against other bacterial strains as compared to the standard drugs ampicillin and clotrimazole. SAR and antibacterial and fungal screening results are presented in **Fig. 14**.⁶⁴



Bromo substitution exhibited favorable activity than chloro, fluoro groups

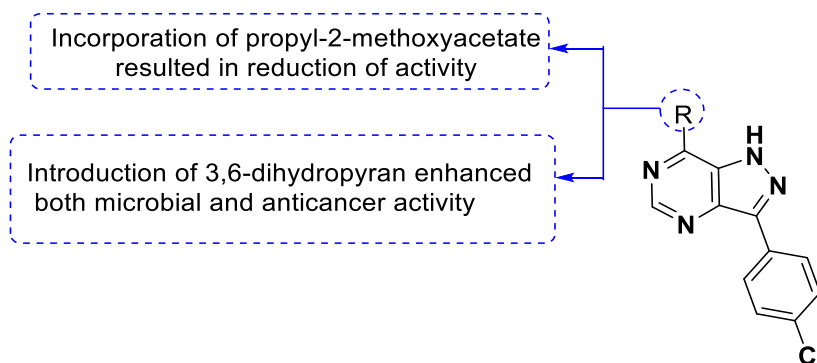
C. No	R	<i>S. aureus</i>		<i>E. Coli</i>		<i>P. aeruginosa</i>		<i>C. albicans</i>	
		(µg mL ⁻¹)		(µg mL ⁻¹)		(µg mL ⁻¹)		(µg mL ⁻¹)	
		MIC	MBC	MIC	MBC	MIC	MBC	MIC	MBC
18	Br	NA	NA	NA	NA	NA	NA	250	250
Clotrimazole		NA	NA	NA	NA	NA	NA	7.81	15.62
Ampicillin		3.9	15.62	7.81	31.25	250	500	NA	NA

NA: No activity.

Fig. 14. Anti-microbial values of 3-(4-bromophenyl)-1,6-dihydro-7H-pyrazolo[4,3-d]pyrimidin-7-one against different bacterial and fungal strains.

In 2016, Hafez and co-workers synthesized a series of novel 6-amino-3-(4-chlorophenyl)-5-methyl-1,6-dihydro-7H-pyrazolo[4,3-d]pyrimidin-7-one derivatives and evaluated them for their antimicrobial properties. All the synthesized molecules exhibited potent activity against gram positive and gram negative bacterial and fungal strains, comparable to that of standard drug. Compounds were also tested against HT29, HePG2 and MCF-7 cancer cell lines. Compounds **19** and **20** showed prominent results for both antimicrobial and anti-cancer activity. **Fig. 15** represents the structures, SAR studies and biological properties of active compounds along with reference drugs.³⁵

Chapter 3



C. No	R	Bacterial Strains				Fungi	
		Gram -ve		Gram +ve		MIC ($\mu\text{g mL}^{-1}$)	
		\forall ZI(mm)/MIC ($\mu\text{g mL}^{-1}$)	<i>C. albicans</i>	<i>A. flavus</i>			
		<i>E. Coli</i>	<i>P. aeruginosa</i>	<i>S. lactis</i>	<i>S. aureus</i>		
19		12/50	10/35	15/35	18/40	22/-	25/-
20		14/40	14/55	20/40	24/40	18/-	24/-
	Cefatoxime	26/13	18/10	30/12	31/15	-/-	-/-
	Nystatin	-/-	-/-	-/-	-/-	25/20	30/25

-/-: No activity; \forall Results expressed as inhibition zone (ZI) diameter in mm./Minimal inhibitory concentration (MIC)

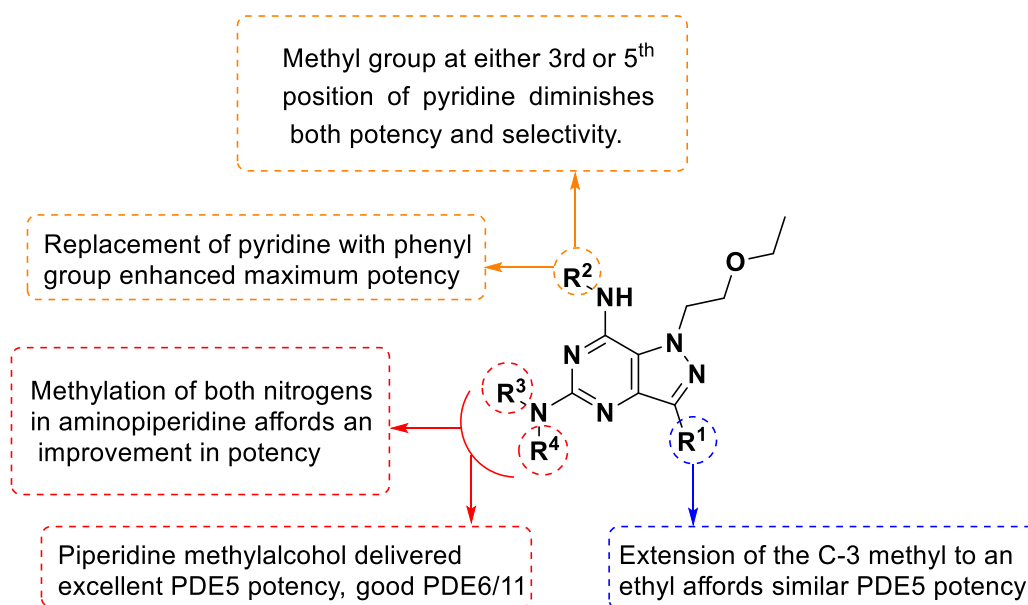
C. No	R	HT-29	HePG-2	MCF-7
		IC ₅₀ ($\mu\text{g mL}^{-1}$)	IC ₅₀ ($\mu\text{g mL}^{-1}$)	IC ₅₀ ($\mu\text{g mL}^{-1}$)
19		1.52 ± 0.09	1.62 ± 0.11	1.77 ± 0.15
20		0.88 ± 0.04	0.42 ± 0.12	0.62 ± 0.03

Fig. 15. Antimicrobial and anti-cancer properties of 6-amino-3-(4-chlorophenyl)-5-methyl-1,6-dihydro-7H-pyrazolo[4,3-*d*]-pyrimidin-7-one derivatives.

3.3. CNS Agents

3.3.1. Phosphodiesterase-5 inhibitor activity

In 2010, Tollefson et al. introduced a series of 1-(2-ethoxyethyl)-1*H*-pyrazolo[4,3-*d*]pyrimidines and determined their biological activity as potent phosphodiesterase-5 inhibitors (PDE5). From SAR study, it was revealed that the substitution of functional groups at C-3, C-5 and C-7 positions are necessary to achieve significant potency. From this series, compounds **21-24** exhibited significant potency, selectivity and efficacy against PDE5 as shown in **Fig. 16**. Further, the most active compound **24** of the series was incubated with human liver microsomes and observed that 87% of compound remained after 30 minutes time.⁸¹



C. No	R ¹	R ²	NR ³ R ⁴	PDE5 IC ₅₀ (nM)	PDE6/PDE5 ^a ratio	PDE11/PDE5 ^a ratio	HLM ^b
21	Et			0.07	140×	160×	81%

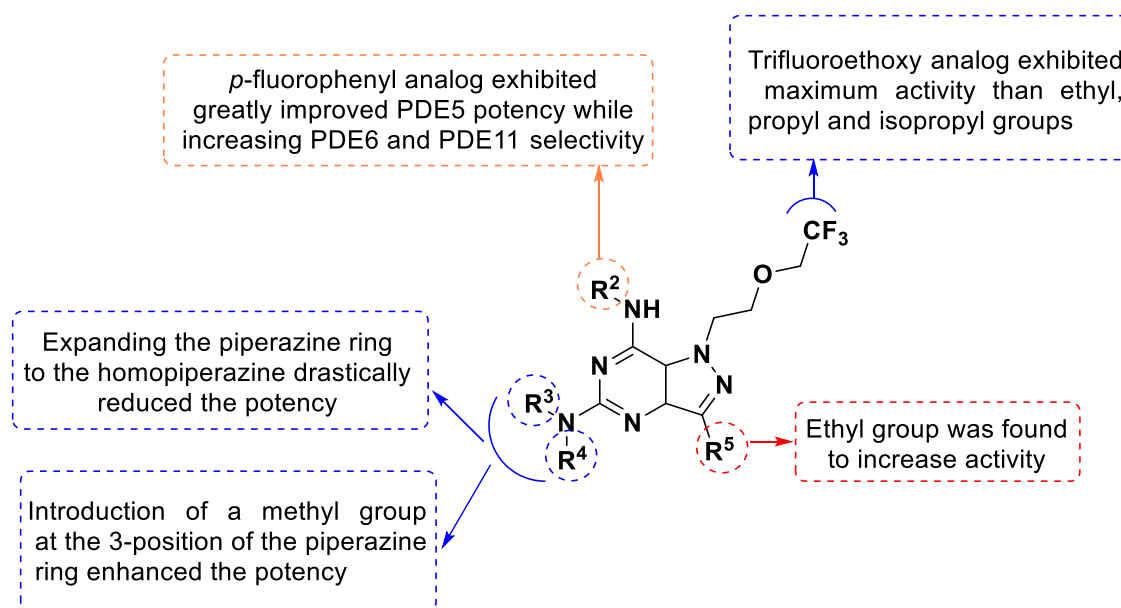
22	Et		0.087	110×	540×	36%
23	Et		0.07	100×	120×	28%
24	Et		0.04	100×	530×	87%

a: Ratios of IC_{50} 's.; b: Human liver microsome stability, % compound remaining after 30 minutes.

Fig. 16. SAR and phosphodiesterase inhibitory abilities of active compounds.

In 2010, Tollefson *et al.* reported the synthesis of a series of 1-(2-(2,2,2-trifluoroethoxy)ethyl)-1H-pyrazolo[4,3-d]pyrimidines as potent phosphodiesterase (PDE5/6/11) inhibitors. Among the series, compounds **25-28** displayed potent activity against PDE5. From SAR studies, it was revealed that the presence of trifluoroethoxyethyl group at N-1 position was necessary for significant PDE5 activity. The pharmacokinetic data of active compounds were examined by using dogs. Apart from these studies, authors also investigated *in vivo* model for efficacy in spontaneously hypertensive rats (SHR) to investigate the compound levels and blood pressure. Results of the active compounds and pharmacokinetic data are represented in **Fig. 17**.³⁴

Chapter 3



C. No	R ²	NR ³ R ⁴	R ⁵	PDE5 IC ₅₀ (nM)	PDE6/PDE5 ^a ratio	PDE11/PDE5 ^a ratio	HLM ^b
25			Me	0.78	420×	440×	83
26			Et	0.15	120×	2800×	96
27			Me	0.14	312×	14,700×	76 min ^c
28			Et	0.07	125×	27,000×	42 min ^c

a: Ratios of IC₅₀'s; b: Human liver microsome stability, % compound remaining after 30 minutes; c: HLM half life.

C. No	Dofetilide ^a (%)	hERG ^b		IV Dog PK ^c		SHR ^d
		IC ₅₀ (μM)	<i>t</i> _{1/2}	Cl	V _{dss}	
25	40.0	5.6	ND	ND	ND	ND

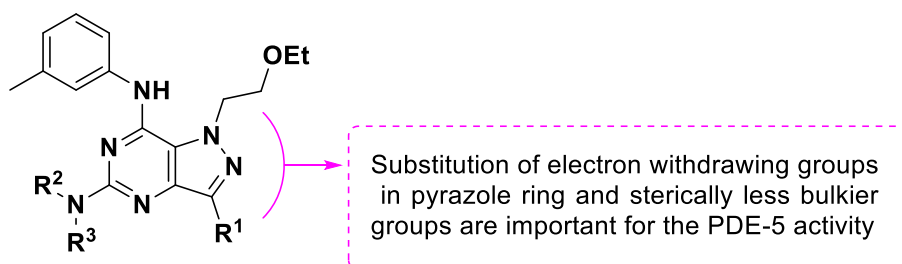
Chapter 3

26	10.7	5.1	6.7	20.2	8.0	+
27	24.7	9.0	4.9	22	9.4	++
28	18.8	1.4	5.1	18.5	7.8	++

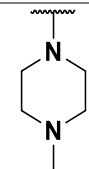
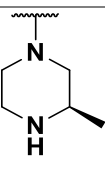
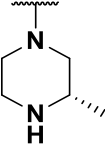
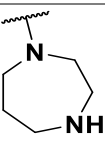
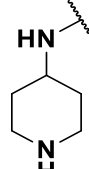
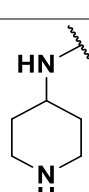
a: Percent inhibition of [3H]-dofetilide binding to the hERG protein stably expressed on HEK-293 cells following a 10 IM dose of test compound; b: hERG patch clamp electrophysiology assay, IC₅₀; c: Compound dosed at 0.2f–0.5e mpk in 10 kg beagles. Half-life (t_{1/2}) in h, clearance (Cl) in mL/min/kg, volume of distribution (V_{dss}) in L/kg; d: Compound dosed orally in spontaneously hypertensive rats (SHR) while monitoring MAP, + = decrease of 10–15 mmHg, ++ decrease of >15 mmHg.

Fig. 17. SAR and pharmacokinetic properties of piperazine linked pyrazolo[4,3-*d*]pyrimidines as potent phosphodiesterase inhibitors.

In 2015, Choudhari *et al.* reported the three dimensional quantitative structure-activity relationship (3D-QSAR), pharmacophore identification studies on a series of 1-(2-ethoxyethyl)-1*H*-pyrazolo[4,3-*d*]pyrimidines as PDE5 inhibitors. Two different QSAR models (multiple linear regression analysis and kNN-MFA analysis) were used to carry out identification studies on 32 molecules and observed that both techniques showed similar results. From the obtained results, they concluded kNN-MFA technique can be utilized for cross validation of the results of multiple linear regression studies. A brief SAR and QSAR results of compounds **29-35** are presented in **Fig. 18**.⁸²



C. No	R ¹	NR ² R ³	3D QSAR by MLR ^a			D QSAR by kNN-MFA ^b		
			Obs. Act [§]	Pre. Act ^ε	Res.	Obs. Act	Pre. Act	Res.
29	Me		-0.41497	-0.50069	0.085718	-0.41497	-0.34802	-0.06696

30	Et		0.05061	0.043787	0.006823	0.05061	-0.07732	0.127927
31	Et		-0.39794	-0.12422	-0.27373	-0.39794	-0.35668	-0.04126
32	Et		-0.07918	-0.03801	-0.04117	-0.07918	-0.2384	0.159214
33	Et		0.119186	0.098904	0.020282	0.119186	-0.08439	0.203571
34	Me		-0.36173	-0.27329	-0.08844	-0.36173	0.03908	0.40075
35	Et		0.69897	0.87657	-0.1776	0.69897	0.47816	0.220824

a: Multiple linear regression; b: k-nearest neighbour molecular field analysis; §: Observed activity; €: previous activity.

Fig. 18. 3D-QSAR studies of 1-(2-ethoxyethyl)-1H-pyrazolo[4,3-d]pyrimidines as PDE5 inhibitors.

In 2016, Rabal and co-workers described the synthesis and biological evaluation of pyrazolo[4,3-*d*]pyrimidines as first-in-class dual acting histone deacetylases (HDACs) and PDE5 inhibitors for the treatment of Alzheimer's disease. Role of functional groups at C-5 position in achieving potent inhibitory activity against PDE-5, HDAC-2 and HDAC-6 has been elaborated in **Fig. 19**. From the tested series, compounds **36-39** showed promising activity with IC₅₀ values ranging from 0.5 to 60 nM against PDE-5, while the hit compound **37** exhibited PDE-5 inhibition at 3 nM. The identified lead compound **39** demonstrated higher selectivity for HDAC-6 (IC₅₀ = 91 nM) over other isoforms of HDAC.⁸³

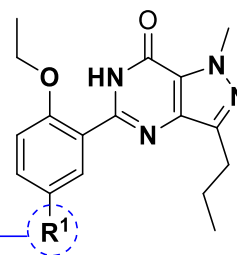
Chapter 3

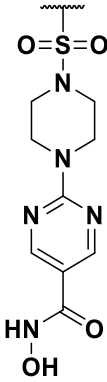
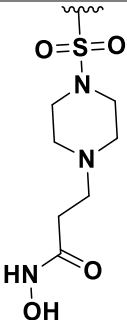
Incorporation of *N*-hydroxy-3-cyclo butane-1-carboxamide moiety through alkyl linker resulted in good activity and selectivity against both PDE-5, HDAC-6

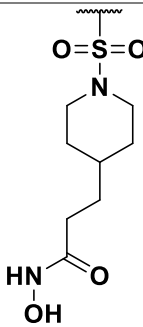
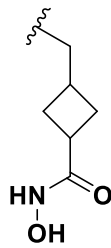
Observed more flexibility between sildenafil core and hydrophobic linker by introducing secondary amine as an attachment point

Pyrimidyl groups presented high potency than phenyl groups

Replacement of the sulfonamide group tended to result in a slight decrease in the potency for PDE-5



C. No	R ¹	IC ₅₀ (nM)				
		PDE-5	HDAC-1	HDAC-2	HDAC-3-NCOR-2	HDAC-6
36		3	8	117	36	268
37		3	10500	>20000	NA	2360

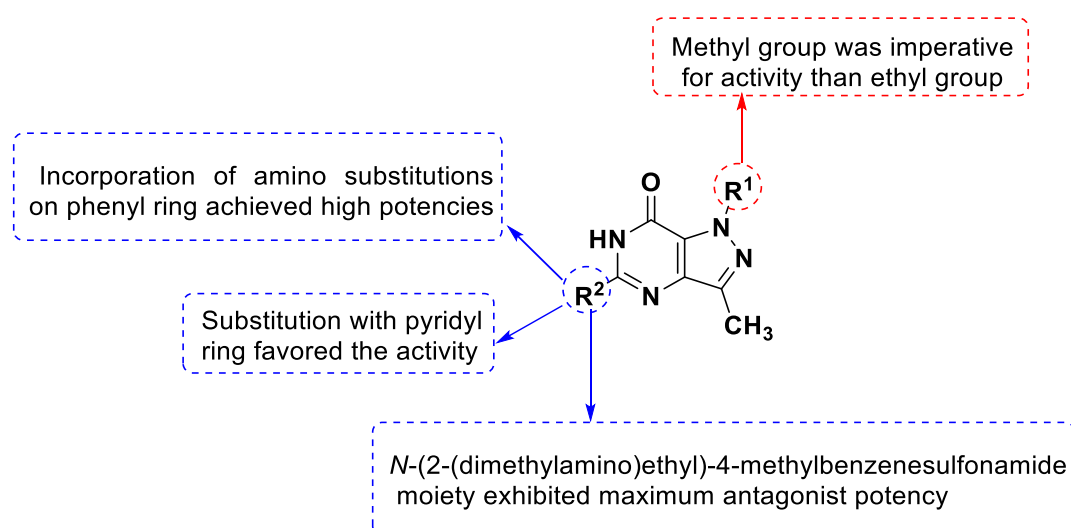
38		0.5	406	1940	NA	87
39		60	310	490	322	91

NA: No activity; HDACs: dual acting histone deacetylases.

Fig. 19. Structures, biological results of active compounds as potent PDE5 inhibitors.

3.3.2. Adenosine receptor antagonist's activity

In 1987, Hamilton and co-workers reported synthesis of 1,3-dialkylpyrazolo[4,3-*d*]pyrimidin-7-ones and evaluated their pharmacological properties for adenosine receptor antagonists. From the synthesized series, compounds **40-42** exhibited excellent potency towards adenosine A₁ receptors. SAR studies indicated that *N*-(2 (dimethylamino)ethyl) benzenesulfonamide group at C-5 and methyl group at C-3 position was responsible for higher activity as depicted **Fig.20**.³¹



C. No	R ¹	R ²	Antagonist activity IC ₅₀ (nM)
-------	----------------	----------------	---

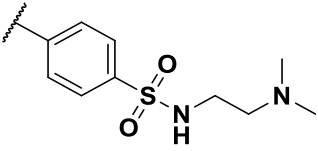
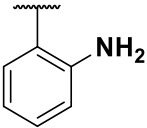
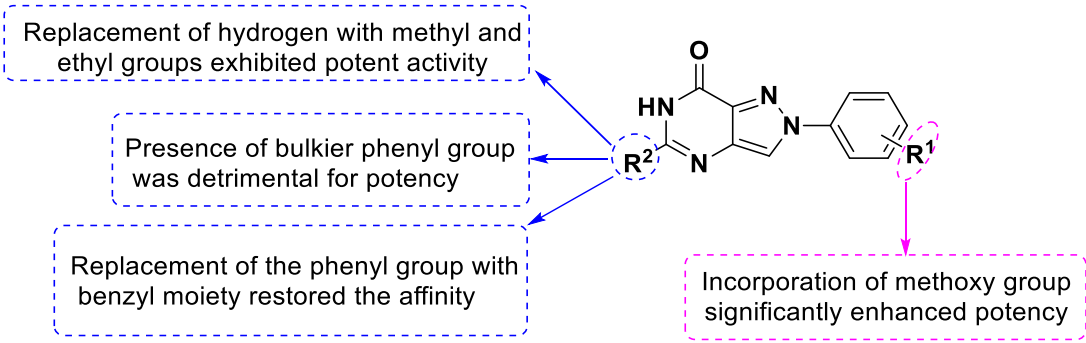
40	CH ₃		68
41	CH ₃		230
42	C ₂ H ₅	4-pyridyl	250

Fig. 20. SAR and adenosine receptor antagonist activity of 1,3-dialkyl pyrazolo[4,3-*d*]pyrimidin-7-ones.

In 2009, Lenzi and co-workers reported synthesis and biological evaluation of 2-phenyl pyrazolo[4,3-*d*]pyrimidines as potent and selective human A₃ adenosine receptor antagonists. SAR studies indicated that presence of small lipophilic substituent at C-5 position was important for significant activity. From series, compound **43** [2-(4-methoxyphenyl)-5-methyl-2,6-dihydro-7*H*-pyrazolo[4,3-*d*]pyrimidin-7-one] exhibited potent activity as represented in **Fig. 21**.⁶²



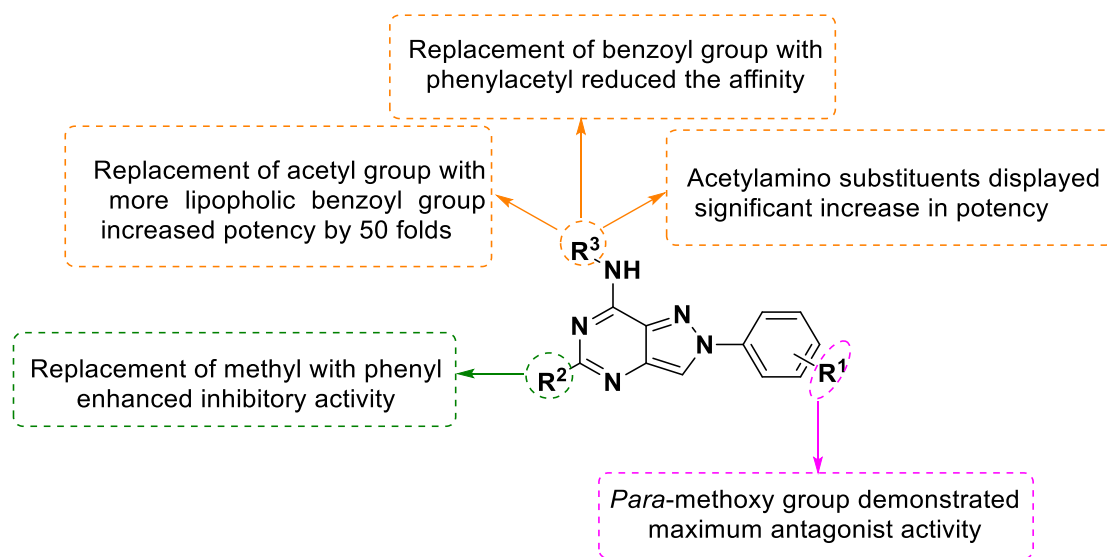
C. No	R ¹	R ²	Binding experiments K _i (nM)			cAMP assays IC ₅₀ (nM)	
			hA ₃ ^a	hA ₁ ^b	hA _{2A} ^c	hA _{2B} ^d	hA ₃ ^e
43	4-OCH ₃	CH ₃	1.2 ± 0.1	5%	1%	2%	5.2 ± 0.5

a: Displacement of specific [¹²⁵I]AB-MECA binding to hA₃ CHO cells, where K_i values are mean values (SEM of four separate assays each performed in duplicate. Percentage of inhibition in [¹²⁵I]AB-MECA competition binding assays to hA₃CHO cells at 1 μM tested compounds; b: Percentage of inhibition in [³H]DPCPX competition binding assays to hA₁CHO cells at 1 μM tested compounds; c: Percentage of inhibition in [³H]ZM241385 competition binding assays to hA_{2A}CHO cells at 1 μM tested compounds; d: Percentage of inhibition on cAMP experiments in hA_{2B}CHO cells, stimulated by 200 nM NECA, at 1 μM examined compounds; e: IC₅₀ values are expressed as mean values (SEM of four separate cAMP experiments in hA₃CHO cells, inhibited by 100 nM Cl-IB-MECA.

Fig. 21. SAR and human A₃ adenosine receptor antagonist activity of 2-(4-methoxyphenyl)-5-methyl-2,6-dihydro-7*H*-pyrazolo[4,3-*d*]pyrimidin-7-one.

Chapter 3

In 2013, Squarcialupi *et al.* reported synthesis, molecular modelling and pharmacological evaluation of 2-arylpyrazolo[4,3-*d*]pyrimidin-7-amino derivatives as human A₃ adenosine receptor antagonists. SAR studies suggested that *para*-methoxy group on 2-phenyl ring at C-2 position, lipophilic groups at C-5 and acyl groups at C-7 position are essential for significant potency. From the set of series synthesized, compounds **44-46** exhibited good activity. A brief SAR along with active most compounds are presented in **Fig. 22**.⁸⁴



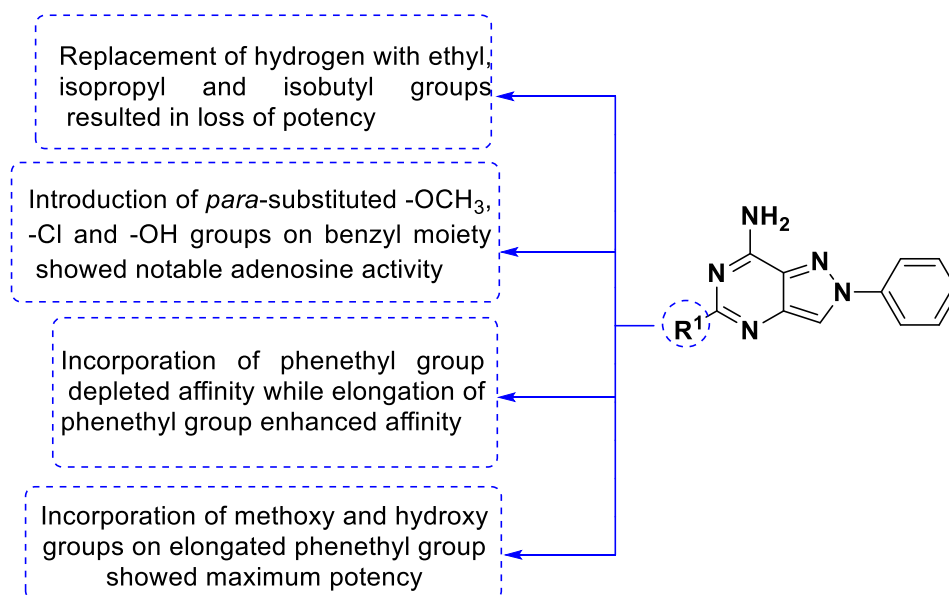
C. No	R ¹	R ²	R ³	Binding experiments ^a				cAMP assays	
				K _i (nM) or I%				IC ₅₀ (nM)	
				hA ₁ ^b	hA _{2A} ^c	hA ₃ ^d	rA ₃ ^e	hA _{2B} ^f	hA ₃ ^g
44	H	CH ₃	CO-C ₆ H ₄ - OCH ₃	4%	1%	2.4 ± 0.2	NIL	1%	NIL
45	H	CH ₃	CO-Ph	30%	1%	5.6 ± 0.5	6%	2%	2.4 ± 0.2
46	OCH ₃	Ph	CO-Ph	3%	1%	18 ± 2	12%	2%	63 ± 5

a: K_i values are means ± SEM of four separate assays each performed in duplicate. Percentage of inhibition (I%) is determined at 1 μM concentration of the tested compounds; b: Displacement of specific [³H]DPCPX competition binding assays to hA₁CHO cells; c: Displacement of specific [³H]ZM241385 competition binding to hA₂ACHO cells; d: Displacement of specific [¹²⁵I]AB-MECA competition binding to hA₃CHO cells; e: Percentage of inhibition (I%) in [¹²⁵I]AB-MECA competition binding assays to rA₃HEK cells. f: cAMP experiments in hA_{2B}CHO cells, stimulated by 200 nM NECA. IC₅₀ values are expressed as means ± SEM of four separate cAMP experiments. Percentage of inhibition (I%) is determined at 1 μM concentration of the tested compounds; g: IC₅₀ values are expressed as means ± SEM of four separate cAMP experiments in hA₃CHO cells, in the presence of 100 nM Cl-IB-MECA.

Fig. 22. Structures, binding results of 7-amino-2-phenylpyrazolo[4,3-*d*]pyrimidines as A₃ adenosine receptor antagonists.

Chapter 3

In 2014, Squarcialupi *et al.* reported molecular modeling and biological properties of 7-amino-2-phenylpyrazolo[4,3-*d*]pyrimidines as A₁ and A_{2A} adenosine receptors. SAR studies revealed that affinity and selectivity were based on the nature of the functional groups at C-5 position as depicted in **Fig. 23**. In this series, compounds **47-52** exhibited potent activity against both human A₁ and A_{2A} adenosine receptors.⁶⁹



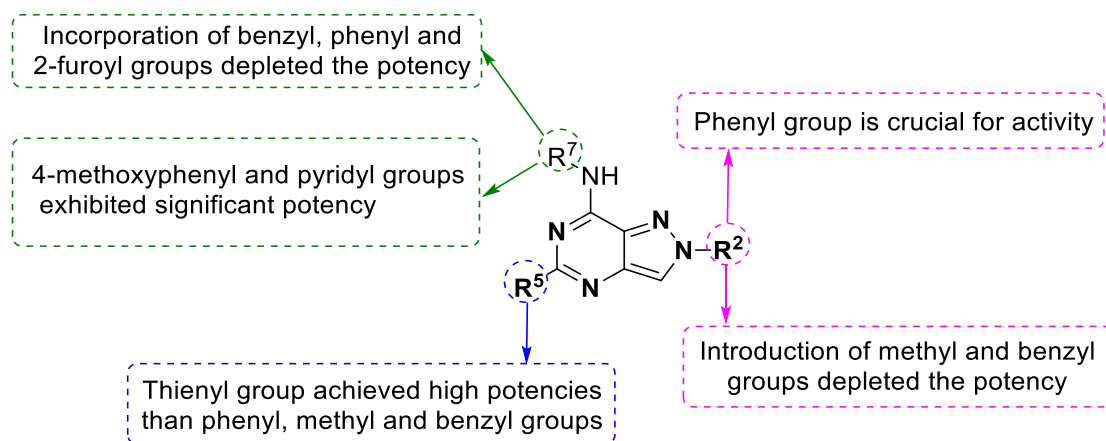
C. No	R ¹	Binding experiments ^a			cAMP assays
		K _i (nM) or I%			IC ₅₀ (nM) or I%
		hA ₁ ^b	hA _{2A} ^c	hA ₃ ^d	hA _{2B} ^e
47	2-F-C ₆ H ₄ -CH ₂ -	35 ± 4	154 ± 13	37%	123 ± 11
48	Ph-(CH ₂) ₃	5.31 ± 0.42	55 ± 5	12%	42%
49	2-OMe-C ₆ H ₄ -(CH ₂) ₃	1.31 ± 0.15	1.53 ± 12	47%	387 ± 36
50	3-OMe-C ₆ H ₄ -(CH ₂) ₃	0.15 ± 0.02	147 ± 13	33%	334 ± 27
51	2-OH-C ₆ H ₄ -(CH ₂) ₃	0.54 ± 0.05	102 ± 9	36%	247 ± 18
52	3-OH-C ₆ H ₄ -(CH ₂) ₃	0.22 ± 0.03	146 ± 15	46%	314 ± 26

a: K_i values are means ± SEM of four separate assays each performed in duplicate. Percentage of inhibition (I%) are determined at 1 μM concentration of the tested compounds; b: Displacement of specific [³H]DPCPX competition binding assays to hA₁CHO cells; c: Displacement of specific [³H]ZM241385 competition binding to hA_{2A}CHO cells; d: Displacement of specific [¹²⁵I]AB-MECA competition binding to hA₃CHO cells; e: cAMP experiments in hA_{2B}CHO cells, stimulated by 200 nM NECA. IC₅₀ values are expressed as means ± SEM of four separate cAMP experiments. Percentage of inhibition (I%) are determined at 1 μM concentration of the tested compounds.

Fig. 23. SAR and A₁ and A_{2A} adenosine receptor activity of pyrazolo[4,3-*d*]pyrimidines.

Chapter 3

In 2016, Squarcialupi *et al.* reported structural refinement of pyrazolo[4,3-*d*]pyrimidine derivatives to obtain potent and selective antagonists for the human A₃ adenosine receptors. SAR studies presented the significance of phenyl group at C-2, 2-thienyl moiety at C-5 and acyl groups at C-7 positions for favorable activity as illustrated in **Fig. 24**. However, outcome of this work concluded that compounds **53-55** exhibited potent activity against A₃ adenosine receptors.⁷³



C. No	R ²	R ⁵	R ⁷	Binding experiments ^a			cAMP assays	
				K _i (nM) or I%			IC ₅₀ (nM) or I%	
				hA ₁ ^b	hA _{2A} ^c	hA ₃ ^d	hA _{2B} ^e	hA ₃ ^f
53	Ph	2-thienyl	C ₆ H ₄ -OMe	1%	1%	0.027 ± 0.003	1%	0.11 ± 0.01
54	Ph	2-thienyl	3-pyridyl	764 ± 68	3%	0.41 ± 0.04	1%	0.01 ± 0.09
55	Ph	C ₆ H ₄ -OMe	C ₆ H ₄ -OMe	3%	1%	1.31 ± 0.12	1%	4.27 ± 0.03

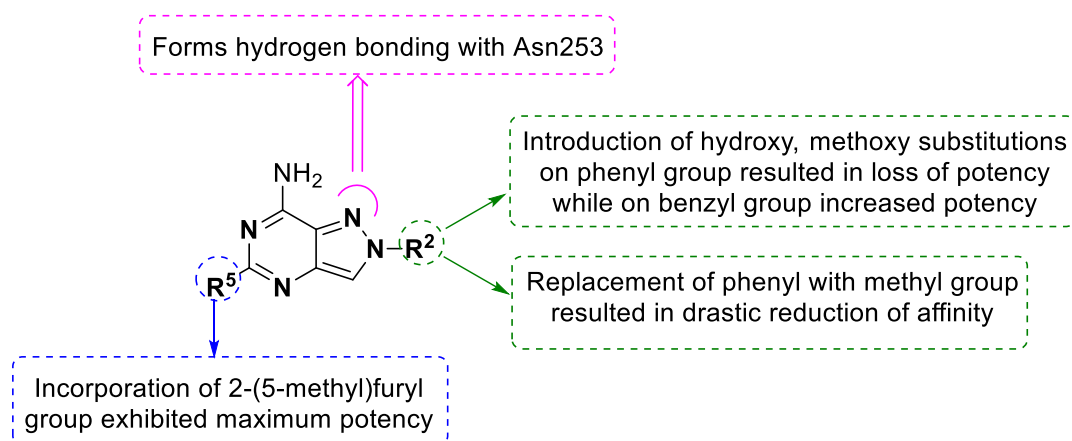
a: K_i values are means ± SEM of four separate assays each performed in duplicate. Percentage of inhibition (I%) are determined at 1 μM concentration of the tested compounds; b: Displacement of specific [³H]DPCPX competition binding assays to hA₁CHO cells; c: Displacement of specific [³H]ZM241385 competition binding to hA_{2A}CHO cells; d: Displacement of specific [¹²⁵I]AB-MECA competition binding to hA₃CHO cells; e: cAMP experiments in hA_{2B}CHO cells, stimulated by 200 nM NECA. IC₅₀ values are expressed as means ± SEM of four separate cAMP experiments. Percentage of inhibition (I%) are determined at 1 μM concentration of the tested compounds.

Fig. 24. SAR and human A₃ adenosine receptor activity of lead compounds consisting pyrazolo[4,3-*d*]pyrimidine.

In 2016, Squarcialupi *et al.* synthesized 7-aminopyrazolo[4,3-*d*]pyrimidines to evaluate structural modification at C-2 and C-5 positions to afford significant activity against human A₁ and A_{2A} adenosine receptors. SAR study revealed that incorporation of 2-methoxybenzyl group at C-2 region and 5-

Chapter 3

methylfuran-2-yl at C-5 region enhanced the adenosine activity as shown in **Fig. 25**. From the series, compounds **56-59** displayed promising activity against both A₁ and A_{2A} receptors.⁷²



C. No	R ²	R ⁵	^a Binding experiments			cAMP assays
			K _i (nM) or I%			IC ₅₀ (nM) or I%
			hA ₁	hA _{2A}	hA ₃	hA _{2B}
56			18 ± 2	3.62 ± 0.34	82 ± 7	30%
57			126 ± 11	5.26 ± 0.47	88 ± 6	293 ± 26
58			308 ± 8	57 ± 6	498 ± 47	354 ± 32
59			252 ± 21	51 ± 5	427 ± 41	421 ± 39

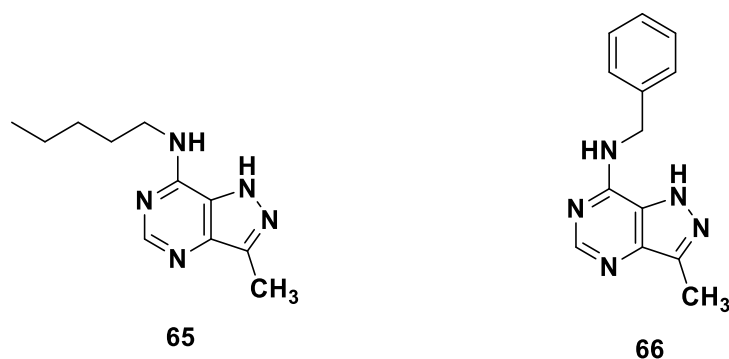
a: K_i values are means ± SEM of four separate assays each performed in duplicate. Percentage of inhibition (I%) are determined at 1 μM concentration of the tested compounds; b: Displacement of specific [³H]DPCPX competition binding assays to hA₁CHO cells; c: Displacement of specific [³H]ZM241385 competition binding to hA_{2A}CHO cells; d: Displacement of specific [¹²⁵I]AB-MECA competition binding to hA₃CHO cells; e: cAMP experiments in hA_{2B}CHO

C. No	R	Range tested	Cytokinin activity IC ₅₀ (μM)		Antagonist activity IC ₅₀ (μM)	
			Detection	Maximum growth	Detection	Lethal dosage
62		0.009-20	NA	NG	0.03	0.2
63		0.009-20	NA	NG	0.03	0.5
64		0.009-20	NA	NG	0.1	0.73

NA: No activity; NG: No growth.

Fig. 27. SAR of 7-substituted 3-methylpyrazolo[4,3-*d*]pyrimidines as cytokinin antagonists in tobacco bioassay.

In 1980, Gregorini and co-workers reported synthesis of 7-(pentylamino), 7-(benzylamino)-3-methylpyrazolo[4,3-*d*]pyrimidines and evaluated them as cytokinin antagonists on suspension-cultured tobacco cells. All molecules were found highly inhibitory to cytokinin-autonomous and cytokinin-requiring tobacco cells. The structures of active compounds (**65**, **66**) and cytokinin activity results are represented in **Fig. 28**.³²



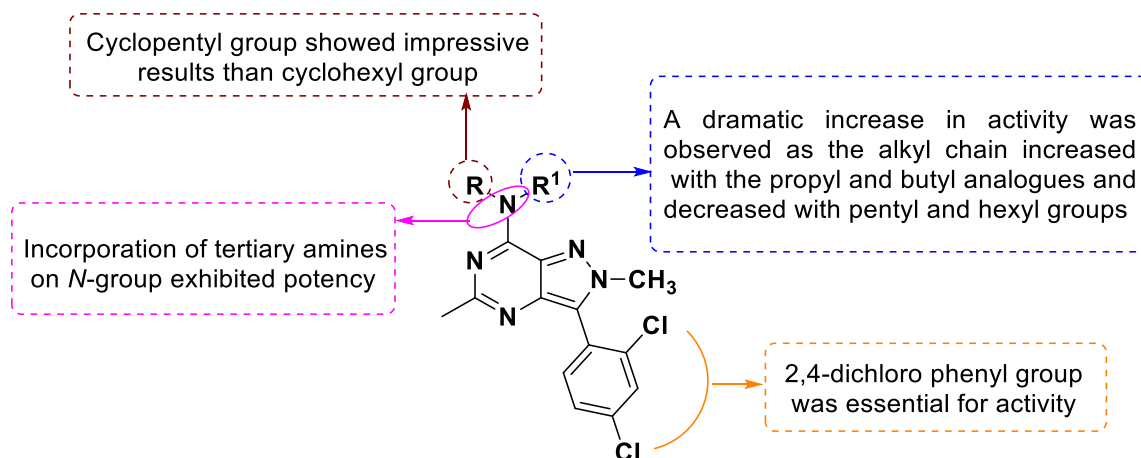
C. No	cytokinin-autonomous tobacco cells		cytokinin-requiring tobacco cells	
	IC ₅₀ (μM)		IC ₅₀ (μM)	
	I ₅₀ *	I ₁₀₀ *	I ₅₀	I ₁₀₀
65	0.025	0.05	0.02	0.05
66	0.03	0.1	0.04	0.15

*I₅₀ and I₁₀₀ correspond to concentrations of analogs which produce 50% and 100% of growth inhibition, respectively.

Fig. 28. Cytokinin activity of pyrazolo[4,3-*d*]pyrimidines on various tobacco cells.

3.5. Miscellaneous agents

In 2002, Yuan and co-workers reported the synthesis and pharmacological evaluation of 3-aryl pyrazolo[4,3-*d*]pyrimidine derivatives as potential corticotropin releasing factor-1 (CRF-1) antagonists. SAR studies reveal the effect of substitutions on nitrogen at C-7 and at C-3 positions as depicted in **Fig. 29**. From the reported series, compounds **67-70** exhibited significant antagonist activity against nonpeptide CRF-1.³³

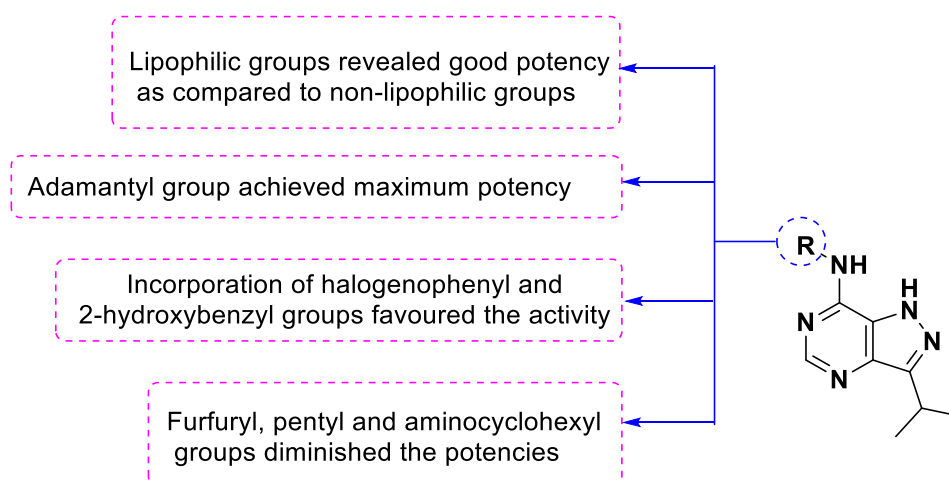


Chapter 3

C. No	R	R ¹	CRF ₁ Binding K _i (nM)
67	<i>n</i> -propyl	<i>n</i> -propyl	2 ± 1
68	(CH ₂) ₂ OCH ₃	(CH ₂) ₂ OCH ₃	3 ± 2
69	Ethyl	<i>n</i> -butyl	2 ± 1
70	Ethyl	<i>n</i> -propyl	3 ± 2

Fig. 29. SAR, structures and CRF-1 binding affinity studies of lead compounds.

In 2011, Jorda *et al.* reported a series of 3,7-disubstituted pyrazolo[4,3-*d*]pyrimidine derivatives and evaluated them for anti-leishmanial and CRK/CYC6 (cdc2-related kinase/ Cyclin 6) kinase activity. Among the tested series, compounds **71-74** exhibited potential activity whose SAR studies revealed that the lipophilic groups (namely adamantyl, halo substituted phenyl and 2-hydroxybenzyl) at C-7 position were responsible for increased activity whereas, non-lipophilic (furyl) and lipophilic (pentyl) groups lowered the activity as discussed in **Fig. 30**.¹⁹



C. No	R	Leishmanial donovani axeaxenicaxenic amastigotes inhibition		CRK/CYC6 kinase inhibition	
		(%) ^a	EC ₅₀ (μM)	(%) ^b	IC ₅₀ (μM) ^c
71	2-hydroxybenzyl	87.4 ± 0.4	35.7	68.0 ± 2.1	11.91
72	Adamantan-1-yl	73.2 ± 0.0	1.22	93.8 ± 0.3	1.82
73	4-F-Ph	75.8 ± 1.7	11.6	78.8 ± 0.4	6.8

74	3-Cl-Ph	73.3 ± 1.1	12.4	81.3 ± 2.3	9.86
----	---------	------------	------	------------	------

a: In the presence of 30 μ M compound; b: In the presence of 15 ATP with 30 μ M compound; c: In the presence of 15 μ M ATP.

Fig. 30. Anti-leishmanial activity and SAR studies of 3,7-disubstituted pyrazolo[4,3-*d*]pyrimidines.

3.6. Patents covering pyrazolo[4,3-*d*]pyrimidine scaffold with diverse biological activities

Pharmacological significance of pyrazolo[4,3-*d*]pyrimidine scaffold is further proved based on several patents registered from 1976 to 2012. Different research groups patented this nucleus for numerous therapeutic sections are briefly presented in **Table-1**.

Research group	Patent number	Target activity	Year
Ratajczyk	US3939161	Anti-convulsant, sedative, anti-inflammatory and gastric anti-secretory agents. ⁸⁷	1976
Hecht	US4282361	Various schemes for synthesis. ⁸⁸	1981
Fujikawa	US4654348	Anti-hyperlipidemic agents. ⁸⁹	1987
Hamilton	US4663326	A ₁ adenosine and cardiovascular. ⁹⁰	1987
Hamilton	US4666908	PDE5 inhibitors. ⁹¹	1987
Hamilton	WO8800192	Anti-anxiety, asthma and allergic agents. ⁹²	1988
Yuan	US5723608	CRF ₁ receptor antagonists. ⁹³	1998
Zhihua	WO0014088	Male erectile dysfunction. ⁹⁴	2000
Lu	US6204383 B1	Synthetic process for preparing sildenafil. ⁹⁵	2001
Yuan	US6211187 B1	CRF ₁ receptor ligands. ⁹⁶	2001
Bunnage	WO0127113 A2	Male erectile dysfunction and female sexual dysfunction. ³⁸	2001
Daniela	EP1348707 A1	Diagnostic agents. ³⁶	2003
Jonas	US6777419 B1	PDE5 inhibitors. ⁹⁷	2004
Eggenweiler	US20040023990	Asthma, allergic and female sexual disorder. ⁹⁸	2004
Eggenweiler	US20040063730 A1	Hypertension, angina and pulmonary hypertension. ⁹⁹	2004
Eggenweiler	US20040077664 A1	Hypertension, angina and bronchitis. ¹⁰⁰	2004

Chapter 3

Hodgetts	CA2537916 A1	CRF ₁ receptor modulators. ¹⁰¹	2005
Hodgetts	WO2005028480 A2	Selective modulators of CRF ₁ receptors. ¹⁰²	2005
Bell	WO2005097799 A1	PDE5 inhibitors. ¹⁰³	2005
Pal	US20060128729 A1	Anti-inflammatory. ³⁷	2006
Acker	WO2006046135 A2	PDE5 inhibitors. ¹⁰⁴	2006
Bell	US7262192 B2	PDE5 inhibitors. ¹⁰⁵	2007
Butora	US7534767 B2	RNA dependent RNA viral polymerase. ¹⁰⁶	2009
Bell	US7569572 B2	PDE5 inhibitors. ¹⁰⁷	2009
Bell	US7572799 B2	PDE5 inhibitors. ¹⁰⁸	2009
Moravcova	US7745450 B2	Cancer. ¹⁰⁹	2010
Bell	US8097621 B2	PDE5 inhibitors. ¹¹⁰	2012

Table 1. Pyrazolo[4,3-*d*]pyrimidine nucleus containing patents having numerous biological Activities.

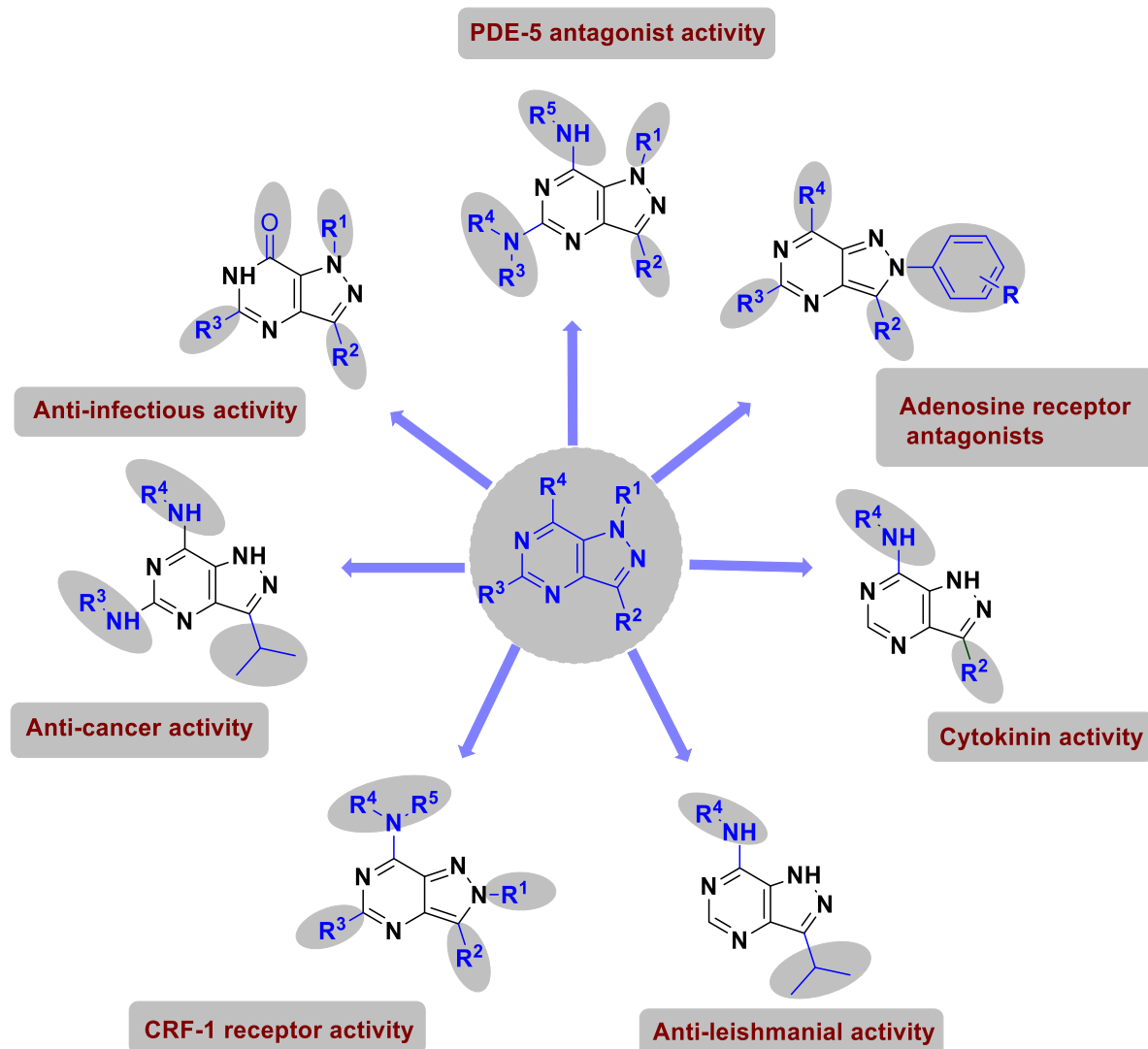


Fig. 31. Summary of structural amendments to influence the biological activity.

4. Conclusion

Nitrogen containing heterocycles have been a versatile class of compounds displaying array of biological properties. Pyrazolo[4,3-*d*]pyrimidine is a significant framework that is being explored exponentially for its multifarious medicinal properties. The present manuscript at the beginning has emphasized numerous methods for synthesizing variously substituted pyrazolo[4,3-*d*]pyrimidines through conventional, multi-component and microwave-assisted reaction methods. Apart from remarkable synthetic evolutions, pyrazolo[4,3-*d*]pyrimidine derivatives have been found to unveil a diverse set of pharmaceutical properties. Numerous applications along with patents (**Table 1**) have been explored based on their biochemical, biophysical and medicinal aspects and much more is yet to be explored. Medicinal properties of pyrazolo[4,3-*d*]pyrimidines have been broadly examined for diverse biological activities such as

antimicrobial, human adenosine antagonists, anticancer, CNS depressant, phosphodiesterase 5 inhibitors and other applications such as anti-leishmanial and cytokinin inhibitors. Many of the researchers have successfully achieved the modifications over the pyrazolo[4,3-*d*]pyrimidine scaffold and have investigated them on diverse biological activities. These activity profiles could be regulated by suitable selection of the fused heterocycles and the substitutions on the pyrazolo[4,3-*d*]pyrimidine scaffold. Substitutions on C-3, C-5 and C-7 positions of pyrazolo[4,3-*d*]pyrimidine showed distinct anti-cancer activity, whereas substitutions at N-1, C-3 and C-5 positions showed antibacterial activity. Further, the sites of modifications on pyrazolo[4,3-*d*]pyrimidine scaffold and variation of biological activity has been represented in **Fig. 31**. A wide range of synthetic pathways and varied biological properties have opened the door for the discovery of novel drug candidates and other target activities. In addition, the current manuscript can be valuable to researchers to find out novel, optimized and target selective pyrazolo[4,3-*d*]pyrimidine compounds and its use in the treatment of some more incurable diseases.

5 Conflicts of Interest

Authors hereby declare that there are no financial/commercial conflicts of interest.

6 Acknowledgement

The authors are thankful to the College of Health Sciences, University of KwaZulu-Natal, Durban, South Africa for the facilities and financial support.

References

- [1] X.F. Wu, H. Neumann, M. Beller, *Chem. Rev.* 2013, 113, 1–35.
- [2] S. P. Singh, Surendra S. Parmar, K. Raman, V. I. Stenberg, *Chem. Rev.* 1981, 81, 175–203.
- [3] K. Bozorov, J-Y. Zhao, B. Elmuradov, A. Pataer, H. A. Aisa, *Eur. J. Med. Chem.* 2015, 102, 552–573.
- [4] T. A. Krenitsky, G. B. Elion, R. A. Strelitz, G. H. Hitchings, *J. Biol. Chem.* 1967, 242, 2675–2682.
- [5] A.S. Hassan, T.S. Hafez, S.A. Osman, *Sci. Pharm.* 2015, 83, 27–39.
- [6] Y. Li, W. Gao, F. Li, J. Wang, J. Zhang, Y. Yang, S. Zhang, L. Yang, *Mol. Biosyst.* 2013, 9, 2266–2281.
- [7] P.B. Yu, C.C. Hong, C. Sachidanandan, J.L. Babitt, D.Y. Deng, S.A. Hoyng, H.Y. Lin, K.D. Bloch, R.T. Peterson, *Nat Chem Biol.* 2008, 4, 33–41.
- [8] M. Drev, U. Groselj, S. Mevec, E. Pusavec, J. Strekelj, A. Golobic, G. Dahmann, B. Stanovnik, J. Svete, *Tetrahedron.* 2014, 70, 8267–8279.
- [9] N. Kato, M. Oka, T. Murase, M. Yoshida, M. Sakairi, S. Yamashita, Y. Yasuda, A. Yoshikawa, Y. Hayashi, M. Makino, M. Takeda, Y. Mirenska, T. Kakigami, *Bioorg. Med. Chem.* 2011, 19, 7221–7227.
- [10] P. Kaswan, K. Pericherla, D. Purohit, A. Kumar, *Tetrahedron Lett.* 2015, 56, 549–553.
- [11] N.K. Terrett, A.S. Bell, D. Brown, P. Ellis, *Bioorg. Med. Chem. Lett.* 1996, 6, 1819–1824.
- [12] B.M. Dean, D. Perrett, *Br. J. Clin. Pharmacol.* 1974, 1, 119–127.
- [13] R. Jorda, L. Havlicek, I.W. McNae, M. D. Walkinshaw, J. Voller, A. Sturc, J. Navratilova, M. Kuzma, M. Mistrik, J. Bartek, M. Strnad, V. Krystof, *J. Med. Chem.* 2011, 54, 2980–2993.
- [14] D. Moravcova, V. Krystof, L. Havlicek, J. Moravec, R. Lenobel, M. Strnad, *Bioorg. Med. Chem. Lett.* 2003, 13, 2989–2992.
- [15] A. Gopalsamy, H. Yang, J. W. Ellingboe, H. R. Tsou, N. Zhang, E. Honores, D. Powell, M. Miranda, J. P. McGinnis, S. K. Rabindran, *Bioorg. Med. Chem. Lett.* 2005, 15, 1591–1594.
- [16] M. Bakavoli, G. Bagherzadeh, M. Vaseghifar, A. Shiri, M. Pordel, M. Mashreghi, P. Pordeli, M. Araghi, *Eur. J. Med. Chem.* 2010, 45, 647–650.
- [17] P.G. Baraldi, D. Simoni, V. Periotto, S. Manfredini, M. Guarneri, R. Manservigi, E. Cassai, *J. Med. Chem.* 1984, 27, 986–990.
- [18] S. Bondock, R. Rabie, H. A. Etman, A. A. Fadda, *Eur. J. Med. Chem.* 2008, 43, 2122–2129.
- [19] R. Jorda, N. Sacerdoti-Sierra, J. Voller, L. Havlicek, K. Kracalikova, M.W. Nowicki, A. Nasereddin, V. Krystof, M. Strnad, M. D. Walkinshaw, C. L. Jaffe, *Bioorg. Med. Chem. Lett.* 2011, 21, 4233–4237.

- [20] S. Selleri, F. Bruni, C. Costagli, A. Costanzo, G. Guerrini, G. Ciciani, B. Costa, C. Martini, *Bioorg. Med. Chem.* 2001, 9, 2661–2671.
- [21] C. Almansa, A. F. D. Arriba, F. L. Cavalcanti, L. A. Gomez, A. Miralles, M. Merlos, J. Garcia-Rafanell, J. Forn, *J. Med. Chem.* 2001, 44, 350–361.
- [22] A. M. Gilbert, S. Caltabiano, F. E. Koehn, Z. Chen, G. D. Francisco, J. W. Ellingboe, Y. Kharode, A. Mangine, R. Francis, M. Trailsmith, D. Gralnick, *J. Med. Chem.* 2002, 45, 2342–2345.
- [23] T. Novinson, B. Bhooshan, T. Okabe, G. R. Revankar, R. K. Robins, K. Senga, H. R. Wilson, *J. Med. Chem.* 1976, 19, 512–516.
- [24] A. V. Ivachtchenko, E. S. Golovina, M. G. Kadieva, V. M. Kysil, O. D. Mitkin, S. E. Tkachenko, I. Okun, *Bioorg. Med. Chem.* 2011, 19, 1482–1491.
- [25] A. V. Ivachtchenko, D. E. Dmitriev, E. S. Golovina, M. G. Kadieva, A. G. Koryakova, V. M. Kysil, O. D. Mitkin, I. M. Okun, S. E. Tkachenko, A. A. Vorobiev, *J. Med. Chem.* 2010, 53, 5186–5196.
- [26] T. Saito, T. Obitsu, C. Minamoto, T. Sugiura, N. Matsumura, S. Ueno, A. Kishi, S. Katsumata, H. Nakai, M. Toda, *Bioorg. Med. Chem.* 2011, 19, 5955–5966.
- [27] A. R. Trivedi, B. H. Dholariya, C. P. Vakhariya, D. K. Dodiya, H. K. Ram, V. B. Kataria, A. B. Siddiqui, V. H. Shah, *Med. Chem. Res.* 2012, 21, 1887–1891.
- [28] J. Xu, H. Liu, G. Li, Y. He, R. Ding, X. Wang, M. Feng, S. Zhang, Y. Chen, S. Li, M. Zhao, Y. Li, C. Qi, *Z. Naturforsch. B. Chem. Sci.* 2012, 67, 827–834.
- [29] M. Chauhan, R. Kumar, *Bioorg. Med. Chem.* 2013, 21, 5657–5668.
- [30] R. K. Robins, *J. Am. Chem. Soc.* 1956, 80, 6671–6679.
- [31] H. W. Hamilton, D. F. Ortwine, D. F. Worth, J. A. Bristol, *J. Med. Chem.* 1987, 30, 91–96.
- [32] G. Gregorini, M. Laloue, *Plant Physiol.* 1980, 65, 363–367.
- [33] J. Yuan, M. Gulianello, S. D. Lombaert, R. Brodbeck, A. Kieltyka, K. J. Hodgetts, *Bioorg. Med. Chem. Lett.* 2002, 12, 2133–2136.
- [34] M. B. Tollefson, B. A. Acker, E. J. Jacobsen, R.O. Hughes, J.K. Walker, D.N.A. Fox, M.J. Palmer, S.K. Freeman, Y. Yu, B.R. Bond, *Bioorg. Med. Chem. Lett.* 2010, 20, 3125–3128.
- [35] H. N. Hafez, Abdul-Rhman. B. A. El-Gazzar, S. A. Al-Hussain, *Bioorg. Med. Chem. Lett.* 26, 2016, 2428–2433.
- [36] M. Daniela, H. Libor, K. Vladimir, L. Rene, S. Miroslav, EP1348707 A1, 2003.
- [37] M. Pal, Y. K. Rao, I. Khanna, N. K. Swamy, V. Subramanian, V. R. Batchu, J. Iqbal, S. Pillarisetti, US20060128729 A1, 2006.
- [38] M. E. Bunnage, K. M. Devries, L. J. Harris, P. C. Levett, J. P. Mathias, J. T. Negri, S. D. Street, A. S. Wood, WO0127113 A2, 2001.
- [39] A. Salonia, P. Rigatti, F. Montorsi, *Curr. Med. Res. Opin.* 2003, 19, 241–62.

- [40] S. Manfredini, R. Bazzanini, P. Giovanni, M. Guarneri, D. Simoni, M. E. Marongiu, A. Pani, E. Tramontane, P. L. Colla, Pyrazole-Related Nucleosides. *J. Med. Chem.* 1992, 35, 917–924.
- [41] S. Cherukupalli, R. Karpoornath, B. Chandrasekaran, G.A. Hampannavar, N. Thapliyal, V. N. Palakollu, *Eur. J. Med. Chem.* 2017, 126, 298–352.
- [42] J. A. Joule, K. Mills, *Heterocyclic chemistry*, fourth edition, 2000, ISBN 0-632-05453-0.
- [43] R.E.Orth, Biologically active pyrazoles, *J. Pharm. Sci.* 1968, 57, 537–556.
- [44] H. Kumar, D. Saini, S. Jain, N. Jain, *Eur. J. Med. Chem.* 2013, 70, 248–258.
- [45] R. K. Robins, L. B. Holum, F. W. Furcht, *J. Org. Chem.* 1956, 21, 833–836.
- [46] R. K. Robins, F. W. Furcht, A. D. Grauer, J. W. Jones, *J. Am. Chem. Soc.* 1956, 78, 2418–2422.
- [47] R. A. Long, F. Cerster, L. B. Townsend, *J. Heterocycl. Chem.* 1970, 7, 2–8.
- [48] E. M. Action, A. N. Fuziwara, L. Goodman, D. W. Henry, *Carbohydr. Res.* 1974, 33, 135–151.
- [49] H. Takei, N. Yasuda, H. Takagaki, *Bull. Chem. Soc. Japan.* 1979, 52, 208–211.
- [50] J. Wierzchowski, J. Kusmierek, J. Giziewicz, D Salvi, D. Shugar, *Acta Biochim. Pol.* 1980, 27, 35–56.
- [51] A. F. Lewis, L. B. Townsend, *J. Am. Chem. Soc.* 1982, 104, 1073–1077.
- [52] H. Ochi, T. Miyasaka, *Chem. Pharm. Bull. (Tokyo).* 1983, 31, 1228–1234.
- [53] E. M. Acton, K. J. Ryan, *J. Org. Chem.* 1984, 49, 528–536.
- [54] J. G. Buchanan, M. Harrison, R. H. Wightman, *J. Chem. Soc. Perkin Trans.* 1989, 71, 925– 930.
- [55] M. E. Haddad, M. Soukri, S. Lazar, A. Bennamara, G. Guillaumet, M. Akssira, *J. Heterocycl. Chem.* 2000, 37, 1247–1252.
- [56] D. J. Dale, P. J. Dunn, C. Golightly, M. L. Hughes, P. C. Levett, A. K. Pearce, P. M. Searle, G. Ward, A. S. Wood, *Org. Process Res. Dev.* 2000, 4, 17–22.
- [57] M. M. El-Abadelah, S. S. Sabri, M. A. Khanfar, H. A. Yasin, *J. Heterocycl. Chem.* 2002, 39, 1055–1059.
- [58] N. R. Reddy, G. M. Reddy, B. S. Reddy, P. P. Reddy, *J. Heterocycl. Chem.* 2005, 42, 751–754.
- [59] K. M. Khan, G. M. Maharvia, M. I. Choudhary, Atta-ur-Rahman, S. Parveen, *J. Heterocycl. Chem.* 2005, 42, 1085–1093.
- [60] V. Krystof, D. Moravcova, M. Paprskarova, P. Barbier, V. Peyrot, A. Hlobilkova, L. Havlicek, M. Strnad, *Eur. J. Med. Chem.* 2006, 41, 1405–1411.
- [61] T. Brady, K. Vu, J. R. Barber, S.C. Ng, Y. Zhou, *Tetrahedron Lett.* 2009, 50, 6223–6227.
- [62] O. Lenzi, V. Colotta, D. Catarzi, F. Varano, D. Poli, G. Filacchioni, K. Varani, F. Vincenzi, P.A. Borea, S. Paoletta, E. Morizzo, S. Moro, *J. Med. Chem.* 2009, 52, 7640–7652.
- [63] N. R. Reddy, G. M. Reddy, P. P. Reddy, *Org. Prep. Proced. Int.* 2004, 36, 92–95.
- [64] D. Geffken, R. Soliman, F. S. G. Soliman, M. M. Abdel-Khalek, D. A. E. Issa, *Med. Chem. Res.* 2011, 20, 408–420.
- [65] M. Nayak, N. Rastogi, S. Batra, *Eur. J. Org. Chem.* 2012, 7, 1360–1366.

- [66] M. K. Bratenko, M. M. Barus, M. V. Vovk, *Chem. Heterocycl. Compd.* 2013, 49, 1345–1351.
- [67] L. Squarzialupi, V. Colotta, D. Catarzi, F. Varano, G. Filacchioni, K. Varani, C. Corciulo, F. Vincenzi, P.A. Borea, C. Ghelardini, L. Di, C. Mannelli, A. Ciancetta, S. Moro, *J. Med. Chem.* 2012, 56, 2256–2269.
- [68] G. L. Reddy, S. K. Guru, M. Srinivas, A. S. Pathania, P. Mahajan, A. Nargotra, S. Bhushan, R. A. Vishwakarma, S. D. Sawant, *Eur. J. Med. Chem.* 2014, 80, 201–208.
- [69] L. Squarzialupi, V. Colotta, D. Catarzi, F. Varano, M. Betti, K. Varani, F. Vincenzi, P. A. Borea, N. Porta, A. Ciancetta, S. Moro, *Eur. J. Med. Chem.* 2014, 84, 614–627.
- [70] R. V. Rote, D. P. Shelar, S. R. Patil, M. N. Jachak, *J. Heterocycl. Chem.* 2014, 51, 815–823.
- [71] S. Mohammed, R. A. Vishwakarma, S. B. Bharate, *J. Org. Chem.* 2015, 80, 6915–6921.
- [72] L. Squarzialupi, M. Falsini, D. Catarzi, F. Varano, M. Betti, K. Varani, F. Vincenzi, D. Dal Ben, C. Lambertucci, R. Volpini, V. Colotta, *Bioorg. Med. Chem.* 2016, 24, 2794–2808.
- [73] L. Squarzialupi, D. Catarzi, F. Varano, M. Betti, M. Falsini, F. Vincenzi, A. Ravani, A. Ciancetta, K. Varani, S. Moro, V. Colotta, *Eur. J. Med. Chem.* 2016, 108, 117–133.
- [74] V. Papesch, R. M. Dodson, *J. Org. Chem.* 1965, 30, 199–203.
- [75] S. Senda, K. Hirota, T. Asao, Y. Yamada, *J. Chem. Soc. Chem. Commun.* 1977, 556–557.
- [76] K. Hirota, Y. Yamada, T. Asao, S. Senda, *J. Chem. Soc. Perkin Trans. 1.* 1982, 277–284.
- [77] S. B. Weitensteiner, J. Liebl, V. Krystof, L. Havlicek, T. Gucky, M. Strnad, R. Furst, A.M. Vollmar, S. Zahler, *PLoS One.* 2013, 8, e54607.
- [78] E. Reznickova, S. Weitensteiner, L. Havlicek, R. Jorda, T. Gucky, K. Berka, V. Bazgier, S. Zahler, V. Krystof, M. Strnad, *Chem. Biol. Drug Des.* 2015, 86, 1528–1540.
- [79] L. Vymetalova, L. Havlicek, A. Sturc, Z. Skraskova, R. Jorda, T. Pospisil, M. Strnad, V. Krystof, *Eur. J. Med. Chem.* 2016, 110, 291–301.
- [80] Y. S. Sanghvi, S. B. Larson, D. F. Smee, G. R. Revankar, R. K. Robins, *Nucleosides & Nucleotides*, 1991, 10, 1417–1427.
- [81] M. B. Tollefson, B. A. Acker, E. J. Jacobsen, R. O. Hughes, J. K. Walker, D. N. A. Fox, M. J. Palmer, S. K. Freeman, Y. Yu, B. R. Bond, *Bioorg. Med. Chem. Lett.* 2010, 20, 3120–3124.
- [82] P. Choudhari, M. Bhatia, *J. Saudi Chem. Soc.* 2012, 19, 265–273.
- [83] O. Rabal, J. A. Sánchez-Arias, M. Cuadrado-Tejedor, I. D. Miguel, M. Marta Pérez-González, C. García-Barroso, A. Ugarte, A. E. H. D. Mendoza, E. Sáez, M. Espelousin, S. Ursua, T. Haizhong, W. Wei, X. Musheng, A. Garcia-Osta, J. Oyarzabal, *J. Med. Chem.* 2016, 59, 8967–9004.
- [84] L. Squarzialupi, V. Colotta, D. Catarzi, F. Varano, G. Filacchioni, K. Varani, C. Corciulo, F. Vincenzi, P. A. Borea, C. Ghelardini, L. D. C. Mannelli, A. Ciancetta, S. Moro, *J. Med. Chem.* 2013, 56, 2256–2269.
- [85] S. M. Hecht, R. M. Bock, R. Y. Schmitzt, F. Skoog, N. J. Leonard, *Proc. Natl. Acad. Sci. U. S.*

- A. 1971, 68, 2608–2610.
- [86] F. Skoog, R. Y. Schmitz, *Phytochemistry*. 1973, 12, 25–37.
- [87] J. D. Ratajczyk, R. G. Stein, R. Swett, US3939161, 1976.
- [88] S. M. Hecht, U. Jordis, US4282361, 1981.
- [89] Y. Fujikawa, M. Suzuki, M. Sakashita, N. Tsuruzoe, T. Miyasaka, US4654348, 1987.
- [90] H. W. Hamilton, US4663326A, 1987.
- [91] H. W. Hamilton, US4666908, 1987.
- [92] H. W. Hamilton, WO8800192A1, 1988.
- [93] J. Yuan, US5723608A, 1998.
- [94] S. Zhihua, G. Jihua, M. Mark, WO0014088A1, 2000.
- [95] Y. F. Lu, C. Antezak, J. Qudenes, Y. Tao, US6204383 B1, 2001.
- [96] J. Yuan, US6211187 B1, 2001.
- [97] R. Jonas, H. M. Eggenweiler, P. Schelling, M. Christadler, N. Beier, US6777419 B1, 2004.
- [98] H. M. Eggenweiler, V. Eiermann, US20040023990A1, 2004.
- [99] H. M. Eggenweiler, V. Eiermann, US20040063730 A1, 2004.
- [100] H. M. Eggenweiler, V. Eiermann, P. Schelling, US20040077664 A1, 2004.
- [101] K. J. Hodgetts, S. John, N. Moorcroft, CA2537916 A1, 2005.
- [102] K. J. Hodgetts, S. John, N. Moorcroft, G. Shutske, B. Kaiser, Y. Yamaguchi, P. Ge, R. F. Horvath, WO2005028480 A2, 2005.
- [103] A. S. Bell, D. G. Brown, D. N. A. Fox, H. F. Lu, I. R. Marsh, A. I. Morrell, D. R. Owen, M. J. Palmer, T. E. Rogers, C. A. Winslow, WO2005097799A1, 2005.
- [104] B. A. Acker, R. O. Hughes, E. J. Jacobsen, H. F. Lu, T. E. Rogers, M. B. Tollefson, J. K. Walker, WO2006046135A2, 2006.
- [105] A. S. Bell, D. G. Brown, D. N. A. Fox, I. R. Marsh, A. I. Morrell, M. J. Palmer, C. A. Winslow, US7262192B2, 2007.
- [106] G. Butora, M. MacCoss, B. Bhat, A. B. Eldrup, US7534767B2, 2009.
- [107] A. S. Bell, D. G. Brown, D. N. A. Fox, I. R. Marsh, A. I. Morrell, D. R. Owen, M. J. Palmer, C. A. Winslow, H. F. Lu, T. E. Rogers, US7569572 B2, 2009.
- [108] A. S. Bell, D. G. Brown, K. Dack, D. N. A. Fox, I. R. Marsh, A. I. Morrell, M. J. Palmer, C. A. Winslow, US7572799B2, 2009.
- [109] D. Maravcova, L. Havlicek, V. Krystof, R. Lenobel, M. Strnad, US7745450 B2, 2010.
- [110] A. S. Bell, D. G. Brown, K. Dack, D. N. A. Fox, I. R. Marsh, A. I. Morrell, M. J. Palmer, C. A. Winslow, US8097621B2, 2012.

Abstract:

A novel series of 4,6-disubstituted pyrazolo[3,4-*d*]pyrimidines (**7-43**) bearing various anilines at C-4 position and thiophenethyl or thiopentane moieties at C-6 position have been designed and synthesized by molecular hybridization approach. All the synthesized compounds were evaluated for *in vitro* CDK2/cyclin E and Abl kinase inhibitory activity as well as anti-proliferative activity against K-562 (chronic myelogenous leukemia), and MCF-7 (breast adenocarcinoma) cell lines. The structure-activity relationship (SAR) studies revealed that compounds with thiophenethyl group at C-6 with mono-substituted anilines at C-4 exhibited better CDK2 inhibitory activity compared to alkyl group (thiopentane) at C-6 and di-substituted anilines at C-4 of the scaffold. In particular, compounds having 2-chloro, 3-nitro and 4-methylthio aniline groups at C-4 displayed significant enzymatic inhibitory activity against CDK2 with single digit micro molar IC₅₀ values. The *in silico* molecular docking studies suggested possible binding orientation and the binding energies were in agreement with the observed SAR as well as experimental results. In addition, some of the synthesized compounds indicated anti-proliferative effects against K-562 and MCF-7 cancer cell lines with IC₅₀ values in a micro molar range. Thus, the synthesized compounds could be considered as new anticancer hits for further lead optimization.

Key words: Pyrazolo[3,4-*d*]pyrimidine; cyclin dependent kinase inhibitor; Anti-proliferative activity; Molecular docking; GLIDE.

1 Introduction

Cancer is an enormous global health burden, affecting almost every region and socio-economic level. It is the second leading cause of death worldwide, accounted for 8.8 million deaths in 2015 and nearly 1 in 6 of all global deaths.¹ The new cancer cases are expected to increase to 15 million per year by 2020, according to the World Health Organization (WHO), unless further precautionary measures are followed.² Wide efforts are being carried out in order to discover new treatment approaches as well as to improve prevention and molecular diagnostic systems.^{3,4} It is becoming noteworthy to investigate new druggable molecular targets, identify and develop their modulators as novel drugs for the treatment of cancer. Amongst others, protein kinases have become an important group of drug targets and number of kinase inhibitors in clinical development is rapidly increasing.⁵

Cyclin-dependent kinases (CDKs) are a group of serine/threonine kinases comprising 20 members, of which some are linked with regulation of cell-cycle progression by phosphorylating proteins involved in cell division. For example, formation of active complex composed of CDK2 and cyclin E enables pRb phosphorylation, activation of transcription factor E2F which initiates S phase of the cell cycle.⁶ CDK2 then also associates with cyclin A, governing continuous DNA replication and properly programmed deactivation of E2F. Deregulations of CDKs or cyclins, as well as the loss of endogenous inhibitory proteins, result in abrogation of cell cycle control, which is connected with development of tumors. Thus CDKs are considered important targets for anticancer drugs.^{7,8} The lack of clarity as to which CDK is the most suitable drug target followed by poor selectivity hindered the clinical development of specific CDK inhibitors.⁹

Initially, the importance of CDK2 as a drug target for cancer therapy was in question since CDK2 knockdown investigations failed to block cell proliferation in a number of tumour cell lines,¹⁰ and by mouse knockout investigations where the animals were viable.^{11,12} Current investigations employing a chemical genetic method in which CDK2 countenance was maintained, but enzymatic activity was inhibited, affords interesting sign that CDK2 is a valid anticancer drug target.⁶ Up to date many CDK2 inhibitors have been developed and some of them (including roscovitine, CYC065, dinaciclib, AT7519, milciclib) undergo clinical evaluation.^{13,14} CDK2 inhibitors are also anticipated to have efficacy in combinations with other drugs or where synthetic lethality can be recognized.¹⁵ Recent study proved that a combination of phosphatidylinositol-3-kinase and CDK2 inhibitors induced apoptosis in malignant glioma xenografts via synthetic-lethal interaction.¹⁶ CDK2 was proved as a therapeutic target in BRCA-deficient cancers,¹⁷ ovarian cancer.¹⁸

Fused pyrimidines have received a great deal of attention due to their immense role as active pharmacophores.¹⁹ The pyrazole annulated on the pyrimidine scaffold leads to pyrazolopyrimidine, which can be looked upon as the bio-isostere of purine.²⁰ The pharmacological significance of purine

nucleus is well established. Oxypurinol and its congeners allopurinol and thiopurine (Tisopurine) which contains pyrazolo[3,4-*d*]pyrimidine scaffold inhibit xanthine oxidase enzyme and interfere with the biosynthesis of uric acid, further allopurinol acting as a causative agent for gout.²¹ Ibrutinib/PCI-32765 was recently approved by the US FDA for the treatment of mantle cell lymphoma, chronic lymphocytic leukemia and Waldenstrom's macroglobulinemia diseases (**Figure 1**).²²

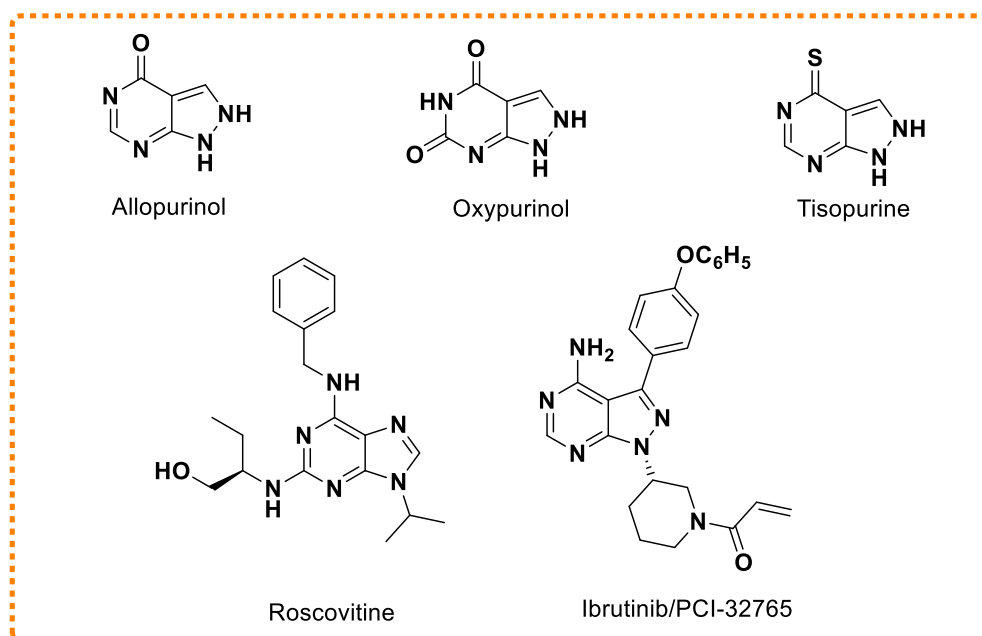


Figure 1. Structures of active drugs containing fused pyrimidine.

Pyrazolo[3,4-*d*]pyrimidine is also reported to encompass biological potential as anticancer, antiviral, antimicrobial, herbicidal, CNS agents (phosphodiesterase 9 and benzodiazepine receptors), anti-inflammatory and cardiovascular activities.²³ **Figure 2** depicts several reported analogs of pyrazolo[3,4-*d*]pyrimidine with anti-cancer activities related to inhibition of various protein kinases.²⁴⁻²⁹

Based on the above mentioned facts and in continuation of our research work on anticancer drug discovery, we envisaged to further exploit the pyrazolo[3,4-*d*]pyrimidine scaffold to synthesize novel CDK2 inhibitors.^{30,31} Thus a series of 4,6-disubstituted pyrazolo[3,4-*d*]pyrimidine was synthesized with a design strategy: a) bioisosteric replacement of purine nucleus, b) incorporation of more lipophilic aromatic amines (C-4) and aliphatic or aromatic groups (C-6). These derivatives were also evaluated against Abl kinase and two cancer cell lines K-562 (chronic myelogenous leukemia) and MCF-7 (breast adenocarcinoma). Further, *in silico* molecular docking studies were performed to calculate the binding energies and orientations of these compounds with respect to the active site of CDK-2 protein. The computational results were in agreement with our experimental observations.

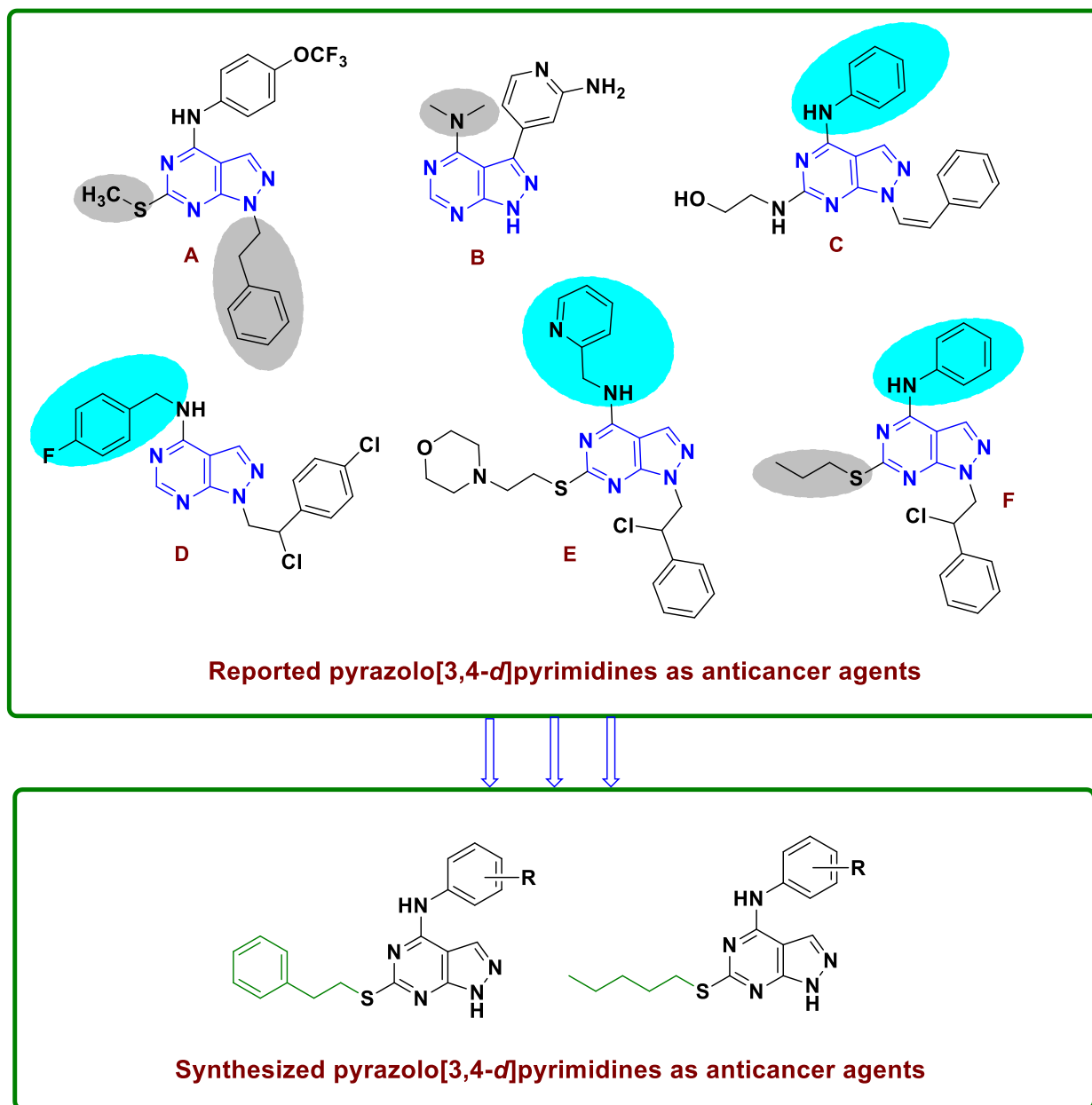


Figure 2. Known derivatives of pyrazolo[3,4-*d*]pyrimidine and their anticancer activities along with the designed molecules. **A:** (K_{i50} against Src, AbIT315I = 0.056, 0.01 μM);²⁴ **B:** (IC_{50} against CDK9 = 17 nM);²⁵ **C:** (IC_{50} against CDK2 = 0.5 μM);²⁶ **D:** (K_{i50} against Abl = 80 nM);²⁷ **E:** (K_{i50} against cSrc, Abl = 0.21 ± 0.02 , 0.15 ± 0.02 μM);²⁸ **F:** (IC_{50} against Src = 1.2 ± 0.4 μM).²⁹

2 Results and discussion

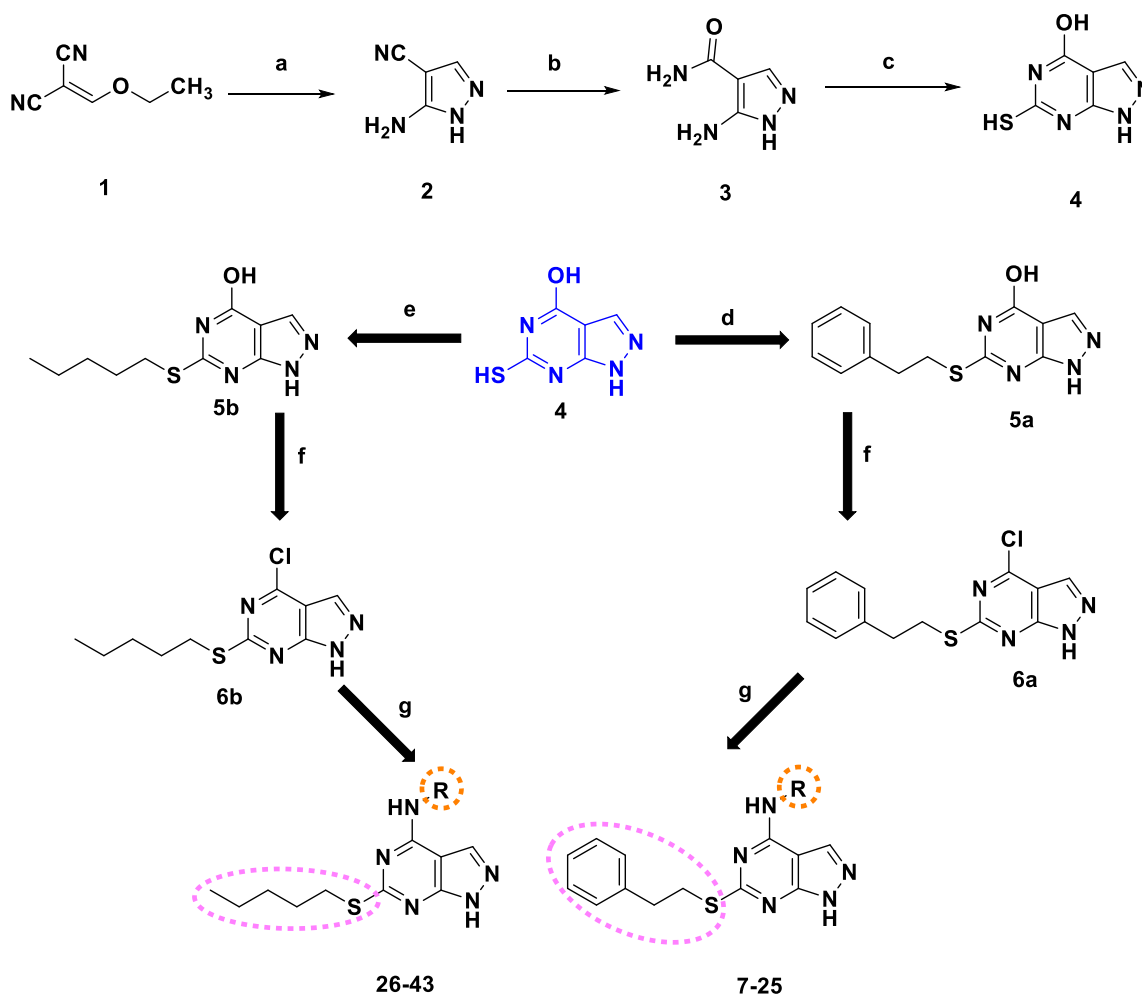
2.1 Chemistry

The synthesis of novel series of pyrazolo[3,4-*d*]pyrimidine hybrids was achieved through an efficient and versatile synthetic route as depicted **Scheme 1**. On the pyrazolopyrimidine scaffold, chloro group was introduced at C-4 as a good leaving group, which acted as a most reactive site for different nucleophiles, while thiophenethyl or thiopentane groups were introduced at C-6 position. With a view

Chapter 4

to prepare the target hybrid molecules (**7-43**), the key intermediates 4-chloro-6-(phenethylthio)-1*H*-pyrazolo[3,4-*d*]pyrimidine (**6a**), 4-chloro-6-(pentylthio)-1*H*-pyrazolo[3,4-*d*]pyrimidine (**6b**) were synthesized from ethoxymethylene malononitrile (**1**) as illustrated in **Scheme 1**.

From the earlier reported literature methods compound **4** was successfully synthesized.³² Further under microwave irradiation alkylation of compound **4** was achieved by reacting with 2-chloroethyl benzene in presence of anhydrous potassium carbonate in *N,N*-dimethylformamide (DMF) to obtain 6-(phenethylthio)-1*H*-pyrazolo[3,4-*d*]pyrimidin-4-ol (**5a**). Similarly reacting **4** with 1-bromopentane in 1M NaOH solution at 70 °C resulted in 6-(pentylthio)-1*H*-pyrazolo[3,4-*d*]pyrimidin-4-ol (**5b**) in moderate yield. Chlorination of **5a** and **5b** was easily achieved with Vilsmeier complex (POCl₃:DMF) to obtain halogenated key intermediates 4-chloro-6-(phenethyl/pentylthio)-1*H*-pyrazolo[3,4-*d*]pyrimidine that is **6a** and **6b**. As displayed in **Scheme 1**, the synthesis of the final hybrid compounds (**7-43**) in good yield (75-95%) was achieved by nucleophilic substitution with various primary amines at C-4. The IR, ¹H and ¹³C NMR spectroscopic data of all the novel compounds were in agreement with the predicted structures, which was further validated by the HR-MS data (Supporting information).



Scheme 1: Synthetic exploration for the preparation of 4,6-disubstituted pyrazolo[3,4-*d*]pyrimidine analogues (**7-43**).

Reagents and conditions: (a) hydrazine hydrate, ethanol, 80 °C, 3h, 92%; (b) Conc. H₂SO₄, NH₄OH, H₂O, 50 °C, 5h, 90%; (c) potassium ethyl xanthogenate, DMF, 120 °C, 6h, 82%; (d) 2-chloroethyl benzene, K₂CO₃, DMF, 70 °C, microwave, 20 min, 76%; (e) 1-bromopentane, NaOH, H₂O, glacial acetic acid, 50 °C, 5h, RT, overnight, 80%; (f) POCl₃, DMF, 80 °C, 2h, 85%; (g) R-NH₂, EtOH, 80 °C, 2h, 75-95%.

The ¹H NMR of compound **4** exhibited very distinct singlet signals resonating at around δ 13.61, 13.03, 11.86 and 8.42 ppm, was attributed to the N-H, S-H, O-H and Ar-H protons of pyrazole ring. Thus, indicating the formation of the fused pyrazolopyrimidine by ring annulation of 5-amino-1*H*-pyrazole-4-carboxamide (**3**) with potassium ethyl xanthogenate. For compounds **5a** and **5b**, the distinctive methylene signals (Ph-CH₂-CH₂-S- and -S-CH₂-CH₂-CH₂-CH₂-) appeared around δ 3.43-3.39, 3.01-2.97 ppm and δ 3.17-2.87, 1.73-1.43, 1.41-1.14 respectively, while the methyl peak for **5b** was observed at δ 0.86-0.80 ppm. In particular, the disappearance of a distinct singlet signal at around δ 13.03 ppm for mercapto (-SH) group evidently indicated the successful alkylation of pyrimidine scaffold. Whereas the most characteristic singlet, doublet and triplet signals at around δ 7.32-7.20 ppm was attributed to the aromatic protons (C₆H₅-CH₂-CH₂-S-) at C-6 of the pyrimidine ring. Further, the absence of characteristic singlet signal at around δ 12.22-12.28 ppm for (-OH) at C-4 of pyrimidine ring confirmed the formation of halogenated (-Cl) key intermediates 4-chloro-6-(phenethyl/pentylthio)-1*H*-pyrazolo[3,4-*d*]pyrimidine (**6a** and **6b**). These findings corroborated with their respective ¹³C NMR, where the methylene carbon peaks at δ 34.61, 31.08 ppm (C₆H₅-CH₂-CH₂-) and δ 30.61-30.37, 30.16-29.69, 29.22-28.11, 21.78-21.73 ppm (-S-CH₂-CH₂-CH₂-CH₂-) were assigned to **5a** and **5b**. The single methyl peak (**5b**) appeared around 13.90-13.83 ppm while the prominent aromatic signals (**5a** and **5b**) resonated around δ 167.89-109.79 ppm.

The IR spectra of the title compounds **7-43** displayed a reasonably sturdy and characteristic bands around 2921-3033 cm⁻¹, 1270-1300 cm⁻¹ accounting for N-H and C-S stretching respectively, while the most prominent band of C-N appearing around 1180-1184 cm⁻¹ indicated the formation of final hybrid molecules. Further, the prominent ¹H-NMR signals of the title compounds **7-43** resonated around δ 13.39-10.28 ppm (exocyclic-N-H), δ 9.94-7.75 ppm (ring-N-H) and 10.02-8.19 ppm (C-3 aromatic proton) while, the singlet or multiplet aromatic proton peaks appeared around δ 8.47-6.84 ppm. For compounds **7-25** the methylene protons (-S-CH₂-CH₂-Ph) were observed around δ 3.43-2.81 ppm while for compounds **26-43** the signals (-S-CH₂-CH₂-CH₂-CH₂-) appeared around δ 3.10-1.20 ppm. The methyl protons for **26-43** resonated around δ 0.87-0.80 ppm. Further the methylthio (-Ph-SCH₃), methyl (Br-Ph-CH₃), methoxy (Ph-OCH₃) and ethynyl-H protons resonated around δ 2.47-2.44 ppm, δ 2.30-

2.18 ppm, δ 3.77-3.71 ppm and 4.18 ppm respectively. The ^{13}C NMR spectra further confirmed the structures of the title compounds. The characteristic carbon signals C-6, C-4 and C-3 of the pyrimidine ring were observed around δ 167.41-166.40, 155.73-153.11 and 132.88-130.56 ppm, while the various aromatic/heteroaromatic carbons resonated between δ 153.62-98.12 ppm. Further, the prominent carbon signals observed around δ 55.66-55.61 ppm δ 21.78-17.74 ppm and 30.17-15.31 ppm were attributed to the methoxy ($-\text{O}\underline{\text{C}}\text{H}_3$), methyl and thiomethyl carbons respectively. Further, for compounds **7-25** the methylene carbon peaks ($-\text{S}-\underline{\text{C}}\text{H}_2-\underline{\text{C}}\text{H}_2-\text{Ph}$) were observed around δ 35.51-31.08 ppm while for compounds **26-43** the signals ($-\text{S}-\underline{\text{C}}\text{H}_2-\underline{\text{C}}\text{H}_2-\underline{\text{C}}\text{H}_2-\underline{\text{C}}\text{H}_2-$) appeared around δ 30.62-21.73 ppm and the methyl peak resonated around δ 13.89-13.83 ppm. In addition, the HR-MS spectrums of the title compounds (**7-43**) displayed accurate molecular ion peaks, which were in agreement with their expected molecular weights (supporting information).

2.2 *In vitro* evaluation for CDK2 and Abl kinase inhibitors

All the final compounds were evaluated for CDK2/cyclin E kinase inhibition and the IC_{50} values of various *in vitro* anticancer profiles of the final compounds are summarized in **Table 1**. Abl kinase inhibition was evaluated as a counter screen, to get a preliminary information about selectivity.

Code	R	IC_{50} (μM) ^a			
		CDK2/Cyclin E	Abl	K-562	MCF-7
7	Ph	>12.5	>12.5	19.9	19.2
8	2-ClPh	7.8	>12.5	>6.25	>6.25
9	3-ClPh	13.3	>25	>25	24.0
10	4-ClPh	>25	>25	>25	>25
11	3-NO ₂ Ph	5.1	>25	24.6	24.3
12	4-NO ₂ Ph	>12.5	>12.5	>6.25	>6.25
13	2-BrPh	>12.5	>12.5	>6.25	>6.25
14	3-BrPh	>25	>25	27.4	23.9
15	4-BrPh	>25	>25	>50	>50
16	2,4-(CH ₃) ₂ Ph	>12.5	>12.5	>6.25	>6.25
17	SCH ₃ Ph	>25	>25	>6.25	>6.25
18	4-Cl-3-CF ₃ Ph	13.4	>25	>6.25	>6.25
19	4-Br-3-CF ₃ Ph	>25	>25	>6.25	>6.25
20	4-Cl-3-NO ₂ Ph	>25	>25	>6.25	>6.25
21	4-F-2-CH ₃ Ph	>12.5	>12.5	>6.25	>6.25
22	3-Br-4-CH ₃ Ph	>25	>25	>6.25	>6.25

23	2-Cl-4-FPh	>12.5	>12.5	>12.5	>12.5
24	3,4-(OCH ₃)Ph	15.9	>12.5	>6.25	>6.25
25	4-(ethynyl)Ph	>25	>25	>12.5	>12.5
26	Ph	>50	>50	>100	>100
27	2-ClPh	8.7	>12.5	>25	>25
28	3-ClPh	>25	>25	>12.5	>12.5
29	4-ClPh	>12.5	>12.5	>6.25	>6.25
30	3-NO ₂ Ph	17.7	>25	>12.5	>12.5
31	4-NO ₂ Ph	>25	>25	>6.25	>6.25
32	2-BrPh	>25	>25	>12.5	>12.5
33	3-BrPh	>25	>25	>6.25	>6.25
34	4-BrPh	>25	>25	>6.25	>6.25
35	2,4-(CH ₃) ₂ Ph	>25	>25	>12.5	>12.5
36	SCH ₃ Ph	8.8	>25	>6.25	>6.25
37	4-Cl-3-CF ₃ Ph	>25	>25	>12.5	>12.5
38	4-Br-3-CF ₃ Ph	>25	>25	>6.25	>6.25
39	4-Cl-3-NO ₂ Ph	>25	>25	>12.5	>12.5
40	4-F-2-CH ₃ Ph	>12.5	>12.5	>12.5	>12.5
41	3-Br-4-CH ₃ Ph	>25	>25	>6.25	>6.25
42	2-Cl-4-FPh	>12.5	>12.5	>6.25	>6.25
43	3,4-(OCH ₃)Ph	>12.5	>12.5	>6.25	>6.25
	Roscovitine	0.1	>100	42	11
	Imatinib	>100	0.2	0.5	>10

^a IC₅₀ values were determined in triplicate in the range of 0.05 to 100 μM. IC₅₀ value indicates concentration (μM) that inhibits activity of the tested enzyme to 50%. For cytotoxic assays, IC₅₀ means the concentration (μM) that inhibits the growth of 50% of cells during a three-day cultivation

Table 1. Anticancer evaluation of novel 4,6-disubstituted pyrazolo[3,4-*d*]pyrimidine derivatives.

Some synthesized compounds displayed an activity in the single digit micro molar range against CDK2/cyclin E. Fascinatingly, it was observed that some compounds containing thiophenethyl group at C-6 displayed prominent anticancer activity (**7**, **9**, **11**, **14**) as compared to compounds **26-43** having thiopentane group. It was also observed that incorporation of phenyl/substituted phenyl groups at C-4 of the pyrazolo[3,4-*d*]pyrimidine nucleus was essential for CDK2 activity. From the tested thiophenethyl series the highest CDK2 inhibitory activity was recorded for compounds **11** (IC₅₀ = 5.1 μM) and **8** (IC₅₀ = 7.8 μM) with 3-nitroaniline and 2-chloroaniline group at C-4 respectively. Notable significant inhibition was also observed for compounds bearing 3-chloroaniline (**9**; IC₅₀ = 13.3 μM), 4-

chloro-3-trifluoromethylaniline (**18**; $IC_{50} = 13.4 \mu M$) and 3,4-dimethoxyaniline (**24**; $IC_{50} = 15.9 \mu M$). For the remaining compounds of this thiophenethyl series, IC_{50} values could not be measured due to a solubility limit (IC_{50} value >12.5 or $>25 \mu M$).

Similarly, some thiopentane derivatives (series **26-43**) also exhibited a reasonable activity profile with IC_{50} starting from $8.7 \mu M$. From this series, compounds with 2-chloroaniline (**27**) and 4-methylthioaniline (**36**) showed the best activity with IC_{50} $8.7 \mu M$ and $8.8 \mu M$, respectively; this was followed by 3-nitroaniline derivative (**30**) with IC_{50} $17.7 \mu M$. The remaining compounds in this series were less soluble and their IC_{50} were not achieved. In addition, all compounds (**7-43**) were also evaluated against Abl kinase but none of the compounds showed any inhibition in the assayed concentration range, confirming reasonable selectivity towards CDK2 over unrelated Abl.

2.3 Anti-proliferative activity against K-562 and MCF-7 cell lines

All the newly synthesized 4,6-disubstituted pyrazolo[3,4-*d*]pyrimidine analogues **7-43** were further evaluated for their *in vitro* anti-proliferative activity against K-562 (chronic myelogenous leukemia) and MCF-7 (breast adenocarcinoma) cell lines. Several compounds are displaying appreciable activity with measurable IC_{50} values against the two cell lines, such as compounds **7** ($IC_{50} = 19.9, 19.2 \mu M$), **9** ($IC_{50} = >25, 24 \mu M$), **11** ($IC_{50} = 24.6, 24.3 \mu M$), and **14** ($IC_{50} = 27.4, 23.9 \mu M$). The remaining compounds were not active in the tested concentration range.

2.4 Structure-activity relationship (SAR) studies

In general, a careful observation of the structure-activity relationship (SAR) indicated that the CDK inhibitory activity was considerably affected by the nature of various substituents present at C-4 (aromatic ring) and C-6 positions on pyrazolo[3,4-*d*]pyrimidine scaffold. From the two series of compounds (phenethyl and pentane at C6), the phenethyl series gave most number of active compounds (8, 9, 11, 18 and 24), while in pentane series only three molecules (**27**, **30** and **36**) were active. Further analysis of both the series revealed that compounds **8**, **9**, **11**, **27**, **30** and **36** with mono substituted phenyl ring (2-Cl-Ph, 3-Cl-Ph, 3-NO₂-Ph, and 4-SCH₃-Ph groups) at C-4 showed better activity than compounds with disubstituted phenyl groups except for compounds **18** and **24** (4Cl-3CF₃-Ph and 3,4-OCH₃-Ph). Compound **11** followed by **8**, **9**, **27**, **30** and **36** presented highest inhibitory activity.

Further, no specific activity was observed for all the compounds against Abl kinase ($IC_{50} = >12.5$ to >50.0). However, compounds **7**, **11** and **14**, displayed specific anti-proliferative activity against K-562 ($IC_{50} = 19.9, 24.6$ and 27.4) and MCF-7 ($IC_{50} = 19.2, 24.3$ and 23.9), indicating that mono-substitutions at C4 with phenethyl at C6 was favorable. In summary, compound **11** was most active,

however due to low solubility profile for most of the compounds a conclusive SAR could not be derived.

Figure 3 provides a brief overview of the SAR.

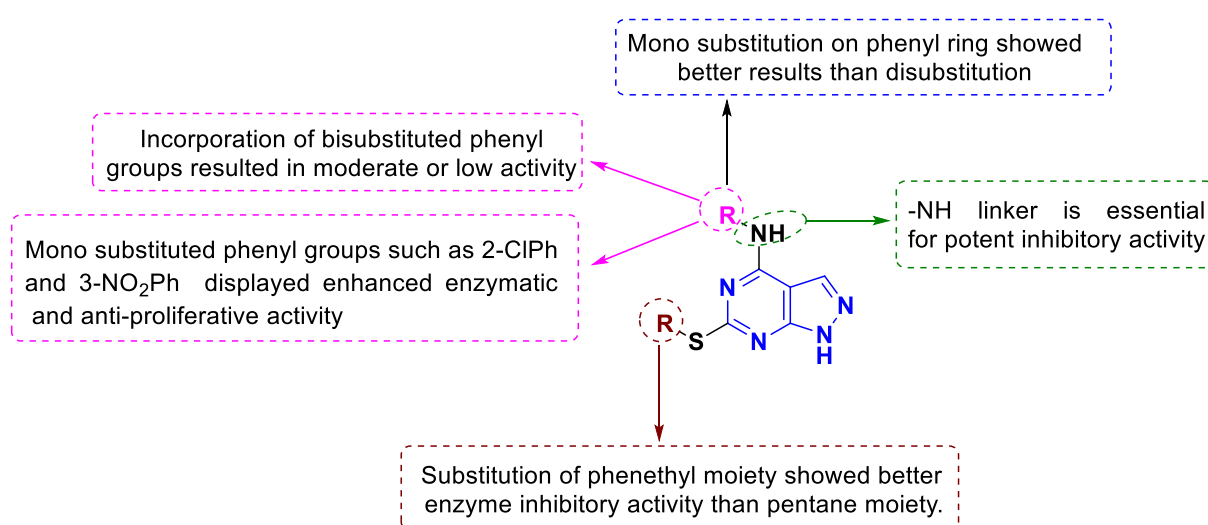


Fig. 3. SAR study of 4,6-disubstituted pyrazolo[3,4-*d*]pyrimidines as potent anticancer agents.

2.5 Molecular docking study

Computational and bioinformatics tools have become essential part for the design and development of therapeutically effective novel chemical entity.³³ Dinaciclib, a pyrazolo[1,5-*a*]pyrimidine compound, displayed higher binding affinity towards CDKs.³⁴ Hence, to further understand and substantiate our observed experimental data, molecular docking simulation was performed for the synthesized compounds with the target CDK2 protein.

To validate the docking protocols and to reproduce the reported orientation of *R*-roscovitine in the predefined binding site of CDK2 (PDB ID: 2A4L), docking studies were performed using Glide program of Schrodinger-Maestro 11.2. From the docking results, the pose of *R*-roscovitine obtained revealed similar molecular interactions as reported.³⁵ The docked complex presented characteristic hydrogen bonding (H-bond) interactions with crucial residues of the active-site, such as Leu83 interacted with roscovitine by forming a strong [C=O with benzylamino NH (1.91 Å)] and a weak [(C=O with ring nitrogen (2.39 Å)] H-bond. Similarly, the residue Asp86 interacted with OH group of roscovitine via a strong H-bond (1.67 Å), whereas Lys89 exhibited π -cation interaction with phenyl ring of the ligand. **Figure 4** represents the reproduced 3D molecular interactions of the docked pose, validating the docking protocols.

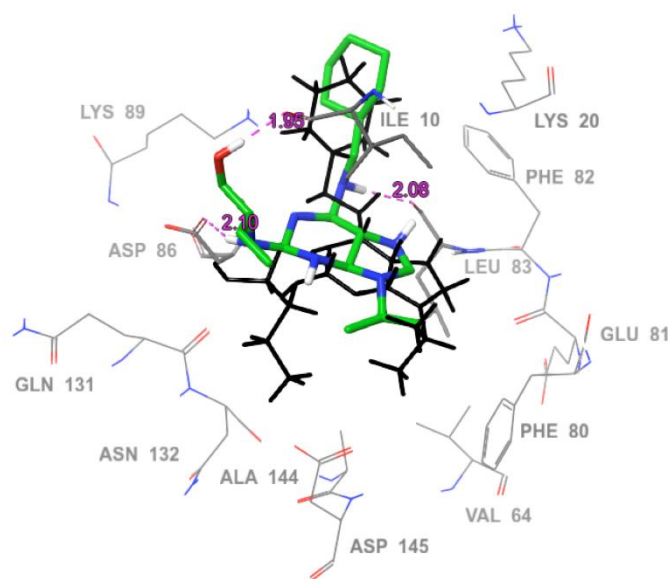


Figure 4: Reported pose of Roscovitine (black thin tube model) and docked pose (thick tube model) into the active-site showing similar interactions (docking validation). Magenta coloured dashed lines indicate hydrogen bonding, while grey-coloured thin tube amino acids are considered as crucial residues.

The docking experimental data with our synthesized compounds revealed that they fit well into the binding-site and display favourable interactions with the crucial amino acid residues. Interestingly, two nitrogen atoms of pyrazole ring of the best active compound **11** ($IC_{50} = 5.1 \mu M$) displayed strong H bond interactions with NH of Leu83 (2.37 \AA) and C=O of Glu81 (2.02 \AA) respectively, signifying these H bond interactions were crucial for the CDK-2 inhibition. The nitro group of the ligand was in close proximity to Lys89 presenting weak vdW interaction, whereas the acidic and basic amino acid residues (Lys129, Glu131, Asn132 and Asp145) surrounded thiophenethyl group. The exocyclic NH and the side chain sulphur displayed no characteristic interactions with the protein (**Figure 5a**). In the case of moderately active compound **27**, the ring NH displayed H bond interaction with Leu83 (1.69 \AA), while the exocyclic NH presented weak H bond interaction (2.59 \AA) with Asp86. The side chain was anchored within the catalytic residues Phe80 and Asp145, whereas the pocket consisting of Val18, Lys33, and Asp145 residues surrounded chlorophenyl ring. While in the case of the least active compound **30**, the orientation of the docked pose was observed to be different with respect to best and the moderately active compounds (**11** and **27**). The nitro group showed weak H bond interactions with the basic residues (Lys33 and Asn 132), which could have contributed to the altered pose of the ligand. Furthermore the aliphatic side chain occupied the hydrophobic region (Val64, Phe80, Leu134, and Ala144) resulting in H-bond interactions of the ring and exocyclic nitrogen with different residues of the active site (Leu83 and Ile10). **Figure 5** presents the different molecular interactions of **11**, **27** and **30** with the active site residues of CDK-2 protein (PDB ID: 2A4L).

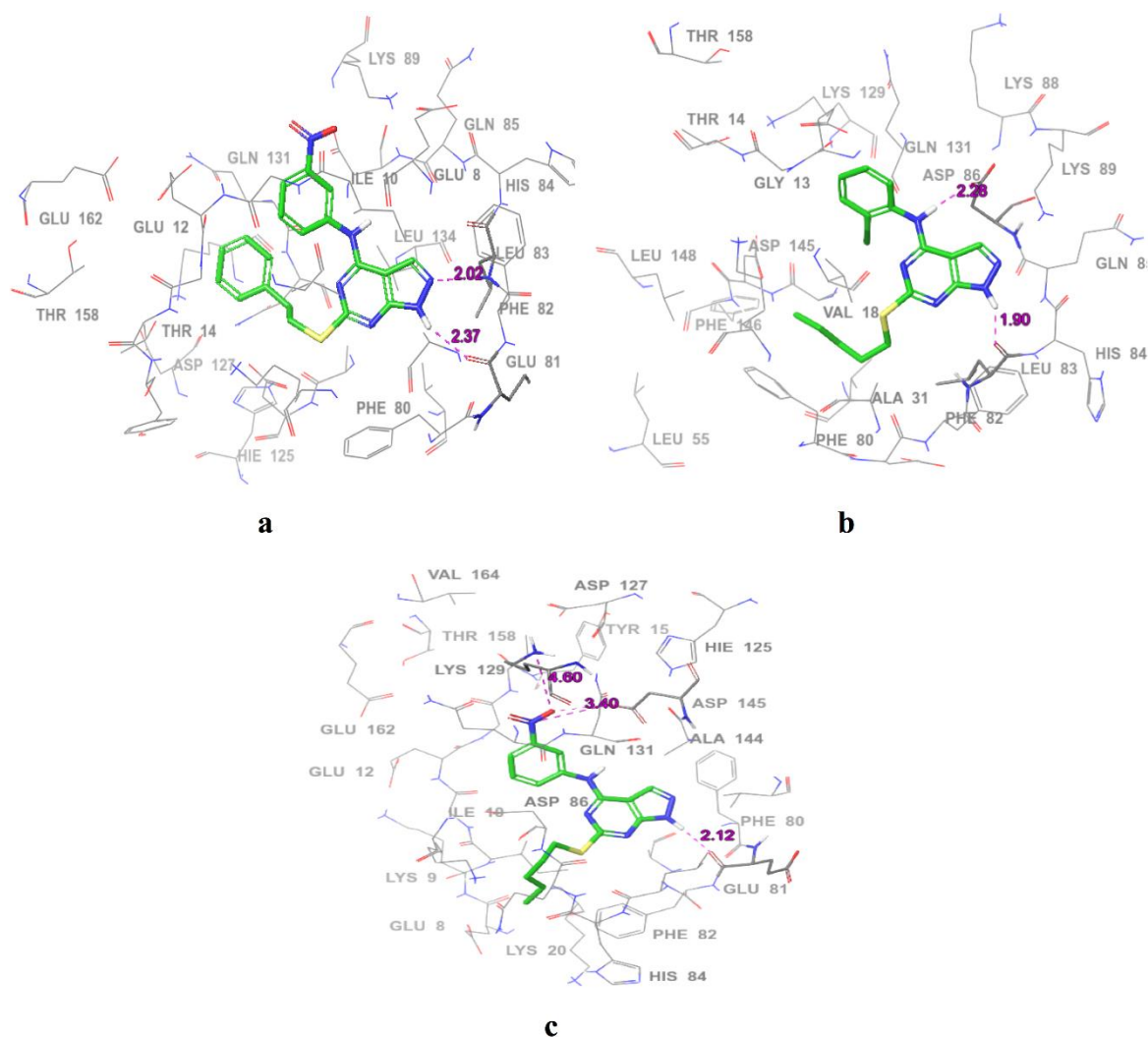


Figure 5. Molecular interactions of a) best active compound **11** b) moderately active compound **27** c) less active compound **30** into the binding site of CDK2/cyclin E protein. Nonpolar hydrogens were hidden for clarity and pink dashed lines indicate H bond.

3 Conclusion

In summary, we have successfully synthesized and characterized a new series of pyrazolo[3,4-*d*]pyrimidine derivatives **7-43** in good yields. The key intermediates 4-chloro-6-(phenethylthio)-1*H*-pyrazolo[3,4-*d*]pyrimidine (**6a**), 4-chloro-6-(pentylthio)-1*H*-pyrazolo[3,4-*d*]pyrimidine (**6b**) allowed us to generate a library of condensed pyrimidines. All synthesized compounds were evaluated for their *in vitro* enzymatic inhibitory activity against CDK2/cyclin E and four compounds (**8**, **11**, **27**, and **36**) were significantly active with IC₅₀ values ranging from 5.1 μM to 8.8 μM. From the SAR, it was clear that the presence of thiophenethyl group at C-6 with mono-substituted anilines at C-4 of the pyrazolo[3,4-*d*]pyrimidine nucleus was essential for anticancer activity. In addition, the binding

energies of the best active compounds were in agreement with the experimental data and supported the SAR studies. However, the moderate to poor activity observed for the majority of the compounds could be attributed to the solubility limit and this is currently being addressed in our laboratory. Thus, these preliminary research findings can further guide the researchers at large in developing novel pyrazolo[3,4-*d*]pyrimidine based CDK2 inhibitors as potential anticancer agents.

4 Experimental Section

All the chemicals used in this research work were purchased from Sigma-Aldrich and Merck Millipore, South Africa. All the solvents, except those of laboratory-reagent grade, were dried and purified when necessary according to previously published methods. The progress of the reactions was monitored by thin-layer chromatography (TLC) on pre-coated silica gel plates procured from E. Merck and Co. (Darmstadt, Germany) using 36% ethyl acetate in *n*-hexane as the mobile phase and iodine vapor as the visualizing agent. Purification of crude compounds were performed by crystallization using appropriate solvent and by flash column chromatography using 100-200 mesh silica gel with Methanol (MeOH) and DCM as solvents. The melting points of the synthesized compounds were determined using a Thermo Fisher Scientific (IA9000, UK) digital melting point apparatus and are uncorrected. The IR spectra were recorded on a Bruker Alpha FT-IR spectrometer (Billerica, MA, USA) using the ATR technique. The ¹H NMR and ¹³C NMR spectra were recorded on a Bruker AVANCE 400 and 600 MHz (Bruker, Rheinstetten/Karlsruhe, Germany) spectrometers using CDCl₃ and DMSO-*d*₆. The chemical shifts are reported in δ ppm units with respect to TMS as an internal standard. HR-MS was recorded on an Autospec mass spectrometer with electron impact at 70 eV.

4.1 Synthesis of 6-(phenethylthio)-1*H*-pyrazolo[3,4-*d*]pyrimidin-4-ol (5a)

To a stirred solution of 6-mercapto-1*H*-pyrazolo[3,4-*d*]pyrimidin-4-ol (compound **4**, 0.3g, 0.00179 mol) in *N,N*-dimethyl formamide (2 mL), K₂CO₃ (0.247 g, 0.00179 mol) was added and stirred at room temperature for 10 min. To this constantly stirred reaction mass, 2-chloroethyl benzene (0.28 mL, 0.002 mol) was slowly added dropwise and heated at 80 °C for 20 min. in a microwave reactor at 150 psi. After completion of reaction (monitored on TLC), the reaction mixture was poured in ice cold water and extracted with dichloromethane (DCM). The extracted organic layer was dried over anhydrous sodium sulphate and concentrated under reduced pressure to obtain crude product (dark brown viscous liquid) which was further purified by flash silica column [MeOH/ DCM, 10:90] to afford the desired compound **5a** as light brown solid. Yield: 76%; mp 210-212 °C; FTIR (ATR, cm⁻¹) ν_{\max} : 3022 (NH Str.), 2920 (Ar-H Str. of Pyr.), 1671 (C=O Str.); ¹H-NMR (400 MHz, DMSO-*d*₆) δ: 13.59 (s, 1H, NH), 12.22 (s, 1H, OH), 8.03 (s, 1H, ArH), 7.31 (t, *J* = 2.52 Hz, 4H, ArH), 7.25-7.20 (m, 1H, ArH), 3.41 (t, *J* = 5.04 Hz, 2H, CH₂), 2.99 (t, *J* = 7.56 Hz, 2H, CH₂) ppm; ¹³C NMR (100 MHz, DMSO-*d*₆) δ: 158.20, 139.93, 128.73, 128.62, 128.41, 126.41, 102.89, 34.61 (CH₂), 31.08 (CH₂) ppm.

4.2 Synthesis of 6-(pentylthio)-1*H*-pyrazolo[3,4-*d*]pyrimidin-4-ol (5b)

To a stirred solution of 6-mercapto-1*H*-pyrazolo[3,4-*d*]pyrimidin-4-ol (compound **4**, 1g, 0.005 mol) in 1M NaOH solution (12 mL), 1-bromopentane (1.48 mL, 0.011 mol) was added dropwise and heated at 70 °C for 6h and later slowly brought to RT and continued stirring for overnight. After completion of reaction (monitored on TLC), glacial acetic acid was added dropwise to yield the crude solid, which further washed with petroleum ether and purified by flash silica column [MeOH/DCM, 05:95] to afford the desired compound **5b** as yellow solid. Yield: 80%; mp 201-203 °C; FTIR (ATR, cm⁻¹) ν_{\max} : 3180 (NH Str.), 2953 (Ar-H Str.), 1678 (C=O Str.); ¹H-NMR (400 MHz, DMSO-*d*₆) δ : 13.54 (s, 1H, NH), 12.28 (s, 1H, OH), 7.93 (s, 1H, ArH), 3.15 (t, *J* = 7.26 Hz, 2H, CH₂), 1.70-1.63 (m, 2H, CH₂), 1.39-1.26 (m, 4H, (CH₂)₂), 0.86 (t, *J* = 7.08 Hz, 3H, CH₃) ppm; ¹³C NMR (100 MHz, DMSO-*d*₆) δ : 159.49, 157.75, 135.24, 30.37 (CH₂), 29.69 (CH₂), 28.24 (CH₂), 21.66 (CH₂), 13.84 (CH₃) ppm.

4.3 Synthesis of 4-chloro-6-(phenethylthio)-1*H*-pyrazolo[3,4-*d*]pyrimidine(6a)

Vilsmeier-Haack reagent was freshly prepared by the careful addition of POCl₃ (3.75 mL, 0.041 mol) in DMF (0.85 mL, 0.011 mol) at 0 °C with constant stirring. To this reaction mixture (maintained at 0 °C), added 6-(phenethylthio)-1*H*-pyrazolo[3,4-*d*]pyrimidin-4-ol (5a, 1g, 0.003 mol) and stirred initially for 30 min and later slowly brought to RT and continued stirring for another 30 min. Finally, the reaction mixture was allowed to reflux at 80 °C for 2 h until the TLC showed full consumption of starting material. The reaction mixture was then poured on ice cold water and neutralized with 10% NaOH solution. Thus, the obtained precipitate was filtered under suction and further purified by flash silica column [MeOH/DCM, 05:95] to afford the desired compound **6a**, as light yellow solid. Yield: 85%; mp 218-220 °C; FTIR (ATR, cm⁻¹) ν_{\max} : 3208 (NH Str.), 2927 (Ar-H Str.); ¹H-NMR (400 MHz, DMSO-*d*₆) δ : 14.24 (s, 1H, NH), 8.30 (s, 1H, ArH), 7.31 (t, *J* = 2.48 Hz, 4H, ArH), 7.25-7.19 (m, 1H, ArH), 3.41 (t, *J* = 7.66 Hz, 2H, CH₂), 3.01 (t, *J* = 7.62 Hz, 2H, CH₂) ppm; ¹³C NMR (100 MHz, DMSO-*d*₆) δ : 167.89, 140.07, 128.73, 128.63, 128.39, 126.36, 109.79, 34.58 (CH₂), 31.93 (CH₂) ppm.

4.4 Synthesis of 4-chloro-6-(pentylthio)-1*H*-pyrazolo[3,4-*d*]pyrimidine (6b)

Vilsmeier-Haack reagent was freshly prepared by the careful addition of POCl₃ (4.29 mL, 0.047 mol) in DMF (0.97 mL, 0.012 mol) at 0 °C with constant stirring. To this reaction mixture (maintained at 0 °C) was added 6-(pentylthio)-1*H*-pyrazolo[3,4-*d*]pyrimidin-4-ol (5b, 1g, 0.004 mol) and stirred initially for 30 min and later slowly brought to RT and continued stirring for another 30 min. Finally, the reaction mixture was allowed to reflux at 80 °C for 2 h until the TLC showed full consumption of starting material. The reaction mixture was then poured in ice cold water and neutralized with 10% NaOH solution. Thus, the generated precipitate was filtered under suction and further purified by flash silica column [MeOH/DCM, 05:95] to afford the desired compound **6b** as light yellow solid. Yield: 85%; mp 194-196 °C; FTIR (ATR, cm⁻¹) ν_{\max} : 3095 (NH Str.), 2956 (Ar-H Str.), 1602, 1556, 1465; ¹H-NMR

(400 MHz, DMSO- d_6) δ : 14.19 (s, 1H, NH), 8.28 (s, 1H, ArH), 3.16 (t, $J = 7.32$ Hz, 2H, $\underline{\text{CH}_2}$), 1.73-1.66 (m, 2H, $\underline{\text{CH}_2}$), 1.42-1.27 (m, 4H, ($\underline{\text{CH}_2}$)₂), 0.87 (t, $J = 7.16$ Hz, 3H, $\underline{\text{CH}_3}$) ppm; ^{13}C NMR (100 MHz, DMSO- d_6) δ : 168.23, 109.70, 30.42 ($\underline{\text{CH}_2}$), 30.38 ($\underline{\text{CH}_2}$), 28.11 ($\underline{\text{CH}_2}$), 21.66 ($\underline{\text{CH}_2}$), 13.84 ($\underline{\text{CH}_3}$) ppm.

4.5 General procedure for the synthesis of 6-(phenethylthio/pentylthio)-*N*-phenyl-1*H* pyrazolo[3,4-*d*]pyrimidin-4-amines (7-43)

To a well stirred solution of compound **6a** or **6b** (0.2g, 1Eq.) in 10 mL absolute ethanol, was added an appropriately substituted anilines (1.1Eq.) and the reaction mixture was refluxed for 2-3 h until TLC showed full consumption of starting materials. The excess of solvent was evaporated under reduced pressure to yield the crude solids, which were further purified by recrystallization with methanol to afford the desired title compounds (7-43).

4.5.1. 6-(phenethylthio)-*N*-phenyl-1*H*-pyrazolo[3,4-*d*]pyrimidin-4-amine (7)

White solid; yield: 90%; mp 226-228 °C; FTIR (ATR, cm^{-1}) $_{\text{vmax}}$: 3363, 3119, 2918, 1621, 1567, 1491, 1470, 1301, 1183; ^1H -NMR (400 MHz, DMSO- d_6) δ : 13.44 (s, 1H, NH), 10.05 (s, 1H, ArH), 8.17 (s, 1H, NH), 7.77 (d, $J = 7.92$ Hz, 2H, ArH), 7.35-7.19 (m, 7H, ArH), 7.10 (t, $J = 7.34$ Hz, 1H, ArH), 3.36 (t, $J = 5.14$ Hz, 2H, $\underline{\text{CH}_2}$), 2.97 (t, $J = 5.14$, 2H, $\underline{\text{CH}_2}$) ppm; ^{13}C NMR (100 MHz, DMSO- d_6) δ : 167.40, 155.51, 153.48, 140.38, 138.90, 128.69, 128.52, 128.31, 126.20, 123.59, 121.34, 98.41, 35.30 ($\underline{\text{CH}_2}$), 31.31 ($\underline{\text{CH}_2}$) ppm; HRMS (ESI) for $\text{C}_{19}\text{H}_{16}\text{N}_5\text{S}$, $[\text{M}+\text{H}]^+$ calcd: 346.1126, found: 346.1126.

4.5.2. *N*-(2-chlorophenyl)-6-(phenethylthio)-1*H*-pyrazolo[3,4-*d*]pyrimidin-4-amine (8)

White solid; yield: 92%; mp 268-270 °C; FTIR (ATR, cm^{-1}) $_{\text{vmax}}$: 3055, 2918, 2718, 1626, 1560, 1379, 1269, 1184; ^1H -NMR (400 MHz, DMSO- d_6) δ : 10.47 (s, 1H, NH), 7.98 (s, 1H, NH), 7.62-7.58 (m, 2H, ArH), 7.41-7.08 (m, 8H, ArH), 3.20 (t, $J = 7.68$ Hz, 2H, $\underline{\text{CH}_2}$), 2.83 (t, $J = 7.56$ Hz, 2H, $\underline{\text{CH}_2}$) ppm; ^{13}C NMR (100 MHz, DMSO- d_6) δ : 166.95, 155.03, 140.21, 134.86, 130.46, 129.95, 129.39, 128.49, 128.29, 127.81, 126.20, 98.12, 35.33 ($\underline{\text{CH}_2}$), 31.37 ($\underline{\text{CH}_2}$) ppm.

4.5.3. *N*-(3-chlorophenyl)-6-(phenethylthio)-1*H*-pyrazolo[3,4-*d*]pyrimidin-4-amine (9)

White solid; yield: 85%; mp 216-218 °C; FTIR (ATR, cm^{-1}) $_{\text{vmax}}$: 3311, 3210, 3132, 3023, 2917, 1635, 1558, 1473, 1388, 1309, 1176; ^1H -NMR (400 MHz, DMSO- d_6) δ : 10.46 (s, 1H, NH), 8.35 (s, 1H, NH), 8.08 (s, 1H, ArH), 7.73 (dd, $J = 8.08, 1.04$ Hz, 1H, ArH), 7.36-7.12 (m, 8H, ArH), 3.39 (t, $J = 7.62$ Hz, 2H, $\underline{\text{CH}_2}$), 2.98 (t, $J = 7.62$ Hz, 2H, $\underline{\text{CH}_2}$) ppm; ^{13}C NMR (100 MHz, DMSO- d_6) δ : 167.27, 155.19, 153.30, 140.47, 140.24, 132.99, 132.48, 130.28, 128.57, 128.32, 126.25, 123.05, 120.55, 119.31, 35.06 ($\underline{\text{CH}_2}$), 31.52 ($\underline{\text{CH}_2}$) ppm; HRMS (ESI) for $\text{C}_{19}\text{H}_{15}\text{N}_5\text{S}\text{Cl}$, $[\text{M}+\text{H}]^+$ calcd: 380.0733, found: 380.0737.

4.5.4. *N*-(4-chlorophenyl)-6-(3-phenylpropyl)-1*H*-pyrazolo[3,4-*d*]pyrimidin-4-amine (10)

White solid; yield: 85%; mp 286-288 °C; FTIR (ATR, cm^{-1}) ν_{max} : 3052, 2911, 2725, 1627, 1566, 1487, 1383, 1276, 1184, 1080, 1015; $^1\text{H-NMR}$ (400 MHz, $\text{DMSO-}d_6$) δ : 10.81 (s, 1H, NH), 8.49 (s, 1H, NH), 7.84 (d, $J = 8.80$ Hz, 2H, ArH), 7.35-7.18 (m, 8H, ArH), 3.37 (t, $J = 7.74$ Hz, 2H, CH_2), 2.95 (t, $J = 7.74$ Hz, 2H, CH_2) ppm; $^{13}\text{C NMR}$ (100 MHz, $\text{DMSO-}d_6$) δ : 166.99, 154.47, 153.53, 140.20, 137.55, 132.23, 128.56, 128.51, 128.31, 127.63, 126.26, 123.16, 98.76, 35.21 (CH_2), 31.38 (CH_2) ppm.

4.5.5. *N*-(3-nitrophenyl)-6-(phenethylthio)-1*H*-pyrazolo[3,4-*d*]pyrimidin-4-amine (11)

Yellow solid; yield: 81%; mp 249-251 °C; FTIR (ATR, cm^{-1}) ν_{max} : 3378, 3100, 3030, 2828, 1629, 1566, 1525, 1478, 1429, 1349, 1250, 1109; $^1\text{H-NMR}$ (400 MHz, $\text{DMSO-}d_6$) δ : 10.63 (s, 1H, NH), 8.91 (t, $J = 2.12$ Hz, 1H, ArH), 8.34 (s, 1H, NH), 8.22 (dd, $J = 8.06, 1.62$ Hz, 1H, ArH), 7.91 (dd, $J = 8.14, 1.98$ Hz, 1H, ArH), 7.61 (t, $J = 8.18$ Hz, 1H, ArH), 7.28-7.17 (m, 6H, ArH), 3.41 (t, $J = 7.62$ Hz, 2H, CH_2), 2.97 (t, $J = 7.60$ Hz, 2H, CH_2) ppm; $^{13}\text{C NMR}$ (100 MHz, $\text{DMSO-}d_6$) δ : 167.38, 155.45, 153.12, 147.90, 140.35, 140.23, 132.53, 130.00, 128.47, 128.29, 126.46, 126.22, 117.51, 114.85, 98.72, 35.03 (CH_2), 31.44 (CH_2) ppm.

4.5.6. *N*-(4-nitrophenyl)-6-(phenethylthio)-1*H*-pyrazolo[3,4-*d*]pyrimidin-4-amine (12)

White solid; yield: 88%; mp 265-267 °C; FTIR (ATR, cm^{-1}) ν_{max} : 3033, 2902, 2820, 2752, 1627, 1570, 1515, 1338, 1274, 1183, 1110; $^1\text{H-NMR}$ (400 MHz, $\text{DMSO-}d_6$) δ : 11.06 (s, 1H, NH), 9.94 (s, 1H, NH), 8.54 (s, 1H, ArH), 8.17 (s, 4H, ArH), 7.29-7.19 (m, 5H, ArH), 3.41 (t, $J = 7.70$ Hz, 2H, CH_2), 3.00 (t, $J = 7.68$ Hz, 2H, CH_2) ppm; $^{13}\text{C NMR}$ (100 MHz, $\text{DMSO-}d_6$) δ : 167.34, 155.39, 153.01, 145.64, 141.83, 140.27, 132.88, 128.51, 128.32, 126.29, 124.72, 120.14, 99.19, 35.08 (CH_2), 31.39 (CH_2) ppm; HRMS (ESI) for $\text{C}_{19}\text{H}_{15}\text{N}_6\text{O}_2\text{S}$, $[\text{M}+\text{H}]^+$ calcd: 391.0974, found: 391.0977.

4.5.7. *N*-(2-bromophenyl)-6-(phenethylthio)-1*H*-pyrazolo[3,4-*d*]pyrimidin-4-amine (13)

White solid; yield: 85%; mp 266-268 °C; FTIR (ATR, cm^{-1}) ν_{max} : 3052, 2921, 2709, 1625, 1585, 1564, 1547, 1507, 1415, 1380, 1268, 1185; $^1\text{H-NMR}$ (400 MHz, $\text{DMSO-}d_6$) δ : 10.57 (s, 1H, NH), 7.96 (s, 1H, NH), 7.76 (dd, $J = 8.0, 1.0$ Hz, 1H, ArH), 7.57 (dd, $J = 7.80, 1.52$ Hz, 1H, ArH), 7.44 (dd, $J = 7.62, 1.16$ Hz, 1H, ArH), 7.32-7.24 (m, 4H, ArH), 7.18 (t, $J = 7.28$ Hz, 1H, ArH), 7.08 (d, $J = 7.28$ Hz, 2H, ArH), 3.19 (t, $J = 7.72$ Hz, 2H, CH_2), 2.82 (t, $J = 7.68$ Hz, 2H, CH_2) ppm; $^{13}\text{C NMR}$ (100 MHz, $\text{DMSO-}d_6$) δ : 166.85, 155.15, 140.18, 136.35, 133.12, 131.87, 129.79, 128.88, 128.50, 128.29, 126.20, 35.32 (CH_2), 31.39 (CH_2) ppm.

4.5.8. *N*-(3-bromophenyl)-6-(phenethylthio)-1*H*-pyrazolo[3,4-*d*]pyrimidin-4-amine (14)

White solid; yield: 81%; mp 265-267 °C; FTIR (ATR, cm^{-1}) ν_{max} : 3053, 2914, 2724, 1625, 1558, 1507, 1472, 1379, 1273, 1184; $^1\text{H-NMR}$ (400 MHz, $\text{DMSO-}d_6$) δ : 10.61 (s, 1H, NH), 8.42 (s, 1H, NH), 8.23 (s, 1H, ArH), 7.80 (t, $J = 2.66$ Hz, 1H, ArH), 7.29-7.20 (m, 8H, ArH), 3.39 (t, $J = 7.58$ Hz, 2H, CH_2), 2.98 (t, $J = 7.56$ Hz, 2H, CH_2) ppm; $^{13}\text{C NMR}$ (100 MHz, $\text{DMSO-}d_6$) δ : 167.16, 153.39, 140.52, 140.17,

132.46, 130.56, 128.59, 128.33, 126.26, 126.09, 123.55, 121.41, 119.85, 98.75, 35.02 ($\underline{\text{C}}\text{H}_2$), 31.56 ($\underline{\text{C}}\text{H}_2$) ppm; HRMS (ESI) for $\text{C}_{19}\text{H}_{15}\text{N}_5\text{SBr}$, $[\text{M}+\text{H}]^+$ calcd: 424.0224, found: 424.0232.

4.5.9. *N*-(4-bromophenyl)-6-(phenethylthio)-1*H*-pyrazolo[3,4-*d*]pyrimidin-4-amine (15)

White solid; yield: 78%; mp 284-286 °C; FTIR (ATR, cm^{-1}) ν_{max} : 3100, 3025, 2917, 1613, 1579, 1495, 1473, 1304, 1225, 1180; ^1H -NMR (400 MHz, $\text{DMSO-}d_6$) δ : 10.84 (s, 1H, NH), 8.51 (s, 1H, NH), 7.79 (d, $J = 8.76$ Hz, 2H, ArH), 7.46 (d, $J = 8.80$ Hz, 2H, ArH), 7.30-7.18 (m, 6H, ArH), 3.37 (t, $J = 5.16$ Hz, 2H, $\underline{\text{C}}\text{H}_2$), 2.95 (t, $J = 7.74$ Hz, 2H, $\underline{\text{C}}\text{H}_2$) ppm; ^{13}C NMR (100 MHz, $\text{DMSO-}d_6$) δ : 166.98, 153.50, 140.20, 137.97, 132.22, 131.47, 128.51, 128.33, 126.27, 123.52, 115.74, 98.81, 35.21 ($\underline{\text{C}}\text{H}_2$), 31.38 ($\underline{\text{C}}\text{H}_2$) ppm.

4.6.0. *N*-(2,4-dimethylphenyl)-6-(phenethylthio)-1*H*-pyrazolo[3,4-*d*]pyrimidin-4-amine (16)

White solid; yield: 76%; mp 238-240 °C; FTIR (ATR, cm^{-1}) ν_{max} : 3100, 3025, 2917, 1613, 1579, 1495, 1473, 1335, 1304, 1225, 1180; ^1H -NMR (400 MHz, $\text{DMSO-}d_6$) δ : 13.29 (s, 1H, NH), 9.66 (s, 1H, NH), 7.29-7.04 (m, 9H, ArH), 3.22 (s, 2H, $\underline{\text{C}}\text{H}_2$), 2.88 (s, 2H, $\underline{\text{C}}\text{H}_2$), 2.31 (s, 3H, $\underline{\text{C}}\text{H}_3$), 2.14 (s, 3H, $\underline{\text{C}}\text{H}_3$) ppm; ^{13}C NMR (100 MHz, $\text{DMSO-}d_6$) δ : 167.40, 155.73, 140.50, 133.89, 132.55, 131.23, 128.51, 128.25, 127.04, 126.13, 35.51 ($\underline{\text{C}}\text{H}_2$), 31.28 ($\underline{\text{C}}\text{H}_2$), 20.64 ($\underline{\text{C}}\text{H}_3$), 17.74 ($\underline{\text{C}}\text{H}_3$) ppm; HRMS (ESI) for $\text{C}_{21}\text{H}_{20}\text{N}_5\text{S}$, $[\text{M}+\text{H}]^+$ calcd: 374.1447, found: 374.1439.

4.6.1. *N*-(4-(methylthio)phenyl)-6-(phenethylthio)-1*H*-pyrazolo[3,4-*d*]pyrimidin-4-amine (17)

White solid; yield: 90%; mp 262-264 °C; FTIR (ATR, cm^{-1}) ν_{max} : 3054, 2921, 2809, 2752, 1625, 1583, 1586, 1488, 1417, 1385, 1274, 1243, 1184; ^1H -NMR (400 MHz, $\text{DMSO-}d_6$) δ : 10.50 (s, 1H, NH), 8.36 (s, 1H, NH), 7.74 (d, $J = 8.52$ Hz, 2H, ArH), 7.31-7.19 (m, 8H, ArH), 3.37 (t, $J = 7.80$ Hz, 2H, $\underline{\text{C}}\text{H}_2$), 2.96 (t, $J = 7.76$ Hz, 2H, $\underline{\text{C}}\text{H}_2$), 2.44 (s, 3H, $\underline{\text{S}}\underline{\text{C}}\underline{\text{H}}_3$); ^{13}C NMR (100 MHz, $\text{DMSO-}d_6$) δ : 167.07, 154.78, 153.49, 140.28, 135.91, 132.20, 128.51, 128.31, 126.70, 126.24, 122.23, 98.58, 35.31 ($\underline{\text{C}}\text{H}_2$), 31.31 ($\underline{\text{C}}\text{H}_2$), 15.31 ($\underline{\text{C}}\text{H}_3$) ppm; HRMS (ESI) for $\text{C}_{20}\text{H}_{18}\text{N}_5\text{S}_2$, $[\text{M}+\text{H}]^+$ calcd: 392.1000, found: 392.1004.

4.6.2. *N*-(4-chloro-3-(trifluoromethyl)phenyl)-6-(phenethylthio)-1*H*-pyrazolo[3,4-*d*]pyrimidin-4-amine (18)

White solid; yield: 89%; mp 273-275 °C; FTIR (ATR, cm^{-1}) ν_{max} : 3033, 2920, 2808, 2752, 1628, 1566, 1507, 1498, 1399, 1315, 1274, 1171, 1153, 1107, 1037; ^1H -NMR (400 MHz, $\text{DMSO-}d_6$) δ : 10.93 (s, 1H, NH), 8.49 (d, $J = 2.52$ Hz, 1H, ArH), 8.47 (s, 1H, NH), 8.18 (dd, $J = 8.82, 2.50$ Hz, 1H, ArH), 7.61 (d, $J = 8.80$ Hz, 1H, ArH), 7.29-7.20 (m, 6H, ArH), 3.37 (t, $J = 7.68$ Hz, 2H, $\underline{\text{C}}\text{H}_2$), 2.96 (t, $J = 7.66$ Hz, 2H, $\underline{\text{C}}\text{H}_2$) ppm; ^{13}C NMR (100 MHz, $\text{DMSO-}d_6$) δ : 167.21, 155.12, 153.17, 140.21, 138.63, 132.61, 131.89, 126.76, 126.46, 125.52, 124.15, 123.86, 121.44, 119.62, 119.57, 98.83, 35.03 ($\underline{\text{C}}\text{H}_2$), 31.40 ($\underline{\text{C}}\text{H}_2$) ppm; HRMS (ESI) for $\text{C}_{20}\text{H}_{15}\text{N}_5\text{F}_3\text{SCl}$, $[\text{M}+\text{H}]^+$ calcd: 449.0689, found: 448.0611.

4.6.3. *N*-(4-bromo-3-(trifluoromethyl)phenyl)-6-(phenethylthio)-1*H*-pyrazolo[3,4-*d*]pyrimidin-4-amine (19)

White solid; yield: 86%; mp 273-275 °C; FTIR (ATR, cm⁻¹)_{v_{max}}: 3033, 2905, 2809, 2752, 1628, 1562, 1507, 1473, 1381, 1315, 1273, 1182, 1131, 1097; ¹H-NMR (400 MHz, DMSO-*d*₆) δ: 10.71 (s, 1H, NH), 8.48 (s, 1H, NH), 8.37 (s, 1H, ArH), 8.08 (t, *J* = 6.48 Hz, 1H, ArH), 7.76 (t, *J* = 7.44 Hz, 1H, ArH), 7.29-7.20 (m, 6H, ArH), 3.37 (t, *J* = 7.66 Hz, 2H, CH₂), 2.96 (t, *J* = 7.54 Hz, 2H, CH₂) ppm; ¹³C NMR (100 MHz, DMSO-*d*₆) δ: 167.27, 153.11, 140.23, 139.12, 135.27, 132.61, 128.50, 128.32, 128.26, 126.26, 125.49, 124.25, 121.53, 119.82, 35.04 (CH₂), 31.38 (CH₂) ppm; HRMS (ESI) for C₂₀H₁₅N₅F₃SBr, [M+H]⁺ calcd: 493.0184, found: 492.0105.

4.6.4. *N*-(4-chloro-3-nitrophenyl)-6-(phenethylthio)-1*H*-pyrazolo[3,4-*d*]pyrimidin-4-amine (20)

White solid; yield: 75%; mp 265-267 °C; FTIR (ATR, cm⁻¹)_{v_{max}}: 3023, 2899, 2827, 2759, 1628, 1557, 1531, 1494, 1432, 1376, 1338, 1275, 1182, 1048; ¹H-NMR (400 MHz, DMSO-*d*₆) δ: 10.95 (s, 1H, NH), 8.75 (s, 1H, ArH), 8.43 (s, 1H, NH), 8.16 (d, *J* = 8.84 Hz, 1H, ArH), 7.68 (dd, *J* = 8.82, 1.66 Hz, 1H, ArH), 7.29-7.18 (m, 6H, ArH), 3.40 (t, *J* = 7.58 Hz, 2H, CH₂), 2.97 (t, *J* = 7.56 Hz, 2H, CH₂) ppm; ¹³C NMR (100 MHz, DMSO-*d*₆) δ: 167.28, 155.29, 153.02, 147.02, 140.21, 139.17, 132.71, 131.82, 128.50, 128.30, 126.25, 125.57, 118.35, 117.18, 98.82, 34.98 (CH₂), 31.45 (CH₂) ppm.

4.6.5. *N*-(4-fluoro-2-methylphenyl)-6-(phenethylthio)-1*H*-pyrazolo[3,4-*d*]pyrimidin-4-amine (21)

White solid; yield: 80 %; mp 268-270 °C; FTIR (ATR, cm⁻¹)_{v_{max}}: 3103, 3026, 3000, 2934, 1593, 1580, 1492, 1313, 1303, 1210, 1180, 1144; ¹H-NMR (400 MHz, DMSO-*d*₆) δ: 13.34 (s, 1H, NH), 9.72 (s, 1H, NH), 7.39 (q, *J* = 4.76 Hz, 1H, ArH), 7.29-7.04 (m, 8H, ArH), 3.20 (s, 2H, CH₂), 2.87 (d, *J* = 6.92 Hz, 2H, CH₂), 2.19 (s, 3H, CH₃) ppm; ¹³C NMR (100 MHz, DMSO-*d*₆) δ: 167.41, 161.66, 155.71, 140.44, 132.79, 132.48, 128.47, 128.24, 126.15, 117.12, 116.89, 113.21, 113.00, 35.50 (CH₂), 31.28 (CH₂), 17.90 (CH₃) ppm; HRMS (ESI) for C₂₀H₁₇N₅FS, [M+H]⁺ calcd: 378.1191, found: 378.1189.

4.6.6. *N*-(3-bromo-4-methylphenyl)-6-(phenethylthio)-1*H*-pyrazolo[3,4-*d*]pyrimidin-4-amine (22)

White solid; yield: 85%; mp 279-281 °C; FTIR (ATR, cm⁻¹)_{v_{max}}: 3056, 2923, 2745, 1626, 1583, 1550, 1487, 1383, 1270, 1184, 1145, 1038; ¹H-NMR (400 MHz, DMSO-*d*₆) δ: 10.67 (s, 1H, NH), 8.43 (s, 1H, NH), 8.19 (d, *J* = 1.84 Hz, 1H, ArH), 7.68 (dd, *J* = 8.24, 2.00 Hz, 1H, ArH), 7.28-7.18 (m, 7H, ArH), 3.38 (t, *J* = 7.66 Hz, 2H, CH₂), 2.96 (t, *J* = 7.62 Hz, 2H, CH₂), 2.30 (s, 3H, CH₃) ppm; ¹³C NMR (100 MHz, DMSO-*d*₆) δ: 167.06, 154.62, 153.45, 140.16, 137.83, 130.85, 128.58, 128.30, 126.25, 124.55, 123.64, 120.54, 119.29, 35.07 (CH₂), 31.56 (CH₂), 21.78 (CH₃) ppm; HRMS (ESI) for C₂₀H₁₈N₅SBr, [M+H]⁺ calcd: 439.0466, found: 438.0388.

4.6.7. *N*-(2-chloro-4-fluorophenyl)-6-(phenethylthio)-1*H*-pyrazolo[3,4-*d*]pyrimidin-4-amine (23)

White solid; yield: 83 %; mp 282-284 °C; FTIR (ATR, cm^{-1}) ν_{max} : 3037, 2907, 2724, 1629, 1569, 1488, 1380, 1269, 1256, 1196, 1180; $^1\text{H-NMR}$ (400 MHz, $\text{DMSO-}d_6$) δ : 10.28 (s, 1H, NH), 8.08 (s, 1H, NH), 7.65-7.57 (m, 2H, ArH), 7.28-7.17 (m, 5H, ArH), 7.09 (d, $J = 10.24$ Hz, 2H, ArH), 3.18 (t, $J = 7.76$ Hz, 2H, CH_2), 2.82 (d, $J = 5.80$ Hz, 2H, CH_2) ppm; $^{13}\text{C NMR}$ (100 MHz, $\text{DMSO-}d_6$) δ : 155.10, 140.17, 131.55, 130.92, 130.82, 128.41, 128.26, 126.21, 117.24, 116.98, 115.09, 114.87, 35.36 (CCH_2), 31.32 (CCH_2) ppm.

4.6.8. *N*-(3,4-dimethoxyphenyl)-6-(phenethylthio)-1H-pyrazolo[3,4-*d*]pyrimidin-4-amine (24)

Light yellow solid; yield: 78%; mp 265-267 °C; FTIR (ATR, cm^{-1}) ν_{max} : 3063, 2930, 2716, 1629, 1584, 1505, 1457, 1388, 1259, 1232, 1204, 1184, 1129; $^1\text{H-NMR}$ (400 MHz, $\text{DMSO-}d_6$) δ : 10.97 (s, 1H, NH), 8.63 (s, 1H, NH), 7.39-7.14 (m, 8H, ArH), 6.85 (d, $J = 8.40$ Hz, 1H, ArH), 3.73 (s, 3H, OCH_3), 3.71 (s, 3H, OCH_3), 3.38 (t, $J = 7.80$ Hz, 2H, CH_2), 2.93 (t, $J = 7.74$ Hz, 2H, CH_2) ppm; $^{13}\text{C NMR}$ (100 MHz, $\text{DMSO-}d_6$) δ : 166.40, 148.58, 140.05, 131.11, 128.52, 128.30, 126.29, 111.69, 55.66 (O-CH_3), 55.51 (O-CH_3), 35.19 (CCH_2), 31.46 (CCH_2) ppm.

4.6.9. *N*-(3-ethynylphenyl)-6-(phenethylthio)-1H-pyrazolo[3,4-*d*]pyrimidin-4-amine (25)

Light yellow solid; yield: 78%; mp 254-256 °C; FTIR (ATR, cm^{-1}) ν_{max} : 3230, 3065, 2914, 2750, 1627, 1571, 1543, 1509, 1381, 1257, 1167, 1051; $^1\text{H-NMR}$ (400 MHz, $\text{DMSO-}d_6$) δ : 10.82 (s, 1H, NH), 8.51 (s, 1H, NH), 8.03 (s, 1H, ArH), 7.86 (d, $J = 4.54$ Hz, 1H, ArH), 7.35-7.18 (m, 8H, ArH), 4.18 (s, 1H, Ethynyl-H), 3.39 (t, $J = 7.54$ Hz, 2H, CH_2), 2.97 (t, $J = 7.52$ Hz, 2H, CH_2) ppm; $^{13}\text{C NMR}$ (100 MHz, $\text{DMSO-}d_6$) δ : 166.99, 153.62, 140.13, 138.92, 129.13, 127.04, 126.27, 124.41, 122.09, 122.04, 98.80, 83.30, 80.75, 35.04 (CCH_2), 31.56 (CCH_2) ppm.

4.7.0. 6-(pentylthio)-*N*-phenyl-1H-pyrazolo[3,4-*d*]pyrimidin-4-amine (26)

White solid; yield: 86%; mp 202-204 °C; FTIR (ATR, cm^{-1}) ν_{max} : 3079, 2924, 1624, 1568, 1540, 1507, 1496, 1309, 1185; $^1\text{H-NMR}$ (400 MHz, $\text{DMSO-}d_6$) δ : 13.39 (s, 1H, NH), 10.02 (s, 1H, ArH), 8.15 (s, 1H, NH), 7.78 (d, $J = 7.88$ Hz, 2H, ArH), 7.38 (t, $J = 7.92$ Hz, 2H, ArH), 7.12 (t, $J = 7.32$ Hz, 1H, ArH), 3.09 (t, $J = 7.38$ Hz, 2H, CH_2), 1.66 (m, 2H, CH_2), 1.25-1.38 (m, 4H, (CH_2)₂), 0.85 (t, $J = 7.16$ Hz, 3H, CH_3) ppm; $^{13}\text{C NMR}$ (100 MHz, $\text{DMSO-}d_6$) δ : 167.73, 155.51, 153.39, 138.96, 128.64, 123.53, 121.22, 98.34, 30.57 (CCH_2), 29.97 (CCH_2), 28.97 (CCH_2), 21.75 (CCH_2), 13.85 (CCH_3) ppm; HRMS (ESI) for $\text{C}_{16}\text{H}_{18}\text{N}_5\text{S}$, $[\text{M}+\text{H}]^+$ calcd: 312.1284, found: 312.1283.

4.7.1. *N*-(2-chlorophenyl)-6-(pentylthio)-1H-pyrazolo[3,4-*d*]pyrimidin-4-amine (27)

White solid; yield: 75%; mp 231-233 °C; FTIR (ATR, cm^{-1}) ν_{max} : 3054, 2924, 2719, 1624, 1571, 1383, 1273, 1185, 1057; $^1\text{H-NMR}$ (400 MHz, $\text{DMSO-}d_6$) δ : 10.48 (s, 1H, NH), 7.99 (s, 1H, NH), 7.57-7.61 (m, 2H, ArH), 7.35-7.44 (m, 2H, ArH), 2.90 (t, $J = 7.44$ Hz, 2H, CH_2), 1.46-1.53 (m, 2H, CH_2), 1.14-1.22 (m, 4H, (CH_2)₂), 0.82 (t, $J = 6.86$ Hz, 3H, CH_3) ppm; $^{13}\text{C NMR}$ (100 MHz, $\text{DMSO-}d_6$) δ : 167.35,

154.87, 134.96, 132.05, 129.84, 129.43, 128.19, 127.70, 97.95, 30.50 ($\underline{\text{CH}_2}$), 29.99 ($\underline{\text{CH}_2}$), 29.11 ($\underline{\text{CH}_2}$), 21.74($\underline{\text{CH}_2}$), 13.87 ($\underline{\text{CH}_3}$) ppm.

4.7.2. *N*-(3-chlorophenyl)-6-(pentylthio)-1*H*-pyrazolo[3,4-*d*]pyrimidin-4-amine (28)

White solid; yield: 92%; mp 224-226 °C; FTIR (ATR, cm^{-1}) $_{\text{vmax}}$: 3099, 2928, 1623, 1558, 1541, 1473, 1386, 1304, 1180; $^1\text{H-NMR}$ (400 MHz, $\text{DMSO-}d_6$) δ : 10.35 (s, 1H, NH), 8.30 (s, 1H, NH), 8.12 (s, 1H, ArH), 7.70 (d, $J = 8.28$ Hz, 1H, ArH), 7.39 (t, $J = 8.10$ Hz, 1H, ArH), 7.15 (dd, $J = 7.90, 1.70$ Hz, 1H, ArH), 3.12 (t, $J = 7.32$ Hz, 2H, $\underline{\text{CH}_2}$), 1.63-1.70 (m, 2H, $\underline{\text{CH}_2}$), 1.21-1.41 (m, 4H ($\underline{\text{CH}_2}$)₂), 0.84 (t, $J = 7.16$ Hz, 3H, $\underline{\text{CH}_3}$) ppm; $^{13}\text{C NMR}$ (100 MHz, $\text{DMSO-}d_6$) δ : 167.64, 155.27, 153.21, 140.53, 132.96, 132.43, 130.28, 123.00, 120.47, 119.19, 98.62, 30.51 ($\underline{\text{CH}_2}$), 30.14 ($\underline{\text{CH}_2}$), 28.75 ($\underline{\text{CH}_2}$), 21.76 ($\underline{\text{CH}_2}$), 13.87 ($\underline{\text{CH}_3}$) ppm.

4.7.3. *N*-(4-chlorophenyl)-6-(pentylthio)-1*H*-pyrazolo[3,4-*d*]pyrimidin-4-amine (29)

White solid; yield: 88%; mp 253-255 °C; FTIR (ATR, cm^{-1}) $_{\text{vmax}}$: 3056, 2923, 2717, 1625, 1567, 1541, 1384, 1267, 1183, 1080, 1013; $^1\text{H-NMR}$ (400 MHz, $\text{DMSO-}d_6$) δ : 10.58 (s, 1H, NH), 8.39 (s, 1H, NH), 7.85 (d, $J = 8.88$ Hz, 2H, ArH), 7.43 (d, $J = 8.88$ Hz, 2H, ArH), 3.09 (t, $J = 7.38$ Hz, 2H, $\underline{\text{CH}_2}$), 1.61-1.68 (m, 2H, $\underline{\text{CH}_2}$), 1.22-1.37 (m, 4H, ($\underline{\text{CH}_2}$)₂), 0.84 (t, $J = 7.16$ Hz, 3H, $\underline{\text{CH}_3}$) ppm; $^{13}\text{C NMR}$ (100 MHz, $\text{DMSO-}d_6$) δ : 167.45, 153.38, 137.76, 132.27, 128.51, 127.40, 122.95, 98.60, 30.58 ($\underline{\text{CH}_2}$), 30.12 ($\underline{\text{CH}_2}$), 28.88 ($\underline{\text{CH}_2}$), 21.76 ($\underline{\text{CH}_2}$), 13.87 ($\underline{\text{CH}_3}$) ppm.

4.7.4. *N*-(3-nitrophenyl)-6-(pentylthio)-1*H*-pyrazolo[3,4-*d*]pyrimidin-4-amine (30)

Brown solid; yield: 84%; mp 210-212 °C; FTIR (ATR, cm^{-1}) $_{\text{vmax}}$: 3080, 2928, 2757, 1625, 1558, 1522, 1348, 1299, 1175, 1072; $^1\text{H-NMR}$ (400 MHz, $\text{DMSO-}d_6$) δ : 10.70 (s, 1H, NH), 8.96 (t, $J = 2.14$ Hz, 1H, ArH), 8.37 (s, 1H, ArH), 8.20-8.23 (m, 1H, ArH), 7.92-7.94 (m, 1H, ArH), 7.66 (t, $J = 8.22$ Hz, 1H, ArH), 3.15 (t, $J = 7.30$ Hz, 2H, $\underline{\text{CH}_2}$), 1.62-1.69 (m, 2H, $\underline{\text{CH}_2}$), 1.21-1.38 (m, 4H, ($\underline{\text{CH}_2}$)₂), 0.82 (t, $J = 7.20$ Hz, 3H, $\underline{\text{CH}_3}$) ppm; $^{13}\text{C NMR}$ (100 MHz, $\text{DMSO-}d_6$) δ : 167.72, 155.34, 153.14, 147.93, 140.40, 132.55, 130.00, 126.49, 117.56, 114.85, 98.72, 30.49 ($\underline{\text{CH}_2}$), 30.16 ($\underline{\text{CH}_2}$), 28.57 ($\underline{\text{CH}_2}$), 21.74 ($\underline{\text{CH}_2}$), 13.86 ($\underline{\text{CH}_3}$) ppm.

4.7.5. *N*-(4-nitrophenyl)-6-(pentylthio)-1*H*-pyrazolo[3,4-*d*]pyrimidin-4-amine (31)

Yellow solid; yield: 93%; mp 268-270 °C; FTIR (ATR, cm^{-1}) $_{\text{vmax}}$: 3108, 2923, 1626, 1568, 1508, 1336, 1297, 1250, 1182, 1111; $^1\text{H-NMR}$ (400 MHz, $\text{DMSO-}d_6$) δ : 10.66 (s, 1H, NH), 8.33 (s, 1H, NH), 8.27 (d, $J = 9.24$ Hz, 2H, ArH), 8.13 (d, $J = 9.24$ Hz, 2H, ArH), 3.14 (t, $J = 7.32$ Hz, 2H, $\underline{\text{CH}_2}$), 1.66-1.73 (m, 2H, $\underline{\text{CH}_2}$), 1.25-1.43 (m, 4H, ($\underline{\text{CH}_2}$)₂), 0.85 (t, $J = 7.18$ Hz, 3H, $\underline{\text{CH}_3}$) ppm; $^{13}\text{C NMR}$ (100 MHz, $\text{DMSO-}d_6$) δ : 167.77, 155.64, 152.77, 145.70, 141.75, 132.57, 124.79, 119.87, 99.00, 30.60 ($\underline{\text{CH}_2}$), 30.12 ($\underline{\text{CH}_2}$), 28.73 ($\underline{\text{CH}_2}$), 21.77 ($\underline{\text{CH}_2}$), 13.86 ($\underline{\text{CH}_3}$) ppm.

4.7.6. *N*-(2-bromophenyl)-6-(pentylthio)-1*H*-pyrazolo[3,4-*d*]pyrimidin-4-amine (32)

White solid; yield: 81%; mp 255-257 °C; FTIR (ATR, cm^{-1}) $_{\text{vmax}}$: 3052, 2924, 2725, 1626, 1570, 1542, 1507, 1379, 1275, 1184, 1044; $^1\text{H-NMR}$ (400 MHz, $\text{DMSO-}d_6$) δ : 10.53 (s, 1H, NH), 7.96 (s, 1H, NH), 7.75-7.78 (m, 1H, ArH), 7.53-7.56 (m, 1H, ArH), 7.45-7.49 (m, 1H, ArH), 7.29-7.33 (m, 1H, ArH), 2.90 (t, $J = 7.42$ Hz, 2H, CH_2), 1.45-1.53 (m, 2H, CH_2), 1.14-1.22 (m, 4H, (CH_2) $_2$), 0.82 (t, $J = 6.98$ Hz, 3H, CH_3) ppm; $^{13}\text{C NMR}$ (100 MHz, $\text{DMSO-}d_6$) δ : 167.15, 155.06, 136.37, 133.01, 131.81, 129.82, 128.80, 128.40, 121.69, 97.97, 30.49 (CH_2), 30.06 (CH_2), 29.15 (CH_2), 21.75 (CH_2), 13.88 (CH_3) ppm.

4.7.7. *N*-(3-bromophenyl)-6-(pentylthio)-1*H*-pyrazolo[3,4-*d*]pyrimidin-4-amine (33)

Brown solid; yield: 76%; mp 232-234 °C; FTIR (ATR, cm^{-1}) $_{\text{vmax}}$: 3099, 2927, 1622, 1557, 1472, 1298, 1178, 1063; $^1\text{H-NMR}$ (400 MHz, $\text{DMSO-}d_6$) δ : 10.41 (s, 1H, NH), 8.32 (s, 1H, NH), 8.26 (t, $J = 1.78$ Hz, 1H, ArH), 7.75 (d, $J = 8.04$ Hz, 1H, ArH), 7.27-7.35 (m, 2H, ArH), 3.12 (t, $J = 7.28$ Hz, 2H, CH_2), 1.63-1.71 (m, 2H, CH_2), 1.23-1.41 (m, 4H, (CH_2) $_2$), 0.84 (t, $J = 7.22$ Hz, 3H, CH_3) ppm; $^{13}\text{C NMR}$ (100 MHz, $\text{DMSO-}d_6$) δ : 167.59, 155.19, 153.18, 140.63, 132.41, 130.56, 125.88, 123.32, 121.39, 119.57, 98.61, 30.49 (CH_2), 30.13 (CH_2), 28.70 (CH_2), 21.75 (CH_2), 13.86 (CH_3) ppm.

4.7.8. *N*-(4-bromophenyl)-6-(pentylthio)-1*H*-pyrazolo[3,4-*d*]pyrimidin-4-amine (34)

White solid; yield: 90%; mp 256-258 °C; FTIR (ATR, cm^{-1}) $_{\text{vmax}}$: 3056, 2924, 2718, 1626, 1559, 1474, 1383, 1269, 1183, 1065; $^1\text{H-NMR}$ (400 MHz, $\text{DMSO-}d_6$) δ : 10.53 (s, 1H, NH), 8.36 (s, 1H, NH), 7.80 (d, $J = 8.64$ Hz, 2H, ArH), 7.55 (d, $J = 8.80$ Hz, 2H, ArH), 3.09 (t, $J = 7.36$ Hz, 2H, CH_2), 1.61-1.68 (m, 2H, CH_2), 1.22-1.37 (m, 4H, (CH_2) $_2$), 0.85 (t, $J = 7.08$ Hz, 3H, CH_3); $^{13}\text{C NMR}$ (100 MHz, $\text{DMSO-}d_6$) δ : 167.48, 153.34, 138.22, 132.27, 131.41, 123.25, 98.61, 30.59 (CH_2), 30.12 (CH_2), 28.89 (CH_2), 21.76 (CH_2), 13.89 (CH_3) ppm; HRMS (ESI) for $\text{C}_{16}\text{H}_{17}\text{N}_5\text{SBr}$, $[\text{M}+\text{H}]^+$ calcd: 390.0383, found: 390.0388.

4.7.9. *N*-(2,4-dimethylphenyl)-6-(pentylthio)-1*H*-pyrazolo[3,4-*d*]pyrimidin-4-amine (35)

Brown solid; yield: 90%; mp 256-258 °C; FTIR (ATR, cm^{-1}) $_{\text{vmax}}$: 3099, 2922, 1614, 1578, 1473, 1315, 1223, 1180; $^1\text{H-NMR}$ (400 MHz, $\text{DMSO-}d_6$) δ : 13.24 (s, 1H, NH), 9.62 (s, 1H, ArH), 7.17 (t, $J = 9.64$ Hz, 2H, ArH), 7.06 (d, $J = 7.68$ Hz, 1H, ArH), 2.95 (s, 2H, CH_2), 2.31 (s, 3H, CH_3), 2.13 (s, 3H, CH_3), 1.56 (s, 2H, CH_2), 1.25 (s, 4H, (CH_2) $_2$), 0.84 (t, $J = 6.68$ Hz, 3H, CH_3) ppm; $^{13}\text{C NMR}$ (100 MHz, $\text{DMSO-}d_6$) δ : 167.72, 155.74, 133.93, 132.51, 131.16, 127.51, 127.00, 30.58 (CH_2), 29.80 (CH_2), 29.10 (CH_3), 21.76 (CH_2), 20.62 (CH_3), 17.72 (CH_2), 13.90 (CH_3) ppm; HRMS (ESI) for $\text{C}_{18}\text{H}_{22}\text{N}_5\text{S}$, $[\text{M}+\text{H}]^+$ calcd: 340.1601, found: 340.1596.

4.8.0. *N*-(4-(methylthio)phenyl)-6-(pentylthio)-1*H*-pyrazolo[3,4-*d*]pyrimidin-4-amine (36)

Brown solid; yield: 77%; mp 242-244 °C; FTIR (ATR, cm^{-1}) ν_{max} : 3064, 2923, 2724, 1624, 1558, 1520, 1507, 1386, 1185, 1083; $^1\text{H-NMR}$ (400 MHz, $\text{DMSO-}d_6$) δ : 10.65 (s, 1H, NH), 8.42 (d, $J = 9.84$, 1H, NH), 7.75 (d, $J = 8.60$ Hz, 2H, ArH), 7.29 (d, $J = 8.64$ Hz, 2H, ArH), 3.09 (t, $J = 7.42$ Hz, 2H, CH_2), 2.47 (s, 3H, SCH_3), 1.60-1.68 (m, 2H, CH_2), 1.21-1.36 (m, 4H, $(\text{CH}_2)_2$), 0.84 (t, $J = 7.12$ Hz, 3H, CH_3) ppm; $^{13}\text{C NMR}$ (100 MHz, $\text{DMSO-}d_6$) δ : 167.25, 153.57, 135.82, 131.96, 126.74, 122.41, 98.61, 30.61 (CH_2), 30.17 (CH_2), 28.98 (CH_2), 21.77 (CH_2), 15.38 (CH_3), 13.90 (CH_3) ppm.

4.8.1. *N*-(4-chloro-3-(trifluoromethyl)phenyl)-6-(pentylthio)-1H-pyrazolo[3,4-d]pyrimidin-4-amine (37)

White solid; yield: 83%; mp 258-260 °C; FTIR (ATR, cm^{-1}) ν_{max} : 3101, 2927, 1628, 1567, 1478, 1437, 1385, 1321, 1256, 1176, 1132; $^1\text{H-NMR}$ (400 MHz, $\text{DMSO-}d_6$) δ : 10.60 (s, 1H, NH), 8.51 (d, $J = 2.52$ Hz, 1H, ArH), 8.32 (s, 1H, ArH), 8.10 (dd, $J = 8.80, 2.52$ Hz, 1H, ArH), 7.71 (d, $J = 8.80$ Hz, 1H, ArH), 3.10 (t, $J = 7.34$ Hz, 2H, CH_2), 1.61-1.68 (m, 2H, CH_2), 1.21-1.38 (m, 4H, $(\text{CH}_2)_2$), 0.84 (t, $J = 7.18$ Hz, 3H, CH_3) ppm; $^{13}\text{C NMR}$ (100 MHz, $\text{DMSO-}d_6$) δ : 167.67, 155.41, 152.99, 138.72, 132.49, 131.94, 126.45, 125.33, 123.73, 119.47, 98.66, 30.48 (CH_2), 30.01 (CH_2), 28.57 (CH_2), 21.73 (CH_2), 13.83 (CH_3) ppm.

4.8.2. *N*-(4-bromo-3-(trifluoromethyl)phenyl)-6-(pentylthio)-1H-pyrazolo[3,4-d]pyrimidin-4-amine (38)

Brown solid; yield: 79%; mp 257-259 °C; FTIR (ATR, cm^{-1}) ν_{max} : 3099, 2926, 1633, 1559, 1541, 1474, 1436, 1257, 1145, 1097; $^1\text{H-NMR}$ (400 MHz, $\text{DMSO-}d_6$) δ : 10.62 (s, 1H, NH), 8.51 (d, $J = 2.52$ Hz, 1H, ArH), 8.34 (s, 1H, NH), 8.03 (dd, $J = 8.74, 2.50$ Hz, 1H, ArH), 7.86 (d, $J = 8.72$ Hz, 1H, ArH), 3.10 (t, $J = 7.32$ Hz, 2H, CH_2), 1.61-1.68 (m, 2H, CH_2), 1.22-1.38 (m, 4H, $(\text{CH}_2)_2$), 0.84 (t, $J = 7.14$ Hz, 3H, CH_3) ppm; $^{13}\text{C NMR}$ (100 MHz, $\text{DMSO-}d_6$) δ : 167.64, 155.37, 152.98, 139.16, 135.28, 132.50, 128.54, 125.39, 124.29, 119.73, 111.31, 98.70, 30.48 (CH_2), 30.00 (CH_2), 28.56 (CH_2), 21.73 (CH_2), 13.83 (CH_3) ppm; HRMS (ESI) for $\text{C}_{17}\text{H}_{16}\text{N}_5\text{F}_3\text{SBr}$, $[\text{M}+\text{H}]^+$ calcd: 458.0258, found: 458.0262.

4.8.3. *N*-(4-chloro-3-nitrophenyl)-6-(pentylthio)-1H-pyrazolo[3,4-d]pyrimidin-4-amine (39)

Yellow solid; yield: 91%; mp 251-253 °C; FTIR (ATR, cm^{-1}) ν_{max} : 3098, 2925, 1626, 1558, 1540, 1473, 1339, 1297, 1265, 1182; $^1\text{H-NMR}$ (400 MHz, $\text{DMSO-}d_6$) δ : 10.73 (s, 1H, NH), 8.78 (d, $J = 2.52$ Hz, 1H, ArH), 8.33 (s, 1H, ArH), 8.08 (dd, $J = 8.92, 2.56$ Hz, 1H, ArH), 7.76 (d, $J = 8.88$ Hz, 1H, ArH), 3.12 (t, $J = 7.26$ Hz, 2H, CH_2), 1.61-1.68 (m, 2H, CH_2), 1.20-1.39 (m, 4H, $(\text{CH}_2)_2$), 0.84 (t, $J = 7.14$ Hz, 3H, CH_3) ppm; $^{13}\text{C NMR}$ (100 MHz, $\text{DMSO-}d_6$) δ : 167.70, 155.45, 152.90, 147.12, 139.23, 132.54, 131.83, 125.33, 118.20, 116.94, 98.71, 30.48 (CH_2), 30.14 (CH_2), 28.50 (CH_2), 21.76 (CH_2), 13.86 (CH_3) ppm.

4.8.4. *N*-(4-fluoro-2-methylphenyl)-6-(pentylthio)-1H-pyrazolo[3,4-d]pyrimidin-4-amine (40)

White solid; yield: 90%; mp 261-263 °C; FTIR (ATR, cm^{-1}) ν_{max} : 3100, 2953, 1577, 1490, 1206, 1181; $^1\text{H-NMR}$ (400 MHz, $\text{DMSO-}d_6$) δ : 13.29 (s, 1H, NH), 9.69 (s, 1H, ArH), 7.33-7.36 (m, 1H, ArH), 7.20 (t, $J = 4.76$ Hz, 1H, ArH), 7.01-7.11 (m, 1H, ArH), 2.93 (s, 2H, CH_2), 2.18 (s, 3H, CH_3), 1.54 (s, 2H, CH_2), 1.22 (s, 4H, $(\text{CH}_2)_2$), 0.84 (t, $J = 6.96$ Hz, 3H, CH_3) ppm; $^{13}\text{C NMR}$ (100 MHz, $\text{DMSO-}d_6$) δ : 167.72, 155.80, 132.83, 132.39, 129.41, 117.01, 116.79, 113.15, 112.90, 30.59 (CH_2), 29.84(CH_2), 29.13 (CH_3), 21.76 (CH_2), 17.87 (CH_2), 13.87 (CH_3) ppm.

4.8.5. *N*-(3-bromo-4-methylphenyl)-6-(pentylthio)-1*H*-pyrazolo[3,4-*d*]pyrimidin-4-amine (41)

Brown solid; yield: 86%; mp 237-239 °C; FTIR (ATR, cm^{-1}) ν_{max} : 3099, 2923, 1623, 1556, 1474, 1395, 1301, 1178; $^1\text{H-NMR}$ (400 MHz, $\text{DMSO-}d_6$) δ : 10.63 (s, 1H, NH), 8.30 (s, 1H, NH), 8.23 (d, $J = 1.84$ Hz, 1H, ArH), 7.65 (dd, $J = 8.28, 2.08$ Hz, 1H, ArH), 7.34 (d, $J = 8.32$ Hz, 1H, ArH), 3.12 (t, $J = 7.28$ Hz, 2H, CH_2), 1.62-1.70 (m, 2H, CH_2), 1.22-1.40 (m, 4H, $(\text{CH}_2)_2$), 0.84 (t, $J = 7.22$ Hz, 3H, CH_3) ppm; $^{13}\text{C NMR}$ (100 MHz, $\text{DMSO-}d_6$) δ : 167.54, 153.23, 138.05, 132.30, 131.98, 130.82, 124.29, 123.61, 120.19, 98.52, 30.50 (CH_2), 30.13 (CH_2), 28.72 (CH_2), 21.75(CH_2), 21.73(CH_3), 13.86 (CH_3) ppm; HRMS (ESI) for $\text{C}_{17}\text{H}_{19}\text{N}_5\text{FS}$, $[\text{M}+\text{H}]^+$ calcd: 344.1348, found: 344.1345.

4.8.6. *N*-(2-chloro-4-fluorophenyl)-6-(pentylthio)-1*H*-pyrazolo[3,4-*d*]pyrimidin-4-amine (42)

White solid; yield: 80%; mp 247-249 °C; FTIR (ATR, cm^{-1}) ν_{max} : 3054, 2925, 2716, 1625, 1573, 1488, 1382, 1257, 1181; $^1\text{H-NMR}$ (400 MHz, $\text{DMSO-}d_6$) δ : 10.44 (s, 1H, NH), 8.04 (s, 1H, ArH), 7.59-7.62 (m, 2H, ArH), 7.29-7.34 (m, 1H, ArH), 2.89 (t, $J = 7.42$ Hz, 2H, CH_2), 1.45-1.52 (m, 2H, CH_2), 1.16-1.22 (m, 4H, $(\text{CH}_2)_2$), 0.82 (t, $J = 6.88$ Hz, 3H, CH_3) ppm; $^{13}\text{C NMR}$ (100 MHz, $\text{DMSO-}d_6$) δ : 167.20, 161.54, 159.08, 155.10, 131.86, 131.01, 117.13, 116.87, 115.01, 114.78, 98.01, 30.59 (CH_2), 30.09 (CH_2), 29.19 (CH_2), 21.76 (CH_2), 13.86 (CH_3) ppm.

4.8.7. *N*-(3,4-dimethoxyphenyl)-6-(pentylthio)-1*H*-pyrazolo[3,4-*d*]pyrimidin-4-amine (43)

Brown solid; yield: 78%; mp 247-249 °C; FTIR (ATR, cm^{-1}) ν_{max} : 3055, 2951, 2725, 1625, 1507, 1260, 1233, 1026; $^1\text{H-NMR}$ (400 MHz, $\text{DMSO-}d_6$) δ : 10.52 (s, 1H, NH), 8.43 (s, 1H, NH), 7.40 (s, 1H, ArH), 7.28 (s, 1H, ArH), 6.97 (d, $J = 8.72$ Hz, 1H, ArH), 3.76 (d, $J = 2.12$ Hz, 6H, $(\text{OCH}_3)_2$), 3.10 (t, $J = 7.38$ Hz, 2H, CH_2), 1.59-1.64 (m, 2H, CH_2), 1.20-1.34 (m, 4H, $(\text{CH}_2)_2$), 0.83 (t, $J = 7.08$ Hz, 3H, CH_3) ppm; $^{13}\text{C NMR}$ (100 MHz, $\text{DMSO-}d_6$) δ : 166.72, 153.97, 148.59, 131.38, 114.58, 111.74, 107.58, 98.57, 55.73 (OCH_3), 55.59 (OCH_3), 30.50 (CH_2), 30.28 (CH_2), 28.81 (CH_2), 21.72 (CH_2), 13.83 (CH_3) ppm; HRMS (ESI) for $\text{C}_{18}\text{H}_{22}\text{N}_5\text{O}_2\text{S}$, $[\text{M}+\text{H}]^+$ calcd: 372.1496, found: 372.1494.

5 Biological activity

5.1 CDK2 and Abl kinase inhibition assays

CDK2/cyclin E and Abl kinases were produced in Sf9 insect cells via baculoviral infection and purified on a NiNTA column. The kinase reactions were assayed with suitable substrates (1 mg/mL histone H1 for CDK2 and 500 μ M peptide GGEAIYAAPFKK for Abl) in the presence of 15 or 10 μ M ATP for CDK2 and Abl, respectively, 0.05 μ Ci [γ - 33 P]ATP, and the test compound in a final volume of 10 μ L, all in a reaction buffer (60 mM HEPES-NaOH, pH 7.5, 3 mM MgCl₂, 3 mM MnCl₂, 3 μ M Na-orthovanadate, 1.2 mM DTT, 2.5 μ g / 50 μ l PEG_{20,000}). The reactions were stopped by adding 5 μ L of 3% aq. H₃PO₄. Aliquots were spotted onto P-81 phosphocellulose (Whatman), washed 3 \times with 0.5% aq. H₃PO₄ and finally air-dried. Kinase inhibition was quantified using a FLA-7000 digital image analyzer. The concentration of the test compounds required to reduce the kinase activity by 50 % was determined from dose-response curves and recorded as their IC₅₀.

5.2 Anti-proliferative evaluation for K-562 and MCF-7 cell lines

The tumor cells (purchased from the American Type Culture Collection) were grown in DMEM medium (Gibco BRL) supplemented with 10% (v/v) fetal bovine serum and L-glutamine (0.3 g/L) and were maintained at 37°C in a humidified atmosphere with 5% CO₂. For anticancer cytotoxicity estimations, 10⁴ cells were seeded into each well of a 96-well plate, allowed to stabilize for 20 h, and the test inhibitors were then added at different concentrations (ranging from 0.1 to 100 μ M or to a solubility limit) in triplicate. Three days after addition of the inhibitors, calcein AM solution (Molecular Probes) was added. One hour later, fluorescence of cells was quantified using a Fluoroskan Ascent (Labsystems) reader and cytotoxic effective concentrations were calculated and expressed as IC₅₀ values from dose-response curves. Roscovitine and imatinib were used as reference drugs.

6 Molecular docking simulation

Molecular docking experiments were performed using Glide software package³⁶ implemented in Schrodinger Suite (2017-2) (Schrödinger, Inc., USA)³⁷ running on Intel CORE i7 based hpZ230 workstation with the Microsoft Windows 10 OS. In this protocol, the protein was kept rigid, while the ligands were allowed to be flexible throughout the docking simulation.

6.1 Protein preparation

The starting X-ray solved protein crystal structure of cyclin dependent kinase-2 bound with R-roscovitine was retrieved from protein data bank (PDB) bearing ID 2A4L.³⁵ The protein was prepared by automatic preparation by Protein Preparation Wizard of Glide employing the Optimized Potentials for Liquid Simulations 3 (OPLS3) forcefield. During the pre-processing stage, crystallographic water molecules were removed and added missing hydrogens to the protein structure corresponding to pH 7.0 was achieved. The protein metal ions and cofactors were viewed and removed from the protein structure. The tool neutralized the side chains that are not close to the binding cavity and do not

participate in salt bridges. The pre-processed protein structure was refined initially by optimizing the sample-water orientation followed by restrained minimization of co-crystallized complex using OPLS3, which reorients side chain hydroxyl groups and alleviates potential steric clashes. Thus, the complex obtained was minimized until it reaches the convergent of heavy atom to RMSD 0.3 Å and taken finally in .mae format.

6.2 Grid file generation

Receptor grid generation protocol of Maestro 11.2 was used to define the binding-site of the protein (2A4L) for docking simulation by excluding any co-crystallized metals, co-factors, water molecules all of which may have crystallized during experimental crystallization of the CDK-2 protein. A grid box was generated around the centroid of the cognate ligand (*R*-roscovitine) specifying the size for the docking ligands (20 Å) with default settings.

6.3 Ligand preparation

The structures of the synthesized ligands and standard *R*-roscovitine were sketched using built panel of Maestro and taken in .mae format. LigPrep is a utility of Schrodinger software suit that combines tools for generating 3D structures from 1D (Smiles) and 2D (SDF) representation, searching for tautomers, steric isomers and perform a geometry minimization of the ligands. By employing Ligprep protocol, all the ligands were prepared using OPLS3 with default settings and the output file was saved in maegz format automatically.

6.4 Docking simulation

For precision and accuracy of the docking protocols, the co-crystallized ligand was extracted from the crystal structure of 2A4L and re-docked using Glide docking algorithm (Schrodinger Inc) in its extra precision (XP) mode with default settings without applying any constraints. A good agreement of the obtained pose of docked *R*-roscovitine with cognate ligand indicated the reliability of the selected docking parameters for docking of the synthesized ligands. Hence, by specifying the ligands against the receptor grid, molecular docking was performed using default settings in Glide XP mode.

6.5 Binding mode analysis

The protein-ligand complexes were analysed to investigate various types of interactions by utilizing XP visualizer protocol. For the best-scored ligands, the 2D and 3D plots of molecular ligand-receptor interactions were analysed for hydrogen bond, halogen bond, salt bridges, π - π stacking, and π -cation interactions.

Conflict of Interest

Authors hereby declare that there are no financial/commercial conflicts of interest.

Acknowledgment

Authors are thankful to Discipline of Pharmaceutical Sciences, College of Health Sciences, University of KwaZulu-Natal (UKZN), South Africa, for their constant support, encouragement and financial assistance. One of the authors (CB) gratefully acknowledges National Research Foundation (DST-NRF), South Africa for research funding in the form of Innovation Post-Doctoral Research Fellowship (UID: 99546). Authors also sincerely thank Centre for High Performance Computing (CHPC), Cape Town, South Africa for computational resources. Authors express heartfelt thanks to Mr. Dilip Jagjivan and Dr. Caryl Janse Van Rensburg (UKZN, South Africa) for their assistance in the NMR and EIMS experiments. Vladimir Krystof was supported by the Ministry of Education, Youth and Sports of the Czech Republic (National Program of Sustainability I, LO1204) and Palacky University Olomouc (IGA_PrF_2017_014 and IGA_PrF_2018_006).

References

1. Cancer Facts and Figures, *American Cancer Society*, 2016.
2. D. Belpomme, P. Irigaray, A.J. Sasco, J.A. Newby, V. Howard, R. Clapp, L. Hardell, The growing incidence of cancer: role of lifestyle and screening detection (Review), *Int. J. Oncol.* 30 (2007) 1037-1049.
3. Y. L. Chen, S. Z. Lin, J. Y. Chang, Y. L. Cheng, N. M. Tsai, S. P. Chen, W. L. Chang and H. J. Harn, In vitro and In vivo studies of novel potential anticancer agent of isochaihulactone on human lung cancer A549 cells, *Biochem. Pharmacol.* 72 (2006) 308-319.
4. M. Nakhjiri, M. Safavi, E. Alipour, S. Emami, A. F. Atash, M. Jafari-Zavareh, S. K. Ardestani, M. Khoshneviszadeh, A. Foroumadi and A. Shafiee, Asymmetrical 2,6-bis(benzylidene)cyclohexanones: Synthesis, cytotoxic activity and QSAR study, *Eur. J. Med. Chem.* 50 (2012) 113-123.
5. a) P. Cohen, Protein kinases-the major drug targets of the twenty-first century, *Nat. Rev. Drug Discov.* 1 (2002) 309-315; b) R. Santos, O. Ursu, A. Gaulton, A. P. Bento, R. S. Donadi, C. G. Bologa, A. Karlsson, B. L. Lazikani, A. Hersey, T. I. Opera, J. P. Overington, A comprehensive map of molecular drug targets, *Nat. Rev. Drug Discov.* 16 (2017) 19-34.
6. D. Horiuchi, N. E. Huskey, L. Kusdra, L. Wohlbold, K. A. Merrick, C. Zhang, K. J. Creasman, K. M. Shokat, R. P. Fisher, A. Goga, Chemical-genetic analysis of cyclin dependent kinase 2 function reveals an important role in cellular transformation by multiple oncogenic pathways, *Proc. Natl. Acad. Sci. U. S. A.* 109 (2012) 1019-1027.
7. D. O. Morgan, Principles of CDK regulation, *Nature*, 374 (1995) 131-134.
8. U. Asghar, A.K. Witkiewicz, N.C. Turner, E.S. Knudsen, The history and future of targeting cyclin dependent kinases in cancer therapy, *Nat. Rev. Drug Discov.* 14 (2015) 130-146.
9. M. Malumbres, M. Barbacid, Cell cycle, CDKs and cancer: a changing paradigm, *Nat. Rev. Cancer* 9 (2009) 153-166.
10. O. Tetsu, F. McCormick, Proliferation of cancer cells despite CDK2 inhibition, *Cancer Cell*, 3 (2003) 233-245.
11. S. Ortega, I. Prieto, J. Odajima, A. Martin, P. Dubus, R. Sotillo, J. L. Barbero, M. Malumbres, M. Barbacid, Cyclin dependent kinase 2 is essential for meiosis but not for mitotic cell division in mice, *Nat. Genet.* 35 (2003) 25-31.
12. C. Berthet, E. Aleem, V. Coppola, L. Tessarollo, P. Kaldis, CDK2 knockout mice are viable, *Curr. Biol.* 13 (2003) 1775-1785.
13. S. R. Whittaker, A. Mallinger, P. Workman, P. A. Clarke, Inhibitors of cyclin-dependent kinases as cancer therapeutics, *Pharmacol. Ther.* 173 (2017) 83-105.
14. T. Otto, P. Sicinski, Cell cycle proteins as promising targets in cancer therapy, *Nat. Rev. Cancer*, 17 (2017) 93-115.

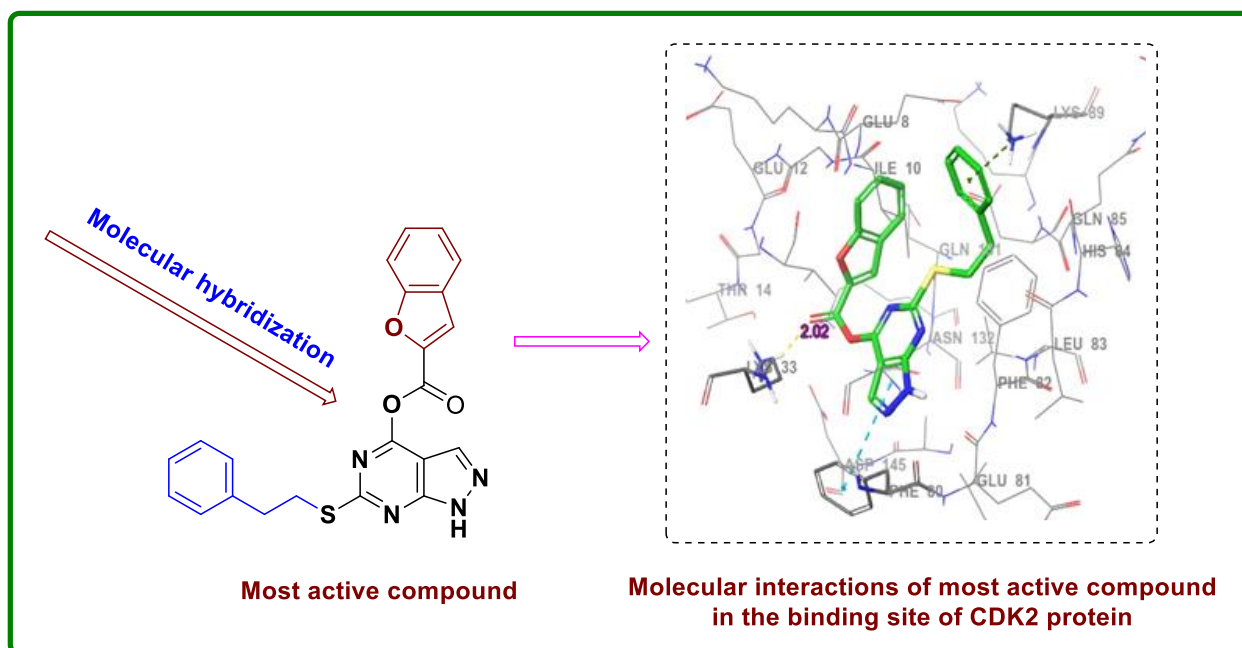
15. L. Vymetalova, V. Krystof, Potential clinical uses of CDK inhibitors: Lessons from synthetic lethality screens, *Med. Chem. Res.* 35 (2015) 1156-1174.
16. C. K. Cheng, W. C. Gustafson, E. Charron, B. T. Houseman, E. Zunder, A. Goga, N. S. Gray, B. Pollok, S. A. Oakes, C. D. James, K. M. Shokat, W. A. Weiss, Q. W. Fan, Dual blockade of lipid and cyclin-dependent kinases induces synthetic lethality in malignant glioma, *Proc. Natl. Acad. Sci. U. S. A.* 109 (2012) 12722-12727.
17. A. J. Deans, K. K. Khanna, C. J. McNees, C. Mercurio, J. Heierhorst, G. McArthur, Cyclin-dependent kinase 2 functions in normal DNA repair and is a therapeutic target in BRCA1-deficient cancers, *Cancer Res.* 66 (2006) 8219-8226.
18. L. Yang, D. Fang, H. Chen, Y. Lu, Z. Dong, H. F. Ding, Q. Jing, S. B. Su, S. Huang, Cyclin dependent 2 kinase is an ideal target for ovary tumors with elevated cyclin E1 expression, *Oncotarget*, 6 (2015) 20801-20812.
19. S. Schenone, M. Radi, F. Musumeci, C. Brullo, M. Botta, Biologically driven synthesis of pyrazolo[3,4-d]pyrimidines as protein kinase inhibitors: an old scaffold as a new tool for medicinal chemistry and chemical biology studies, *Chem. Rev.* 114 (2014) 7189-7238.
20. R. Jorda, K. Paruch, V. Krystof, Cyclin dependent kinase inhibitors inspired by roscovitine: purine bioisosteres, *Curr. Pharm. Des.* 18 (2012) 2974-2980.
21. L. L. Thomas, A. W. David, F. R. Victoria, S. W. Zito, Foye's principles of medicinal chemistry: seventh edition, Wolters Kluwer Health Adis, 2013.
22. L. A. Honigberg, A. M. Smith, M. Sirisawad, E. Verner, D. Loury, B. Chang, S. Li, Z. Pan, D. H. Thamm, R. A. Miller, J. J. Buggy, The bruton tyrosine kinase inhibitor PCI-32765 blocks B-cell activation and is efficacious in models of autoimmune disease and B-cell malignancy, *Proc. Natl. Acad. Sci. U. S. A.* 107 (2010) 13075-13080.
23. M. Chauhan, R. Kumar, Medicinal attributes of pyrazolo[3,4-*d*]pyrimidines: A review, *Bioorg. Med. Chem.* 21 (2013) 5657-5668.
24. D. A. Ibrahim, A. M. El-Metwally, E. E. Al-Arab, Structure-based design of a new class of highly selective pyrazolo[3,4-*d*]pyrimidines based inhibitors of cyclin dependent kinases, *Arkivoc*, 7 (2009) 12-25.
25. J. A. Markwalder, M. R. Arnone, P. A. Benfield, M. Boisclair, C. R. Burton, C. H. Chang, S. S. Cox, P. M. Czerniak, C. L. Dean, D. Doleniak, R. Grafstrom, B. A. Harrison, R. F. Kaltenbach, D. A. Nugiel, K. A. Rossi, S. R. Sherk, L. M. Sisk, P. Stouten, G. L. Trainor, P. Worland, S. P. Seitz, Synthesis and biological evaluation of 1-aryl-4,5-dihydro-1*H*-pyrazolo[3,4-*d*]pyrimidin-4-one inhibitors of cyclin-dependent kinases, *J. Med. Chem.* 47 (2004) 5894-5911.
26. S. Bahceci, B. Chan, D. S. Chan, J. Chen, T. P. Forsyth, M. Franzini, V. Jammalamadaka, J. W. Jeong, L. R. Jones, R. M. Kelley, WO Patent 2010003133 (2010).

27. F. Manetti, C. Brullo, M. Magnani, F. Mosci, B. Chelli, E. Crespan, S. Schenone, A. Naldini, O. Bruno, M. L. Trincavelli, G. Maga, F. Carraro, C. Martini, F. Bondavalli, M. Botta, Structure-based optimization of pyrazolo[3,4-d]pyrimidines as Abl inhibitors and anti-proliferative agents toward human leukemia cell lines, *J. Med. Chem.* 51 (2008) 1252-1259.
28. J. Y. L. Brazidec, A. Pasis, B. Tam, C. Boykin, C. Black, D. Wang, G. Claassen, J. H. Chong, J. Chao, J. Fan, K. Nguyen, L. Silvian, L. Ling, L. Zhang, M. Choi, M. Teng, N. Pathan, S. Zhao, T. Li, A. Taveras, Synthesis, SAR and biological evaluation of 1,6-disubstituted-1*H*-pyrazolo[3,4-d]pyrimidines as dual inhibitors of aurora kinases and CDK1, *Bioorg. Med. Chem. Lett.* 22 (2012) 2070-2074.
29. A. Burchat, D. W. Borhani, D. J. Calderwood, G. C. Hirst, B. Li, R. F. Stachlewitz, Discovery of A-770041, a src-family selective orally active lck inhibitor that prevents organ allograft rejection, *Bioorg. Med. Chem. Lett.* 16 (2006) 118-122.
30. H. M. Patel, B. Sing, V. Bhardwaj, M. Palkar, R. Rane, W. S. Alwan, A. K. Gadak, M. N. Noolvi, R. Karpoormath, Design, synthesis and evaluation of small molecule imidazo[2,1-*b*][1,3,4] thiadiazoles as inhibitors of transforming growth factor- β type-1 receptor kinase (ALK5), *Eur. J. Med. Chem.* 26 (2015) 599-613.
31. S. Cherukupalli, R. Karpoormath, B. Chandrasekaran, G.A. Hampannavar, N. Thapliyal, V.N. Palakollu, An insight on synthetic and medicinal aspects of pyrazolo[1,5-*a*]pyrimidine scaffold, *Eur. J. Med. Chem.* 126 (2017) 298-352.
32. R. J. Bentems, J. D. Anderson, D. F. Smee, A. J. Jin, H. A. Alaghamandan, B. S. Sharma, W. B. Jolley, R. K. Robins, H. B. Cottam, Guanosine analogs. Synthesis of nucleosides of certain 3-substituted 6-aminopyrazolo[3,4-d]pyrimidin-4(5*H*)-ones as potential immunotherapeutic agents, *J. Med. Chem.* 33 (1990) 2174-2178.
33. G. Sliwoski, S. K. Kothiwale, J. Meiler, E. W. Lowe, Computational methods in drug discovery, *Pharmacol Rev.* 66 (2014) 334-395.
34. D. Parry, T. Guzi, F. Shanahan, N. Davis, D. Prabhavalkar, D. Wiswell, W. Seghezzi, K. Paruch, M. P. Dwyer, R. Doll, A. Nomeir, W. Windsor, T. Fischmann, Y. Wang, M. Oft, T. Chen, P. Kirschmeier, and E. M. Lees, Dinaciclib (SCH 727965), a novel and potent cyclin-dependent kinase inhibitor, *Mol. Cancer Ther.* 9 (2010) 2344-2353.
35. W. F. D. Azevedo, S. Leclerc, L. Meijer, L. Havlicek, M. Strnad, S. H. Kim, Inhibition of cyclin-dependent kinases by purine analogues, *Eur. J. Biochem.* 243 (1997) 518-526.
36. R. A. Friesner, R. B. Murphy, M. P. Repasky, L. L. Frye, J. R. Greenwood, T. A. Halgren, P. C. Sanschagrin, D. T. Mainz, Extra precision glide: Docking and scoring incorporating a model of hydrophobic enclosure for protein-ligand complexes, *J. Med. Chem.* 49 (2006) 6177-6196.
37. Schrodinger Release 2017-2: Glide, Schrodinger, LLC, New York, NY, 2017.

CHAPTER 5

Synthesis of 4,6-disubstituted pyrazolo[3,4-*d*]pyrimidine analogues: molecular docking, anticancer evaluation as cyclin dependent kinase 2 (CDK2) inhibitors

Department of Pharmaceutical Chemistry, College of Health Sciences, University of KwaZulu-Natal, Durban 4000, South Africa.

Graphical Abstract

Abstract:

A series of novel 4,6-disubstituted pyrazolo[3,4-*d*]pyrimidines (**5a-5h**, **6a-6d**, **7a-7c**) bearing different mono & bicyclic heterocycles at C-4 position in a combination of pentane/phenethyl/hexane substituents at C-6 position has been designed and synthesized. All the novel compounds were evaluated for *in vitro* CDK2/cyclin E and Abl kinase inhibitory activity as well as anti-proliferative activity against K-562 (chronic myelogeneous leukemia), MCF-7 (breast adenocarcinoma) cell lines. The structure-activity relationship studies (SAR) revealed that the compounds with pentane/phenethyl group at C-6 with heteroatom containing bicyclic moiety at C-4 exhibited commendable CDK2 inhibitory compared to hexane group at C-6 with monocyclic groups at C-4 of the scaffold. From the tested results, compounds having benzofuran moiety at C-4 showed single digit micro molar IC₅₀ values. Further from *in silico* molecular docking studies, it was suggested that possible binding orientations and binding energies were in agreement with the observed SAR as well as experimental results. In addition, some of the synthesized compounds indicated anti-proliferative effects against K-562 and MCF-7 cancer cell lines with IC₅₀ values in a micromolar range. Thus, the research findings on the pyrazolo[3,4-*d*]pyrimidine hybrids specified the prospective greatness of molecular hybridization and strongly encouraged us for further lead optimization with an aim to develop potential anticancer agents.

Key words: Pyrazolo[3,4-*d*]pyrimidine; Cyclin dependent kinase inhibitor; Anti-proliferative activity; Molecular docking; GLIDE.

1 Introduction

Cancer is one of the most serious health burden touching all over the world. After the cardiovascular, cancer is the second leading cause of death.¹ The understanding of the molecular mechanism of cancer improved strongly in recent years and has deeply impacted on experimental, slowly also on clinical tumor therapy.² Predominant efforts are being carried out in order to identify advanced treatments and developments in prevention and chemotherapeutic organization.^{3,4} Apart from surgical treatment and irradiation methods, chemotherapy remains a significant route for cancer therapy by the progress of molecular targets that exactly interfere with the vital mechanisms involved in expansion and progression of various types of cancer.⁵ Among others, protein kinases have become a significant group of drug targets and number of kinase inhibitors in clinical development is rapidly increasing.⁶

Cyclin-dependent kinases (CDKs) are a family of serine/threonine kinase comprising 20 members, which participates in regulation of cell-cycle progression by phosphorylating proteins in cell division. These enzymes play a crucial role in cell division, transcription, post-transcriptional modification and controlling cell cycle.⁷ Among the 20 existing CDK proteins, CDK2 actively participates in the G1/S checkpoint and initiates the cell cycle through S-phase results in apoptosis.⁸ For example, formation of active complex composed of CDK2 and cyclin E enables pRb phosphorylation, activation of transcription factor E2F which and initiation of S phase of the cell cycle. CDK2 then also associates with cyclin A, governing continuous DNA replication and properly programmed deactivation of E2F. Thus, CDK2 became as prospective target for the treatment of tumors by initiation of apoptotic pathways as contrasting to cell cycle arrest.⁹ Up to date many CDK2 have been developed and some of them (including roscovitine, CYC065, dinaciclib, AT7519, milciclib) undergo clinical evaluation.^{10,11} To support these findings, recent research study evidenced that both phosphatidylinositol-3-kinase and CDK2 inhibitors together induced apoptosis in malignant glioma xenografts via a synthetic-lethal interaction.¹² In addition, CDK2 inhibitor also proved as a therapeutic target in ovarian cancer,¹³ neuroblastoma¹⁴ and BRCA-deficient cancers.¹⁵ Positively these results, taken together with clinical data, have led to a revival of interest in CDK2 inhibitors as anti-cancer agents.

It is a well-known fact that, broad range of investigations have been conducted on pyrazolo[3,4-*d*]pyrimidines due to their enormous role as potent pharmacophore. Fusion of pyrazole on pyrimidine leads to bicyclic system known as pyrazolopyrimidine, which can be looked upon as the bioisostere of purine, thus exhibits promising antitumor activity by acting as ATP competitive inhibitor for several kinase enzymes.^{16,17} Several compounds of this family were found to induce apoptosis and/or reduce cell proliferation in various solid tumor and leukemia cell lines.¹⁸⁻²¹ Their cytotoxic activities might be accredited to inhibition of various enzymes such as mammalian target of rapamycin (mTOR),²² Src/Abl kinase,²³ glycogen synthase kinase (GSK),²⁴ tyrosine kinase,²⁵ cyclin dependent kinase (CDK)²⁶ and

xanthine oxidase inhibitors.²⁷ Also reported to encompass biological potential as CNS agents, antiviral, anti-inflammatory, herbicidal, anticancer, antimicrobial and cardiovascular activities.²⁸ **Fig. 2** depicts several reported derivatives of pyrazolo[3,4-*d*]pyrimidine with anticancer activities related to inhibition of different protein kinases.^{25, 29-34}

Based on the above mentioned facts and in continuation of our research work on anticancer drug discovery,^{35,36} we envisaged to further exploit the pyrazolo[3,4-*d*]pyrimidine scaffold to synthesize novel CDK2 inhibitors. In the present study a novel series of pyrazolo[3,4-*d*]pyrimidine derivatives (**scheme-1**) has been synthesized by substituting various chemical entities at C-4 and C-6 positions through efficient synthetic method. Further, these synthesized molecules were also evaluated against Abl kinase as well as K562 and MCF7 cancer cell lines. In addition, the *in silico* molecular docking studies were performed to analyze the binding energies and orientations of these compounds with respect to the active site of CDK-2 protein. The computational results were in agreement with our experimental observations.

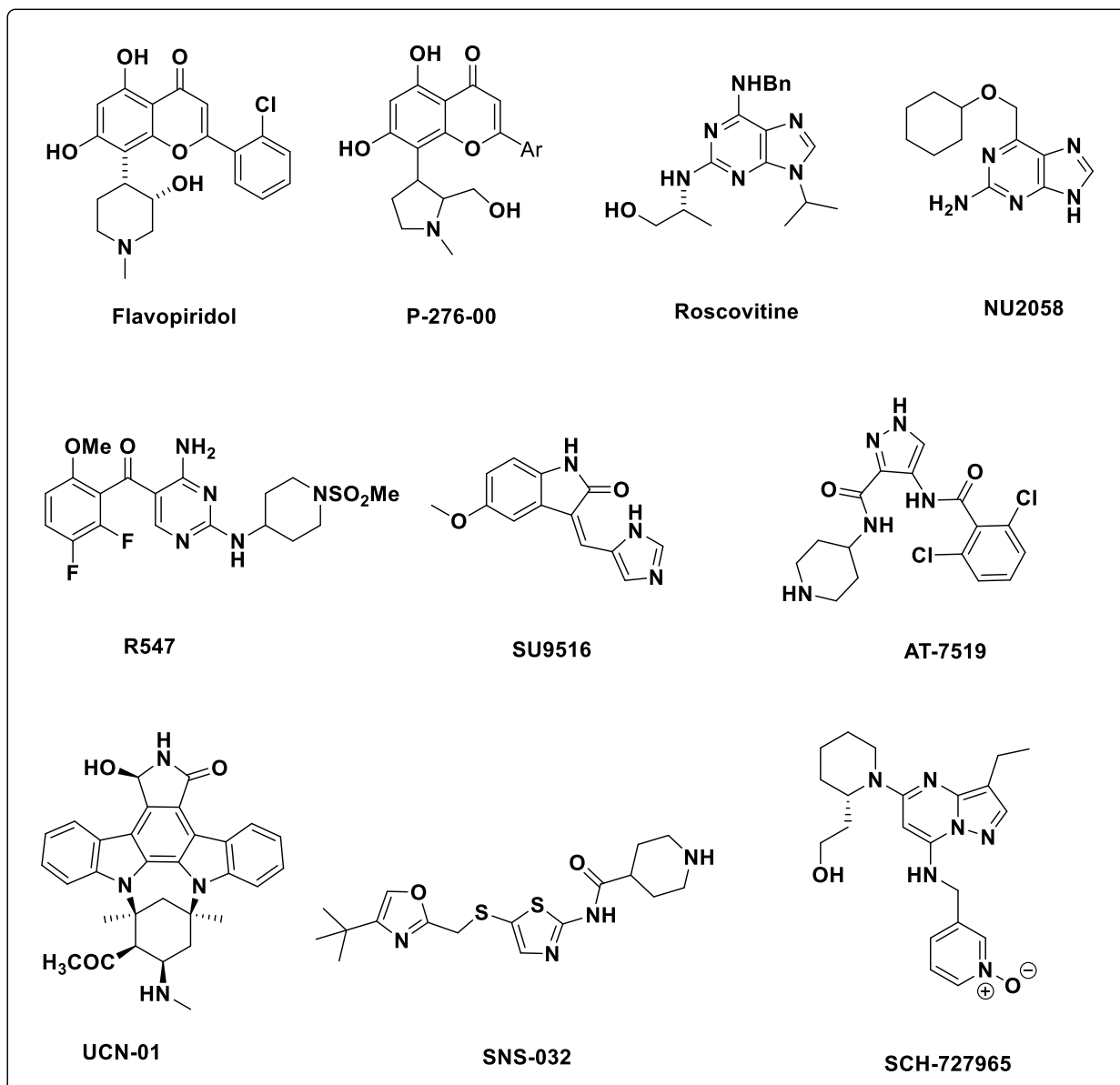


Fig. 1. Structures of the CDK2 inhibitors in clinical trials.

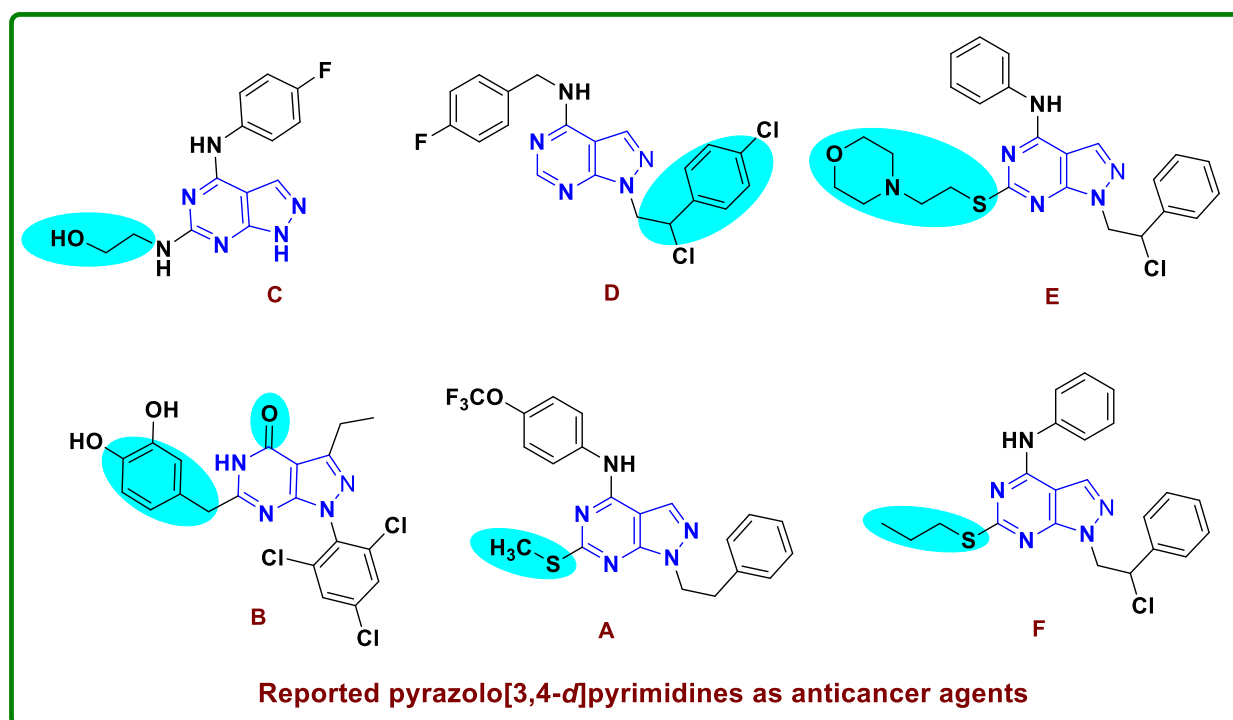


Fig. 2. Known derivatives of pyrazolo[3,4-*d*]pyrimidine and their anticancer activities. Compound **A**: (K_{i50} against Src, AblT315I = 0.056, 0.01 μM)²⁹; **B**: (IC_{50} against CDK2 = 0.020 μM)³⁰; **C**: (IC_{50} against CDK2 = 0.5 μM)³¹; **D**: (K_{i50} against Abl = 80 nM)³²; **E**: (K_{i50} against cSrc, Abl = 0.21 \pm 0.02, 0.15 \pm 0.02 μM)³³; **F**: (IC_{50} against Src = 1.2 \pm 0.4 μM)³⁴.

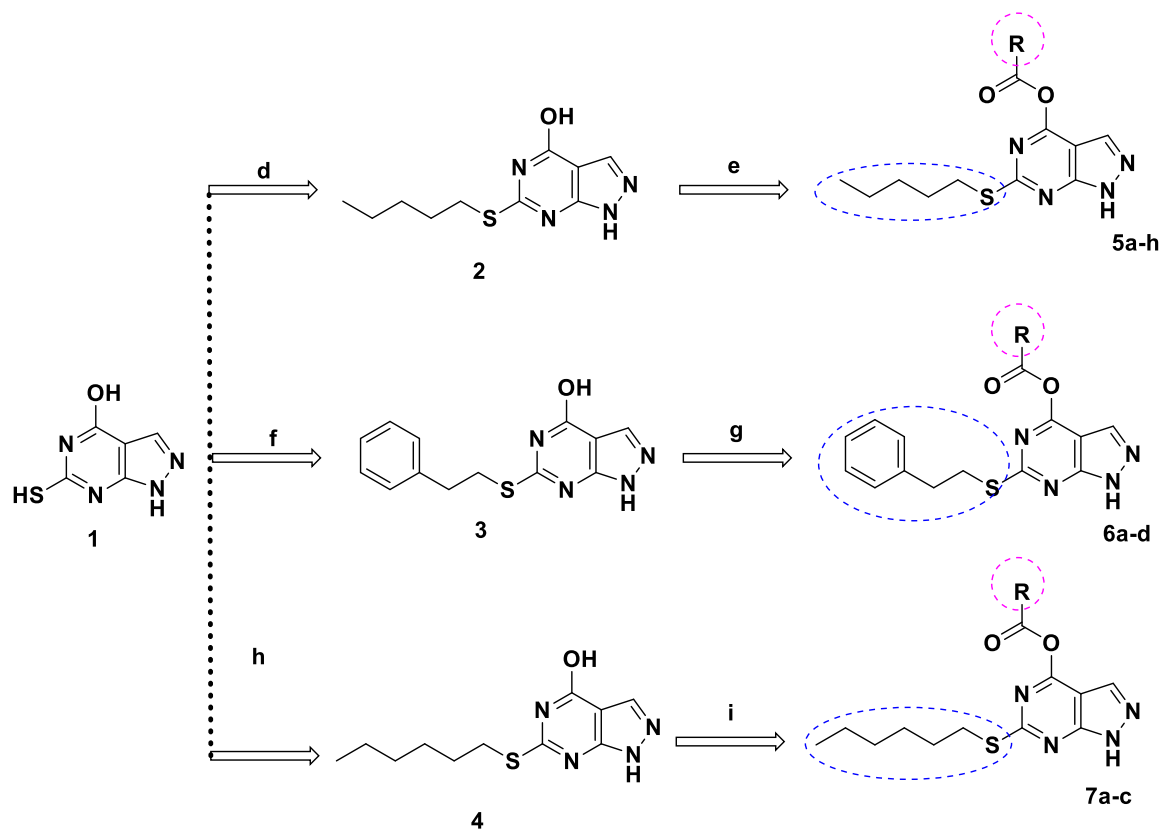
2 Results and discussion

2.1 Chemistry

6-mercapto-1*H*-pyrazolo[3,4-*d*]pyrimidin-4-ol (**1**), is a key intermediate for the synthesis of desired hybrid molecules as shown in **Scheme 1**. On the pyrazolopyrimidine scaffold, the hydroxy group was introduced at C-4 as a nucleophilic substituent, which acted as a most reactive site for different nucleophiles, while mercapto group was introduced at C-6 as a precursor to perform the alkylation with different aliphatic and aromatic substituents.

From the previous reported literature methods compound **1** was successfully synthesized.³⁷ Further, to increase the structural exploration around the nucleus, alkylation of compound **1** was done with 1-bromopentane to achieve 6-(pentylthio)-1*H*-pyrazolo[3,4-*d*]pyrimidin-4-ol (**2**) and also with 2-chloroethyl benzene, 1-bromohexane to obtain 6-(phenethylthio)-1*H*-pyrazolo[3,4-*d*]pyrimidin-4-ol (**3**) and 6-(hexylthio)-1*H*-pyrazolo[3,4-*d*]pyrimidin-4-ol (**4**) respectively. As displayed in **scheme 1** the nucleophilic substitution of compounds **2**, **3** and **4** at C-4 with acid chlorides was successfully accomplished the final compounds (**5a-5h**, **6a-6d** and **7a-7c**) in THF containing catalytic amount of

pyridine in good yield (70-85%). The IR, ^1H and ^{13}C NMR spectroscopic data of all the novel compounds were in agreement with the predicted structures and were further corroborated by HR-MS information, which is precised in supporting information.



Scheme 1: Synthesis of 4,6-disubstituted pyrazolo[3,4-*d*]pyrimidine derivatives.

Reagents and conditions: (a) hydrazine hydrate, ethanol, 80 °C, 3h, 92%; (b) Conc. H_2SO_4 , NH_4OH , H_2O , 50 °C, 5h, 90%; (c) potassium ethyl xanthogenate, DMF, 120 °C, 6h, 82%; (d) 1-bromopentane, NaOH, H_2O , glacial acetic acid, 50 °C, 5h, RT, overnight, 80%; (e) acid chlorides, pyridine, RT, 2h, 75-85%; (f) 2-chloroethyl benzene, K_2CO_3 , DMF, 70 °C, microwave, 20 min, 76%; (g) acid chlorides, pyridine, THF, RT, 2h, 70-85%; (h) 1-bromohexane, NaOH, H_2O , glacial acetic acid, 50 °C, 5h, RT, overnight, 70%; (i) acid chlorides, pyridine, RT, 2h, 65-85%.

The ^1H NMR of compound **1** exhibited the presence of a very distinct singlet signals resonating at around δ 13.61, 13.03, 11.86 and 8.42 ppm for N-H proton, S-H proton, O-H proton and Ar-H proton of pyrazole ring. Thus, indicated the formation of bicyclic moiety by fusion of 5-amino-1H-pyrazole-4-carboxamide with potassium ethyl xanthogenate. ^1H NMR of compounds **2**, **3** and **4** displayed the characteristic methylene signals ($-\text{S}-\underline{\text{CH}_2}-\underline{\text{CH}_2}-\underline{\text{CH}_2}-\underline{\text{CH}_2}-$, $\text{Ph}-\underline{\text{CH}_2}-\underline{\text{CH}_2}-\text{S}-$ and $-\text{S}-\underline{\text{CH}_2}-\underline{\text{CH}_2}-\underline{\text{CH}_2}-$

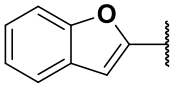
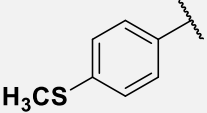
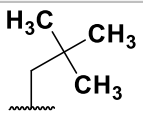
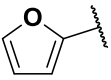
CH₂-CH₂-) around δ 3.17-2.87, 1.73-1.43, 1.41-1.14 ppm; δ 3.43-3.39, 3.01-2.97 ppm; δ 3.17-3.13, 1.69-1.62, 1.41-1.36, 1.34-1.26 ppm respectively, while the methyl signals for **2** and **4** were observed at around δ 0.86-0.80 ppm. In particular, the disappearance of a distinct singlet signal at around δ 13.60-13.54 ppm for mercapto (-SH) group evidently indicated the successful alkylation of pyrimidine scaffold. Whereas most distinctive singlet, doublet and triplet signals at around δ 7.32-7.20 ppm was attributed to the aromatic protons of **11** (C₆H₅-CH₂-CH₂-) at C-6 of pyrazolopyrimidine ring. These findings were further validated with their respective ¹³C NMR, where the most prominent methylene carbon signal resonated at around δ 30.37, 29.69, 28.24, 21.66 ppm (-S-CH₂-CH₂-CH₂-CH₂-), δ 34.61 and 31.08 ppm (-C₆H₅-CH₂-CH₂) and δ 30.74, 29.75, 28.50, 27.85, 22.00 ppm (-S-CH₂-CH₂-CH₂-CH₂-CH₂-) were assigned for compounds **2**, **3** and **4**. The distinctive methyl peaks (**2** and **4**) appeared around δ 13.84 and 13.88 ppm while the prominent aromatic signals (**2**, **3** and **4**) resonated around δ 173.28-130.19 ppm. Further, the characteristic singlet signal disappeared at around δ 12.28-12.31 ppm, which was accounted for (-OH) at C-4 evidently indicated the formation of title compounds (**5a-5h**, **6a-6d** and **7a-7c**) with ester linkage as displayed in **scheme 2**.

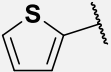
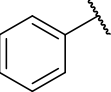
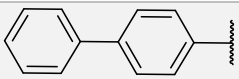
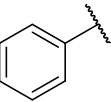
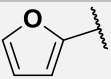
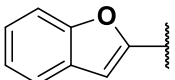
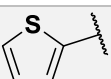
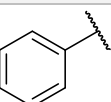
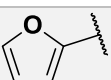
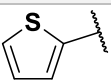
The IR spectra of the title compounds (**5a-5h**, **6a-6d** and **7a-7c**) showed a reasonably sturdy and distinctive bands around 2904-3290 cm⁻¹, 1232-1292 cm⁻¹ accounting for N-H and C-S stretching respectively, while the most distinctive bands of both ester carbonyl group (-O-C=O) and ketone carbonyl (-C=O) were appearing around 1667-1715 cm⁻¹ indicated the formation of title molecules. Further, the ¹H NMR signals of the title compounds displayed distinctive singlet signal around δ 12.36-12.17 ppm for cyclic -NH proton, while the hydroxyl proton (-OH) resonated around at δ 11.47-10.65 ppm. For the title compounds the singlet signal resonated around δ 10.78-8.96 ppm for C-3 proton while, the doublet or multiplet aromatic peaks existed around δ 8.61-6.87 ppm. Further, for compounds **5a-5h**, **6a-6d** and **7a-7c** the methylene protons were appeared around δ 3.52-1.23 ppm while, the methyl protons for **5a-5h** and **7a-7c** were resonated around δ 0.90-0.83 ppm. Further, the most characteristic singlet signals resonated at δ 4.27 ppm, δ 2.57 ppm and δ 1.05 ppm for cyclobutane C-H (**5d**), methylthio and -CH₃₃ (**5c**) protons respectively. The ¹³C NMR spectra was further confirmed the structures of the final compounds. The characteristic carbon peaks for C-3, C-4 and C-6 of pyrazolopyrimidine ring were appeared at around δ 131.96-130.19, 158.87-158.19 and 173.28-161.87 ppm while, different aromatic carbons were observed between δ 159.78-107.87 ppm. Further, the methylene peaks observed for compounds **5a-5h** (-S-CH₂-CH₂-CH₂-CH₂: δ 30.37-21.66 ppm), **6a-6d** (-S-CH₂-CH₂-Ph: δ 34.24-31.20 ppm) and for **7a-7c** (-S-CH₂-CH₂-CH₂-CH₂-CH₂: δ 30.74-22.00 ppm) respectively. The methyl peak for **5a-5h** and **7a-7c** appeared around δ 13.84-13.36 ppm while, the prominent carbon peaks resonated around δ 13.88 ppm (-S-CH₃), δ 44.80 and 31.04-29.86 ppm (**13c**: -CH₂-C(CH₃)₃). In addition, the HR-MS spectrums of the final compounds (**5a-5h**, **6a-6d** and **7a-7c**)

showed accurate molecular ion peaks, which were in agreement with their expected molecular weights (supporting information).

2.2 *In vitro* evaluation for CDK2 and Abl kinase inhibitors

All the final compounds were evaluated for CDK2/cyclin E kinase inhibition and the IC₅₀ values of various *in vitro* anticancer profiles are summarized in **Table 1**. Abl kinase inhibition was evaluated as a counter screen, to get a preliminary information about selectivity. We carried a considerable effort in optimizing the tail groups at both C-4 and C-6 of the pyrazolo[3,4-*d*]pyrimidine scaffold. Thus, substituted various bioactive groups such as pentane, phenethyl, hexane groups at C-6 as well as mono and bicyclic aromatic/heteroaromatic groups at C-4 through ester linkage (**Scheme 1**). The tested compounds from **scheme 1** belongs to three series; pentane (**5a-5h**), phenethyl (**6a-6d**) and hexane series (**7a-7c**). Interestingly, it was observed that the compounds from phenethyl series (**6a-6d**) showed prominent anticancer activity as compared to pentane (**5a-5h**) and hexane (**7a-7c**) series, also observed that the incorporation of aromatics/heteroaromatics at C-4 of the nucleus is necessary for potent activity. From the tested pentane/phenethyl/hexane series, compounds **5a** and **6c** bearing benzofuran moiety at C-4 indicated the best CDK2 activity profile with IC₅₀ = 8.8 μM and 6.8 μM respectively. Further, notable activity profile was also observed for compounds bearing 3,3-dimethylbutane (**5c**: IC₅₀ = 16.9 μM), phenyl (**7a**: IC₅₀ = 14.8 μM) and 2-furan (**7b**: IC₅₀ = 21.2 μM) groups. In addition, these pentane/phenethyl/hexane series of compounds were evaluated against Abl kinase, but none of the compounds showed any inhibition in the assayed concentration range, confirming reasonable selectivity towards CDK2 over unrelated Abl.

C. No	R	IC ₅₀ (μM) ^a			
		CDK2	Abl	K-562	MCF-7
5a		8.8	>12.5	>50	>50
5b		>12.5	>12.5	>50	>50
5c		16.9	>50	73.4	89.3
5d		>25	>25	25.0	23.0
5e		>12.5	>12.5	>25	>25

5f		>12.5	>12.5	>25	>25
5g		>12.5	>12.5	>12.5	>12.5
5h		>12.5	>12.5	>50	>50
6a		>12.5	>12.5	>12.5	>12.5
6b		>12.5	>12.5	20.4	25
6c		6.8	>12.5	19.8	18.9
6d		>12.5	>12.5	23.2	18.9
7a		14.8	>12.5	>50	>50
7b		21.2	>25	>12.5	>12.5
7c		>25	>25	>6.25	>6.25
	Roscovitine	0.1	>100	42	11
	Imatinib	>100	0.2	0.5	>10

^a IC₅₀ values were determined in triplicate in the range of 0.05 to 100 μM. IC₅₀ value indicates concentration (μM) that inhibits activity of tested enzyme to 50% or for cytotoxic assays, concentration (μM) that reduces 50% of cells during a three-day cultivation

Table 1. Anticancer evaluation of novel 4,6-disubstituted pyrazolo[3,4-*d*]pyrimidine derivatives.

2.3 Anti-proliferative activity against K-562 and MCF-7 cell line

All the novel mono and disubstituted pyrazolo[3,4-*d*]pyrimidine analogues (**5a-5h**, **6a-6d** and **7a-7c**) were evaluated for their *in vitro* anti-proliferative activity against K-562 (chronic myelogenous leukemia) and MCF-7 (breast adenocarcinoma) cell lines. Several compounds displaying appreciable activity with measurable IC₅₀ values against the two cell lines, such as compounds **6c** (IC₅₀ = 19.8, 18.9 μM), **6d** (IC₅₀ = 23.2, 18.9 μM) and **6b** (IC₅₀ = 20.4, 25 μM). Further, notable anti-proliferative profile

was observed for compounds **5d** ($IC_{50} = 25.0, 23.0 \mu M$), and **5c** ($IC_{50} = 73.4, 89.3 \mu M$) respectively. The remaining compounds were not active in the tested concentration range.

2.4 Structure-activity relationship (SAR) Studies

In general, careful observation of the structure-activity relationship (SAR) indicated that the anticancer activity was considerably affected by the nature of different substituents present at C-4 and C-6 positions on pyrazolo[3,4-*d*]pyrimidine scaffold. Initially it was observed that the compounds only substituted at C-6 showed least activity whereas compounds substituted at both C-4 and C-6 positions exhibited potent activity, indicated that the incorporation of heterocyclic moieties at C-4 resulted in significant activity. Further analyses of the data revealed that benzofuran group (**5a**, **6c**) at C-4 was more favorable for anticancer and anti-proliferative activity than furan (**5e**) and thiophene (**6d**) indicated that the presence of bi-heterocyclic moiety at C-4 was resulted in best activity. Surprisingly from **scheme 1**, it was observed that phenethyl pentane groups at C-6 showed better activity results than hexane group as illustrated in **Fig. 3**.

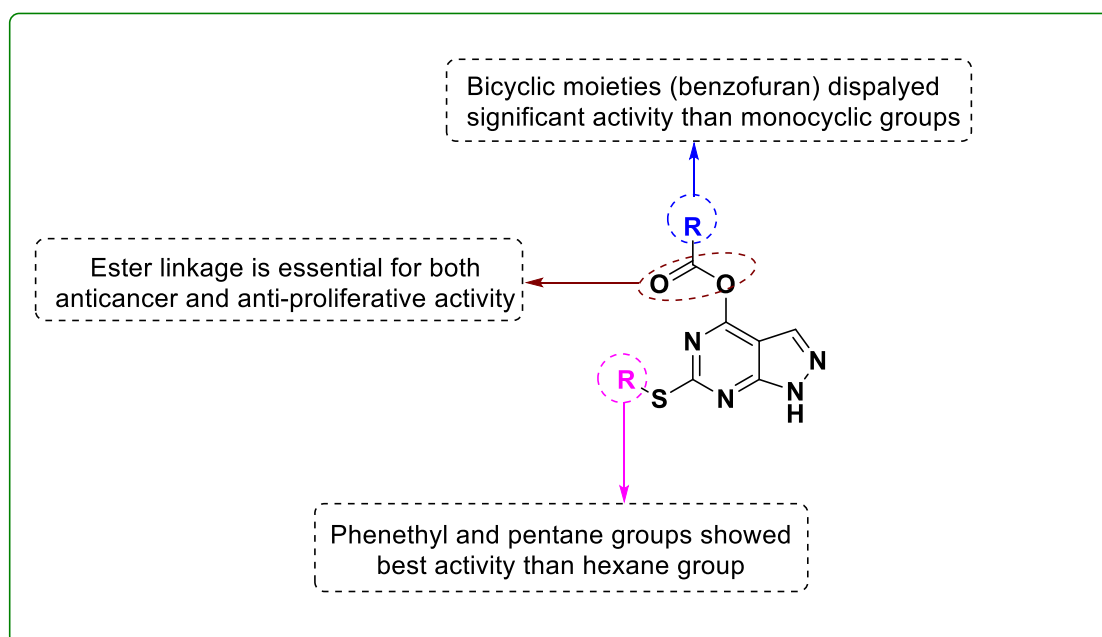


Fig. 3. SAR study around pyrazolo[3,4-*d*]pyrimidine scaffold towards potent activity.

2.5 Molecular docking study

Bioinformatics has become an essential part in the design of therapeutically active novel chemical entity (NCE).³⁸ From the literature, higher binding affinity reported for a pyrazolo[1,5-*a*]pyrimidine-based experimental drug (dinaciclib) towards CDKs motivated us to conduct molecular docking of our synthesized compounds to further understand and substantiate our observed *in vitro* experimental data.³⁹

To validate the docking protocols and to reproduce the protein data bank (PDB) reported orientation of *R*-roscovitine (PDB ID: 2A4L),⁴⁰ docking studies were performed using Glide program of Schrodinger-Maestro 11.2. From the docking experiments, the obtained pose of *R*-roscovitine revealed similar molecular interactions as reported in the PDB. The docked complex presented characteristic hydrogen bonding (H-bond) interactions with crucial residues of the active-site, such as Leu83 with roscovitine by forming a strong [C=O with benzylamino NH (1.91 Å)] and a weak [(C=O with ring nitrogen (2.39 Å)] H-bonds. Similarly, the residue Asp86 interacted with OH group of roscovitine *via* a strong H-bond (1.67 Å), whereas Lys89 exhibited π -cation interaction with phenyl ring of *R*-roscovitine. **Fig. 4** represents the reproduced 3D molecular interactions of the docked pose together with the reported pose of *R*-roscovitine.

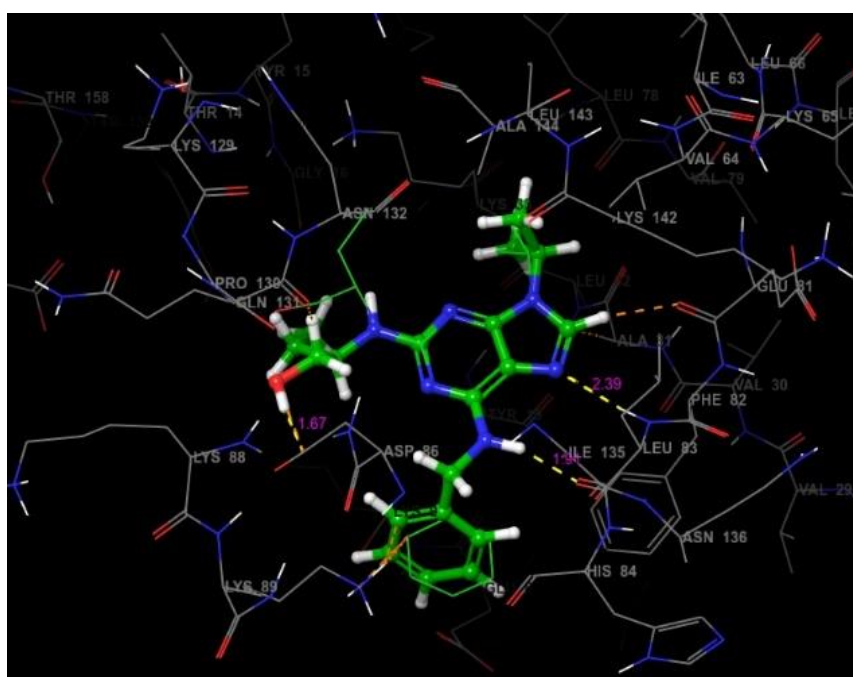
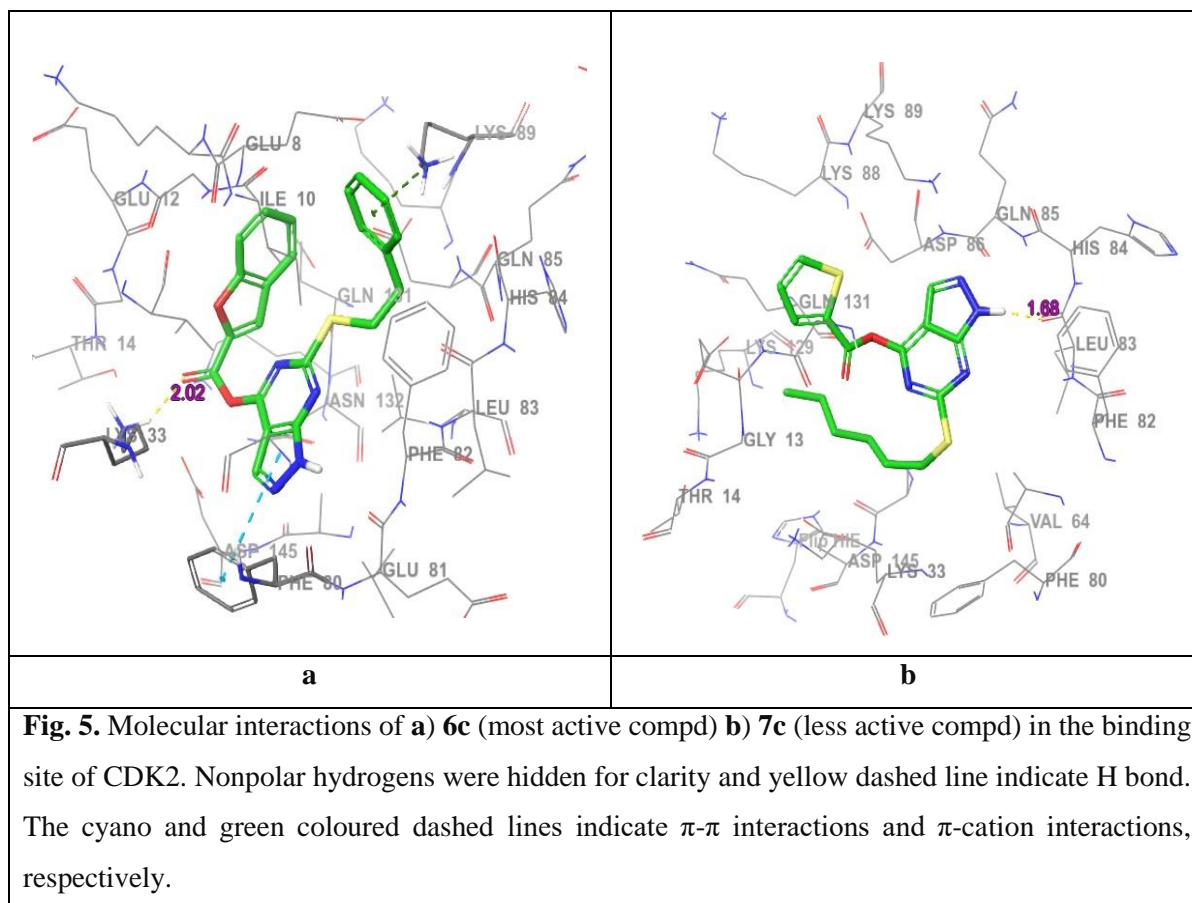


Fig. 4. Reported pose (wire-frame model) and Docked pose (thick tube model) into the active-site showing similar interactions (docking validation).

The docking experimental data of our synthesized compounds revealed that they docked well into the binding-site and displayed favourable interactions with the crucial amino acid residues. Interestingly, the most active compound **6c** showed three significant molecular interactions with crucial amino acid residues of CDK2. The carbonyl oxygen (C=O) of **6c** exhibited a strong H-bond interaction with NH of the basic residue Lys33 (2.02 Å). Further, the pyrazole ring and phenyl ring of thiophenethyl substitution were presented π - π (Phe80) and π -cation (Lys89) interactions, respectively (**Fig. 5a**). Hence, these three molecular interactions were considered as crucial which might have contributed significantly to the potent *in vitro* CDK-2 inhibition.

In the case of less active compound **7c**, the orientation of the docked pose was observed to be different wherein the pyrazole NH presented a strong H-bond interaction with Leu83 (1.68 Å). There is no other characteristic molecular interactions observed for **7c** with active-site residues of CDK2. Hence, lacking of two of the crucial interactions may have contributed to the less *in vitro* CDK-2 inhibition potential of **7c**, while comparing with the most active **6c**. **Fig. 5** presents different molecular interactions of **6c** and **7c** with the active site residues of CDK-2 (PDB ID: 2A4L).



3 Conclusion

In summary, we have successfully synthesized and characterized a new series of 4,6-disubstituted pyrazolo[3,4-*d*]pyrimidine derivatives with good yields. The key intermediates 6-mercapto-1*H*-pyrazolo[3,4-*d*]pyrimidin-4-ol (**1**), 6-(pentylthio)-1*H*-pyrazolo[3,4-*d*]pyrimidin-4-ol (**2**), 6-(phenethylthio)-1*H*-pyrazolo[3,4-*d*]pyrimidin-4-ol (**3**) and 6-(hexylthio)-1*H*-pyrazolo[3,4-*d*]pyrimidin-4-ol (**4**) allowed us to increase a library of total 34 fused pyrimidine derivatives (**5a-5h**, **6a-6d**, **7a-7c**). All synthesized compounds were evaluated for *in vitro* enzymatic activity against CDK2/cyclin E, Abl kinases as well as anti-proliferative activity against K-562 and MCF-7 cancer cell lines. Interestingly, it was observed that compounds **6c**, **5a**, **7a**, **5c** and **7b** showed most potent CDK2/cyclin E activity with IC₅₀ values ranging from 6.8 to 21.2 μ M. Further, compounds **6b** (IC₅₀=

20.4, 25 μM), **6c** (IC_{50} = 19.8, 18.9 μM) and **6d** (IC_{50} = 23.2, 18.9 μM) displayed appreciable anti-proliferative activity at specific IC_{50} values. From the SAR study, it was clear that the presence of bi heterocyclic group (benzofuran) at C-4 of the scaffold led to prominent activity. In addition, the *in silico* binding interaction and energies of the best active compound (**6c**) were in agreement with the experimental data and supported the SAR studies. Thus, these research outcomes can further guide the researchers in emerging novel pyrazolo[3,4-*d*]pyrimidine based CDK-2 inhibitors as potential anticancer agents.

4 Experimental Section

4.1 Chemistry protocol

All the chemicals used in this research work were purchased from Sigma-Aldrich and Merck Millipore, South Africa. All the solvents, except those of laboratory-reagent grade, were dried and purified when necessary according to previously published methods. The progress of the reactions and the purity of the compounds were monitored by thin-layer chromatography (TLC) on pre-coated silica gel plates procured from E. Merck and Co. (Darmstadt, Germany) using 36% ethyl acetate in n-hexane as the mobile phase and iodine vapor as the visualizing agent. The melting points of the synthesized compounds were determined using a Thermo Fisher Scientific (IA9000, UK) digital melting point apparatus and are uncorrected. The IR spectra were recorded on a Bruker Alpha FT-IR spectrometer (Billerica, MA, USA) using the ATR technique. The ^1H NMR and ^{13}C NMR spectra were recorded on a Bruker AVANCE 400 and 600 MHz (Bruker, Rheinstetten/Karlsruhe, Germany) spectrometers using CDCl_3 and $\text{DMSO-}d_6$. The chemical shifts are reported in δ ppm units with respect to TMS as an internal standard. HRMS spectra was recorded on an Autospec mass spectrometer with electron impact at 70 eV.

4.2 Synthesis of 6-(pentylthio)-1*H*-pyrazolo[3,4-*d*]pyrimidin-4-ol (2)

To a stirred solution of 6-mercapto-1*H*-pyrazolo[3,4-*d*]pyrimidin-4-ol (compound **1**, 1 g, 0.00595 mol) in 1M NaOH solution (12 mL), 1-bromopentane (1.48 mL, 0.01190 mol) was added dropwise and heated at 70^o C for 6h and later slowly brought to RT and continued stirring for overnight. After completion of reaction (monitored on TLC), glacial acetic acid was added dropwise to yield the crude solid, which further washed with petroleum ether and purified by flash silica column [MeOH/DCM, 05:95] to afford the desired compound (**2**), as yellow solid. Yield: 80 %; mp 201-203 $^{\circ}\text{C}$; FTIR (ATR, cm^{-1}) ν_{max} : 3180.27 (NH Str.), 2953 (Ar C-H Str.), 2925, 1678 (C=O Str.), 1556, 1390, 1240, 1154, 1123, 961, 874, 773, 665, 588, 534; ^1H -NMR (400 MHz, $\text{DMSO-}d_6$) δ : 13.54 (s, 1H, NH), 12.28 (s, 1H, OH), 7.93 (s, 1H, ArH), 3.15 (t, $J = 7.26$ Hz, 2H, CH_2), 1.70-1.63 (m, 2H, CH_2), 1.39-1.26 (m, 4H, $(\text{CH}_2)_2$), 0.86 (t,

$J = 7.08$ Hz, 3H, CH_3) ppm; ^{13}C NMR (100 MHz, $\text{DMSO-}d_6$) δ : 159.49, 157.75, 135.24, 30.37 (CH_2), 29.69 (CH_2), 28.24 (CH_2), 21.66 (CH_2), 13.84 (CH_3).

4.3 Synthesis of 6-(phenethylthio)-1*H*-pyrazolo[3,4-*d*]pyrimidin-4-ol (3)

To a stirred solution of 6-mercapto-1*H*-pyrazolo[3,4-*d*]pyrimidin-4-ol (compound **1**, 0.3g, 0.00179mol) in *N,N*-dimethyl formamide (2mL), K_2CO_3 (0.247g, 0.00179mol) was added and stirred at room temperature for 10 min. To this constantly stirred reaction mass, 2-chloroethyl benzene (0.28 mL, 0.00214mol) was slowly added dropwise and heated at 80 °C for 20 minutes in microwave reactor at 150 psi. After completion of reaction (monitored on TLC), the reaction mixture was poured on ice cold water and extracted with dichloromethane (DCM). The extracted organic layer was dried over anhydrous sodium sulphate and concentrated under reduced pressure to obtain dark brown gel liquid, was further purified by flash silica column [MeOH/DCM, 10:90] to afford the desired compound (**3**), as light brown solid. Yield: 72 %; mp 210-212 °C; FTIR (ATR, cm^{-1}) ν_{max} : 3022 (NH Str.), 2920 (Ar C-H Str. of Pyr.), 1671 (C=O Str.), 1571, 1239, 1144, 963, 952, 774, 757, 701, 617; $^1\text{H-NMR}$ (400 MHz, $\text{DMSO-}d_6$) δ : 13.59 (s, 1H, NH), 12.22 (s, 1H, OH), 8.03 (s, 1H, ArH), 7.31 (t, $J = 2.52$ Hz, 4H, ArH), 7.25-7.20 (m, 1H, ArH), 3.41 (t, $J = 5.04$ Hz, 2H, CH_2), 2.99 (t, $J = 7.56$ Hz, 2H, CH_2) ppm; ^{13}C NMR (100 MHz, $\text{DMSO-}d_6$): δ 158.20, 139.93, 128.73, 128.62, 128.41, 126.41, 102.89, 34.61 (CH_2), 31.08 (CH_2) ppm.

4.4 6-(hexylthio)-1*H*-pyrazolo[3,4-*d*]pyrimidin-4-ol (4)

To a stirred solution of 6-mercapto-1*H*-pyrazolo[3,4-*d*]pyrimidin-4-ol (compound **1**, 1g, 0.00595mol) in 1M NaOH solution (12 mL), 1-bromohexane (1.65 mL, 0.01190mol) was added dropwise and heated at 70 °C for 6h and later slowly brought to RT and continued stirring for overnight. After completion of reaction (monitored on TLC), glacial acetic acid was added dropwise to yield the crude solid, which further washed with petroleum ether and purified by flash silica column [MeOH/DCM, 05:95] to afford the desired compound (**4**), as yellow solid. Yield: 75 %; mp 211-213 °C; FTIR (ATR, cm^{-1}) ν_{max} : 3174 (NH Str.), 2925 (Ar C-H Str.), 2851, 1670 (C=O Str.), 1595, 1395, 1240, 1151, 1053, 961, 876, 780, 538; $^1\text{H-NMR}$ (400 MHz, $\text{DMSO-}d_6$) δ : 13.54 (s, 1H, NH), 12.28 (s, 1H, OH), 7.93 (s, 1H, ArH), 3.15 (t, $J = 7.22$ Hz, 2H, CH_2), 1.69-1.62 (m, 2H, CH_2), 1.41-1.34 (m, 2H, CH_2), 1.27 (t, $J = 3.62$ Hz, 4H, (CH_2)₂), 0.85 (t, $J = 6.96$ Hz, 3H, CH_3) ppm; ^{13}C NMR (100 MHz, $\text{DMSO-}d_6$) δ : 159.48, 157.72, 153.37, 135.23, 102.54, 30.74 (CH_2), 29.75 (CH_2), 28.50 (CH_2), 27.85 (CH_2), 22.00 (CH_2), 13.88 (CH_3) ppm.

4.5 General procedure for synthesis of final compounds (5a-5h, 6a-6d and 7a-7c)

To a constantly stirred solution of compounds 6-(pentylthio)-1*H*-pyrazolo[3,4-*d*]pyrimidin-4-ol (**5**), 6-(phenethylthio)-1*H*-pyrazolo[3,4-*d*]pyrimidin-4-ol (**7**) 6-(hexylthio)-1*H*-pyrazolo[3,4-*d*]pyrimidin-4-ol (**9**) (0.2g, 0.00074mol) in THF was added pyridine (0.060ml, 0.00047mol) and stirred for 10 min. To this reaction mixture were added different acid chlorides (0.00074mol), continued stirring for 60 min. Progress of the reaction was monitored on TLC. On completion, the reaction mixture was poured into ice cold water to yield the crude solids, which were further purified by recrystallization with ethanol to afford the desired title compounds (**5a-5h**, **6a-6d** and **7a-7c**).

4.5.1 6-(pentylthio)-1*H*-pyrazolo[3,4-*d*]pyrimidin-4-yl benzofuran-2-carboxylate (**5a**)

White solid; yield: 80 %; mp 205-207 °C; FTIR (ATR, cm^{-1}) ν_{max} : 2954 (NH Str.), 2927 (Ar C-H Str.), 2865 (alkane C-H Str.), 1714 (ester C=O Str.), 1442, 1371, 1291, 1177, 1129, 946, 877, 735; $^1\text{H-NMR}$ (400 MHz, $\text{DMSO-}d_6$) δ : 2.36 (s, 1H, NH), 9.18 (s, 1H, ArH), 8.58 (s, 1H, ArH), 7.99 (d, $J = 7.80$ Hz, 1H, ArH), 7.79 (d, $J = 8.52$ Hz, 1H, ArH), 7.61 (t, $J = 7.80$ Hz, 1H, ArH), 7.41 (t, $J = 7.50$ Hz, 1H, ArH), 3.19 (t, $J = 7.24$ Hz, 2H, CH_2), 1.73-1.66 (m, 2H, CH_2), 1.41-1.28 (m, 4H, $(\text{CH}_2)_2$), 0.88 (t, $J = 7.08$ Hz, 3H, CH_3) ppm; $^{13}\text{C NMR}$ (100 MHz, $\text{DMSO-}d_6$) δ : 162.14 (C=O), 159.78, 158.33, 155.54, 155.32, 144.07, 130.46, 129.52, 126.81, 124.62, 124.39, 121.83, 112.17, 108.27, 30.38 (CH_2), 29.93 (CH_2), 27.99 (CH_2), 21.69 (CH_2), 13.83 (CH_3) ppm; HRMS (ESI, m/z) $[\text{M}+\text{H}]^+$; calculated for $\text{C}_{19}\text{H}_{18}\text{N}_4\text{O}_3\text{S}$, 381.1027; found 381.1021.

4.5.2 6-(pentylthio)-1*H*-pyrazolo[3,4-*d*]pyrimidin-4-yl 4-(methylthio)benzoate (**5b**)

White solid; yield: 78 %; mp 187-189 °C; FTIR (ATR, cm^{-1}) ν_{max} : 3056 (NH Str.), 2923 (Ar C-H Str.), 2854 (alkane C-H Str.), 1686 (ester C=O Str.), 1586, 1453, 1355, 1239, 1093, 966, 896, 774, 741; $^1\text{H-NMR}$ (400 MHz, $\text{DMSO-}d_6$) δ : 12.31 (s, 1H, NH), 9.10 (s, 1H, ArH), 8.06 (d, $J = 8.56$ Hz, 2H, ArH), 7.45 (d, $J = 8.56$ Hz, 2H, ArH), 3.16 (t, $J = 7.24$ Hz, 2H, CH_2), 2.57 (s, 3H, S- CH_3), 1.70-1.63 (m, $J = 7.26$ Hz, 2H, CH_2), 1.40-1.25 (m, 4H, $(\text{CH}_2)_2$), 0.86 (t, $J = 7.08$ Hz, 3H, CH_3) ppm; $^{13}\text{C NMR}$ (100 MHz, $\text{DMSO-}d_6$) δ : 165.32, 161.52 (C=O), 159.28, 158.54, 146.95, 132.19, 130.61, 125.76, 124.46, 107.90, 30.36 (CH_2), 29.86 (CH_2), 28.13 (CH_2), 21.67 (CH_2), 13.88 (S- CH_3), 13.81 (CH_3) ppm; HRMS (ESI, m/z) $[\text{M}+\text{H}]^+$; calculated for $\text{C}_{18}\text{H}_{20}\text{N}_4\text{O}_2\text{S}_2$, 387.0944; found 387.0949.

4.5.3 6-(pentylthio)-1*H*-pyrazolo[3,4-*d*]pyrimidin-4-yl 3,3-dimethylbutanoate (**5c**)

Light brown solid; yield: 75 %; mp 174-176 °C; FTIR (ATR, cm^{-1}) ν_{max} : 3191 (C-H Str. of CH_3), 3090 (N-H Str.), 2929 (Ar C-H Str.), 2856 (alkane C-H Str.), 1667 (ester C=O Str.), 1575, 1388, 1245, 1221, 1155, 964, 938, 750, 664; $^1\text{H-NMR}$ (400 MHz, $\text{DMSO-}d_6$) δ : 12.28 (s, 1H, NH), 9.00 (s, 1H, ArH), 3.16 (t, $J = 7.26$ Hz, 2H, CH_2), 3.12 (s, 2H, (CH_2)), 1.71-1.63 (m, 2H, CH_2), 1.41-1.26 (m, 4H, $(\text{CH}_2)_2$), 1.05 (s, 9H, $(\text{CH}_3)_3$), 0.87 (t, $J = 7.12$ Hz, 3H, CH_3) ppm; $^{13}\text{C NMR}$ (100 MHz, $\text{DMSO-}d_6$) δ : 170.74,

161.41 (C=O), 158.87, 158.62, 127.94, 108.30, 44.80, 31.04, 30.38 ($\underline{\text{CH}_2}$), 29.86 ($\underline{\text{CH}_2}$), 29.23, 28.20 ($\underline{\text{CH}_2}$), 21.70 ($\underline{\text{CH}_2}$), 13.84 ($\underline{\text{CH}_3}$) ppm.

4.5.4 6-(pentylthio)-1H-pyrazolo[3,4-d]pyrimidin-4-yl cyclobutanecarboxylate (5d)

White solid; yield: 75 %; mp 165-167 °C; FTIR (ATR, cm^{-1}) ν_{max} : 3057 (Ar C-H Str.), 2917 (N-H Str.), 2855 (alkane C-H Str.), 1698 (ester C=O Str.), 1599, 1452, 1367, 1249, 1136, 965, 779; $^1\text{H-NMR}$ (400 MHz, $\text{DMSO-}d_6$) δ : 12.27 (s, 1H, NH), 8.95 (s, 1H, ArH), 4.29-4.20 (m, 1H, alicyclic $\underline{\text{CH}}$), 3.16 (t, $J = 7.24$ Hz, 2H, $\underline{\text{CH}_2}$), 2.35-2.29 (m, 4H, alicyclic ($\underline{\text{CH}_2}$)₂), 2.11-2.00 (m, 1H, alicyclic $\underline{\text{CH}}$), 1.91-1.82 (m, 1H), 1.71-1.63 (m, 2H, $\underline{\text{CH}_2}$), 1.41-1.28 (m, 4H, ($\underline{\text{CH}_2}$)₂), 0.87 (t, $J = 7.04$ Hz, 3H, $\underline{\text{CH}_3}$) ppm; $^{13}\text{C NMR}$ (100 MHz, $\text{DMSO-}d_6$) δ : 173.28, 161.32 (C=O), 159.13, 158.57, 128.25, 108.12, 37.41, 30.38 ($\underline{\text{CH}_2}$), 29.84 ($\underline{\text{CH}_2}$), 28.18 ($\underline{\text{CH}_2}$), 24.70, 21.69 ($\underline{\text{CH}_2}$), 17.82, 13.84 ($\underline{\text{CH}_3}$) ppm.

4.5.5 6-(pentylthio)-1H-pyrazolo[3,4-d]pyrimidin-4-yl furan-2-carboxylate (5e)

White solid; yield: 80 %; mp 197-199 °C; FTIR (ATR, cm^{-1}) ν_{max} : 3058 (Ar C-H Str.), 2974 (N-H Str.), 2887 (alkane C-H Str.), 1688 (ester C=O Str.), 1603, 1459, 1373, 1285, 1084, 936, 863, 763; $^1\text{H-NMR}$ (400 MHz, $\text{DMSO-}d_6$) δ : 12.33 (s, 1H, NH), 9.12 (s, 1H, ArH), 8.25 (d, $J = 0.80$ Hz, 1H, ArH), 8.11 (d, $J = 3.60$ Hz, 1H, ArH), 6.88 (dd, $J = 3.68, 1.64$ Hz, 1H, ArH), 3.19 (t, $J = 7.24$ Hz, 2H, $\underline{\text{CH}_2}$), 1.73-1.65 (m, 2H, $\underline{\text{CH}_2}$), 1.40-1.29 (m, 4H, ($\underline{\text{CH}_2}$)₂), 0.88 (t, 7.08 Hz, 3H, $\underline{\text{CH}_3}$) ppm; $^{13}\text{C NMR}$ (100 MHz, $\text{DMSO-}d_6$) δ : 161.91 (C=O), 159.68, 158.43, 154.15, 150.64, 143.50, 130.19, 126.39, 113.50, 108.03, 30.37 ($\underline{\text{CH}_2}$), 29.91 ($\underline{\text{CH}_2}$), 28.09 ($\underline{\text{CH}_2}$), 21.66 ($\underline{\text{CH}_2}$), 13.83 ($\underline{\text{CH}_3}$) ppm; HRMS (ESI, m/z) $[\text{M}+\text{H}]^+$; calculated for $\text{C}_{15}\text{H}_{16}\text{N}_4\text{O}_3\text{S}$, 331.0854; found 331.0865.

4.5.6 6-(pentylthio)-1H-pyrazolo[3,4-d]pyrimidin-4-yl thiophene-2-carboxylate (5f)

White solid; yield: 85 %; mp 205-207 °C; FTIR (ATR, cm^{-1}) ν_{max} : 3040 (Ar C-H Str.), 2927 (N-H Str.), 2854 (alkane C-H Str.), 1691 (ester C=O Str.), 1608, 1452, 1352, 1242, 1088, 887, 773, 426; $^1\text{H-NMR}$ (400 MHz, $\text{DMSO-}d_6$) δ : 12.34 (s, 1H, NH), 9.12 (s, 1H, ArH), 8.44 (d, $J = 3.24$ Hz, 1H, ArH), 8.26 (d, $J = 4.32$ Hz, 1H, ArH), 7.34 (t, $J = 4.42$ Hz, 1H, ArH), 3.20 (t, $J = 7.22$ Hz, 2H, $\underline{\text{CH}_2}$), 1.73-1.66 (m, 2H, $\underline{\text{CH}_2}$), 1.42-1.28 (m, 4H, ($\underline{\text{CH}_2}$)₂), 0.88 (t, $J = 7.02$ Hz, 3H, $\underline{\text{CH}_3}$) ppm; $^{13}\text{C NMR}$ (100 MHz, $\text{DMSO-}d_6$) δ : 161.97 (C=O), 159.33, 158.39, 158.35, 140.13, 139.59, 130.95, 129.92, 128.25, 108.37, 30.33 ($\underline{\text{CH}_2}$), 29.89 ($\underline{\text{CH}_2}$), 28.00 ($\underline{\text{CH}_2}$), 21.62 ($\underline{\text{CH}_2}$), 13.80 ($\underline{\text{CH}_3}$) ppm; HRMS (ESI, m/z) $[\text{M}+\text{H}]^+$; calculated for $\text{C}_{15}\text{H}_{16}\text{N}_4\text{O}_2\text{S}_2$, 347.0634; found 347.0636.

4.5.7 6-(pentylthio)-1H-pyrazolo[3,4-d]pyrimidin-4-yl benzoate (5g)

White solid; yield: 76 %; mp 168-170 °C; FTIR (ATR, cm^{-1}) ν_{max} : 3040 (Ar C-H Str.), 2927 (N-H Str.), 2854 (alkane C-H Str.), 1687 (ester C=O Str.), 1597, 1452, 1363, 1238, 1090, 898, 773, 706; $^1\text{H-NMR}$

(400 MHz, DMSO-*d*₆) δ : 12.32 (s, 1H, NH), 9.13 (s, 1H, ArH), 8.06 (d, $J = 7.40$ Hz, 2H, ArH), 7.74 (t, $J = 7.42$ Hz, 1H, ArH), 7.60 (t, $J = 7.70$ Hz, 2H, ArH), 3.16 (t, $J = 7.22$ Hz, 2H, $\underline{\text{CH}}_2$), 1.70-1.63 (m, 2H, $\underline{\text{CH}}_2$), 1.39-1.23 (m, 4H, ($\underline{\text{CH}}_2$)₂), 0.85 (t, $J = 7.04$ Hz, 3H, $\underline{\text{CH}}_3$) ppm; ¹³C NMR (100 MHz, DMSO-*d*₆) δ : 166.24, 161.61 (C=O), 159.33, 158.53, 133.65, 131.44, 130.64, 130.45, 128.29, 108.11, 30.33 ($\underline{\text{CH}}_2$), 29.84 ($\underline{\text{CH}}_2$), 28.11 ($\underline{\text{CH}}_2$), 21.64 ($\underline{\text{CH}}_2$), 13.79 ($\underline{\text{CH}}_3$) ppm; HRMS (ESI, *m/z*) [M+H]⁺; calculated for C₁₇H₁₈N₄O₂S, 341.1071; found 341.1072.

4.5.8 6-(pentylthio)-1H-pyrazolo[3,4-d]pyrimidin-4-yl [1,1'-biphenyl]-4-carboxylate (5h)

White solid; yield: 84 %; mp 173-175 °C; FTIR (ATR, cm⁻¹) ν_{max} : 3036 (Ar C-H Str.), 2904 (N-H Str.), 2873 (alkane C-H Str.), 1691 (ester C=O Str.), 1604, 1448, 1367, 1283, 1253, 1137, 903, 735, 692; ¹H-NMR (400 MHz, DMSO-*d*₆) δ : 12.17 (s, 1H, NH), 9.09 (s, 1H, ArH), 8.21 (d, $J = 8.34$ Hz, 2H, ArH), 7.90 (d, $J = 8.34$ Hz, 2H, ArH), 7.79 (d, $J = 7.56$ Hz, 2H, ArH), 7.53 (t, $J = 7.59$ Hz, 2H, ArH), 7.45 (t, $J = 7.47$ Hz, 1H, ArH), 3.20 (t, $J = 7.26$ Hz, 2H, $\underline{\text{CH}}_2$), 1.73-1.68 (m, 2H, $\underline{\text{CH}}_2$), 1.42-1.30 (m, 4H, ($\underline{\text{CH}}_2$)₂), 0.87 (t, $J = 7.20$ Hz, 3H, $\underline{\text{CH}}_3$) ppm; ¹³C NMR (100 MHz, DMSO-*d*₆) δ : 165.51, 161.43 (C=O), 159.17, 158.19, 144.98, 138.50, 131.96, 128.92, 128.82, 128.29, 126.79, 126.23, 107.87, 30.04 ($\underline{\text{CH}}_2$), 29.75 ($\underline{\text{CH}}_2$), 27.84 ($\underline{\text{CH}}_2$), 21.27 ($\underline{\text{CH}}_2$), 13.36 ($\underline{\text{CH}}_3$) ppm.

4.5.9 6-(phenethylthio)-1H-pyrazolo[3,4-d]pyrimidin-4-yl benzoate (6a)

White solid; yield: 80 %; mp 198-200 °C; FTIR (ATR, cm⁻¹) ν_{max} : 3061 (Ar C-H Str.), 2982 (N-H Str.), 2880 (alkane C-H Str.), 1704 (ester C=O Str.), 1684, 1597, 1455, 1362, 1232, 1135, 898, 698; ¹H-NMR (400 MHz, DMSO-*d*₆) δ : 12.34 (s, 1H, NH), 9.15 (s, 1H, ArH), 8.08 (d, $J = 7.32$ Hz, 1H, ArH), 7.74 (t, $J = 7.46$ Hz, 1H, ArH), 7.61 (t, $J = 7.74$ Hz, 2H, ArH), 7.32-7.26 (m, 4H, ArH), 7.23-7.19 (m, 1H, ArH), 3.45 (t, $J = 7.34$ Hz, 2H, $\underline{\text{CH}}_2$), 3.0 (t, $J = 7.34$ Hz, 2H, $\underline{\text{CH}}_2$) ppm; ¹³C NMR (100 MHz, DMSO-*d*₆) δ : 166.26, 161.41 (C=O), 159.35, 158.55, 139.77, 133.72, 131.51, 130.75, 130.45, 128.60, 128.40, 128.33, 126.42, 108.15, 34.23 ($\underline{\text{CH}}_2$), 31.20 ($\underline{\text{CH}}_2$) ppm; HRMS (ESI, *m/z*) [M+H]⁺; calculated for C₂₀H₁₆N₄O₂S, 375.0920; found 375.0916.

4.6.0 6-(phenethylthio)-1H-pyrazolo[3,4-d]pyrimidin-4-ylfuran-2-carboxylate (6b)

White solid; yield: 78 %; mp 230-232 °C; FTIR (ATR, cm⁻¹) ν_{max} : 3072 (Ar C-H Str.), 2927 (N-H Str.), 2855 (alkane C-H Str.), 1688 (ester C=O Str.), 1608, 1453, 1419, 1368, 1271, 1243, 1139, 1090, 865, 773, 693; ¹H-NMR (400 MHz, DMSO-*d*₆) δ : 12.34 (s, 1H, NH), 9.14 (s, 1H, ArH), 8.27 (d, $J = 0.96$ Hz, 1H, ArH), 8.14 (d, $J = 3.44$ Hz, 1H, ArH), 7.32 (d, $J = 4.48$ Hz, 4H, ArH), 7.23 (m, 1H, ArH), 6.89 (dd, $J = 3.7, 1.6$ Hz, 1H, ArH), 3.47 (t, $J = 7.42$ Hz, 2H, $\underline{\text{CH}}_2$), 3.03 (t, $J = 7.44$ Hz, 2H, $\underline{\text{CH}}_2$) ppm; ¹³C NMR (100 MHz, DMSO-*d*₆) δ : 161.65 (C=O), 159.64, 158.38, 154.11, 150.63, 143.49, 139.85, 130.22, 128.63, 128.43, 126.42, 113.52, 108.05, 34.27 ($\underline{\text{CH}}_2$), 31.28 ($\underline{\text{CH}}_2$) ppm.

4.6.1 6-(phenethylthio)-1H-pyrazolo[3,4-d]pyrimidin-4-yl benzofuran-2-carboxylate (6c)

White solid; yield: 75 %; mp 230-232 °C; FTIR (ATR, cm⁻¹) ν_{\max} : 3120 (Ar C-H Str.), 3028 (N-H Str.), 2876 (alkane C-H Str.), 1706 (ester C=O Str.), 1604, 1542, 1542, 1454, 1373, 1292, 1141, 946, 866, 742, 694; ¹H-NMR (400 MHz, DMSO-*d*₆) δ : 12.37 (s, 1H, NH), 9.21 (s, 1H, ArH), 8.61 (s, 1H, ArH), 8.01 (d, *J* = 7.84 Hz, 1H, ArH), 7.80 (d, *J* = 8.36 Hz, 1H, ArH), 7.61 (t, *J* = 7.78 Hz, 1H, ArH), 7.42 (t, *J* = 7.54 Hz, 1H, ArH), 7.33 (d, *J* = 4.36 Hz, 4H, ArH), 7.24 (m, 1H, ArH), 3.50 (t, *J* = 7.36 Hz, 2H, CH₂), 3.04 (t, *J* = 7.40 Hz, 2H, CH₂) ppm; ¹³C NMR (100 MHz, DMSO-*d*₆) δ : 161.92 (C=O), 159.78, 158.32, 155.55, 155.33, 144.09, 139.81, 130.53, 129.53, 128.64, 128.44, 126.83, 126.46, 124.68, 124.39, 121.87, 112.17, 108.30, 34.13 (CH₂), 31.30 (CH₂) ppm.

4.6.2 6-(phenethylthio)-1H-pyrazolo[3,4-d]pyrimidin-4-yl thiophene-2-carboxylate (6d)

White solid; yield: 80 %; mp 252-254 °C; FTIR (ATR, cm⁻¹) ν_{\max} : 3124 (Ar C-H Str.), 3027 (N-H Str.), 2879 (alkane C-H Str.), 1693 (ester C=O Str.), 1606, 1454, 1374, 1350, 1244, 1093, 887, 742, 725, 693; ¹H-NMR (400 MHz, DMSO-*d*₆) δ : 12.35 (s, 1H, NH), 9.14 (s, 1H, ArH), 8.45 (d, *J* = 2.80 Hz, 1H, ArH), 8.26 (d, *J* = 4.40 Hz, 1H, ArH), 7.32 (d, *J* = 3.92 Hz, 5H, ArH), 7.23 (d, *J* = 3.84 Hz, 1H, ArH), 3.48 (t, *J* = 7.18 Hz, 2H, CH₂), 3.03 (t, *J* = 7.14 Hz, 2H, CH₂); ¹³C NMR (100 MHz, DMSO-*d*₆) δ : 161.76 (C=O), 159.30, 158.37, 140.21, 139.86, 139.62, 130.95, 129.93, 128.62, 128.43, 128.25, 126.43, 108.40, 34.24 (CH₂), 31.34 (CH₂) ppm; HRMS (ESI, *m/z*) [M+H]⁺; calculated for C₁₈H₁₄N₄O₂S₂, 381.0481; found 381.0480.

4.6.3 6-(hexylthio)-1H-pyrazolo[3,4-d]pyrimidin-4-yl benzoate (7a)

White solid; yield: 76 %; mp 167-169 °C; FTIR (ATR, cm⁻¹) ν_{\max} : 3140 (Ar C-H Str.), 2924 (N-H Str.), 2847 (alkane C-H Str.), 1713 (ester C=O Str.), 1610, 1449, 1368, 1285, 1203, 1090, 900, 705; ¹H-NMR (400 MHz, DMSO-*d*₆) δ : 12.33 (s, 1H, NH), 9.14 (s, 1H, ArH), 8.06 (d, *J* = 7.32 Hz, 2H, ArH), 7.74 (t, *J* = 7.40 Hz, 1H, ArH), 7.60 (t, *J* = 7.76 Hz, 2H, ArH), 3.16 (t, *J* = 7.24 Hz, 2H, CH₂), 1.69-1.62 (m, 2H, CH₂), 1.41-1.34 (m, 2H, CH₂), 1.28-1.24 (m, 4H, (CH₂)₂), 0.84 (t, *J* = 6.74 Hz, 3H, CH₃) ppm; ¹³C NMR (100 MHz, DMSO-*d*₆) δ : 166.27, 161.63 (C=O), 159.34, 158.55, 133.67, 131.46, 130.67, 130.46, 128.30, 108.12, 30.71 (CH₂), 29.87 (CH₂), 28.40 (CH₂), 27.83 (CH₂), 21.96 (CH₂), 13.87 (CH₃) ppm.

4.6.4 6-(hexylthio)-1H-pyrazolo[3,4-d]pyrimidin-4-yl thiophene-2-carboxylate (7b)

White solid; yield: 78 %; mp 205-207 °C; FTIR (ATR, cm⁻¹) ν_{\max} : 3143 (Ar C-H Str.), 2915 (N-H Str.), 2850 (alkane C-H Str.), 1692 (ester C=O Str.), 1606, 1453, 1372, 1350, 1243, 1140, 1088, 887, 853, 724; ¹H-NMR (400 MHz, DMSO-*d*₆) δ : 12.35 (s, 1H, NH), 9.14 (s, 1H, ArH), 8.45 (d, *J* = 3.28 Hz, 1H, ArH), 8.26 (d, *J* = 4.68 Hz, 1H, ArH), 7.35 (t, *J* = 4.34 Hz, 1H, ArH), 3.21 (t, *J* = 7.14 Hz, 2H, CH₂),

1.73-1.66 (m, 2H, $\underline{\text{CH}_2}$), 1.40 (d, $J = 6.00$ Hz, 2H, $\underline{\text{CH}_2}$), 1.29 (d, $J = 3.36$ Hz, 4H, $(\underline{\text{CH}_2})_2$), 0.87 (t, $J = 6.42$ Hz, 3H, $\underline{\text{CH}_3}$) ppm; ^{13}C NMR (100 MHz, DMSO- d_6) δ : 161.99 (C=O), 159.35, 158.41, 158.37, 140.15, 139.61, 130.97, 129.98, 128.29, 108.38, 30.70 ($\underline{\text{CH}_2}$), 29.93 ($\underline{\text{CH}_2}$), 28.30 ($\underline{\text{CH}_2}$), 27.82 ($\underline{\text{CH}_2}$), 21.97 ($\underline{\text{CH}_2}$), 13.90 ($\underline{\text{CH}_3}$) ppm; HRMS (ESI, m/z) $[\text{M}+\text{H}]^+$; calculated for $\text{C}_{16}\text{H}_{18}\text{N}_4\text{O}_2\text{S}_2$, 361.0793; found 361.0793.

4.6.5 6-(hexylthio)-1H-pyrazolo[3,4-d]pyrimidin-4-yl furan-2-carboxylate (7c)

White solid; yield: 78 %; mp 152-154 °C; FTIR (ATR, cm^{-1}) ν_{max} : 3092 (Ar C-H Str.), 2924 (N-H Str.), 2849 (alkane C-H Str.), 1712 (ester C=O Str.), 1604, 1462, 1376, 1288, 1263, 1146, 936, 865, 772; ^1H -NMR (400 MHz, DMSO- d_6) δ : 12.34 (s, 1H, NH), 9.14 (s, 1H, ArH), 8.27 (s, 1H, ArH), 8.13 (d, $J = 3.60$ Hz, 1H, ArH), 6.89 (s, 1H, ArH), 3.22-3.13 (m, 2H, $\underline{\text{CH}_2}$), 1.73-1.62 (m, 2H, $\underline{\text{CH}_2}$), 1.40 (s, 2H, $\underline{\text{CH}_2}$), 1.29 (d, $J = 3.60$ Hz, 4H, $(\underline{\text{CH}_2})_2$), 0.86 (d, $J = 5.60$ Hz, 3H, $\underline{\text{CH}_3}$); ^{13}C NMR (100 MHz, DMSO- d_6) δ : 161.87 (C=O), 159.65, 158.41, 158.38, 154.12, 143.48, 130.21, 129.98, 126.34, 113.46, 108.02, 30.69 ($\underline{\text{CH}_2}$), 29.89 ($\underline{\text{CH}_2}$), 28.35 ($\underline{\text{CH}_2}$), 27.82 ($\underline{\text{CH}_2}$), 21.95 ($\underline{\text{CH}_2}$), 13.88 ($\underline{\text{CH}_3}$) ppm; HRMS (ESI, m/z) $[\text{M}+\text{H}]^+$; calculated for $\text{C}_{16}\text{H}_{18}\text{N}_4\text{O}_3\text{S}$, 345.1017; found 345.1021.

5 Biological activity protocol

5.1 CDK2 and Abl kinase inhibition assays

CDK2/cyclin E and Abl kinases were produced in Sf9 insect cells via baculoviral infection and purified on a NiNTA column. The kinase reactions were assayed with suitable substrates (1 mg/mL histone H1 for CDK2 and 500 μM peptide GGEAIYAAPFCK for Abl) in the presence of 15 or 10 μM ATP for CDK2 and Abl, respectively, 0.05 μCi [γ - ^{33}P]ATP, and the test compound in a final volume of 10 μL , all in a reaction buffer (60 mM HEPES-NaOH, pH 7.5, 3 mM MgCl_2 , 3 mM MnCl_2 , 3 μM Na-orthovanadate, 1.2 mM DTT, 2.5 μg / 50 μl PEG_{20,000}). The reactions were stopped by adding 5 μL of 3% aq. H_3PO_4 . Aliquots were spotted onto P-81 phosphocellulose (Whatman), washed 3 \times with 0.5% aq. H_3PO_4 and finally air-dried. Kinase inhibition was quantified using a FLA-7000 digital image analyzer. The concentration of the test compounds required to reduce the kinase activity by 50 % was determined from dose-response curves and recorded as their IC_{50} .

5.2 Anti-proliferative (K-562 and MCF-7) activity assays

The tumor cells (purchased from the American Type Culture Collection) were grown in DMEM medium supplemented with 10% (v/v) fetal bovine serum and L-glutamine (0.3 g/L) and were maintained at 37 °C in a humidified atmosphere with 5% CO_2 . For anticancer cytotoxicity estimations, 10^4 cells were seeded into each well of a 96-well plate, allowed to stabilize for 20 h, and the test

inhibitors were then added at different concentrations (ranging from 0.1 to 100 μM or to a solubility limit) in triplicate. Three days after addition of the inhibitors, calcein AM solution (Molecular Probes) was added. One hour later, fluorescence of cells was quantified using a Fluoroskan Ascent (Labsystems) reader and cytotoxic effective concentrations were calculated and expressed as IC_{50} values from dose-response curves. Roscovitine and imatinib were used as reference drugs.

6 Molecular docking simulation

Molecular docking experiments were performed using Glide software package⁴¹ implemented in Schrodinger Suite (2017-2) (Schrödinger, Inc., USA)⁴² running on Intel CORE i7 based hpZ230 workstation with the Microsoft Windows 10 OS. In this protocol, the protein was kept rigid, while the ligands were allowed to be flexible throughout the docking simulation.

6.1 Protein preparation

The starting X-ray solved protein crystal structure of cyclin dependent kinase-2 bound with *R*-roscovitine was retrieved from protein data bank (PDB) bearing ID 2A4L.⁴³ The protein was prepared by automatic preparation by Protein Preparation Wizard of Glide employing the Optimized Potentials for Liquid Simulations 3 (OPLS3) forcefield. During the pre-processing stage, crystallographic water molecules were removed and added missing hydrogens to the protein structures corresponding to pH 7.0 was achieved. The protein metal ions and cofactors were viewed and removed from the protein structure. The tool neutralized the side chains that are not close to the binding cavity and do not participate in salt bridges. The pre-processed protein structure was refined initially by optimizing the sample-water orientation followed by restrained minimization of co-crystallized complex using OPLS3, which reorients side chain hydroxyl groups and alleviates potential steric clashes. Thus, the complex obtained was minimized until it reaches the convergent of heavy atom to RMSD 0.3 Å and taken finally in .mae format.

6.2 Grid file generation

Receptor grid generation protocol of Maestro 11.2 was used to define the binding-site of the protein (2A4L) for docking simulation by excluding any co-crystallized metals, co-factors, water molecules all of which may have crystallized during experimental crystallization of the CDK-2 protein. A grid box was generated around the centroid of the cognate ligand (*R*-roscovitine) specifying the size for the docking ligands (20 Å) with default settings.

6.3 Ligand preparation

The Structures of the synthesized ligands and standard *R*-roscovitine were sketched using built panel of Maestro and taken in .mae format. LigPrep is a utility of Schrodinger software suit that combines tools for generating 3D structures from 1D (Smiles) and 2D (SDF) representation, searching for tautomers, steric isomers and perform a geometry minimization of the ligands. By employing Ligprep protocol, all the ligands were prepared using OPLS3 with default settings and the output file was saved in .maegz format automatically.

6.4 Docking simulation

For precision and accuracy of the docking protocols, the co-crystallized ligand was extracted from the crystal structure of 2A4L and re-docked using Glide docking algorithm (Schrodinger Inc) in its extra precision (XP) mode with default settings without applying any constraints. A good agreement of the obtained pose of docked *R*-roscovitine with cognate ligand indicated the reliability of the selected docking parameters for docking of the synthesized ligands. Hence, by specifying the ligands against the receptor grid, molecular docking was performed using default settings in Glide XP mode.

6.5 Binding mode analysis

The protein-ligand complexes were analysed to investigate various types of interactions by utilizing XP visualizer protocol. For the best-scored ligands, the 2D and 3D plots of molecular ligand-receptor interactions were analysed for hydrogen bond, halogen bond, salt bridges, π - π stacking, and π -cation interactions. G-score and relevant docking descriptors were computed for each of the best docked pose.

Conflict of Interest

Authors hereby declare that there are no financial/commercial conflicts of interest.

Acknowledgment

Authors are thankful to Discipline of Pharmaceutical Sciences, College of Health Sciences, University of KwaZulu-Natal (UKZN), South Africa, for their constant support, encouragement and financial assistance. One of the authors (CB) gratefully acknowledges National Research Foundation (DST-NRF), South Africa for research funding in the form of Innovation Post-Doctoral Research Fellowship (UID: 99546). Authors also sincerely thank Centre for High Performance Computing (CHPC), Cape Town, South Africa for computational resources. Authors express heartfelt thanks to Mr. Dilip Jagjivan and Dr. Caryl Janse Van Rensburg (UKZN, South Africa) for their assistance in the NMR and EIMS experiments.

References

1. American Cancer Society: Cancer Facts and Figs 2012, *American Cancer Society: Atlanta*, 2012.
2. K. Neet, T. Hunter, *Genes Cells* 1996, 1, 147-169.
3. Y. L. Chen, S. Z. Lin, J. Y. Chang, Y. L. Cheng, N. M. Tsai, S. P. Chen, W. L. Chang, H. J. Harn, *Biochem. Pharmacol.* 2006, 72, 308.
4. M. Nakhjiri, M. Safavi, E. Alipour, S. Emami, A. F. Atash, M. Jafari-Zavareh, S. K. Ardestani, M. Khoshneviszadeh, A. Foroumadi, A. Shafiee, *Eur. J. Med. Chem.* 2012, 50, 113.
5. T. Hunter, *Harvey Lect.* 1998, 94, 81-119.
6. a) P. Cohen, *Nat. Rev. Drug Discov.* 2002, 1, 309-315; b) R. Santos, O. Ursu, A. Gaulton, A. P. Bento, R. S. Donadi, C. G. Bologa, A. Karlsson, B. L. Lazikani, A. Hersey, T. I. Opera, J. P. Overington, *Nat. Rev. Drug Discov.* 2017, 16, 19-34.
7. D. O. Morgan, *Nature.* 1995, 374, 131-134.
8. A. B. Pardee, *Science.* 1989, 246, 603-608.
9. J. W. Harbour, R. X. Luo, A. D. Santi, A. A. Postigo, D. C. Dean, *Cell*, 1999, 98, 859-869
10. S. R. Whittaker, A. Mallinger, P. Workman, P. A. Clarke, *Pharmacol. Ther.* 2017, 173, 83-105.
11. T. Otto, P. Sicinski, *Nat. Rev. Cancer*, 2017, 17, 93-115.
12. L. Yang, D. Fang, H. Chen, Y. Lu, Z. Dong, H. F. Ding, Q. Jing, S. B. Su, S. Huang, *Oncotarget* 2015, 6, 20801-20812.
13. J. J. Molenaar, M. E. Ebus, D. Geerts, J. Koster, F. Lamers, L. J. Valentijn, E. M. Westerhout, R. Versteeg, H. N. Caron, *Proc. Natl. Acad. Sci. U. S. A.* 2009, 106, 12968-12973.
14. A. J. Deans, K. K. Khanna, C. J. McNeese, C. Mercurio, J. Heierhorst, G. McArthur, *Cancer Res.* 2006, 66, 8219-8226.
15. M. K. A. E. Hamid, M. D. Mihovilovic, H. B. El-Nassan, *Eur. J. Med. Chem.* 2012, 57, 323-328.
16. D. J. Richard, J. C. Verheijen, K. Curran, J. Kaplan, L. Toral-Barza, I. Hollander, J. Lucas, K. Yu, A. Zask, *Bioorg. Med. Chem. Lett.* 2009, 19, 6830.
17. R. Jorda, K. Paruch, V. Krystof, *Curr. Pharm. Des.* 2012, 18, 2974-2980.
18. P. Traxler, G. Bold, J. Frei, M. Lang, N. Lydon, H. Mett, E. Buchdunger, T. Meyer, M. Mueller, Furet, *P. J. Med. Chem.* 1997, 40, 3601.
19. M. Radi, E. Dreassi, C. Brullo, E. Crespan, C. Tintori, V. Bernardo, M. Valoti, C. Zamperini, H. Daigl, F. Musumeci, F. Carraro, A. Naldini, I. Filippi, G. Maga, S. Schenone, M. Botta, *J. Med. Chem.* 2011, 54, 2610-26.
20. A. Angelucci, S. Schenone, G. L. Gravina, P. Muzi, C. Festuccia, C. Vicentini, M. Botta, M. Bologna, *Eur. J. Cancer* 2006, 42, 2838.

21. K. J. Curran, J. C. Verheijen, J. Kaplan, D. J. Richard, L. Toral-Barza, I. Hollander, J. Lucas, S. Ayral-Kaloustian, K. Yu, A. Zask, *Bioorg. Med. Chem. Lett.* 2010, 20, 1440-1444.
22. A. Kumar, I. Ahmad, B. S. Chhikara, R. Tiwari, D. Mandal, K. Parang, *Bioorg. Med. Chem. Lett.* 2011, 21, 1342-1346.
23. C. Luma, J. Kahl, L. Kessler, J. Kucharski, J. Lundstrm, S. Miller, H. Nakanishi, Y. Pei, K. Pryor, E. Roberts, L. Sebo, R. Sullivan, J. Urban, Z. Wang, *Bioorg. Med. Chem. Lett.* 2008, 18, 3578-3581
24. R. Ducray, P. Ballard, B. C. Barlaam, M. D. Hickinson, J. G. Kettle, D. J. Ogilvie, C. B. Trigwell, *Bioorg. Med. Chem. Lett.* 2008, 18, 959-962.
25. C. Wang, H. Liu, Z. Song, Y. Ji, L. Xing, X. Peng, X. Wang, J. Ai, M. Geng, A. Zhang, *Bioorg. Med. Chem. Lett.* 2017, 27, 2544-2548.
26. S. Gupta, L. M. Rodrigues, A. P. Esteves, A. M. F. Oliveira-Campos, M. S. J. Nascimento, N. Nazareth, H. Cidade, M. P. Neves, E. Fernandes, M. Pinto, N. M. Cerqueira, N. Bras, *Eur. J. Med. Chem.* 2008, 43, 771.
27. M. Chauhan, R. Kumar, *Bioorg. Med. Chem.* 2013, 21, 5657-5668.
28. G. Vignaroli, M. Mencarelli, D. Sementa, E. Crespan, M. Kissova, G. Maga, S. Schenone, M. Radi, M. Botta, *ACS Combi. Sci.* 2014, 16, 168-175.
29. J. A. Markwalder, M. R. Arnone, P. A. Benfield, M. Boisclair, C. R. Burton, C. H. Chang, S. S. Cox, P. M. Czerniak, C. L. Dean, D. Doleniak, R. Grafstrom, B. A. Harrison, R. F. Kaltenbach, D. A. Nugiel, K. A. Rossi, S. R. Sherk, L. M. Sisk, P. Stouten, G. L. Trainor, P. Worland, S. P. Seitz, *J. Med. Chem.* 2004, 47, 5894-5911.
30. D. C. Kim, Y. R. Lee, B. S. Yang, K. J. Shin, D. J. Kim, B. Y. Chung, K. H. Yoo, *Eur. J. Med. Chem.* 2003, 38, 525-532.
31. F. Manetti, C. Brullo, M. Magnani, F. Mosci, B. Chelli, E. Crespan, S. Schenone, A. Naldini, O. Bruno, M. L. Trincavelli, G. Maga, F. Carraro, C. Martini, F. Bondavalli, M. Botta, *J. Med. Chem.* 2011, 54, 2610-2626.
32. M. Radi, E. Dreassi, C. Brullo, E. Crespan, C. Tintori, V. Bernardo, M. Valoti, C. Zamperini, H. Daigl, F. Musumeci, F. Carraro, A. Naldini, I. Filippi, G. Maga, S. Schenone, M. Botta, *J. Med. Chem.* 2012, 22, 2070.
33. F. Manetti, A. Santucci, G. A. Lucatelli, G. Maga, A. Spreafico, T. Serchi, M. Orlandini, G. Bernardini, N. P. Caradonna, A. Spallarossa, C. Brullo, S. Schenone, O. Bruno, A. Ranise, F. Bondavalli, O. Hoffmann, M. Bologna, A. Angelucci, M. Botta, *J. Med. Chem.* 2007, 50, 5579-5588.
34. M. S. Abaza, A. M. Bahman, R. J. Al-Attiyah, *World J. Gastroenterol.* 2008, 14, 5162-5175.
35. H. M. Patel, B. Sing, V. Bhardwaj, M. Palkar, R. Rane, W. S. Alwan, A. K. Gadak, M. N. Noolvi, R. Karpoormath, *Eur. J. Med. Chem.* 2015, 26, 599-613.

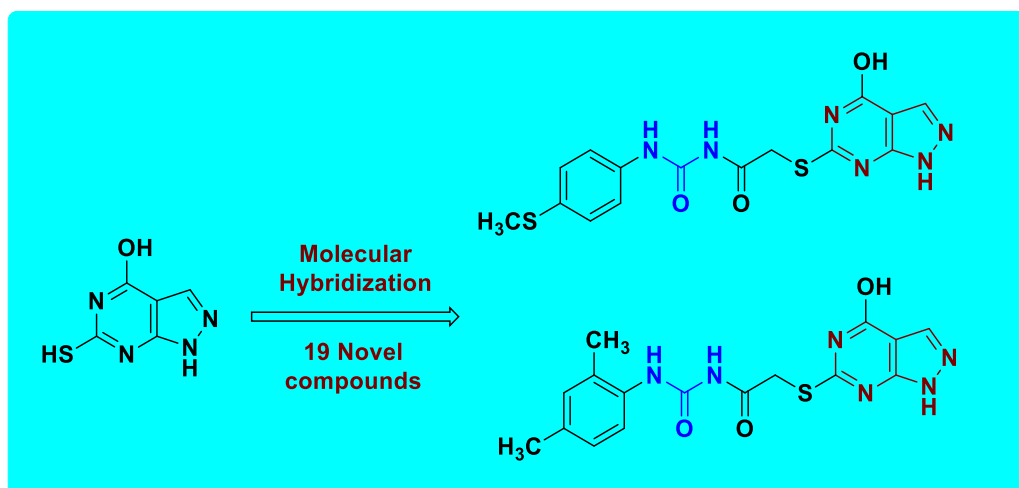
36. S. Cherukupalli, R. Karpoornath, B. Chandrasekaran, G. A. Hampannavar, N. Thapliyal, V. N. Palakollu, *Eur. J. Med. Chem.* 2017, 126, 298–352.
37. R. J. Bentems, J. D. Anderson, D. F. Smee, A. J. Jin, H. A. Alaghamandan, B. S. Sharma, W. B. Jolley, R. K. Robins, H. B. Cottam, *J. Med. Chem.* 1990, 33, 2174-2178.
38. Gregory Sliwoski, Sandeepkumar Kothiwale, Jens Meiler, and Edward W. Lowe, *Pharmacol Rev.* 2014, 66, 334-395.
39. D. Parry, T. Guzi, F. Shanahan, N. Davis, D. Prabhavalkar, D. Wiswell, W. Seghezzi, K. Paruch, M. P. Dwyer, R. Doll, A. Nomeir, W. Windsor, T. Fischmann, Y. Wang, M. Oft, T. Chen, P. Kirschmeier, and E. M. Lees. *Mol Cancer Ther.* 2010, 9, 2344-2353.
40. W. F. D. Azevedo, S. Leclerc, L. Meijer, L. Havlicek, M. Strnad, S. H. Kim, *Eur. J. Biochem.* 1997, 243, 518-526.
41. R. A. Friesner, R. B. Murphy, M. P. Repasky, L. L. Frye, J. R. Greenwood, T. A. Halgren, P. C. Sanschagrin, D. T. Mainz, *J. Med. Chem.* 2006, 49, 6177–6196.
42. Schrodinger Release 2017-2: Glide, Schrödinger, LLC, New York, NY, 2017.
43. L. M. Schang, A. Rosenberg, P. A. Chaffer, *J. Virol.* 2000, 74, 2107–2120.

CHAPTER 6

Design, synthesis and biological evaluation of novel pyrazolo[3,4-*d*]pyrimidine analogues as anticancer agents

Department of Pharmaceutical Chemistry, College of Health Sciences, University of KwaZulu-Natal, Durban 4000, South Africa.

Graphical Abstract



Abstract:

A new series of pyrazolo[3,4-*d*]pyrimidine (**9a-9s**) possessing phenylcarbamoyl acetamide at C-6 position were designed and synthesized. The synthesized compounds were evaluated for anticancer activity against CDK2/Cyclin E and Abl kinase enzymes and further evaluated for anti-proliferative activity against K-562 (chronic myelogenous leukemia) and MCF-7 (breast adenocarcinoma) cell lines. The structure-activity relationship studies (SAR) revealed that the compounds with mono substitution on phenylcarbamoyl acetamide moiety exhibited commendable activity compared to disubstitution. For all the synthesized molecules from this series, IC₅₀ values could not be measured due to solubility limit (IC₅₀ > 12.5 μM or > 25 μM). Therefore, the observed findings on the pyrazolo[3,4-*d*]pyrimidine scaffold with phenylcarbamoyl acetamide group seems to suggest need for further lead optimization with an aim to improve solubility and anticancer activity.

Key words: Pyrazolo[3,4-*d*]pyrimidine; cyclin-dependent kinase inhibitor; Anti-proliferative activity.

1 Introduction

Cancer is a multifaceted disease characterized by uncontrolled growth of the malignant cell population. Cancer is considered as the most serious health burden touching every region of the world.¹ It is a second leading cause of the death worldwide, accounted for 8.8 million death in 2015. According to the World Health Organization (WHO), the new cancer cases are anticipated to rise by as much as 15 million per year by 2020 unless actions that are more preventive.² Although, chemotherapy is the key remedy for cancer treatment, but the use of existing chemotherapeutics is often limited due to existing of limited anticancer drugs and detrimental side effects.³ It is thus momentous to identify new targets and agents for the cure of cancer. Thus, a substantial research for innovative anticancer agents has been fueled by many academics and industries to unveil novel targets and mechanisms based on the lead candidates of various classes of compounds.⁴

Cyclin-dependent kinases (CDKs) are a group of serine/threonine kinase comprising more than 20 members that are associated with regulation of cell-cycle progression by phosphorylating proteins involved in cell division. Controlling subunits of these enzymes play a key role in regulatory cell cycle, cell division and transcription mechanism in both eukaryotes and prokaryotes.⁵ From historic point of view, the first CDK2 inhibitor to be known as 6-dimethylaminopurine (IC_{50} : 120 μ M).^{6,7} From the existing CDK2 inhibitors only few molecules are in different levels of clinical trials. The molecules AT7519, R547 and SNS-032 have reached to phase-I; flavopiridol, roscovitine, P-276-00 and CSH727965 have touched phase-II, while PHA-793887 and AG-024322 have been dismissed in phase-I clinical trials for either the insufficiency of perspicacity from other treatment modalities⁸ or the causing of simple hepatic toxicity.⁹ **Fig. 1** represents the structures of CDK inhibitors under clinical trials. To support these findings, a study proved that both phosphatidylinositol-3-kinase and CDK2 inhibitors together induced apoptosis in malignant glioma xenografts via a synthetic-lethal interaction.¹⁰ Further, CDK2 inhibitors also evidenced as therapeutic target in neuroblastoma¹¹ BRCA-deficient cancers¹² and ovarian cancer.¹³

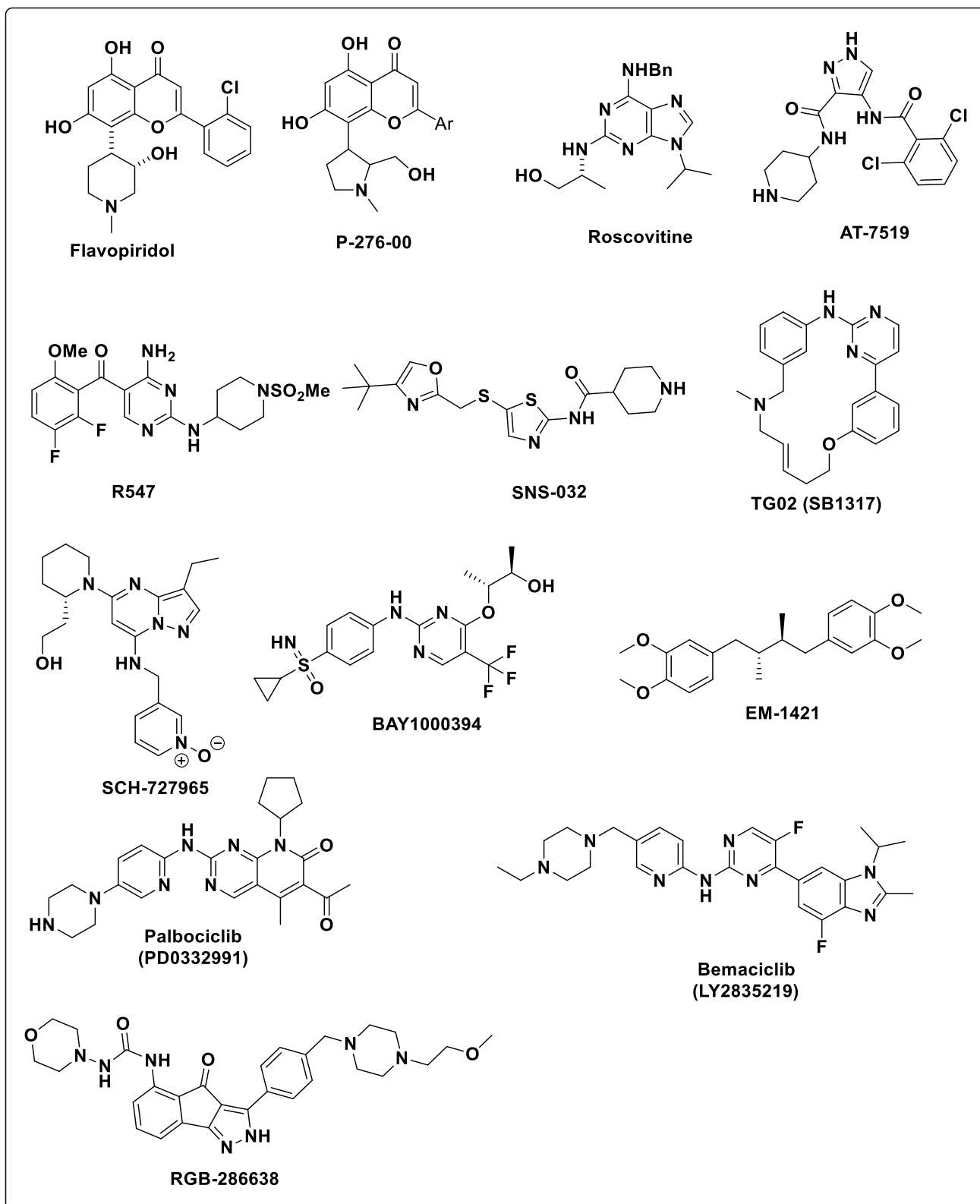


Fig. 1. Structures of the CDK2 inhibitors in clinical trials.

In the past few years, significant amount of contemporary investigations have been conducted on aza-heterocycles for producing wide range of chemical libraries/drug-like candidates. Among all,

pyrazolopyrimidine is one such important drug-like nucleus synthesized by fusion of pyrazole with pyrimidine.¹⁴ Several isomeric forms of pyrazolo pyrimidine namely pyrazolo[3,4-*d*]pyrimidines, pyrazolo[5,1-*b*]pyrimidines, pyrazolo[5,1-*a*]pyrimidines, pyrazolo[1,5-*c*]pyrimidines, pyrazolo[4,3-*d*]pyrimidines are known.¹⁵ From the existing isomers, pyrazolo[3,4-*d*]pyrimidine is an bioisostere of purines with many pharmacological applications as Src/Abl kinase,¹⁶ glycogen synthase kinase (GSK),¹⁷ mammalian target of rapamycin (mTOR),¹⁸ xanthine oxidase inhibitors,¹⁹ tyrosine kinase²⁰ and cyclin dependent kinase (CDK).²¹ Many pyrazolo[3,4-*d*]pyrimidine derivatives bearing different substitutions on nucleus are stated for diverse cancer targets as illustrated in **Fig. 2**.²²⁻²⁷

Inspired by the important findings of pyrazolo[3,4-*d*]pyrimidines as anticancer agents and in continuation of our research work involving the identification of novel anticancer analogues,^{28,29} in the current study a novel series of pyrazolo[3,4-*d*]pyrimidine derivatives have been synthesized and evaluated for *in vitro* anticancer activity towards CDK2, Abl kinase inhibitors and K-562, MCF-7 cell lines. In this work we carried out chemical modifications at C-6 of the pyrazolo[3,4-*d*]pyrimidine nucleus (**scheme-1**) by efficient synthetic method.

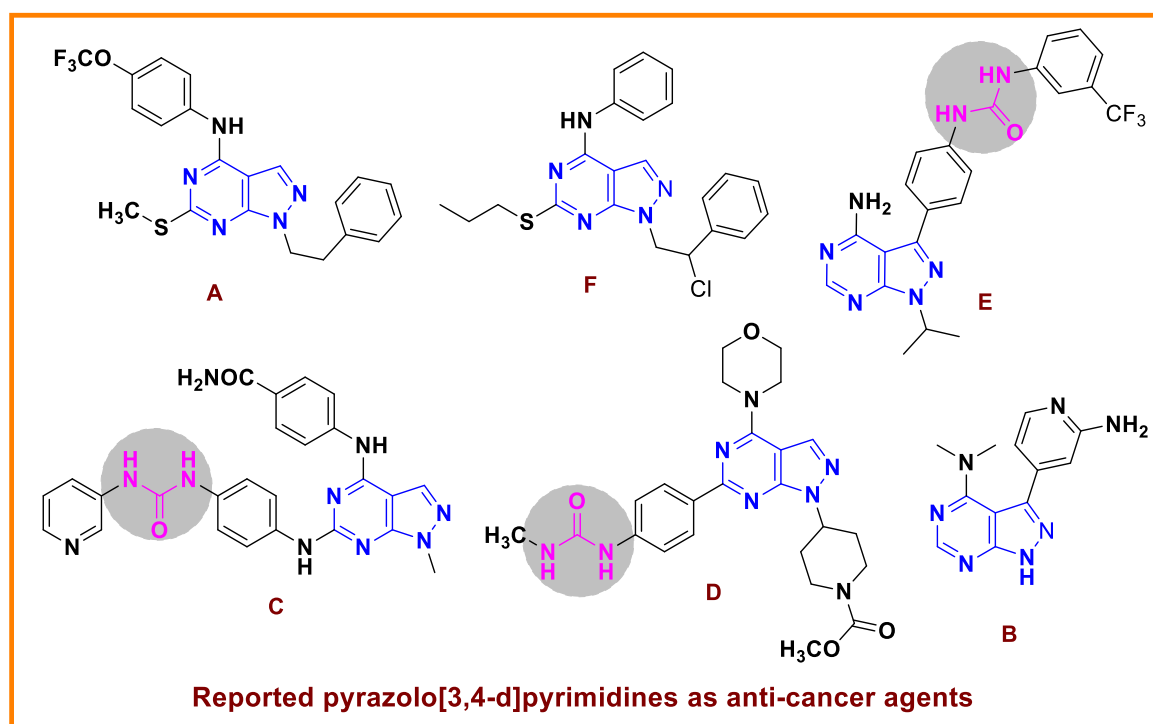
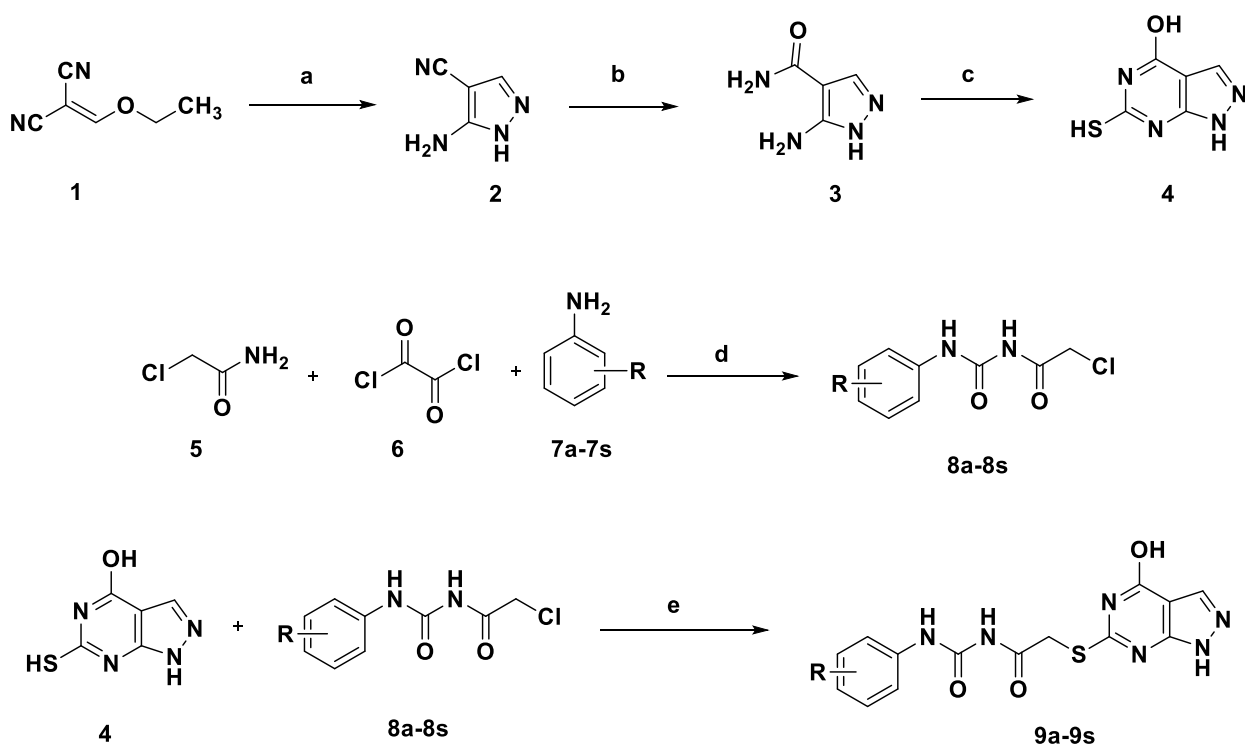


Fig. 2. Known derivatives of pyrazolo[3,4-*d*]pyrimidine analogues and their anticancer activities. **A:** (K_{i50} against Src, AblT315I = 0.056, 0.01 μ M);²² **B:** (IC_{50} against CDK9 = 17 nM);²³ **C:** (IC_{50} against mTOR = 13 nM);²⁴ **D:** (IC_{50} against mTOR = 9 nM);²⁵ **E:** (K_{i50} against cSrc, Abl = 25, 41 nM);²⁶ **F:** (IC_{50} against Src = 1.2 \pm 0.4 μ M).²⁷

2 Results and discussion

2.1 Chemistry

6-mercapto-1*H*-pyrazolo[3,4-*d*]pyrimidin-4-ol (**4**), as a key intermediate for the synthesis of desired hybrid molecules was accomplished from 2-(ethoxymethylene)malononitrile (**1**) by the sequence of reactions shown in **Fig. 1**. The synthesis was performed in a process that the five membered pyrazole ring was first accomplished and the pyrimidine ring formation was followed. In pyrazolopyrimidine scaffold, the hydroxy group as nucleophilic substituent was introduced at C-4 and the methylmercapto group was employed at C-6 as a precursor to perform the nucleophilic substitution with different phenylcarbamoyl acetamides.



Scheme 1. Synthesis of 4-substituted pyrazolo[3,4-*d*]pyrimidine hybrid molecules.

Reagents and conditions: (a) hydrazine hydrate, ethanol, 80⁰ C, 3h, 92%; (b) Conc. H₂SO₄, NH₄OH, H₂O, 50⁰ C, 5h, 90%; (c) potassium ethyl xanthogenate, DMF, 120⁰ C, 6h, 82%; (d) 1,2-dichloroethane, 90⁰ C, 6h, 90%; (e) 1M KOH, acetone, 60⁰ C, 2-3h, 80-96%.

Nucleophilic substitution of commercially available 2-(ethoxymethylene) malononitrile (**1**) with hydrazine hydrate in ethanol under reflux conditions afforded 5-amino-1*H*-pyrazole-4-carbonitrile (**2**) which underwent partial hydrolysis of nitrile group with 98% sulfuric acid to attain 5-amino-1*H*-pyrazole-4-carboxamide (**3**) in excellent yield (90%). Subsequent fusion of carboxamide (**2**) with potassium ethyl xanthogenate in *N,N*-dimethylformamide accomplished the cyclic product 6-mercapto-1*H*-pyrazolo[3,4-*d*]pyrimidin-4-ol (**4**) in good yield (82%).³⁰ Further, various substituted

phenylcarbamoyl acetamides (**8a-8s**) were prepared by allowing the reaction of 2-chloroacetamide (**5**) and oxalyl chloride (**6**) with different amines (**7a-7s**) in anhydrous 1,2-dichloroethane under reflux conditions as reported in literature.³¹ The nucleophilic substitution of compound **4** at C-6 with substituted phenylcarbamoyl acetamides (**8a-8s**) was carried out in presence of 1M KOH solution under heat conditions to attain the desired final products (**9a-9s**) as presented in **scheme 1**. The anticipated structures of newly prepared final compounds were in agreement with physicochemical and spectral (IR, ¹H NMR and ¹³C NMR) data attained and were further sub-stantiated by HR-MS information, which is precised in supporting information.

The ¹H NMR of compound **4** exhibited the presence of a very distinct singlet signals resonating at around δ 13.61, 13.03, 11.86 and 8.42 ppm attributed for N-H proton, S-H proton, O-H proton and C-3 Ar-H protons respectively, indicating its formation of bicyclic system (pyrazolopyrimidine) by a process of simple condensation reaction by ring annulation of 5-amino-1*H*-pyrazole-4-carboxamide with potassium ethyl xanthogenate. Further, from ¹H NMR of compounds **9a-9s**, we observed most informative singlet signals at around δ 13.57-13.07, 12.51-12.16, 8.00-7.94 ppm accounted for three -NH protons, while the characteristic singlet signal appearing at δ 4.28-4.20 ppm attributing to methylene group (-S-CH₂-NH-NH-). Thus confirmed the alkylation of mercapto group (-SH-) with substituted phenylcarbamoyl acetamides (**8a-8s**) to achieve the desired final products (**9a-9s**) as represented in **scheme 1**.

Further, from the IR spectra of the title compounds (**9a-9s**) we observed a reasonably sturdy and characteristic bands around 2904.93-3290.96cm⁻¹, 1232.49-1292.89cm⁻¹ accounting for N-H and C-S groups respectively, while most characteristic band of -C=O appearing around 1667.34-1715.29 cm⁻¹ indicated the formation of final hybrid molecules. Further, the ¹H NMR spectrum of the final compounds displayed some characteristic singlet signals at around δ 12.36-12.17 ppm for ring N-H, δ 13.57-13.07, 8.00-7.94 ppm for two exocyclic -NH protons (-NH-CO-NH-Ph), while the hydroxyl proton (-OH) on aromatic ring resonated as singlet signal around at δ 11.47-10.65 ppm. Further, the most informative singlet signals resonated around δ 10.78-8.96 ppm (C-3 aromatic proton), δ 4.28-4.20 ppm for methylene protons of carbamoyl acetamide chain (-S-CH₂-NH-CO-NH-). Further, various signals appeared as doublet or multiplets at around δ 8.61-6.87 ppm accounted for other aromatic protons. The ¹³C NMR spectra further confirmed the structures of the title compounds. The characteristic carbon signals resonated at around δ 173.28-161.87, 158.87-158.19 and 131.96-130.19 ppm were assigned to C-6, C-4 and C-3 carbons of pyrazolopyrimidine ring. Further, other aromatic/heteroaromatic carbons resonated between δ 159.78-107.87 ppm while, the prominent carbon peaks observed at around δ 34.43-34.29 ppm for methylene (-S-CH₂-NH-CO-NH-), δ 55.76 ppm for methoxy (-OCH₃) and δ 20.03-17.05 ppm for methyl groups respectively. In addition, the formation of

the final pyrazolo[3,4-*d*]pyrimidine derivatives (**9a-9s**) was confirmed by calculating their individual mass spectrums (HR-MS), which displayed accurate molecular ion peaks that were in agreement with their expected molecular weights (supporting information).

2.2 *In vitro* evaluation for anti-cancer (CDK2 & Abl) and anti-proliferative (K-562 & MCF-7) activity

All the final compounds were evaluated for CDK2/cyclin E kinase inhibition and the IC₅₀ values of various *in vitro* anticancer profiles are summarized in **Table 1**. Abl kinase inhibition was evaluated as a counter screen, to get a preliminary information about selectivity. In addition, to explore the biological significance, these compounds were further evaluated for their *in vitro* anti-proliferative activity against K-562 (chronic myelogenous leukemia) and MCF-7 (breast adenocarcinoma) cell lines. We studied the effect of various substitutions on phenyl ring of the phenylcarbamoyl acetamide moiety at C-6, which was in turn connected to pyrazolopyrimidine nucleus through a sulphur bridge. From the obtained results, it was observed that for all the synthesized molecules from this series, IC₅₀ values could not be measured due to solubility limit (IC₅₀ >12.5 μM or >25 μM).

C. No	R	IC ₅₀ (μM)			
		CDK2	Abl	K-562	MCF-7
9a	2,4-CH ₃	>12.5	>12.5	>25	>25
9b	2-Cl	>25	>25	>25	>25
9c	3-Cl	>12.5	>12.5	>25	>25
9d	4-Cl	>25	>25	>25	>25
9e	2-Br	>25	>25	>25	>25
9f	3-Br	>25	>25	>12.5	>12.5
9g	4-Br	>12.5	>12.5	>100	>100
9h	2-NO ₂	>25	>25	>25	>25
9i	3-NO ₂	>25	>25	>25	>25
9j	4-NO ₂	>50	>50	>100	>100

9k	4-Cl-3-NO ₂	>25	>25	>50	>50
9l	4-Br-3-CF ₃	>25	>25	>50	>50
9m	4-SCH ₃	>12.5	>12.5	>12.5	>12.5
9n	4-F-2-CH ₃	>25	>25	>12.5	>12.5
9o	2-Cl-4-F	>25	>25	>50	>50
9p	4-OCH ₃ -2-NO ₂	>12.5	>12.5	>50	>50
9q	2-Cl-5-NO ₂	>25	>25	>25	>25
9r	H	>25	>25	>50	>50
9s	N	>25	>25	49.9	>50
	Roscovitine	0.1	>100	42	11
	Imatinib	>100	0.2	0.5	>10

^a IC₅₀ values were determined in triplicate in the range of 0.05 to 100 μM. IC₅₀ value indicates concentration (μM) that inhibits activity of tested enzyme to 50% or for cytotoxic assays, concentration (μM) that reduces 50% of cells during a three-day cultivation

Table 1. Anticancer evaluation of novel mono substituted pyrazolo[3,4-*d*]pyrimidines against CDK2/Abl kinases and K-562/MCF-7 cell lines.

3 Conclusion

In summary, a series of new mono substituted pyrazolo[3,4-*d*]pyrimidines with substituted phenylcarbamoyl acetamide side chain at C-4 position has been designed and synthesized. The key intermediate 6-mercapto-1*H*-pyrazolo[3,4-*d*]pyrimidin-4-ol allowed us to increase our library of compounds. All synthesized compounds were evaluated for *in vitro* enzymatic activity against CDK2/cyclin E, Abl kinases as well as anti-proliferative activity against K-562 (chronic myelogenous leukemia) and MCF-7 (breast adenocarcinoma) cell lines. From the obtained results, it was observed that for all the synthesized molecules from this series, IC₅₀ values could not be measured due to solubility limit (IC₅₀ >12.5 μM or >25 μM). This research outcome promotes the advantage of interaction of phenylcarbamoyl acetamides to pyrazolopyrimidine scaffold through sulphur linkage, thus

offers an idea for further compound optimization and functionalization to enhance the solubility and anticancer activity, which deserves further investigation.

4 Experimental Section

All the chemicals used in this research work were purchased from Sigma-Aldrich and Merck Millipore, South Africa. All the solvents, except those of laboratory-reagent grade, were dried and purified when necessary according to previously published methods. The progress of the reactions and the purity of the compounds were monitored by thin-layer chromatography (TLC) on pre-coated silica gel plates procured from E. Merck and Co. (Darmstadt, Germany) using 36% ethyl acetate in n-hexane as the mobile phase and iodine vapor as the visualizing agent. The melting points of the synthesized compounds were determined using a Thermo Fisher Scientific (IA9000, UK) digital melting point apparatus and are uncorrected. The IR spectra were recorded on a Bruker Alpha FT-IR spectrometer (Billerica, MA, USA) using the ATR technique. The ¹H NMR and ¹³C NMR spectra were recorded on a Bruker AVANCE 600 and 600 MHz (Bruker, Rheinstetten/Karlsruhe, Germany) spectrometers using CDCl₃ and DMSO-*d*₆. The chemical shifts are reported in δ ppm units with respect to TMS as an internal standard. HRMS spectra were recorded on an Autospec mass spectrometer with electron impact at 70 eV.

4.1 General procedure for the synthesis of compounds (9a-9s)

To a well-stirred solution of compound **4** (0.5g, 0.00298mol) in 1M KOH solution, added equimolar amount of a solution of compounds **8s-8s** in acetone (10mL) was added. The reaction mixture was stirred for 1h at room temperature then heated at 50 °C for 2h. Upon completion, the precipitated product was filtered off to afford the crude product. The crude product was recrystallized from THF to yield the appropriate pure product.

4.1.1 *N*-((2,4-dimethylphenyl)carbamoyl)-2-((4-hydroxy-1H-pyrazolo[3,4-d]pyrimidin-6-yl)thio)acetamide (9a)

Brown solid; yield: 84 %; mp 212-214°C; FTIR (ATR, cm⁻¹) ν_{\max} : 3487.05, 3101.10, 2930.55, 1687.76, 1585.78, 1521.91, 1444.10, 1244.37, 1155.79, 966.32, 840.46, 748.54, 676.59, 553.68; ¹H-NMR (600 MHz, DMSO-*d*₆): δ 13.46 (s, 1H, NH), 12.27 (s, 1H, NH), 10.80 (s, 1H, OH), 9.99 (s, 1H, ArH), 7.99 (s, 1H, NH), 7.72 (d, *J* = 8.22 Hz, 1H, ArH), 7.02 (s, 1H, ArH), 6.97 (d, *J* = 8.28 Hz, 1H, ArH), 4.24 (s, 2H, CH₂), 2.23 (s, 3H, CH₃), 2.16 (s, 3H, CH₃); ¹³C NMR (100 MHz, DMSO-*d*₆): δ 169.85 (C=O), 150.20, 133.00, 132.87, 130.52, 127.72, 126.48, 121.22, 34.37 (CH₂), 20.03 (CH₃), 17.05 (CH₃) ppm.

4.1.2 *N*-((2-chlorophenyl)carbamoyl)-2-((4-hydroxy-1H-pyrazolo[3,4-d]pyrimidin-6-yl)thio)acetamide (9b)

White solid; yield: 90%; mp 216-218°C; FTIR (ATR, cm⁻¹) ν_{\max} : 3487.05, 3101.10, 2952.37, 1687.76, 1585.78, 1521.91, 1444.10, 1296.62, 1244.37, 1155.79, 966.32, 863.26, 748.54, 676.59; ¹H-NMR (600 MHz, DMSO-*d*₆): δ 13.41 (s, 1H, NH), 12.20 (s, 1H, NH), 10.95 (s, 1H, OH), 10.65 (s, 1H, ArH), 8.21 (dd, *J* = 8.28, 1.32 Hz, 1H, ArH), 7.96 (s, 1H, NH), 7.47 (dd, *J* = 8.22, 1.32 Hz, 1H, ArH), 7.34-7.31 (m, *J* = 4.27 Hz, 1H, ArH), 7.12-7.10 (m, *J* = 3.43 Hz, 1H, ArH), 4.25 (s, 2H, CH₂); ¹³C NMR (100 MHz, DMSO-*d*₆): δ 169.92 (C=O), 149.99, 134.30, 128.91, 127.39, 124.46, 122.43, 121.43, 34.35 (CH₂) ppm.

4.1.3 *N*-((3-chlorophenyl)carbamoyl)-2-((4-hydroxy-1H-pyrazolo[3,4-d]pyrimidin-6-yl)thio)acetamide (9c)

White solid; yield: 87 %; mp 211-213°C; FTIR (ATR, cm⁻¹) ν_{\max} : 3290.67, 3055.43, 2976.09, 1672.71, 1487.68, 14783.48, 1245.54, 1148.70, 966.87, 772.62, 657.05, 532.95; ¹H-NMR (600 MHz, DMSO-*d*₆): δ 13.41 (s, 1H, NH), 12.16 (s, 1H, NH), 10.75 (s, 1H, OH), 10.19 (s, 1H, ArH), 8.00 (s, 1H, NH), 7.72 (s, 1H, ArH), 7.37 (d, *J* = 7.74 Hz, 1H, ArH), 7.32 (t, *J* = 8.01 Hz, 1H, ArH), 7.11 (d, *J* = 8.52 Hz, 1H, ArH), 4.25 (s, 2H, CH₂); ¹³C NMR (100 MHz, DMSO-*d*₆): δ 169.51 (C=O), 150.08, 138.78, 133.00, 123.14, 119.14, 118.05, 34.40 (CH₂) ppm.

4.1.4 *N*-((4-chlorophenyl)carbamoyl)-2-((4-hydroxy-1H-pyrazolo[3,4-d]pyrimidin-6-yl)thio)acetamide (9d)

White solid; yield: 85%; mp 244-246°C; FTIR (ATR, cm⁻¹) ν_{\max} : 3242.17, 3137.95, 2975.08, 1704.19, 1675.55, 1599.49, 1556.21, 1493.47, 1231.28, 1152.00, 949.78, 776.09, 708.23, 509.89; ¹H-NMR (600 MHz, DMSO-*d*₆): δ 13.57 (s, 1H, NH), 12.48 (s, 1H, NH), 11.00 (s, 1H, OH), 10.29 (s, 1H, ArH), 7.95 (s, 1H, NH), 7.56 (d, *J* = 8.88 Hz, 2H, ArH), 7.36 (d, *J* = 8.88 Hz, 2H, ArH), 4.23 (s, 2H, CH₂); ¹³C NMR (100 MHz, DMSO-*d*₆): δ 169.43 (C=O), 157.57, 150.04, 136.24, 128.35, 128.26, 127.23, 121.90, 121.15, 102.74, 34.39 (CH₂) ppm.

4.1.5 *N*-((2-bromophenyl)carbamoyl)-2-((4-hydroxy-1H-pyrazolo[3,4-d]pyrimidin-6-yl)thio)acetamide (9e)

Brown solid; yield: 84%; mp 240-242°C; FTIR (ATR, cm⁻¹) ν_{\max} : 3488.26, 3117.93, 2916.20, 1692.18, 1580.58, 1511.78, 1295.08, 1228.77, 1156.20, 966.88, 739.17, 616.56, 546.38; ¹H-NMR (600 MHz, DMSO-*d*₆): δ 13.07 (s, 1H, NH), 11.67 (s, 1H, OH), 10.78 (s, 1H, ArH), 8.19 (dd, *J* = 8.28, 1.28 Hz,

1H, ArH), 7.83 (s, 1H, NH), 7.64 (dd, $J = 8.00, 1.12$ Hz, 1H, ArH), 7.39-7.35 (m, $J = 4.21$ Hz, 1H, ArH), 7.06-7.02 (m, $J = 3.35$ Hz, 1H, ArH), 4.05 (s, 2H, $\underline{\text{CH}_2}$); ^{13}C NMR (100 MHz, DMSO- d_6): δ 150.09, 135.69, 132.15, 131.69, 127.85, 127.82, 124.91, 122.01, 117.20, 115.25, 113.07, 107.33, 34.36 ($\underline{\text{CH}_2}$) ppm.

4.1.6 *N*-((3-bromophenyl)carbamoyl)-2-((4-hydroxy-1H-pyrazolo[3,4-d]pyrimidin-6-yl)thio)acetamide (9f)

White solid; yield: 87 %; mp 226-228°C; FTIR (ATR, cm $^{-1}$) ν_{max} : 3251.64, 2874.39, 2824.05, 1686.84, 1595.07, 1551.77, 1491.77, 1259.54, 1218.24, 1158.08, 769.81, 534.27; ^1H -NMR (600 MHz, DMSO- d_6): δ 13.41 (s, 1H, NH), 12.18 (s, 1H, NH), 10.74 (s, 1H, OH), 10.18 (s, 1H, ArH), 8.01 (s, 1H, NH), 7.87 (s, 1H, ArH), 7.41 (m, $J = 2.19$ Hz, 1H, ArH), 7.26 (t, $J = 2.91$ Hz, 2H, ArH), 4.25 (s, 2H, $\underline{\text{CH}_2}$); ^{13}C NMR (100 MHz, DMSO- d_6): δ 169.48 (C=O), 150.05, 138.89, 130.34, 126.4, 121.97, 121.28, 118.44, 34.38 ($\underline{\text{CH}_2}$) ppm.

4.1.7 *N*-((4-bromophenyl)carbamoyl)-2-((4-hydroxy-1H-pyrazolo[3,4-d]pyrimidin-6-yl)thio)acetamide (9g)

Brown solid; yield: 81%; mp 232-234°C; FTIR (ATR, cm $^{-1}$) ν_{max} : 3236.82, 3133.87, 2922.02, 1702.62, 1672.40, 1547.00, 1489.02, 1392.06, 1311.37, 1227.97, 1118.73, 775.66, 665.01, 506.53; ^1H -NMR (600 MHz, DMSO- d_6): δ 13.41 (s, 1H, NH), 12.19 (s, 1H, NH), 10.72 (s, 1H, OH), 10.15 (s, 1H, ArH), 7.98 (s, 1H, NH), 7.48 (s, 4H, ArH), 4.25 (s, 2H, $\underline{\text{CH}_2}$); ^{13}C NMR (100 MHz, DMSO- d_6): δ 169.44 (C=O), 150.01, 136.67, 131.28, 121.52, 115.13, 34.38 ($\underline{\text{CH}_2}$) ppm.

4.1.8 2-((4-hydroxy-1H-pyrazolo[3,4-d]pyrimidin-6-yl)thio)-*N*-((2-nitrophenyl)carbamoyl)acetamide (9h)

White solid; yield: 82%; mp 227-229°C; FTIR (ATR, cm $^{-1}$) ν_{max} : 3216.47, 2872.46, 1680.99, 1581.77, 1483.18, 1436.94, 1339.98, 1243.75, 1157.59, 857.52, 743.68, 529.26; ^1H -NMR (600 MHz, DMSO- d_6): δ 13.42 (s, 1H, NH), 12.17 (s, 1H, NH), 11.59 (s, 1H, OH), 11.01 (s, 1H, ArH), 8.39 (d, $J = 8.22$ Hz, 1H, ArH), 8.10 (dd, $J = 8.25, 1.05$ Hz, 1H, ArH), 8.03 (s, 1H, NH), 7.74-7.72 (m, $J = 4.26$ Hz, 1H, ArH), 7.32-7.30 (m, $J = 4.19$ Hz, 1H, ArH), 4.25 (s, 2H, $\underline{\text{CH}_2}$); ^{13}C NMR (100 MHz, DMSO- d_6): δ 169.33 (C=O), 15138.55, 134.52, 132.41, 129.77, 125.00, 123.67, 123.17, 117.85, 34.36 ($\underline{\text{CH}_2}$) ppm.

4.1.9 2-((4-hydroxy-1H-pyrazolo[3,4-d]pyrimidin-6-yl)thio)-*N*-((3-nitrophenyl)carbamoyl)acetamide (9i)

Brown solid; yield: 90%; mp 210-212°C; FTIR (ATR, cm⁻¹) ν_{\max} : 3514.66, 3244.67, 3128.20, 2885.63, 1694.75, 1659.36, 1598.09, 1524.26, 1346.53, 1234.93, 1156.82, 735.81, 671.97; ¹H-NMR (600 MHz, DMSO-*d*₆): δ 13.42 (s, 1H, NH), 12.19 (s, 1H, NH), 10.84 (s, 1H, OH), 10.41 (s, 1H, ArH), 8.56 (s, 1H, ArH), 7.99 (s, 1H, NH), 7.91 (dd, *J* = 8.25, 1.95 Hz, 1H, ArH), 7.82 (d, *J* = 8.28 Hz, 1H, ArH), 7.58 (t, *J* = 8.19 Hz, 1H, ArH), 4.27 (s, 2H, CH₂); ¹³C NMR (100 MHz, DMSO-*d*₆): δ 169.50 (C=O), 150.29, 147.97, 138.61, 129.78, 125.73, 117.86, 113.82, 34.43 (CH₂) ppm.

4.2.0 2-((4-hydroxy-1H-pyrazolo[3,4-d]pyrimidin-6-yl)thio)-N-((4-nitrophenyl) carbamoyl acetamide (9j)

White solid; yield: 95%; mp 232-234°C; FTIR (ATR, cm⁻¹) ν_{\max} : 3226.58, 2874.63, 1685.85, 1595.53, 1487.60, 1336.76, 1244.88, 1215.59, 1161.94, 1111.08, 853.82, 770.56, 715.98, 534.24; ¹H-NMR (600 MHz, DMSO-*d*₆): δ 13.41 (s, 1H, NH), 12.17 (s, 1H, NH), 10.90 (s, 1H, OH), 10.53 (s, 1H, ArH), 8.18 (d, *J* = 9.06 Hz, 2H, ArH), 7.98 (s, 1H, NH), 7.78 (d, *J* = 9.12 Hz, 2H, ArH), 4.27 (s, 2H, CH₂); ¹³C NMR (100 MHz, DMSO-*d*₆): δ 169.64 (C=O), 150.01, 143.58, 142.59, 124.44, 124.24, 120.38, 119.27, 34.47 (CH₂) ppm.

4.2.1 N-((4-chloro-3-nitrophenyl)carbamoyl)-2-((4-hydroxy-1H-pyrazolo[3,4-d] pyrimidin-6-yl)thio)acetamide (9k)

Brown solid; yield: 92%; mp 214-216°C; FTIR (ATR, cm⁻¹) ν_{\max} : 3523.06, 3231.76, 2920.69, 1693.28, 1656.76, 1595.61, 1527.54, 1303.35, 1246.28, 1155.31, 969.66, 824.35, 764.03, 699.69; ¹H-NMR (600 MHz, DMSO-*d*₆): δ 13.41 (s, 1H, NH), 12.20 (s, 1H, NH), 10.90 (s, 1H, OH), 10.42 (s, 1H, ArH), 8.35 (d, *J* = 2.46 Hz, 1H, ArH), 7.96 (s, 1H, NH), 7.79 (dd, *J* = 8.79, 2.37 Hz, 1H, ArH), 7.67 (d, *J* = 8.88 Hz, 1H, ArH), 4.26 (s, 2H, CH₂); ¹³C NMR (100 MHz, DMSO-*d*₆): δ 169.39 (C=O), 150.20, 147.22, 137.44, 131.68, 131.46, 125.22, 124.53, 118.56, 115.90, 34.37 (CH₂) ppm.

4.2.2 N-((4-bromo-3-(trifluoromethyl)phenyl)carbamoyl)-2-((4-hydroxy-1H-pyrazolo [3,4-d]pyrimidin-6-yl)thio)acetamide (9l)

Brown solid; yield: 83%; mp 225-227°C; FTIR (ATR, cm⁻¹) ν_{\max} : 3488.74, 3100.86, 2930.06, 1691.15, 1597.49, 1521.09, 1419.88, 1305.27, 1227.40, 1134.94, 827.90, 775.05, 730.96; ¹H-NMR (600 MHz, DMSO-*d*₆): δ 13.39 (s, 1H, NH), 12.16 (s, 1H, NH), 10.81 (s, 1H, OH), 10.34 (s, 1H, ArH), 8.11 (d, *J* = 2.58 Hz, 1H, ArH), 7.96 (s, 1H, NH), 7.78 (d, *J* = 8.70 Hz, 1H, ArH), 7.70 (dd, 8.73, 2.55 Hz, 1H, ArH), 4.26 (s, 2H, CH₂); ¹³C NMR (100 MHz, DMSO-*d*₆): δ 169.36 (C=O), 150.18, 137.39, 135.06, 128.56, 128.36, 124.67, 123.30, 121.49, 118.89, 118.85, 111.71, 34.35 (CH₂) ppm.

4.2.3 2-((4-hydroxy-1H-pyrazolo[3,4-d]pyrimidin-6-yl)thio)-N-((4-(methylthio)phenyl)carbamoyl)acetamide (9m)

Yellow solid; yield: 88%; mp 236-238°C; FTIR (ATR, cm⁻¹) ν_{\max} : 3251.97, 3152.40, 2916.97, 1673.16, 1578.09, 1541.67, 1492.36, 1313.17, 1222.84, 1152.68, 966.09, 801.32, 687.63, 665.54, 507.81; ¹H-NMR (600 MHz, DMSO-*d*₆): δ 13.41 (s, 1H, NH), 12.21 (s, 1H, NH), 10.66 (s, 1H, OH), 10.08 (s, 1H, ArH), 7.94 (s, 1H, NH), 7.46 (d, *J* = 8.76 Hz, 2H, ArH), 7.24 (d, *J* = 8.52 Hz, 2H, ArH), 4.24 (s, 2H, CH₂), 2.44 (s, 3H, CH₃); ¹³C NMR (100 MHz, DMSO-*d*₆): δ 169.39 (C=O), 149.96, 134.83, 132.29, 127.34, 120.24, 34.34 (CH₂), 15.49 (CH₃) ppm.

4.2.4 N-((4-fluoro-2-methylphenyl)carbamoyl)-2-((4-hydroxy-1H-pyrazolo[3,4-d]pyrimidin-6-yl)thio)acetamide (9n)

Yellow solid; yield: 81%; mp 237-239°C; FTIR (ATR, cm⁻¹) ν_{\max} : 3230.66, 2822.22, 1684.11, 1598.02, 1554.55, 1491.53, 1267.43, 1162.90, 1267.43, 1162.90, 867.32, 772.26, 675.14, 536.08; ¹H-NMR (600 MHz, DMSO-*d*₆): δ 13.42 (s, 1H, NH), 12.24 (s, 1H, NH), 10.77 (s, 1H, OH), 9.97 (s, 1H, ArH), 7.93 (s, 1H, NH), 7.80 (q, *J* = 4.82 Hz, 1H, ArH), 7.06 (dd, *J* = 9.48, 2.94 Hz, 1H, ArH), 7.00-6.97 (m, *J* = 4.06 Hz, 1H, ArH), 4.25 (s, 2H, CH₂), 2.21 (s, 3H, CH₃); ¹³C NMR (100 MHz, DMSO-*d*₆): δ 169.79 (C=O), 159.17, 157.57, 150.26, 131.77, 131.11, 131.06, 123.26, 116.30, 112.15, 34.31 (CH₂), 16.98 (CH₃) ppm.

4.2.5 N-((2-chloro-4-fluorophenyl)carbamoyl)-2-((4-hydroxy-1H-pyrazolo[3,4-d]pyrimidin-6-yl)thio)acetamide (9o)

White solid; yield: 92%; mp 236-238°C; FTIR (ATR, cm⁻¹) ν_{\max} : 3231.76, 2871.85, 1681.96, 1595.75, 1545.77, 1483.91, 1383.91, 1246.39, 1158.54, 1050.89, 862.59, 770.91, 697.93; ¹H-NMR (600 MHz, DMSO-*d*₆): δ 13.40 (s, 1H, NH), 12.25 (s, 1H, NH), 10.97 (s, 1H, OH), 10.56 (s, 1H, ArH), 8.18 (q, *J* = 5.00 Hz, 1H, ArH), 7.93 (s, 1H, NH), 7.44 (dd, *J* = 8.34, 2.94 Hz, 1H, ArH), 7.23-7.19 (m, *J* = 4.06 Hz, 1H, ArH), 4.25 (s, 2H, CH₂); ¹³C NMR (100 MHz, DMSO-*d*₆): δ 169.86 (C=O), 158.34, 156.71, 150.06, 131.01, 130.99, 123.56, 122.96, 116.10, 115.92, 114.31, 114.17, 34.29 (CH₂) ppm.

4.2.6 2-((4-hydroxy-1H-pyrazolo[3,4-d]pyrimidin-6-yl)thio)-N-((4-methoxy-2-nitrophenyl)carbamoyl)acetamide (9p)

Yellow solid; yield: 96%; mp 213-215°C; FTIR (ATR, cm⁻¹) ν_{\max} : 3433.23, 3132.91, 2945.11, 1693.03, 1506.83, 1441.97, 1267.52, 1150.08, 1035.73, 831.13, 774.25, 527.88; ¹H-NMR (600 MHz, DMSO-*d*₆): δ 13.57 (s, 1H, NH), 12.51 (s, 1H, NH), 11.47 (s, 1H, OH), 11.18 (s, 1H, ArH), 8.24 (d, *J* = 9.20

Hz, 1H, ArH), 7.94 (s, 1H, NH), 7.58 (d, $J = 3.00$ Hz, 1H, ArH), 7.36 (dd, $J = 9.28, 3.00$ Hz, 1H, ArH), 4.22 (s, 2H, CH₂), 3.82 (s, 3H, CH₃); ¹³C NMR (100 MHz, DMSO-*d*₆): δ 169.27 (C=O), 154.97, 150.28, 139.68, 125.21, 121.27, 108.86, 55.76 (CH₃), 34.34 (CH₂) ppm.

4.2.7 *N*-((2-chloro-5-nitrophenyl)carbamoyl)-2-((4-hydroxy-1H-pyrazolo[3,4-*d*]pyrimidin-6-yl)thio)acetamide (9q)

Brown solid; yield: 81%; mp 214-216°C; FTIR (ATR, cm⁻¹) ν_{\max} : 3251.94, 3129.53, 2962.12, 1691.89, 1659.73, 1565.17, 1344.81, 1227.89, 1150.27, 1060.79, 830.04, 738.55; ¹H-NMR (600 MHz, DMSO-*d*₆): δ 13.39 (s, 1H, NH), 12.18 (s, 1H, NH), 11.23 (s, 1H, OH), 11.01 (s, 1H, ArH), 9.13 (d, $J = 2.52$ Hz, 1H, ArH), 8.00 (s, 1H, NH), 7.94 (m, $J = 3.84$ Hz, 1H, ArH), 7.79 (d, $J = 8.88$ Hz, 1H, ArH), 4.28 (s, 2H, CH₂); ¹³C NMR (100 MHz, DMSO-*d*₆): δ 170.30, 150.11, 146.44, 135.41, 130.01, 128.47, 118.54, 115.01, 34.34 (CH₂) ppm.

4.2.8 2-((4-hydroxy-1H-pyrazolo[3,4-*d*]pyrimidin-6-yl)thio)-*N*-(phenylcarbamoyl) acetamide (9r)

Brown solid; yield: 80%; mp 222-224°C; FTIR (ATR, cm⁻¹) ν_{\max} : 3244.88, 3140.28, 2976.12, 1700.27, 1672.42, 1548.77, 1490.83, 1449.90, 1223.68, 1152.02, 948.72, 857.35, 760.69, 700.47, 532.97; ¹H-NMR (600 MHz, DMSO-*d*₆): δ 13.41 (s, 1H, NH), 12.19 (s, 1H, NH), 10.65 (s, 1H, OH), 10.10 (s, 1H, ArH), 7.99 (s, 1H, NH), 7.49 (d, $J = 8.04$ Hz, 2H, ArH), 7.31 (t, $J = 7.92$ Hz, 2H, ArH), 7.08 (t, $J = 7.44$ Hz, 1H, ArH), 4.25 (s, 2H, CH₂); ¹³C NMR (100 MHz, DMSO-*d*₆): δ 169.49 (C=O), 150.03, 137.23, 128.52, 123.41, 119.53, 34.39 (CH₂) ppm.

4.2.9 2-((4-hydroxy-1H-pyrazolo[3,4-*d*]pyrimidin-6-yl)thio)-*N*-(pyridin-2-ylcarbamoyl) acetamide (9s)

Brown solid; yield: 89%; mp 215-217°C; FTIR (ATR, cm⁻¹) ν_{\max} : 3160.39, 2981.81, 2865.05, 1729.62, 1688.34, 1575.47, 1504.97, 1434.23, 1299.93, 1162.51, 778.15; ¹H-NMR (600 MHz, DMSO-*d*₆): δ 13.40 (s, 1H, NH), 12.20 (s, 1H, NH), 10.92 (s, 1H, OH), 10.46 (s, 1H, ArH), 8.27 (t, $J = 2.94$ Hz, 1H, ArH), 7.91 (d, $J = 8.34$ Hz, 2H, ArH + NH), 7.80-7.77 (m, $J = 4.33$ Hz, 1H, ArH), 7.11-7.09 (m, $J = 3.92$ Hz, 4.27 (s, 2H, CH₂); ¹³C NMR (100 MHz, DMSO-*d*₆): δ 169.54 (C=O), 150.65, 149.82, 147.70, 138.01, 119.17, 112.82, 34.60 (CH₂) ppm.

5 Biological activity protocol

5.1 CDK and Abl kinase inhibition assays

CDK2/cyclin E and Abl kinases were produced in Sf9 insect cells via baculoviral infection and purified on a NiNTA column. The kinase reactions were assayed with suitable substrates (1 mg/mL histone H1 for CDK2 and 500 μ M peptide GGEAIYAAPFKK for Abl) in the presence of 15 or 10 μ M ATP for CDK2 and Abl, respectively, 0.05 μ Ci [γ - 33 P]ATP, and the test compound in a final volume of 10 μ L, all in a reaction buffer (60 mM HEPES-NaOH, pH 7.5, 3 mM MgCl₂, 3 mM MnCl₂, 3 μ M Na-orthovanadate, 1.2 mM DTT, 2.5 μ g / 50 μ l PEG_{20,000}). The reactions were stopped by adding 5 μ L of 3% aq. H₃PO₄. Aliquots were spotted onto P-81 phosphocellulose (Whatman), washed 3 \times with 0.5% aq. H₃PO₄ and finally air-dried. Kinase inhibition was quantified using a FLA-7000 digital image analyzer. The concentration of the test compounds required to reduce the kinase activity by 50 % was determined from dose-response curves and recorded as their IC₅₀.

5.2 Anti-proliferative (K-562 and MCF-7) activity assays

The tumor cells (purchased from the American Type Culture Collection) were grown in DMEM medium supplemented with 10% (v/v) fetal bovine serum and L-glutamine (0.3 g/L) and were maintained at 37 °C in a humidified atmosphere with 5% CO₂. For anticancer cytotoxicity estimations, 10⁴ cells were seeded into each well of a 96-well plate, allowed to stabilize for 20 h, and the test inhibitors were then added at different concentrations (ranging from 0.1 to 100 μ M or to a solubility limit) in triplicate. Three days after addition of the inhibitors, calcein AM solution (Molecular Probes) was added. One hour later, fluorescence of cells was quantified using a Fluoroskan Ascent (Labsystems) reader and cytotoxic effective concentrations were calculated and expressed as IC₅₀ values from dose-response curves. Roscovitine and imatinib were used as reference drugs.

Conflict of Interest

Authors hereby declare that there are no financial/commercial conflicts of interest.

Acknowledgment

Authors are thankful to Discipline of Pharmaceutical Sciences, College of Health Sciences, University of KwaZulu-Natal (UKZN), South Africa, for their constant support, encouragement and financial assistance. Authors express heartfelt thanks to Mr. Dilip Jagjivan and Dr. Caryl Janse Van14 Rensburg (UKZN, South Africa) for their assistance in the NMR and EIMS experiments.

One of the authors (CB) gratefully acknowledges National Research Foundation (DST-NRF), South Africa for research funding in the form of Innovation Post-Doctoral Research Fellowship (UID: 99546). Authors also sincerely thank Centre for High Performance Computing (CHPC), Cape Town, South Africa for computational resources.

References

1. Cancer Facts & Figs, *American Cancer Society*, 2016.
2. D. Belpomme, P. Irigaray, A. J. Sasco, J. A. Newby, V. Howard, R. Clapp, L. Hardell, *Int. J. Oncol.* 2007, 30, 1037-1049.
3. (a) J. B. Gibbs, *Science*, 2000, 287, 1969-1971 (b) C. Unger, *Drug Future*, 1997, 22, 1337-1345.
4. J. E. Dancey, H. X. Chen, *Nat. Rev. Drug Discov.* 2006, 5, 649-659.
5. D. O. Morgan, *Nature*. 1995, 374, 131-134.
6. Y. Dai, S. Grant, *Clin. Cancer Res.* 2010, 16, 376-383.
7. S. Wadler, *Drug Resist. Updates*, 2001, 46, 347-367.
8. J. Cicens and M. Valius, *J. Cancer Res. Clin. Oncol.* 2011, 137, 1409-1418.
9. C. Massard, J. C. Soria, D. A. Anthony, A. Proctor, A. Scaburri, M. A. Pacciarini, B. Laffranchi, C. Pellizzoni, G. Kroemer, J. P. Armand, R. Balheda and C. J. Twelves, *Cell Cycle*, 2011, 10, 963-970.
10. C. K. Cheng, W. C. Gustafson, E. Charron, B. T. Houseman, E. Zunder, A. Goga, N. S. Gray, B. Pollok, S. A. Oakes, C. D. James, K. M. Shokat, W. A. Weiss, Q. W. Fan, *Proc. Natl. Acad. Sci. U. S. A.* 2012, 109, 12722-12727
11. J. J. Molenaar, M. E. Ebus, D. Geerts, J. Koster, F. Lamers, L. J. Valentijn, E. M. Westerhout, R. Versteeg, H. N. Caron, *Proc. Natl. Acad. Sci. U. S. A.* 2009, 106, 12968-12973.
12. A. J. Deans, K. K. Khanna, C. J. McNeese, C. Mercurio, J. Heierhorst, G. McArthur, *Cancer Res.* 2006, 66, 8219-8226.
13. L. Yang, D. Fang, H. Chen, Y. Lu, Z. Dong, H. F. Ding, Q. Jing, S. B. Su, S. Huang, *Oncotarget* 2015, 6, 20801-20812.
14. M. Drev, U. Groselj, S. Mevec, E. Pusavec, J. Strekelj, A. Golobic, G. Dahmann, B. Stanovnik, J. Svete, *Tetrahedron*. 2014, 70, 8267-8279.
15. M. Chauhan, R. Kumar, *Bioorg. Med. Chem.* 2013, 21, 5657-5668.
16. A. Kumar, I. Ahmad, B. S. Chhikara, R. Tiwari, D. Mandal, K. Parang, *Bioorg. Med. Chem. Lett.* 2011, 21, 1342-1346.

17. C. Luma, J. Kahl, L. Kessler, J. Kucharski, J. Lundstrm, S. Miller, H. Nakanishi, Y. Pei, K. Pryor, E. Roberts, L. Sebo, R. Sullivan, J. Urban, Z. Wang, *Bioorg. Med. Chem. Lett.* 2008, 18, 3578-3581.
18. K. J. Curran, J. C. Verheijen, J. Kaplan, D. J. Richard, L. Toral-Barza, I. Hollander, J. Lucas, S. Ayral-Kaloustian, K. Yu, A. Zask, *Bioorg. Med. Chem. Lett.* 2010, 20, 1440-1444.
19. S. Gupta, L. M. Rodrigues, A. P. Esteves, A. M. F. Oliveira-Campos, M. S. J. Nascimento, N. Nazareth, H. Cidade, M. P. Neves, E. Fernandes, M. Pinto, N. M. Cerqueira, N. Bras, *Eur. J. Med. Chem.* 2008, 43, 771-780.
20. R. Ducray, P. Ballard, B. C. Barlaam, M. D. Hickinson, J. G. Kettle, D. J. Ogilvie, C. B. Trigwell, *Bioorg. Med. Chem. Lett.* 2008, 18, 959-962.
21. D. C. Kim, Y. R. Lee, B. S. Yang, K. J. Shin, D. J. Kim, B. Y. Chung, K. H. Yoo, *Eur. J. Med. Chem.* 2003, 38, 525-532.
22. D. A. Ibrahim, A. M. El-Metwally, E. E. Al-Arab, *Arkivoc*, 2009, 7, 12-25.
23. J. A. Markwalder, M. R. Arnone, P. A. Benfield, M. Boisclair, C. R. Burton, C. H. Chang, S. Cox, P. M. Czerniak, C. L. Dean, D. Doleniak, R. Grafstrom, B. A. Harrison, R. F. Kaltenbach, D. A. Nugiel, K. A. Rossi, S. R. Sherk, L. M. Sisk, P. Stouten, G. L. Trainor, P. Worland, S. P. Seitz, *J. Med. Chem.* 2004, 47, 5894.
24. M. G. Bursavich, P. W. Nowak, D. Malwitz, S. Lombardi, A. M. Gilbert, N. Zhang, S. Ayral-Kaloustian, J. T. Anderson, N. Brooijmans, *U.S. Patent*, 2010, 20100015141,
25. K. Yu, L. Toral-Barza, C. Shi, W. G. Zhang, J. Lucas, B. Shor, J. Kim, J. Verheijen, K. Curran, D. J. Malwitz, D. C. Cole, J. Ellingboe, S. Ayral-Kaloustian, T. S. Mansour, J. J. Gibbons, R. T. Abraham, P. Nowak, A. Zask, *Cancer Res.* 2009, 69, 6232-6240.
26. A. C. Dar, M. S. Lopez, K. M. Shokat, *Chem. Biol.* 2008, 15, 1015.
27. A. Burchat, D. W. Borhani, D. J. Calderwood, G. C. Hirst, B. Li, R. F. Stachlewitz, *Bioorg. Med. Chem. Lett.* 2006, 16, 118-122.
28. H. M. Patel, B. Sing, V. Bhardwaj, M. Palkar, R. Rane, W. S. Alwan, A. K. Gadak, M. N. Noolvi, R. Karpoormath, *Eur. J. Med. Chem.* 2015, 26, 599-613.
29. S. Cherukupalli, R. Karpoormath, B. Chandrasekaran, G.A. Hampannavar, N. Thapliyal, V. N. Palakollu, *Eur. J. Med. Chem.* 2017, 126, 298-352.
30. R. J. Bentems, J. D. Anderson, D. F. Smee, A. J. Jin, H. A. Alaghamandan, B. S. Sharma, W. B. Jolley, R. K. Robins, H. B. Cottam, *J. Med. Chem.* 1990, 33, 2174-2178.
31. L. Y. Ma, B. Wang, L. P. Pang, M. Zhang, S. Q. Wang, Y. C. Zheng, K.P. Shao, D. Q. Xue, H. M. Liu, *Bioorg. Med. Chem. Lett.* 2015, 25, 1124-1128.

CHAPTER 7

1 Summary and conclusion

Cancer is a disease caused by an uncontrolled growth of abnormal cells. Recent advancement in understanding the molecular mechanism of cancer and the factors causing it has deeply impacted in the innovation of cancer chemotherapy. Predominant efforts are being carried out in order to identify advanced treatments through enhanced imaging, molecular diagnostic approaches and improvements in prevention and chemotherapeutic organization. Every year the number people with cancer is drastically increasing world over. Thus, it is becoming imperative to investigate and discover new agents and targets for the treatment of cancer.

Cyclin-dependent kinases (CDK/Cyclins) constitute a family of serine/threonine kinases that involve in the regulation of cell cycle progression, transcription by phosphorylating proteins involved in cell division. Twenty different CDKs have been reported in mammalian cells till date. Among them, CDK1, CDK2 and their associated Cyclins A, B, D, E are considered as *bona fide* cell cycle regulators. For example, formation of active complex composed of CDK2 and cyclin E enables pRb phosphorylation, activation of transcription factor E2F which and initiation of S phase of the cell cycle. CDK2 then also associates with cyclin A, governing continuous DNA replication and properly programmed deactivation of E2F. Deregulations of CDKs or cyclins, as well as the loss of endogeneous inhibitory proteins, result in abrogation of cell cycle control, which is connected with development of tumors, thus CDKs are considered important targets for anticancer drugs.

The aim of the present study was to design and identify newer potential anticancer leads by bioisosteric replacement of purine by pyrazolopyrimidines. There are almost five different structural isomers of this bicyclic system (pyrazolo[5,1-*b*]pyrimidines, pyrazolo[5,1-*a*]pyrimidines, pyrazolo[4,3-*d*]pyrimidines, pyrazolo[1,5-*c*]pyrimidines and pyrazolo[3,4-*d*]pyrimidines), which exists due to the varying position of nitrogen, degree of saturation or unsaturation, or the number of nitrogen's on the pyrazole nucleus. Pyrazolo[3,4-*d*]pyrimidine scaffold was substituted with various five/six membered heterocycles to yield novel multifarious pyrazolo[3,4-*d*]pyrimidine derivatives. This research work resulted in 71 novel derivatives as CDK2 inhibitors and the novel desired structures were confirmed by thin layer chromatography (TLC), infrared spectroscopy (IR), nuclear magnetic resonance spectroscopy (^1H , ^{13}C NMR), and high resolution mass spectrometry (HRMS). These compounds were evaluated for their inhibitory activity against CDK2 and Abl kinase enzymes as well as for their anti-proliferative activity (K-562 and MCF-7 cell lines). The pharmacological activity data indicated that the designed some

compounds were explicitly active against CDK2 enzyme. Thus indicating that the pyrazolo[3,4-*d*]pyrimidine nucleus as potential building block in further designing newer anticancer agents.

In chapter 2, we have extensively performed literature assessment on pyrazolo[1,5-*a*]pyrimidine for its various reported pharmacological activities. From our literature search, it was quite evident that pyrazolo[1,5-*a*]pyrimidine is a privileged scaffold, which was evident from the its marketed drugs (zeleplon, indiplon, dinaciclib, dorsomorphin, etc.) that have this scaffold. In addition, several research groups worldwide have exploited this scaffold as a building block for developing drug-like candidates with broad range of medicinal properties such as anticancer, CNS agents, anti-infectious, anti-inflammatory, CRF₁ antagonists and radio diagnostics etc. Apparently, there were no concised review article on pyrazolo[1,5-*a*]pyrimidine and its application in medicinal chemistry. Thus we envisaged in writing a review on pyrazolo[1,5-*a*]pyrimidine and its derivatives describing its biological properties with special emphasis on structure-activity relationship (SAR) studies. This work was published as a review article in *European Journal of Medicinal Chemistry* journal published in **2017**, volume **126** and page number **298** to **352**. <https://doi.org/10.1016/j.ejmech.2016.11.019>.

Similarly in chapter 3, we have performed comprehensive literature survey on another exploited scaffold that is pyrazolo[4,3-*d*]pyrimidine which has demonstrated numerous pharmacological activities particularly, anti-cancer, anti-infectious, phosphodiesterase inhibitors, adenosine antagonists and cytokinin antagonists etc. This extensive review unveils the synthetic and pharmacological diversity with special emphasis on structural variations around pyrazolo[4,3-*d*]pyrimidine scaffold indicating the medicinal worthiness of pyrazolo[4,3-*d*]pyrimidine framework. This review was published in *Bioorganic and medicinal chemistry* journal, **2017**, <https://doi.org/10.1016/j.bmc.2017.10.012>.

In chapter 4, inspired by the biological significance of pyrazolopyrimidine isomers, we synthesized novel derivatives of pyrazolo[3,4-*d*]pyrimidine by attaching aromatics at C-4 position through -NH linkage and phenethyl & pentane functional groups at C-6 via sulphur linkage by effectual synthetic route. This strategic synthetic scheme was more pragmatic in producing decent yields (75-95%) of final compounds. Synthesis of novel derivatives was achieved by nucleophilic substitution reaction of compound 4-chloro-6-(phenethylthio)-1*H*-pyrazolo[3,4-*d*]pyrimidine (**6a**), 4-chloro-6-(pentylthio)-1*H*-pyrazolo[3,4-*d*]pyrimidine (**6b**) with various appropriately substituted anilines at C-4 position as depicted in scheme 1 of chapter 4. Structures of synthesized compounds were characterized by spectral data (IR, ¹H NMR, ¹³C NMR and HRMS). Laboratory of Growth Regulators, Palacky University, Slechtitelu 27, 78371, Olomouc, Czech Republic, performed anticancer screening against CDK2 & Abl kinase inhibitors and K-562 & MCF-7 human cancer cell lines. Compounds **8**, **11** and **36** having 2-chloro, 3-nitro and 4-methylthio aniline groups at C-4 respectively displayed significant enzymatic

inhibitory activity against CDK2 (IC_{50} = 5.1 μ M, 7.8 μ M, 8.8 μ M) and Abl (IC_{50} = >25 μ M, >12.5 μ M, >25 μ M) as well as prominent anti-proliferative effects against K-562 and MCF-7 cancer cell lines with IC_{50} value ranging from 19.2 to 27.4 μ M. Further, the *in silico* molecular docking studies displayed good binding interactions and the binding energies were in agreement with the observed SAR as well as experimental results as discussed in chapter 4. This work This review was published in *Bioorganic Chemistry* journal, 2018, <https://doi.org/10.1016/j.bioorg.2018.02.030>.

In chapter 5, as a continued effort in synthesizing pyrazolo[3,4-*d*]pyrimidine inspired anticancer compounds (CDK2 and Abl kinase inhibitors), pyrazolo[3,4-*d*]pyrimidine with different substituted heterocyclic moieties at C-4 position through ester linkage and phenethyl, pentane and hexane functional groups at C-6 via sulphur linkage for their anticancer activity. Diverse novel compounds of 4,6-disubstituted pyrazolo[3,4-*d*]pyrimidine derivatives (**5a-5h**, **6a-6d** and **7a-7c**) were synthesized by efficient and adaptable synthetic route (scheme 1) as described in chapter 5. These compounds were well characterized by IR, 1H , ^{13}C NMR, and HRMS. Laboratory of Growth Regulators, Palacký University, Slechtitelu 27, 78371, Olomouc, Czech Republic, evaluated obtained compounds for their *in vitro* anticancer activity against CDK2 & Abl kinase inhibitors and K-562 & MCF-7 human cancer cell lines. From the tested series, compounds **5a** (CDK2: IC_{50} = 8.8 μ M) and **6c** (CDK2: IC_{50} = 6.8 μ M) displayed significant enzymatic inhibitory activity and prominent anti-proliferative effects against K-562 and MCF-7 cancer cell lines with IC_{50} value ranging from 18.9 to 89.3 μ M. In addition, the binding energies of the best active compounds were in agreement with the experimental data and supported the SAR studies as discussed in chapter 5. This work has been communicated for publication in *Chemical Biology and Drug Design*.

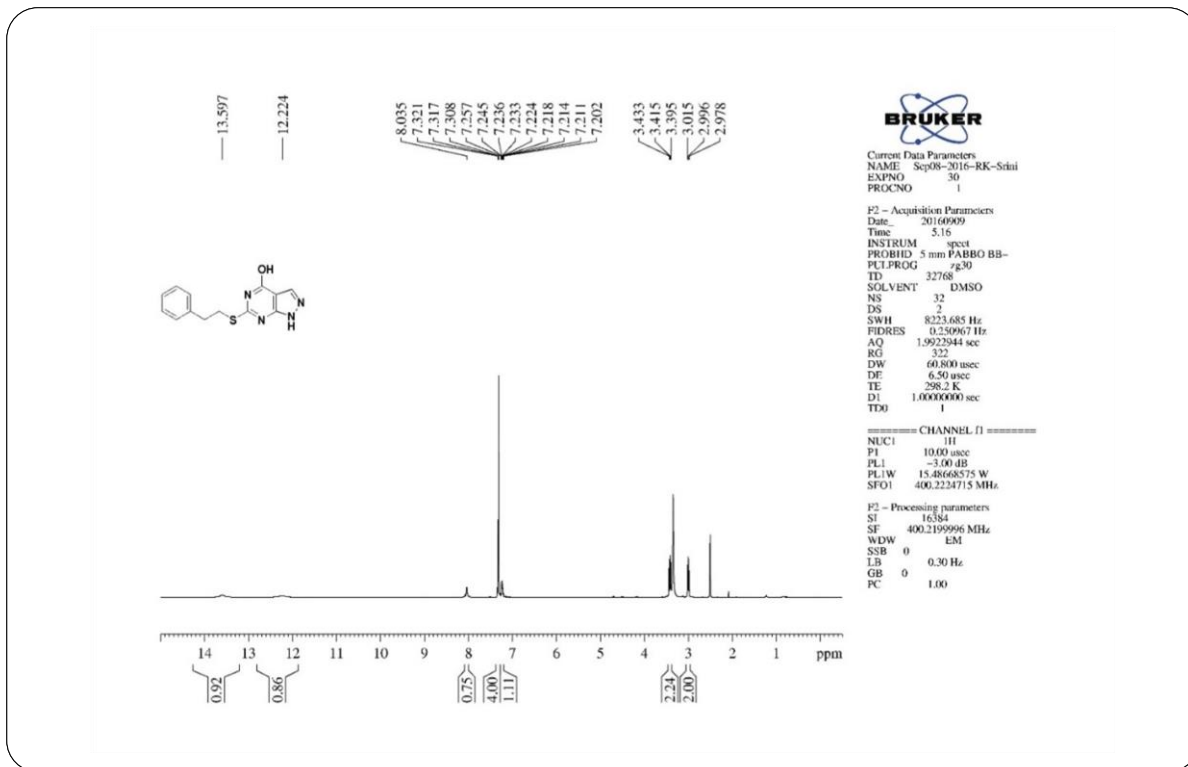
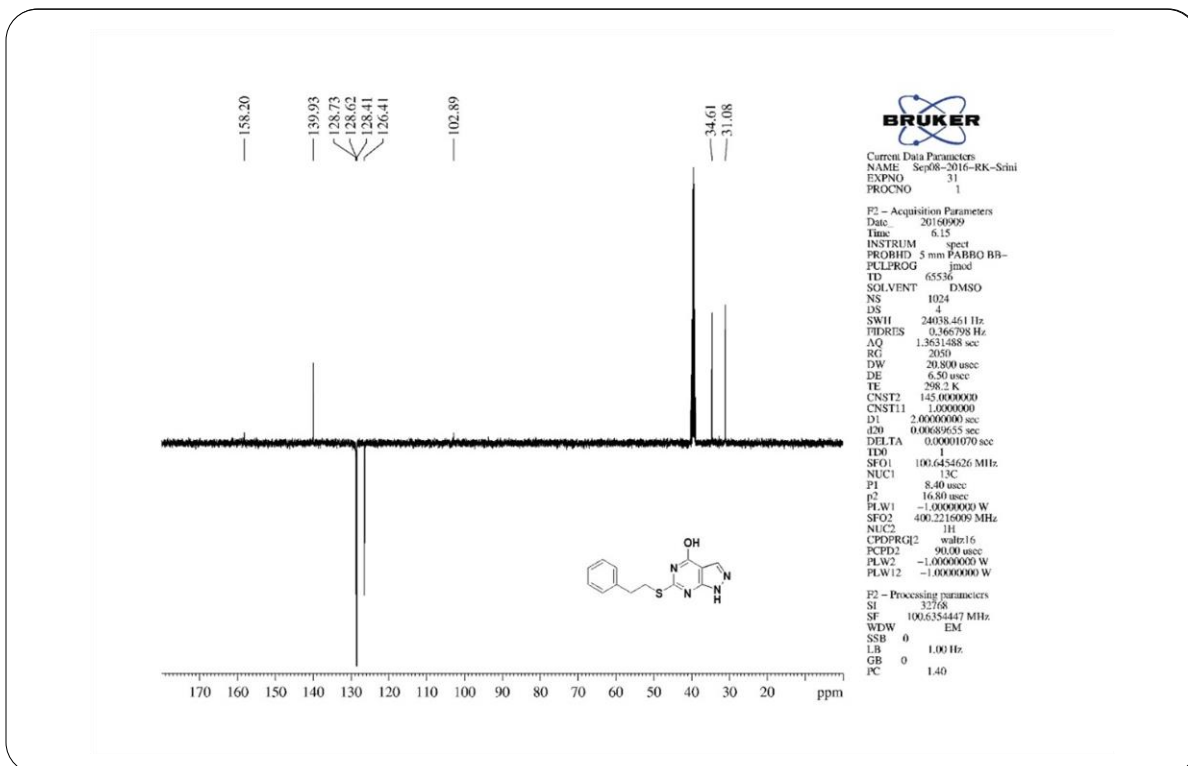
Finally, in chapter 6, as an ongoing endeavour in synthesizing pyrazolo[3,4-*d*]pyrimidine inspired anticancer compounds, we have synthesized phenylcarbamoyl acetamide fused pyrazolo[3,4-*d*]pyrimidines. Compounds **9a-9s** were synthesized with diverse structural variations by simple and effective synthetic route as described in chapter 6. Several phenylcarbamoyl acetamides (**8a-8s**) were efficiently synthesized and used for synthesis of desired final derivatives. All the final compounds were well characterized by IR, 1H , ^{13}C NMR and HRMS, thus conforming their formation. *In vitro* anticancer screening was performed at Laboratory of Growth Regulators, Palacký University, Slechtitelu 27, 78371, Olomouc, Czech Republic. For all the synthesized molecules from this series, IC_{50} values could not be measured due to solubility limit (IC_{50} >12.5 μ M or >25 μ M) as described in chapter 6. The overall finds suggest the significance of hybridisation to achieve fused pyrazolopyrimidines as anticancer agents. The manuscript for this work has been drafted and is ready for communication to an appropriate peer reviewed international journal.

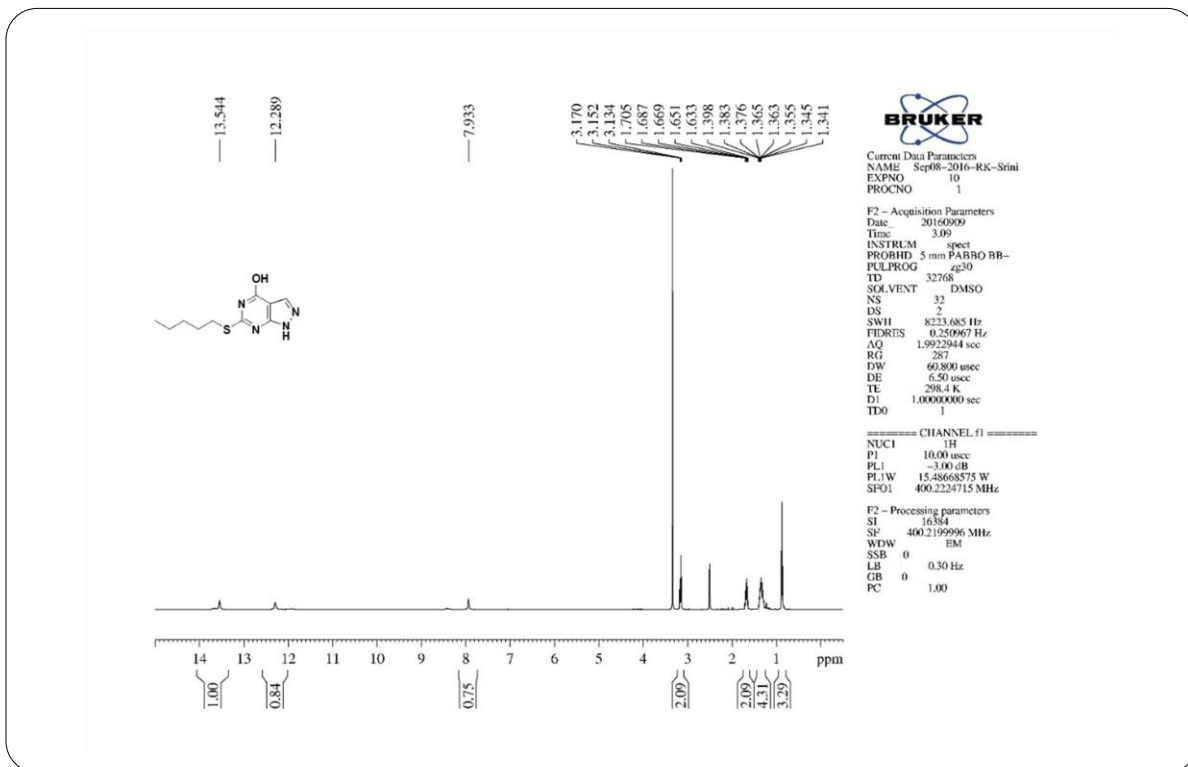
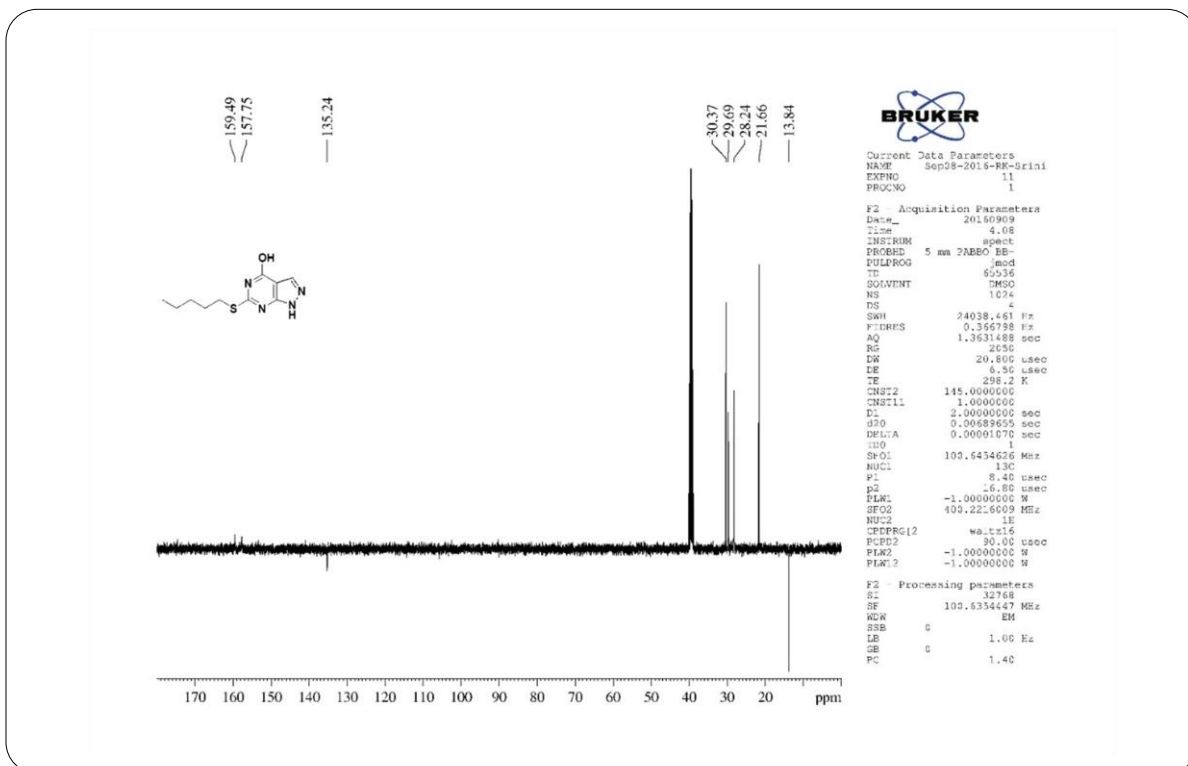
2 Future work

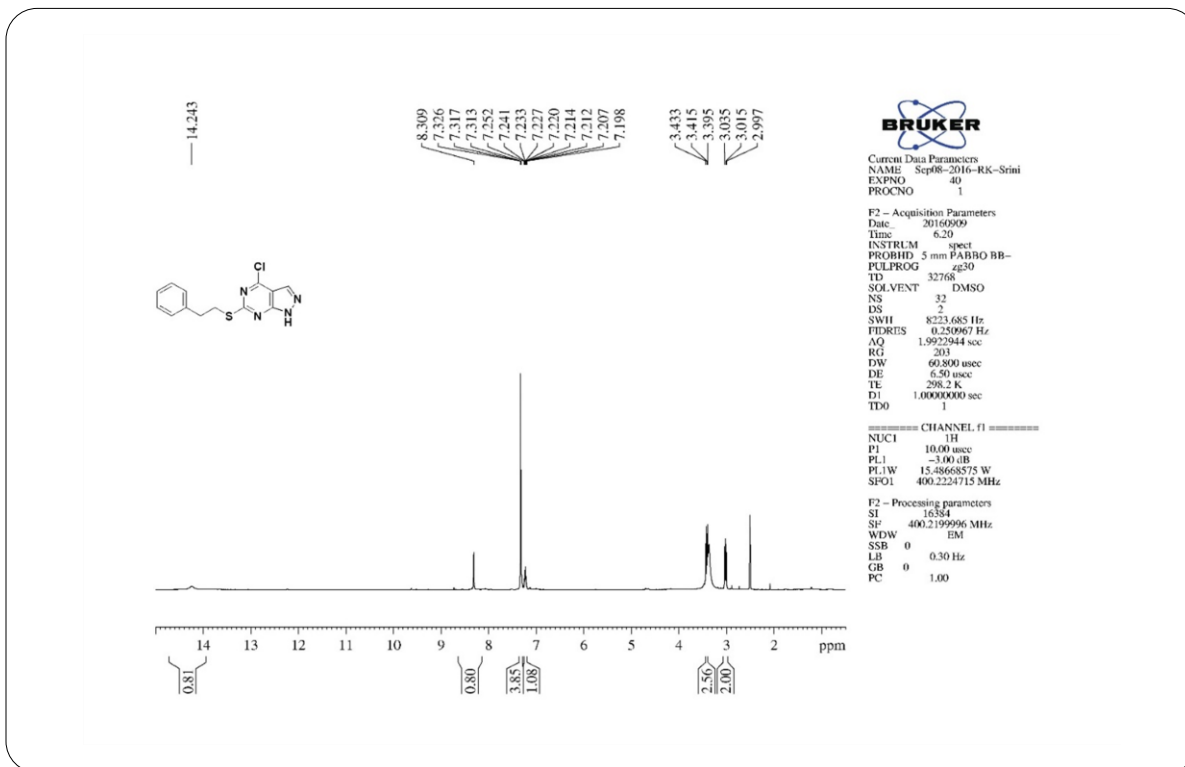
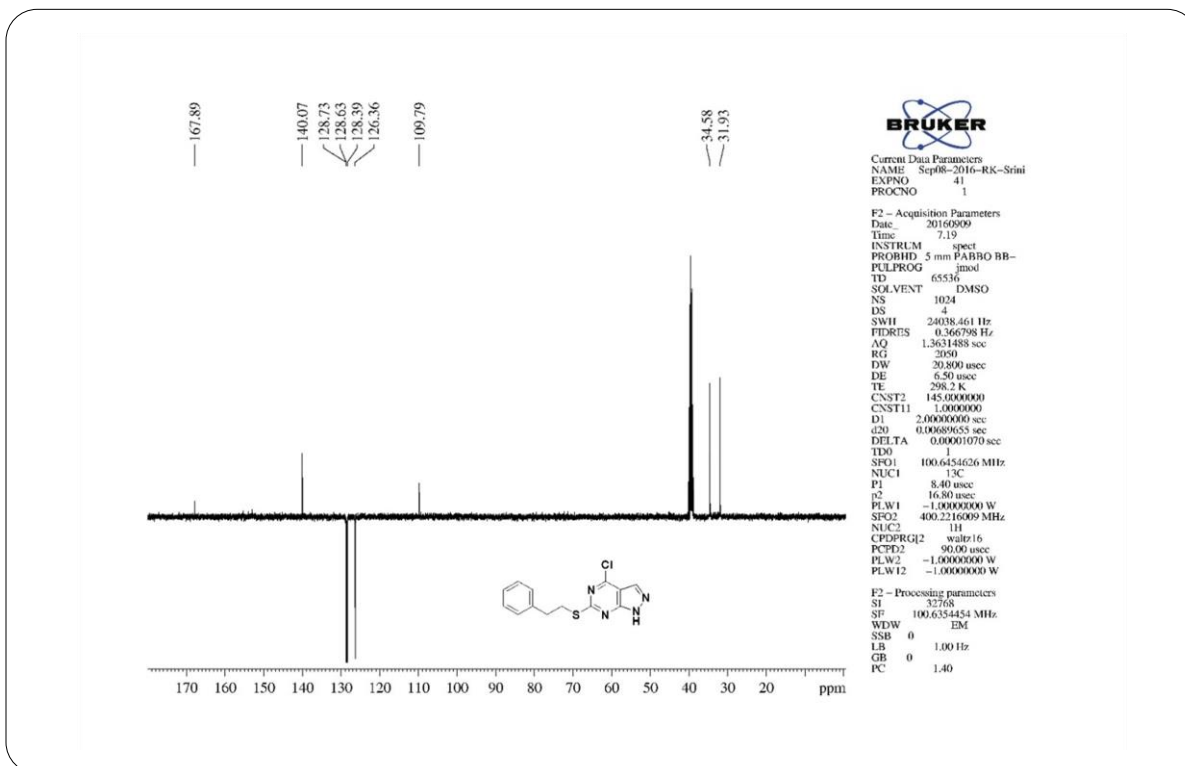
A comprehensive literature review and the anticancer activity data of the synthesized molecules displayed the significance of the pyrazolo[3,4-*d*]pyrimidine scaffold. However, one of the drawbacks of these molecules was the solubility, which could have affected their activity profile. For better pharmacological activity, bioavailability, and efficacy profiles further design and optimization of pyrazolo[3,4-*d*]pyrimidine based molecules is needed. This could be achieved by carefully substitution of hydrophilic and charged bioactive moieties at various positions of the pyrazolo[3,4-*d*]pyrimidine scaffold through efficient synthetic methods. In parallel, 3D-QSAR-based pharmacophore models could be generated from the available dataset molecules and validated using the test set ligands. Thus, ligand-based virtual screening of the best pharmacophore model against drug-like database (ZINC, Maybridge, Chembridge and NCI) can be performed to identify new set of anticancer hits which can also be considered for strategic chemical synthesis. Further, molecular docking studies (structure-based drug design) can also offer comparatively enhanced solutions for optimization of anticancer leads. Thus, the presented work will contribute existing literature on pyrazolo[3,4-*d*]pyrimidine scaffold and assist in developing novel class of pyrazolo[3,4-*d*]pyrimidine based anticancer compounds as potential drug candidates.

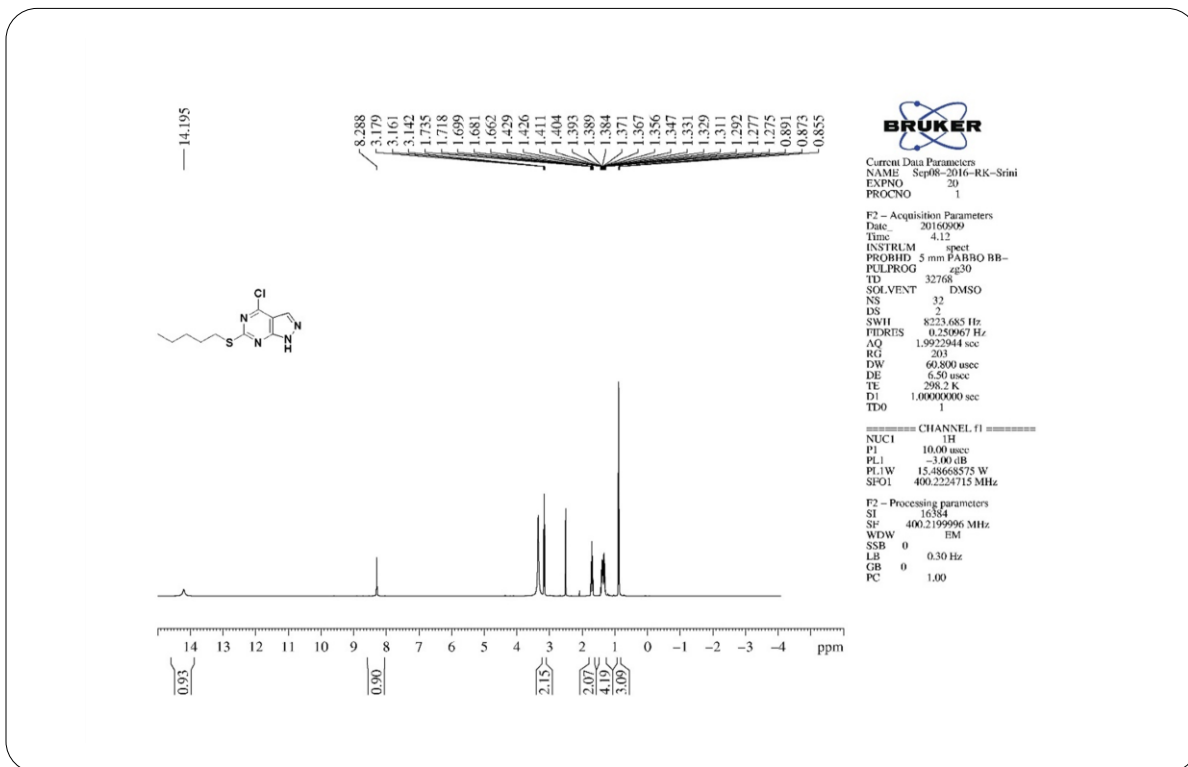
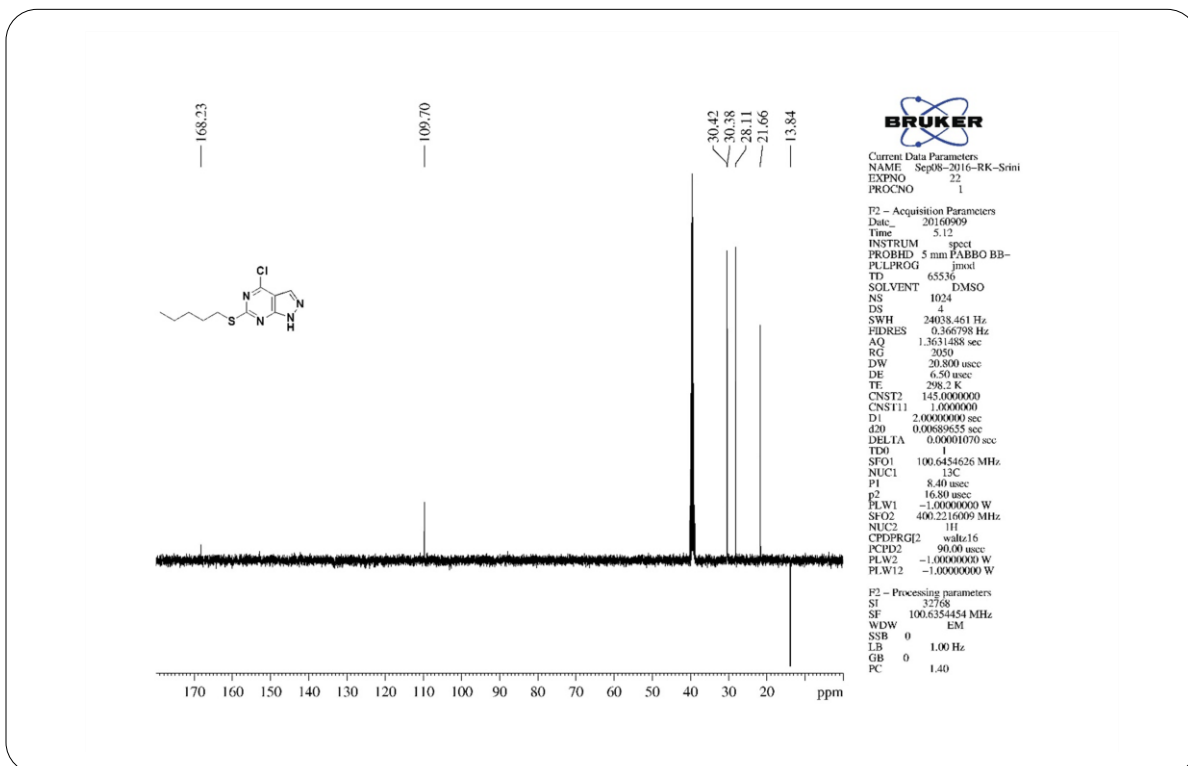
APPENDIX – I**SUPPLEMENTARY INFORMATION****CHAPTER 4****Synthesis, anticancer evaluation, and molecular docking studies of some novel 4,6-disubstituted pyrazolo[3,4-*d*]pyrimidines as cyclin dependent kinase 2 (CDK2) inhibitors**

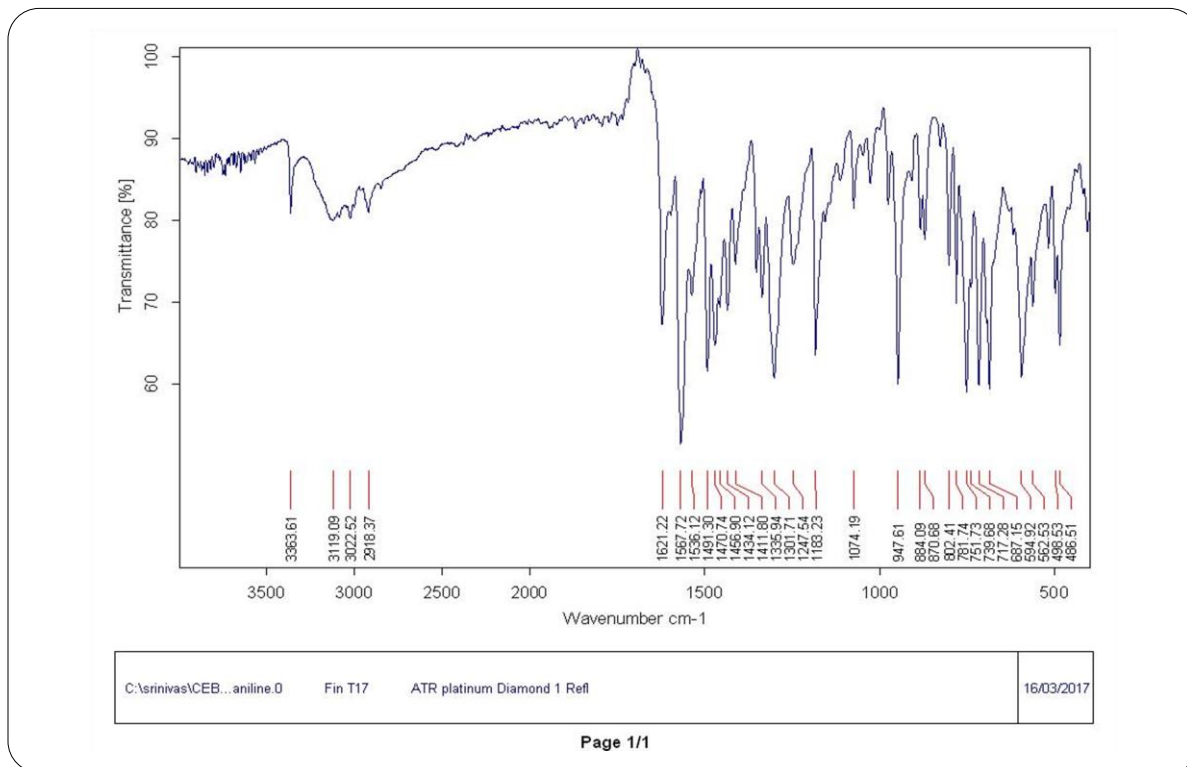
Department of Pharmaceutical Chemistry, College of Health Sciences, University of KwaZulu-Natal, Durban 4000, South Africa.

**¹H NMR Spectrum of Compound 5a****¹³C NMR Spectrum of Compound 5a**

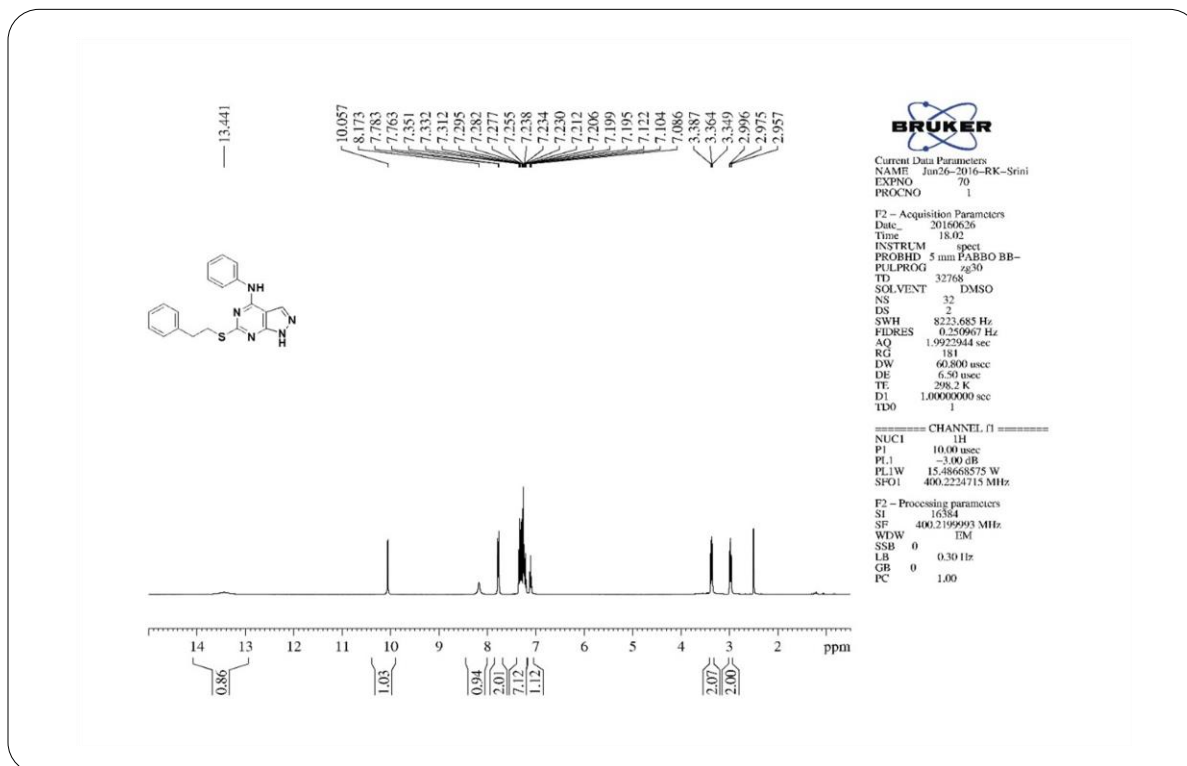
**¹H NMR Spectrum of Compound 5b****¹³C NMR Spectrum of Compound 5b**

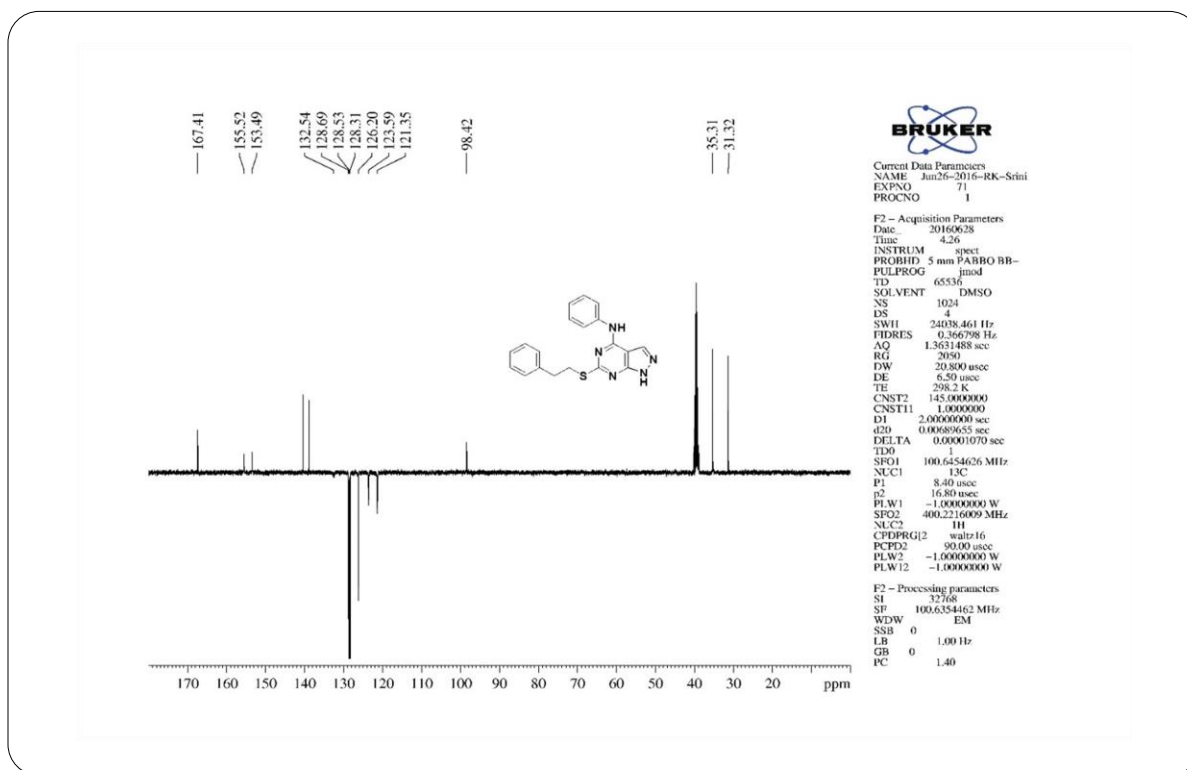
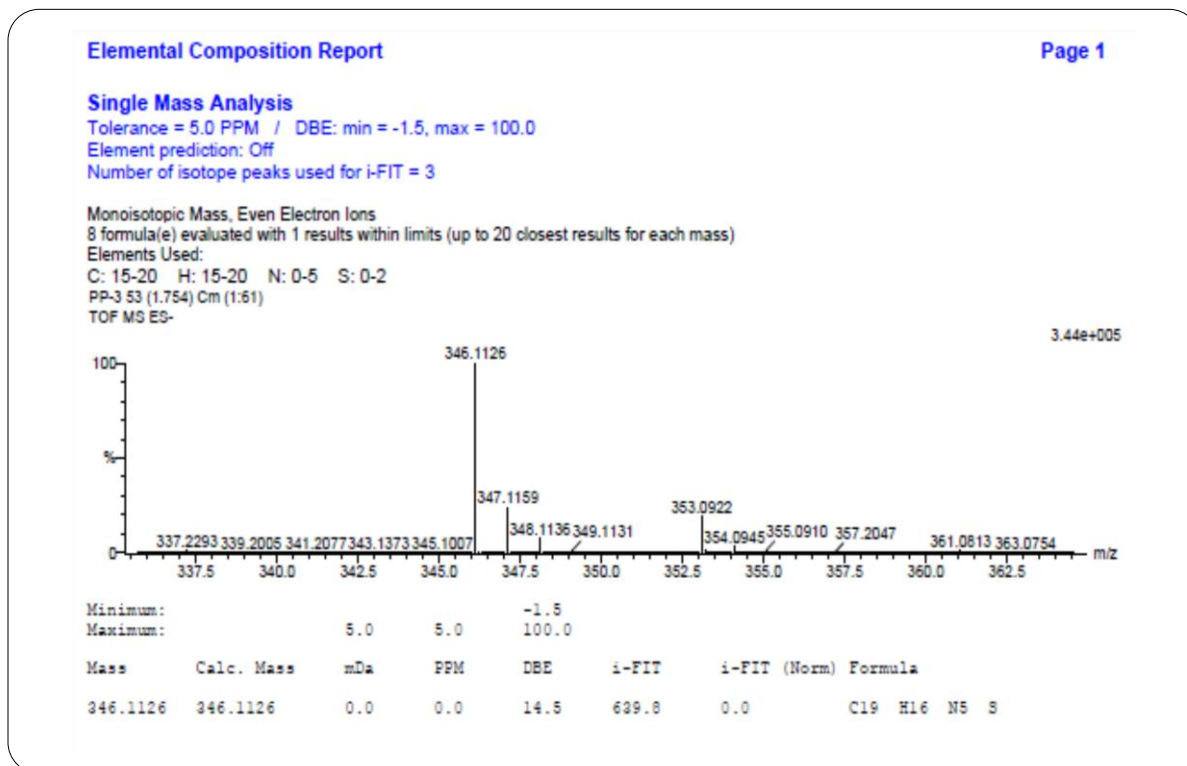
¹H NMR Spectrum of Compound 6a¹³C NMR Spectrum of Compound 6a

**¹H NMR Spectrum of Compound 6b****¹³C NMR Spectrum of Compound 6b**

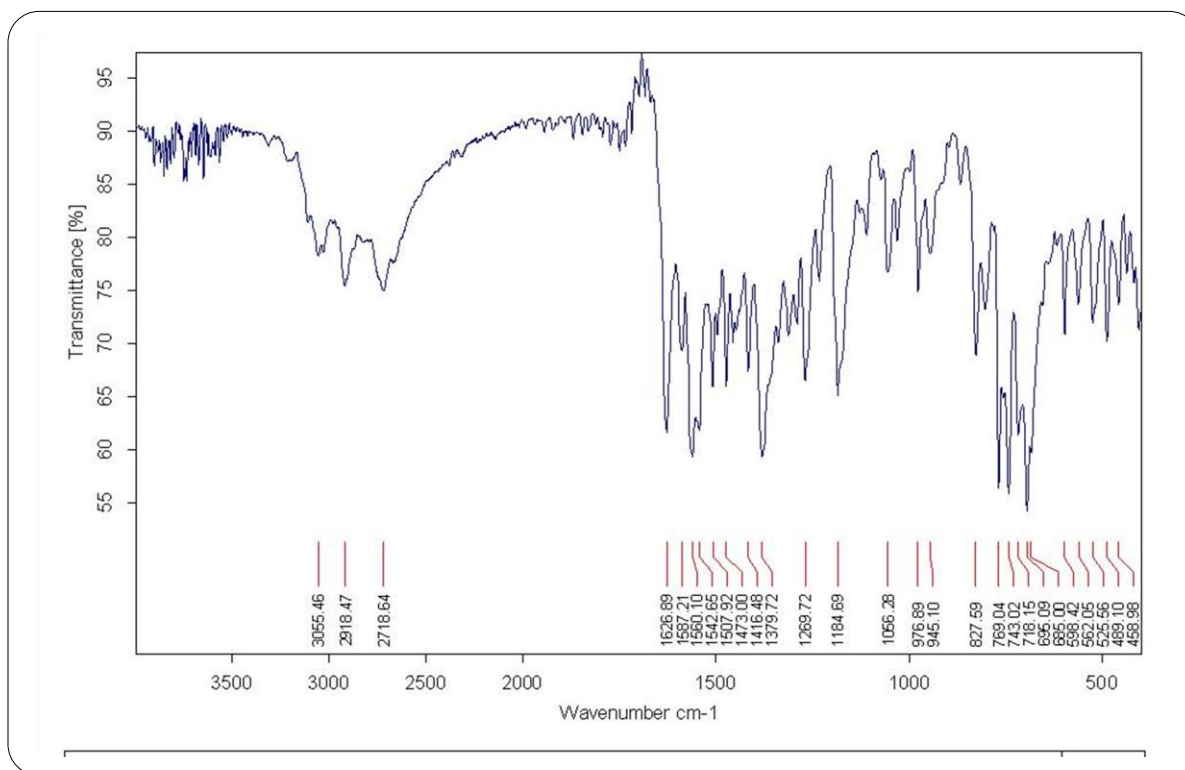


IR Spectrum of Compound 7

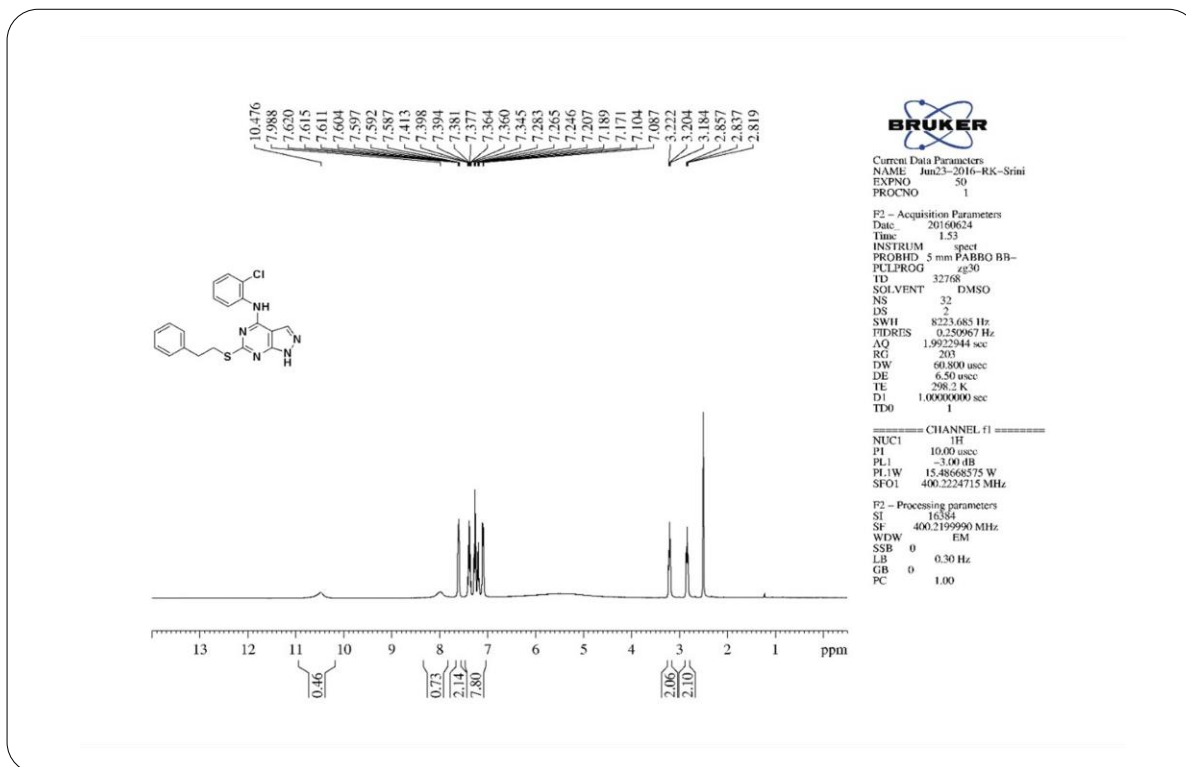
¹H NMR Spectrum of Compound 7

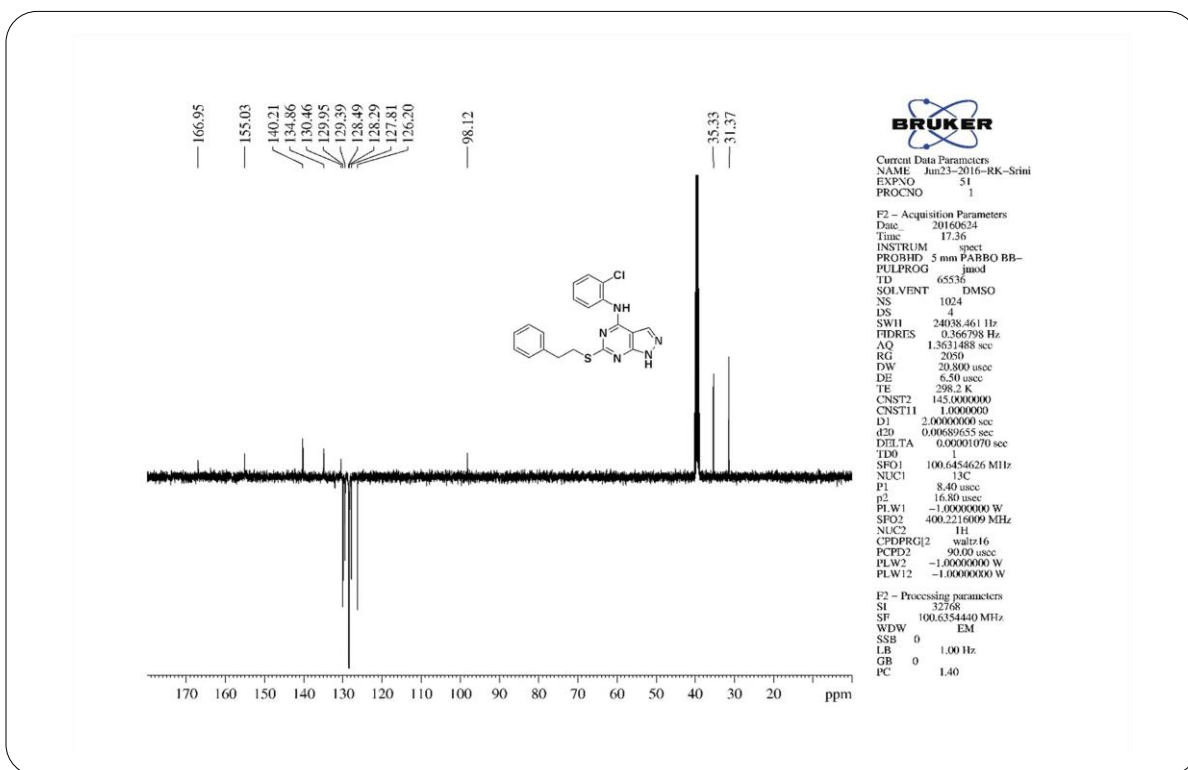
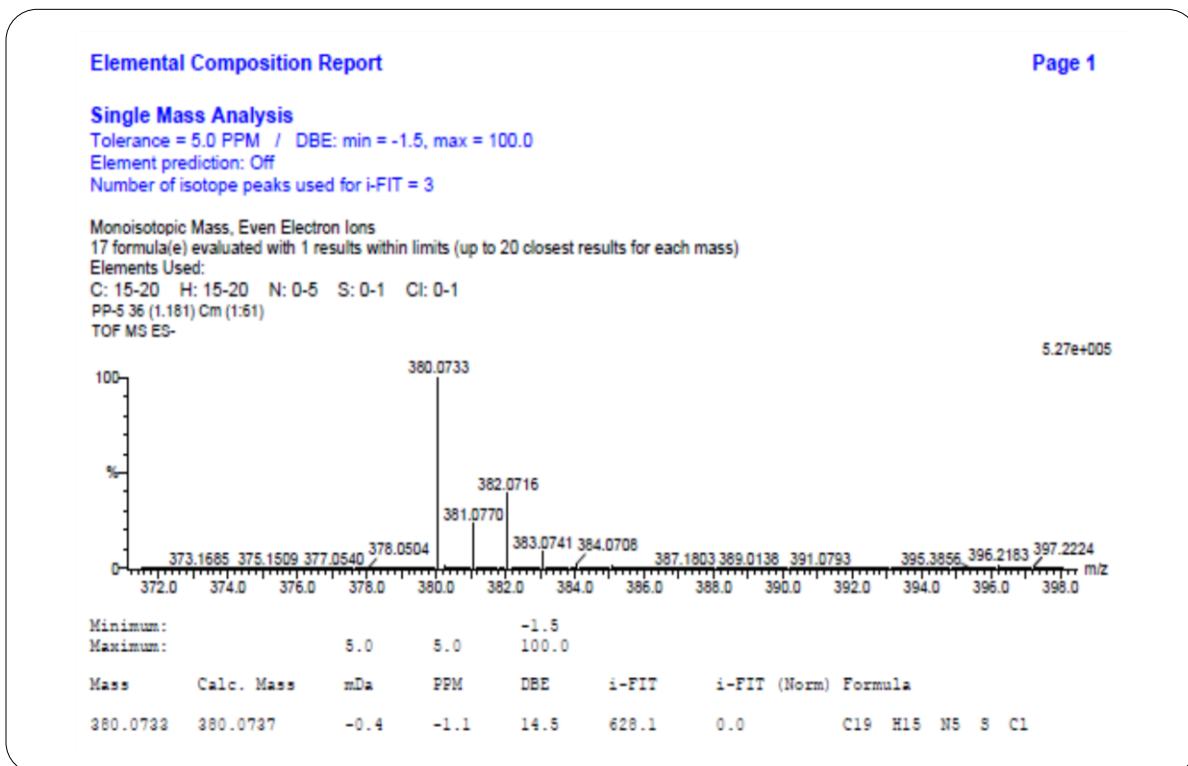
¹³C NMR Spectrum of Compound 7

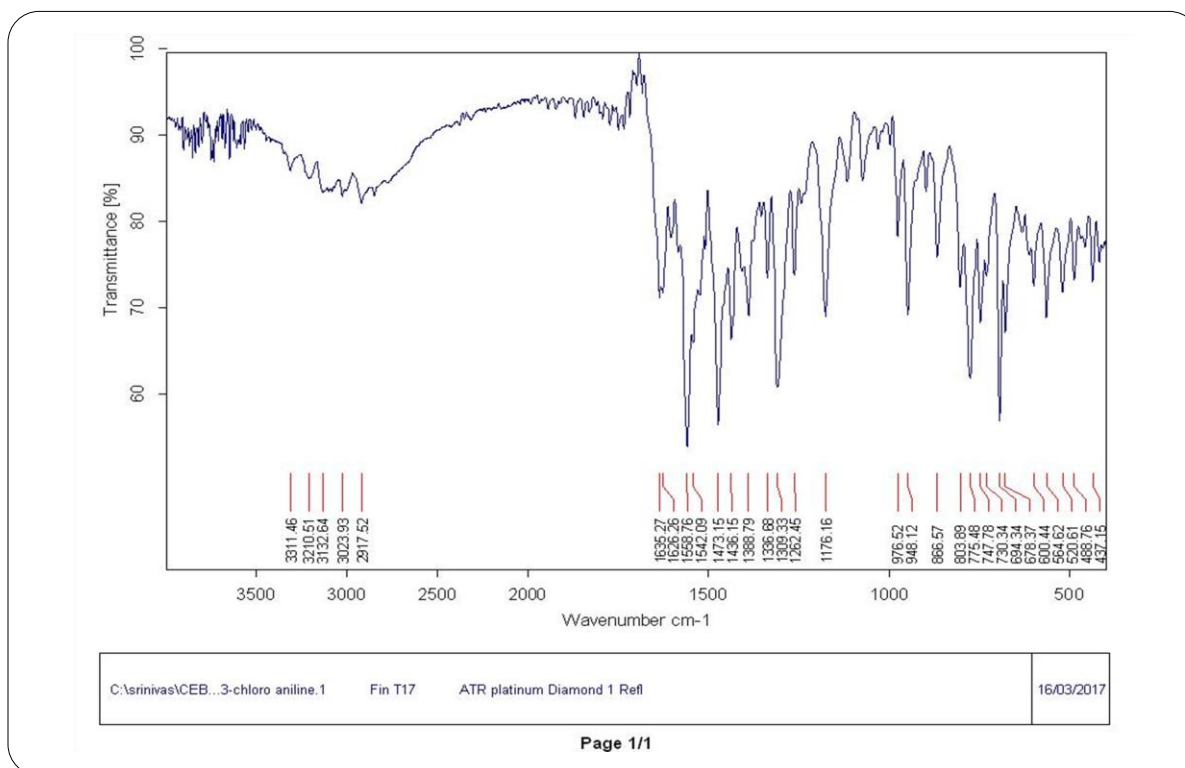
HRMS Spectrum of Compound 7



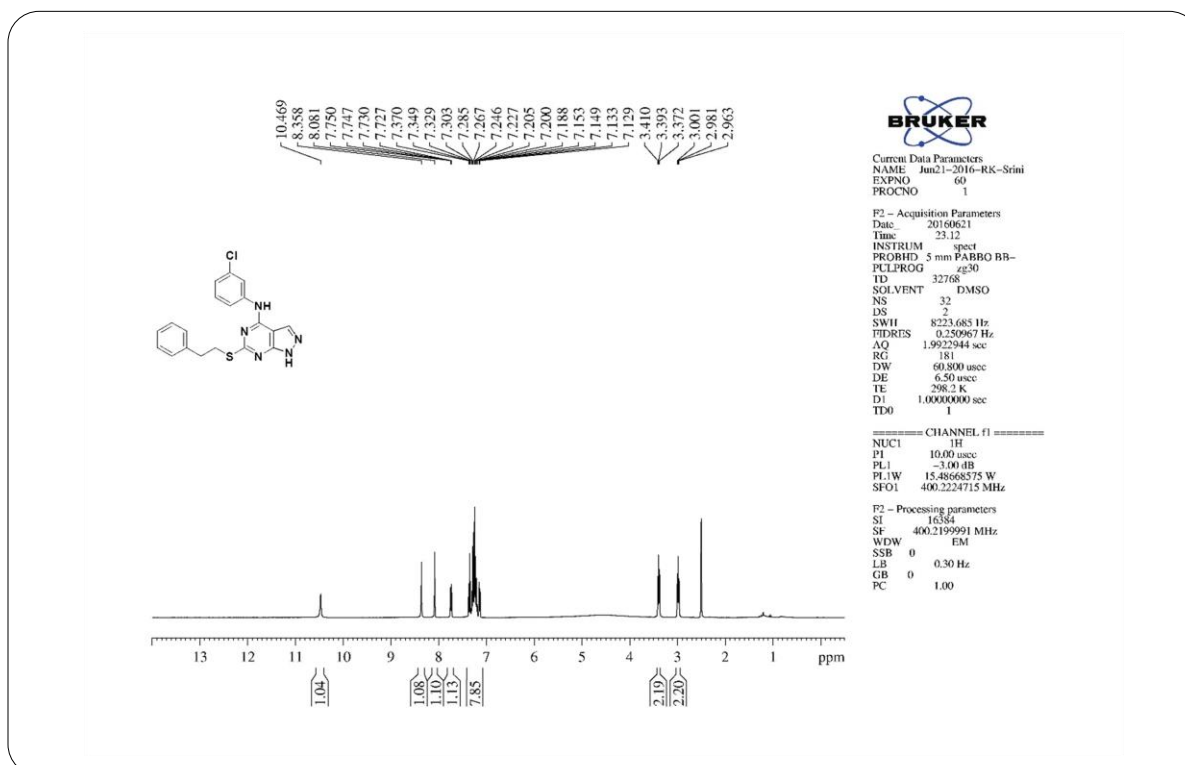
IR Spectrum of Compound 8

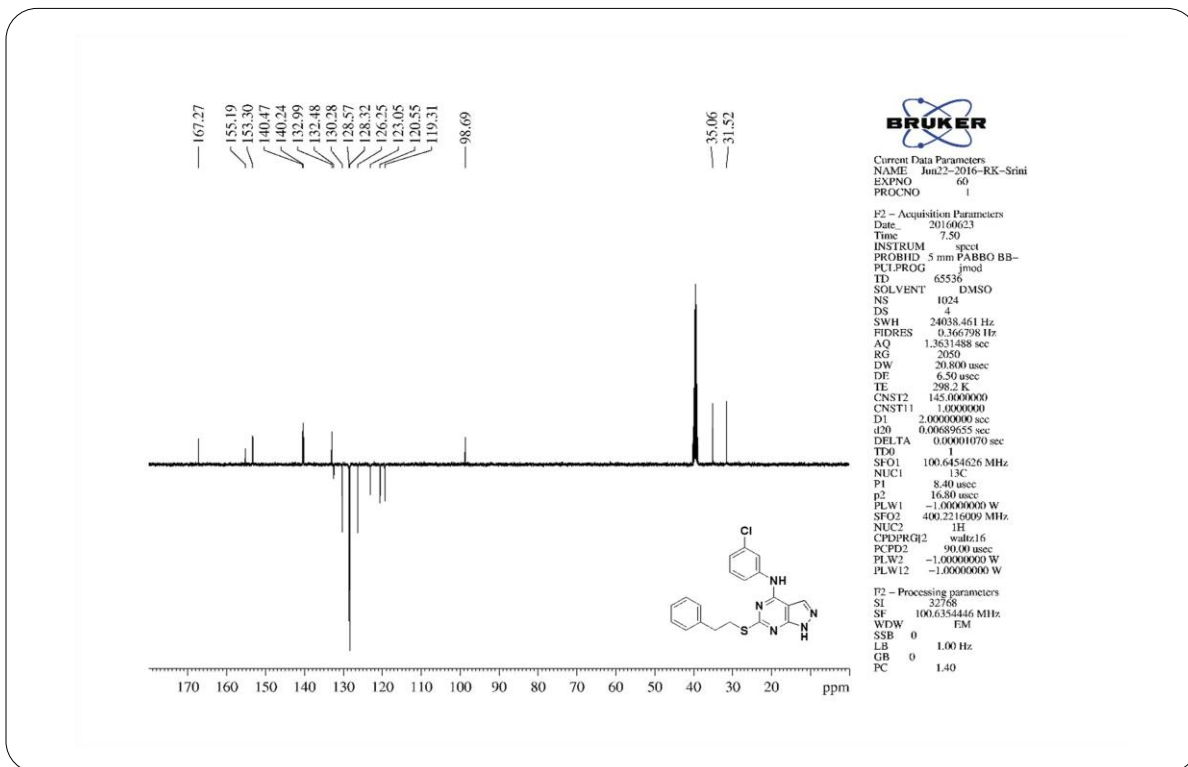
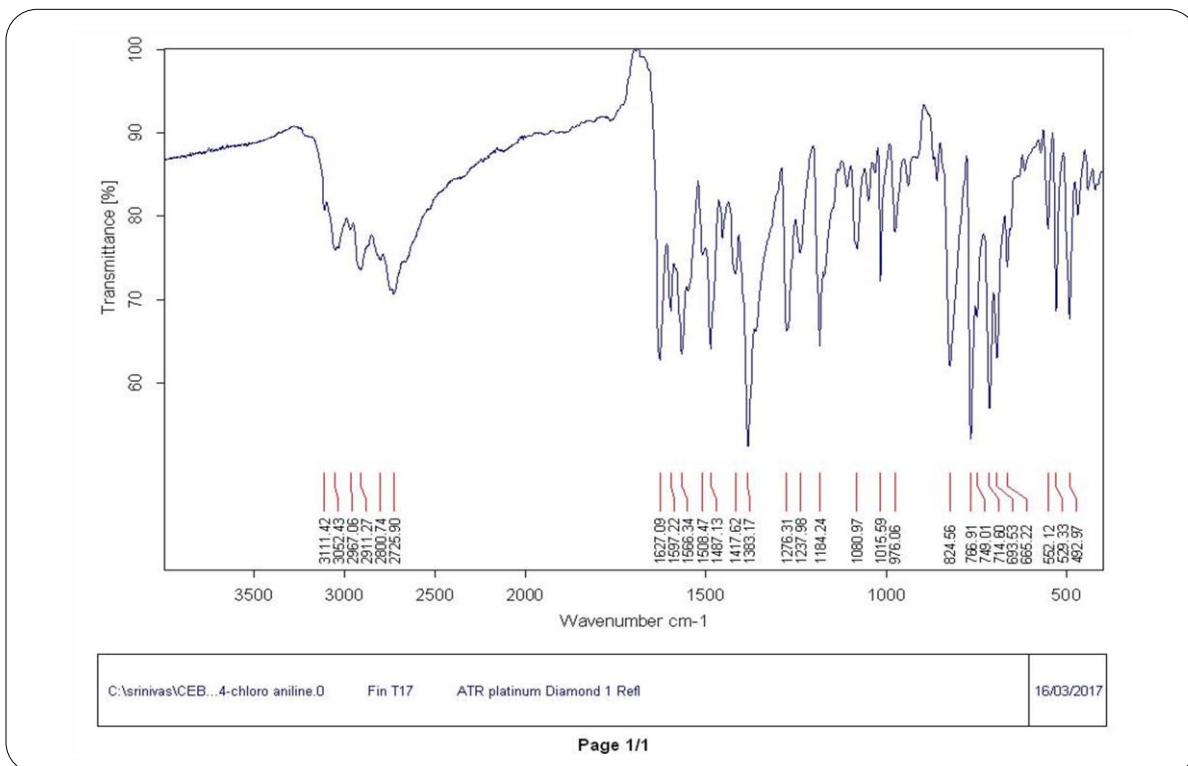
¹H NMR Spectrum of Compound 8

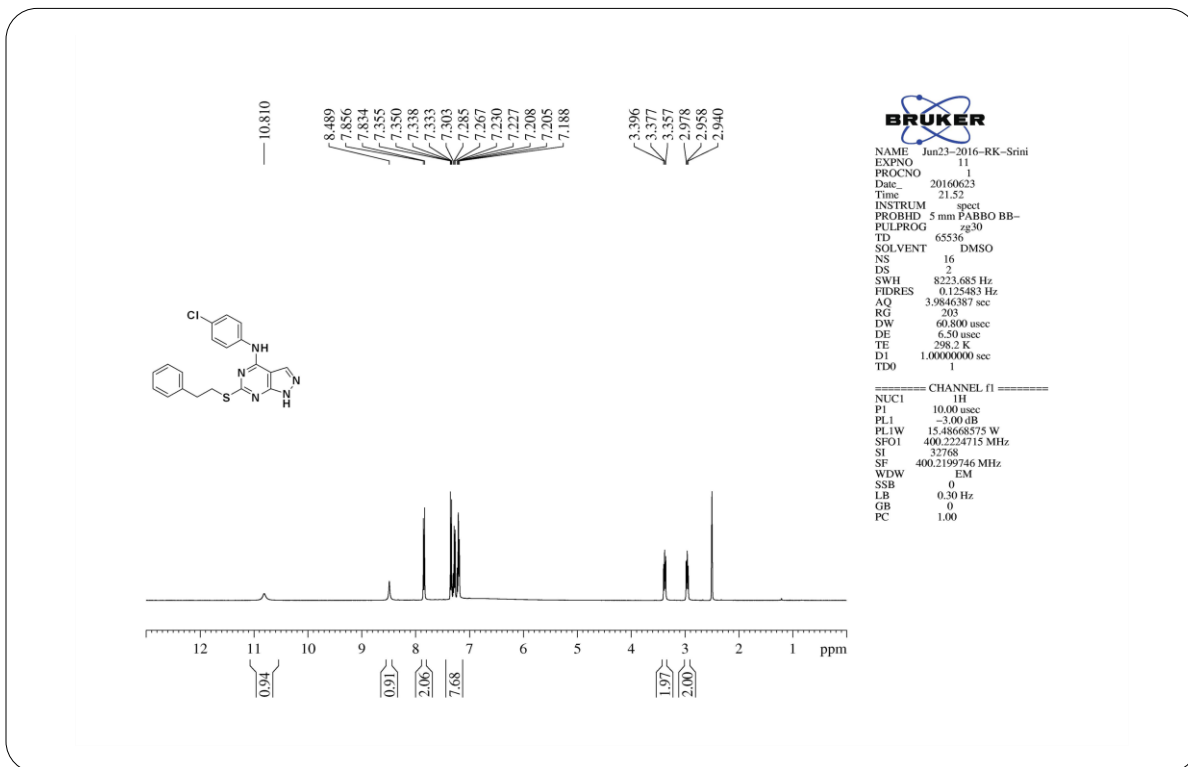
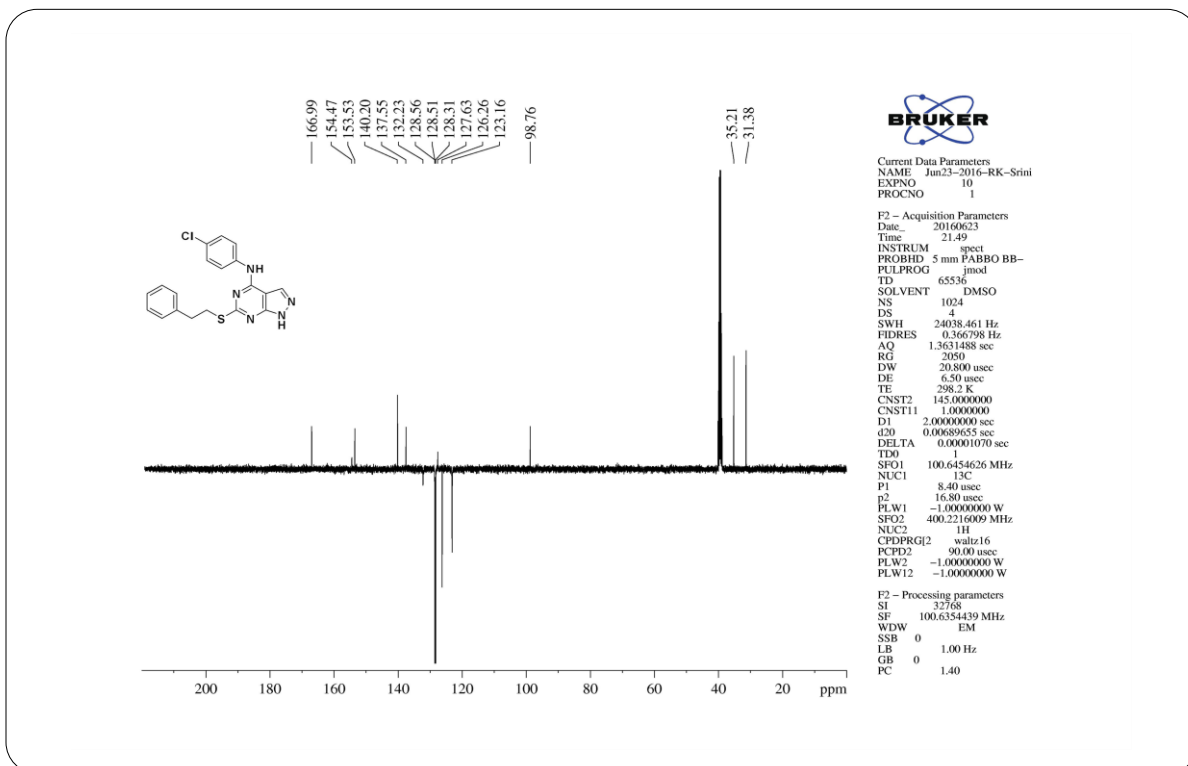
**¹³C NMR Spectrum of Compound 8****HRMS Spectrum of Compound 8**

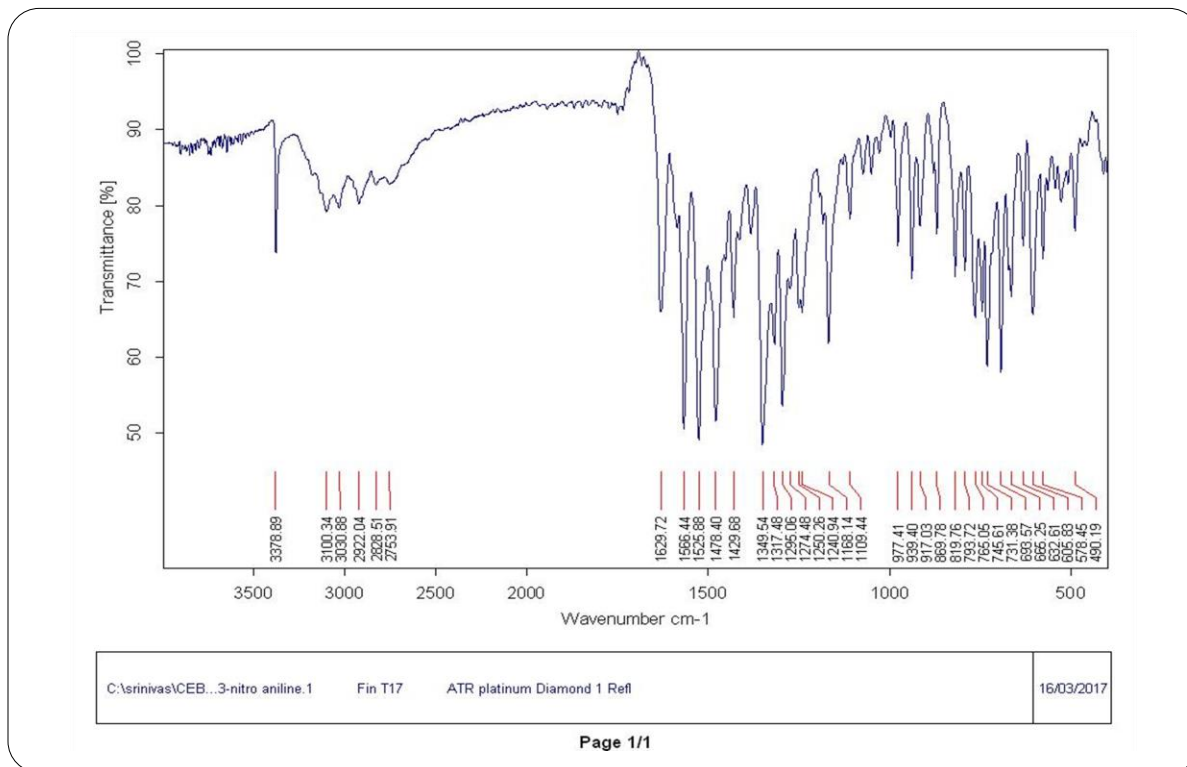


IR Spectrum of Compound 9

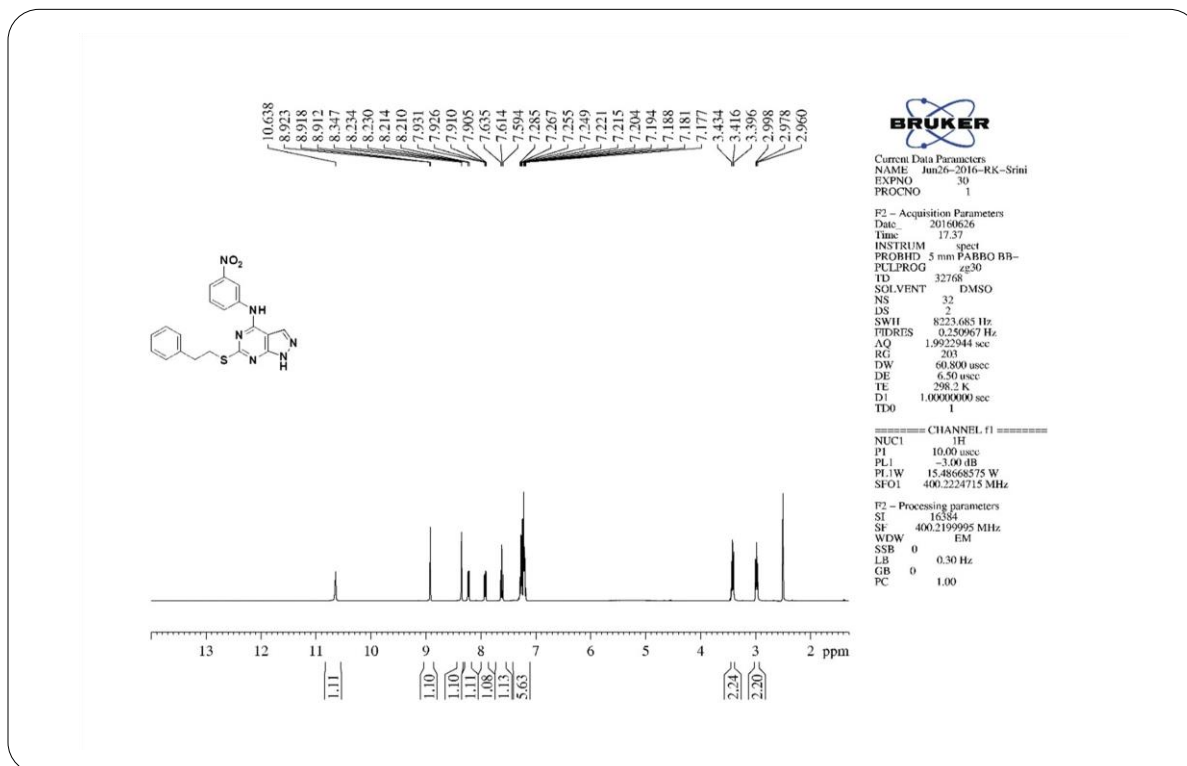
¹H NMR Spectrum of Compound 9

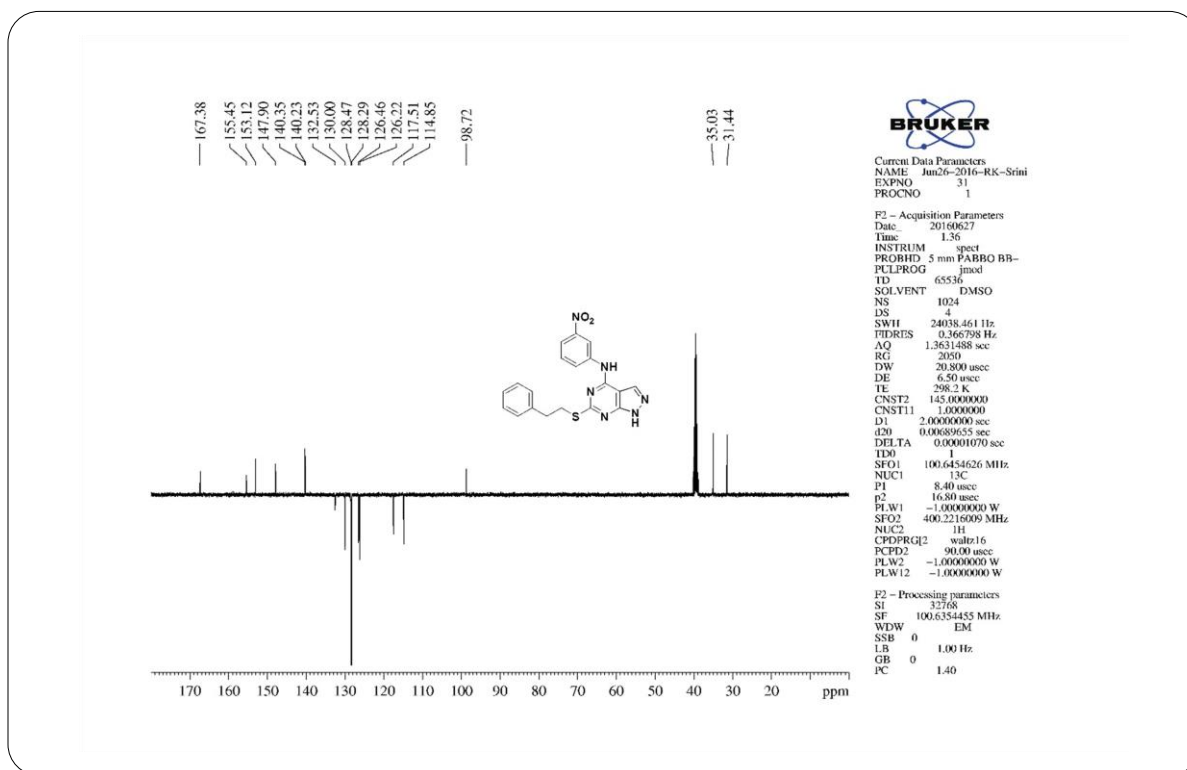
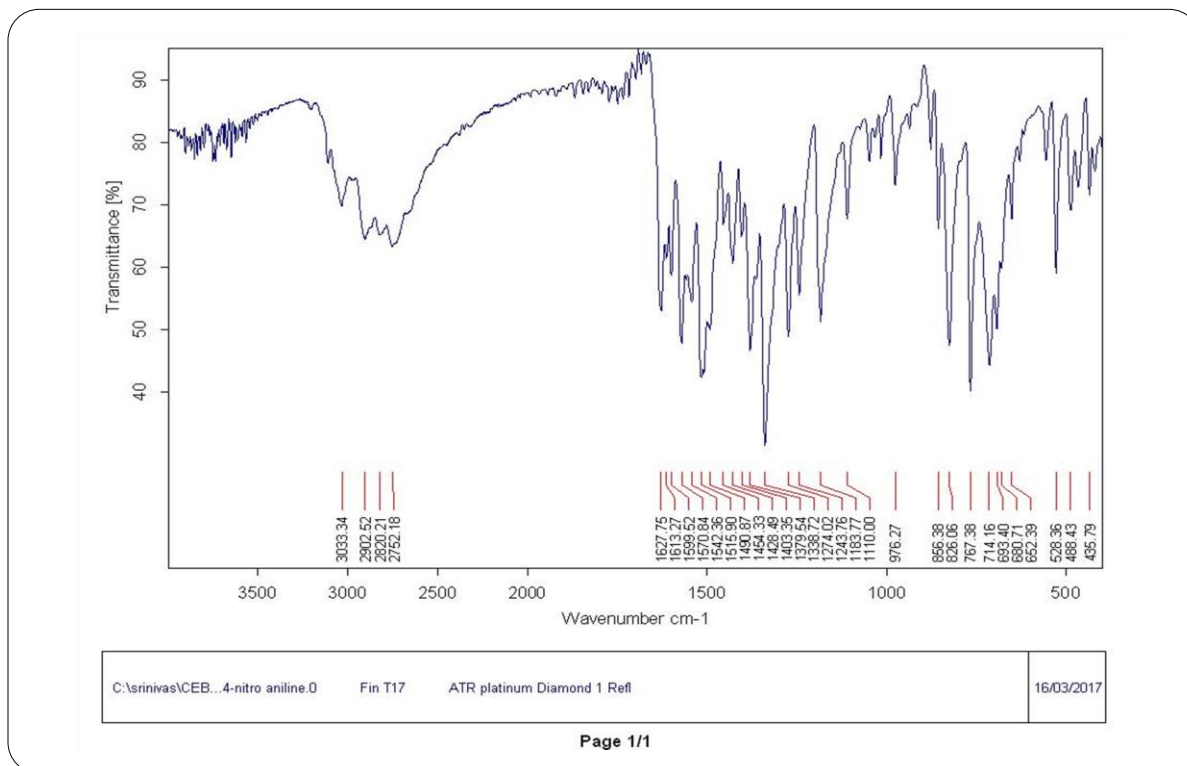
**¹³C NMR Spectrum of Compound 9****IR Spectrum of Compound 10**

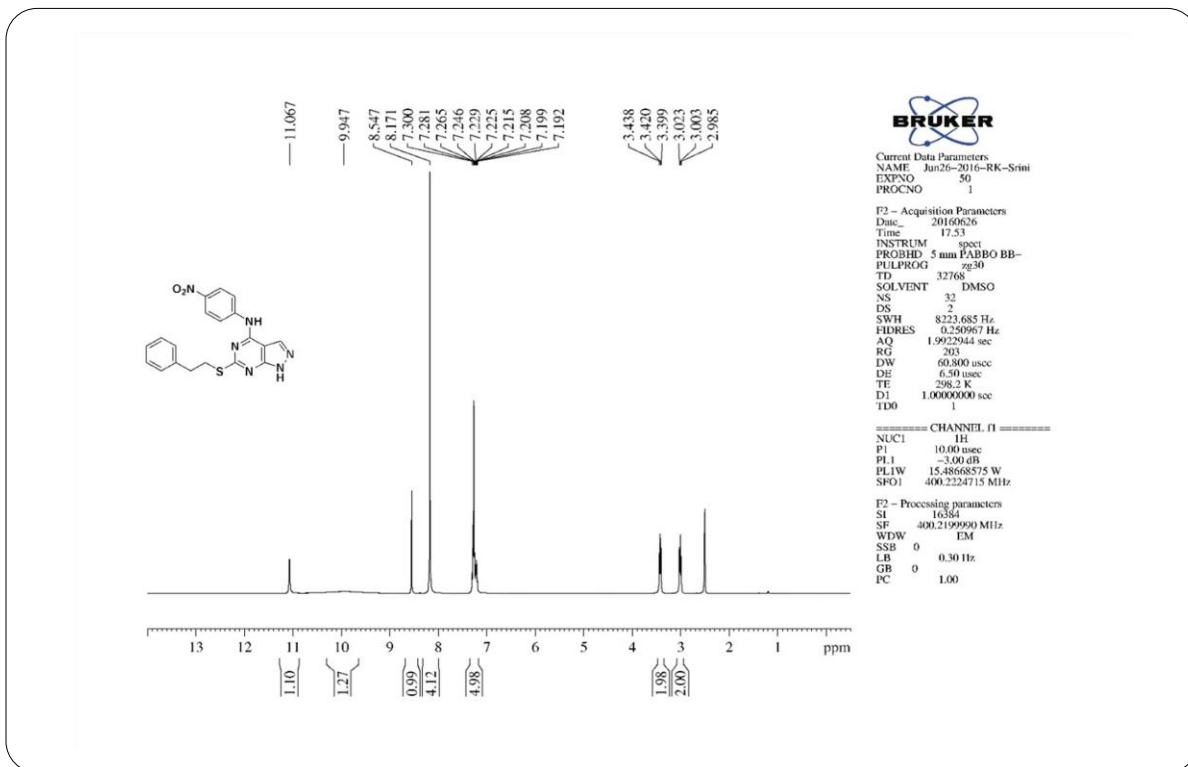
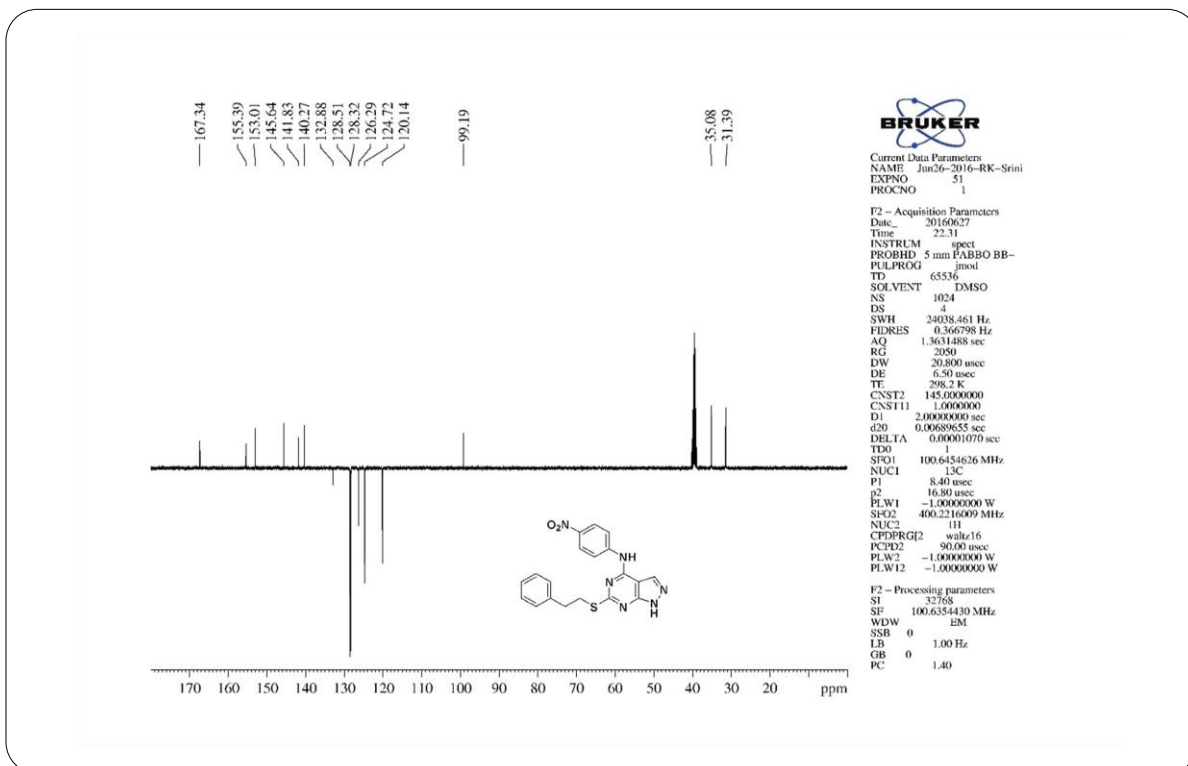
**¹H NMR Spectrum of Compound 10****¹³C NMR Spectrum of Compound 10**

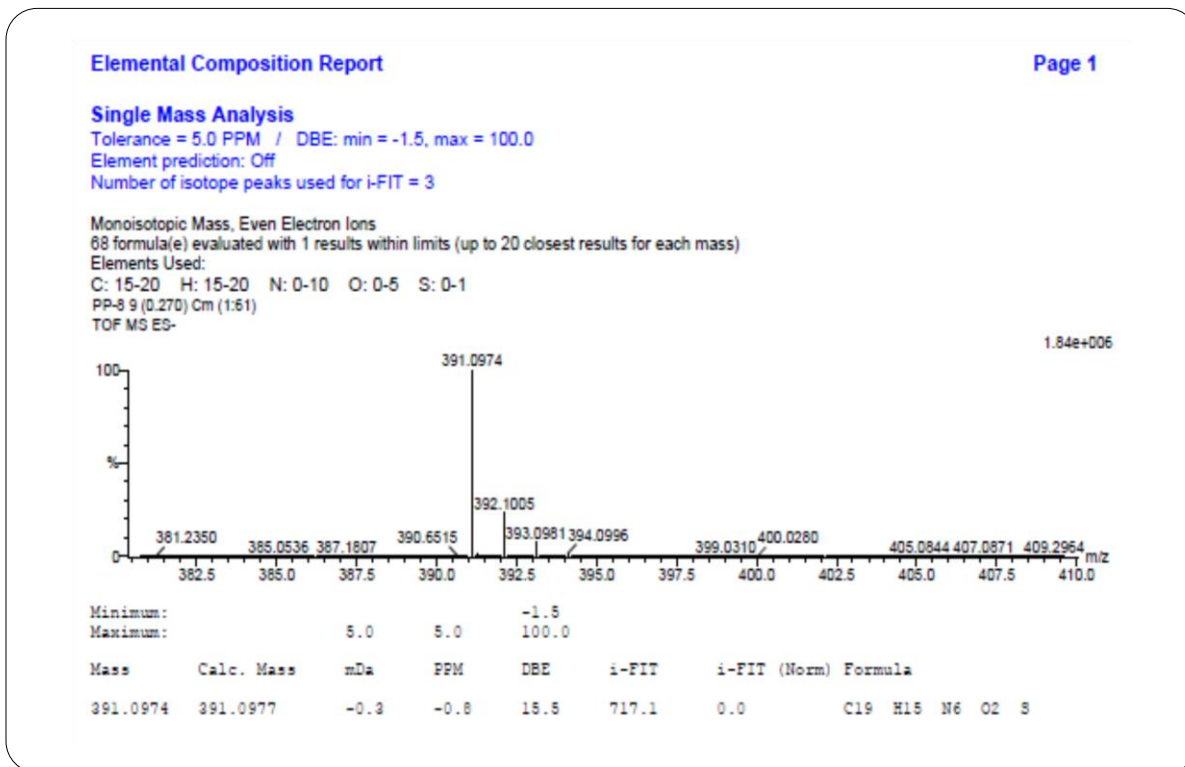


IR Spectrum of Compound 11

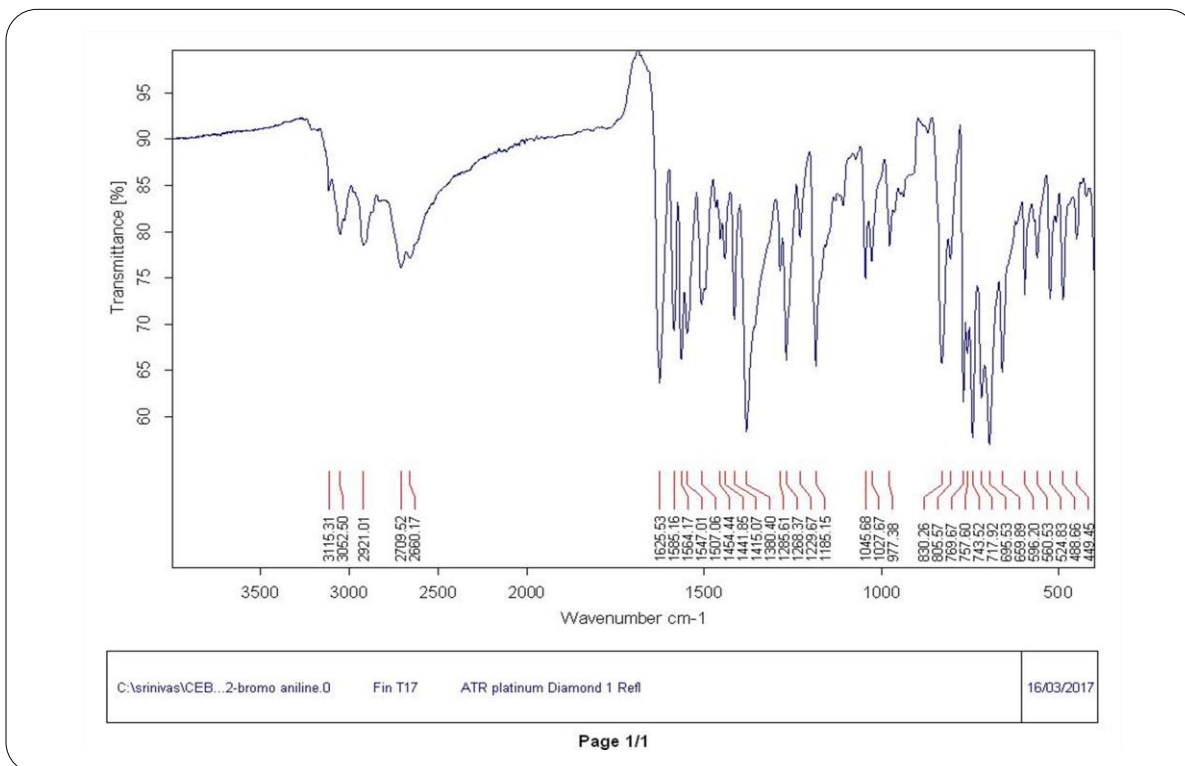
¹H NMR Spectrum of Compound 11

**¹³C NMR Spectrum of Compound 11****IR Spectrum of Compound 12**

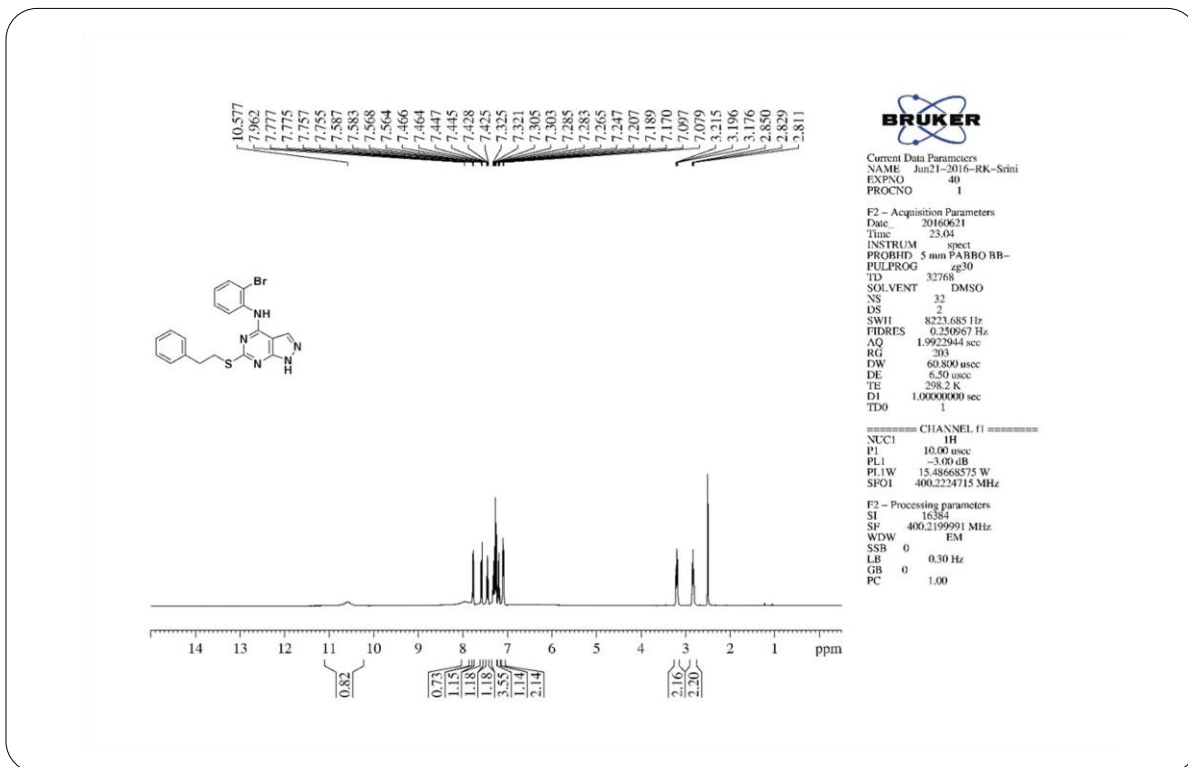
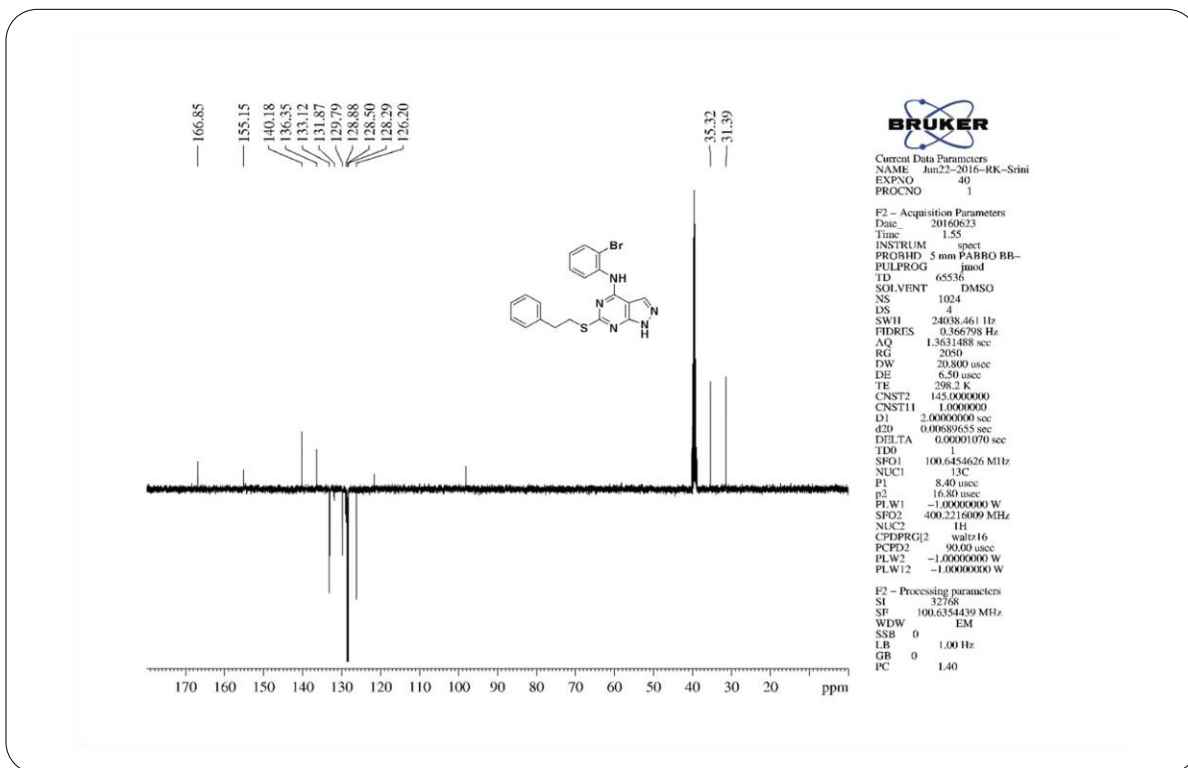
**¹H NMR Spectrum of Compound 12****¹³C NMR Spectrum of Compound 12**

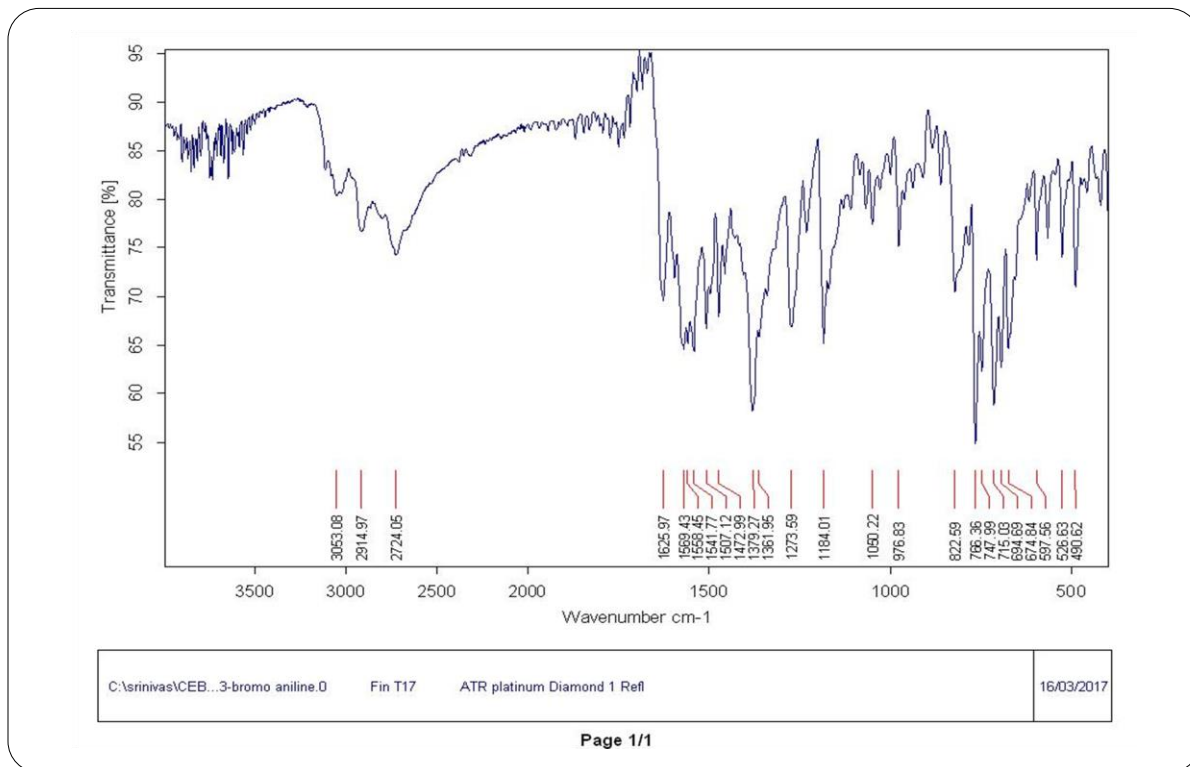


HRMS Spectrum of Compound 12

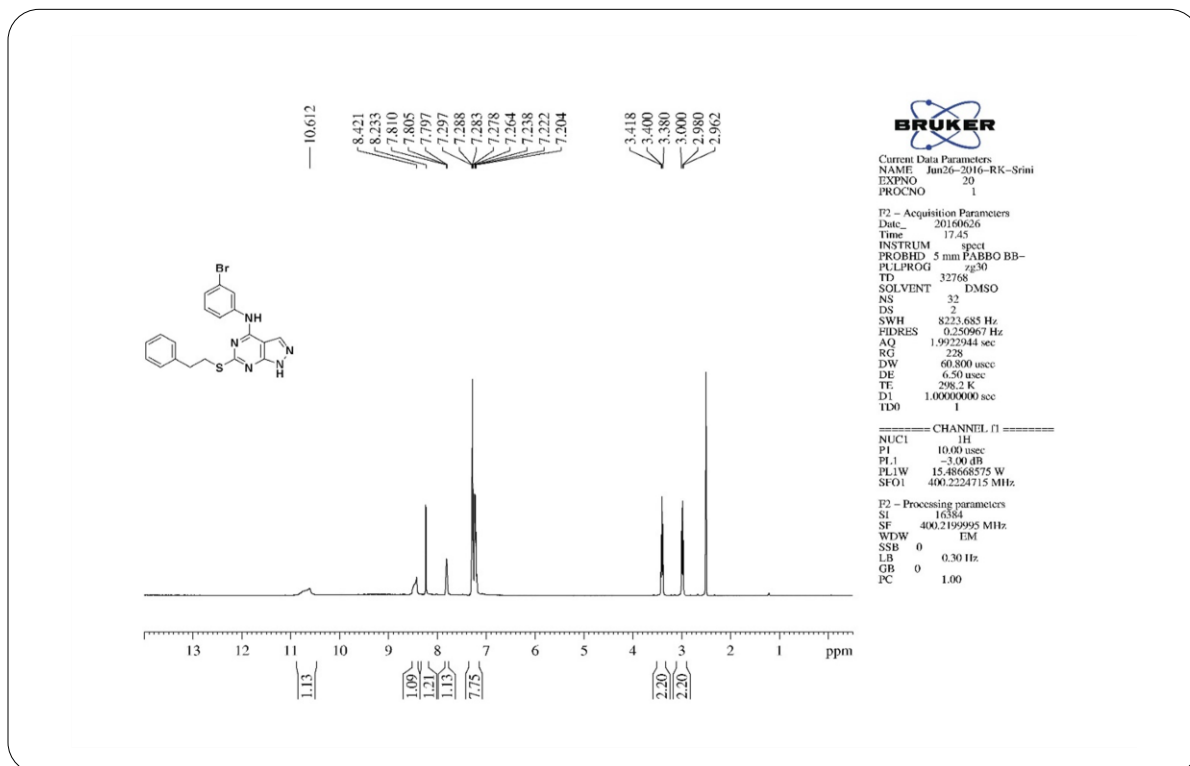


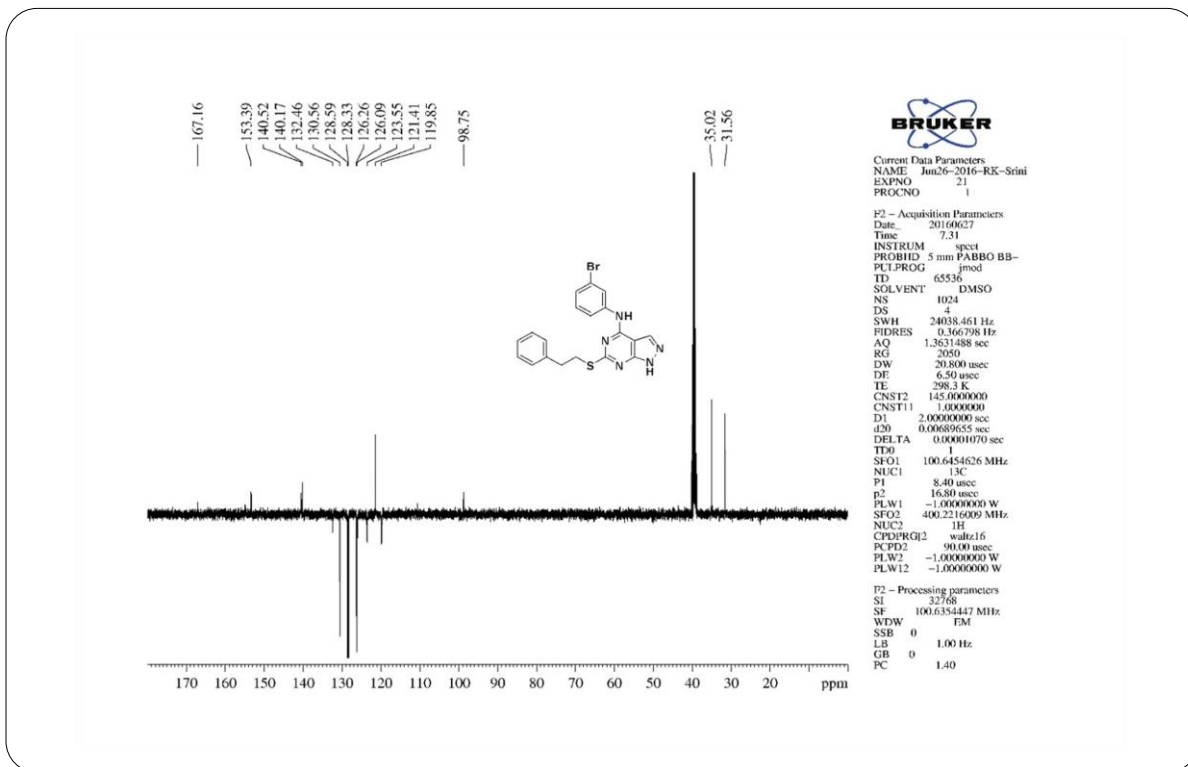
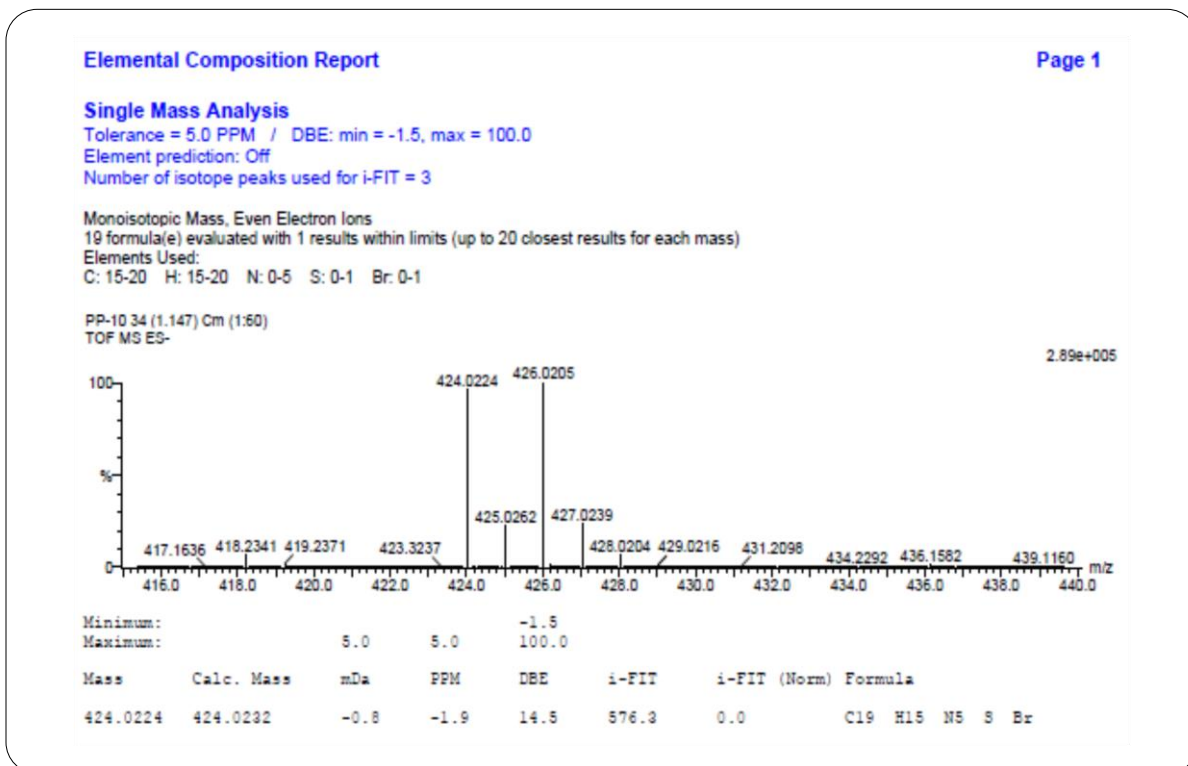
IR Spectrum of Compound 13

**¹H NMR Spectrum of Compound 13****¹³C NMR Spectrum of Compound 13**

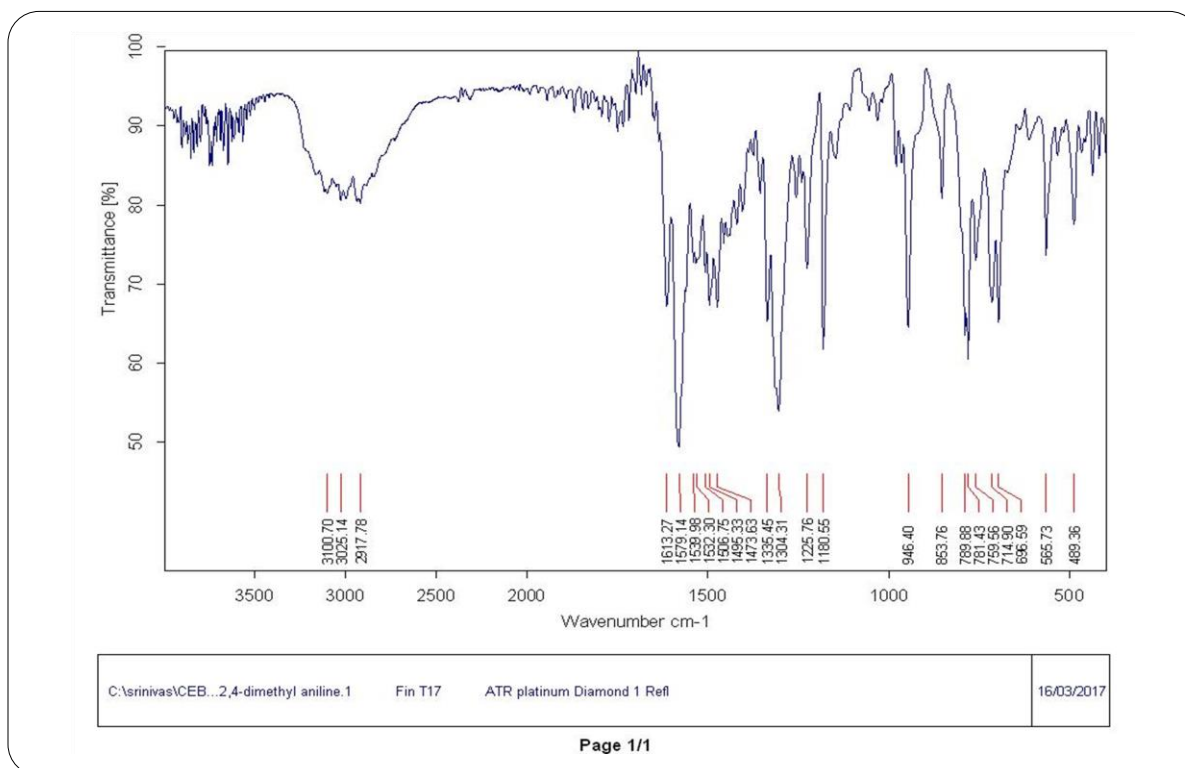


IR Spectrum of Compound 14

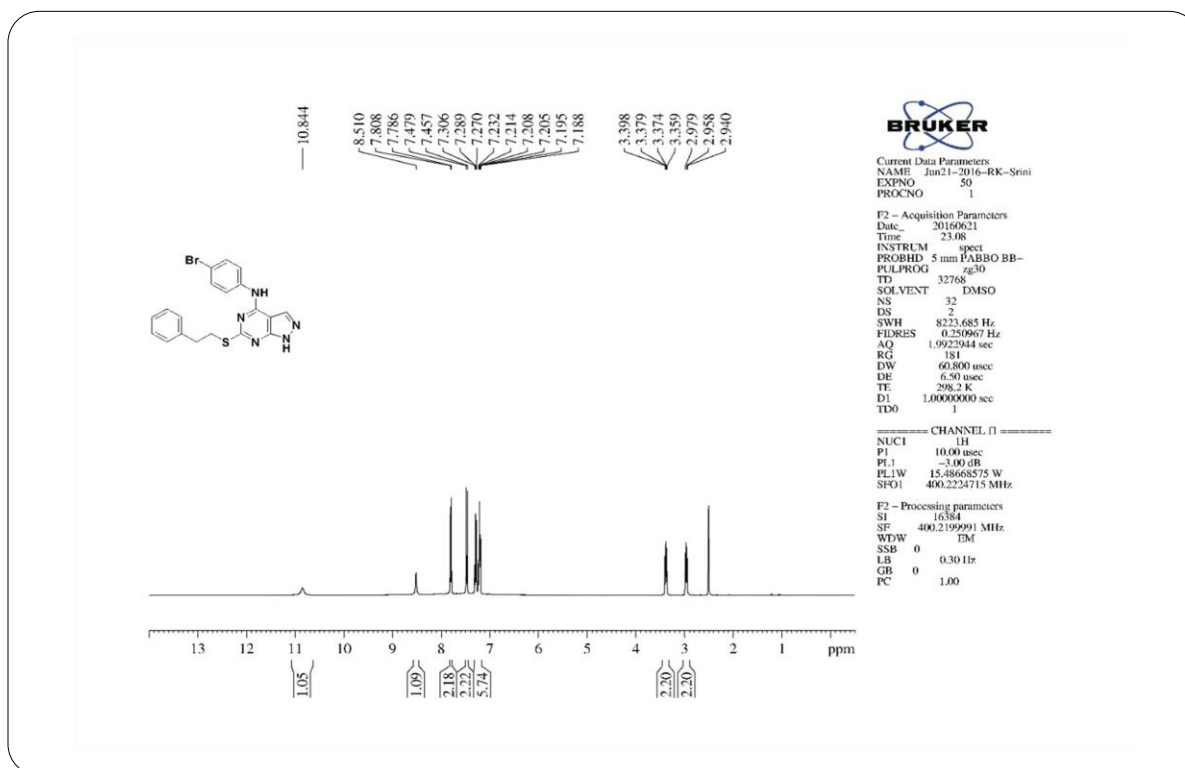
¹H NMR Spectrum of Compound 14

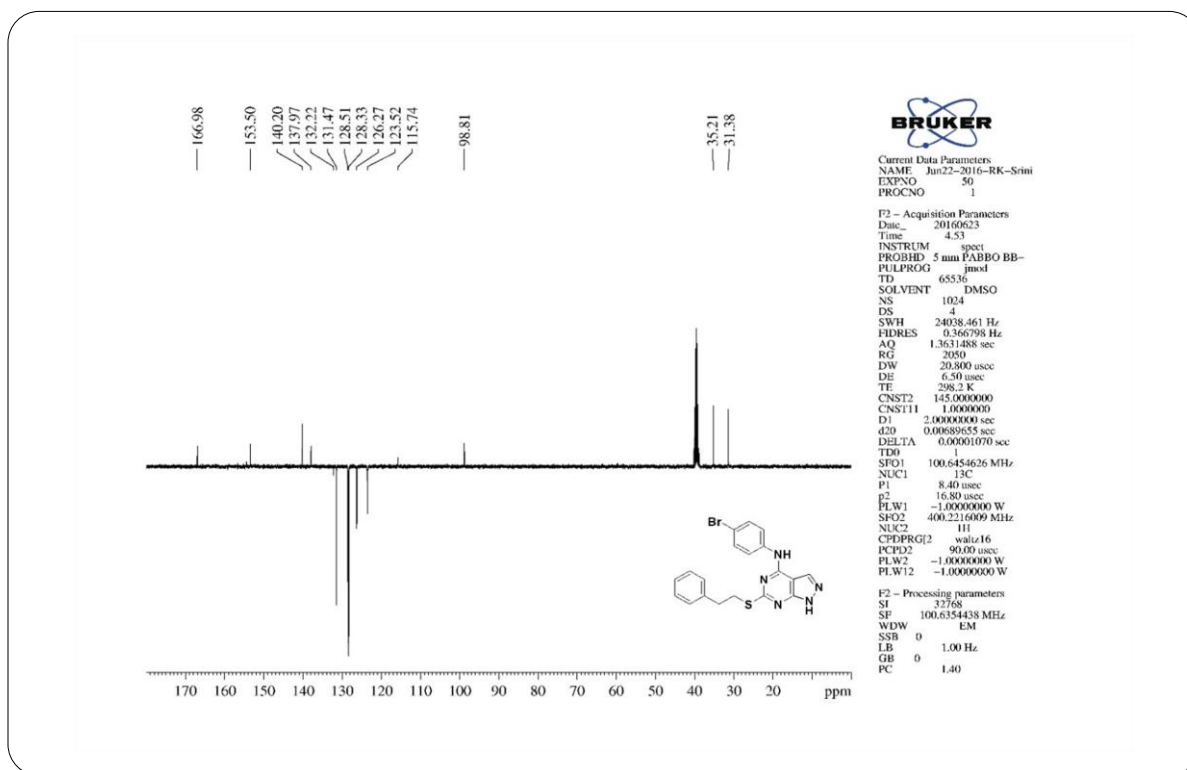
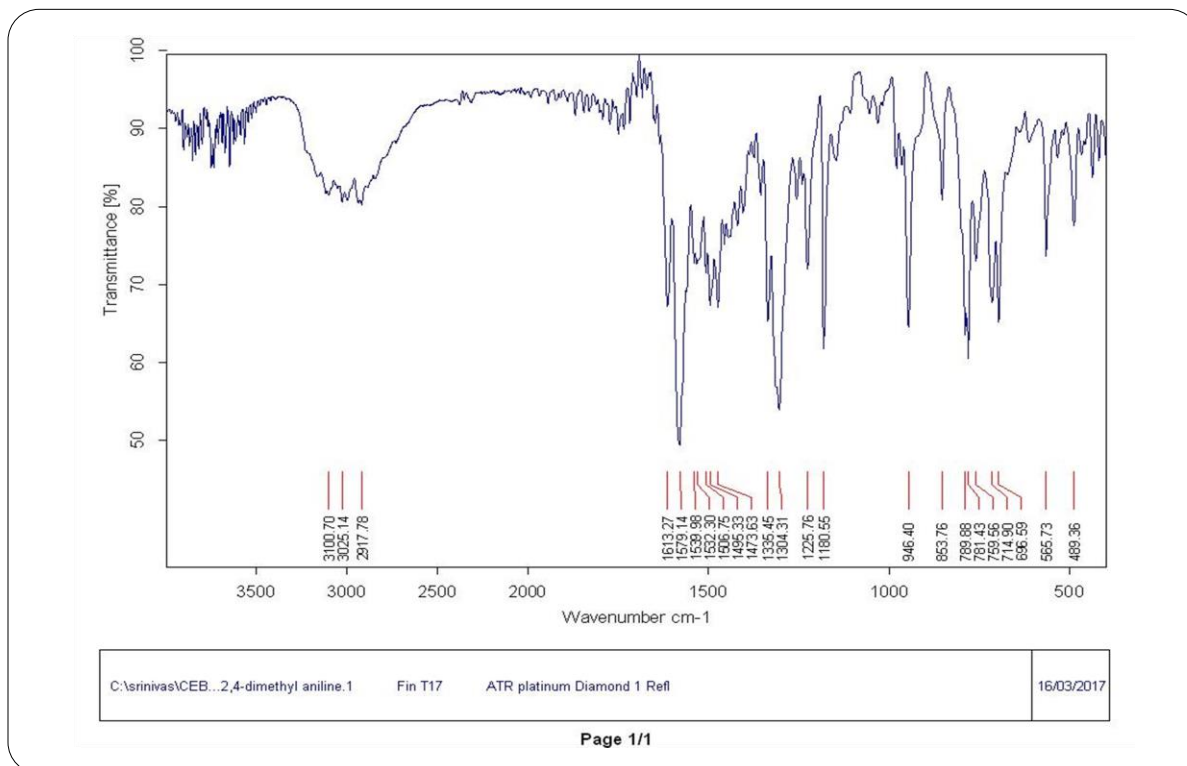
¹³C NMR Spectrum of Compound 14

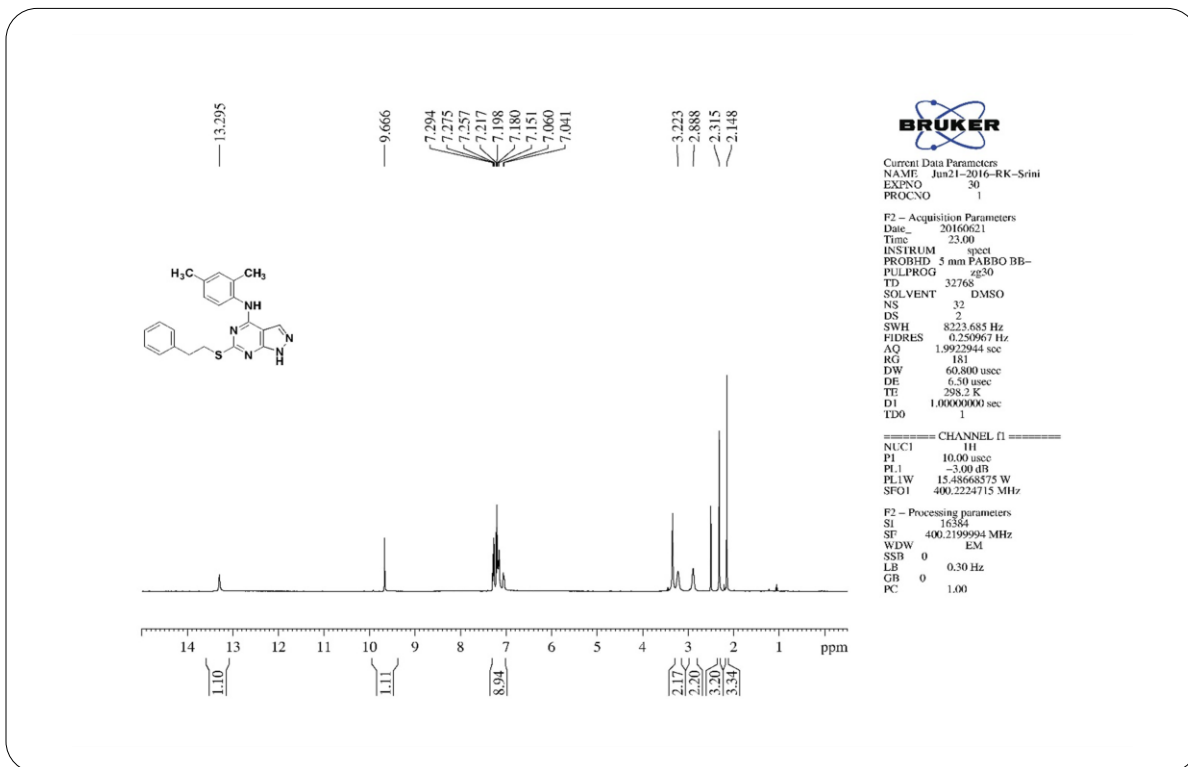
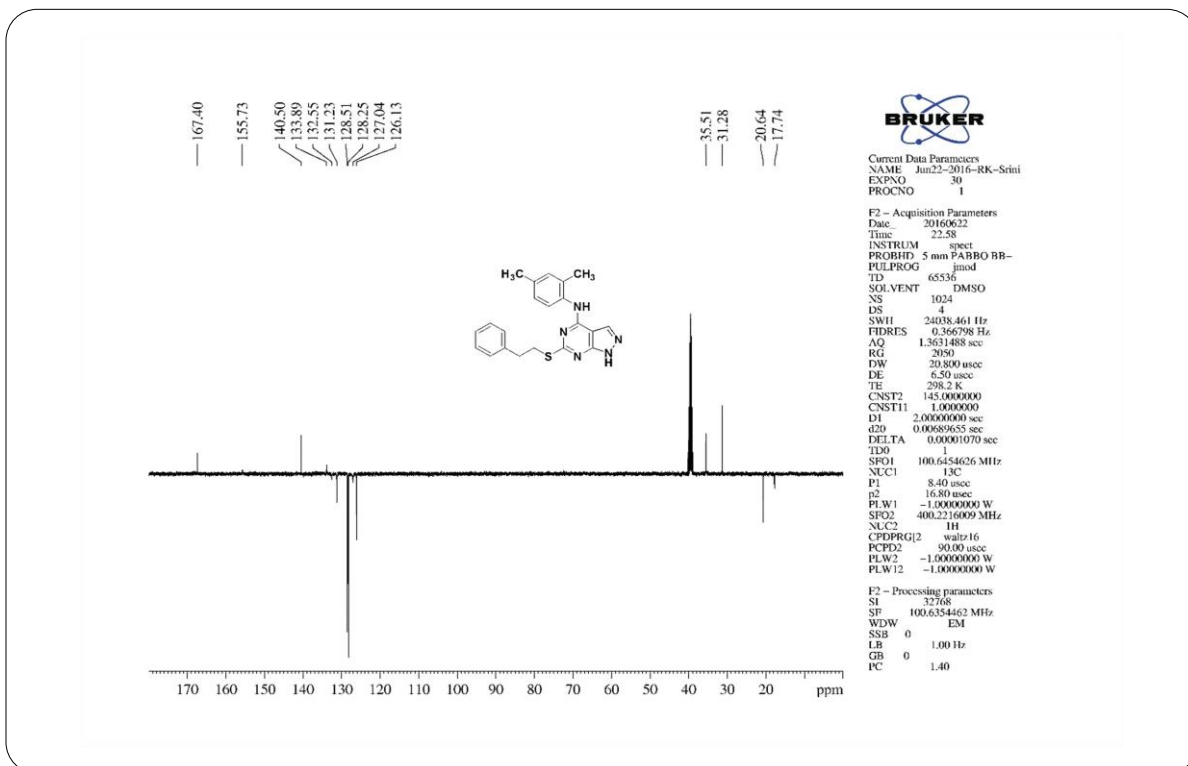
HRMS Spectrum of Compound 14



IR Spectrum of Compound 15

¹H NMR Spectrum of Compound 15

**¹³C NMR Spectrum of Compound 15****IR Spectrum of Compound 16**

¹H NMR Spectrum of Compound 16¹³C NMR Spectrum of Compound 16

Elemental Composition Report

Page 1

Single Mass Analysis

Tolerance = 5.0 PPM / DBE: min = -1.5, max = 100.0

Element prediction: Off

Number of isotope peaks used for i-FIT = 3

Monoisotopic Mass, Even Electron Ions

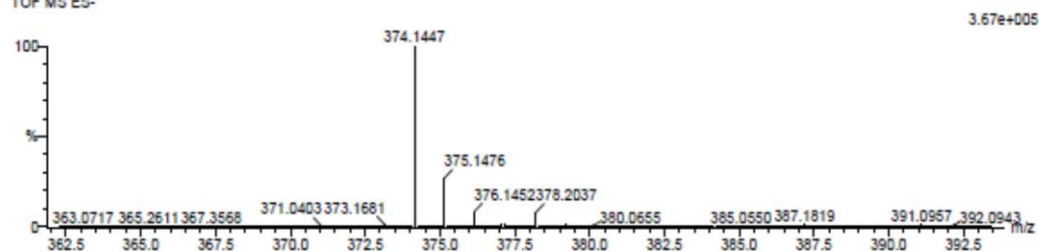
4 formula(e) evaluated with 1 results within limits (up to 20 closest results for each mass)

Elements Used:

C: 15-25 H: 15-20 N: 0-5 S: 0-1

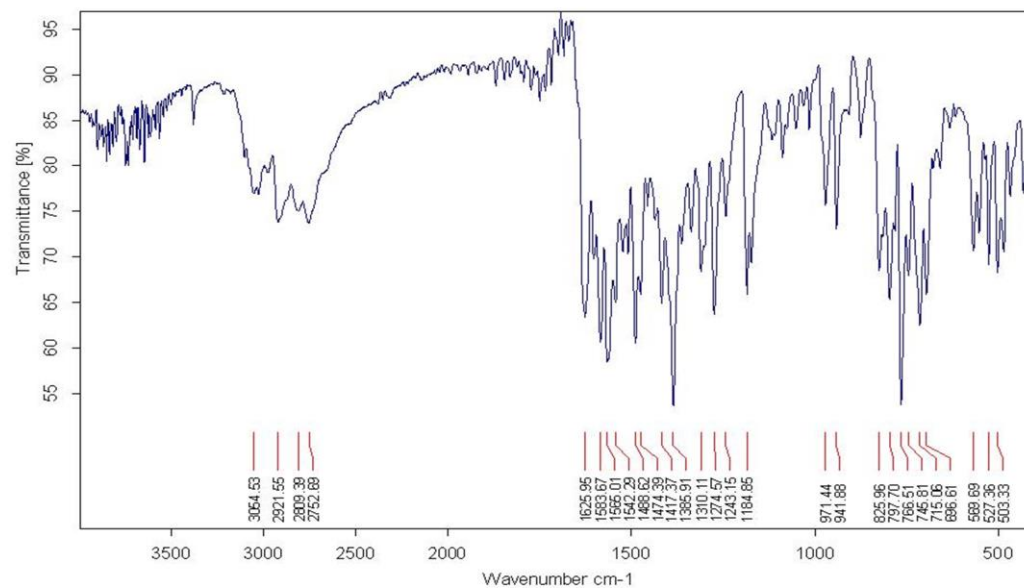
PP-12 34 (1.114) Cm (1:61)

TOF MS ES-



Mass	Calc. Mass	mDa	PPM	DBE	i-FIT	i-FIT (Norm)	Formula
374.1447	374.1439	0.8	2.1	14.5	699.2	0.0	C21 H20 N5 S

HRMS Spectrum of Compound 16

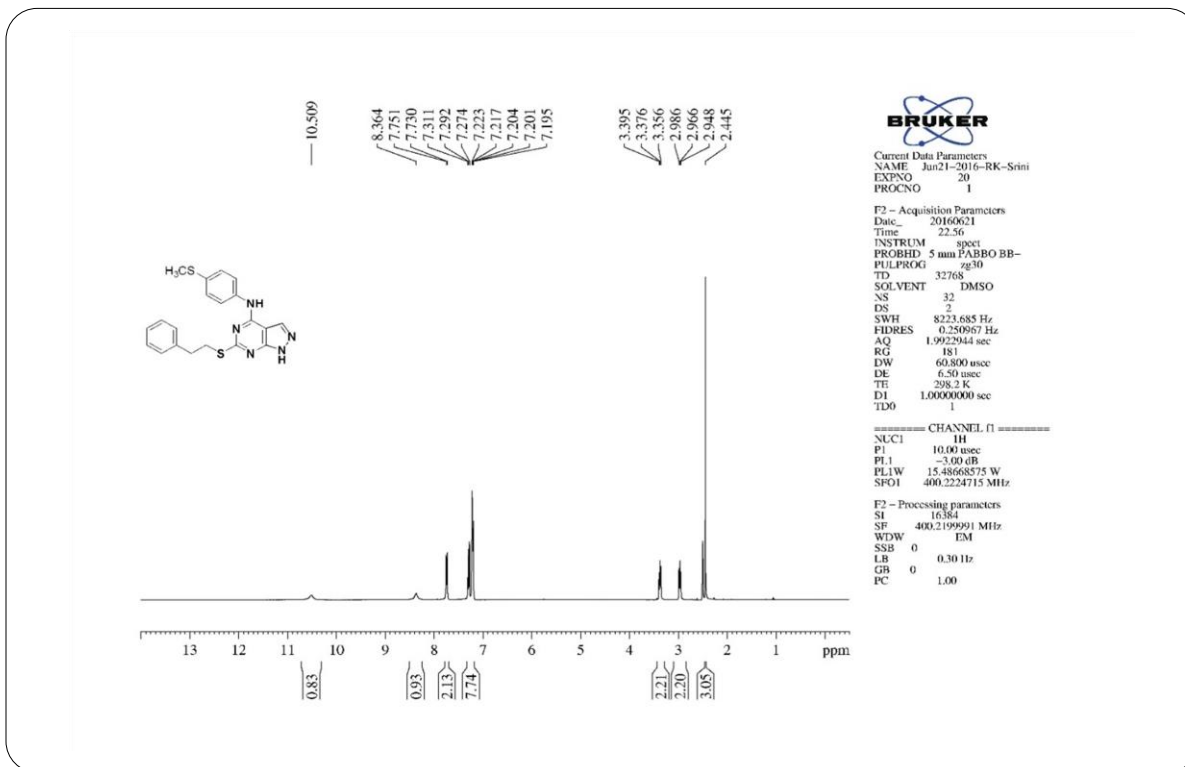
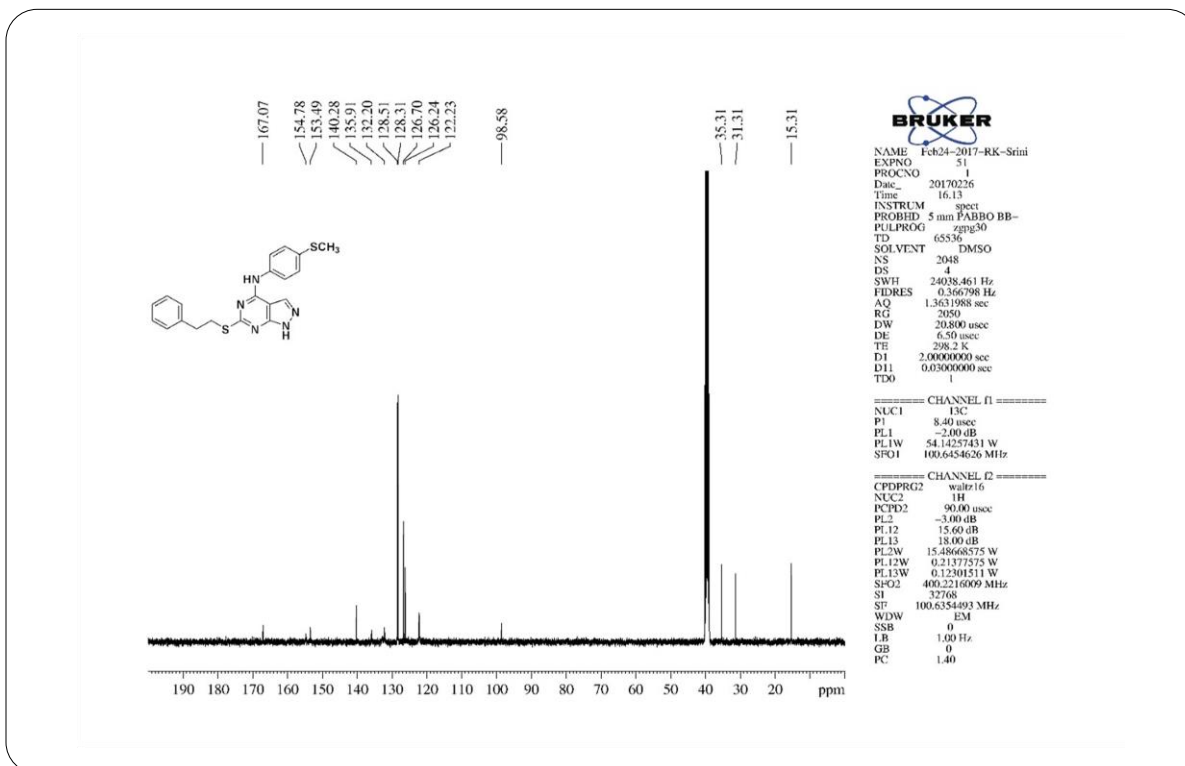


C:\srinivas\CEB...4-methylthio aniline.D Fin T17 ATR platinum Diamond 1 Ref

16/03/2017

Page 1/1

IR Spectrum of Compound 17

**¹H NMR Spectrum of Compound 17****¹³C NMR Spectrum of Compound 17**

Elemental Composition Report

Page 1

Single Mass Analysis

Tolerance = 5.0 PPM / DBE: min = -1.5, max = 100.0

Element prediction: Off

Number of isotope peaks used for i-FIT = 3

Monoisotopic Mass, Even Electron Ions

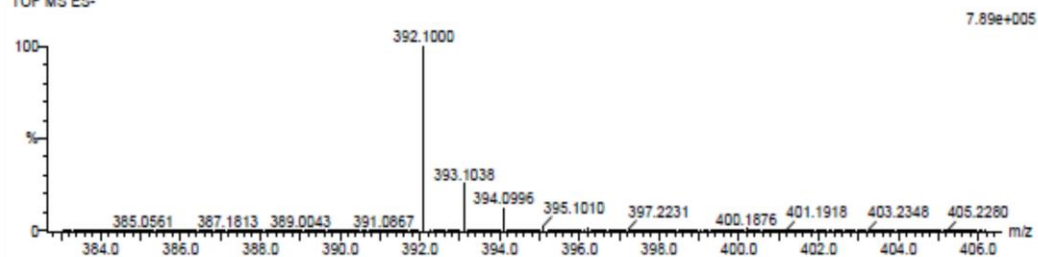
14 formula(e) evaluated with 1 results within limits (up to 20 closest results for each mass)

Elements Used:

C: 15-20 H: 15-20 N: 0-5 S: 0-2

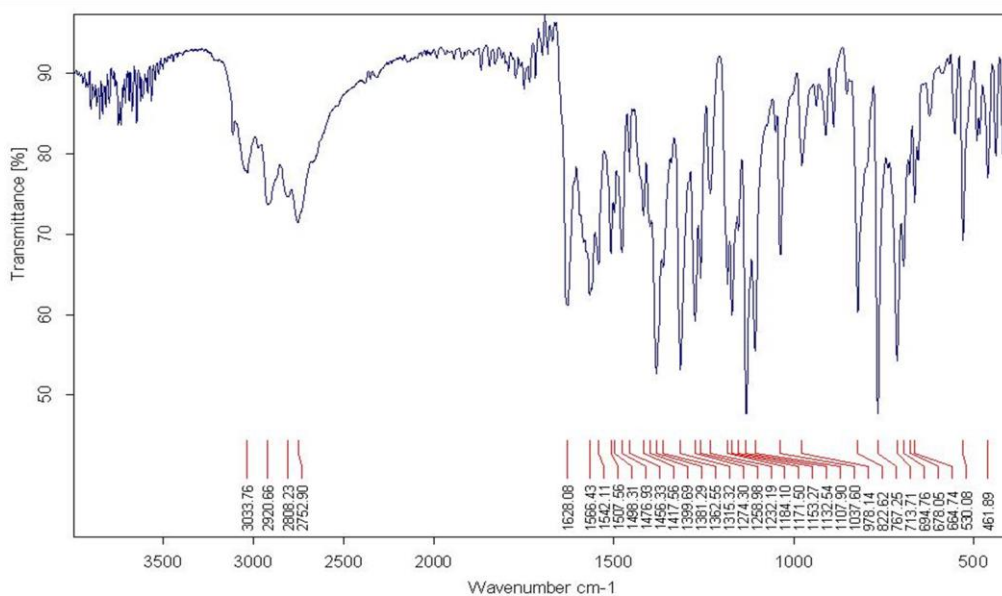
PP-13 2 (0.034) Cm (1.61)

TOF MS ES-



Mass	Calc. Mass	mDa	PPM	DBE	i-FIT	i-FIT (Norm)	Formula
392.1000	392.1004	-0.4	-1.0	14.5	675.3	0.0	C20 H18 N5 S2

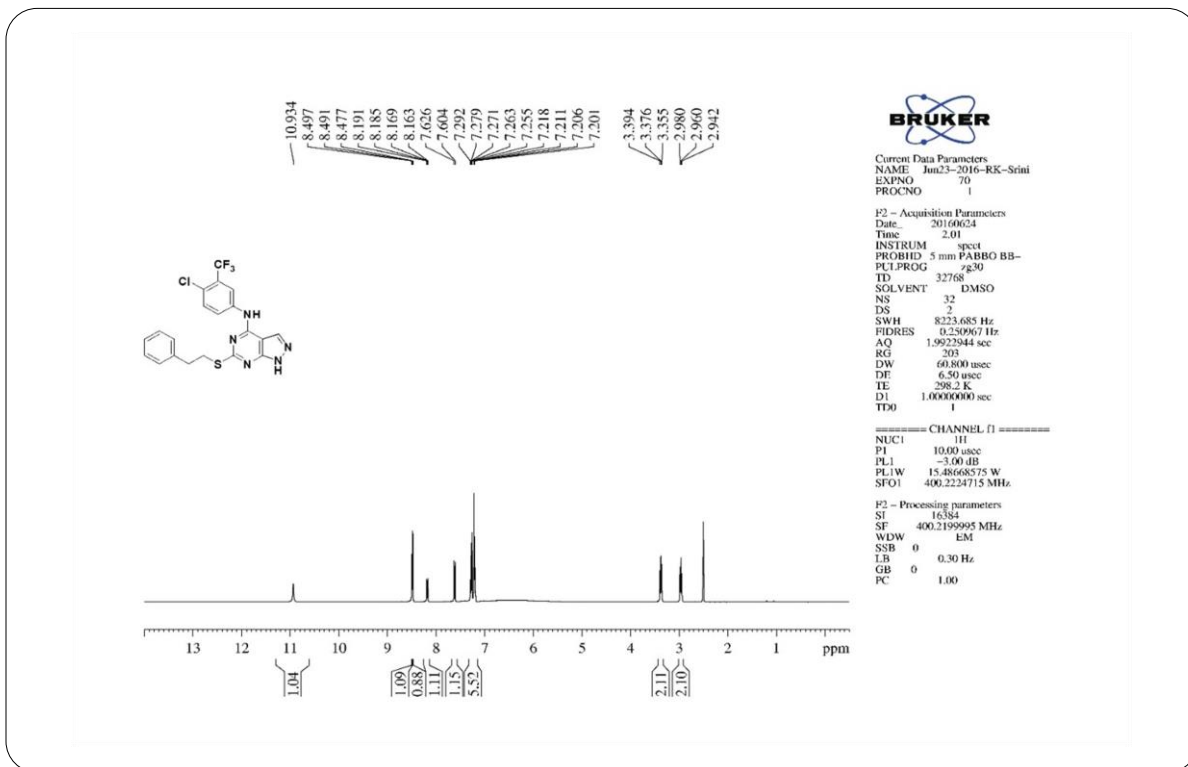
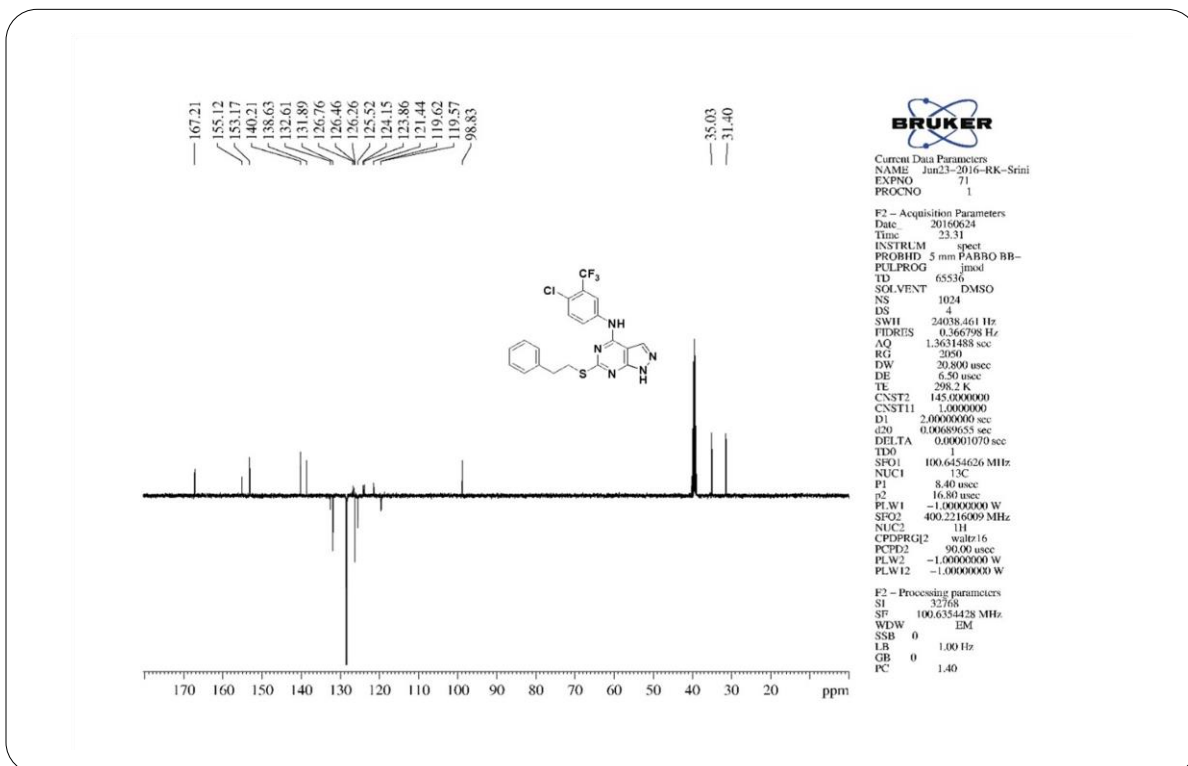
HRMS Spectrum of Compound 17

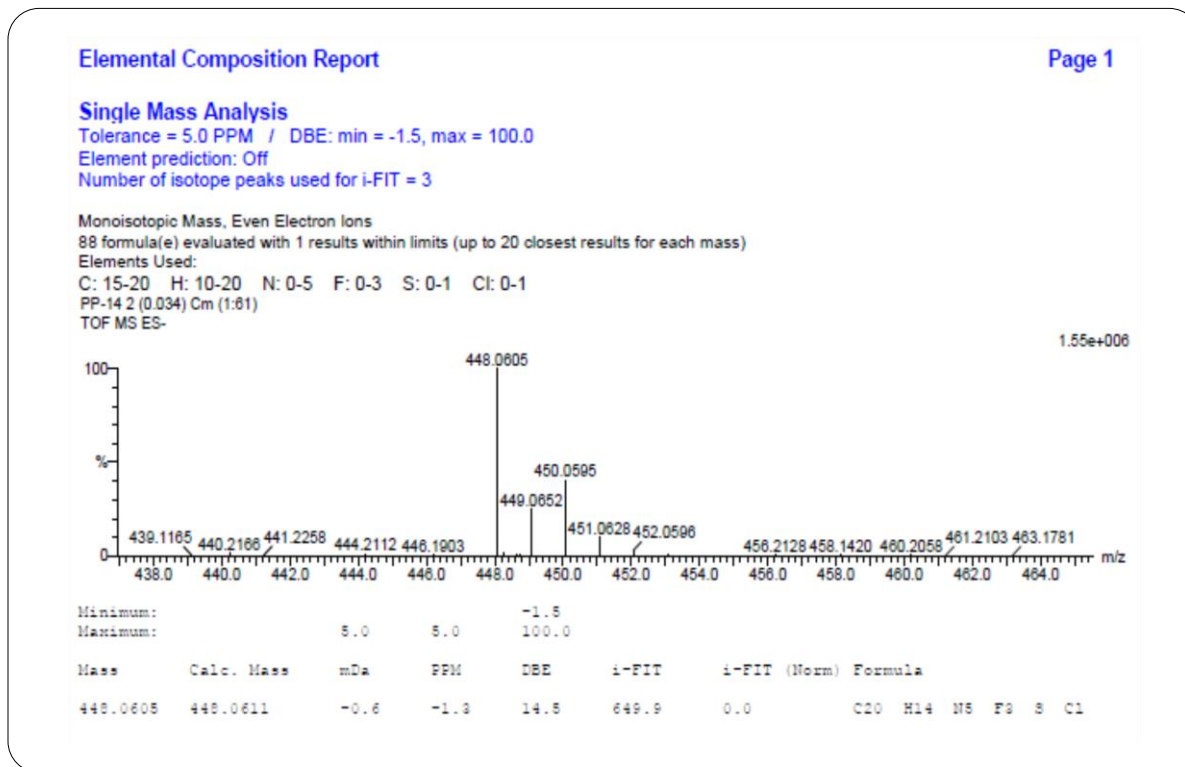


C:\srinivas\CEB...4-chloro-3-CF3 aniline.D Fin T17 ATR platinum Diamond 1 Refl 16/03/2017

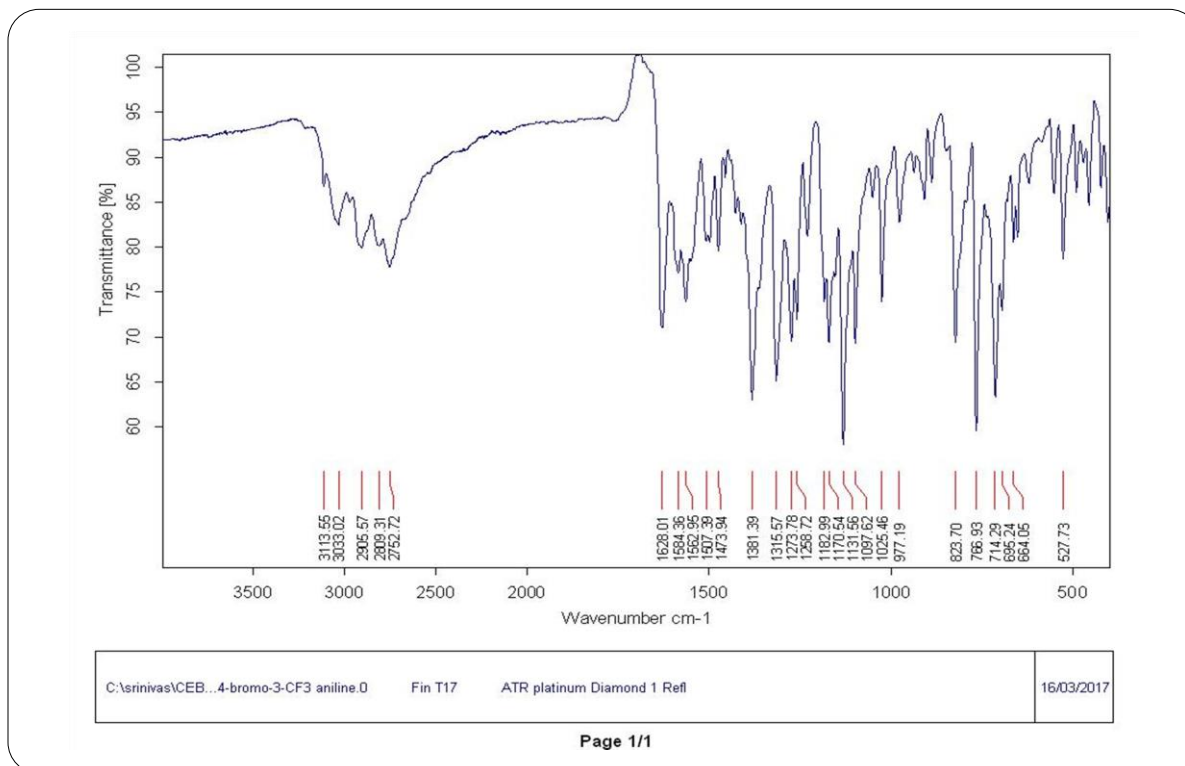
Page 1/1

IR Spectrum of Compound 18

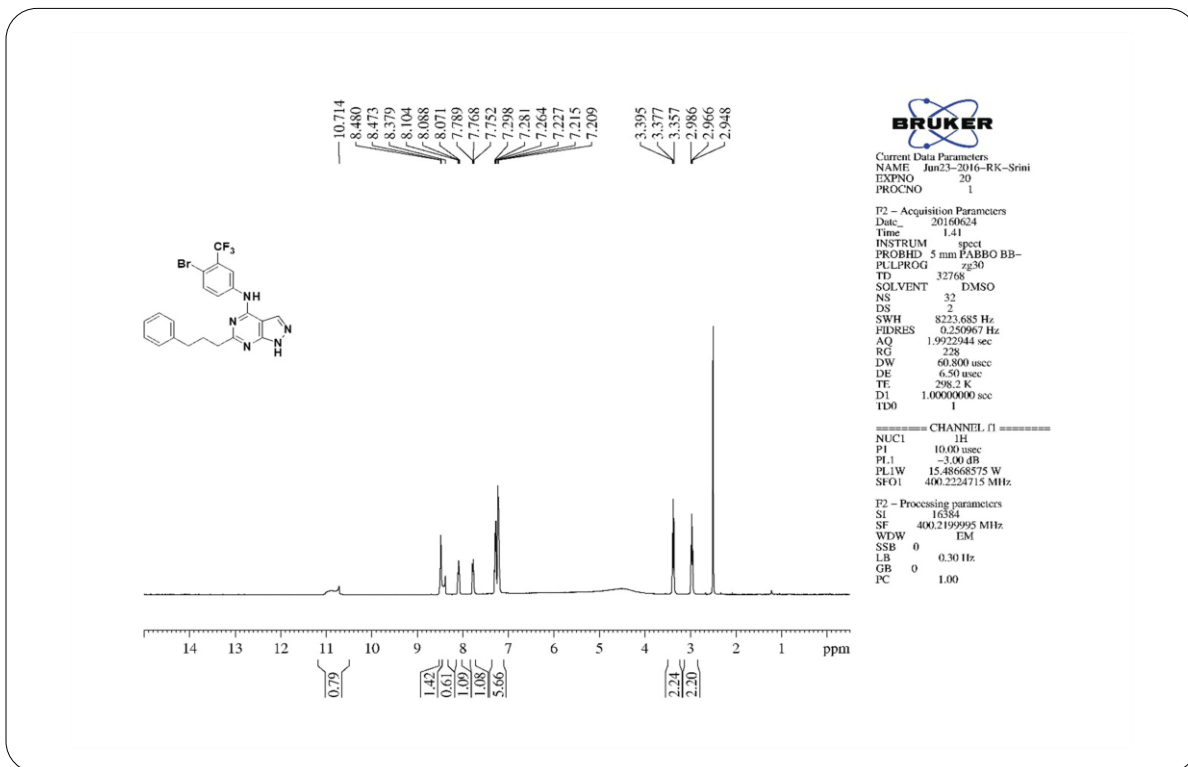
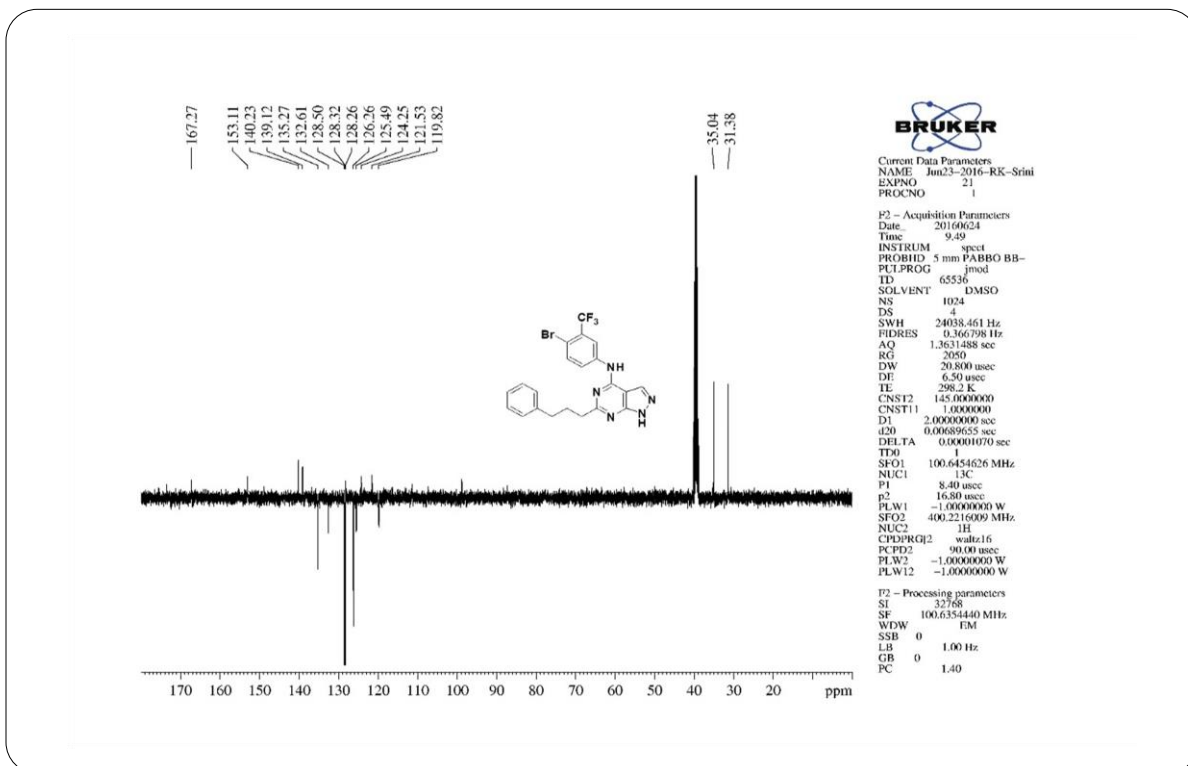
**¹H NMR Spectrum of Compound 18****¹³C NMR Spectrum of Compound 18**

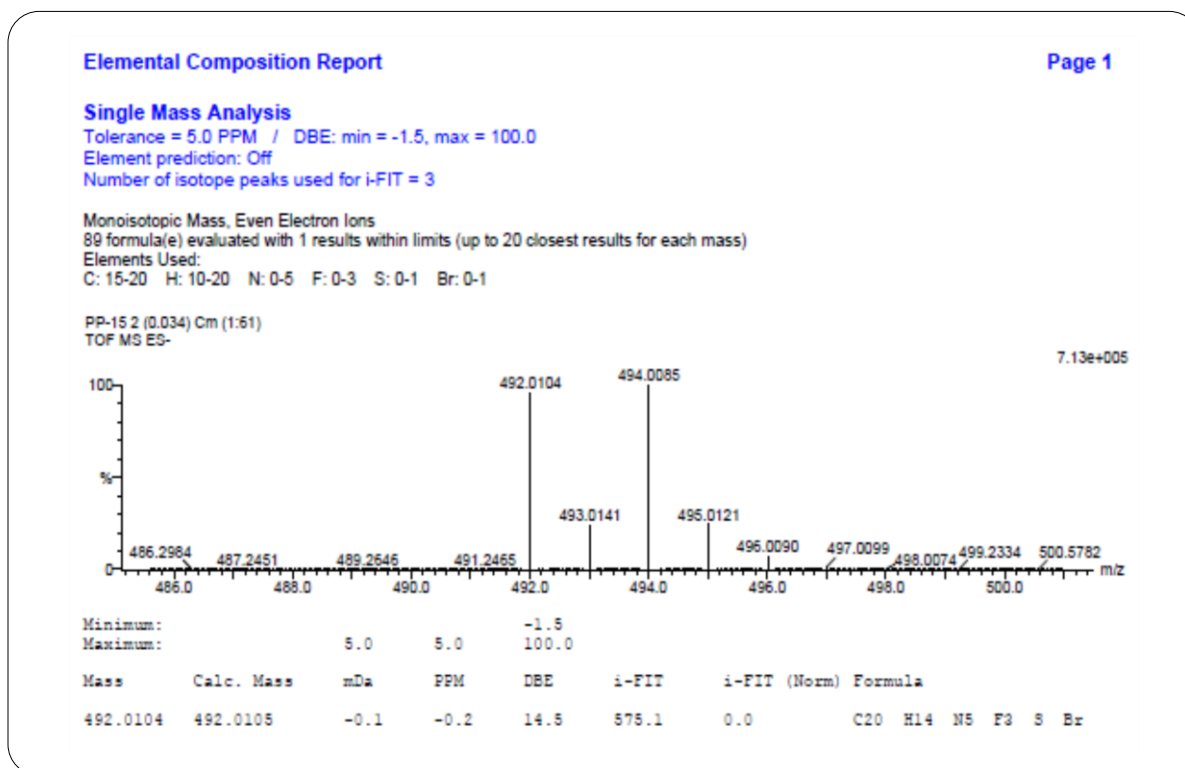


HRMS Spectrum of Compound 18

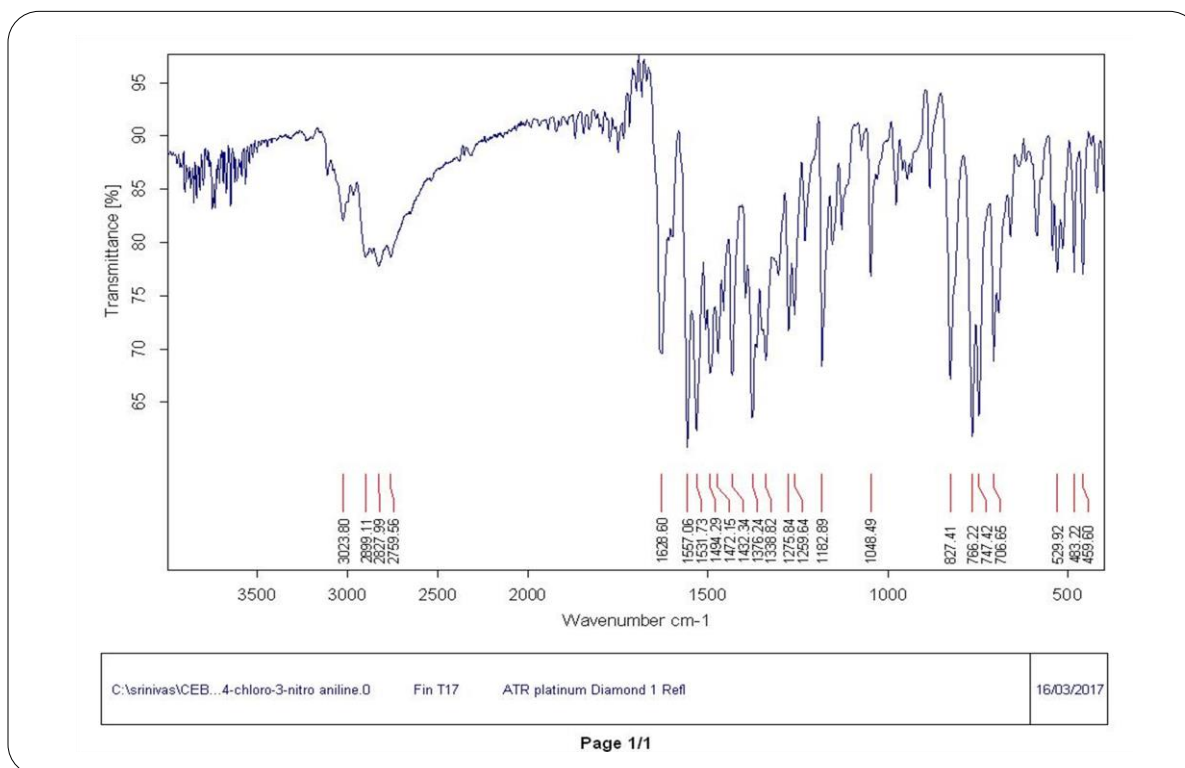


IR Spectrum of Compound 19

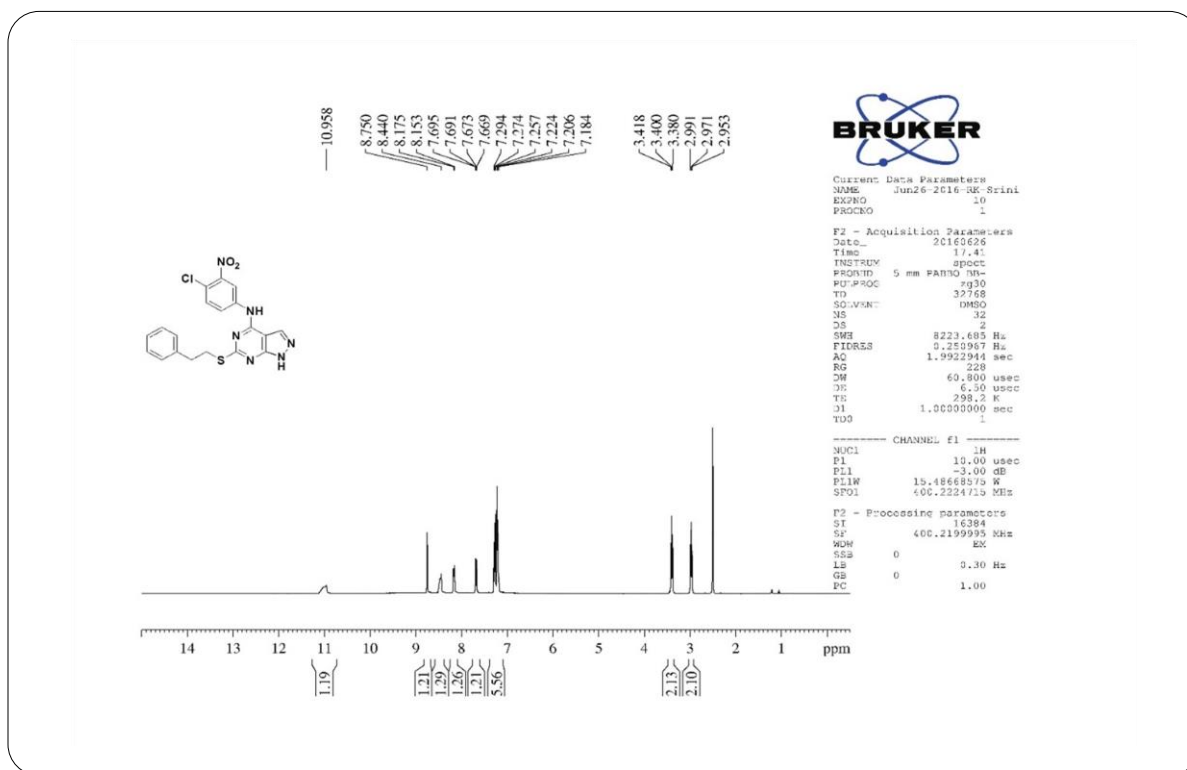
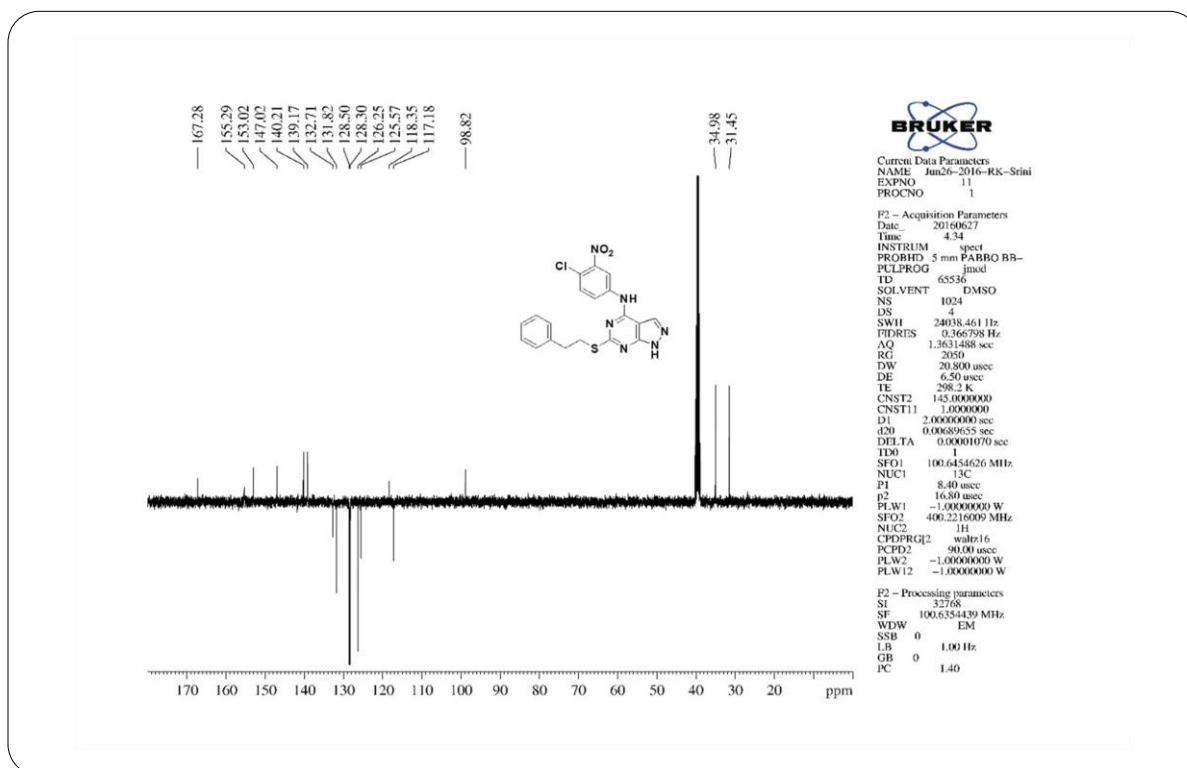
**¹H NMR Spectrum of Compound 19****¹³C NMR Spectrum of Compound 19**

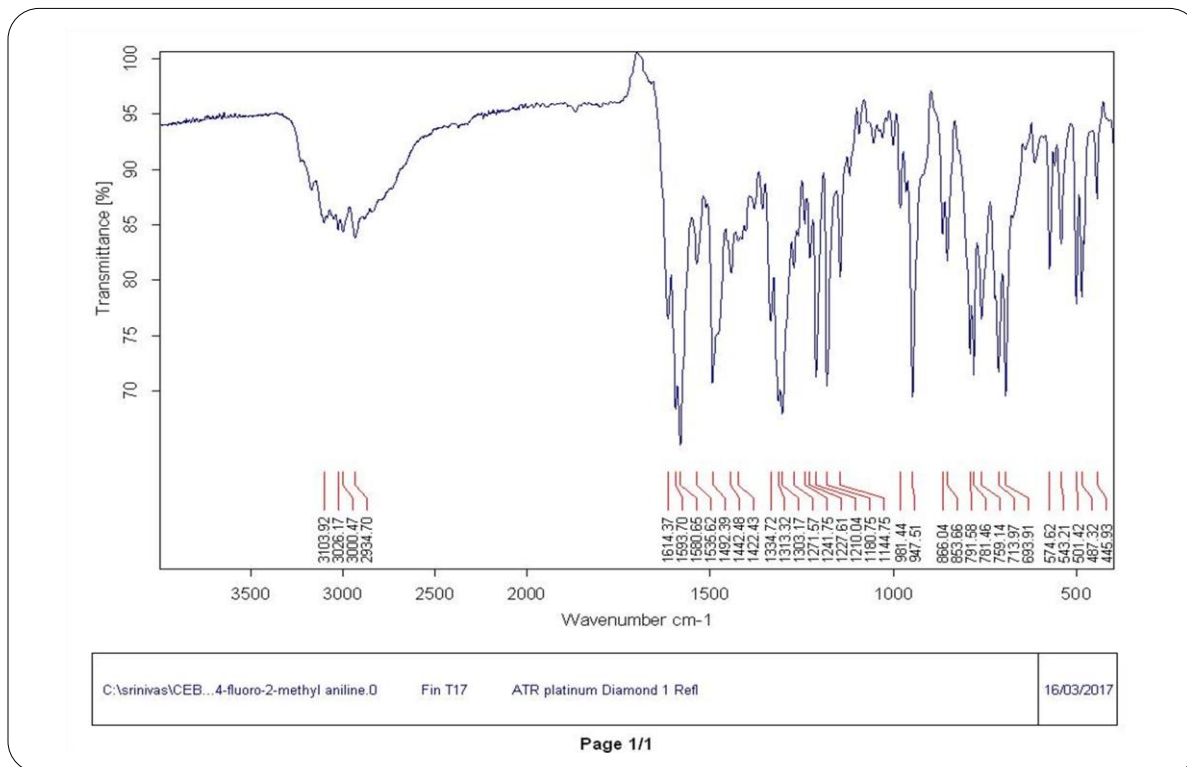


HRMS Spectrum of Compound 19

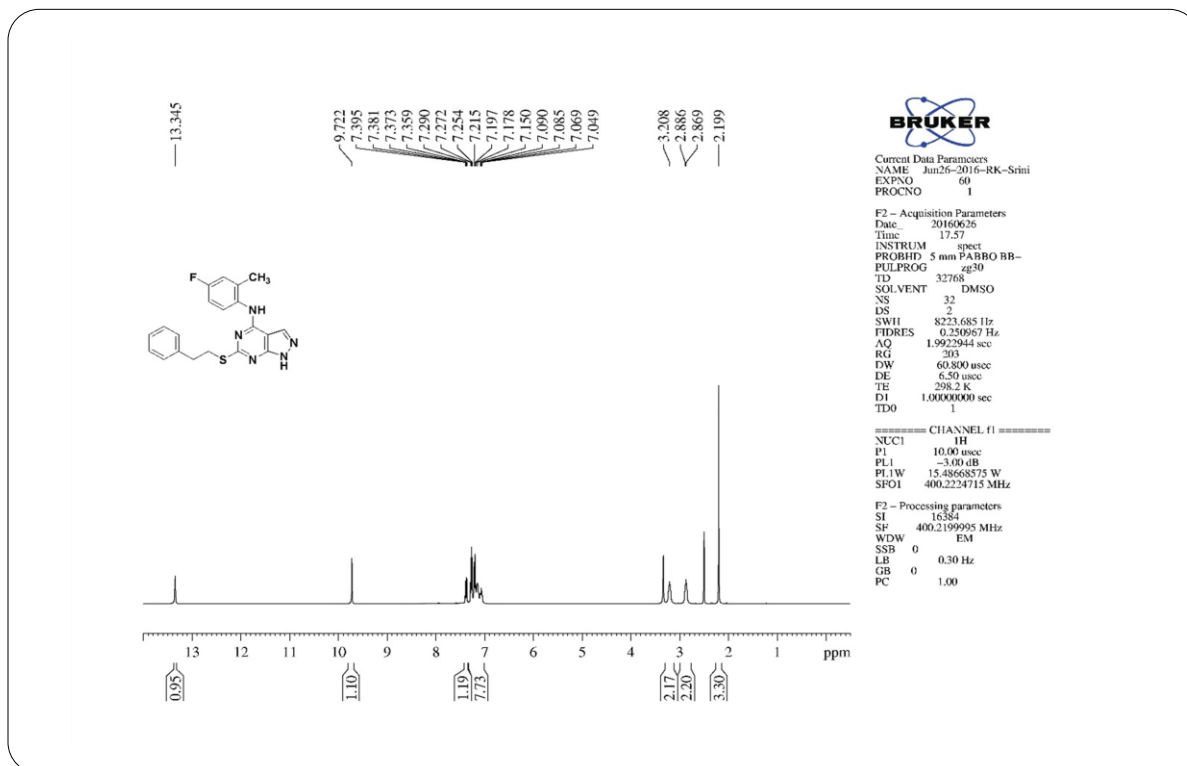


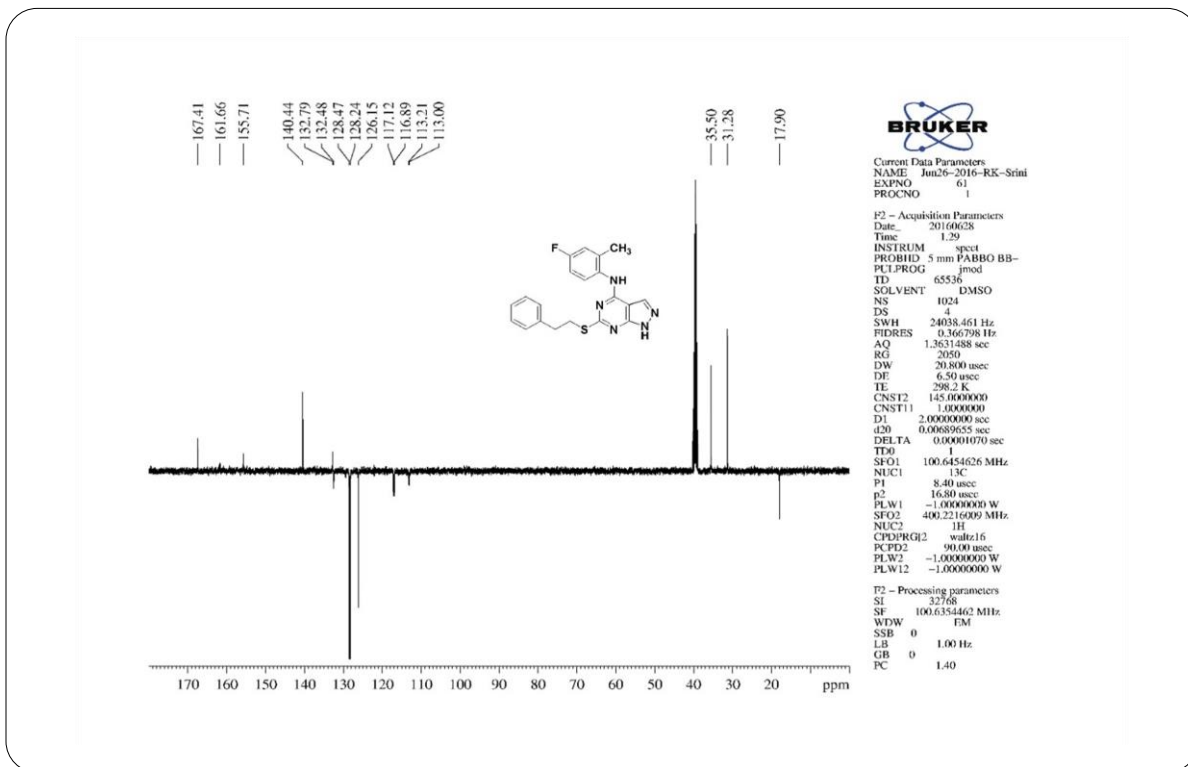
IR Spectrum of Compound 20

**¹H NMR Spectrum of Compound 20****¹³C NMR Spectrum of Compound 20**



IR Spectrum of Compound 21

¹H NMR Spectrum of Compound 21

¹³C NMR Spectrum of Compound 21

Elemental Composition Report

Page 1

Single Mass Analysis

Tolerance = 5.0 PPM / DBE: min = -1.5, max = 100.0

Element prediction: Off

Number of isotope peaks used for i-FIT = 3

Monoisotopic Mass, Even Electron Ions

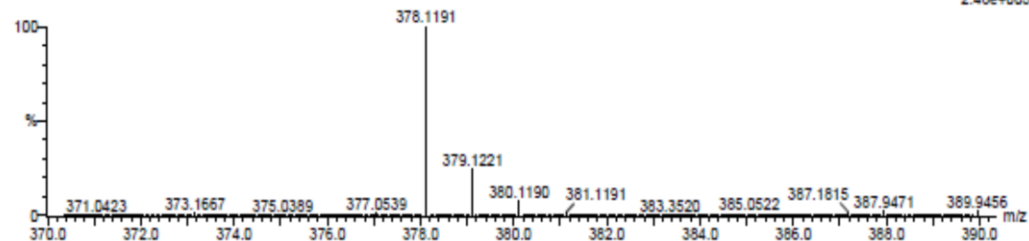
32 formula(e) evaluated with 1 results within limits (up to 20 closest results for each mass)

Elements Used:

C: 15-20 H: 10-20 N: 0-5 F: 0-3 S: 0-1

PP-17 44 (1.451) Cm (1:51)

TOF MS ES-



Minimum:

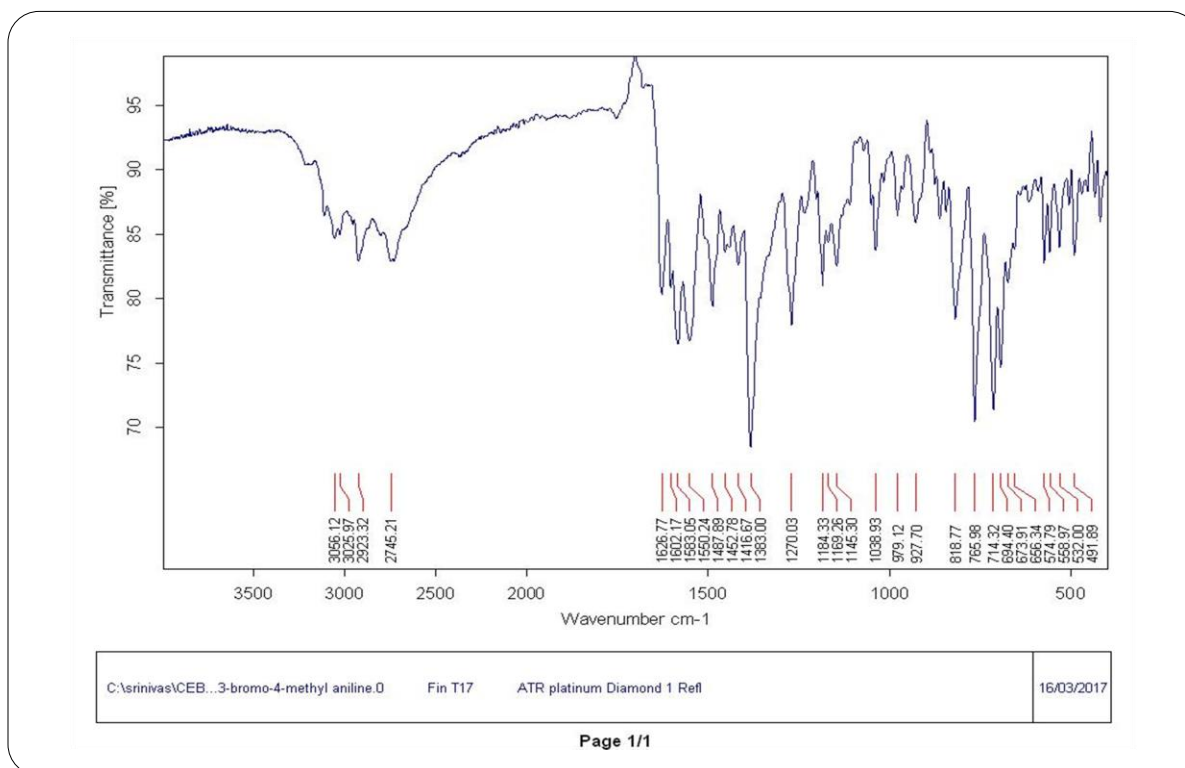
-1.5

Maximum:

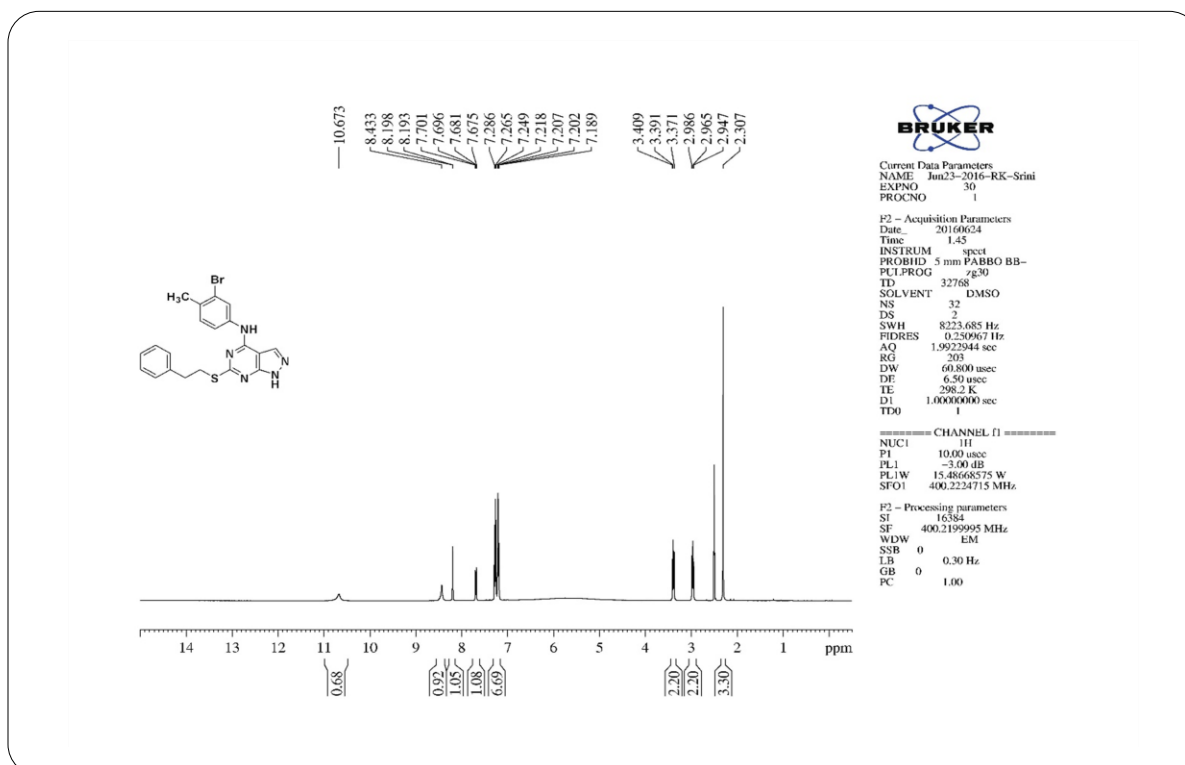
100.0

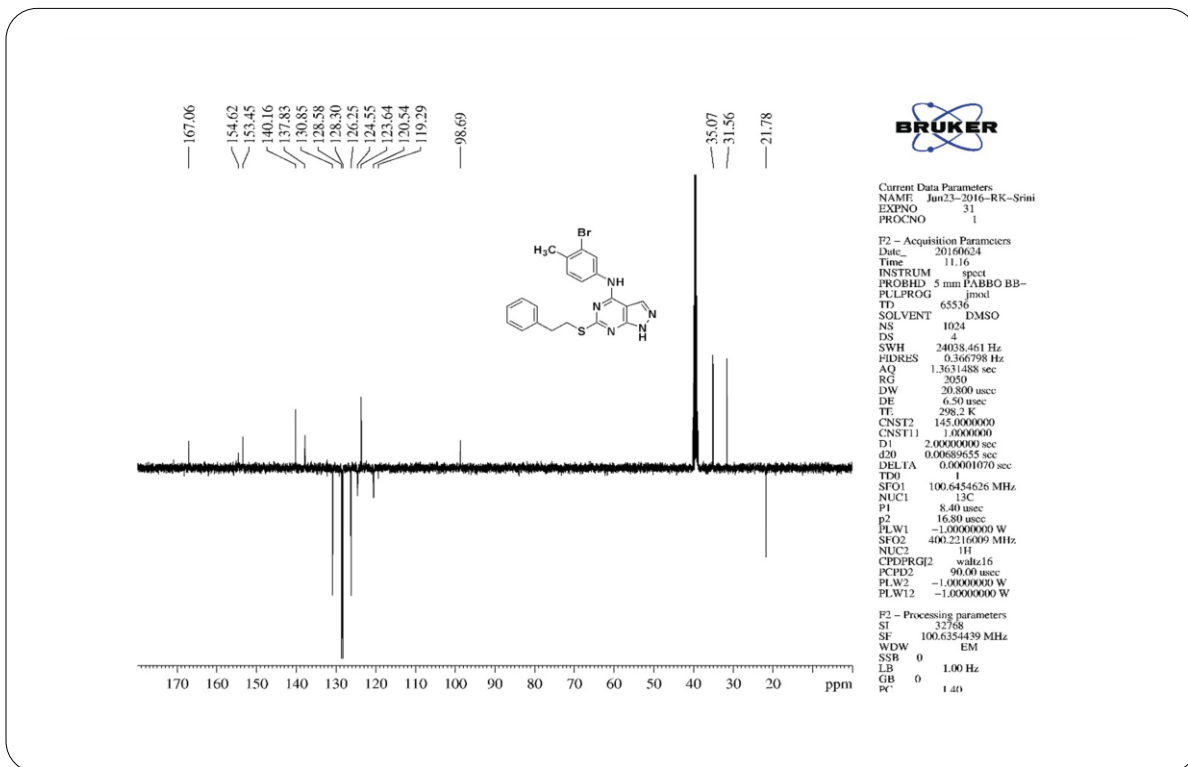
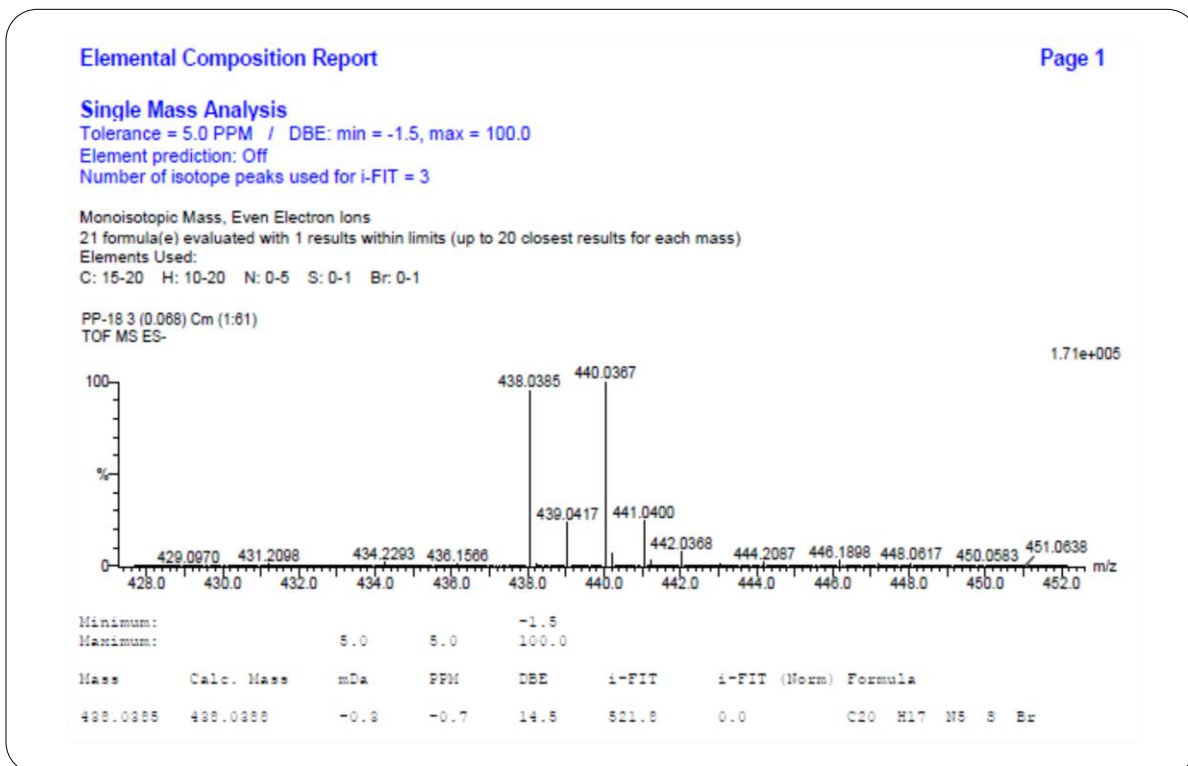
Mass	Calc. Mass	mDa	PPM	DBE	i-FIT	i-FIT (Norm)	Formula
378.1191	378.1189	0.2	0.5	14.5	603.9	0.0	C20 H17 N5 F S

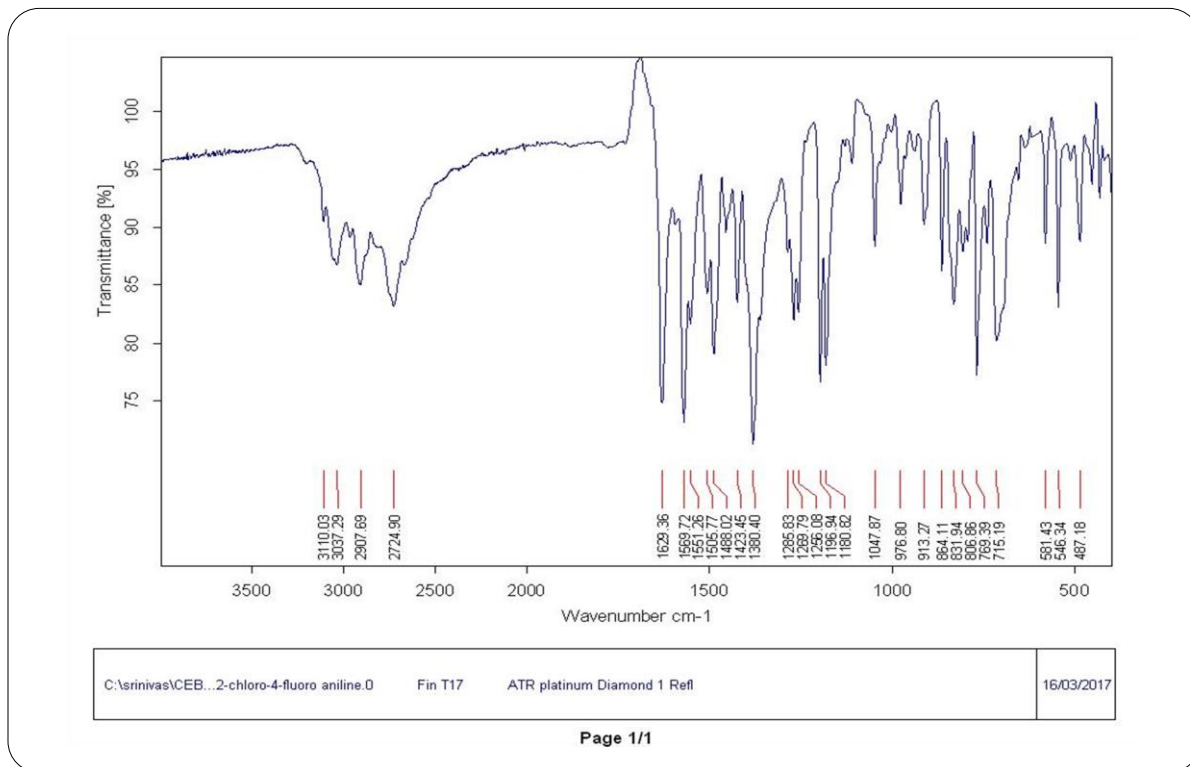
HRMS Spectrum of Compound 21



IR Spectrum of Compound 22

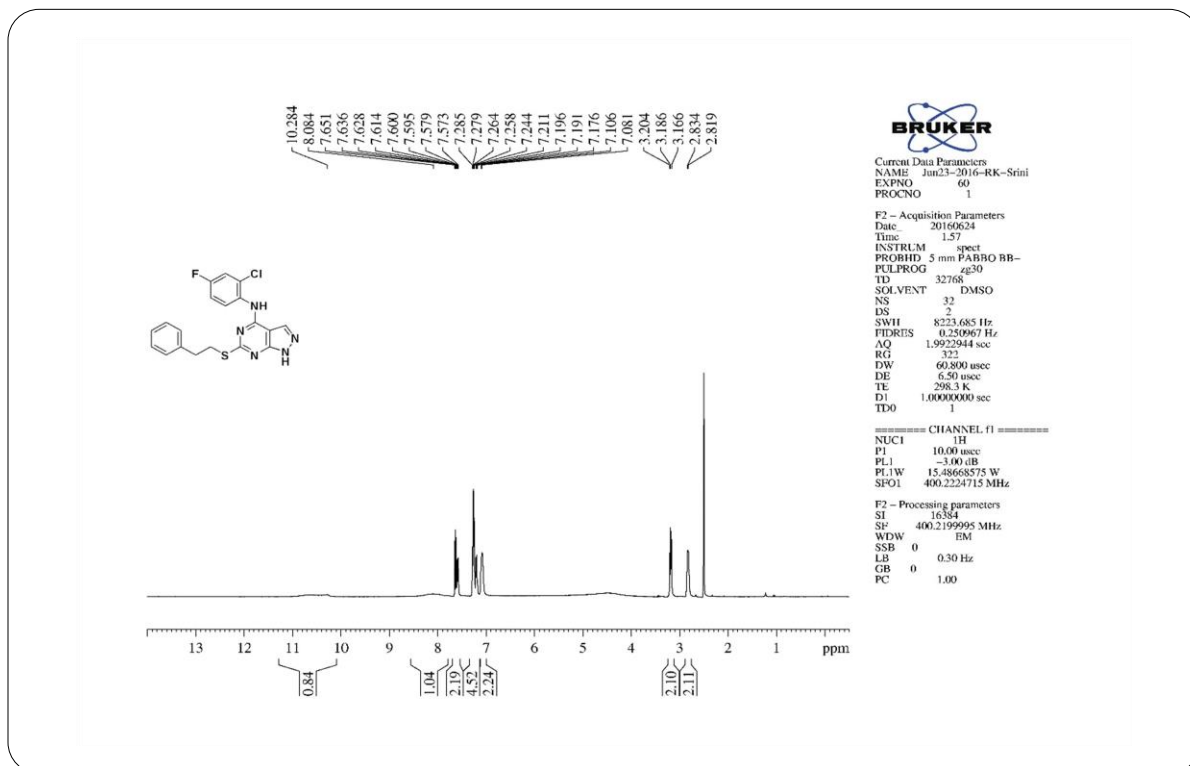


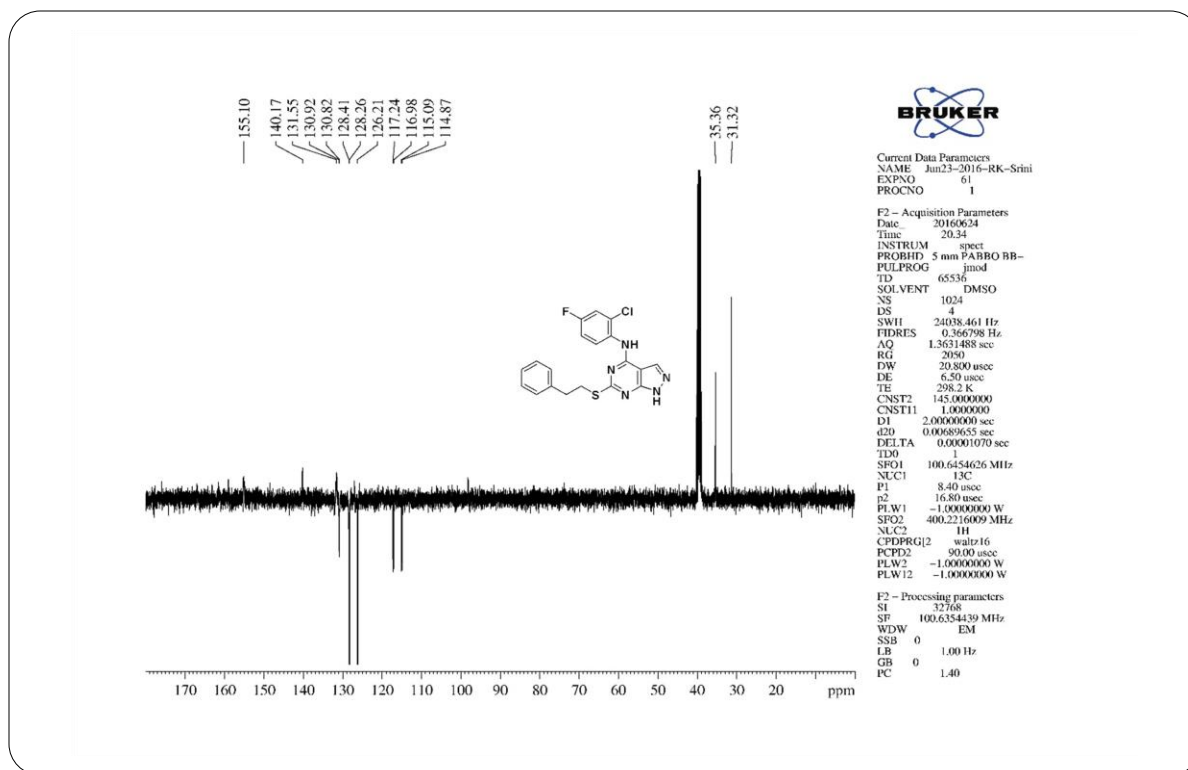
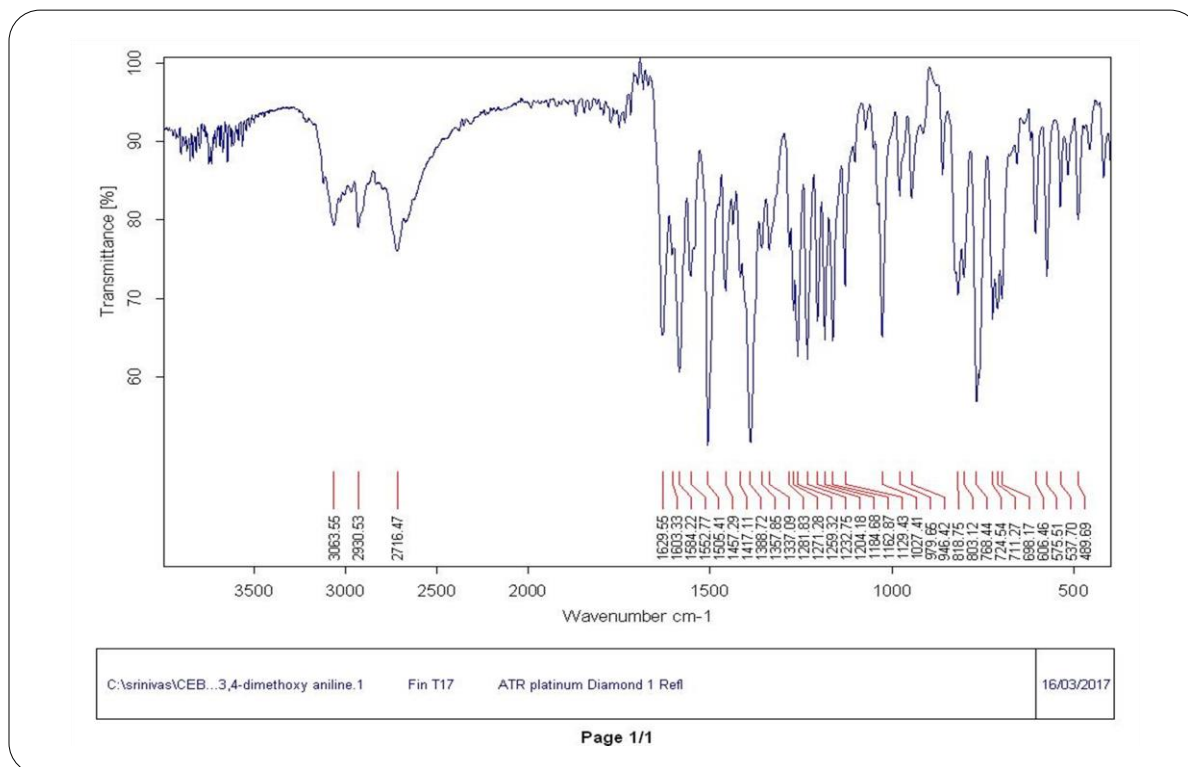
**¹³C NMR Spectrum of Compound 22****HRMS Spectrum of Compound 22**

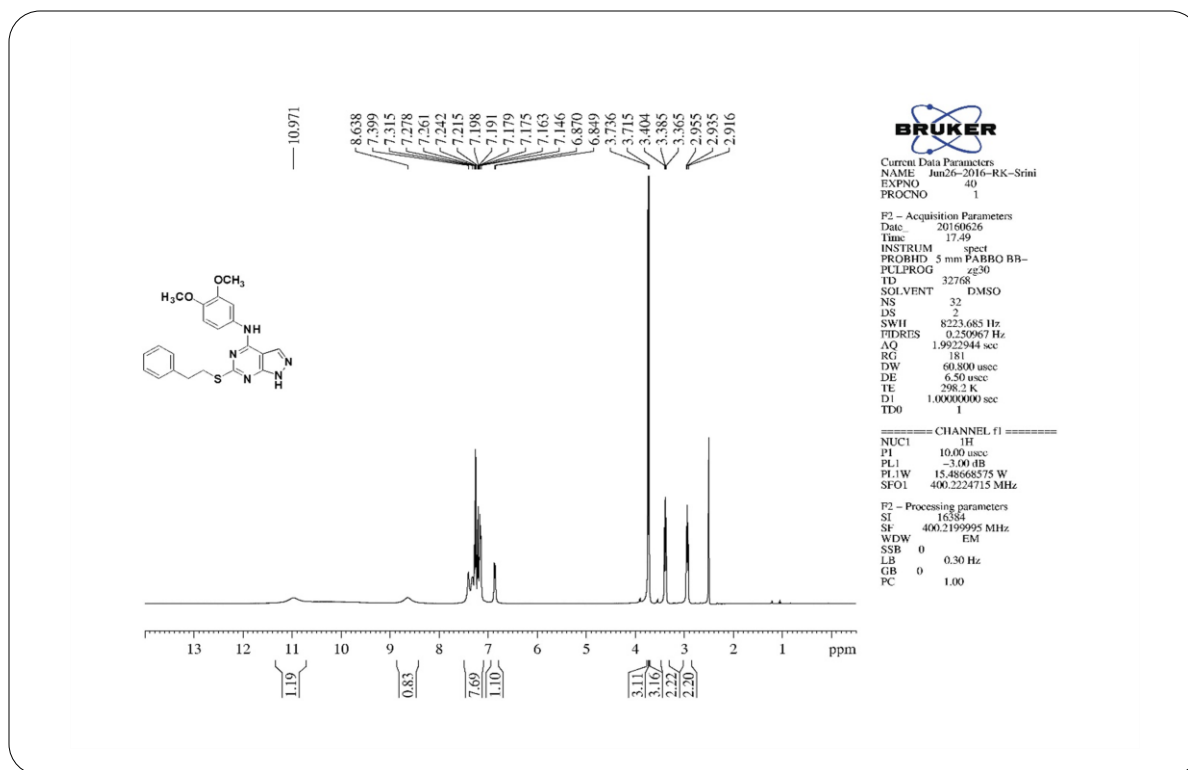
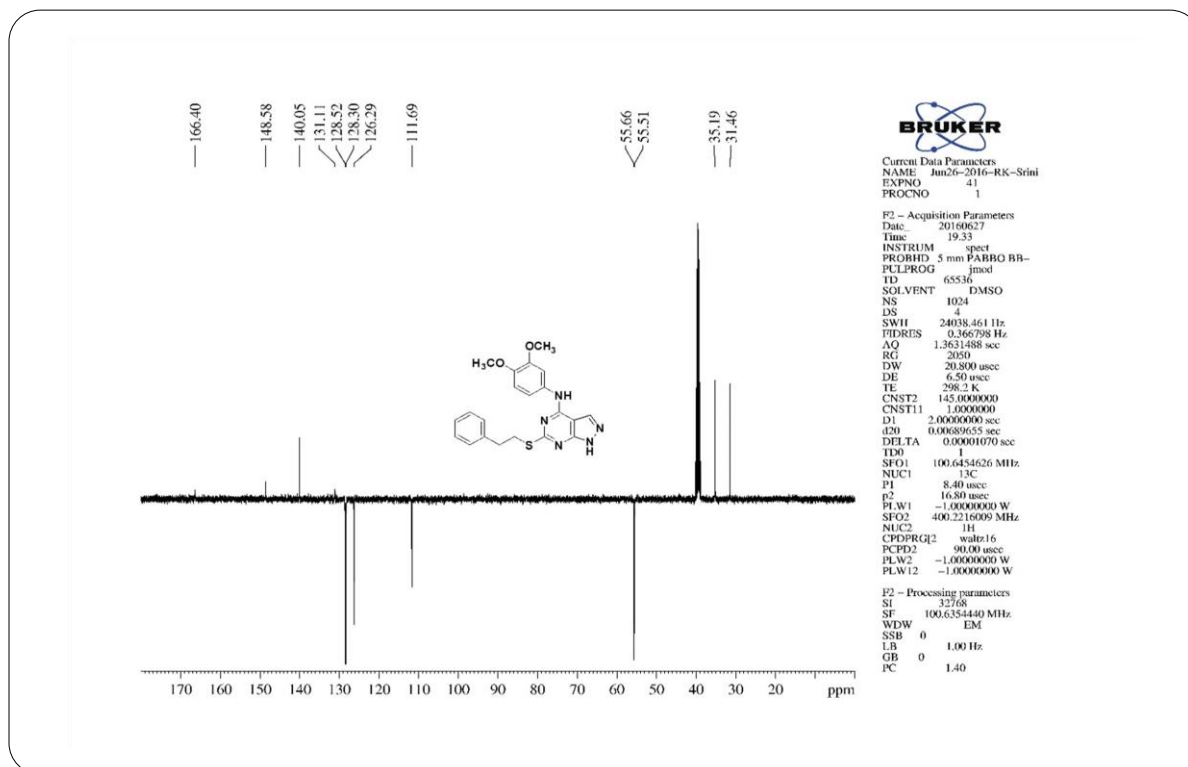


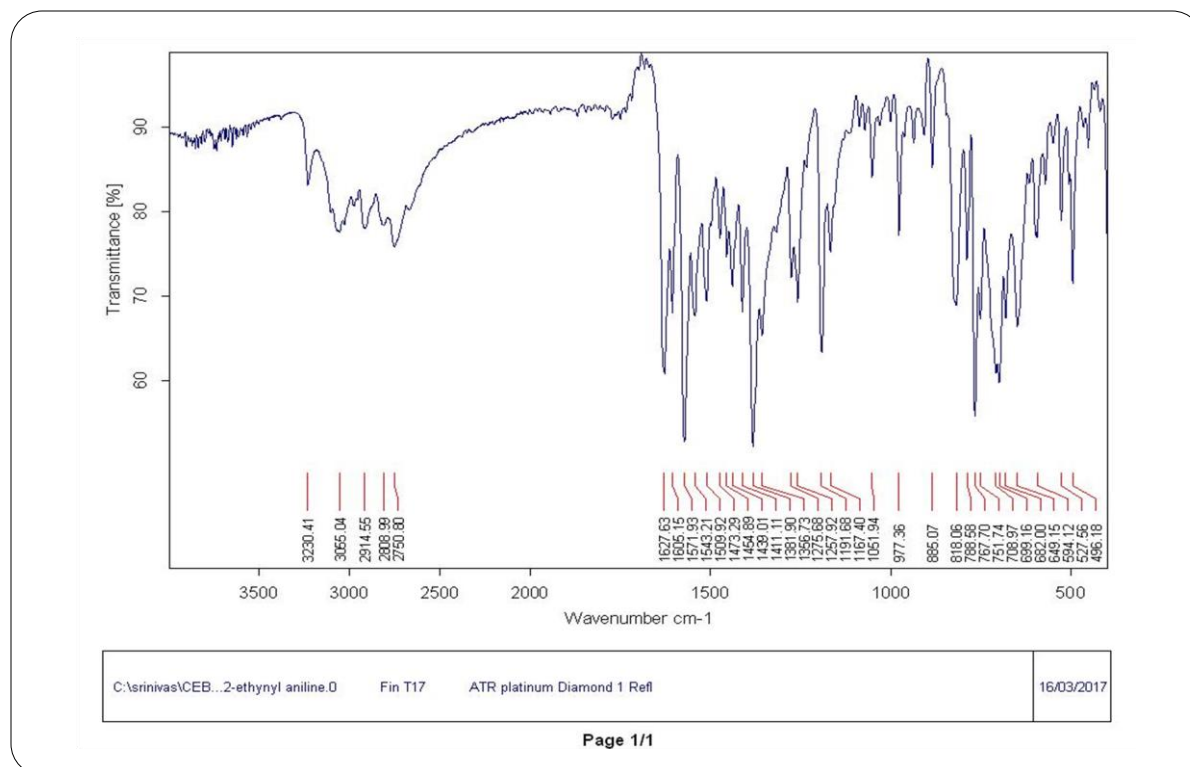
Page 1/1

IR Spectrum of Compound 23

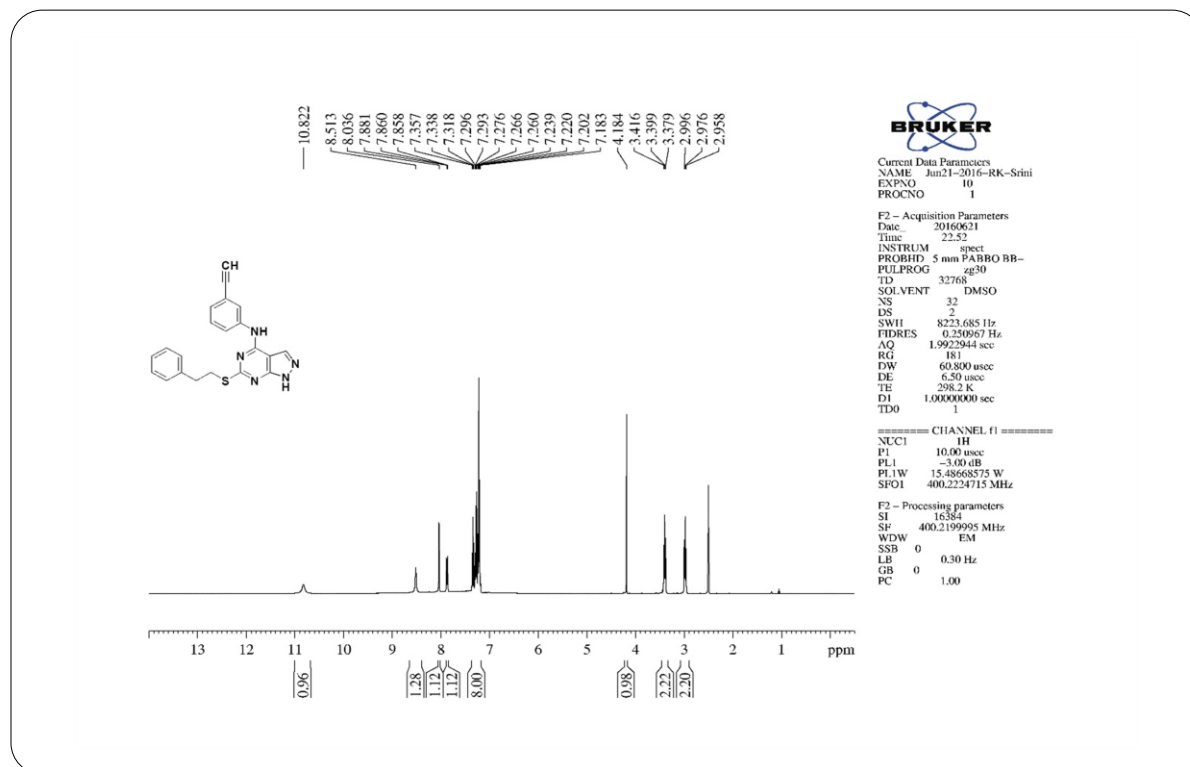
¹H NMR Spectrum of Compound 23

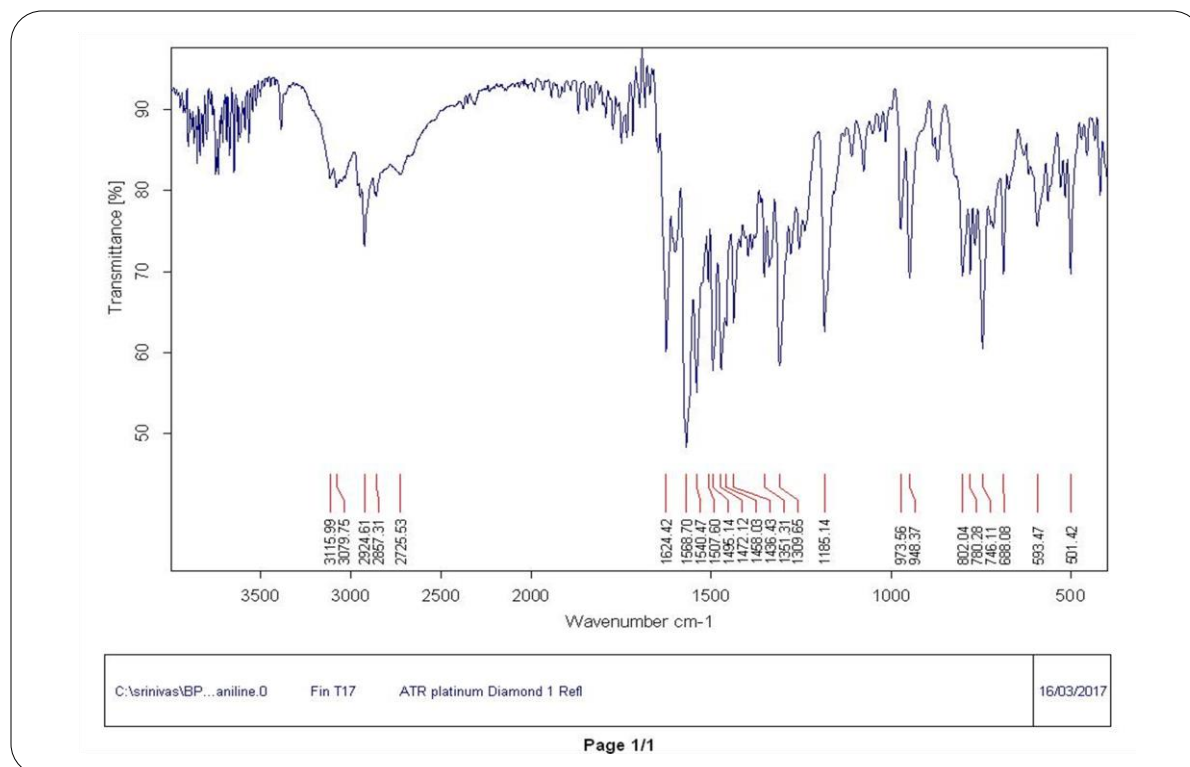
**¹³C NMR Spectrum of Compound 23****IR Spectrum of Compound 24**

**¹H NMR Spectrum of Compound 24****¹³C NMR Spectrum of Compound 24**

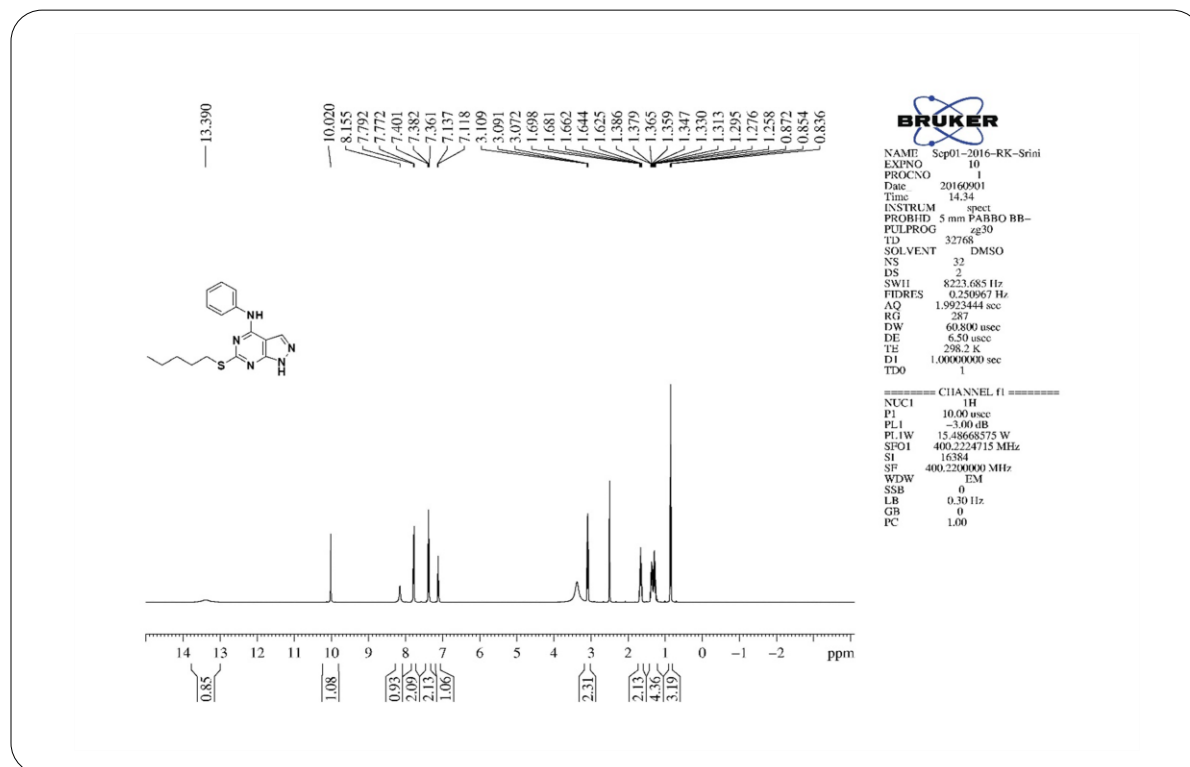


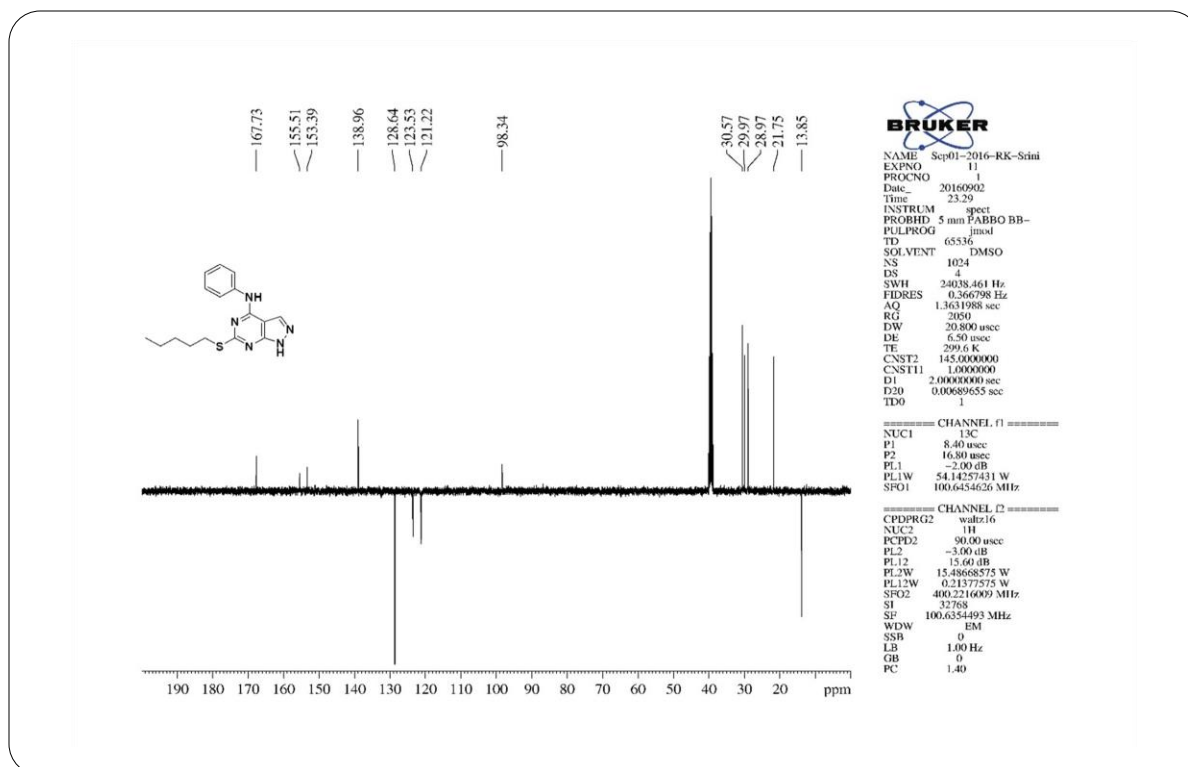
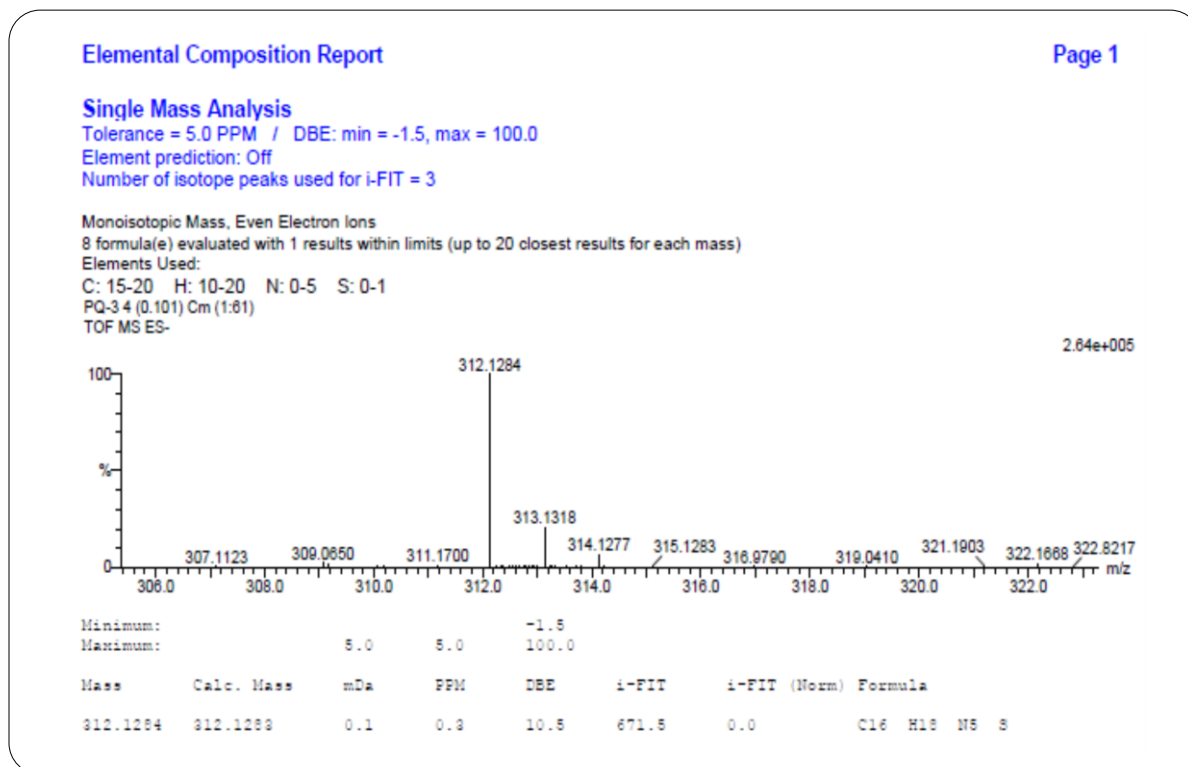
IR Spectrum of Compound 25

¹H NMR Spectrum of Compound 25

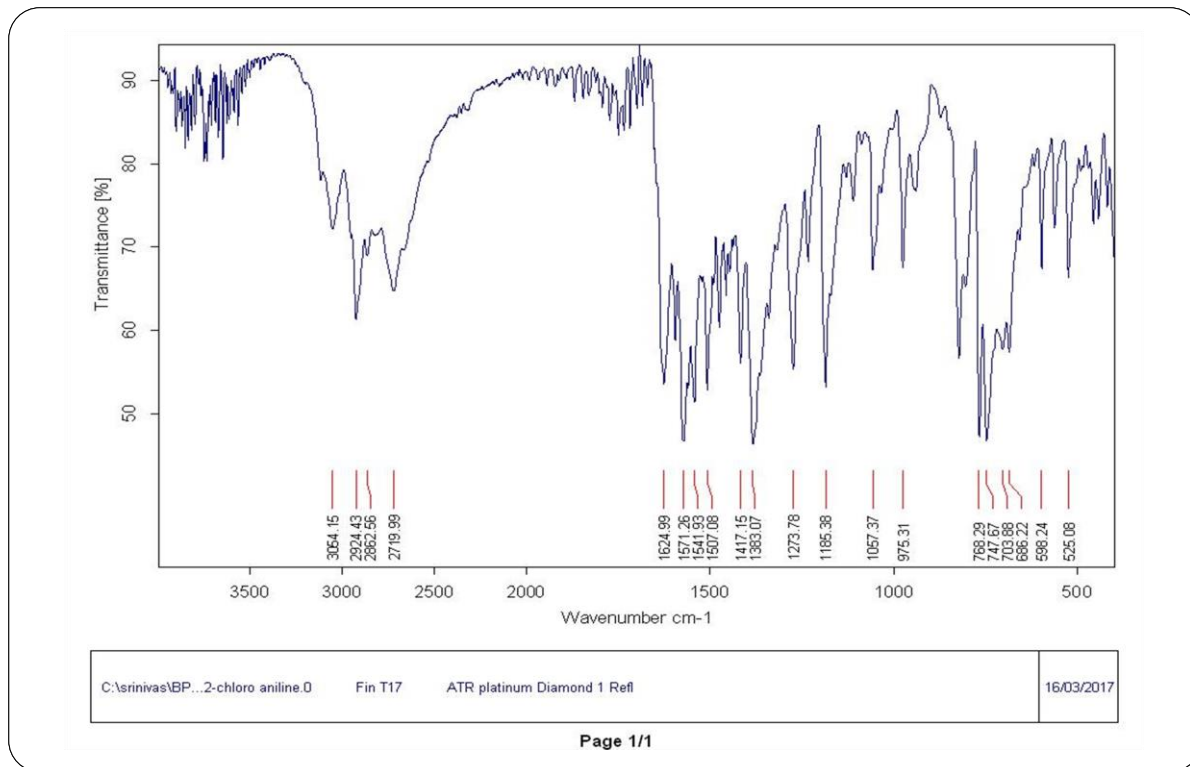


IR Spectrum of Compound 26

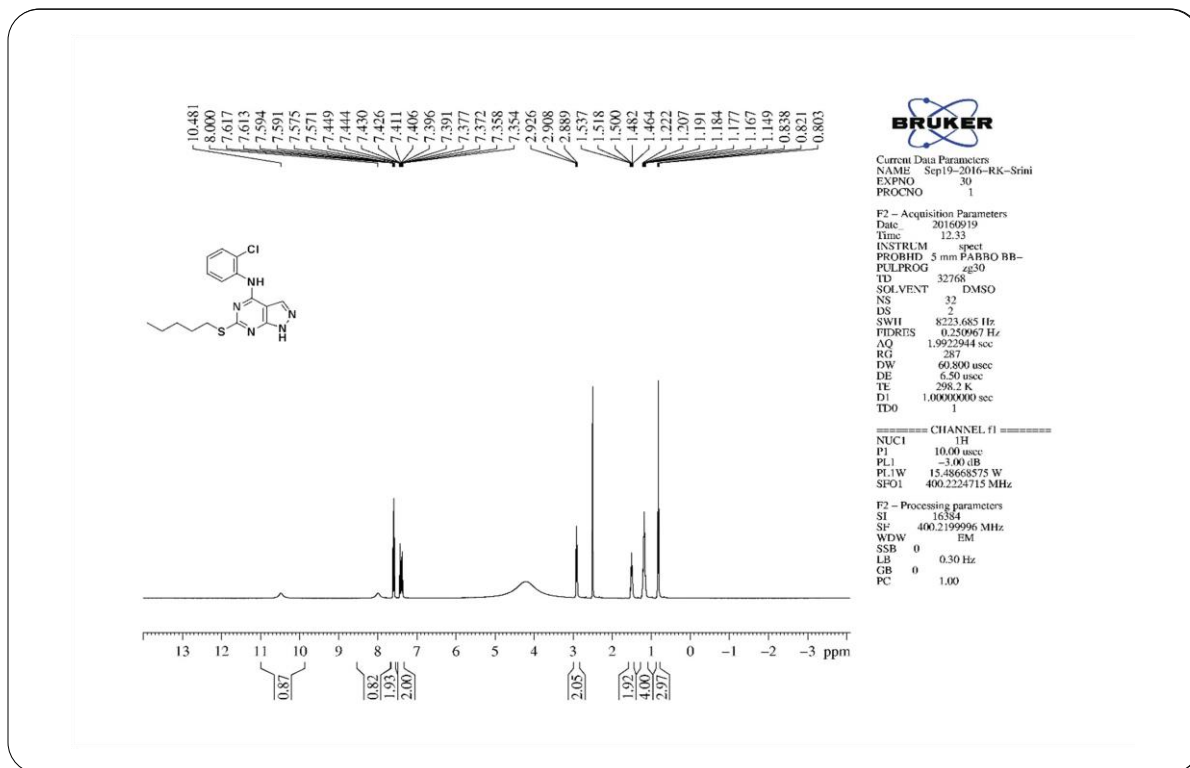
¹H NMR Spectrum of Compound 26

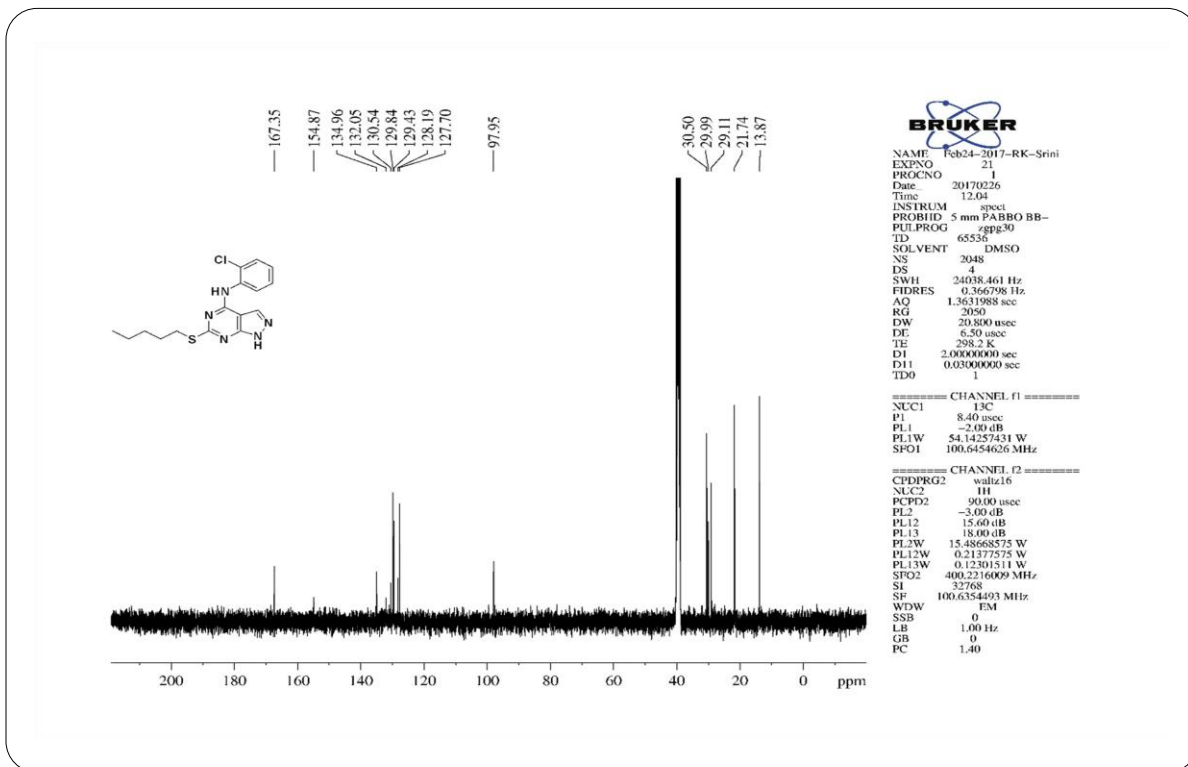
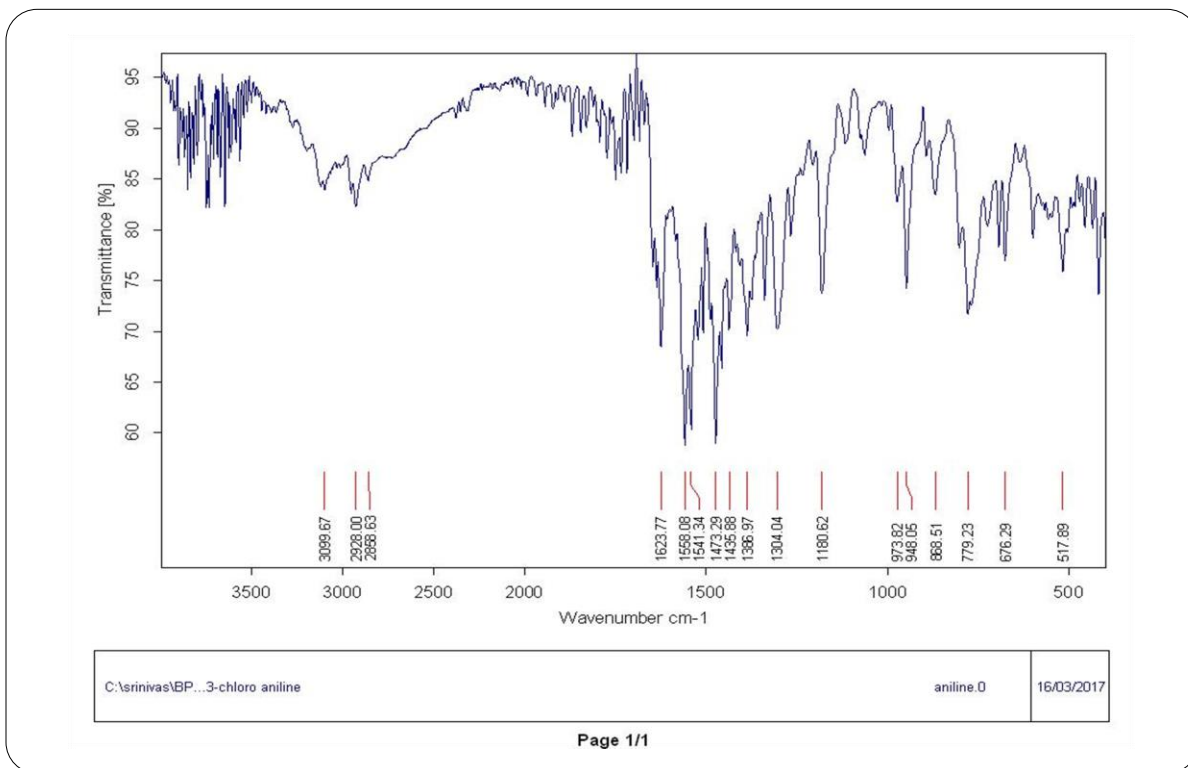
¹³C NMR Spectrum of Compound 26

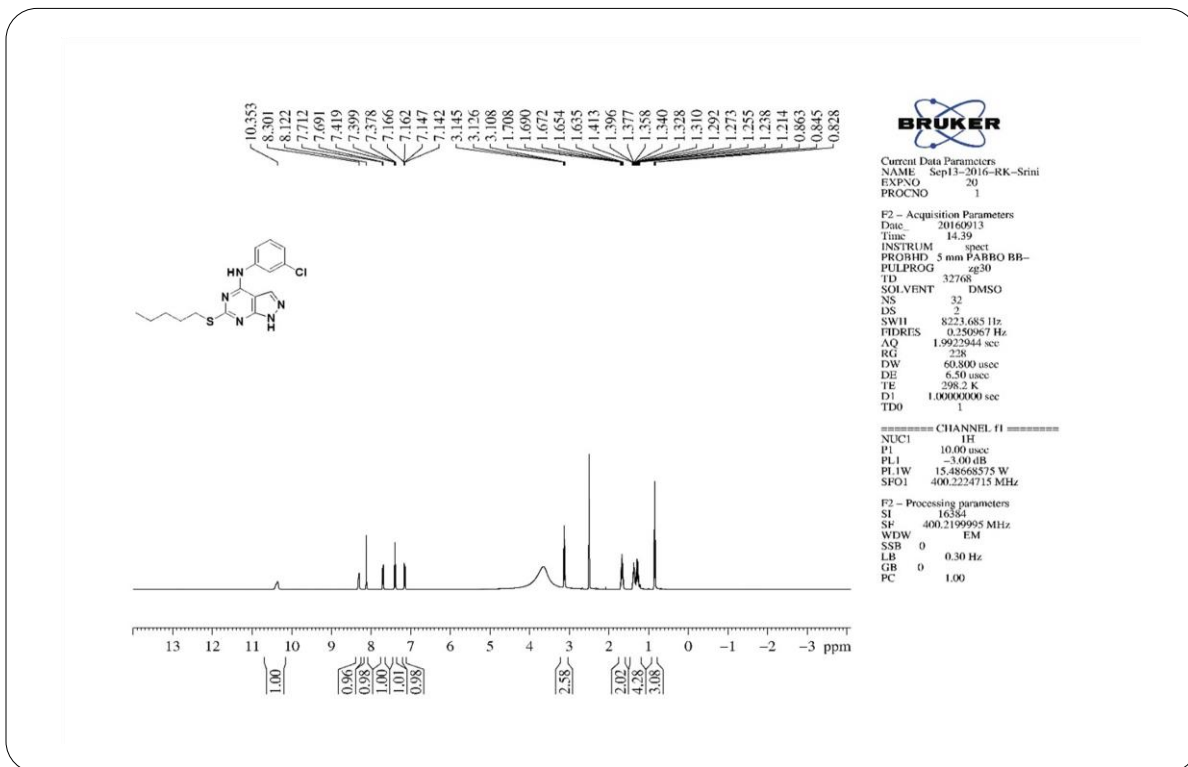
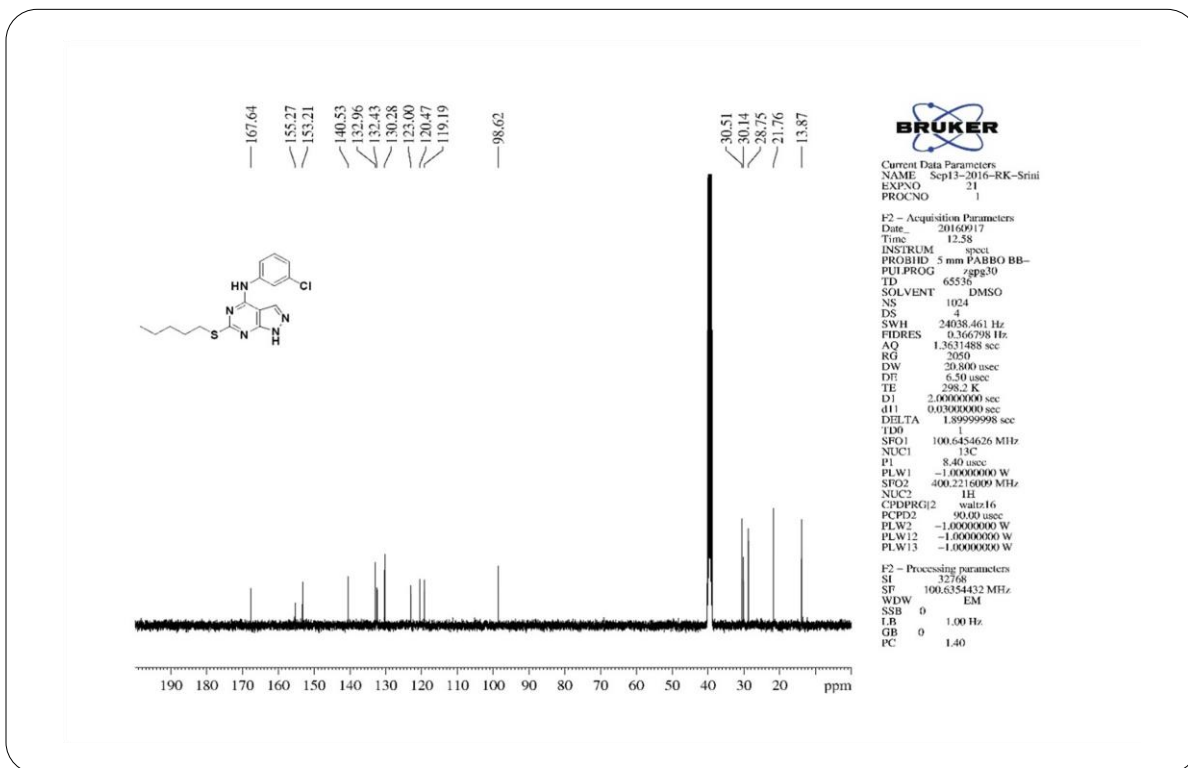
HRMS Spectrum of Compound 26

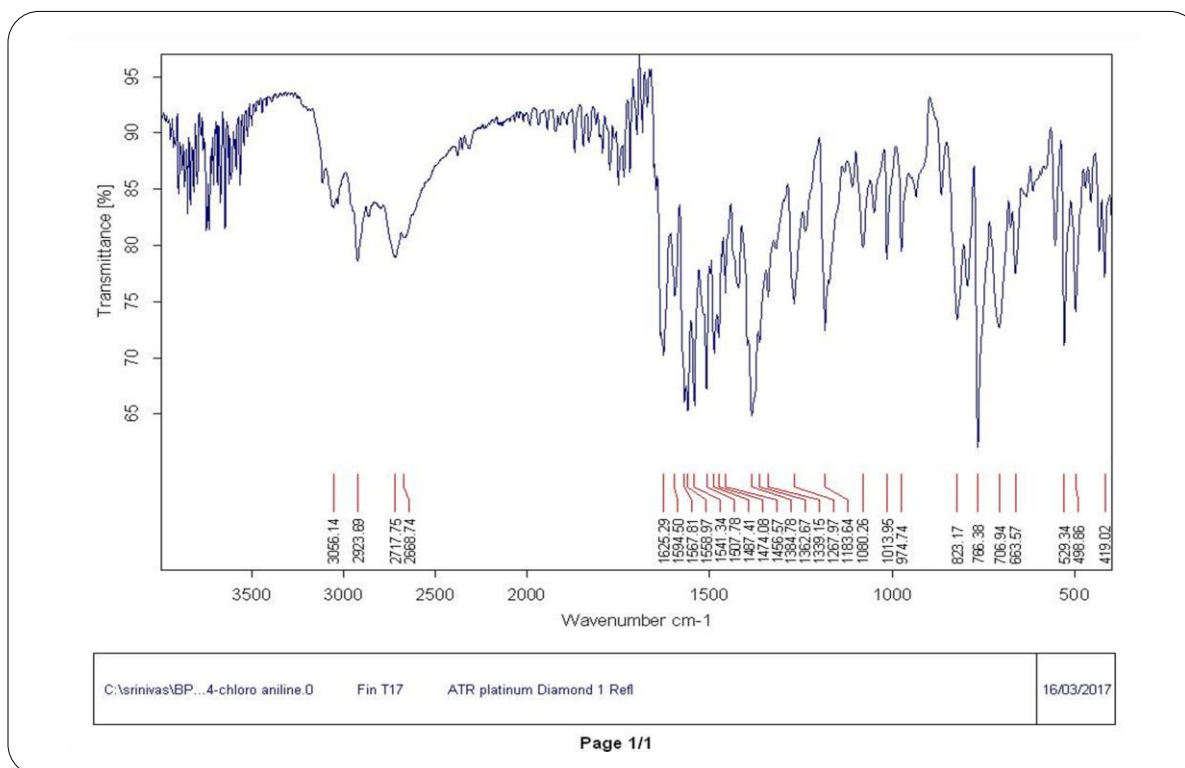


IR Spectrum of Compound 27

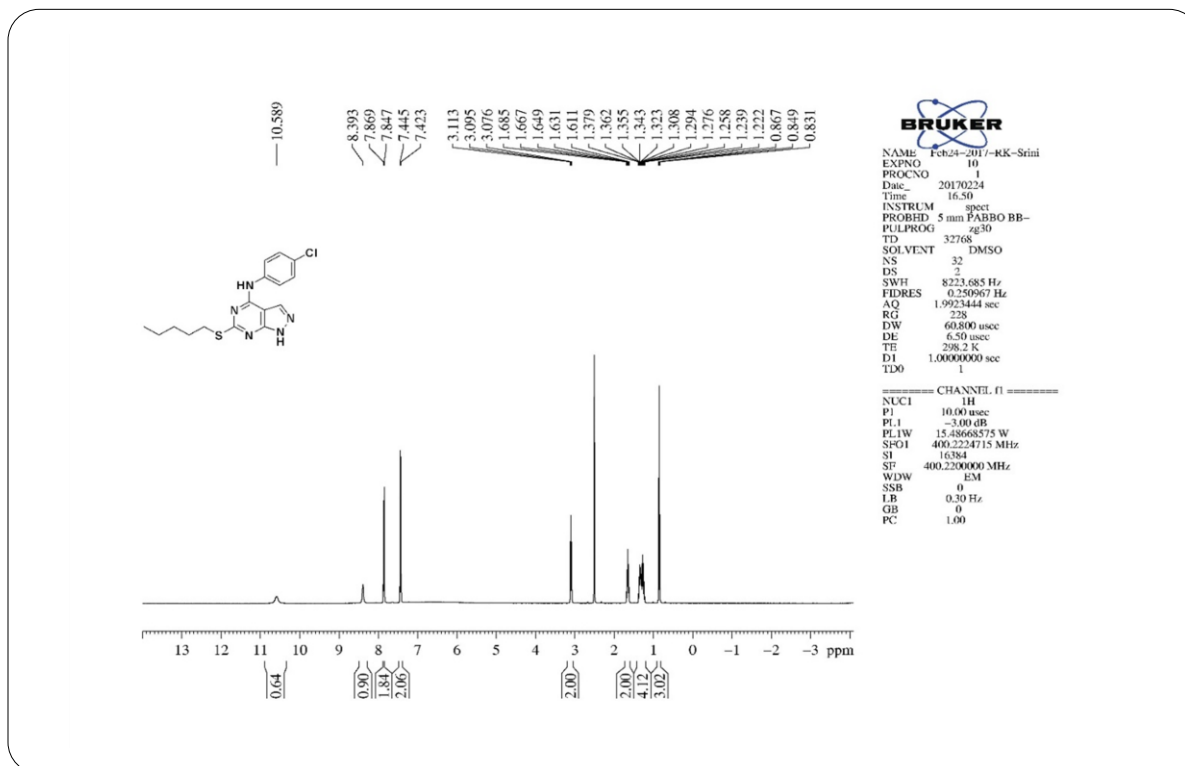
¹H NMR Spectrum of Compound 27

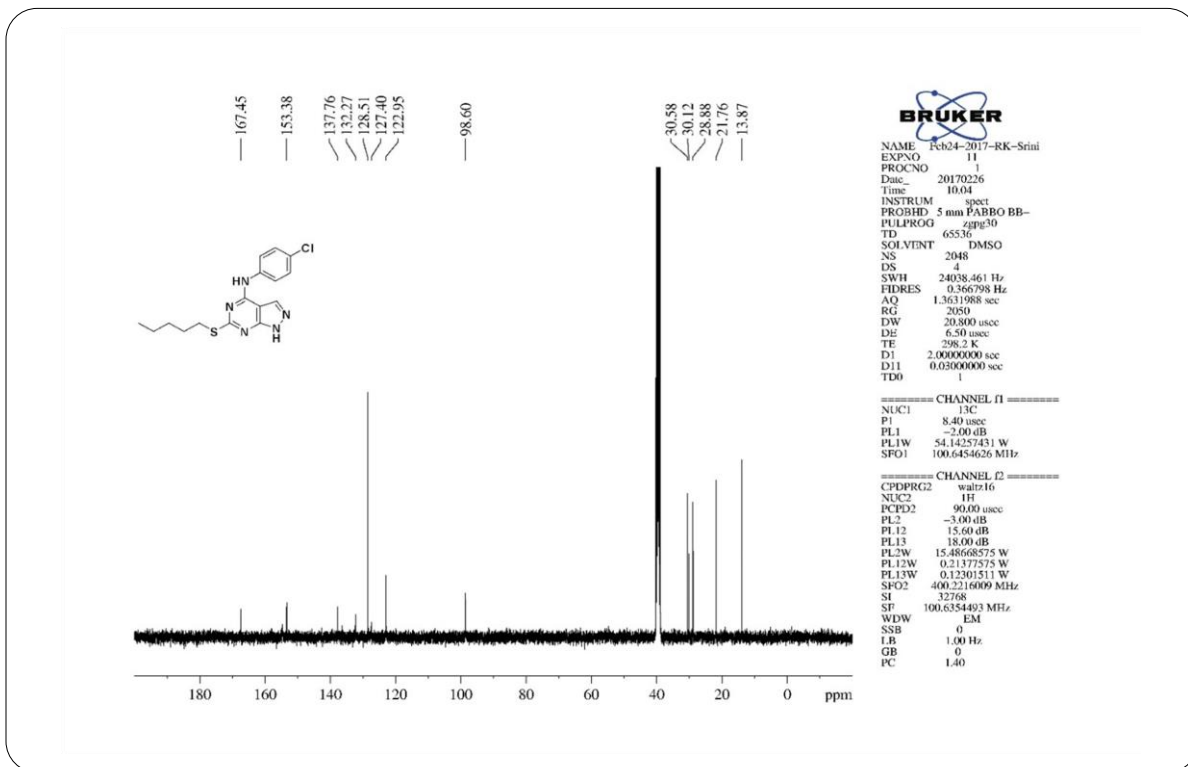
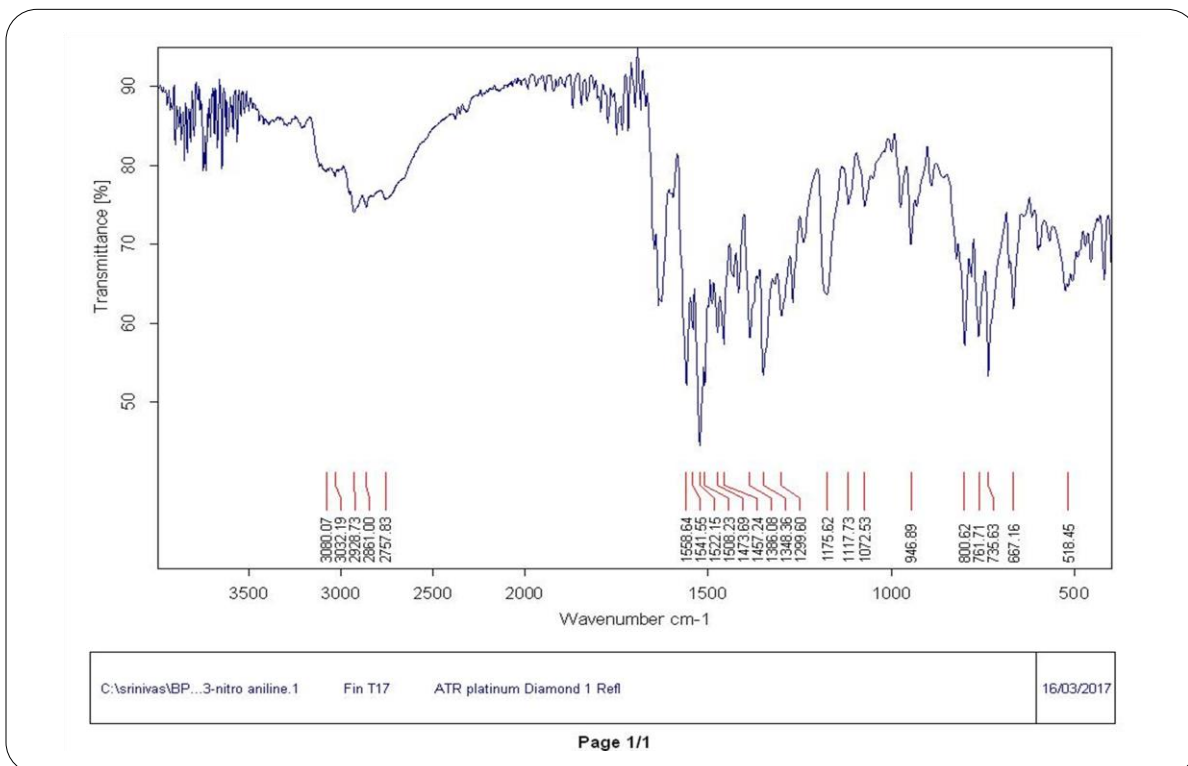
**¹³C NMR Spectrum of Compound 27****IR Spectrum of Compound 28**

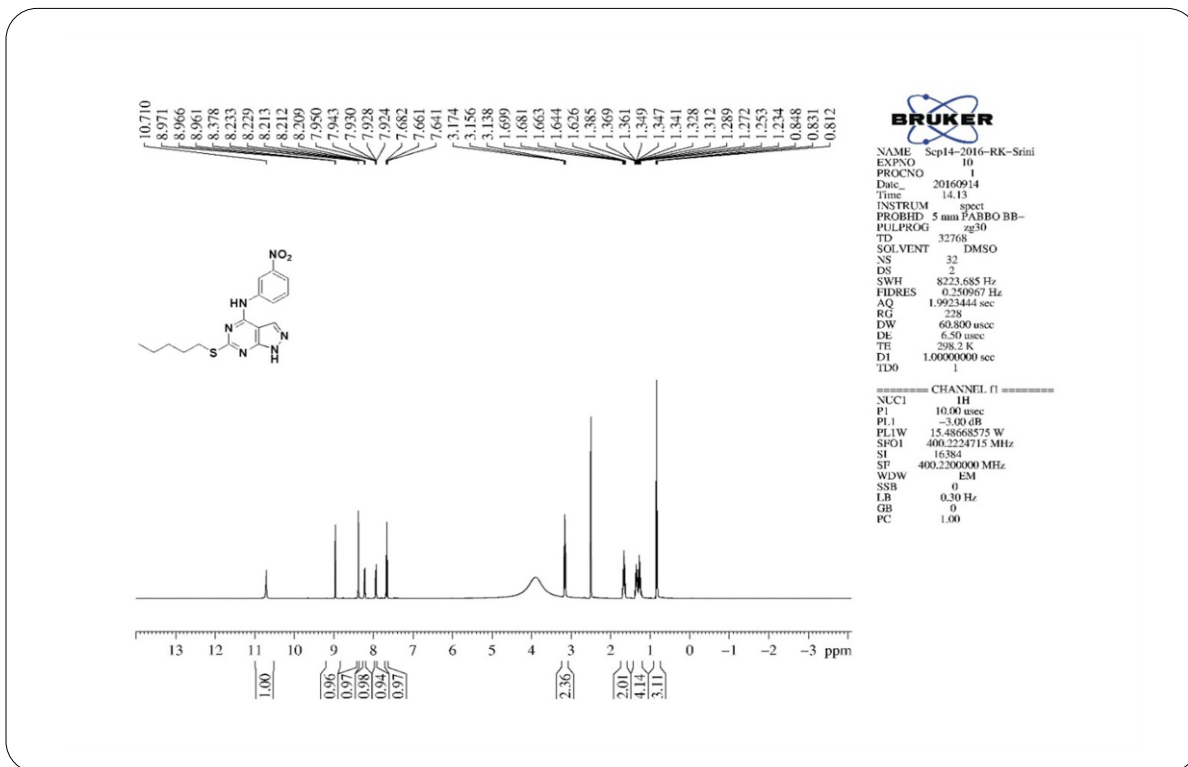
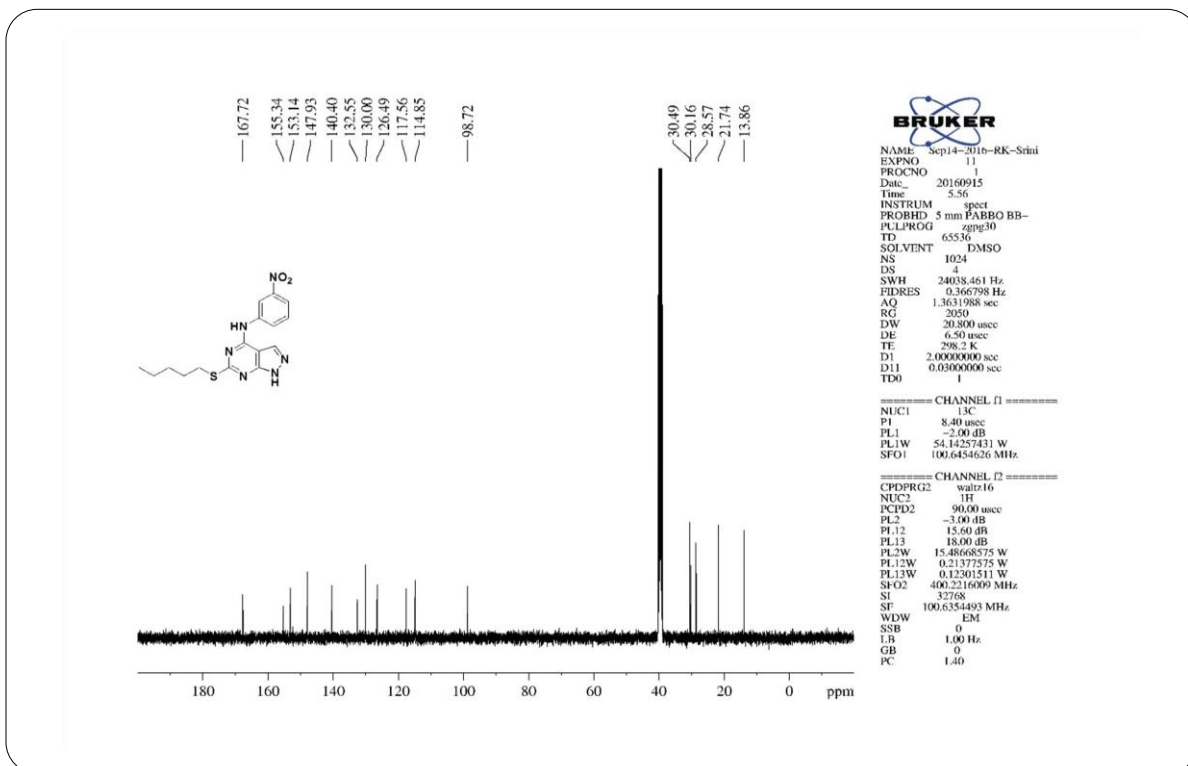
**¹H NMR Spectrum of Compound 28****¹³C MNR Spectrum of Compound 28**

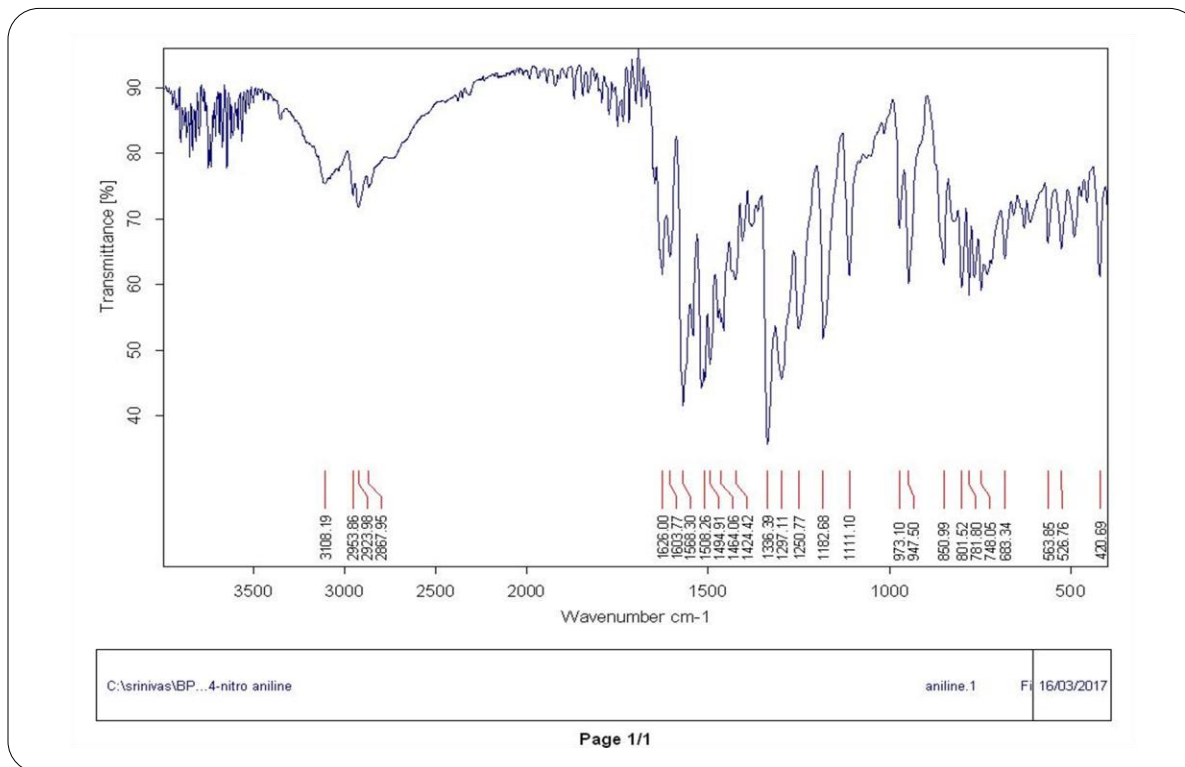


IR Spectrum of Compound 29

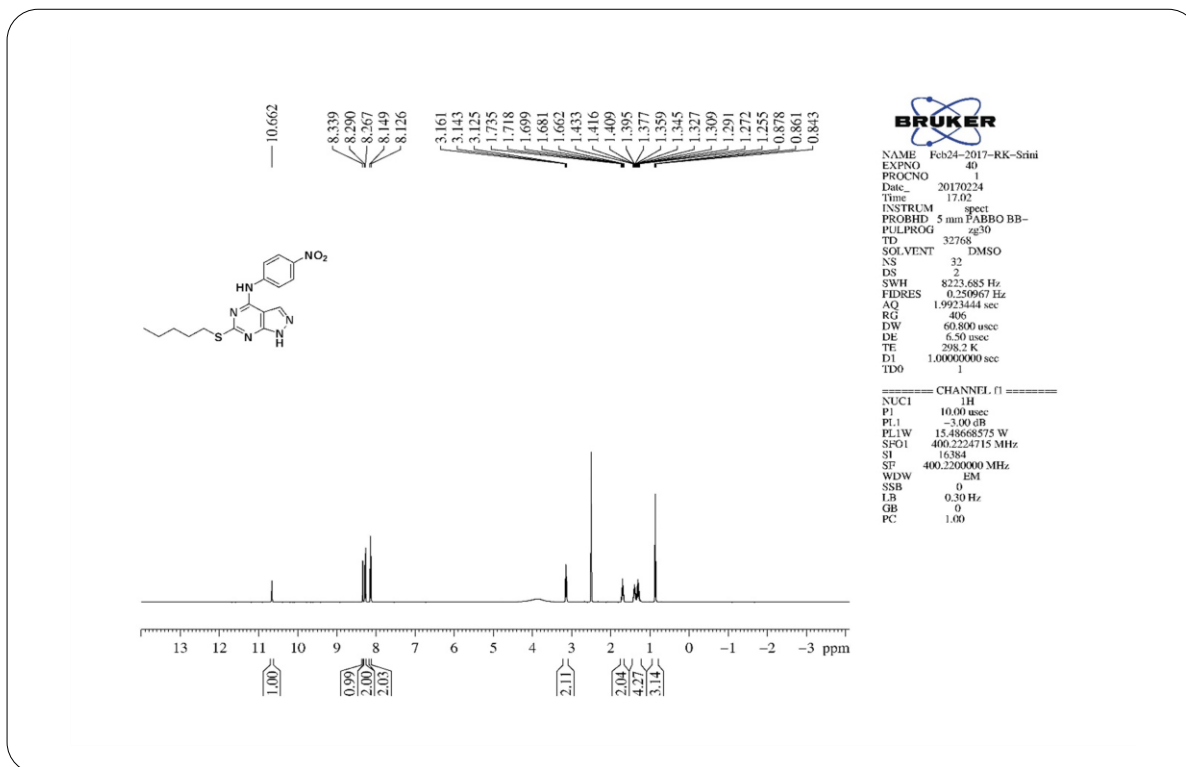
¹H NMR Spectrum of Compound 29

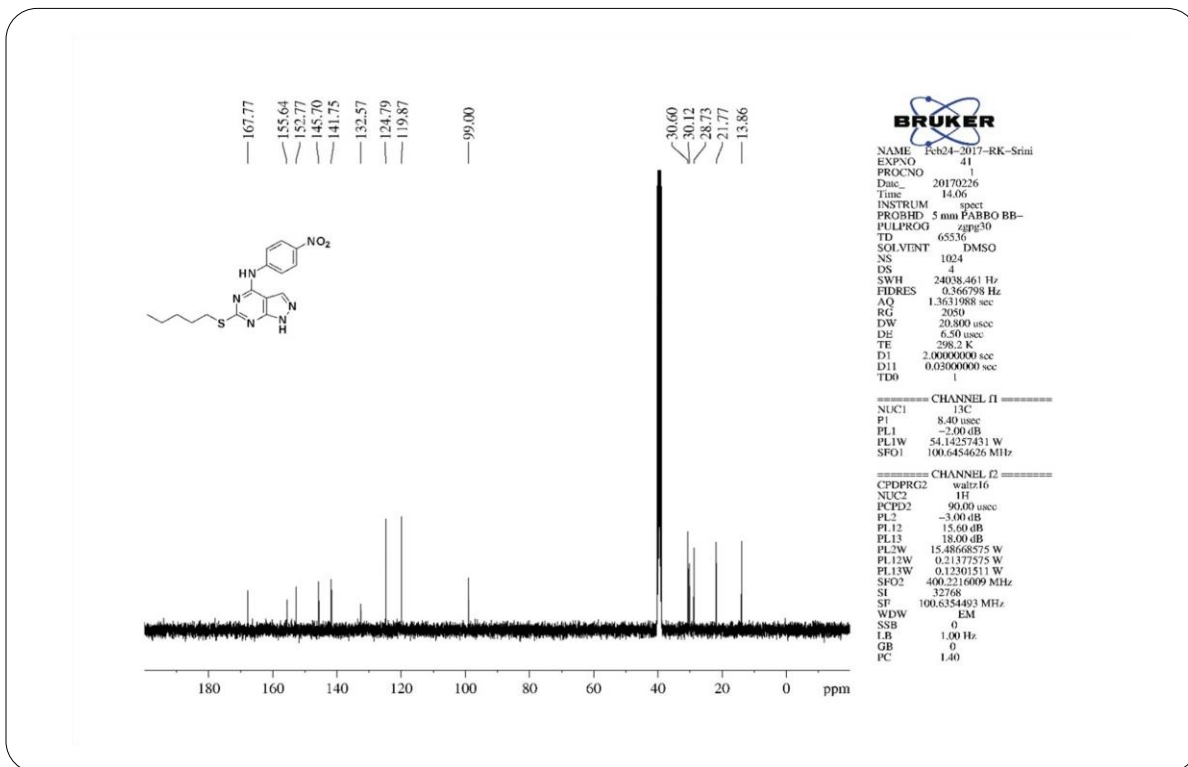
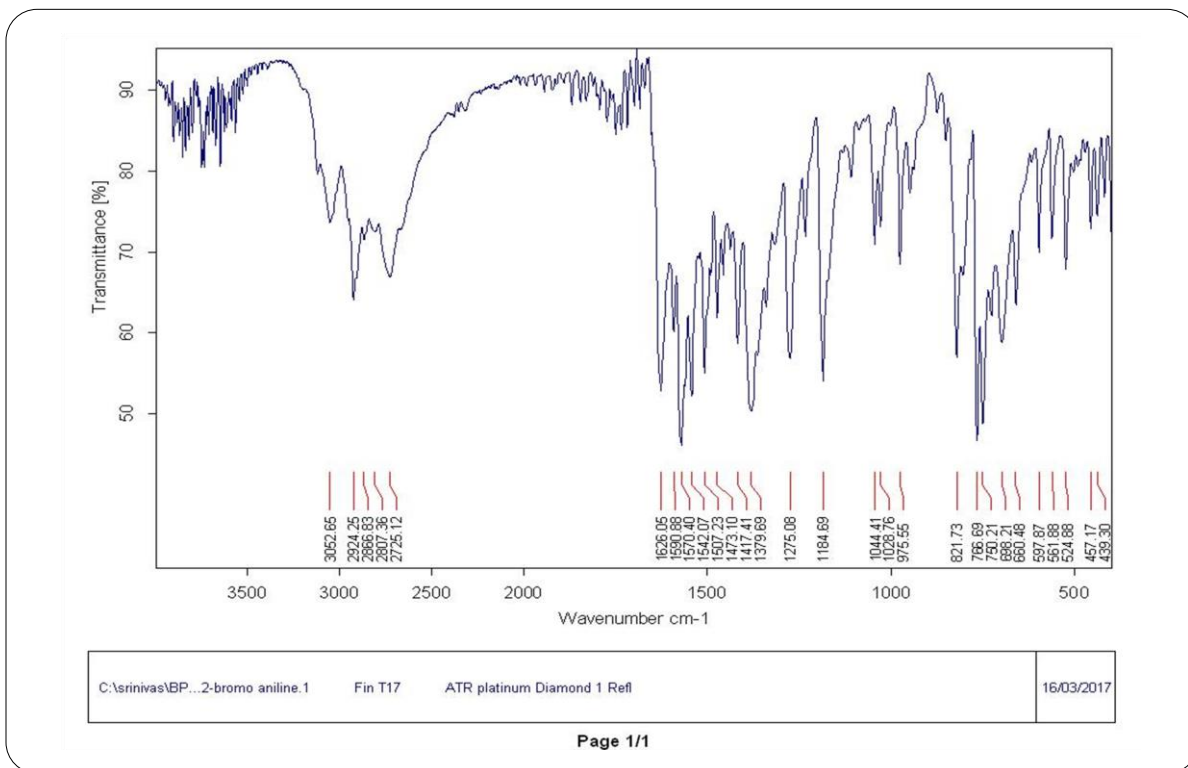
**¹³C NMR Spectrum of Compound 29****IR Spectrum of Compound 30**

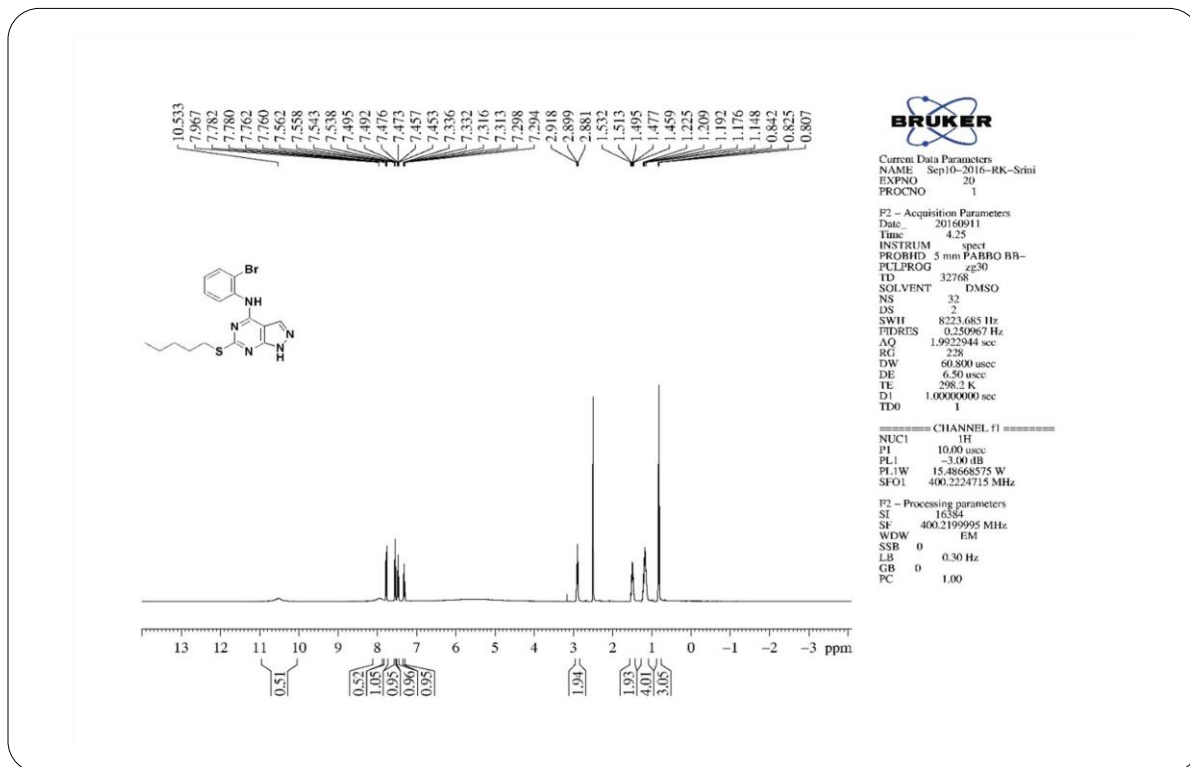
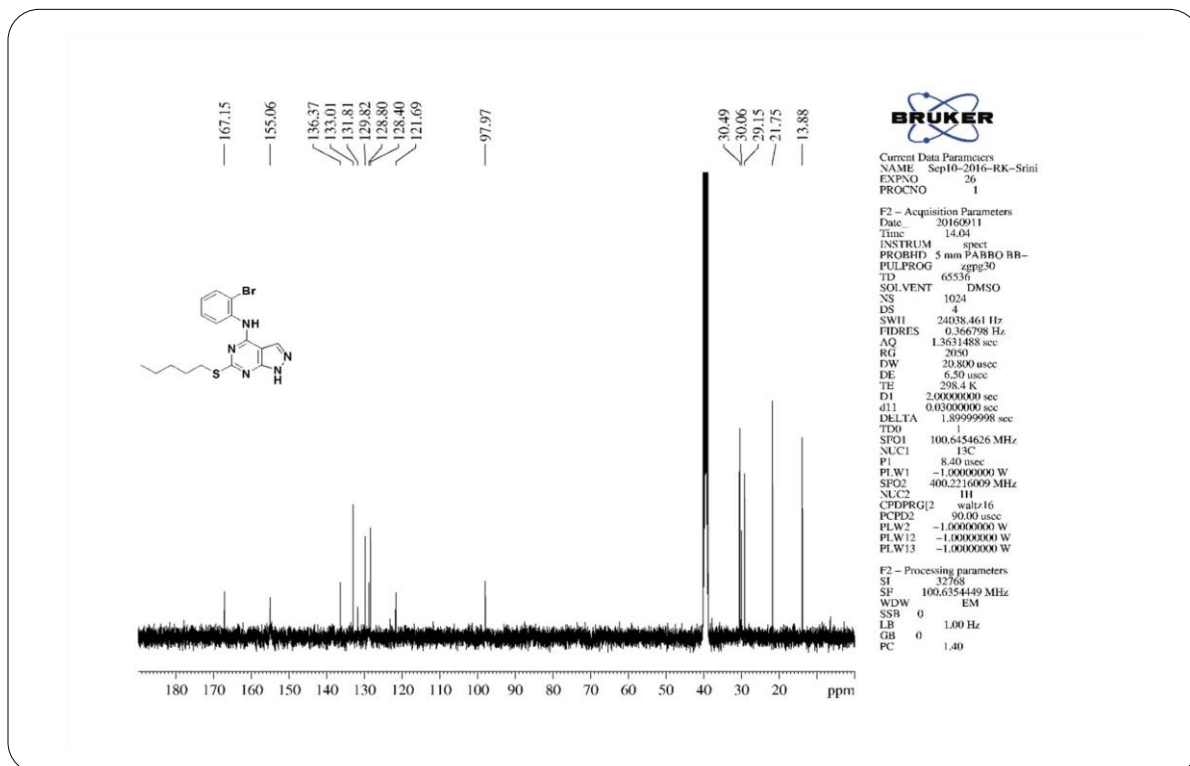
**¹H NMR Spectrum of Compound 30****¹³C NMR Spectrum of Compound 30**

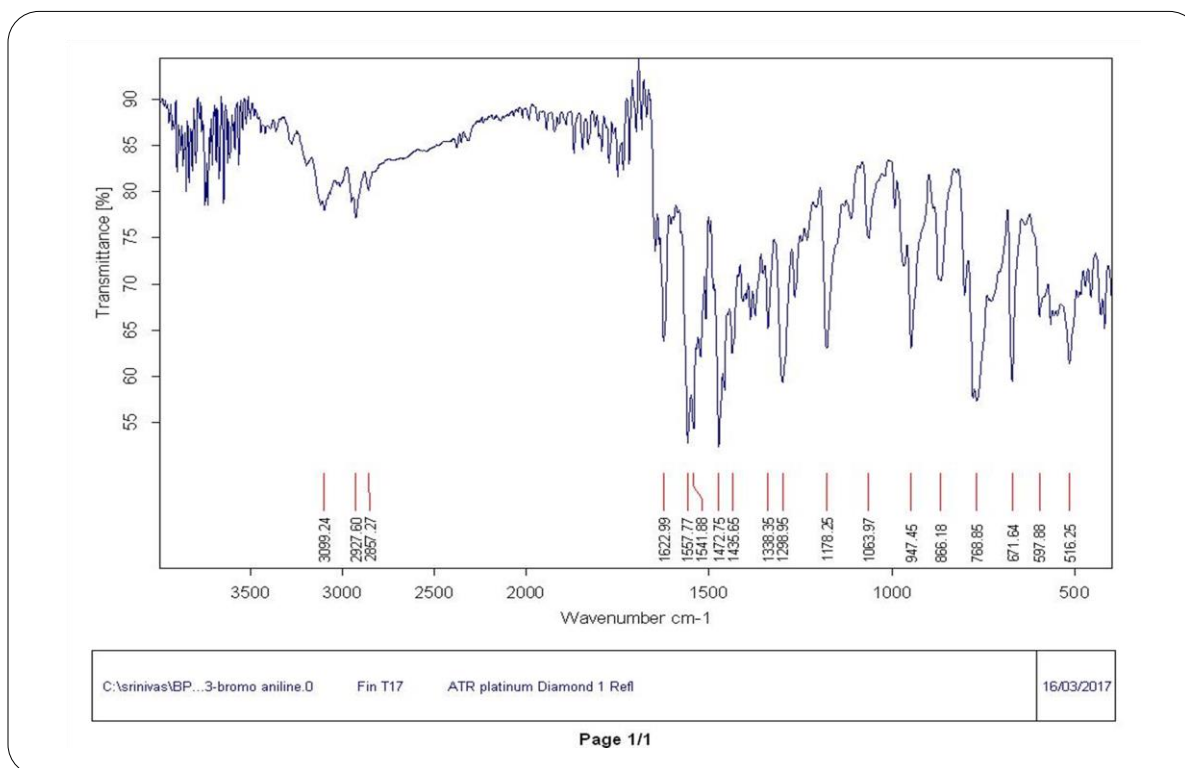


IR Spectrum of Compound 31

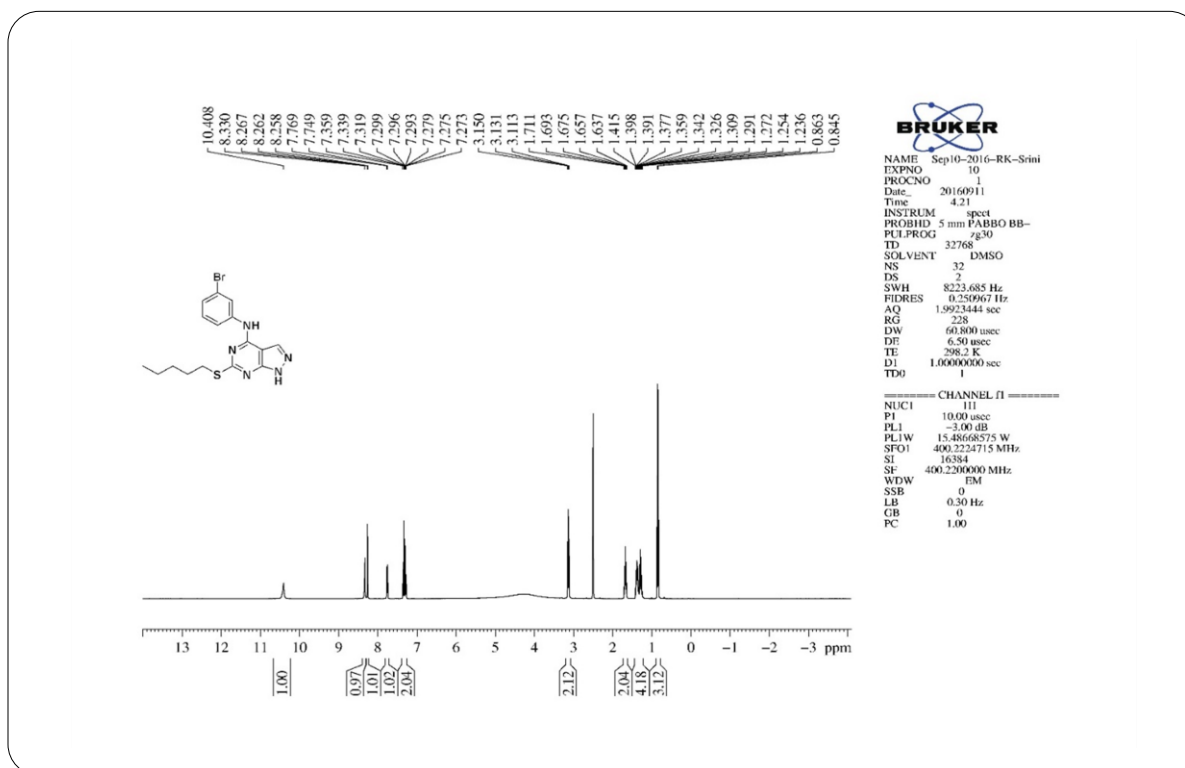
¹H NMR Spectrum of Compound 31

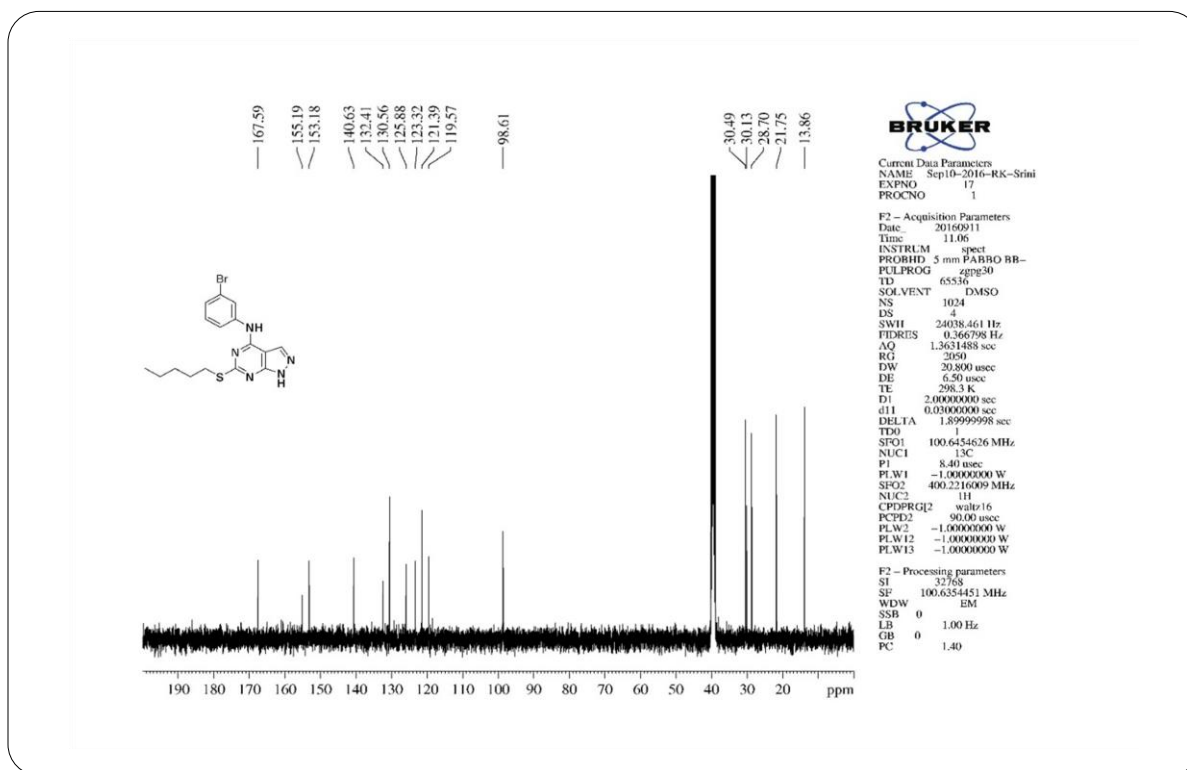
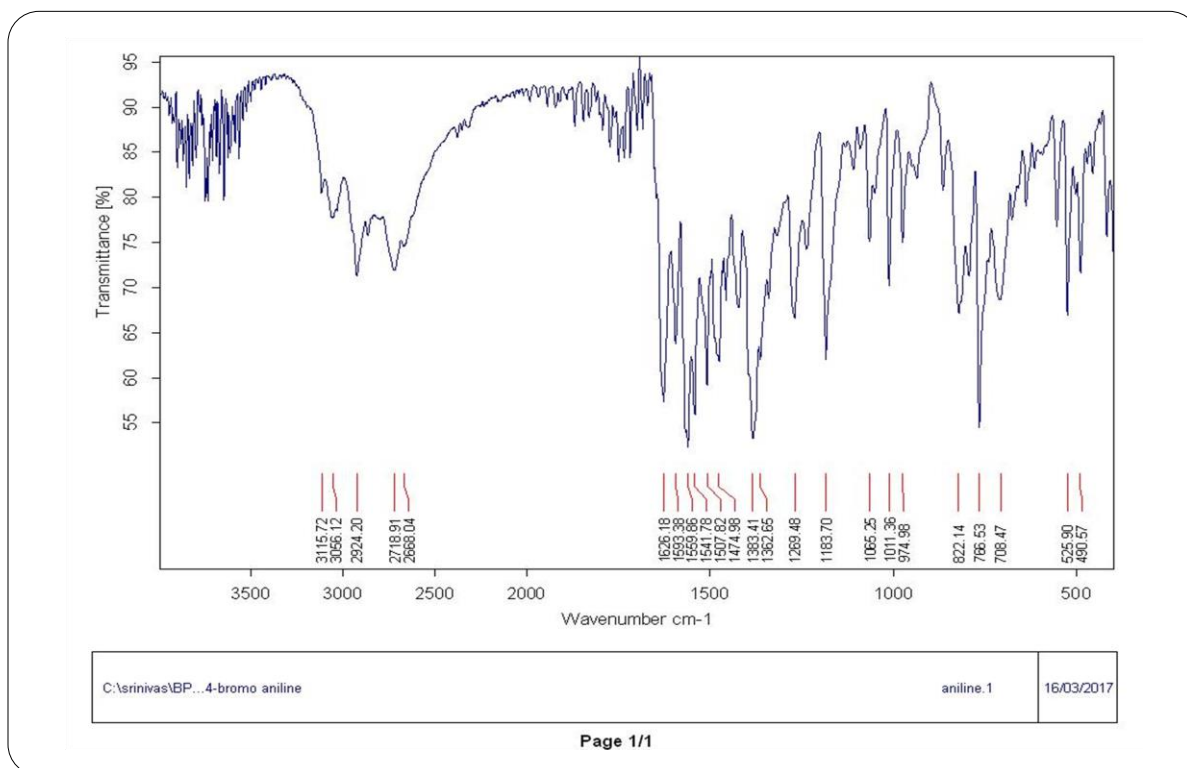
**¹³C NMR Spectrum of Compound 31****IR Spectrum of Compound 32**

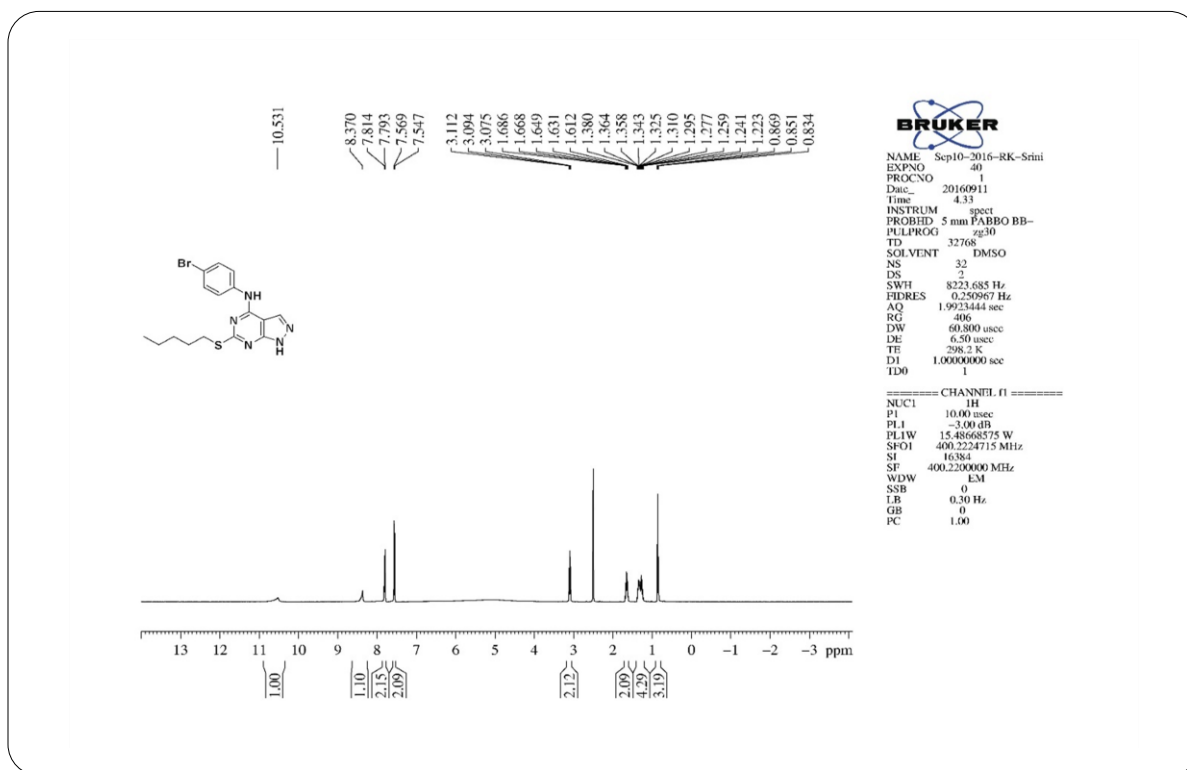
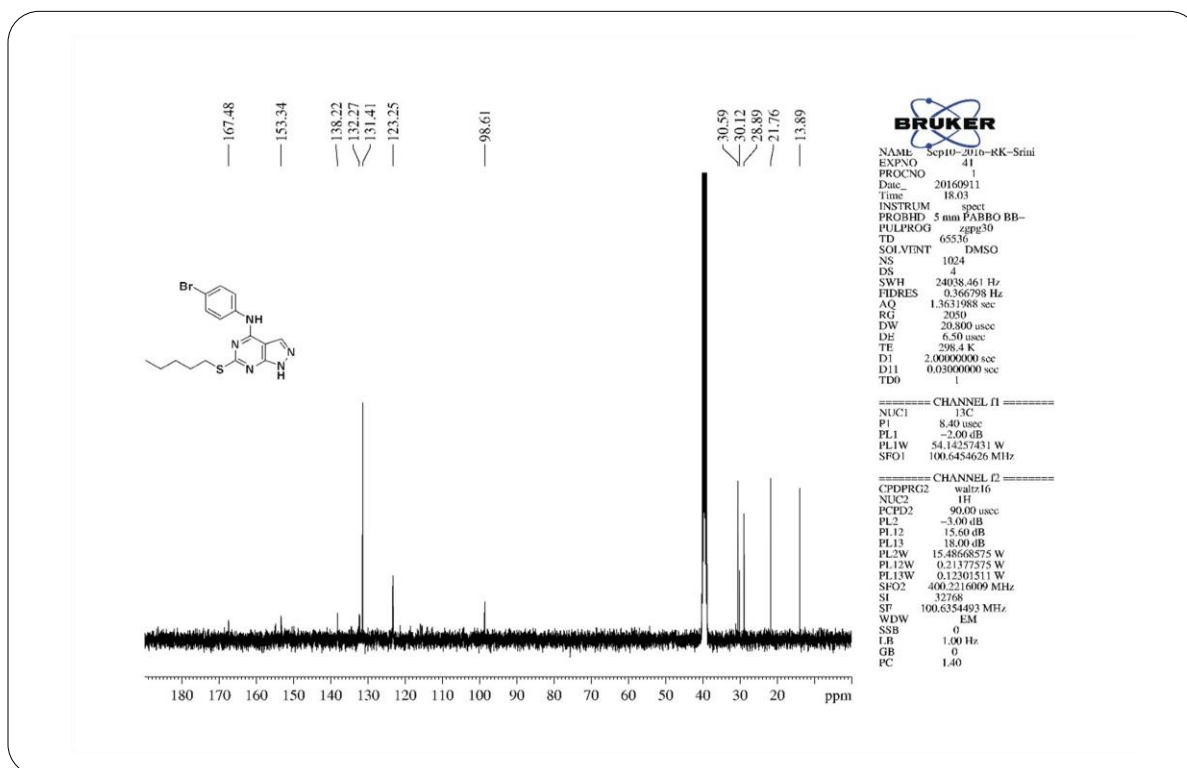
**¹H NMR Spectrum of Compound 32****¹³C NMR Spectrum of Compound 32**

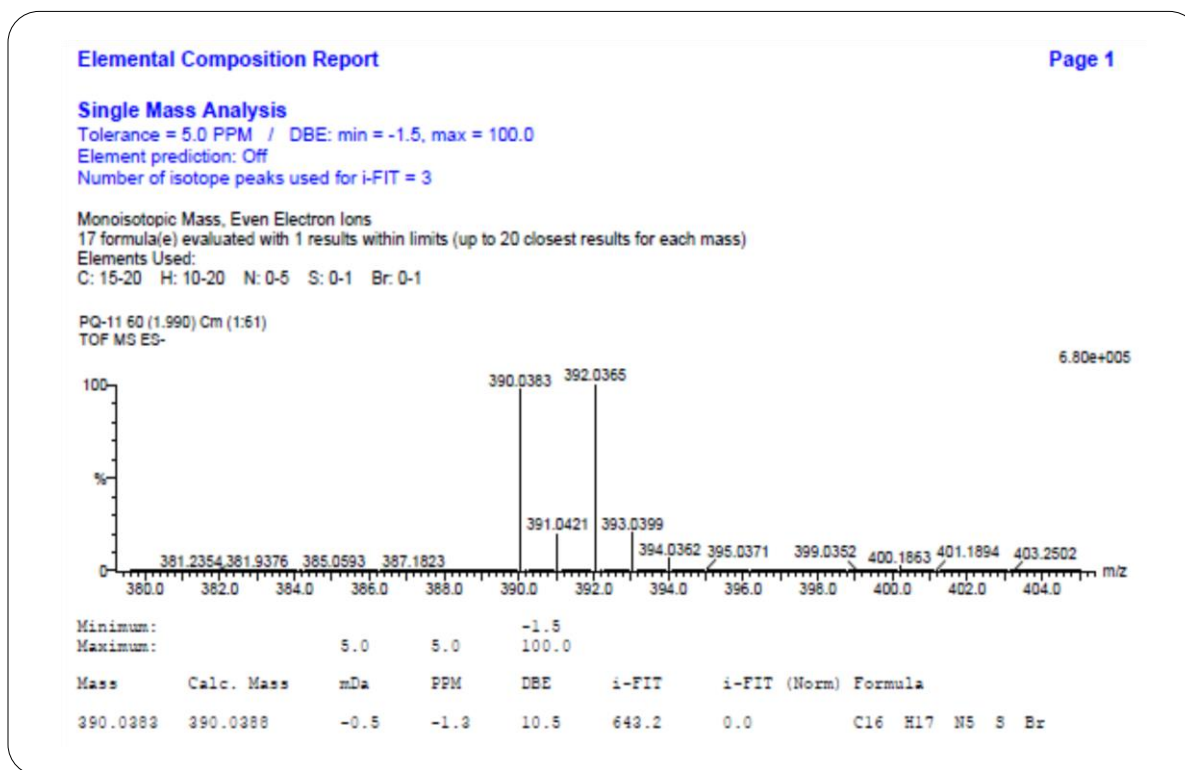


IR Spectrum of Compound 33

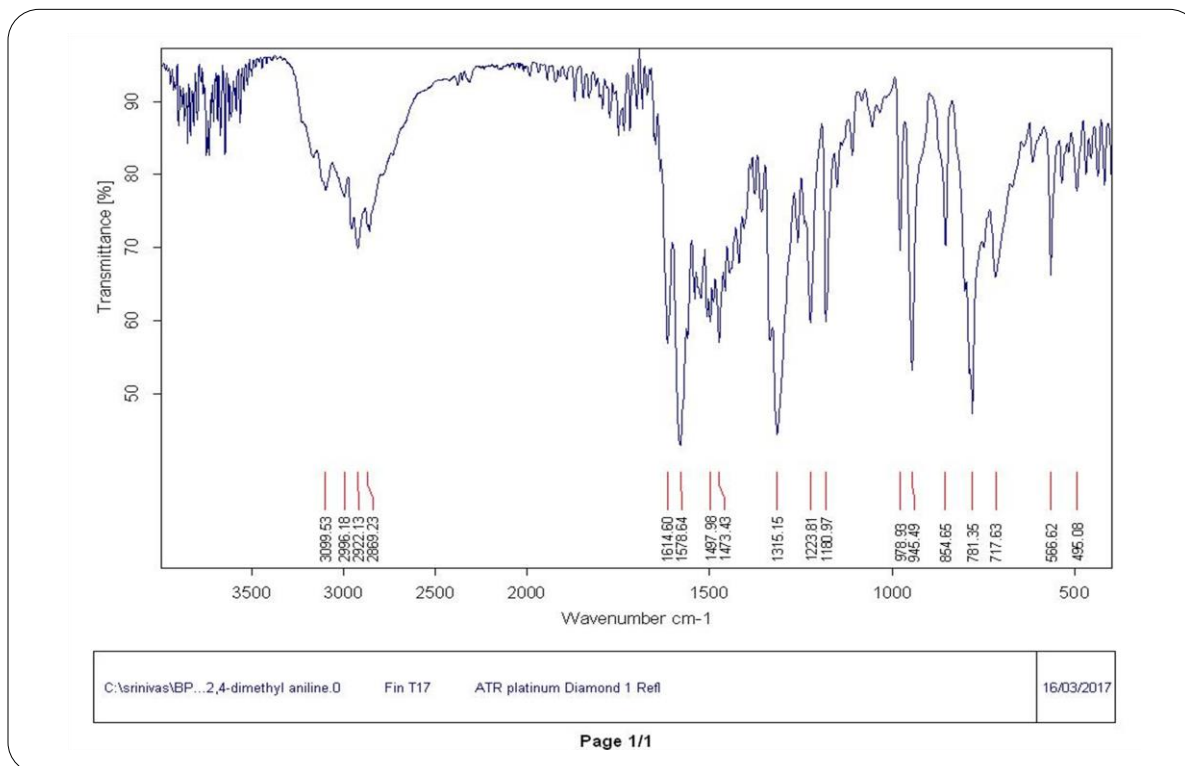
¹H NMR Spectrum of Compound 33

**¹³C NMR Spectrum of Compound 33****IR Spectrum of Compound 34**

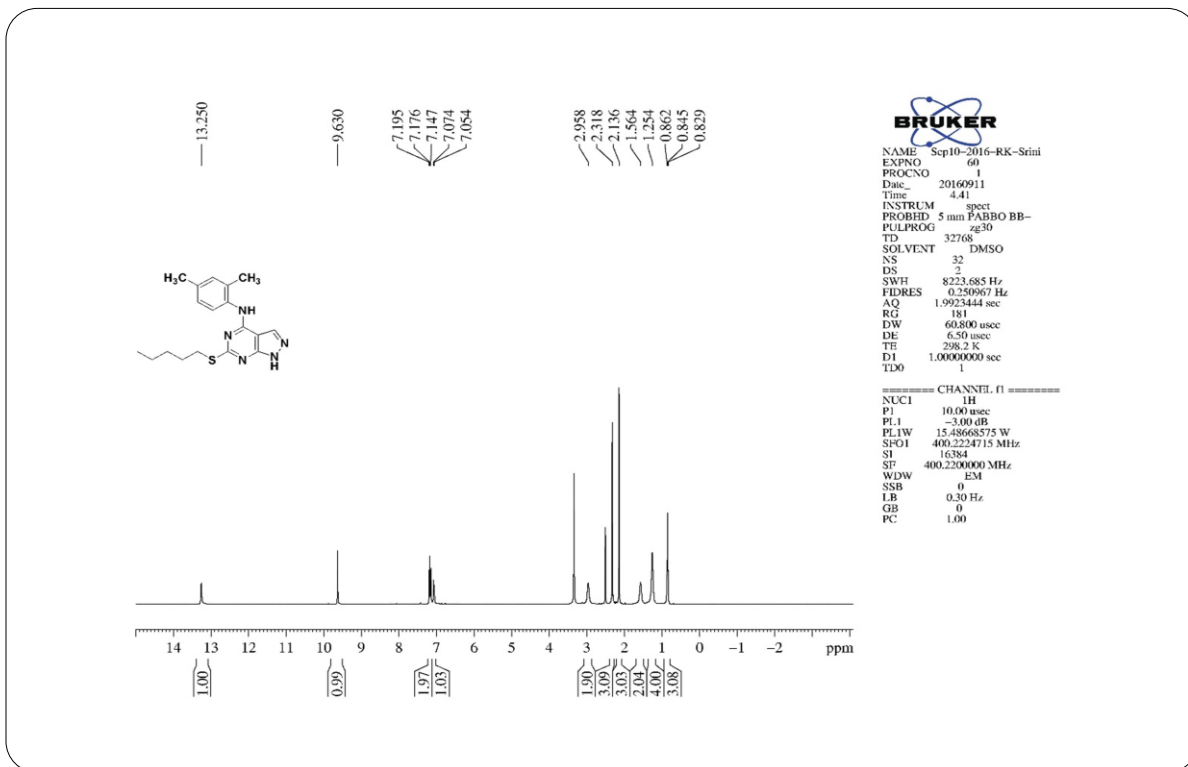
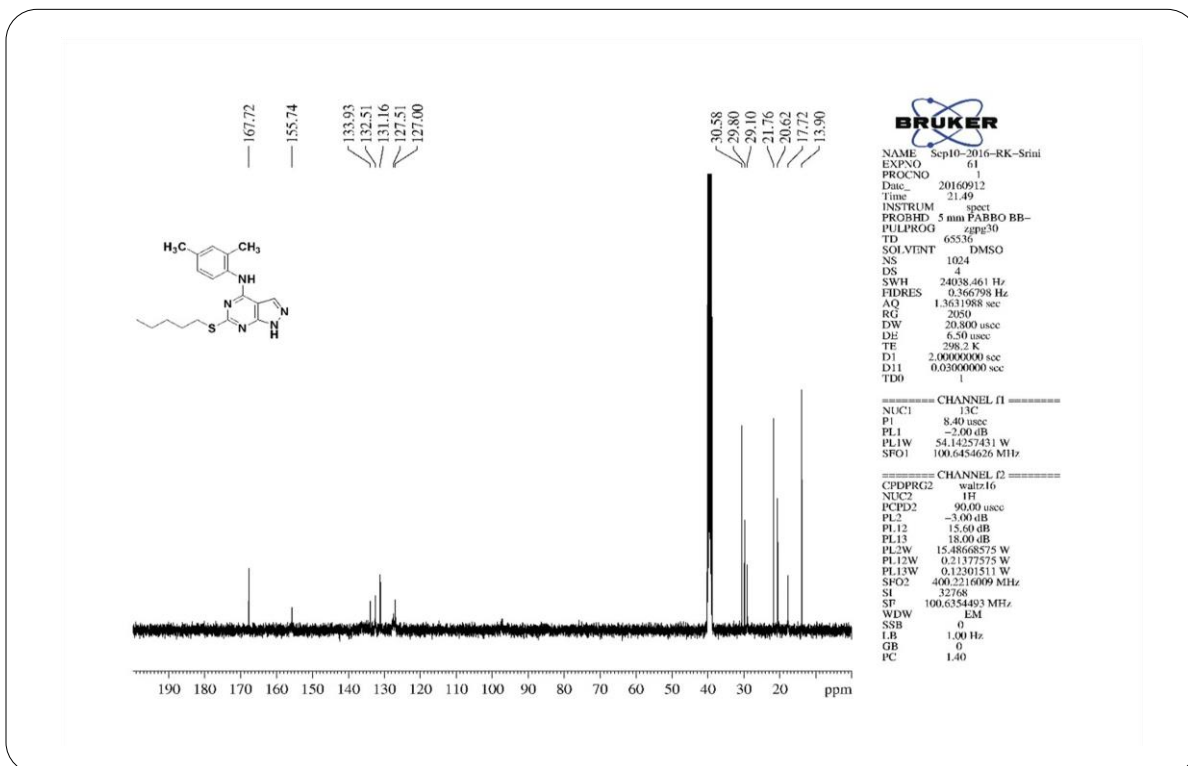
**¹H NMR Spectrum of Compound 34****¹³C NMR Spectrum of Compound 34**

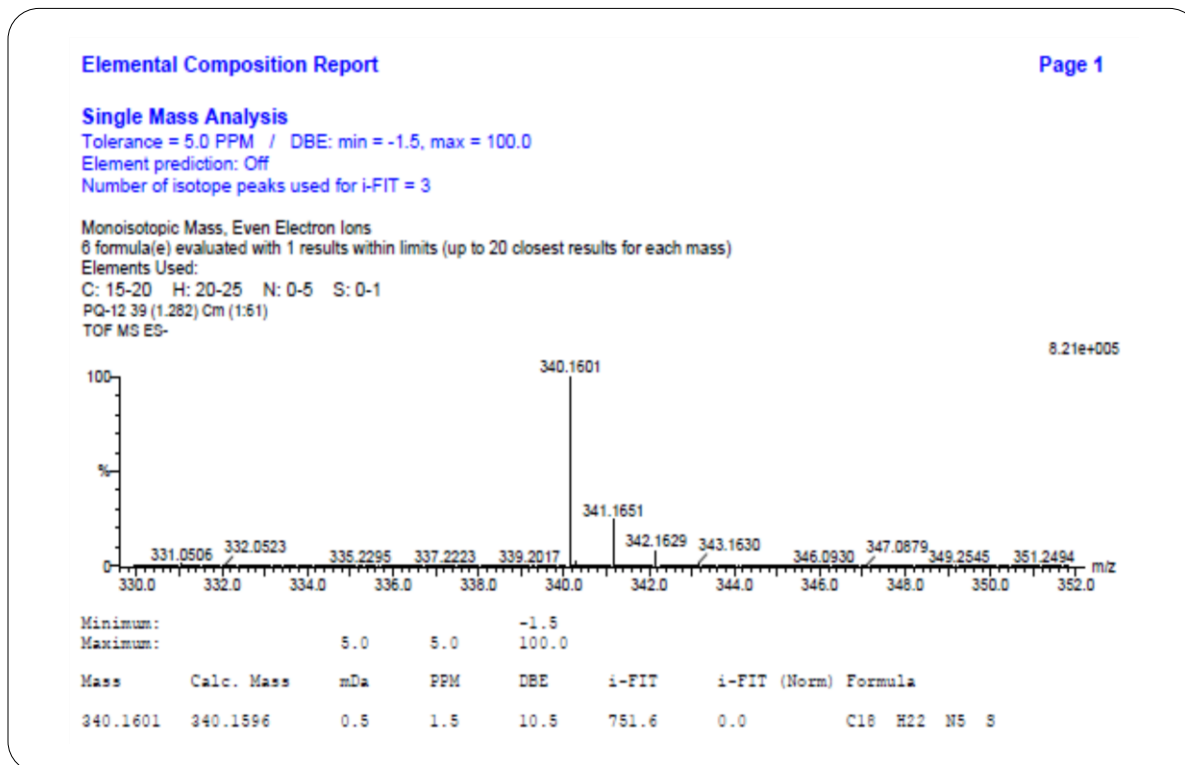


HRMS Spectrum of Compound 34

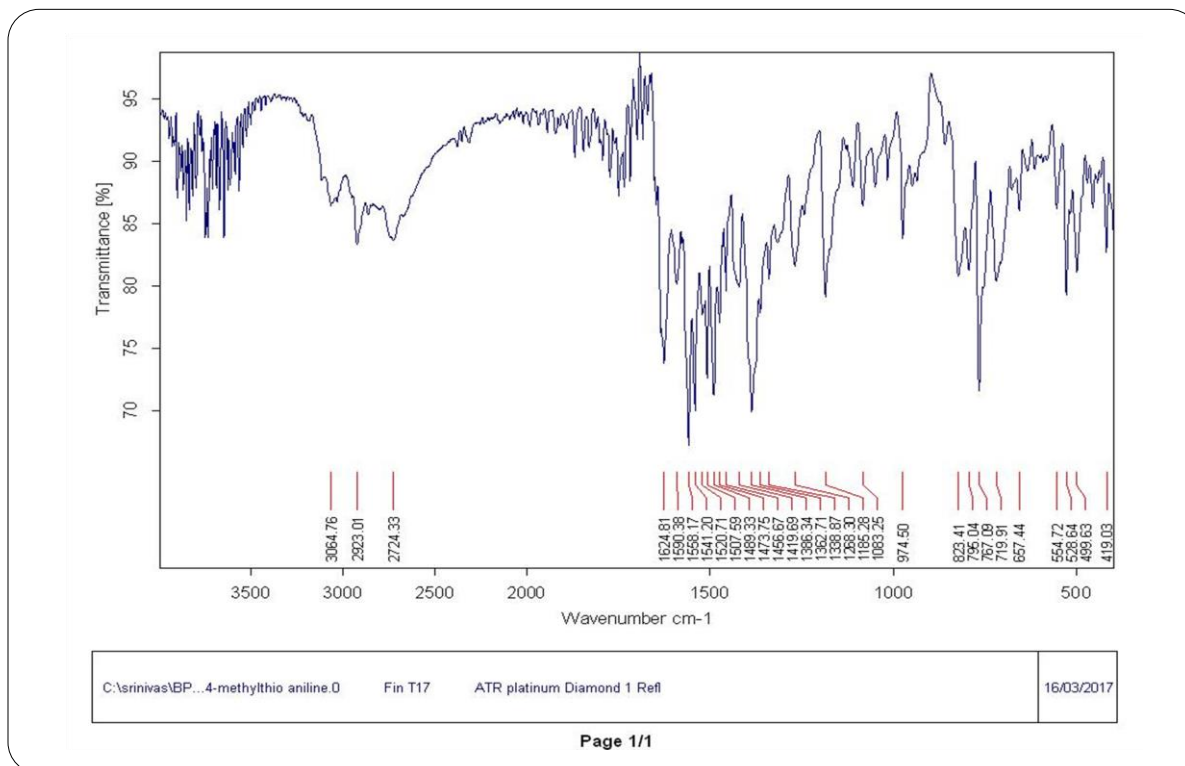


IR Spectrum of Compound 35

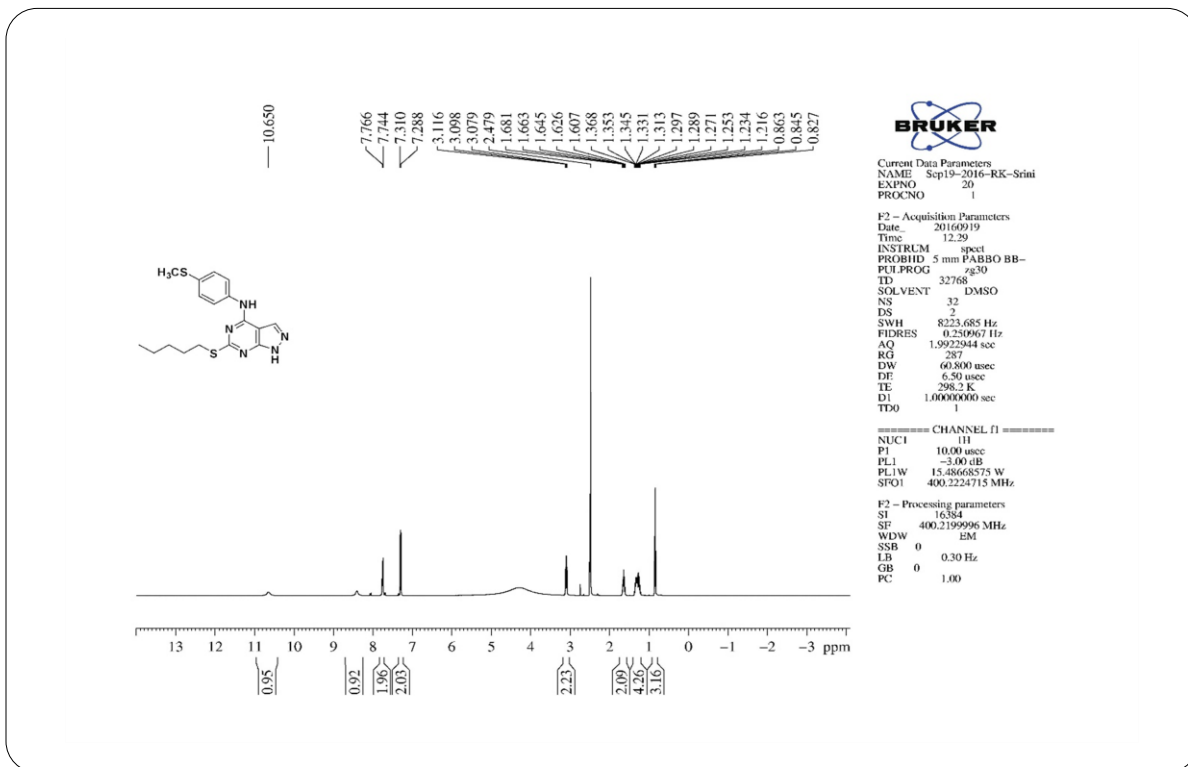
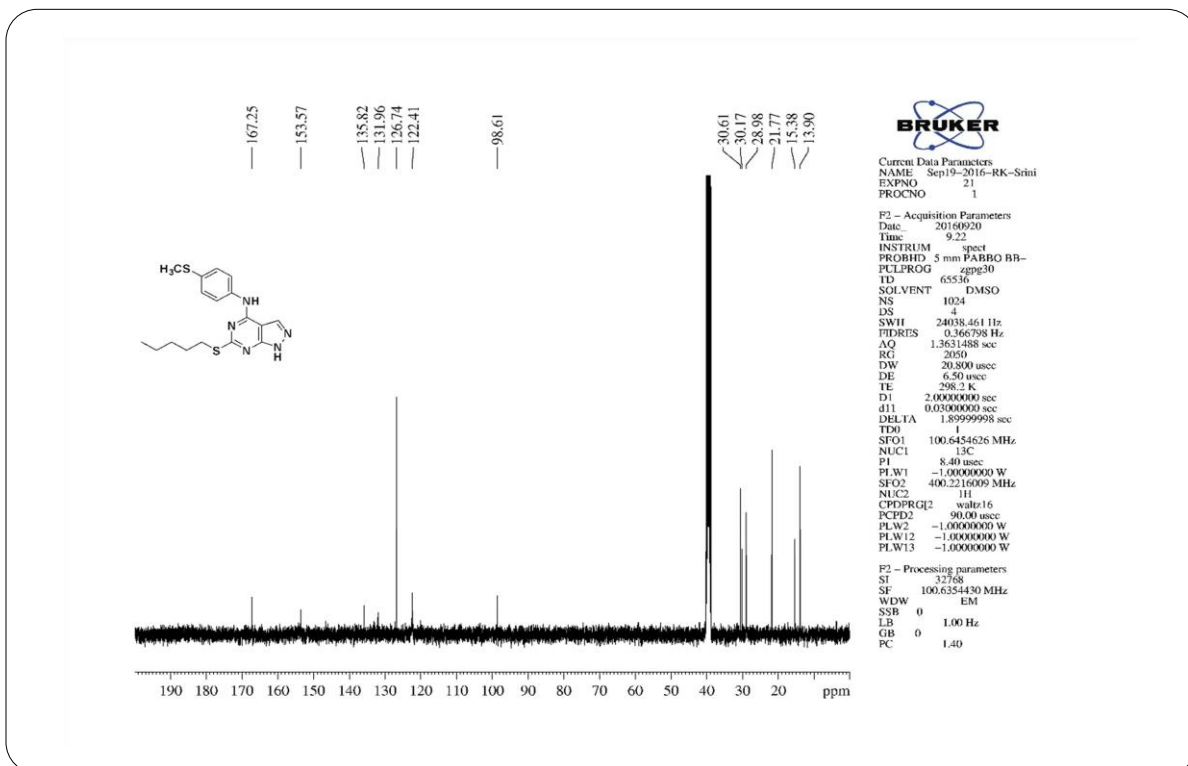
**¹H NMR Spectrum of Compound 35****¹³C NMR Spectrum of Compound 35**

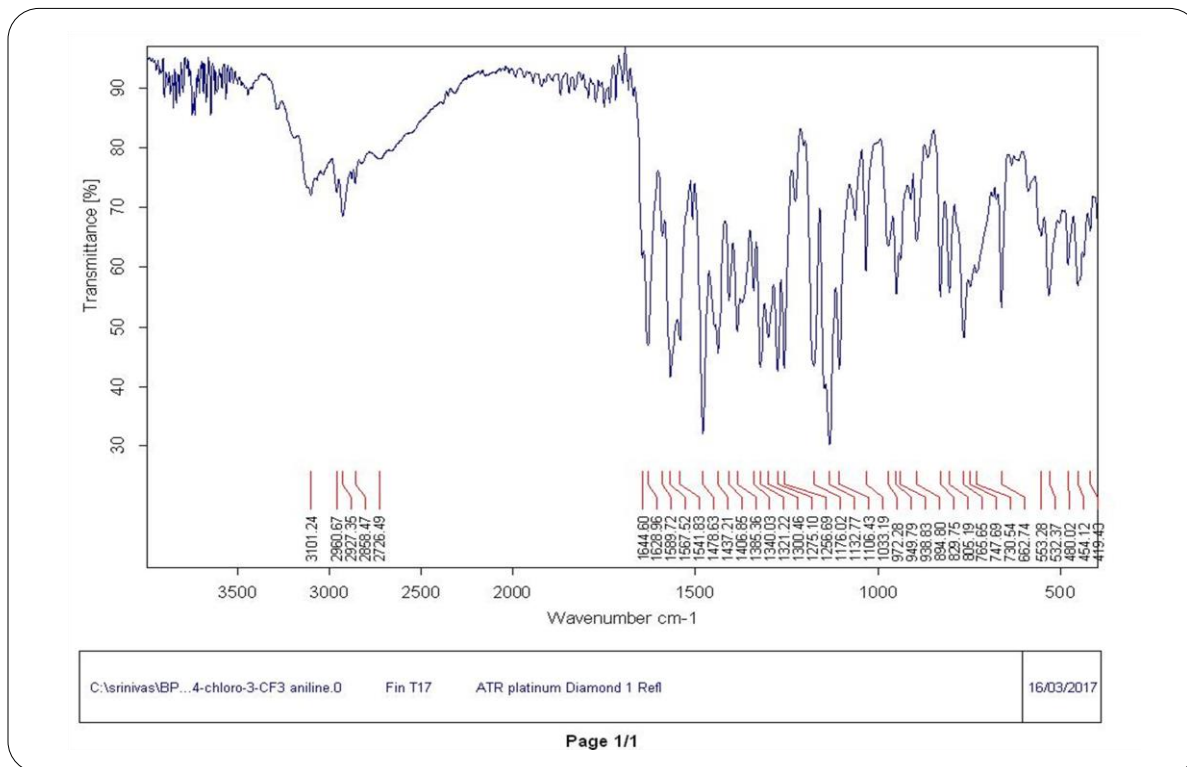


HRMS Spectrum of Compound 35

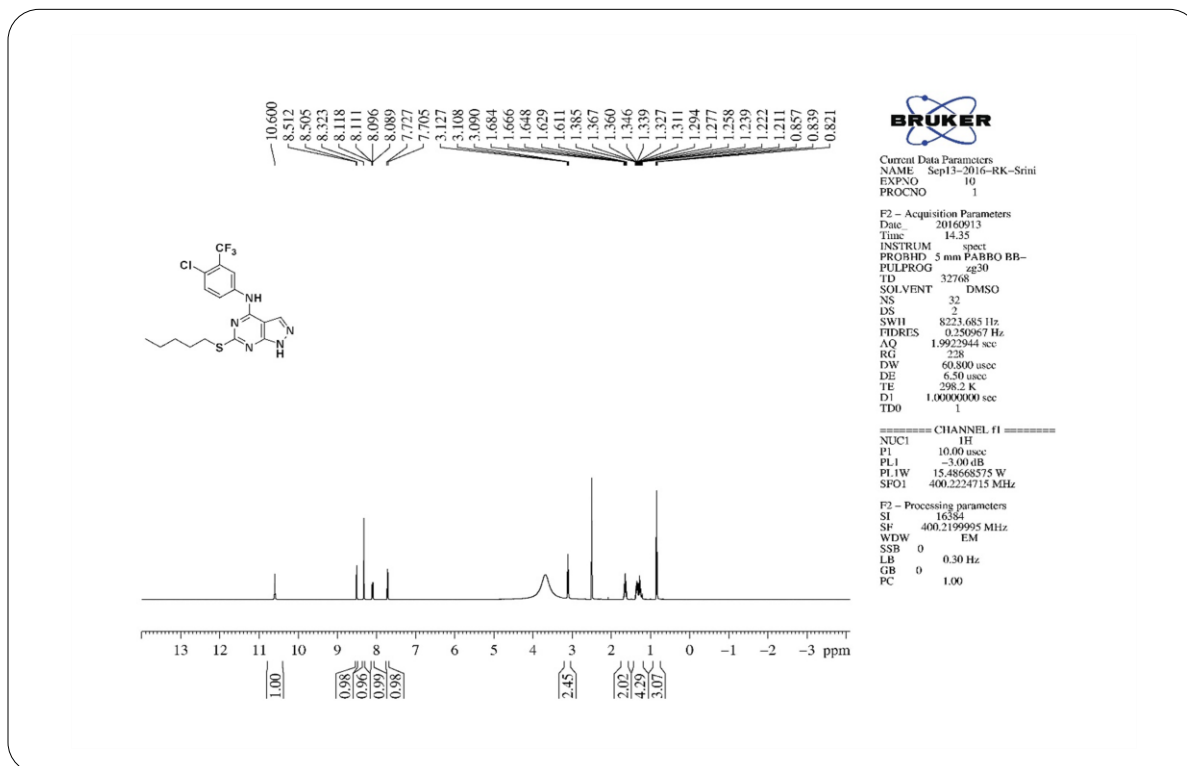


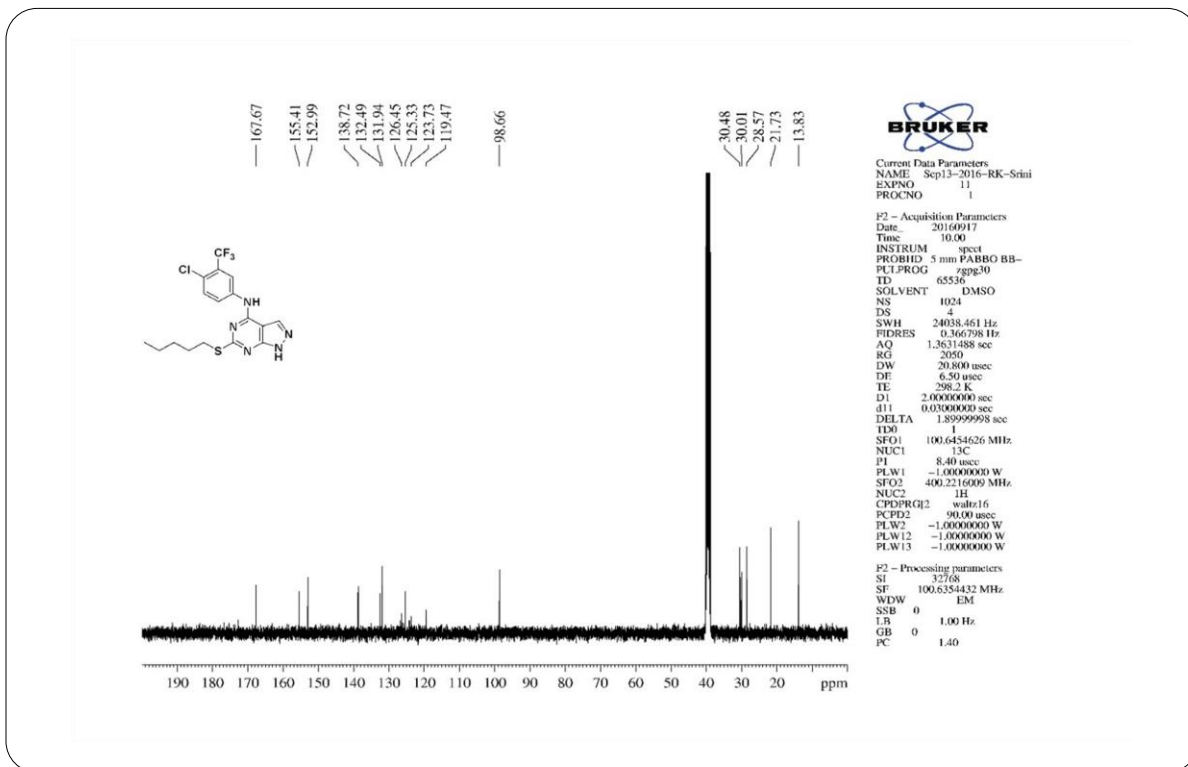
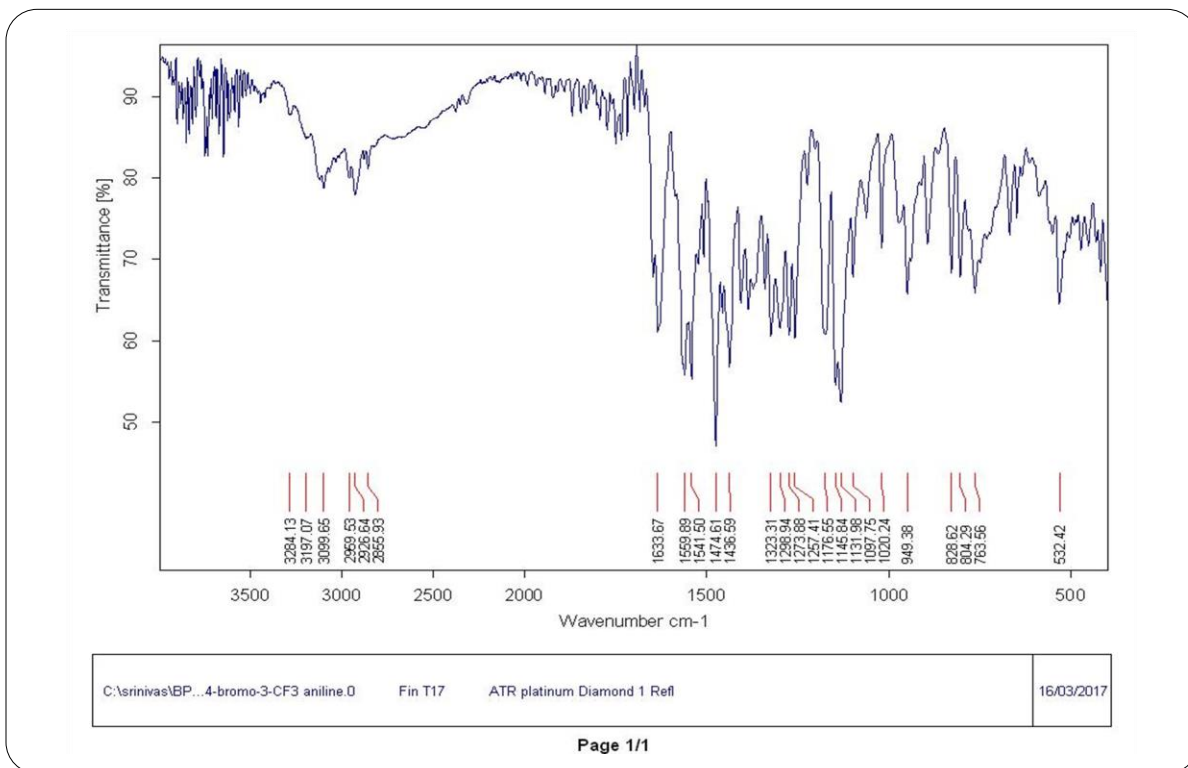
IR Spectrum of Compound 36

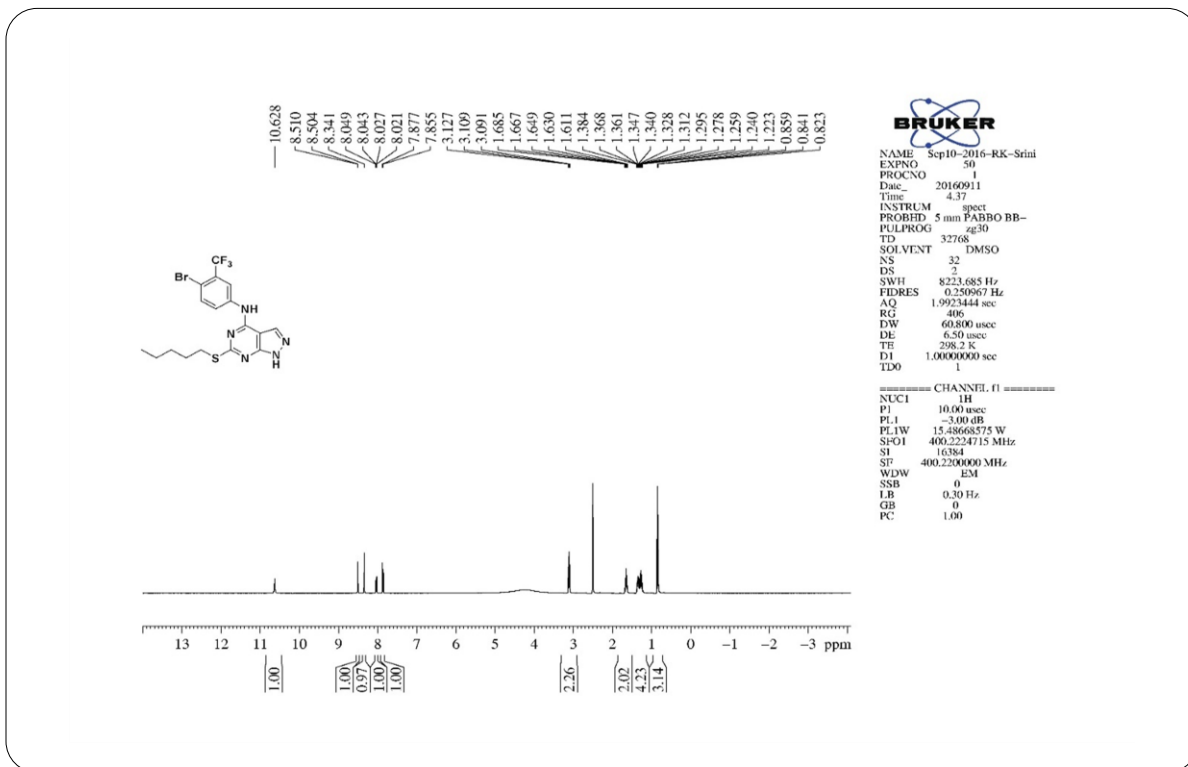
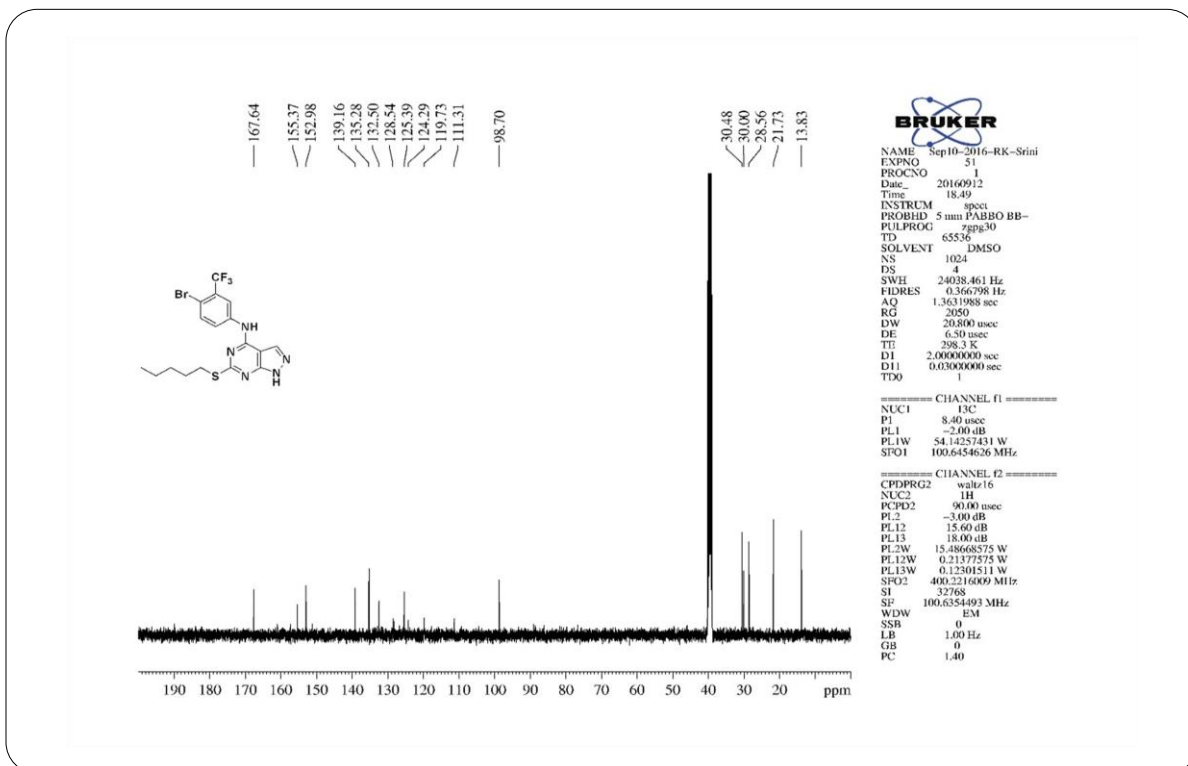
**¹H NMR Spectrum of Compound 36****¹³C NMR Spectrum of Compound 36**



IR Spectrum of Compound 37

¹H NMR Spectrum of Compound 37

**¹³C NMR Spectrum of Compound 37****IR Spectrum of Compound 38**

**¹H NMR Spectrum of Compound 38****¹³C NMR Spectrum of Compound 38**

Elemental Composition Report

Page 1

Single Mass Analysis

Tolerance = 5.0 PPM / DBE: min = -1.5, max = 100.0

Element prediction: Off

Number of isotope peaks used for i-FIT = 3

Monoisotopic Mass, Even Electron Ions

74 formula(e) evaluated with 1 results within limits (up to 20 closest results for each mass)

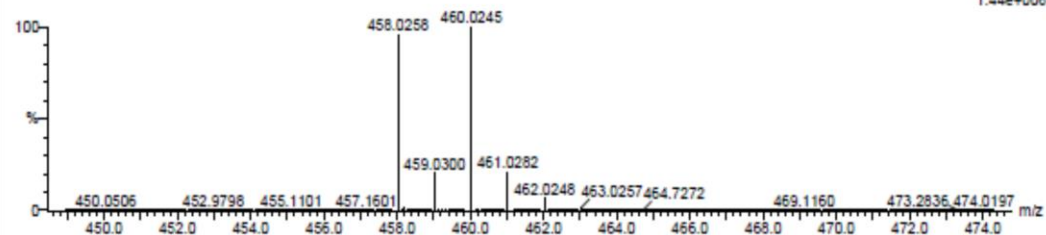
Elements Used:

C: 15-20 H: 15-20 N: 0-5 F: 0-3 S: 0-1 Br: 0-1

PQ-15 2 (0.034) Cm (1:61)

TOF MS ES-

1.44e+006



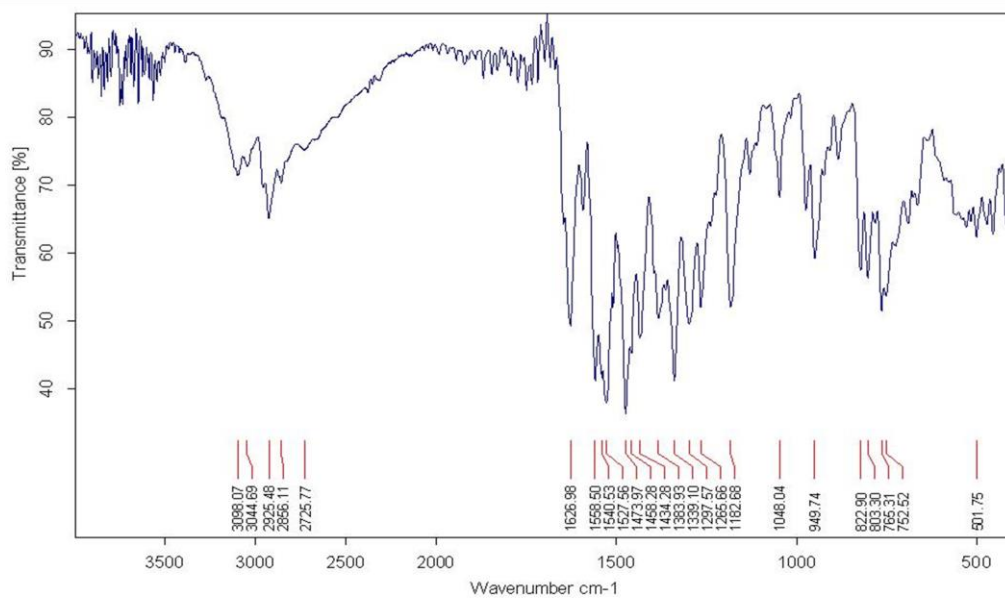
Minimum:

Maximum: 5.0 5.0 -1.5

Mass Calc. Mass mDa PPM DBE i-FIT i-FIT (Norm) Formula

Mass	Calc. Mass	mDa	PPM	DBE	i-FIT	i-FIT (Norm)	Formula
458.0258	458.0262	-0.4	-0.9	10.5	673.0	0.0	C17 H16 N5 F3 S Br

HRMS Spectrum of Compound 38

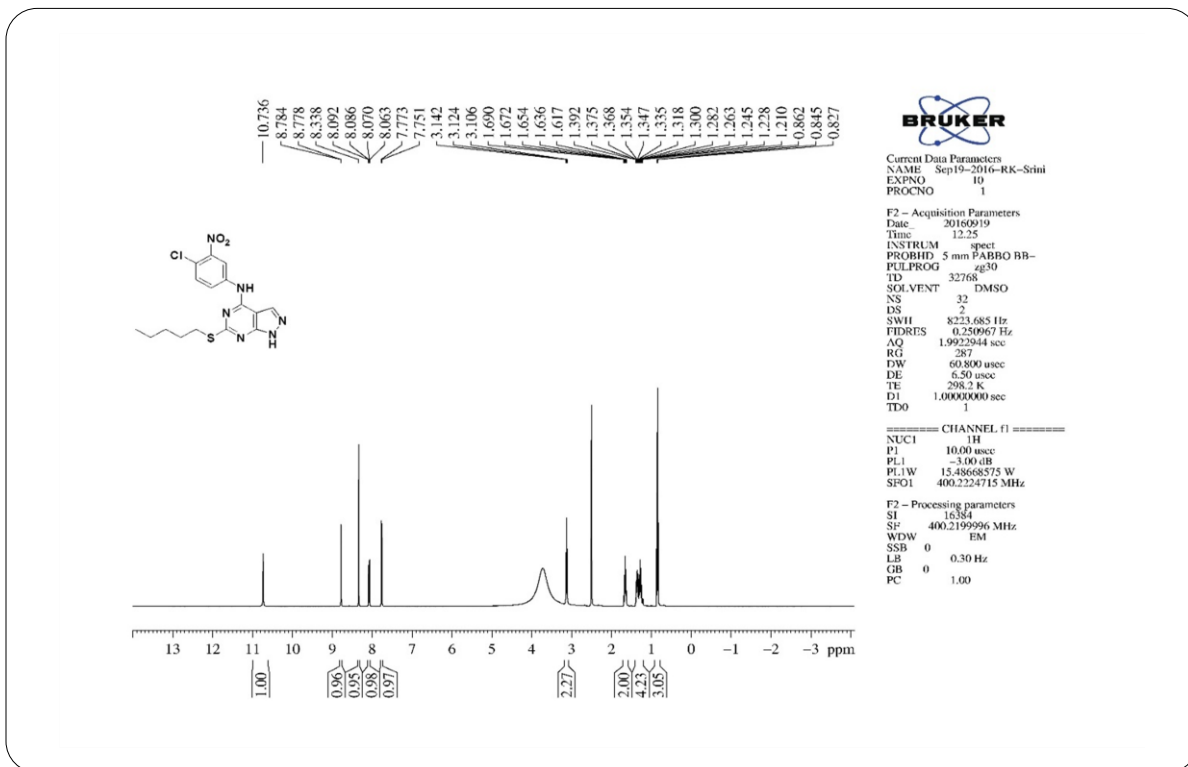
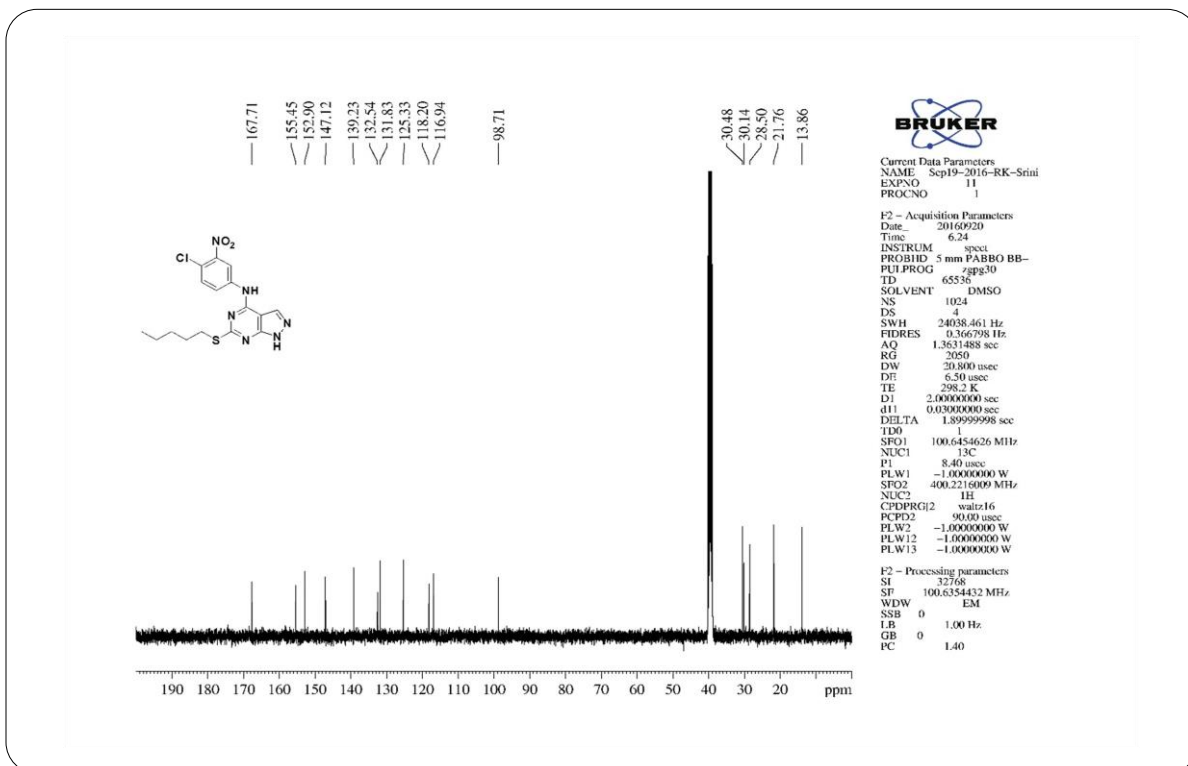


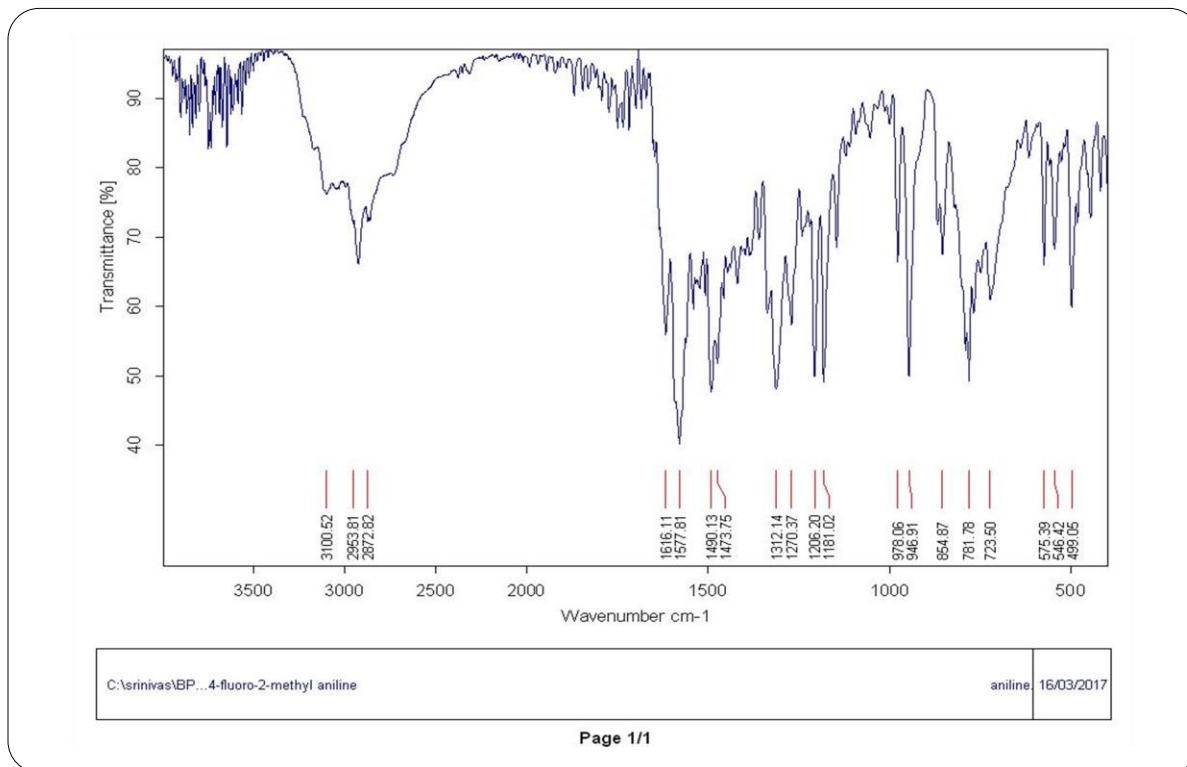
C:\srinivas\BP...4-chloro-3-nitro aniline.D Fin T17 ATR platinum Diamond 1 Ref

16/03/2017

Page 1/1

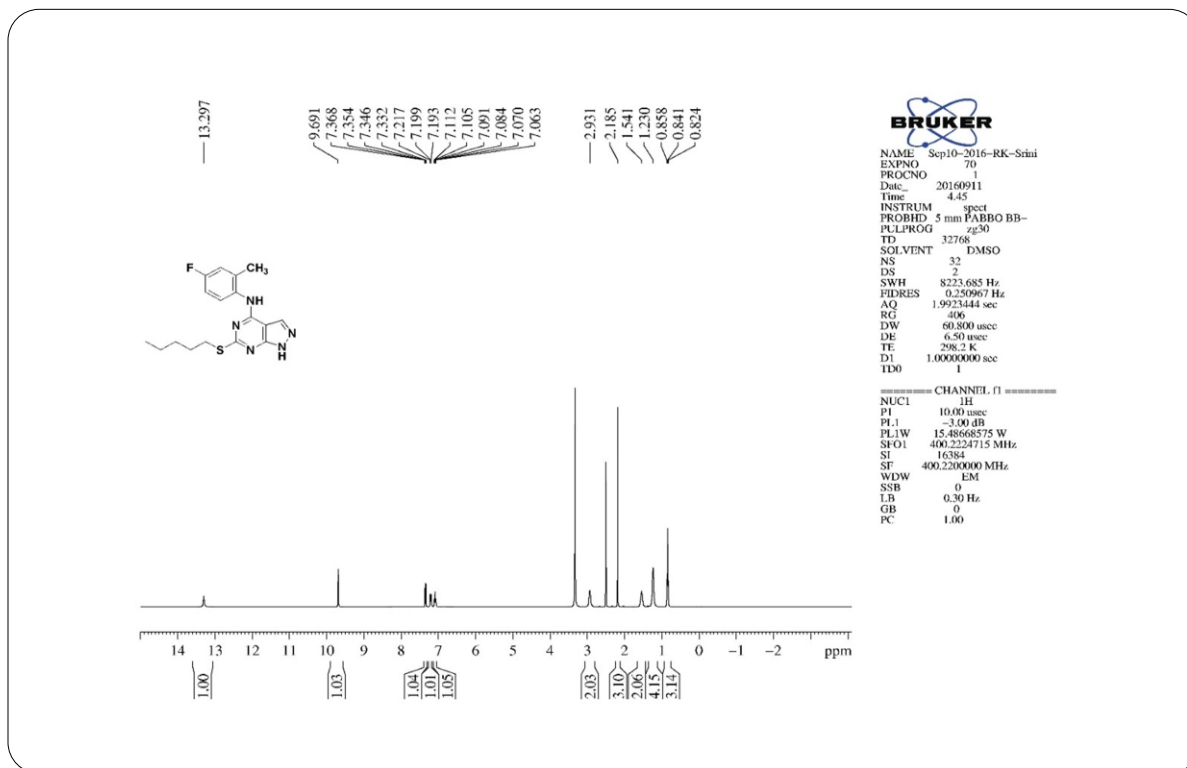
IR Spectrum of Compound 39

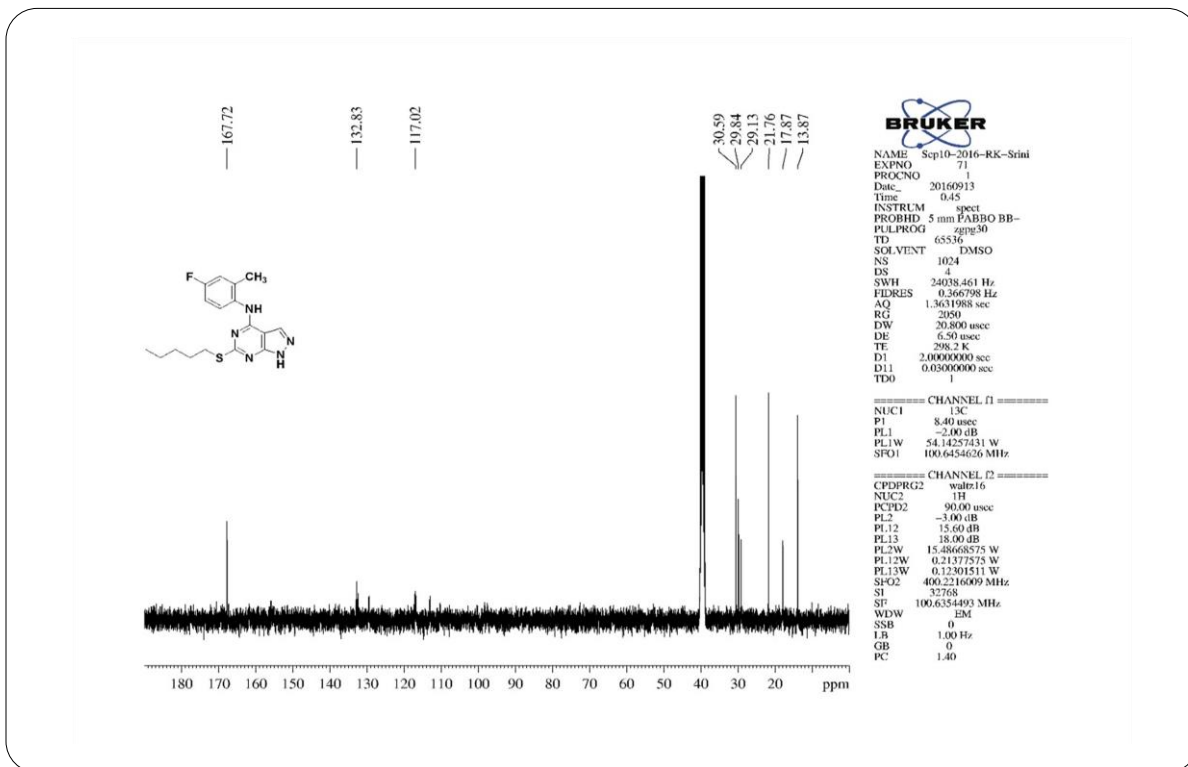
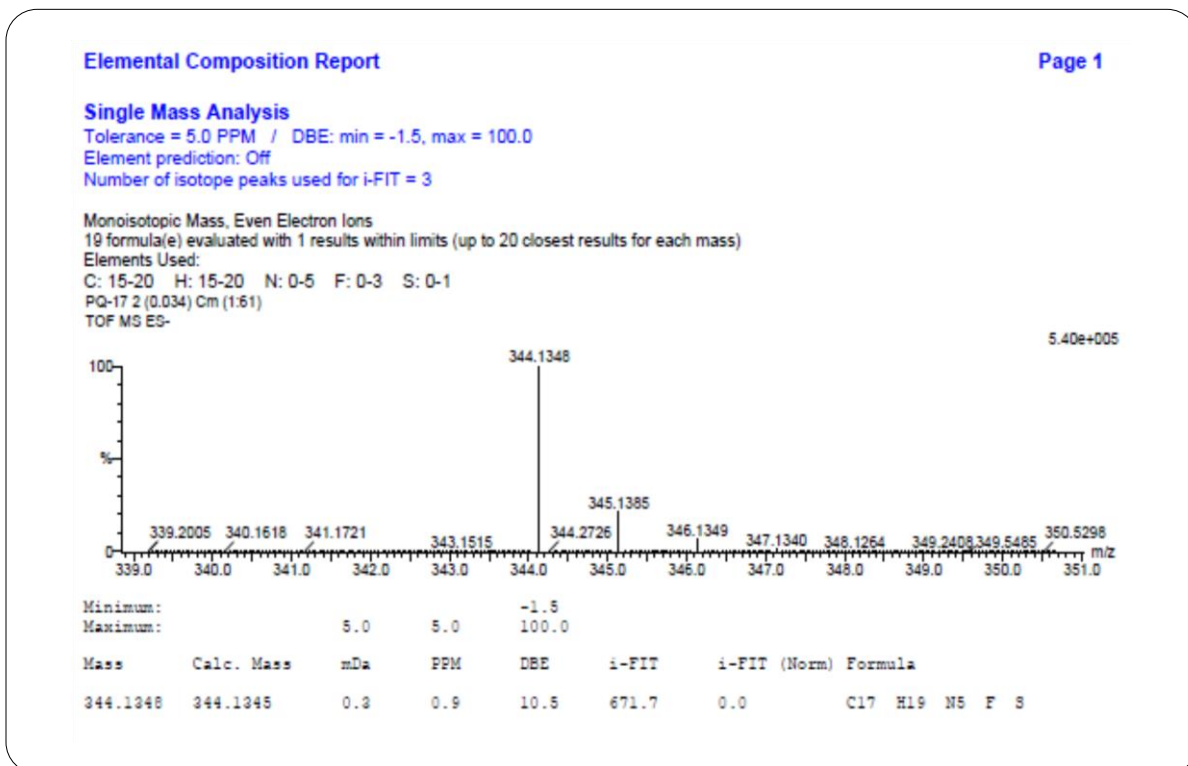
**¹H NMR Spectrum of Compound 39****¹³C NMR Spectrum of Compound 39**



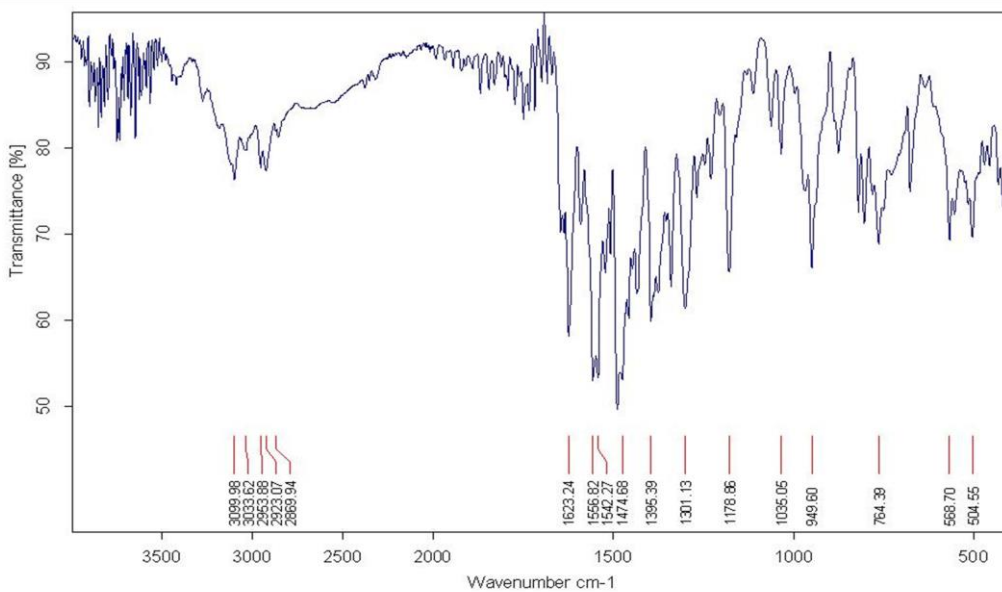
Page 1/1

IR Spectrum of Compound 40

¹H NMR Spectrum of Compound 40

¹³C NMR Spectrum of Compound 40

HRMS Spectrum of Compound 40



C:\srinivas\BP...3-bromo-4-methyl aniline.1

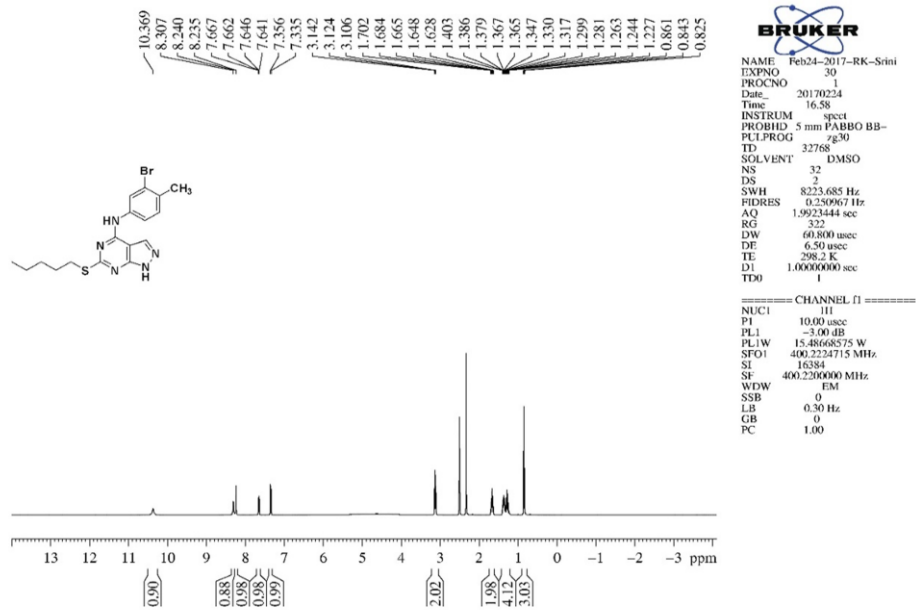
Fin T17

ATR platinum Diamond 1 Refl

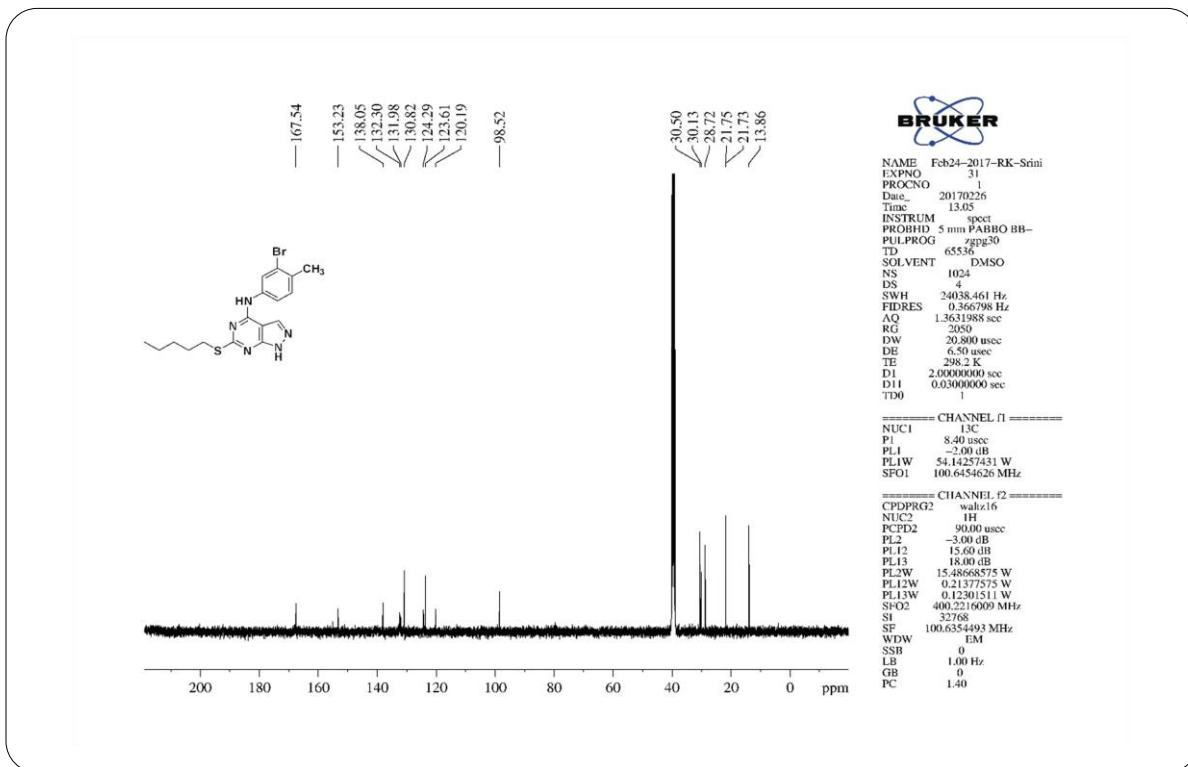
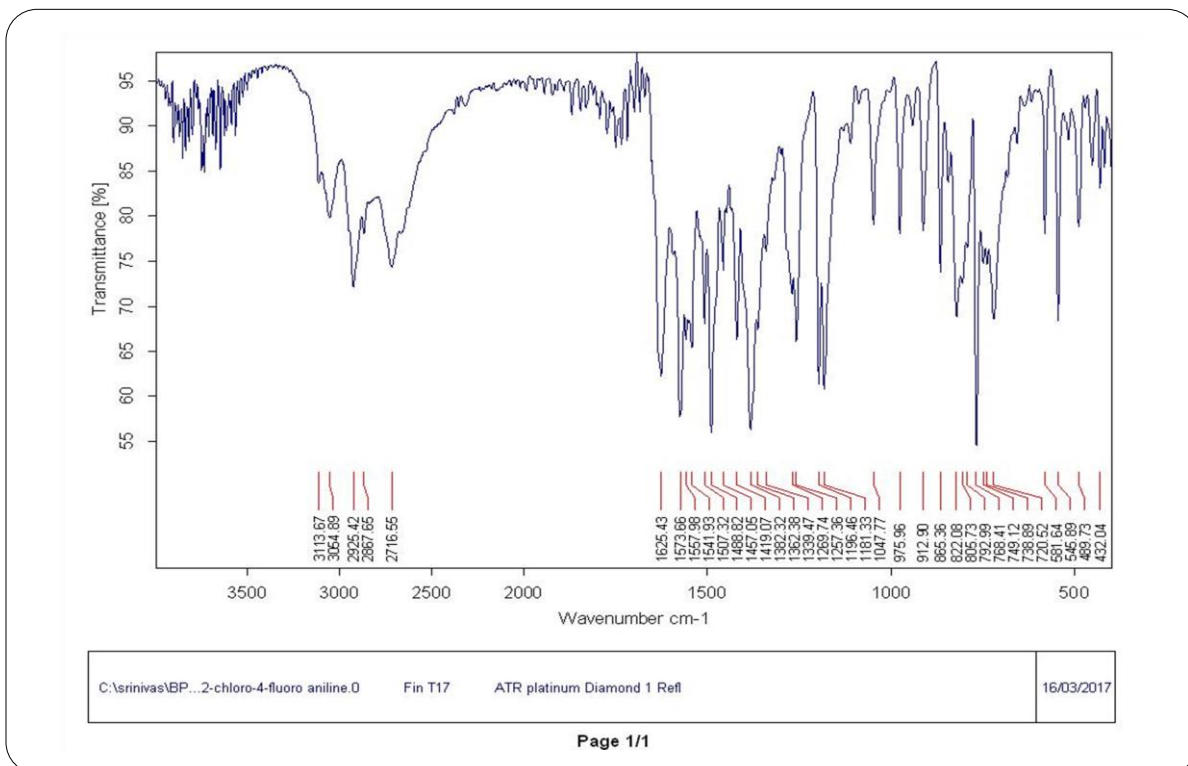
16/03/2017

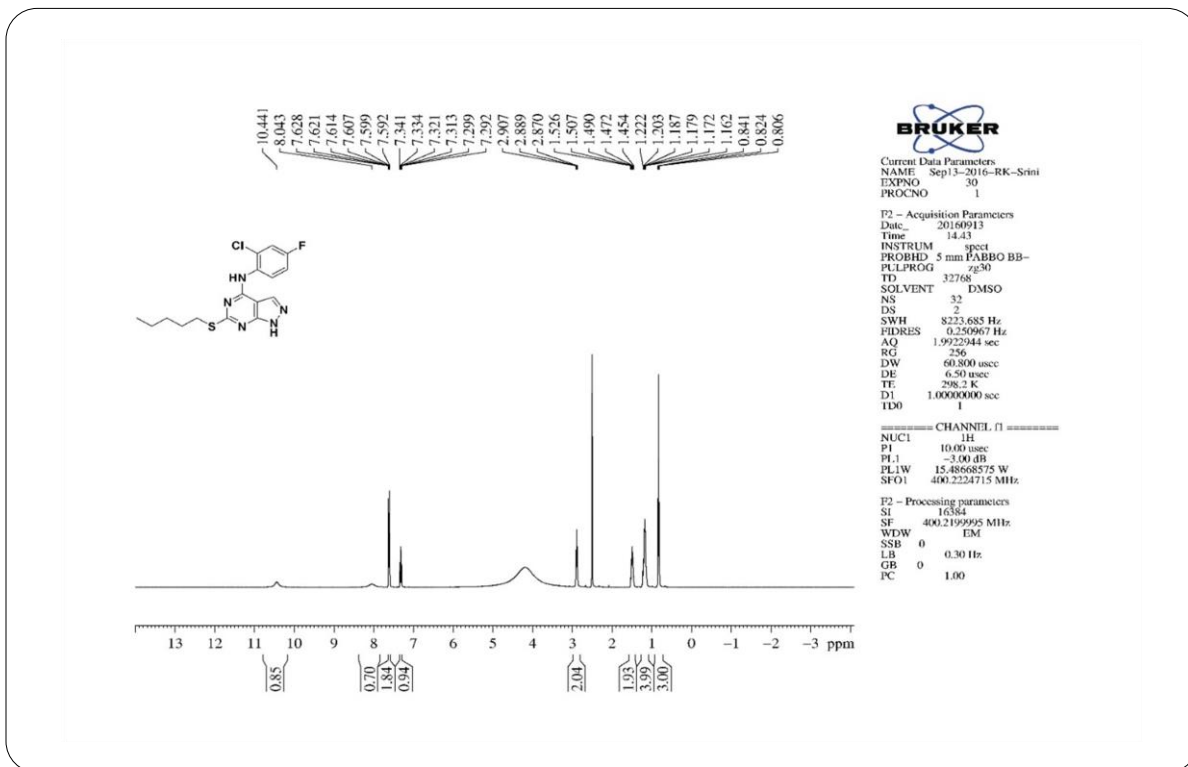
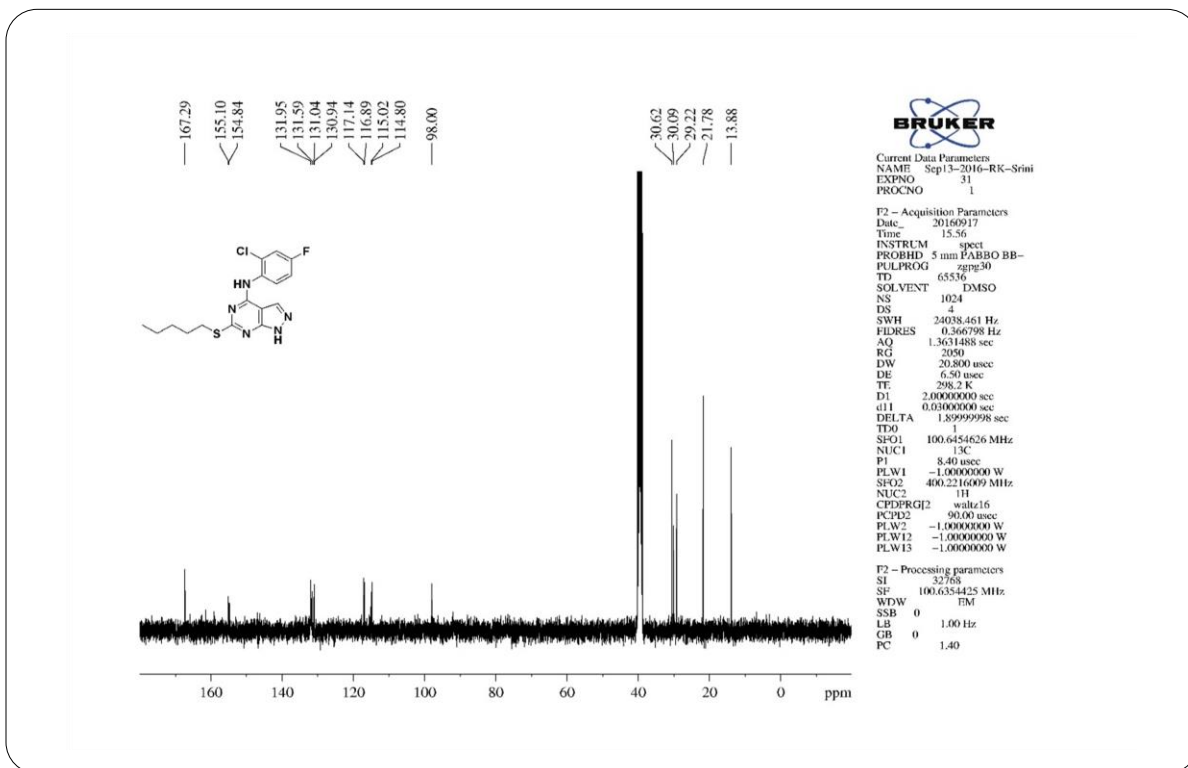
Page 1/1

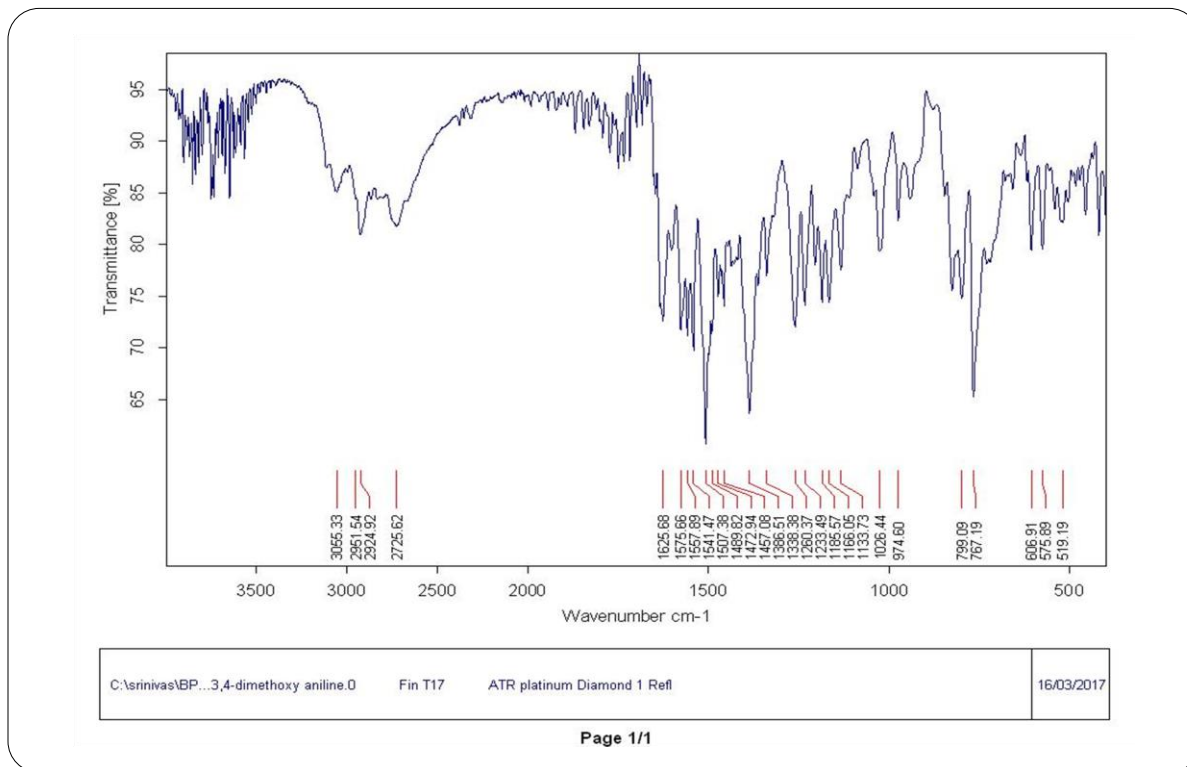
IR Spectrum of Compound 41



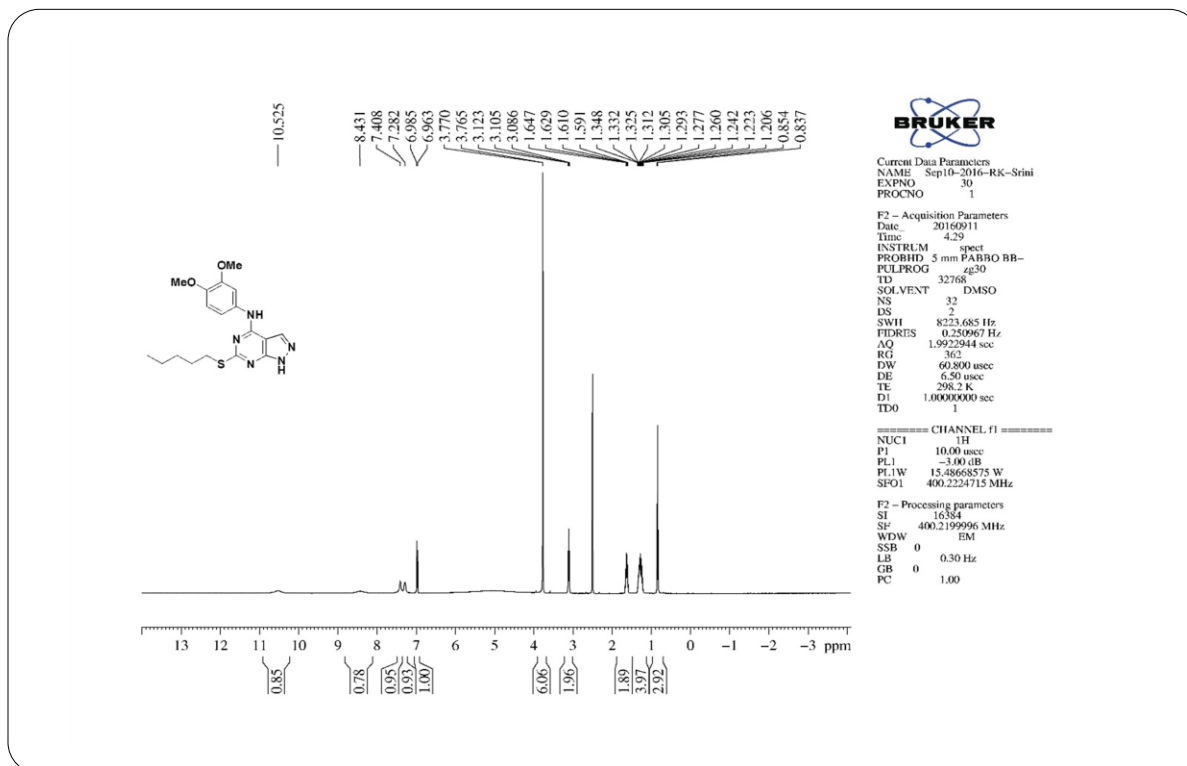
¹H NMR Spectrum of Compound 41

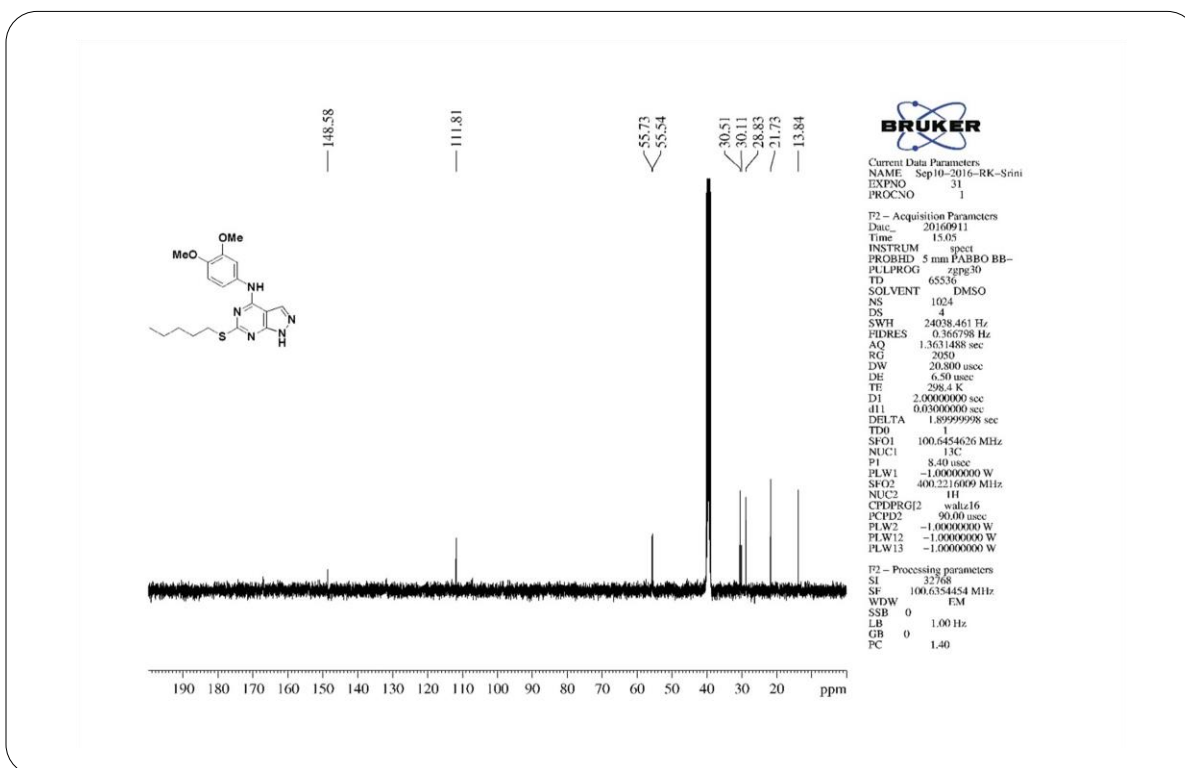
**¹³C NMR Spectrum of Compound 41****IR Spectrum of Compound 42**

**¹H NMR Spectrum of Compound 42****¹³C NMR Spectrum of Compound 42**



IR Spectrum of Compound 43

¹H NMR Spectrum of Compound 43

¹³C NMR Spectrum of Compound 43

Elemental Composition Report

Page 1

Single Mass Analysis

Tolerance = 5.0 PPM / DBE: min = -1.5, max = 100.0

Element prediction: Off

Number of isotope peaks used for i-FIT = 3

Monoisotopic Mass, Even Electron Ions

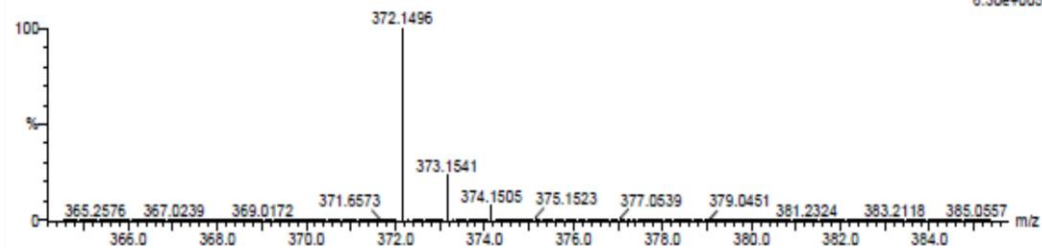
35 formula(e) evaluated with 1 results within limits (up to 20 closest results for each mass)

Elements Used:

C: 15-20 H: 20-25 N: 0-5 O: 0-5 S: 0-1

PQ-20 42 (1.384) Cm (1:61)

TOF MS ES-



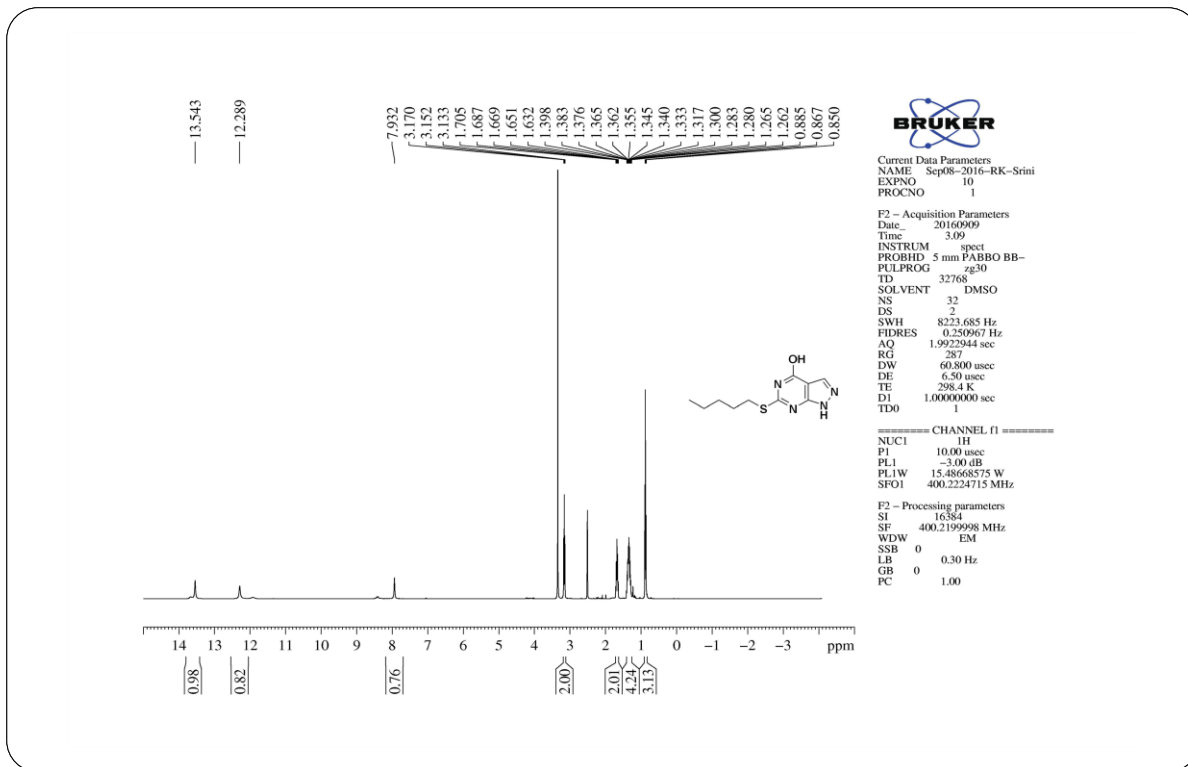
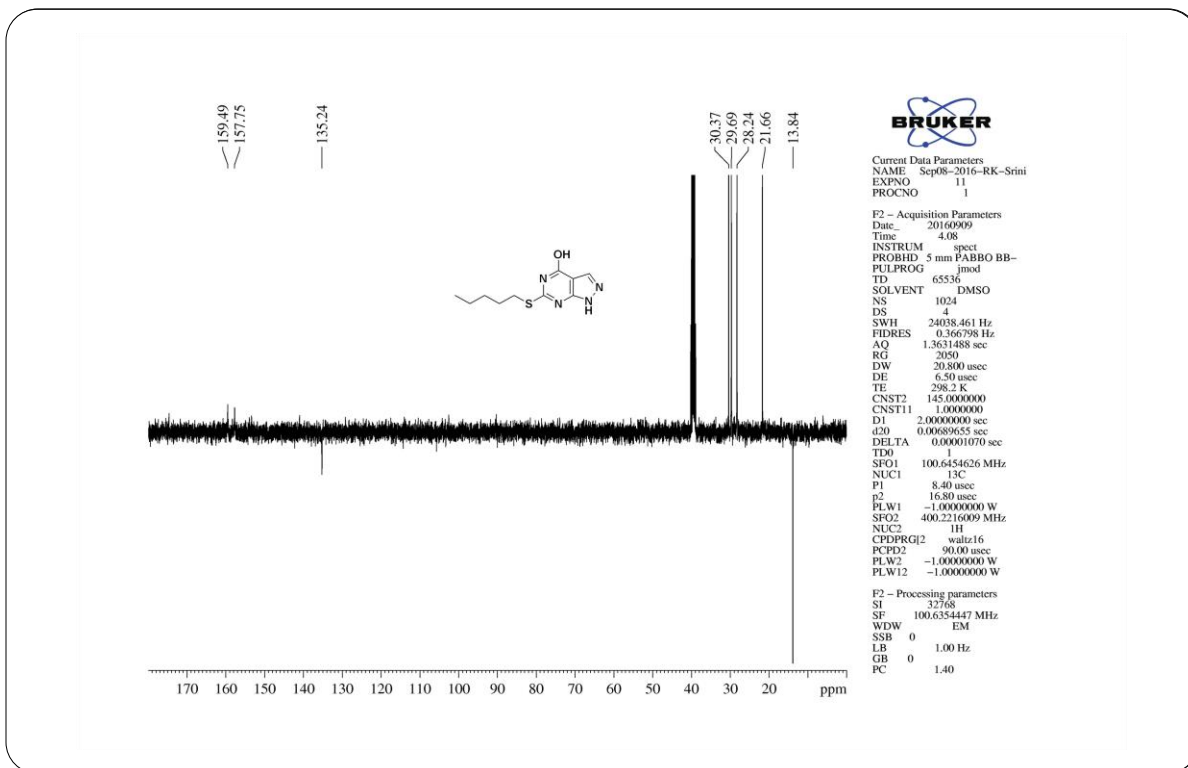
Minimum: -1.5
 Maximum: 5.0 5.0 100.0

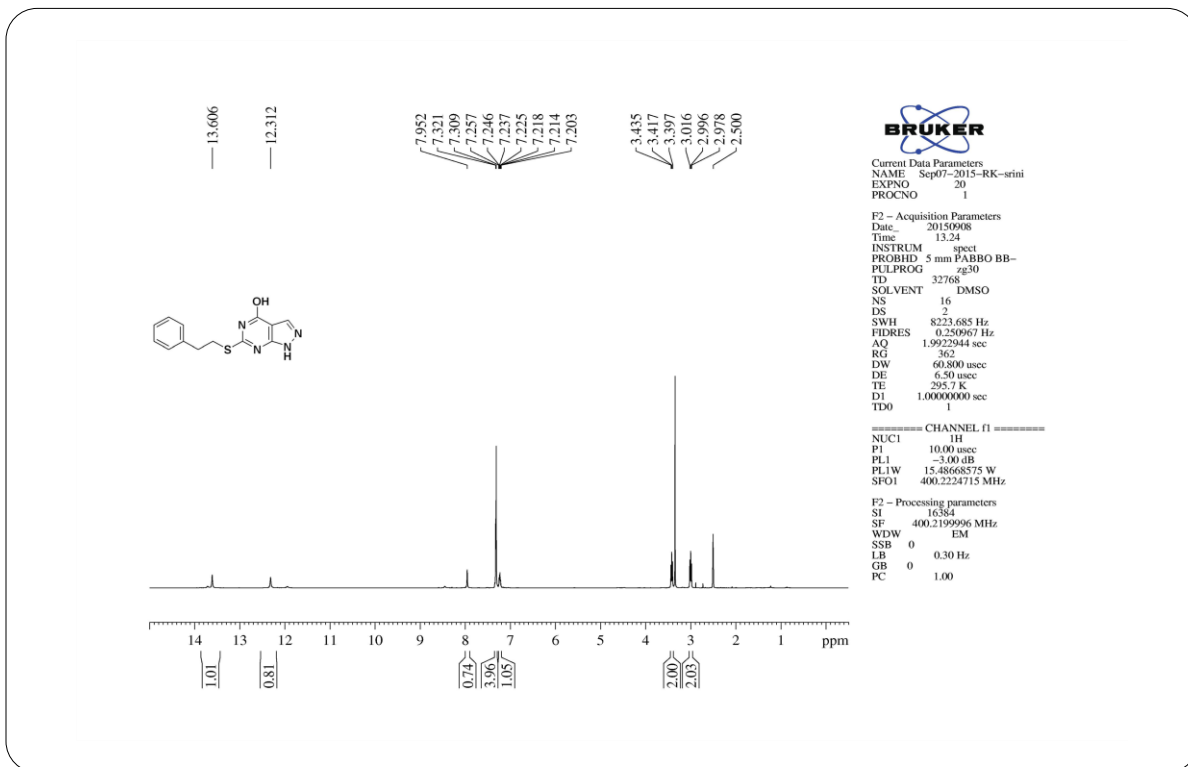
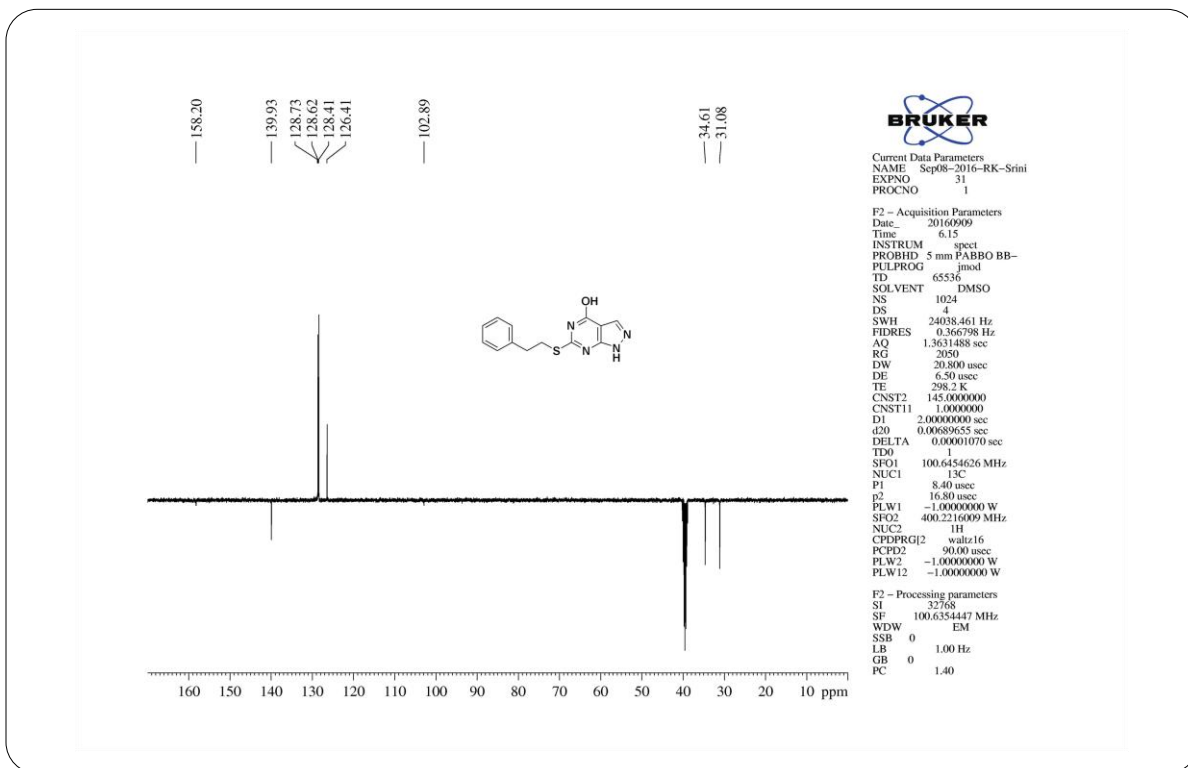
Mass	Calc. Mass	mDa	PPM	DBE	i-FIT	i-FIT (Norm)	Formula
372.1496	372.1494	0.2	0.5	10.5	674.1	0.0	C18 H22 N5 O2 S

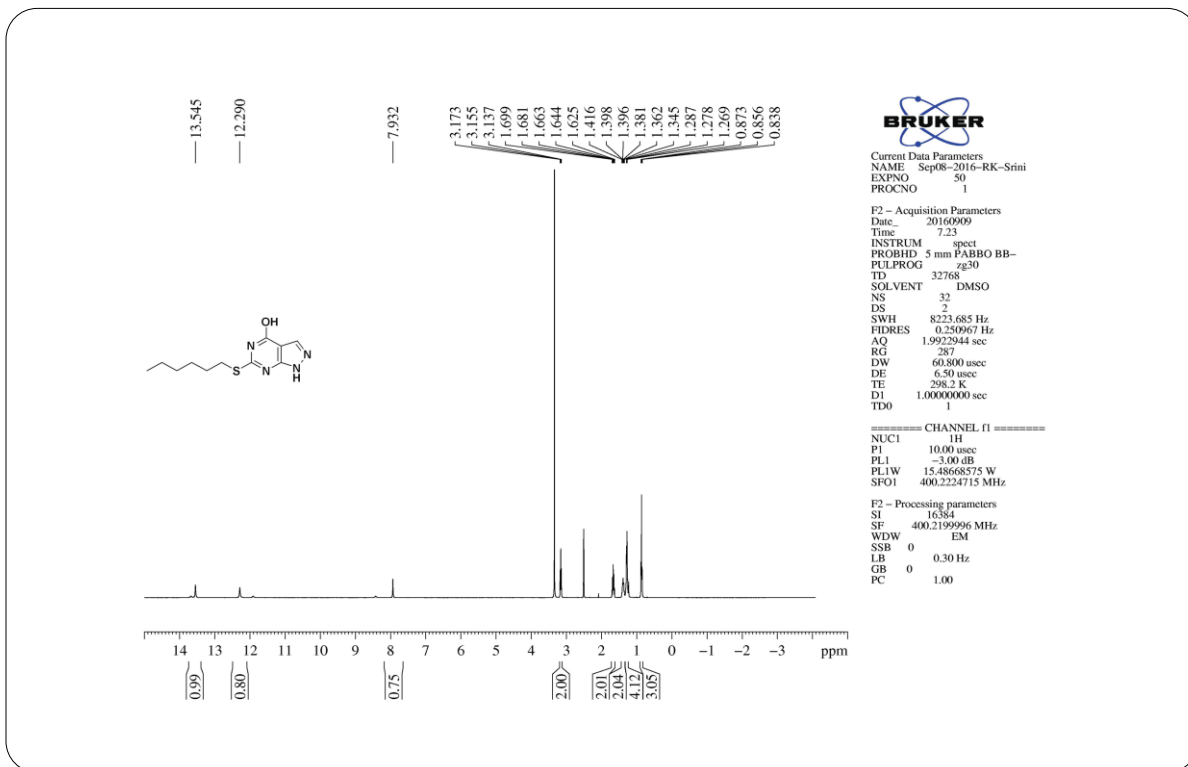
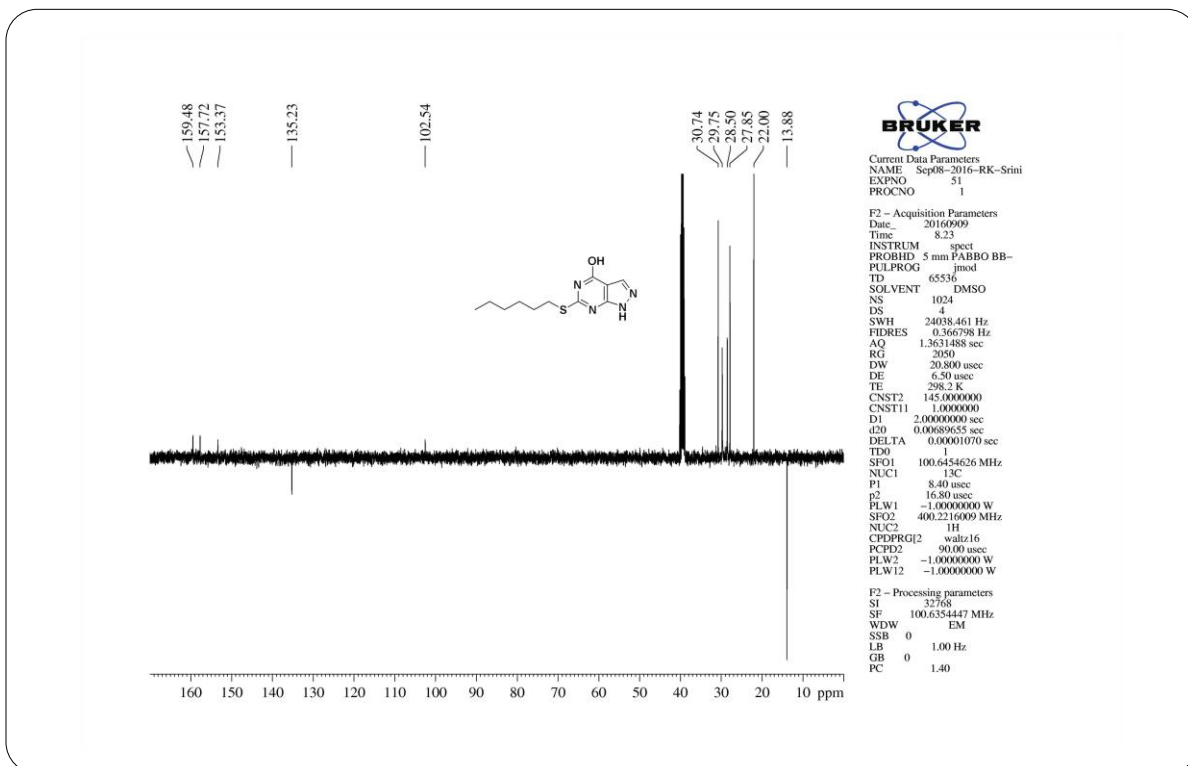
HRMS Spectrum of Compound 43

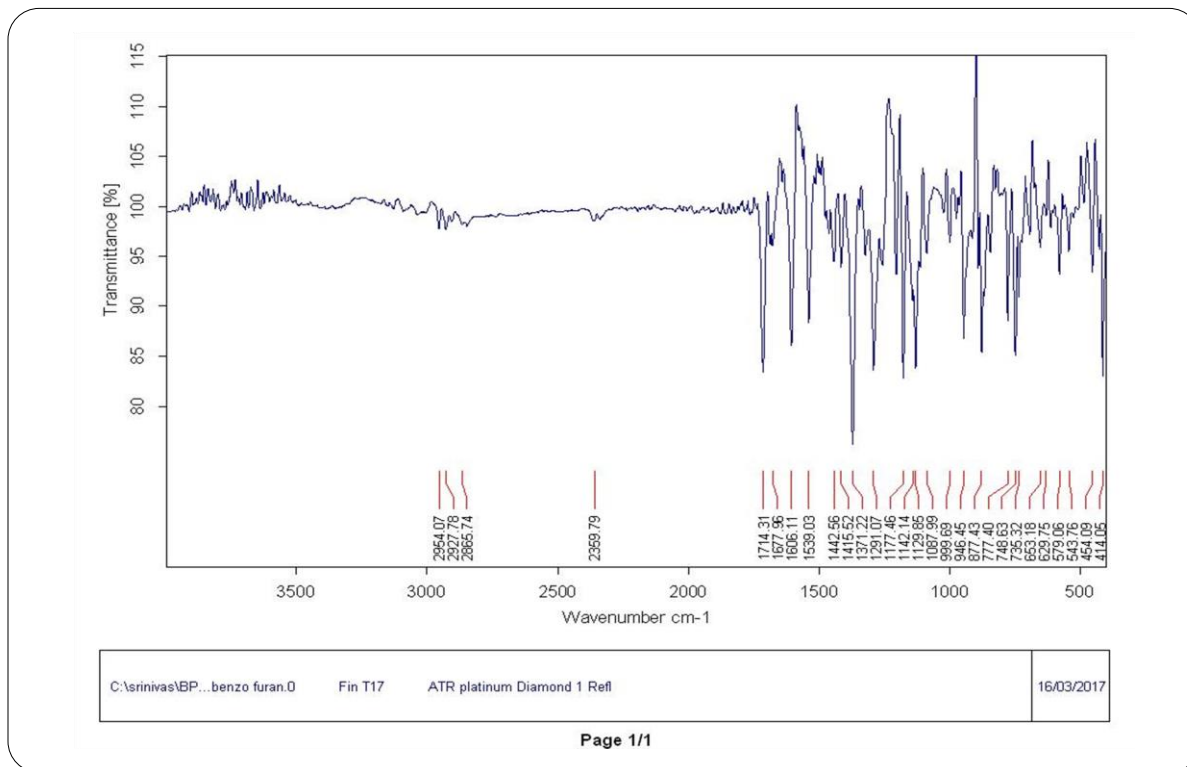
APPENDIX – II**SUPPLEMENTARY INFORMATION****CHAPTER 5****Synthesis of 4,6-disubstituted pyrazolo[3,4-*d*]pyrimidine analogues: molecular docking, anticancer evaluation as cyclin dependent kinase 2 (CDK2) inhibitors**

Department of Pharmaceutical Chemistry, College of Health Sciences, University of KwaZulu-Natal, Durban 4000, South Africa.

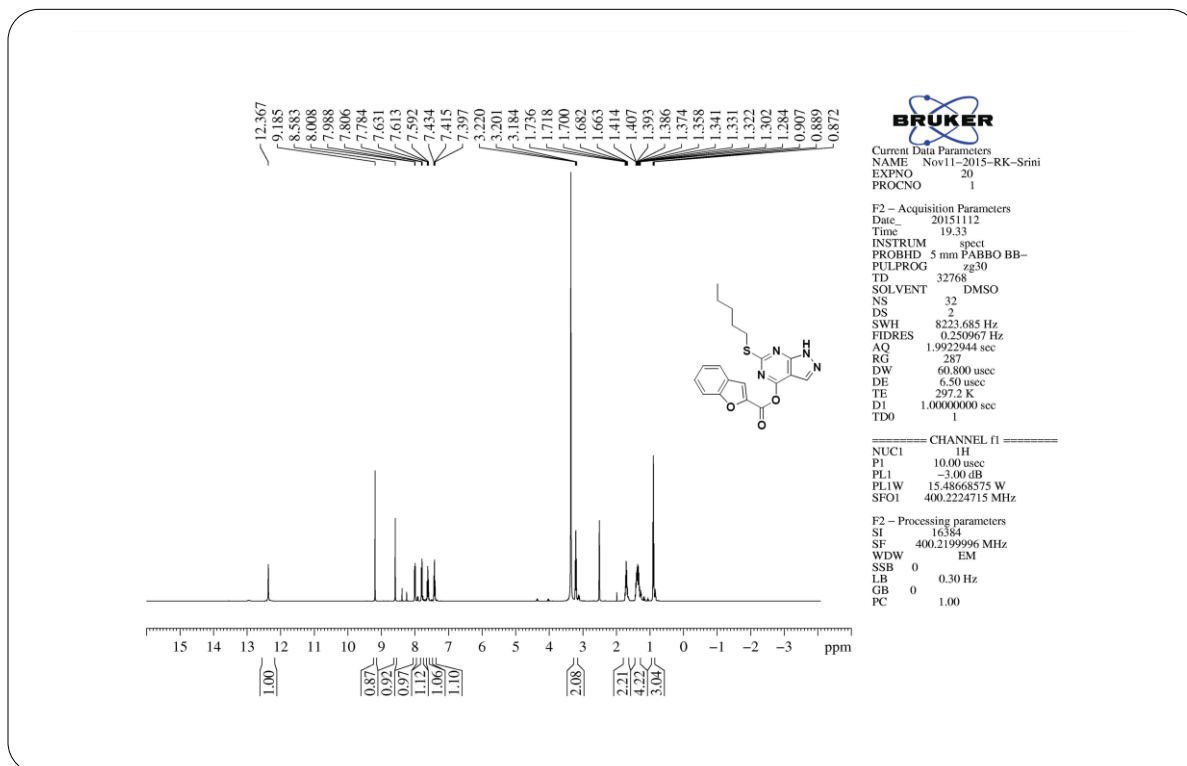
**¹H NMR Spectrum of Compound 2****¹³C NMR Spectrum of Compound 2**

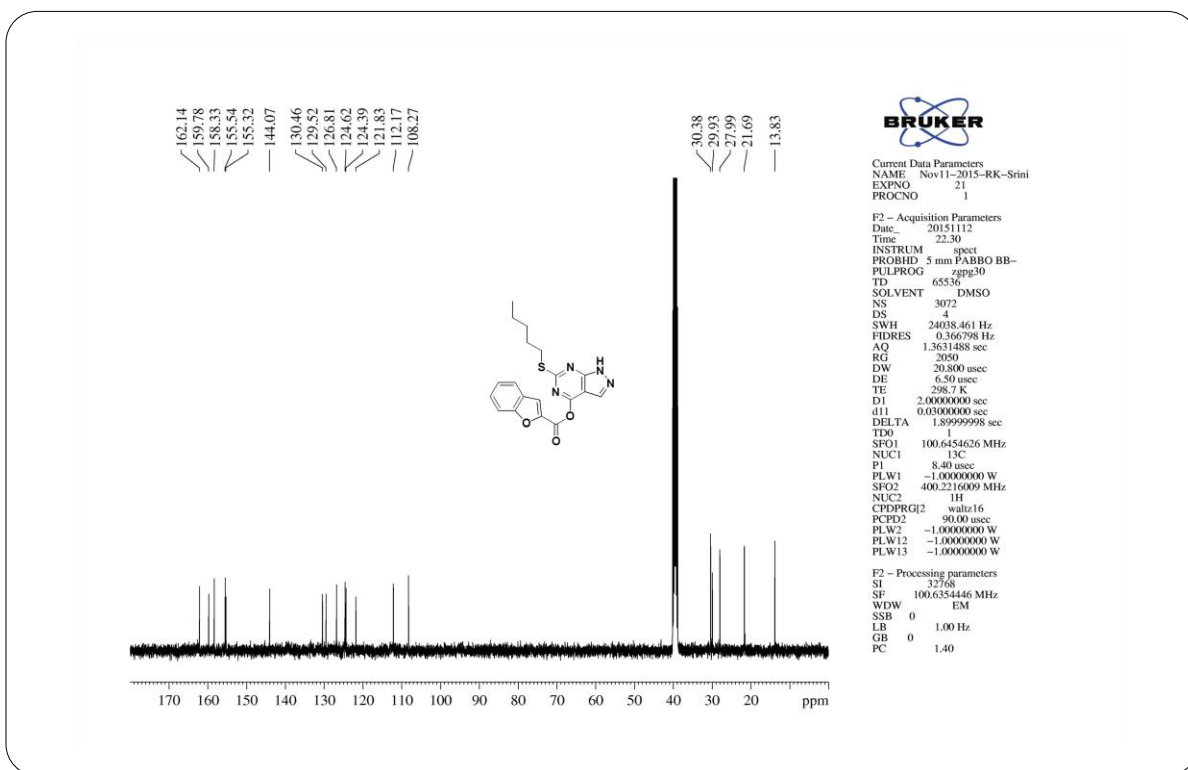
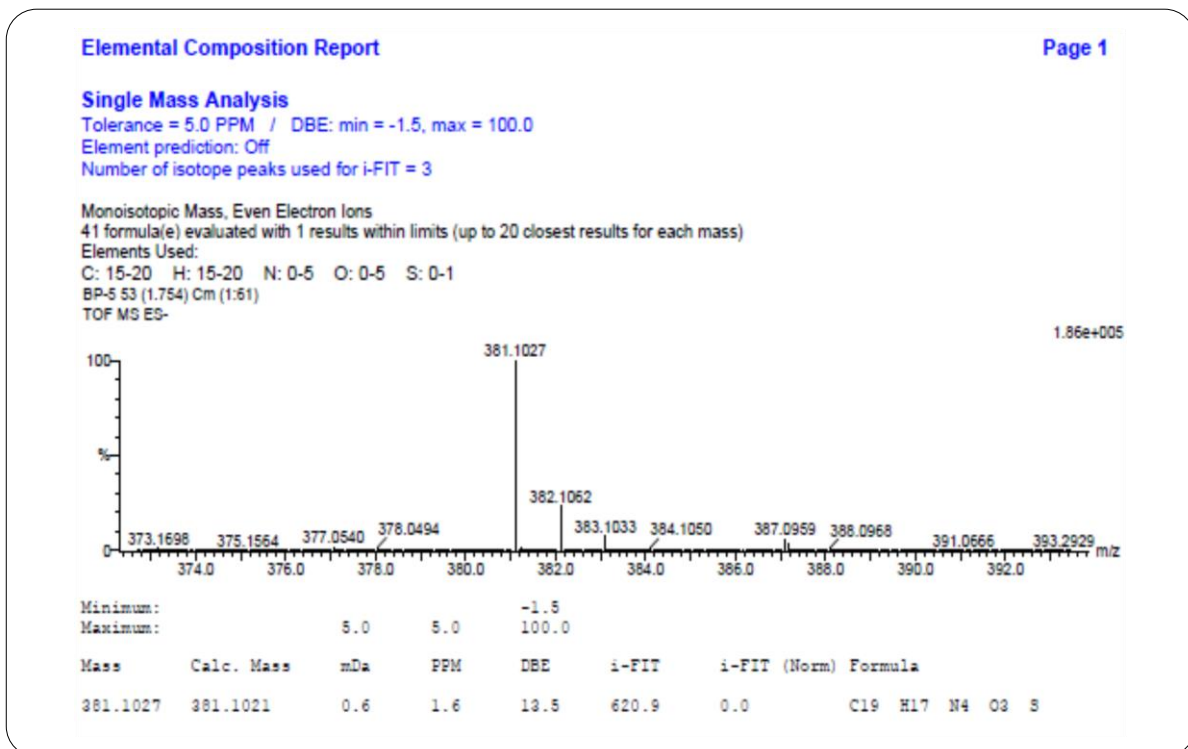
**¹H NMR Spectrum of Compound 3****¹³C NMR Spectrum of Compound 3**

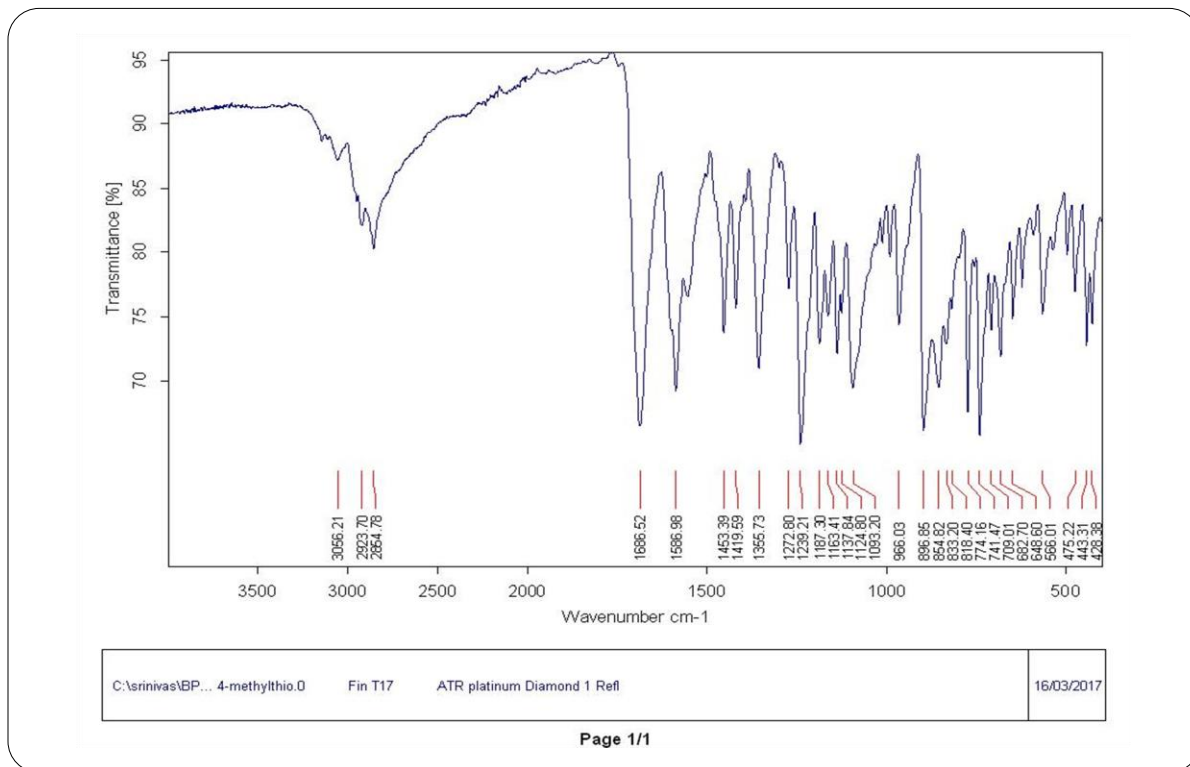
**¹H NMR Spectrum of Compound 4****¹³C MNR Spectrum of Compound 4**



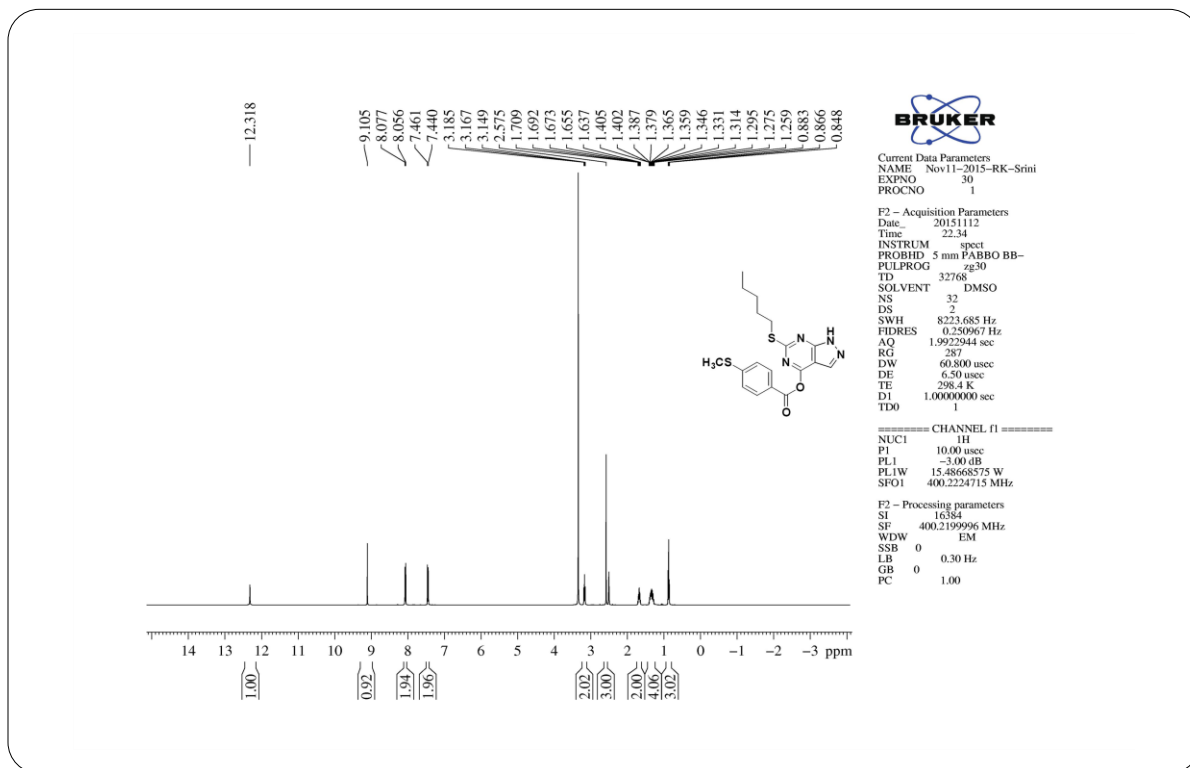
IR Spectrum of Compound 5a

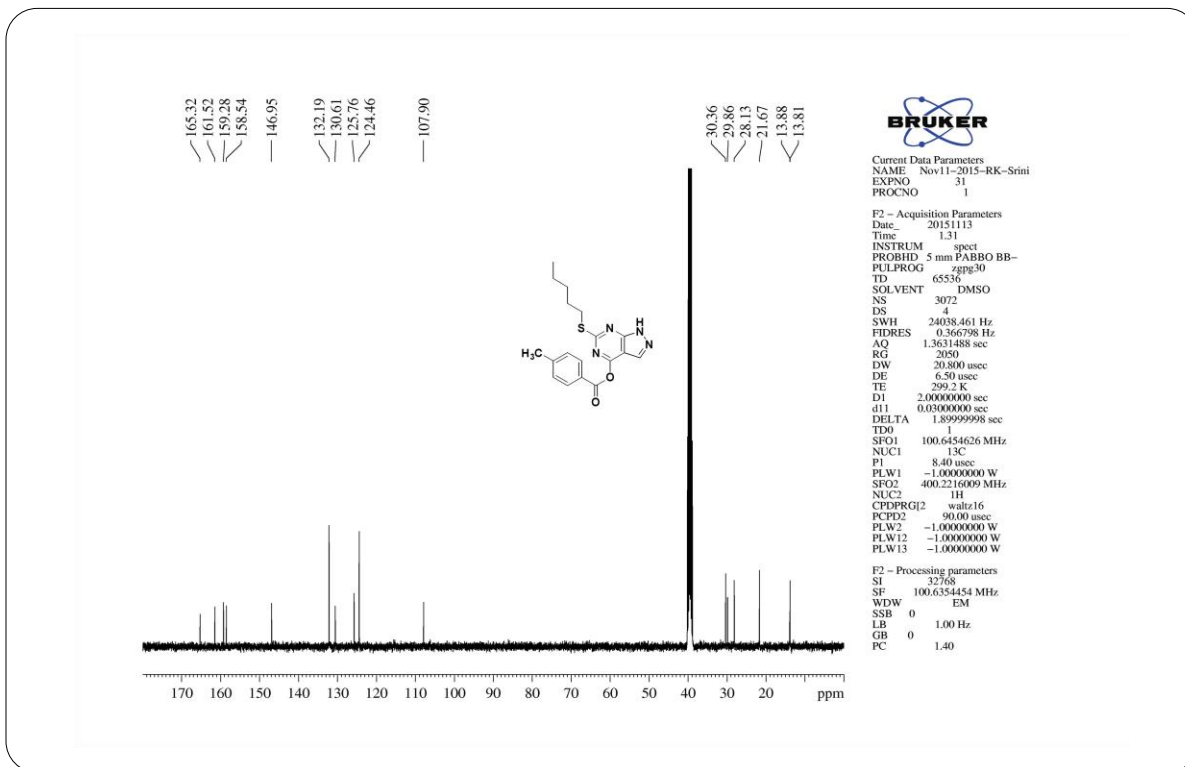
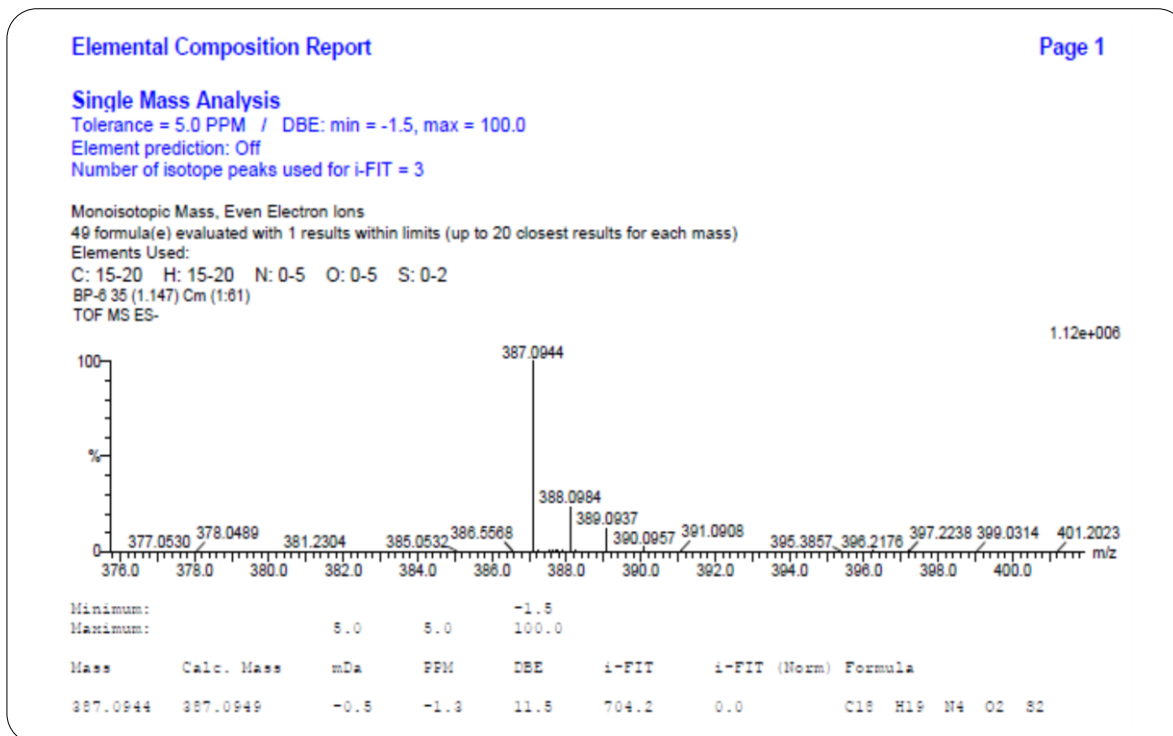
¹H NMR Spectrum of Compound 5a

**¹³C NMR Spectrum of Compound 5a****HRMS Spectrum of Compound 5a**

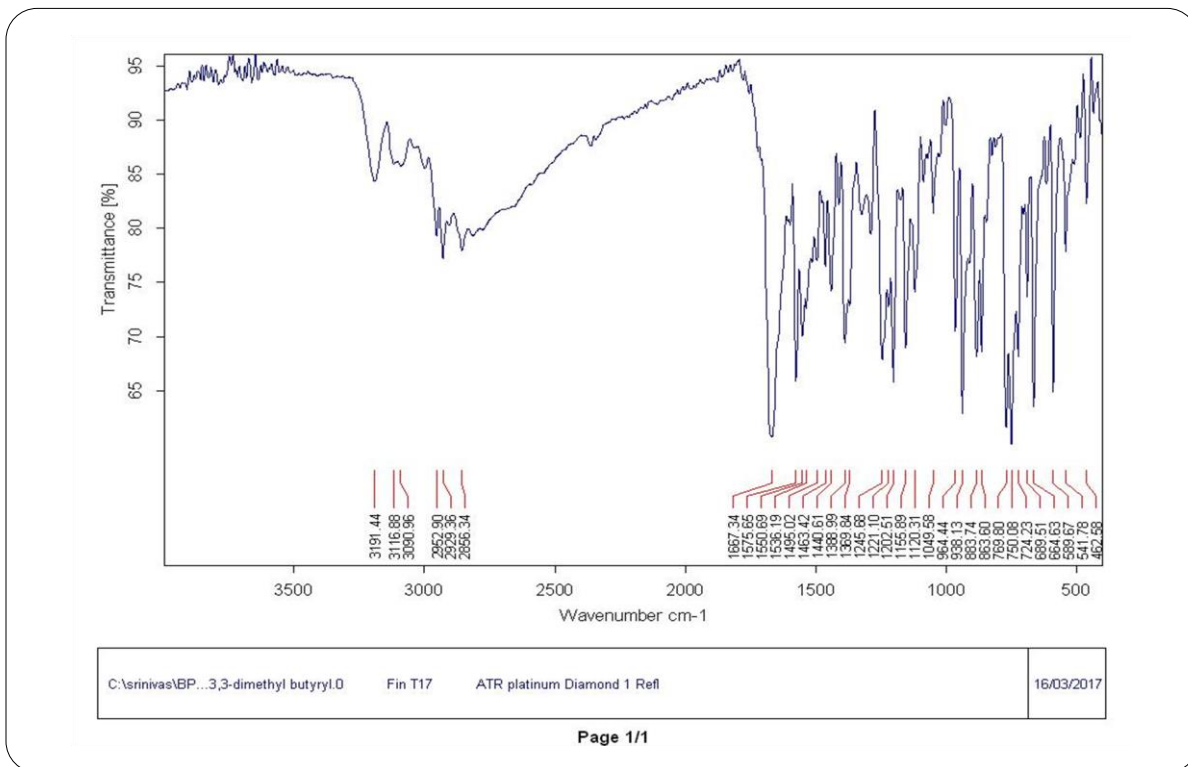


IR Spectrum of Compound 5b

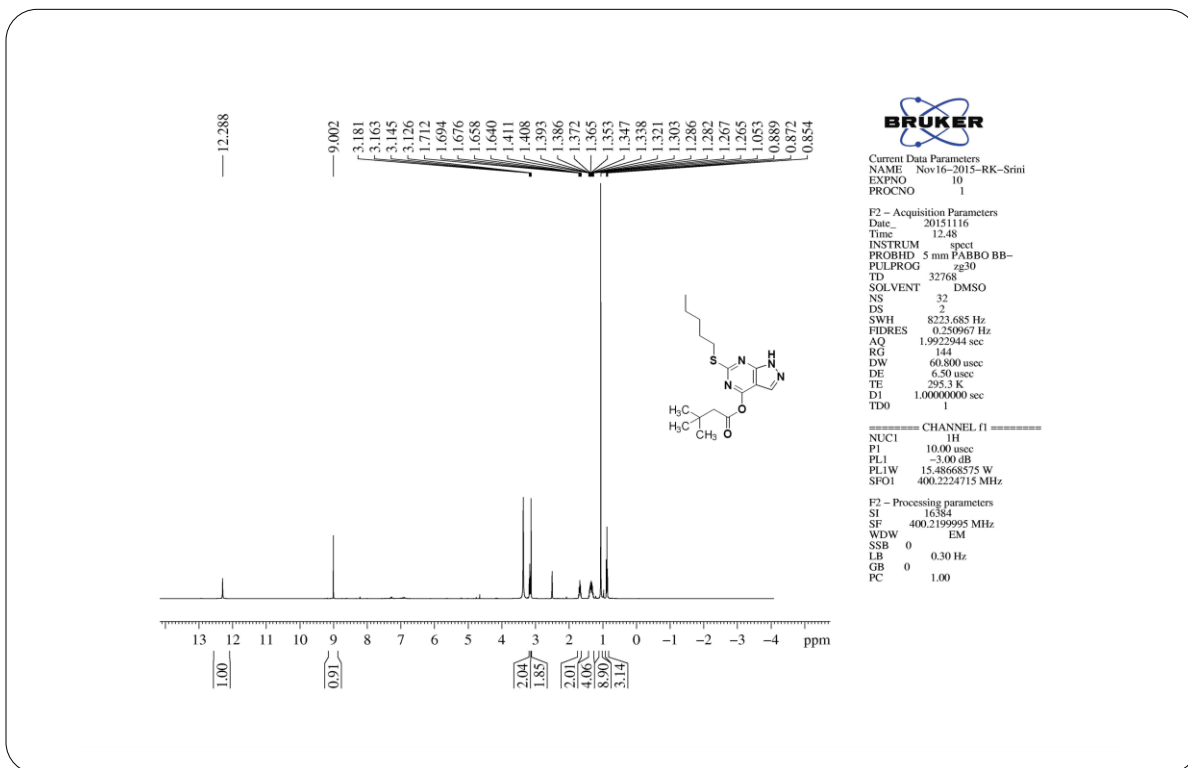
¹H NMR Spectrum of Compound 5b

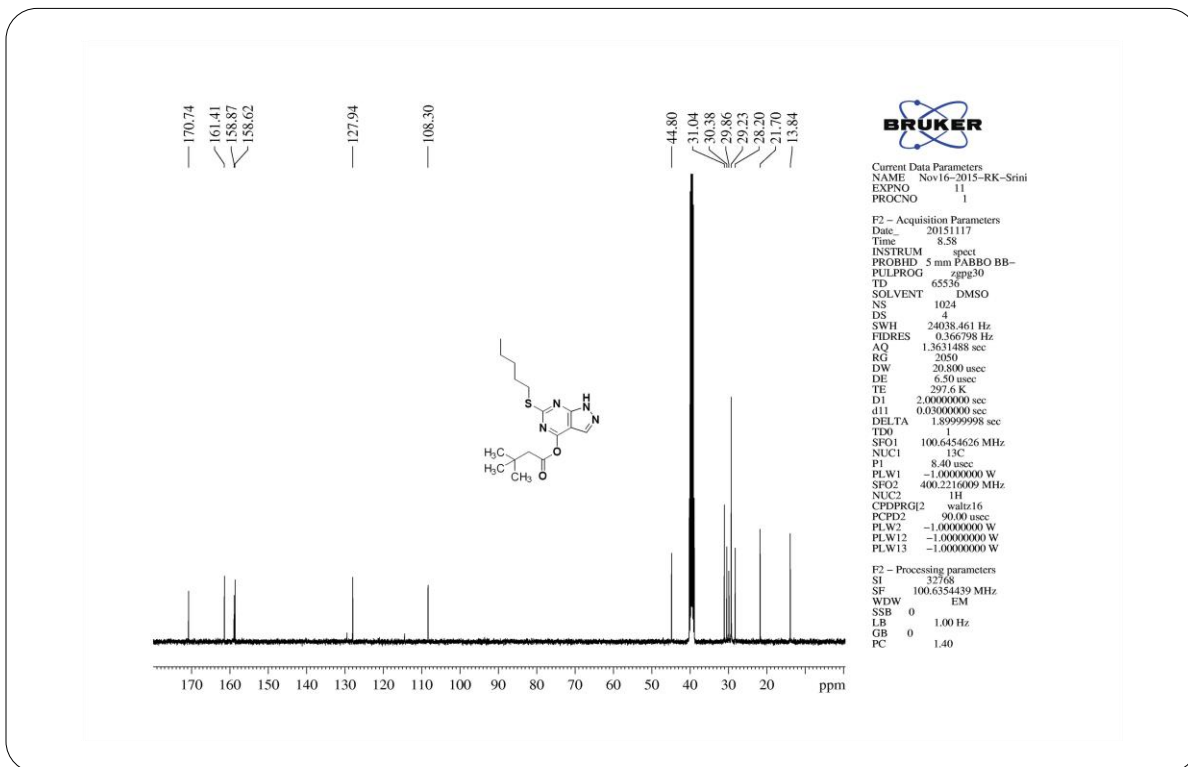
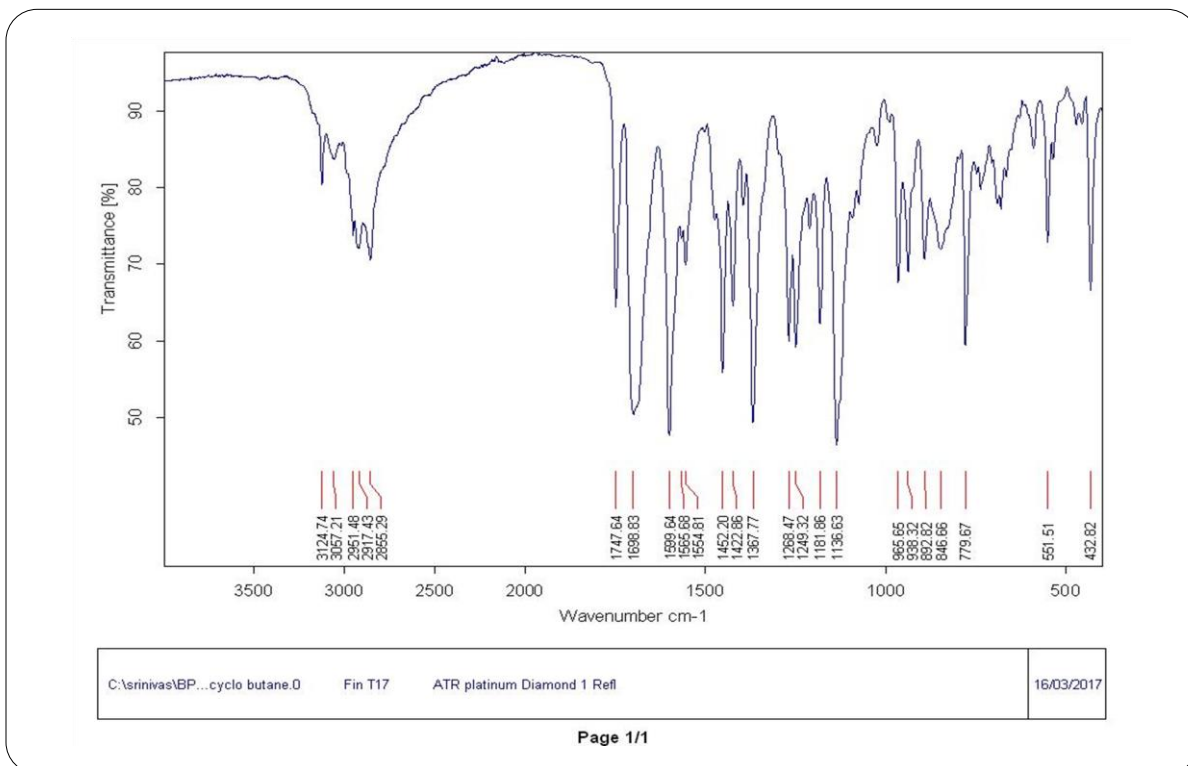
¹³C NMR Spectrum of Compound 5b

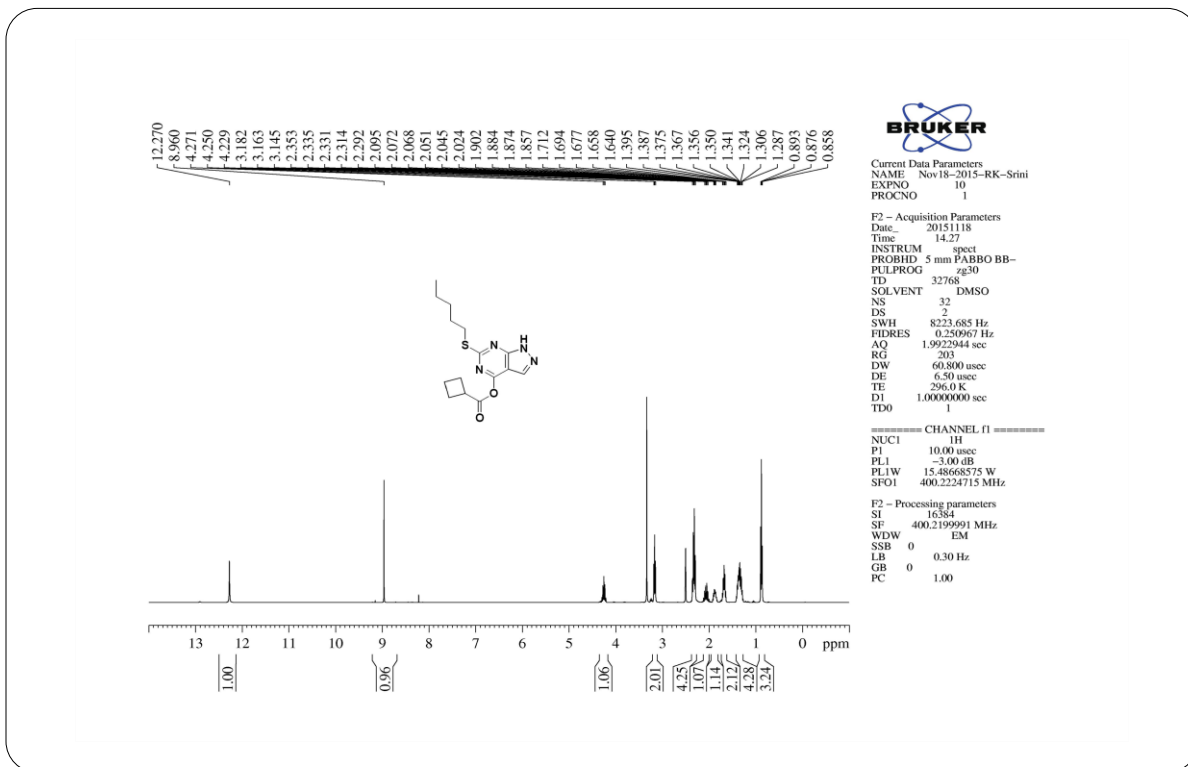
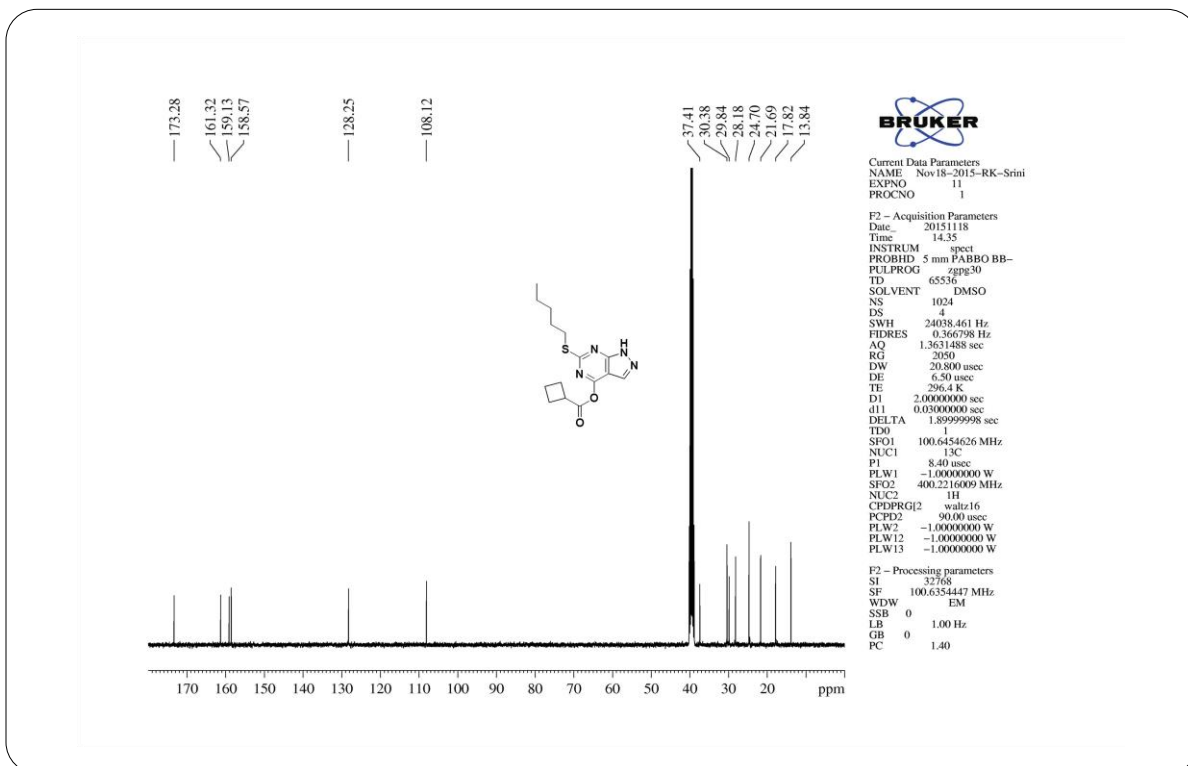
HRMS Spectrum of Compound 5b

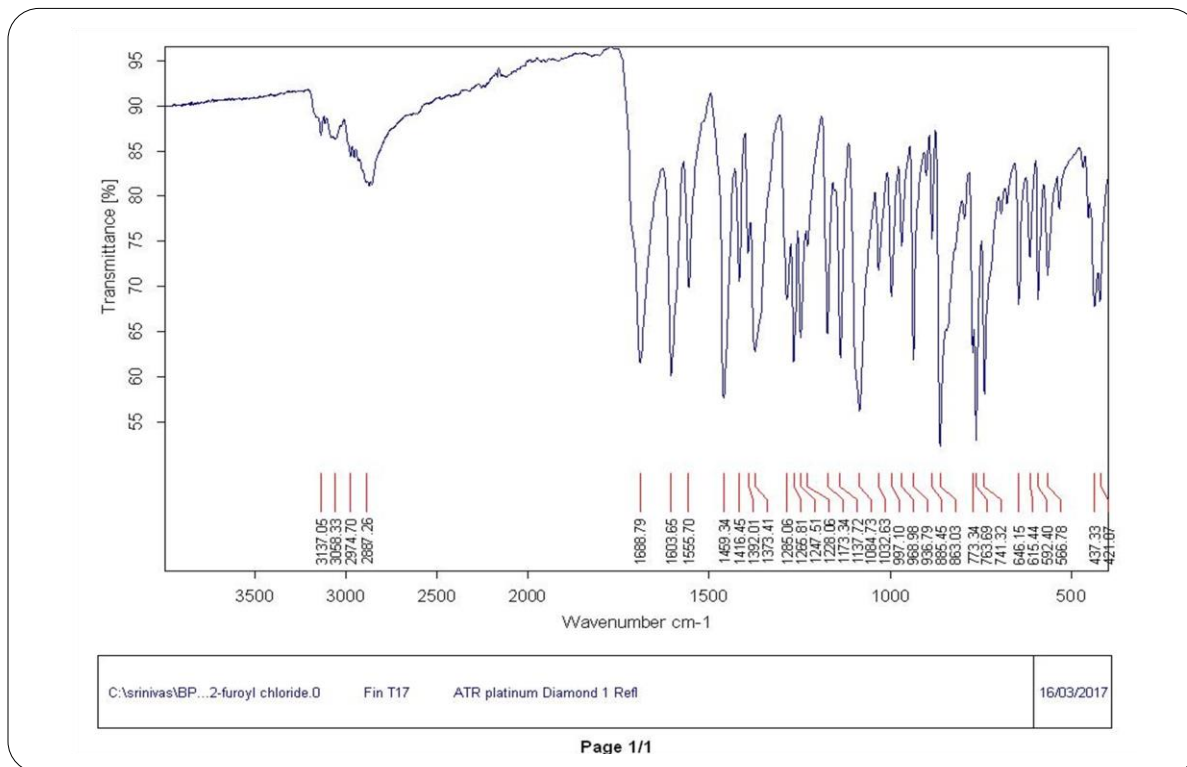


IR Spectrum of Compound 5c

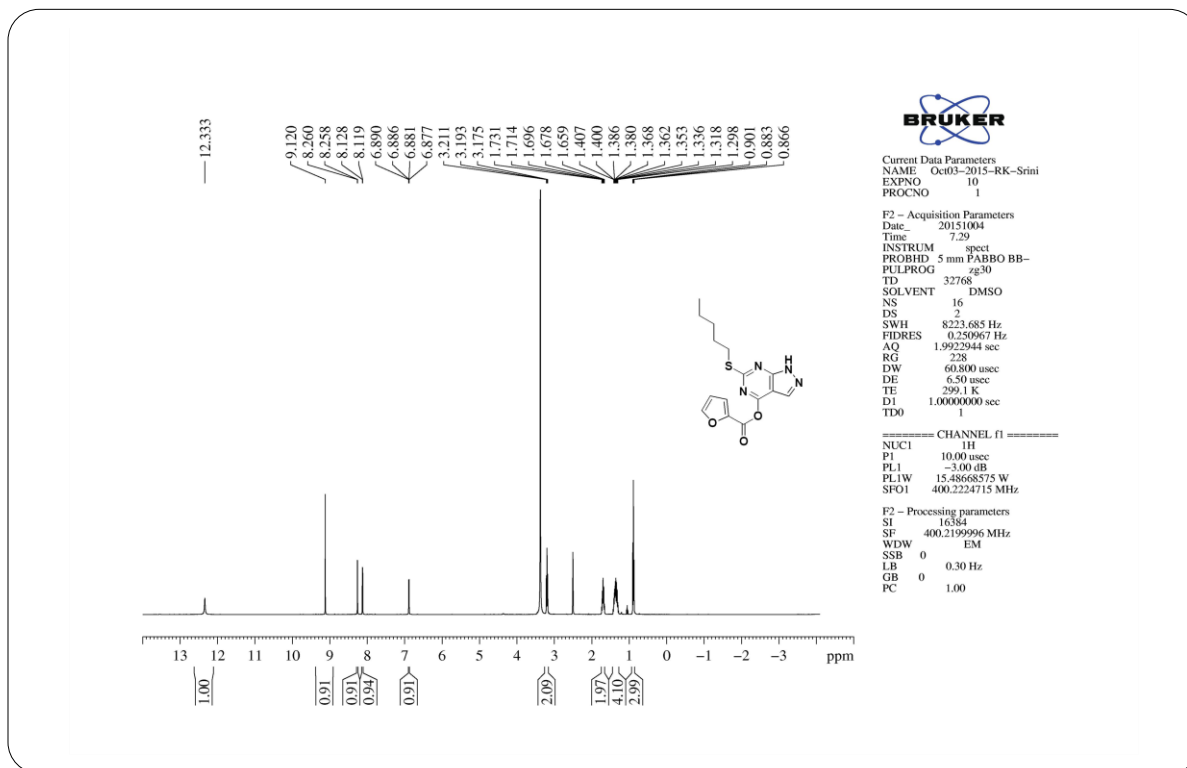
¹H NMR Spectrum of Compound 5c

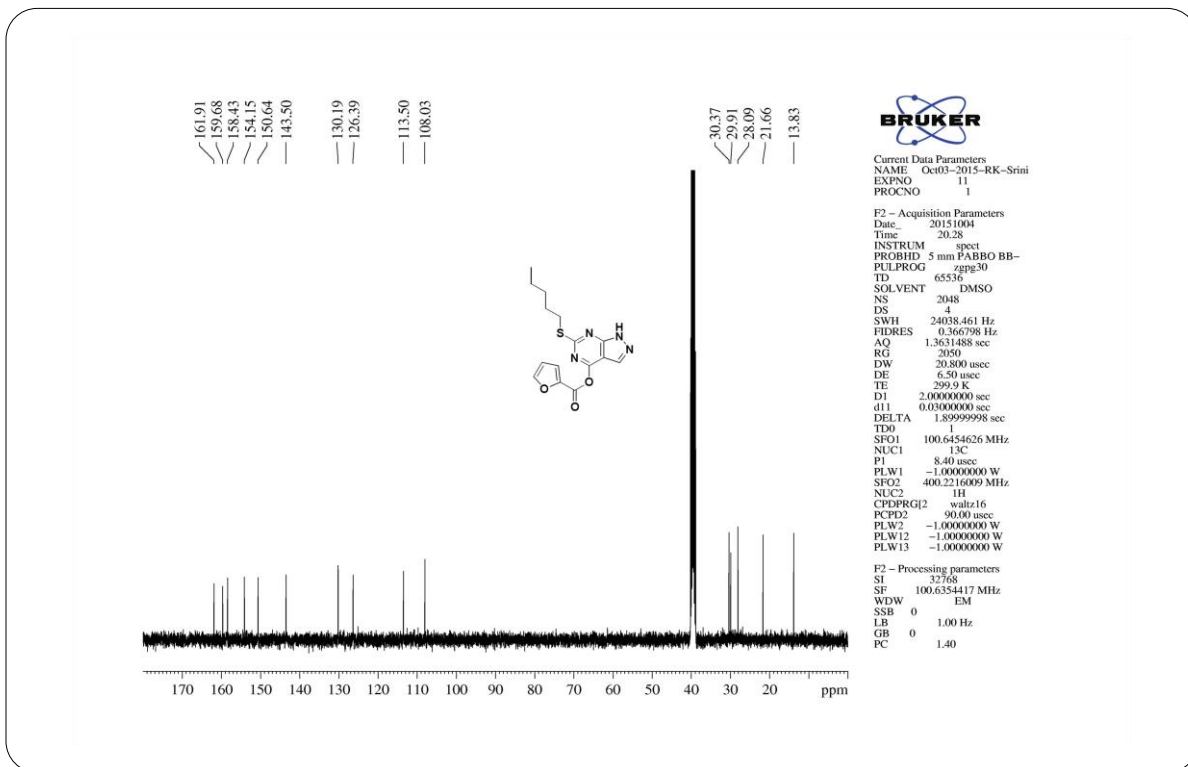
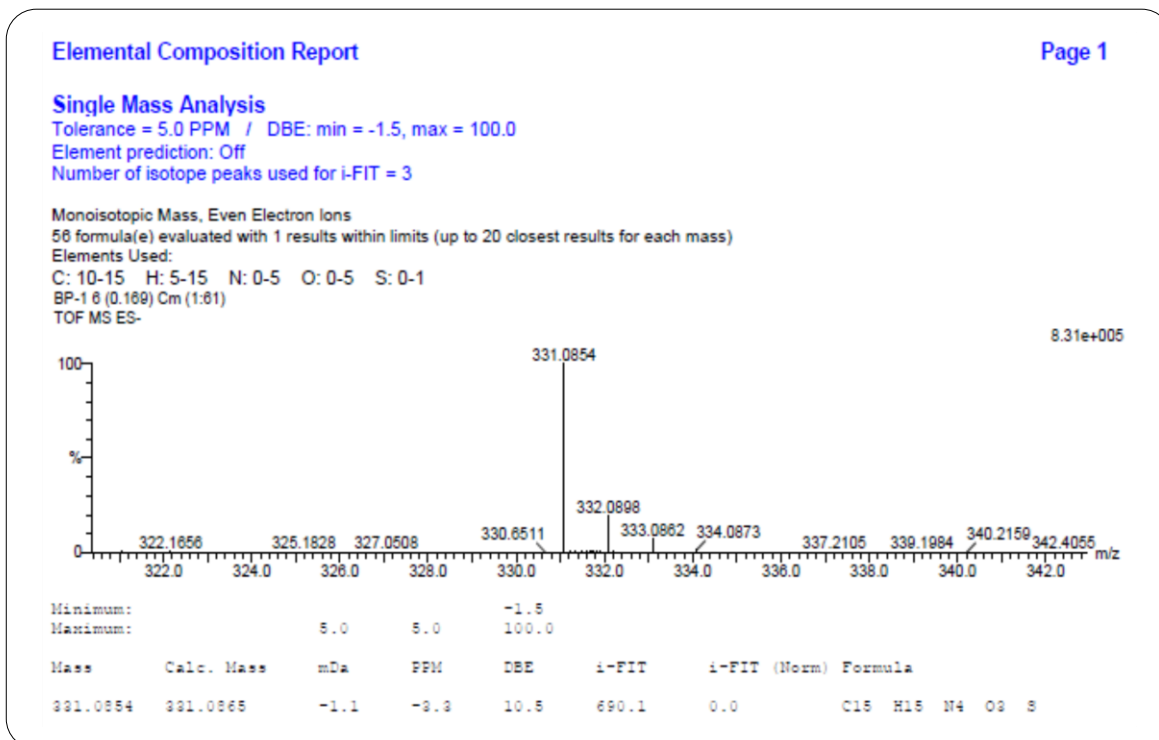
**¹³C NMR Spectrum of Compound 5c****IR Spectrum of Compound 5d**

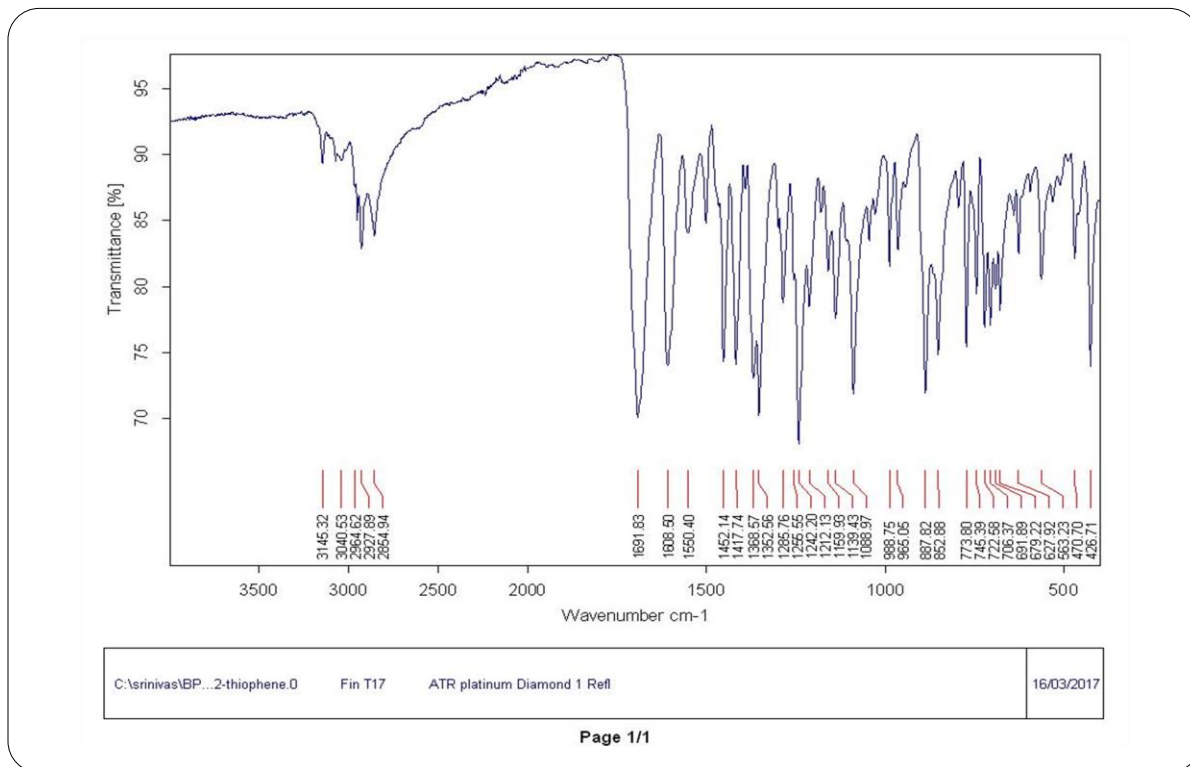
**¹H NMR Spectrum of Compound 5d****¹³C NMR Spectrum of Compound 5d**



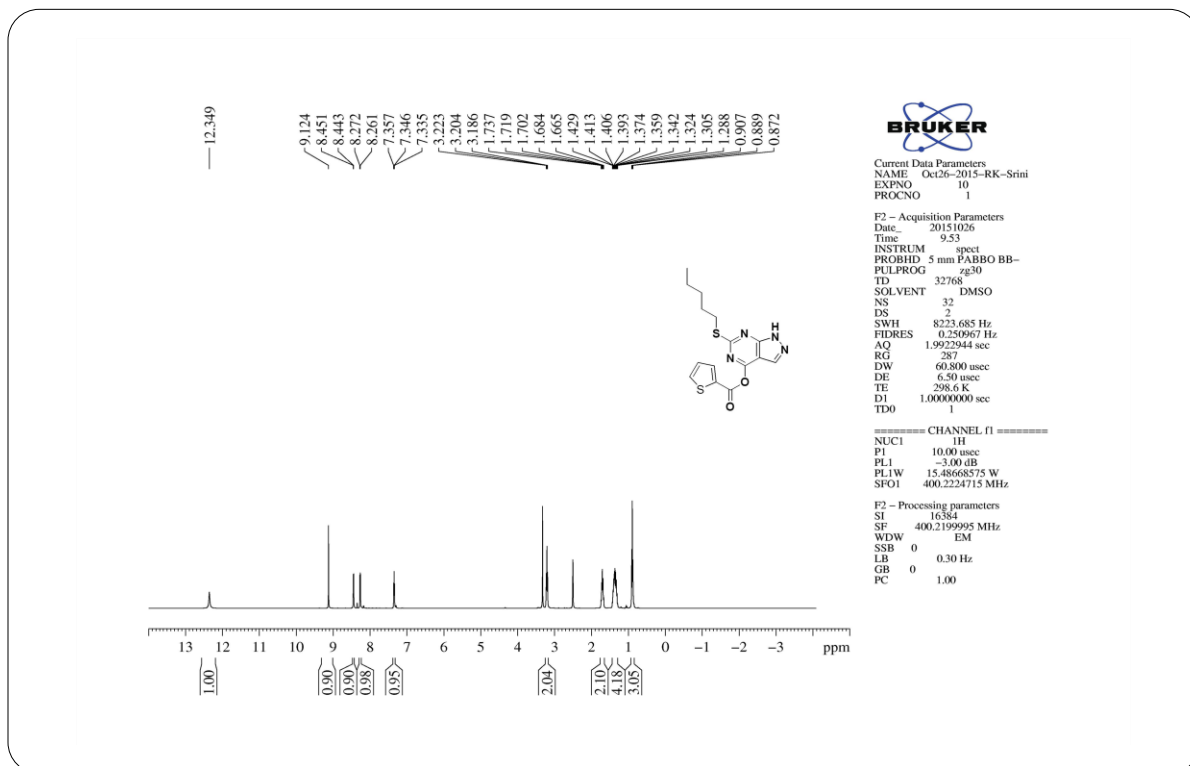
IR Spectrum of Compound 5e

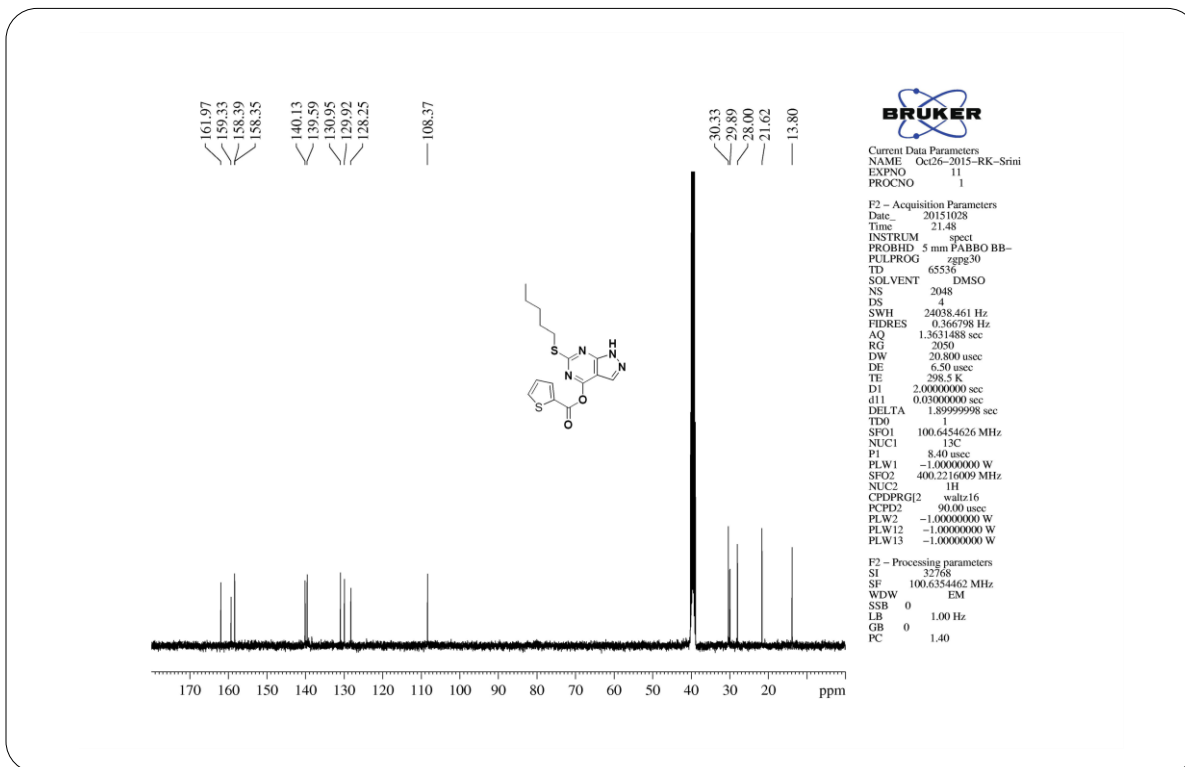
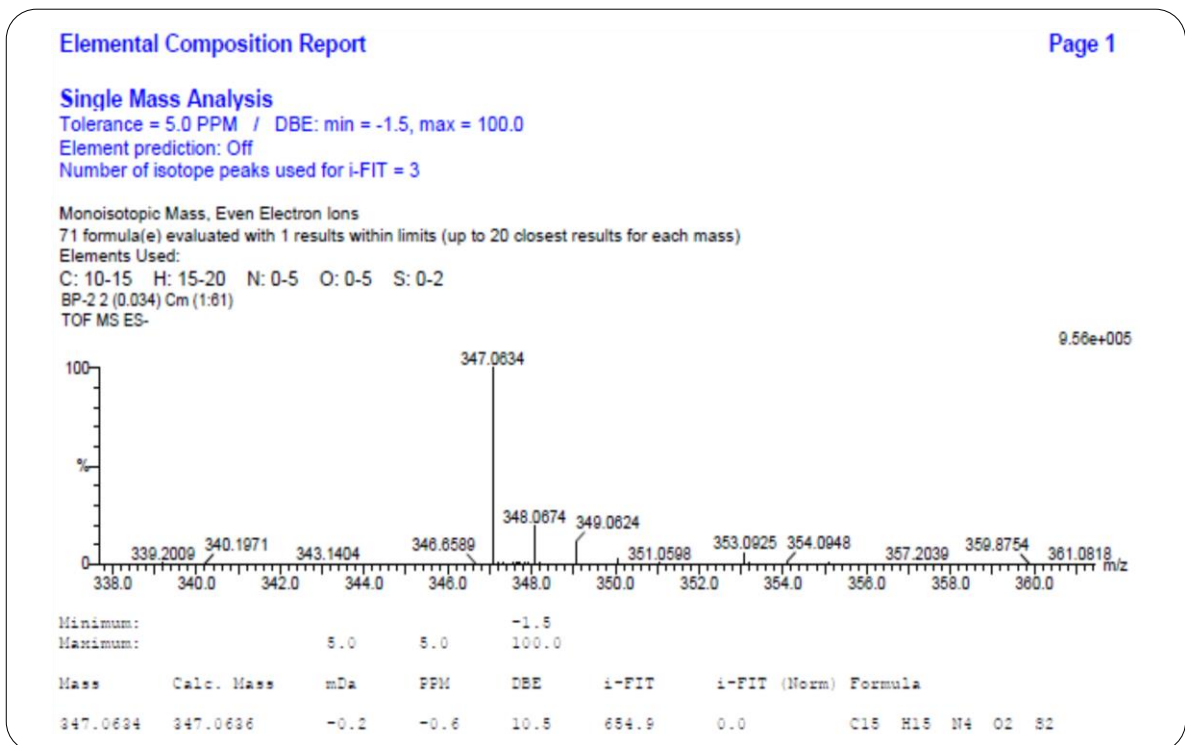
¹H NMR Spectrum of Compound 5e

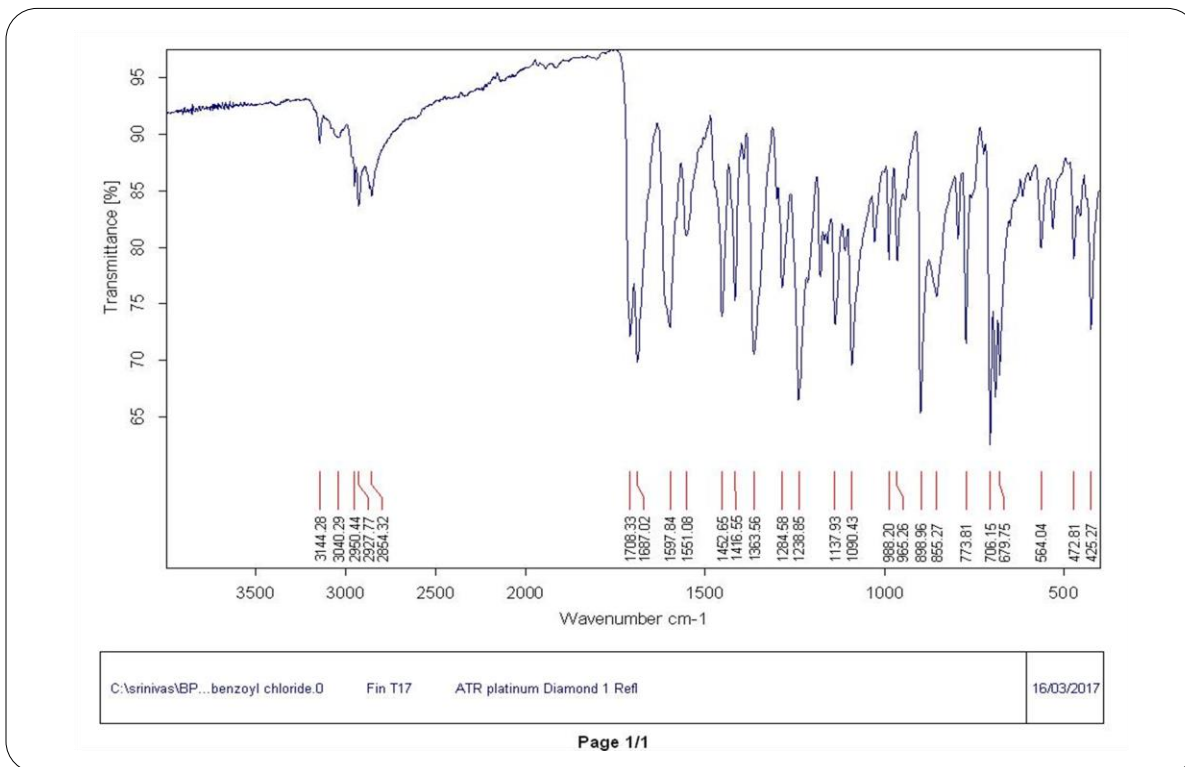
**¹³C NMR Spectrum of Compound 5e****HRMS Spectrum of Compound 5e**



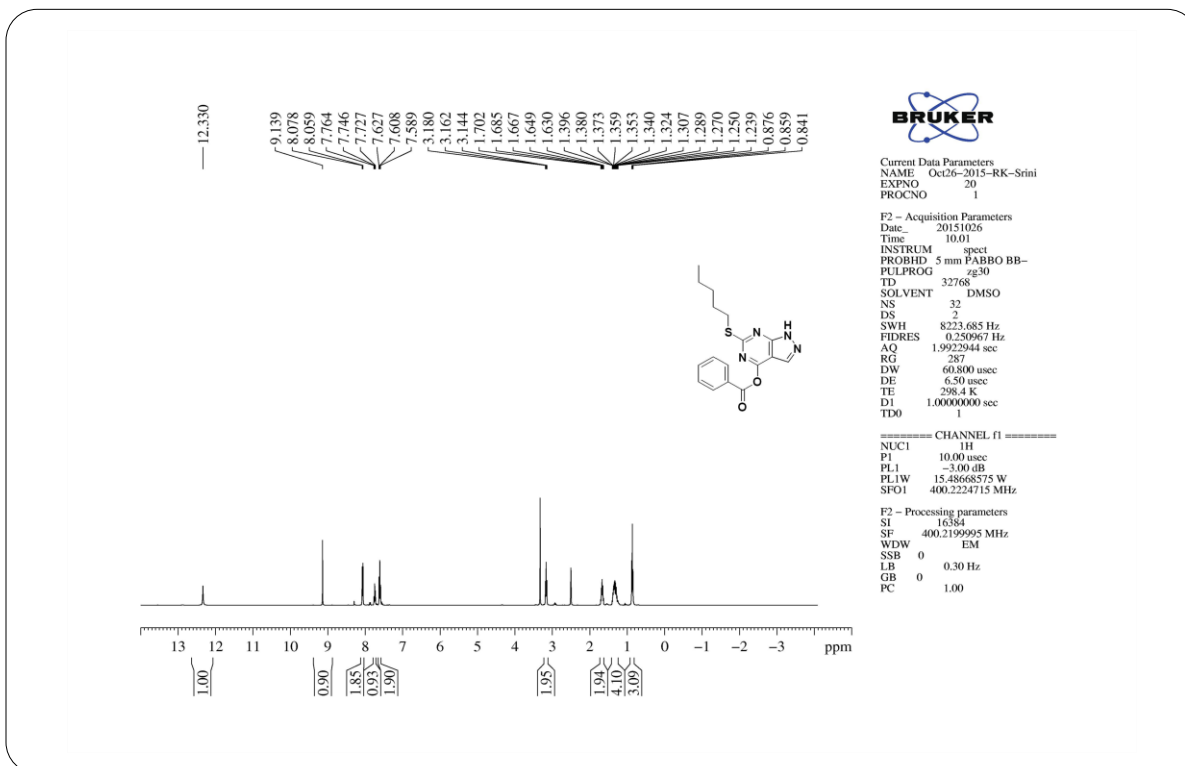
IR Spectrum of Compound 5f

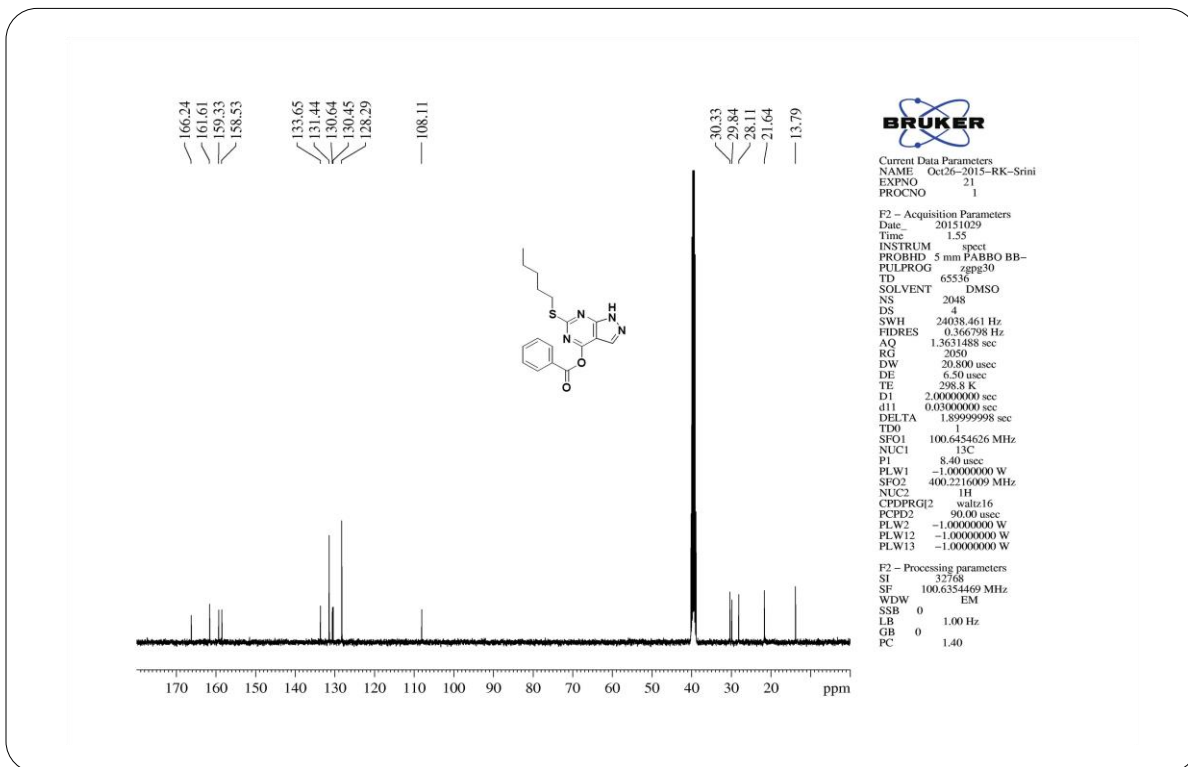
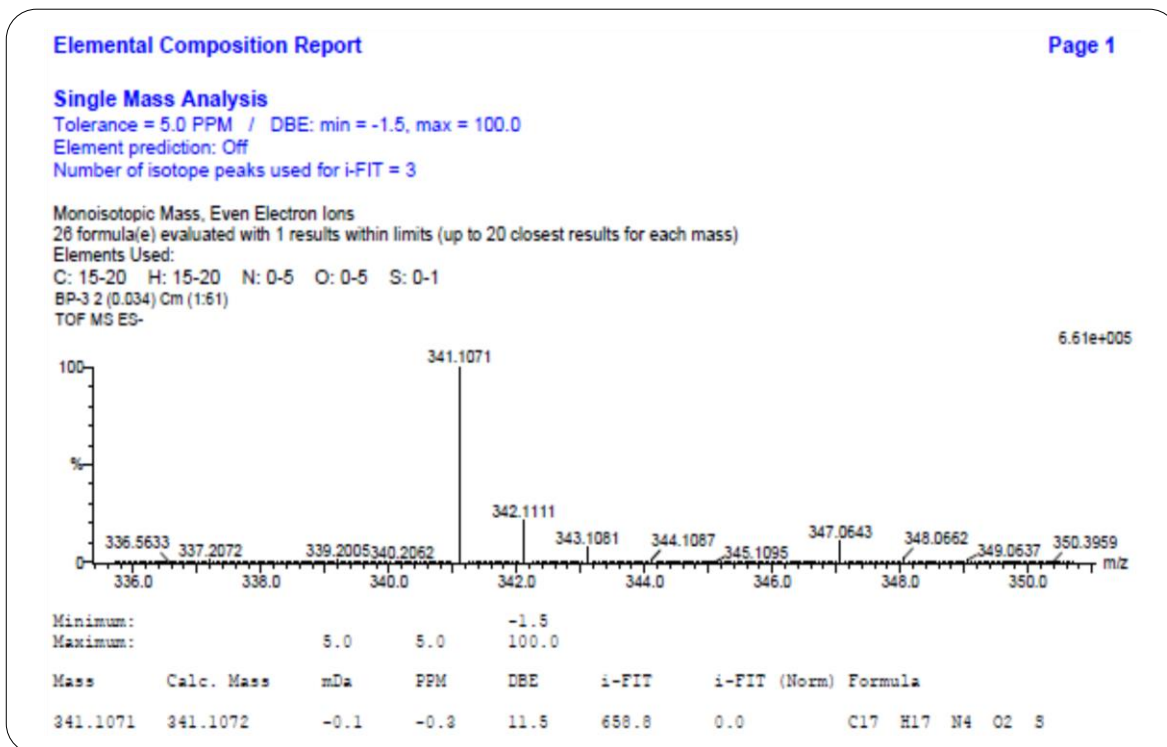
¹H NMR Spectrum of Compound 5f

**¹³C NMR Spectrum of Compound 5f****HRMS Spectrum of Compound 5f**

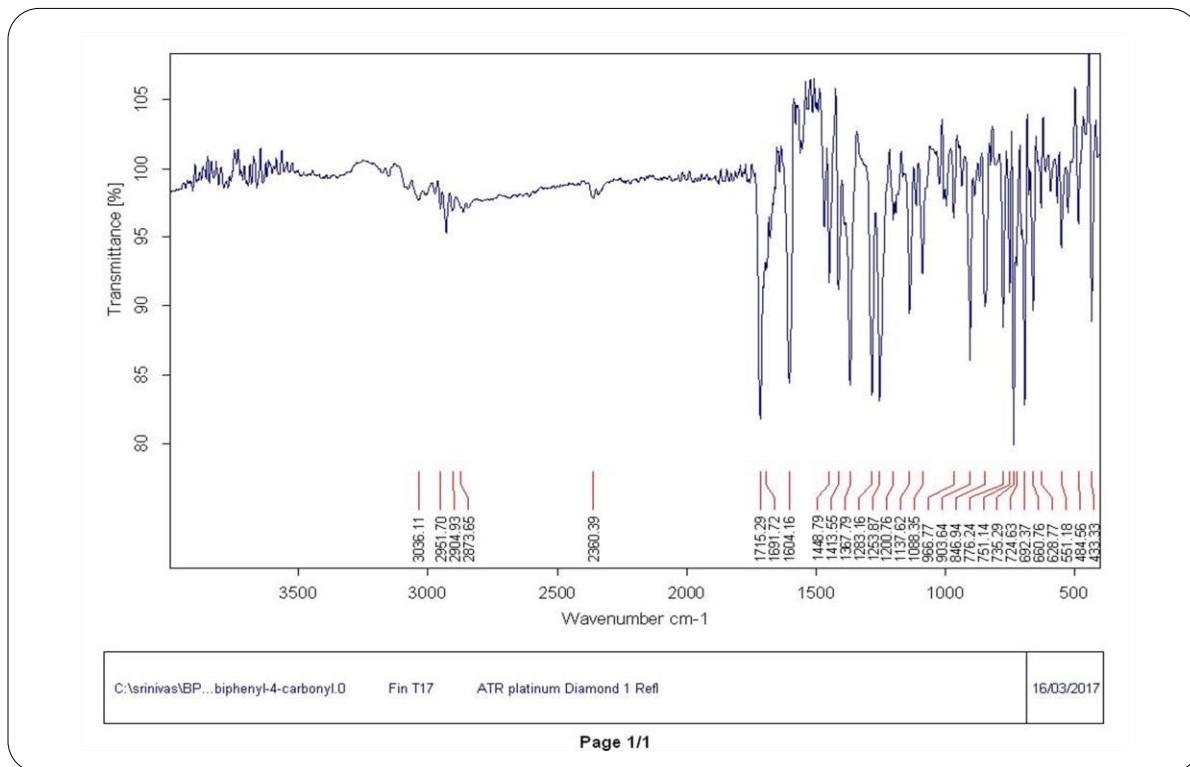


IR Spectrum of Compound 5g

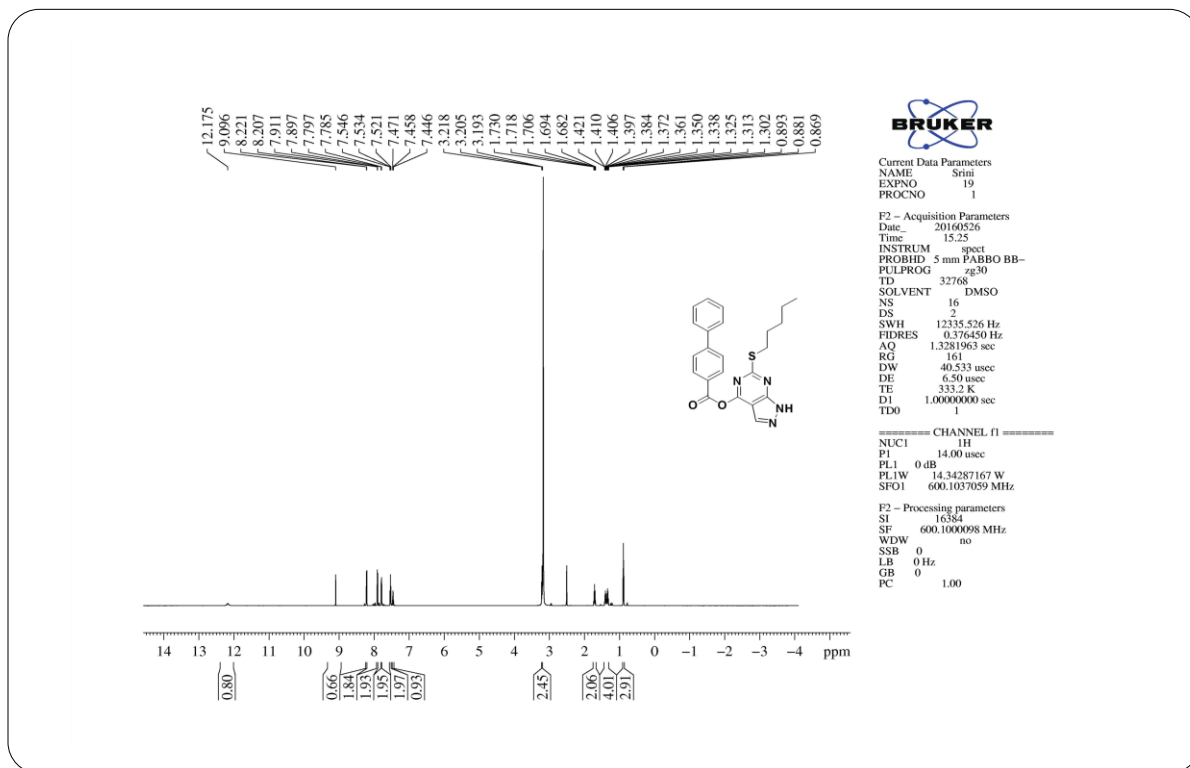
¹H NMR Spectrum of Compound 5g

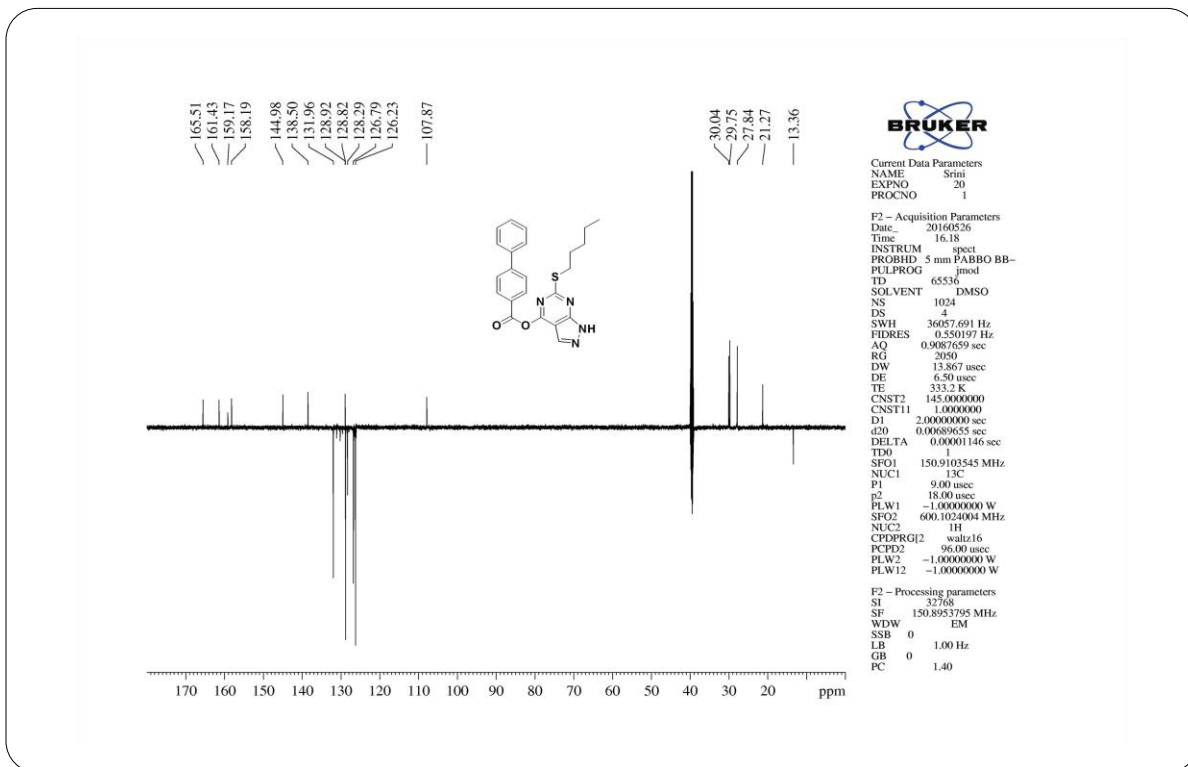
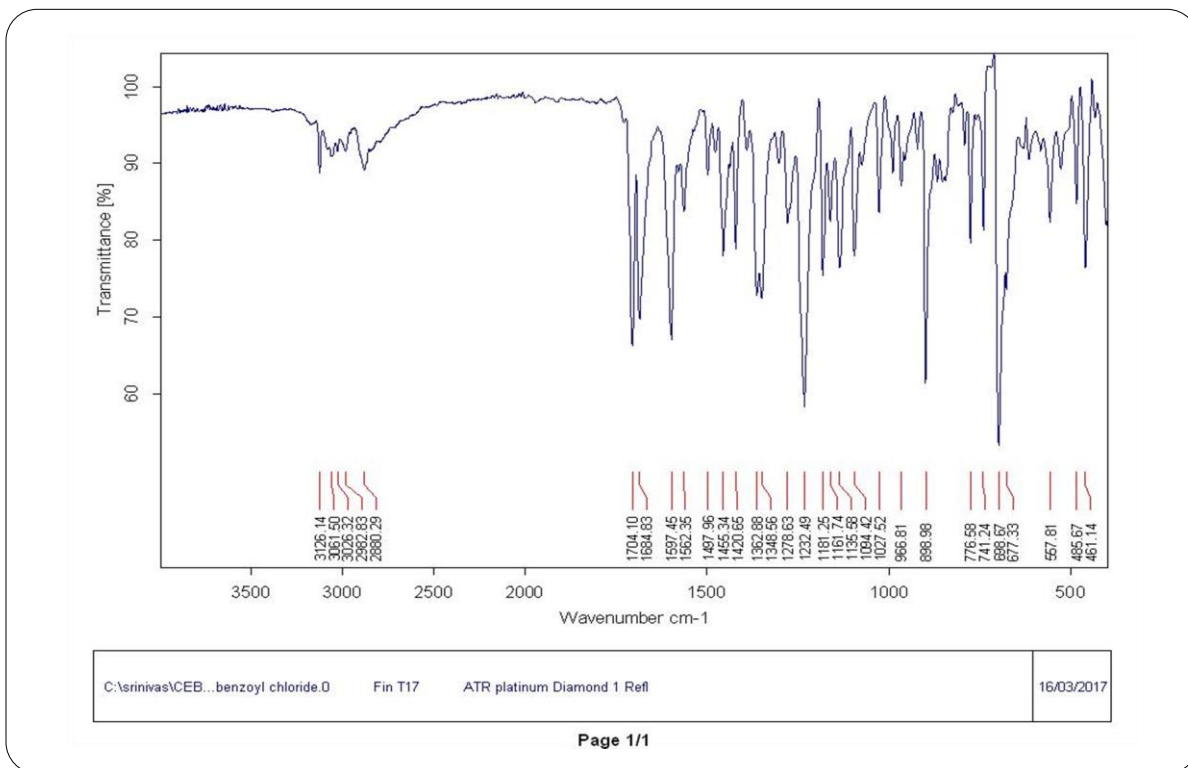
¹³C NMR Spectrum of Compound 5g

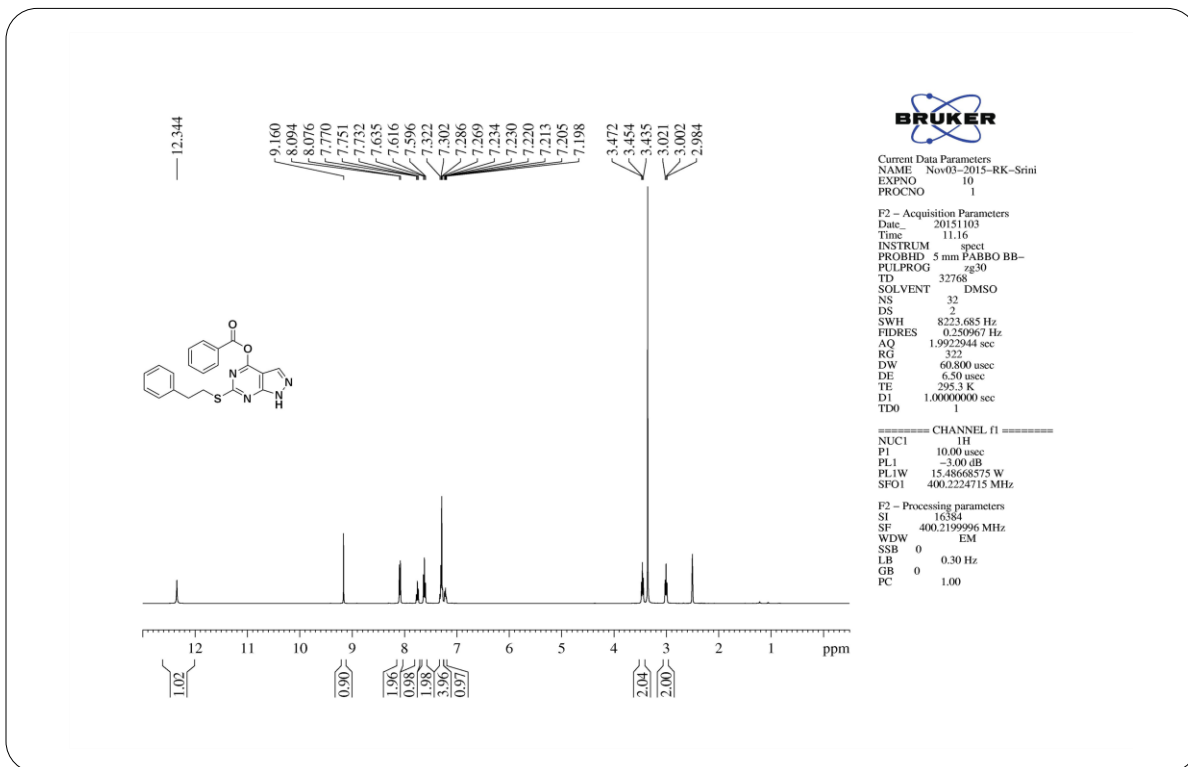
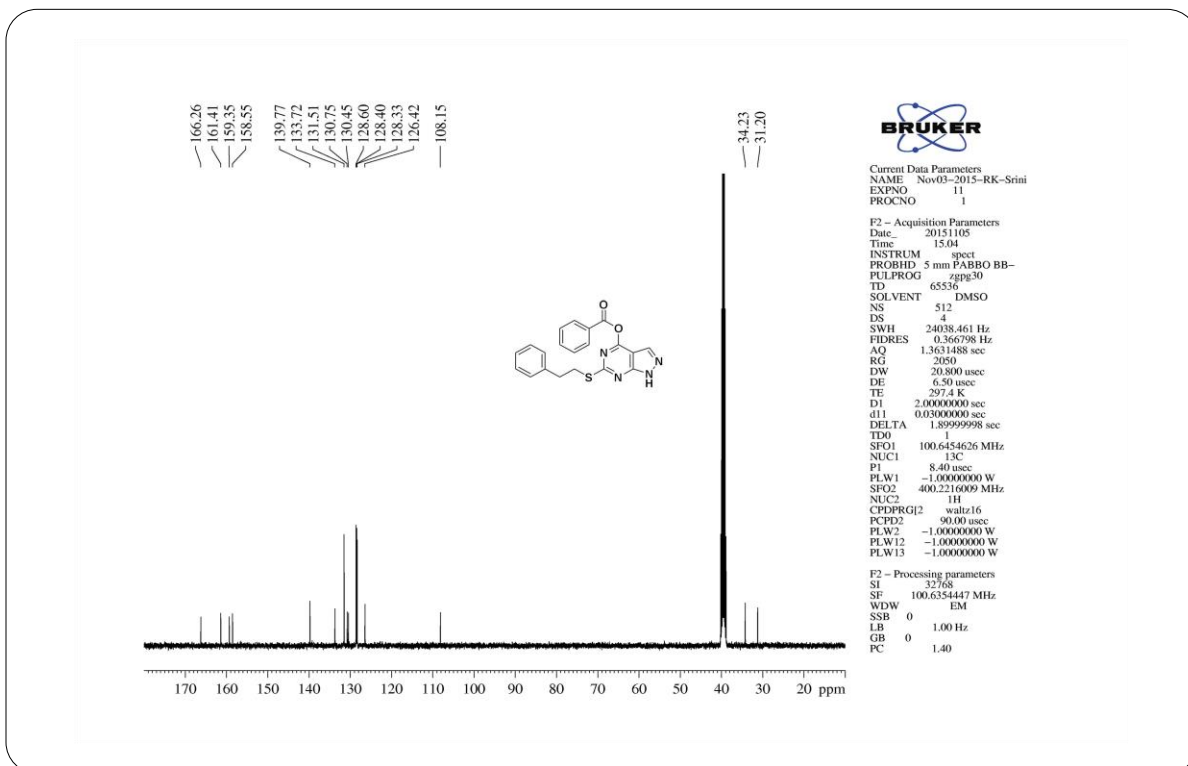
HRMS Spectrum of Compound 5g

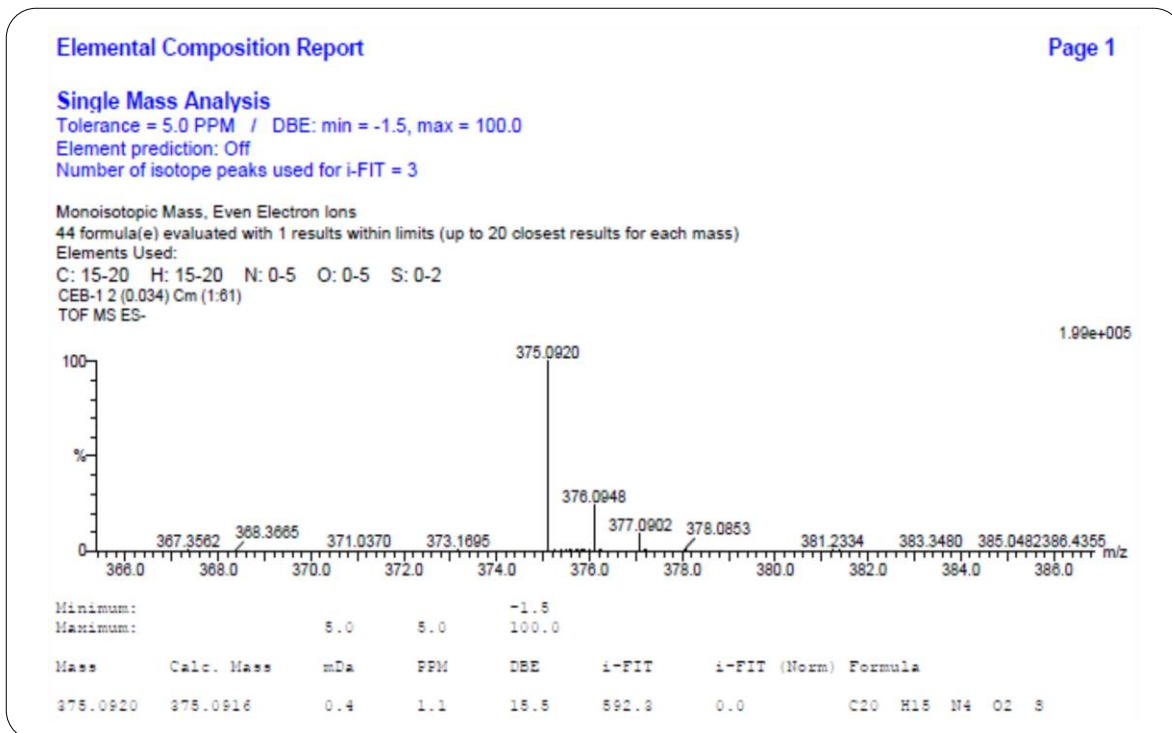


IR Spectrum of Compound 5h

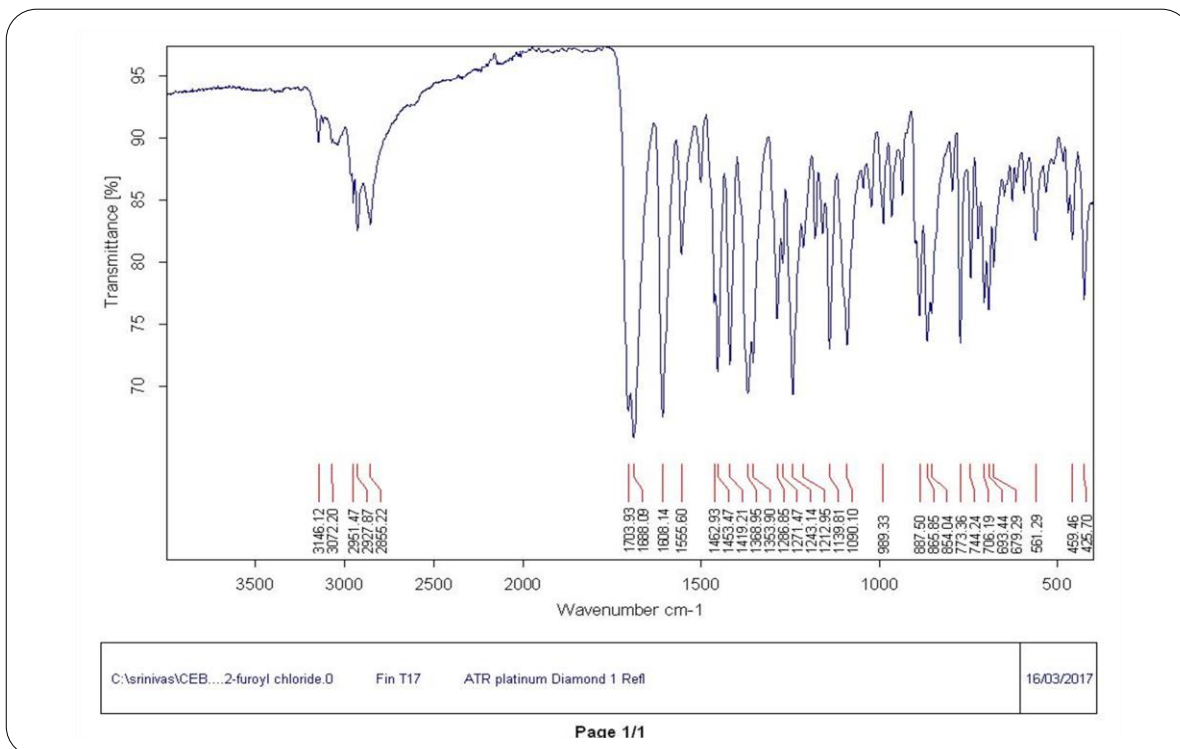
¹H NMR Spectrum of Compound 5h

**¹³C NMR Spectrum of Compound 5h****IR Spectrum of Compound 6a**

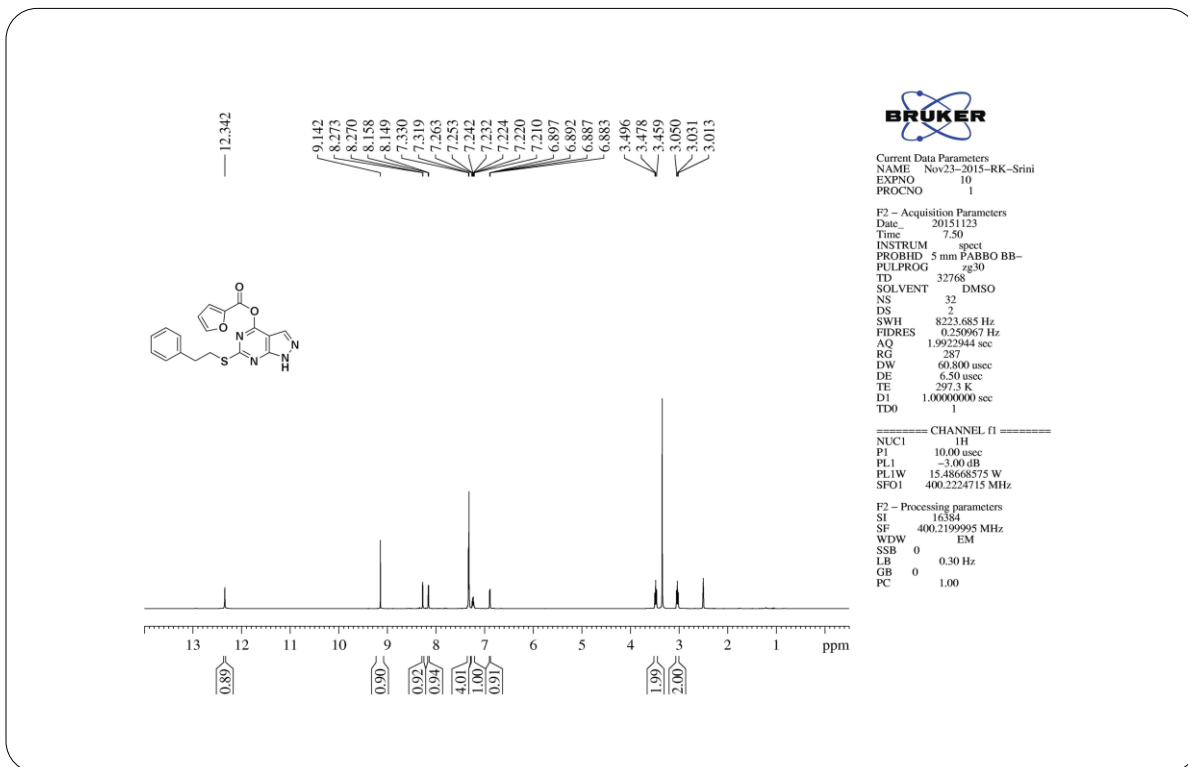
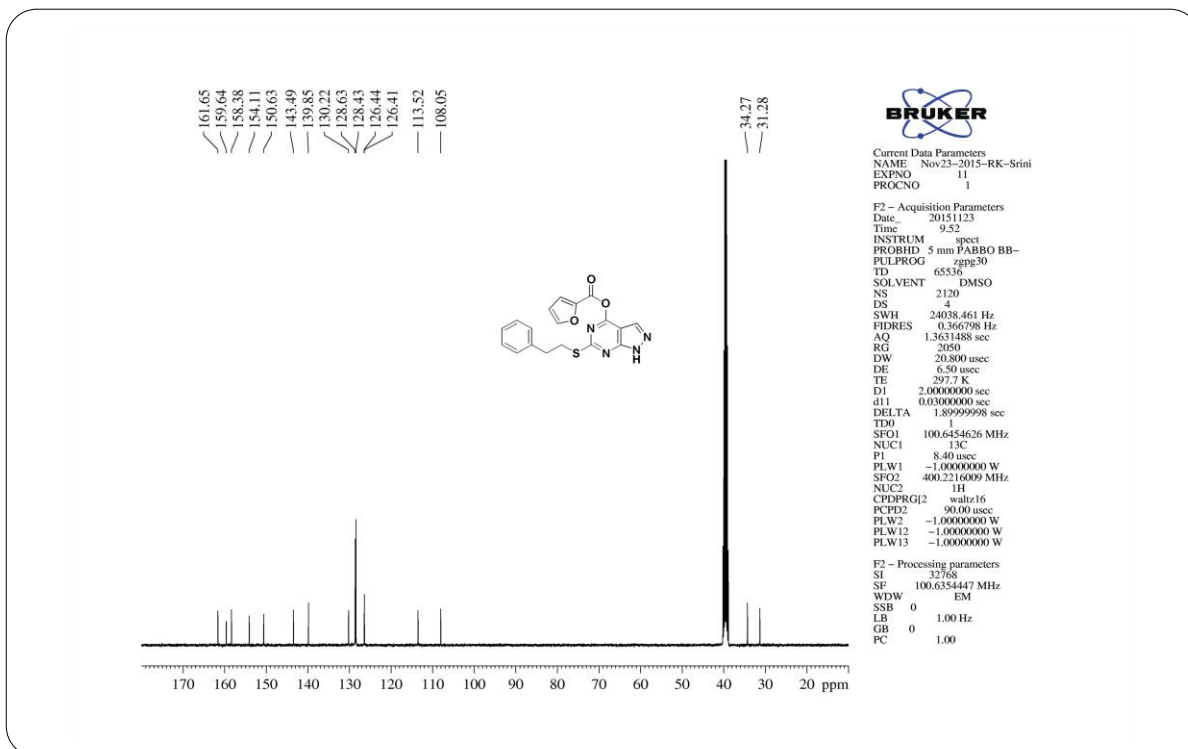
**¹H NMR Spectrum of Compound 6a****¹³C NMR Spectrum of Compound 6a**

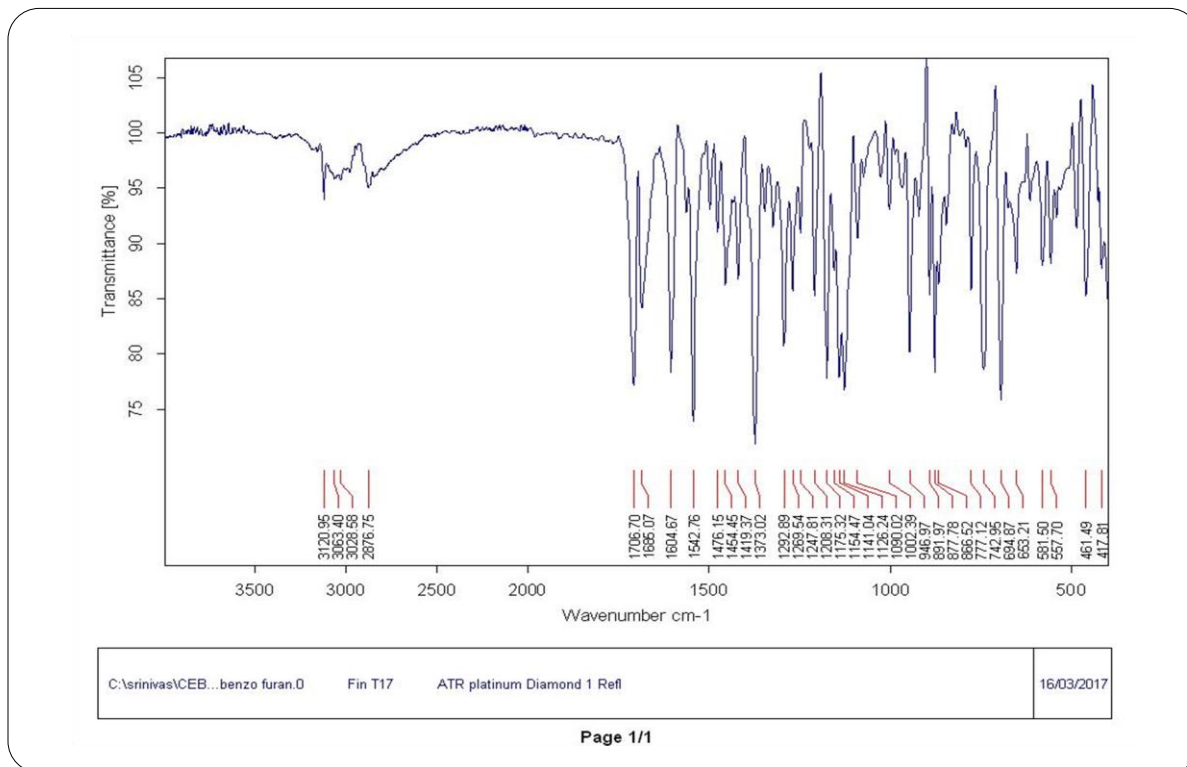


HRMS Spectrum of Compound 6a

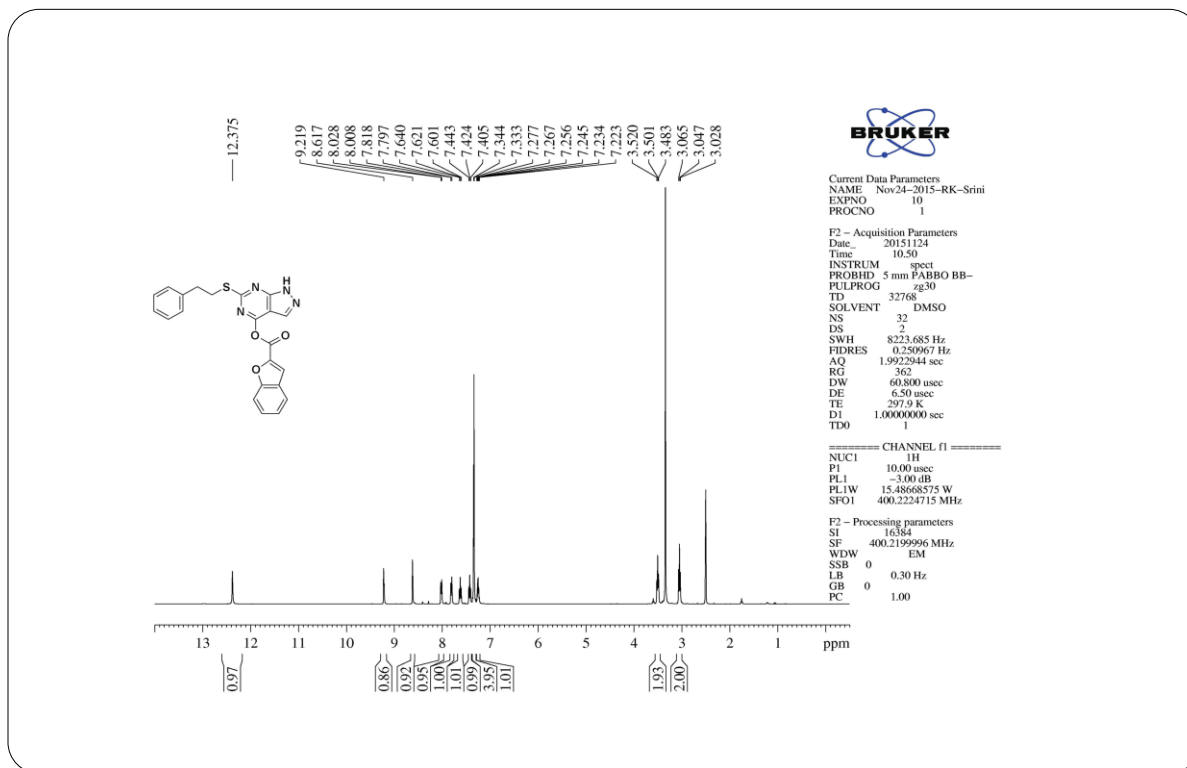


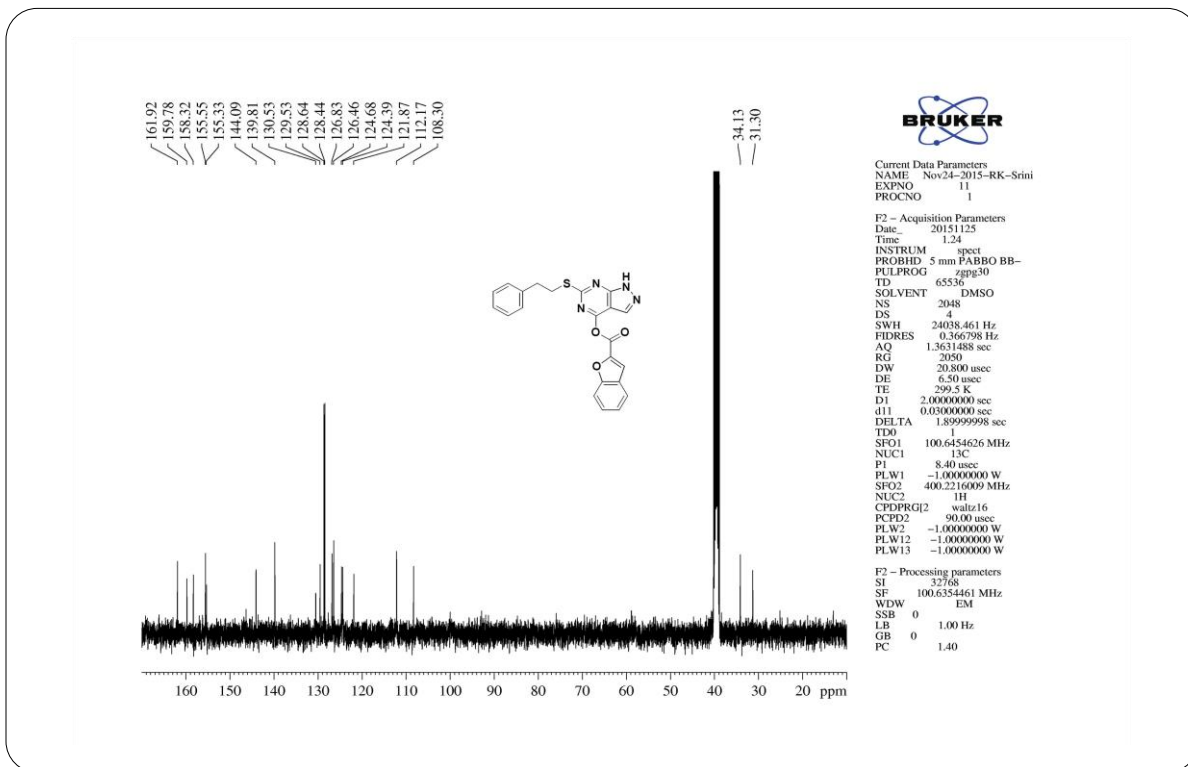
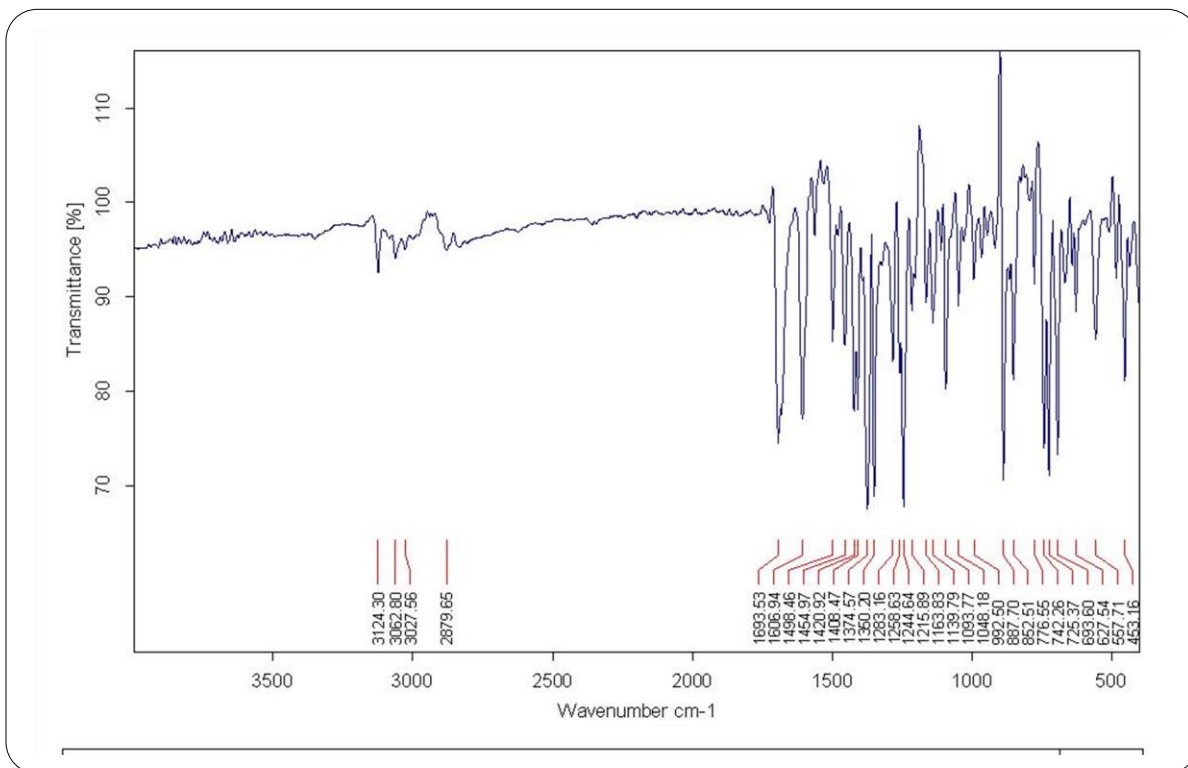
IR Spectrum of Compound 6b

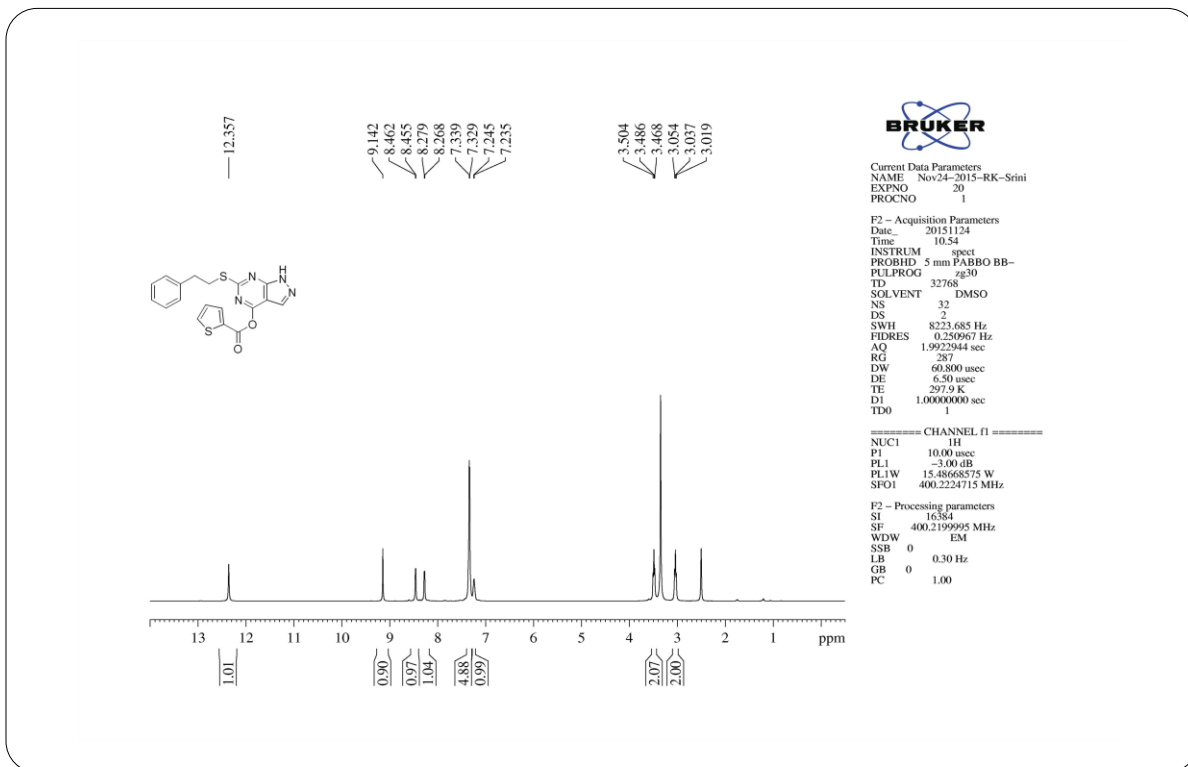
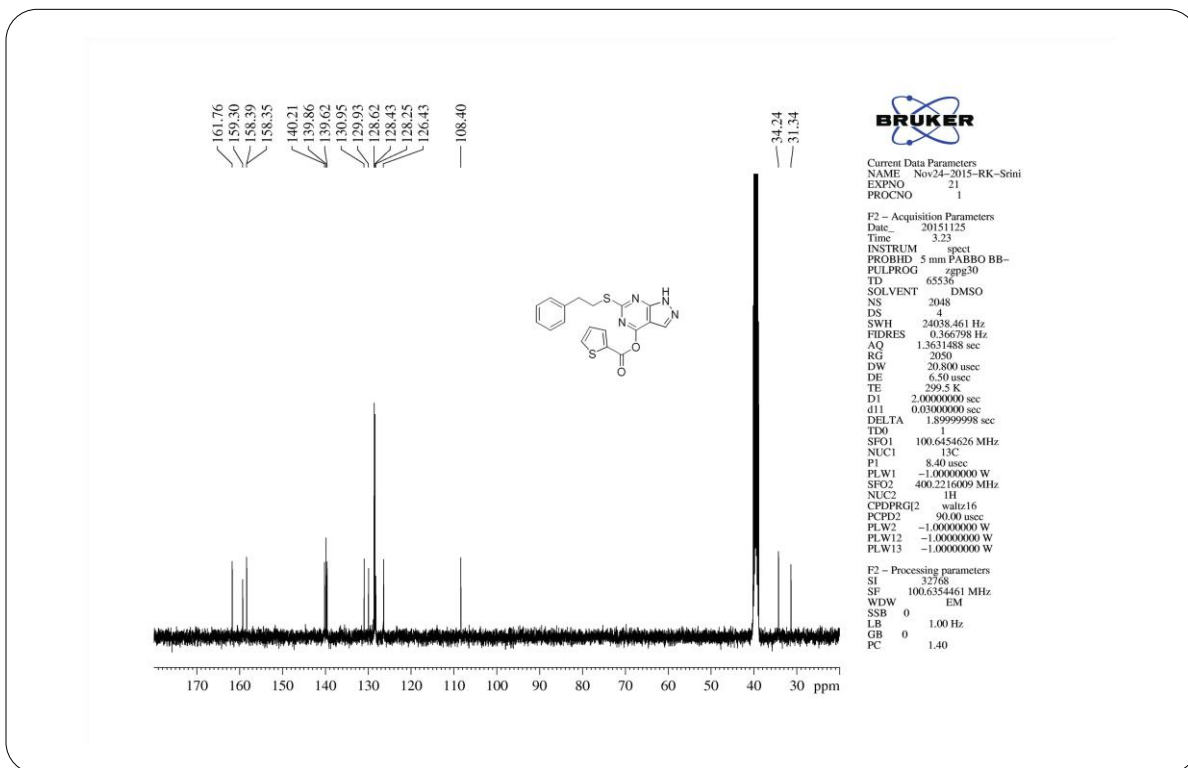
**¹H NMR Spectrum of Compound 6b****¹³C NMR Spectrum of Compound 6b**

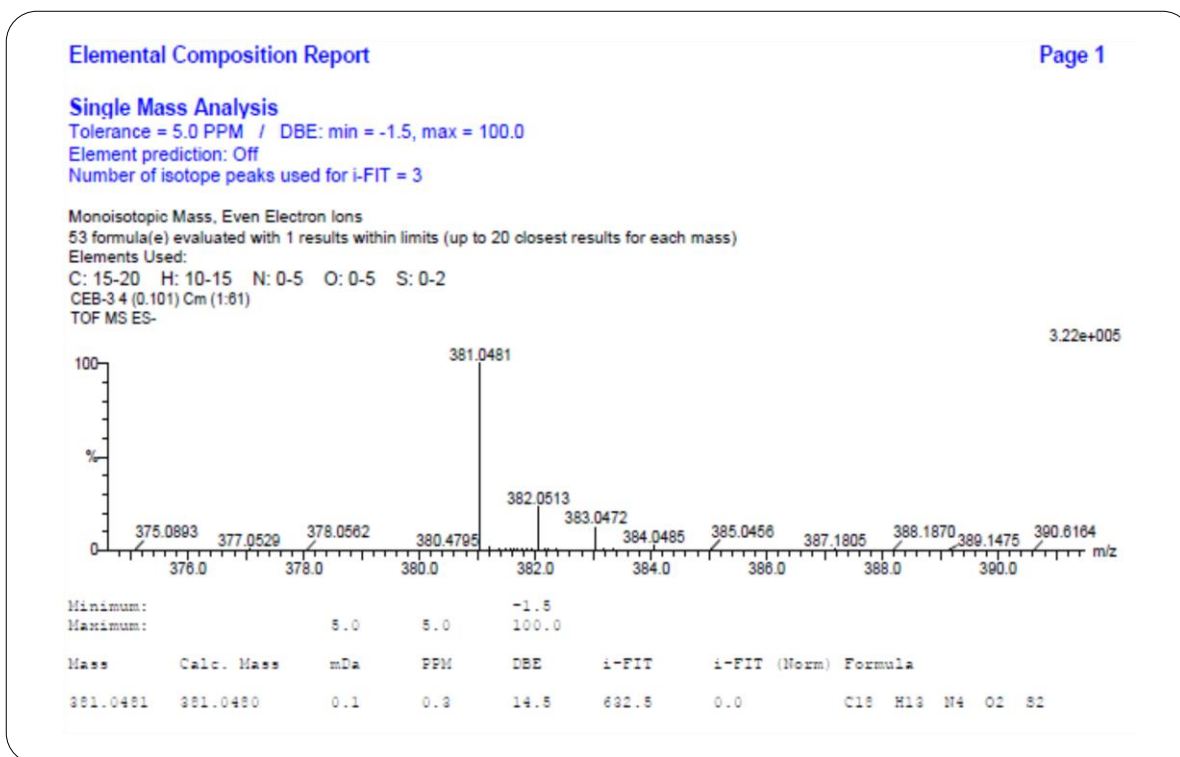


IR Spectrum of Compound 6c

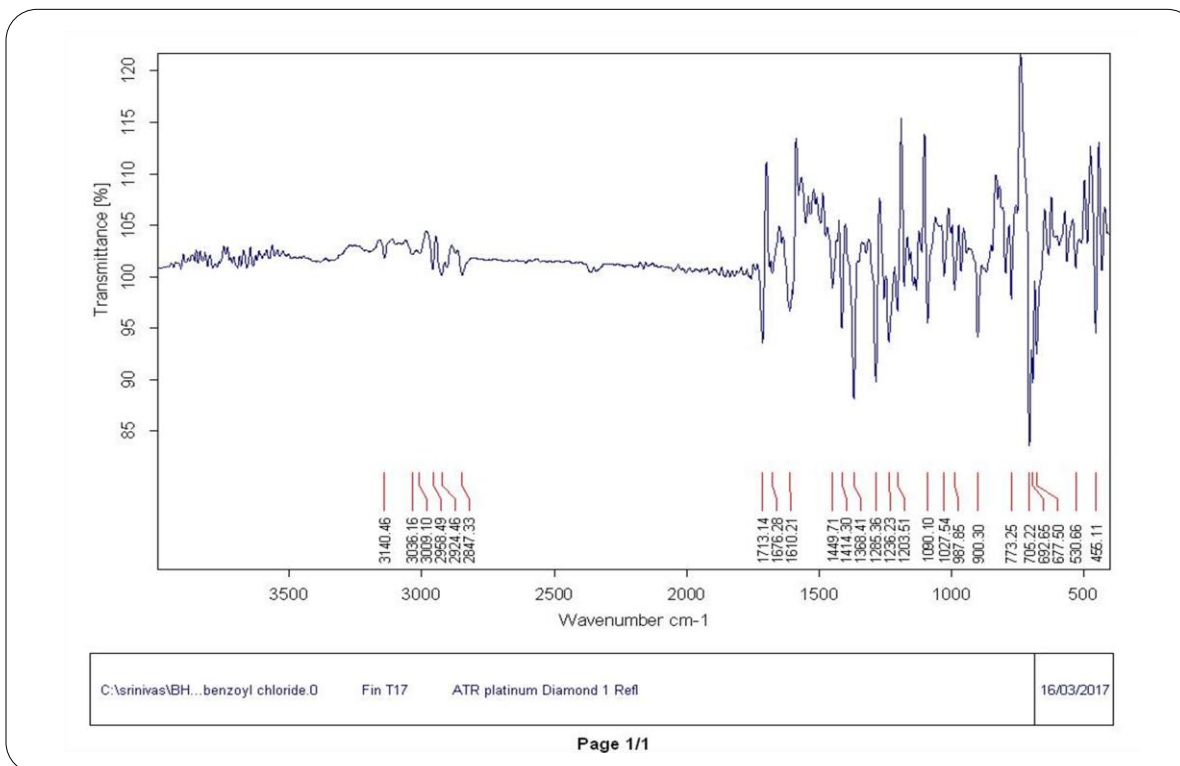
¹H NMR Spectrum of Compound 6c

**¹³C NMR Spectrum of Compound 6c****IR Spectrum of Compound 6d**

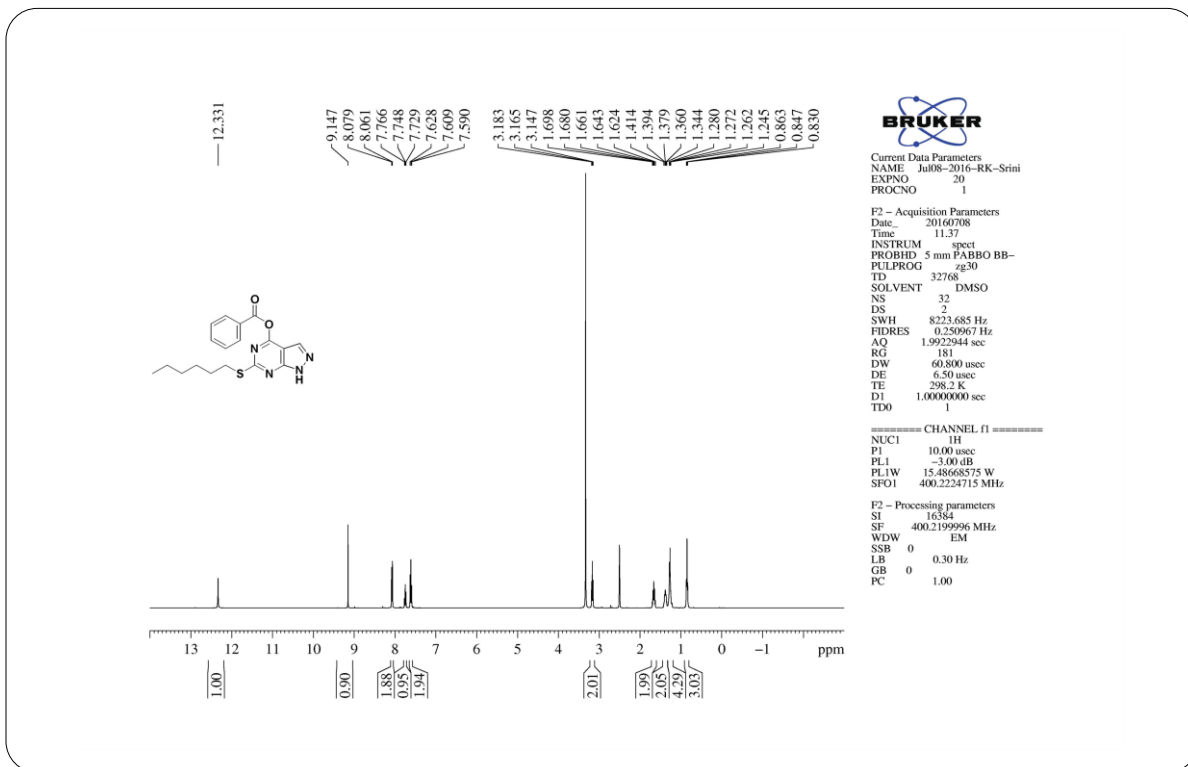
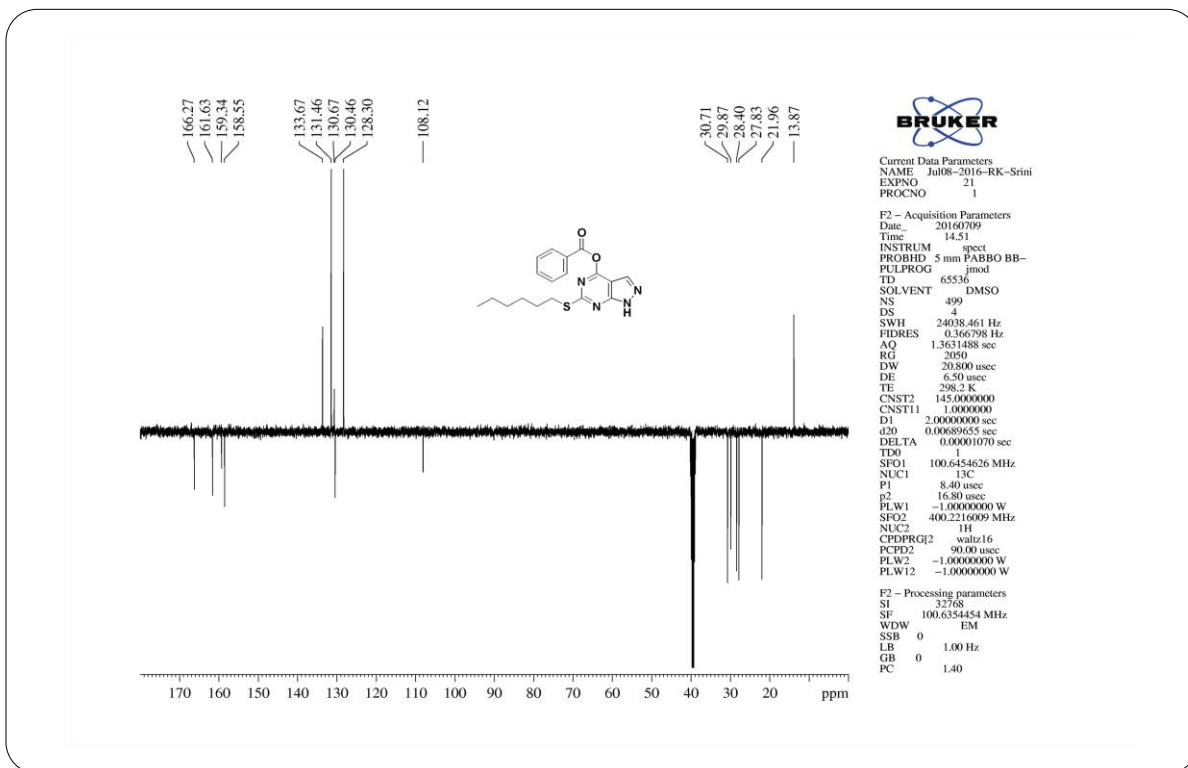
**¹H NMR Spectrum of Compound 6d****¹³C NMR Spectrum of Compound 6d**

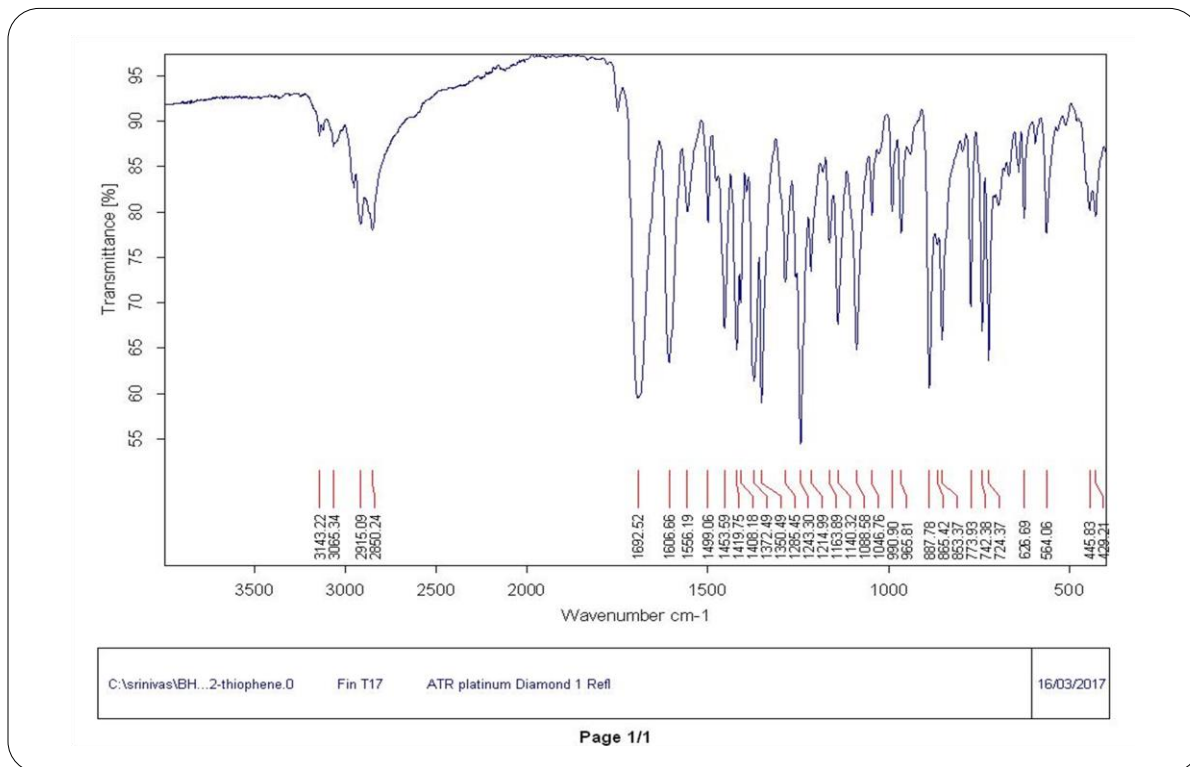


HRMS Spectrum of Compound 6d

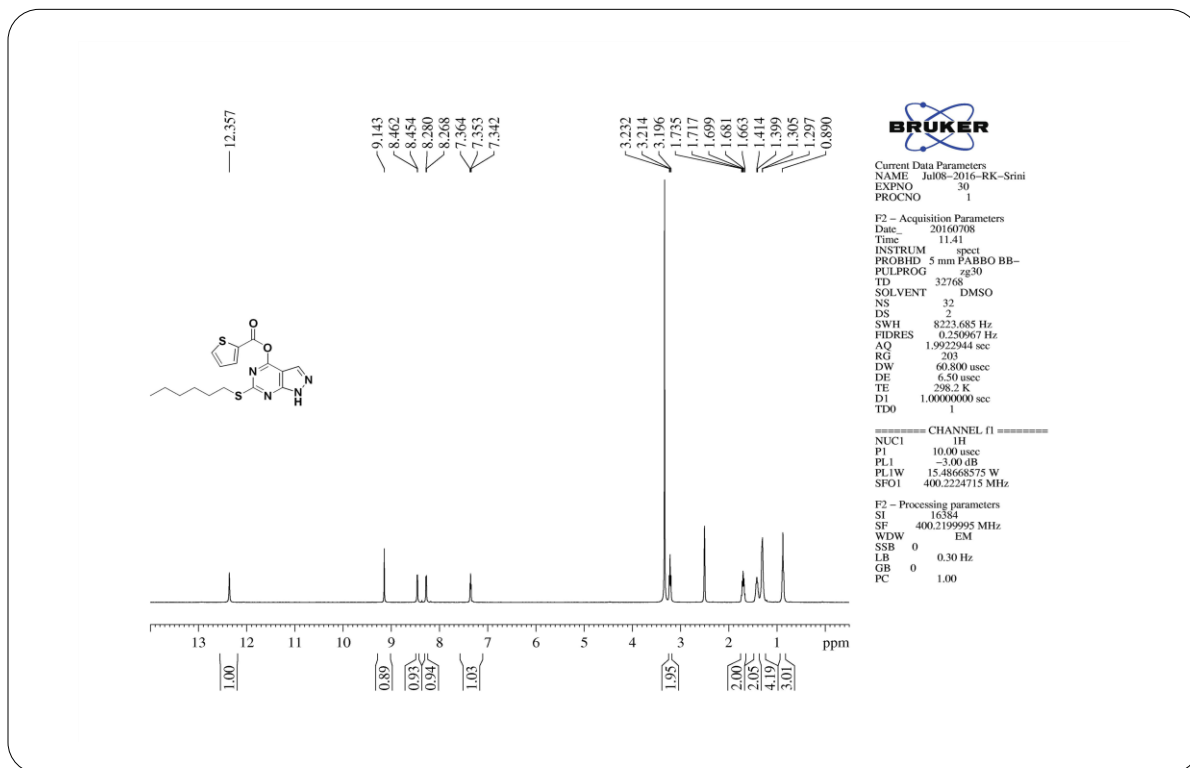


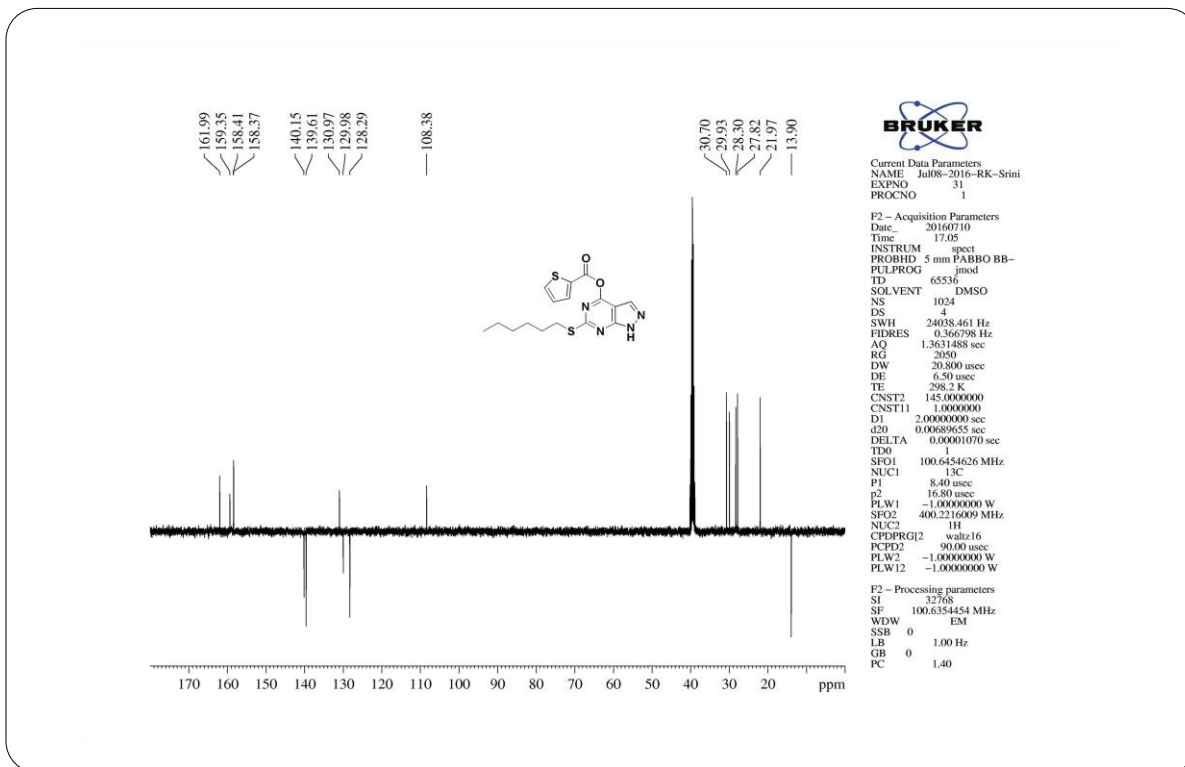
IR Spectrum of Compound 7a

**¹H NMR Spectrum of Compound 7a****¹³C NMR Spectrum of Compound 7a**



IR Spectrum of Compound 7b

¹H NMR Spectrum of Compound 7b

**¹³C NMR Spectrum of Compound 7b****Elemental Composition Report**

Page 1

Single Mass Analysis

Tolerance = 5.0 PPM / DBE: min = -1.5, max = 100.0

Element prediction: Off

Number of isotope peaks used for i-FIT = 3

Monoisotopic Mass, Even Electron Ions

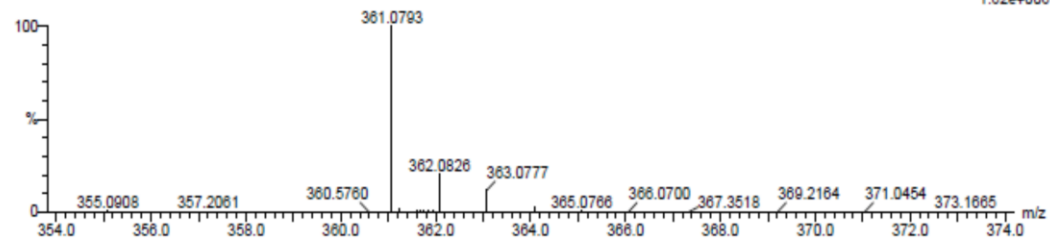
44 formula(e) evaluated with 1 results within limits (up to 20 closest results for each mass)

Elements Used:

C: 15-20 H: 15-20 N: 0-5 O: 0-5 S: 0-2

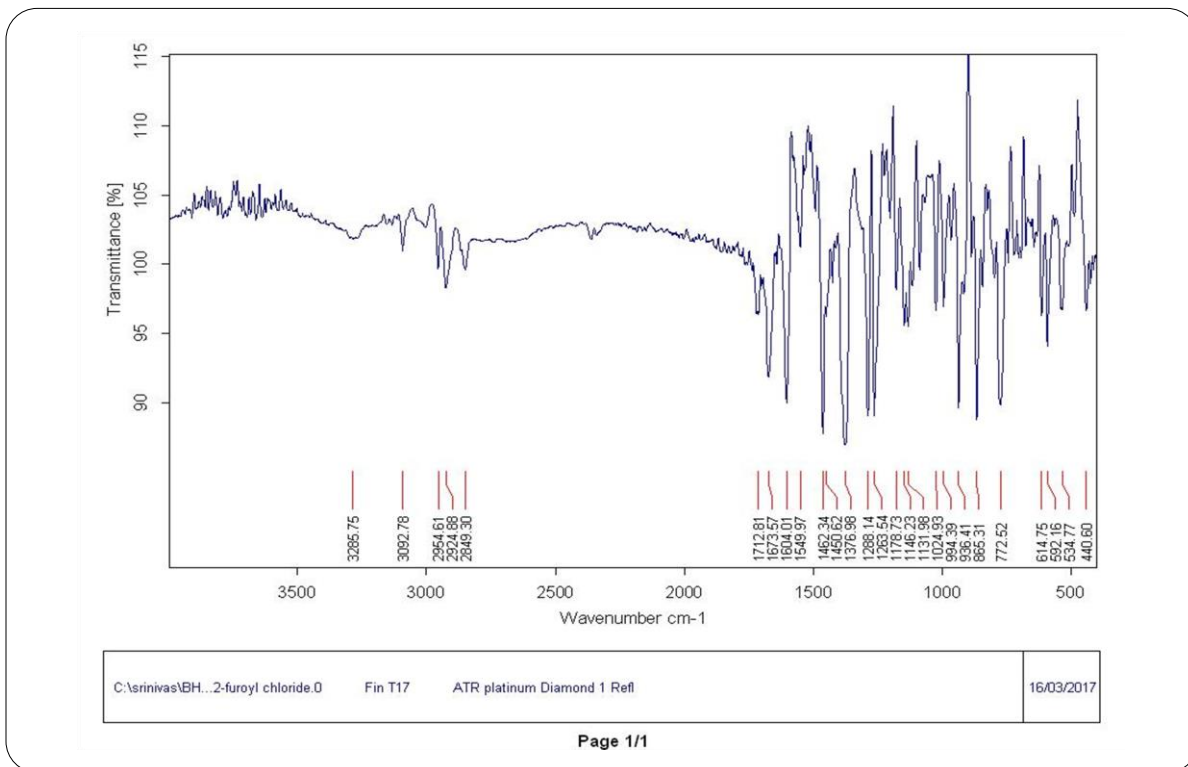
BH-3 49 (1.819) Cm (1.81)

TOF MS ES-

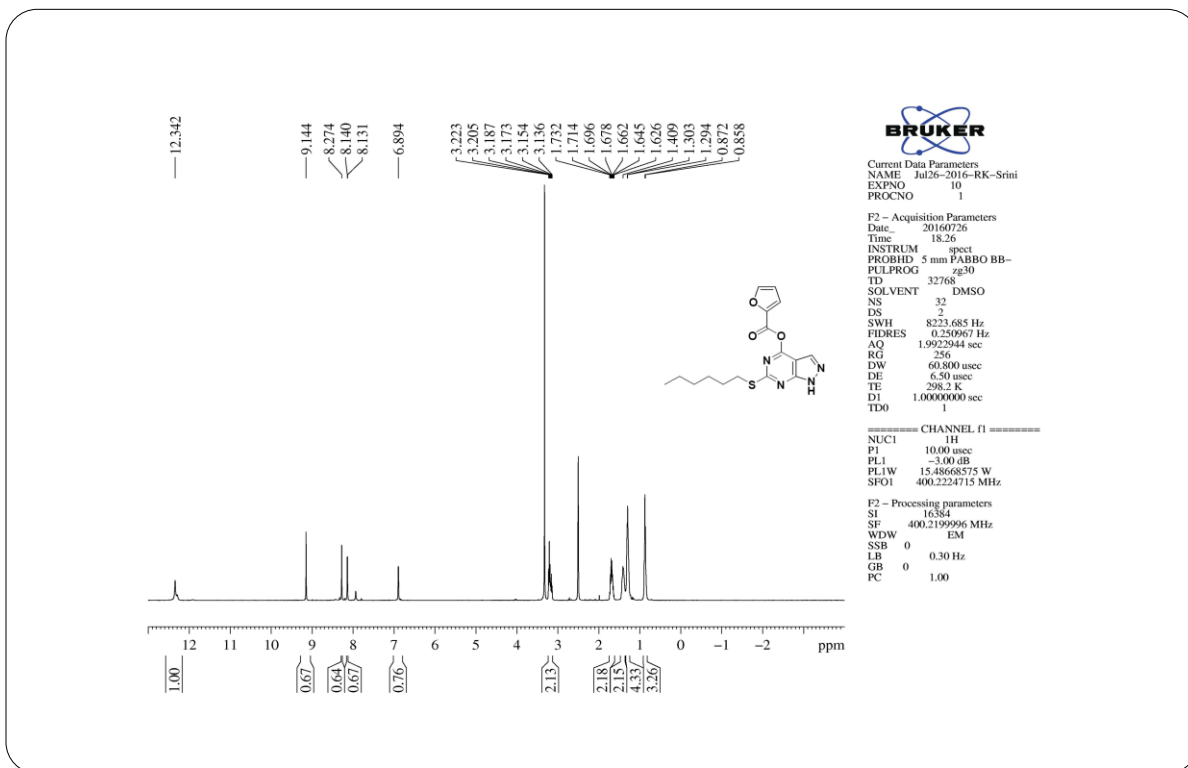


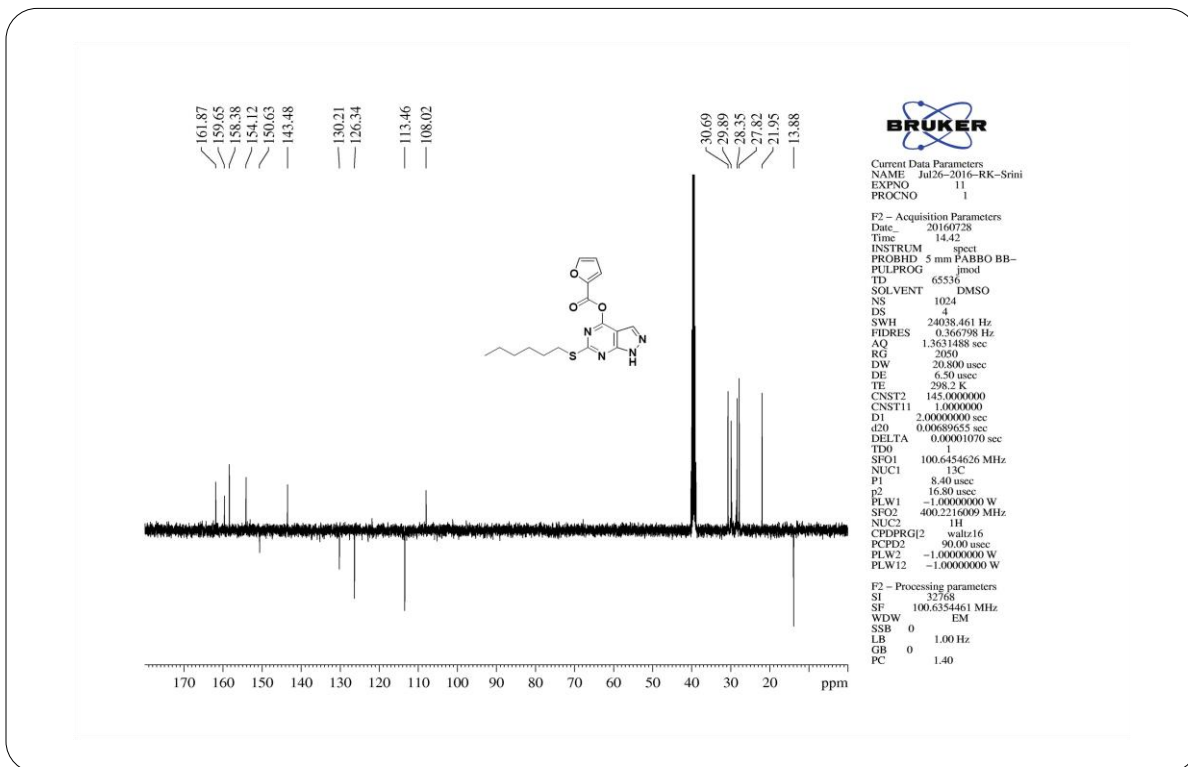
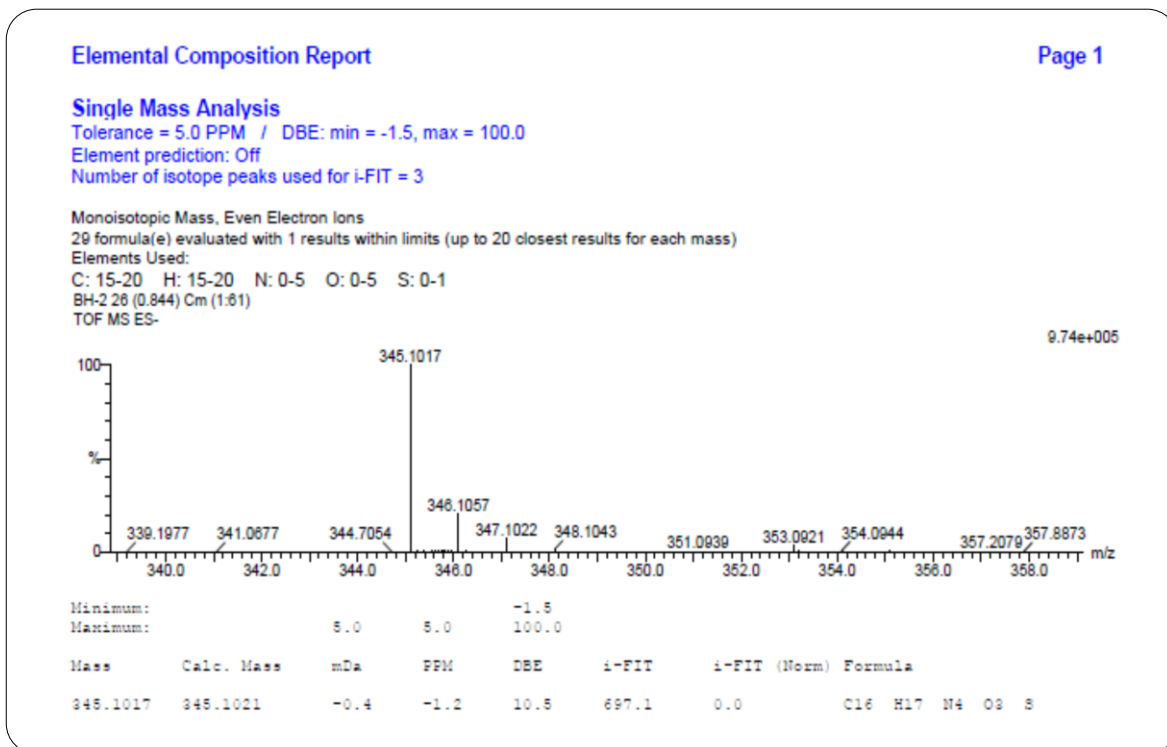
Mass	Calc. Mass	mDa	PPM	DBE	i-FIT	i-FIT (Norm)	Formula
361.0793	361.0793	0.0	0.0	10.5	714.8	0.0	C16 H17 N4 O2 S2

HRMS Spectrum of Compound 7b



IR Spectrum of Compound 7c

¹H NMR Spectrum of Compound 7c

¹³C NMR Spectrum of Compound 7c

HRMS Spectrum of Compound 7c

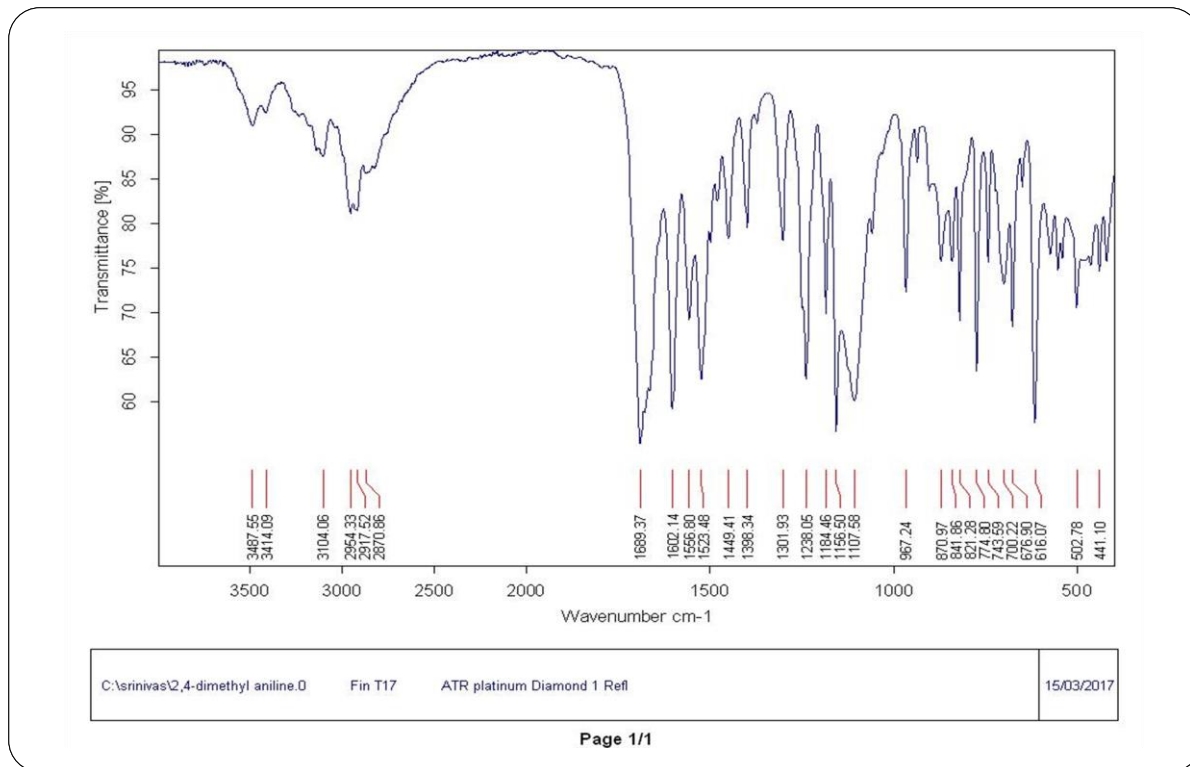
APPENDIX – III

SUPPLEMENTARY INFORMATION

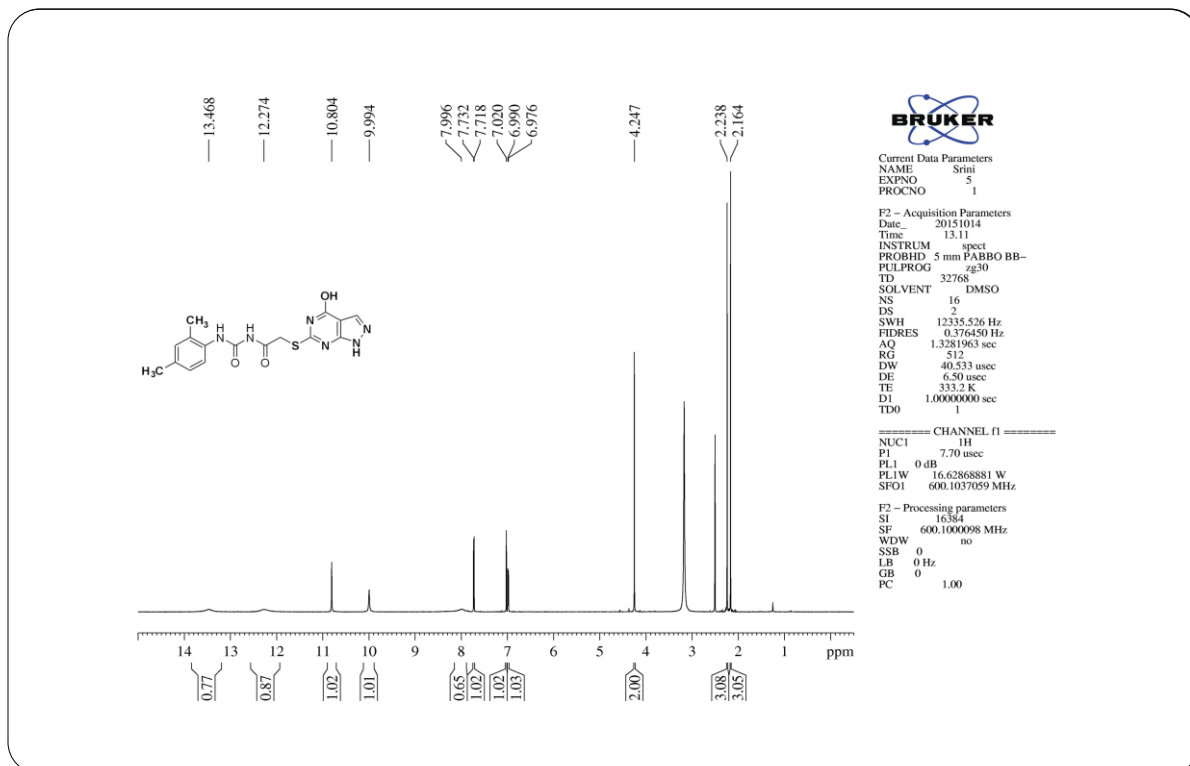
CHAPTER 6

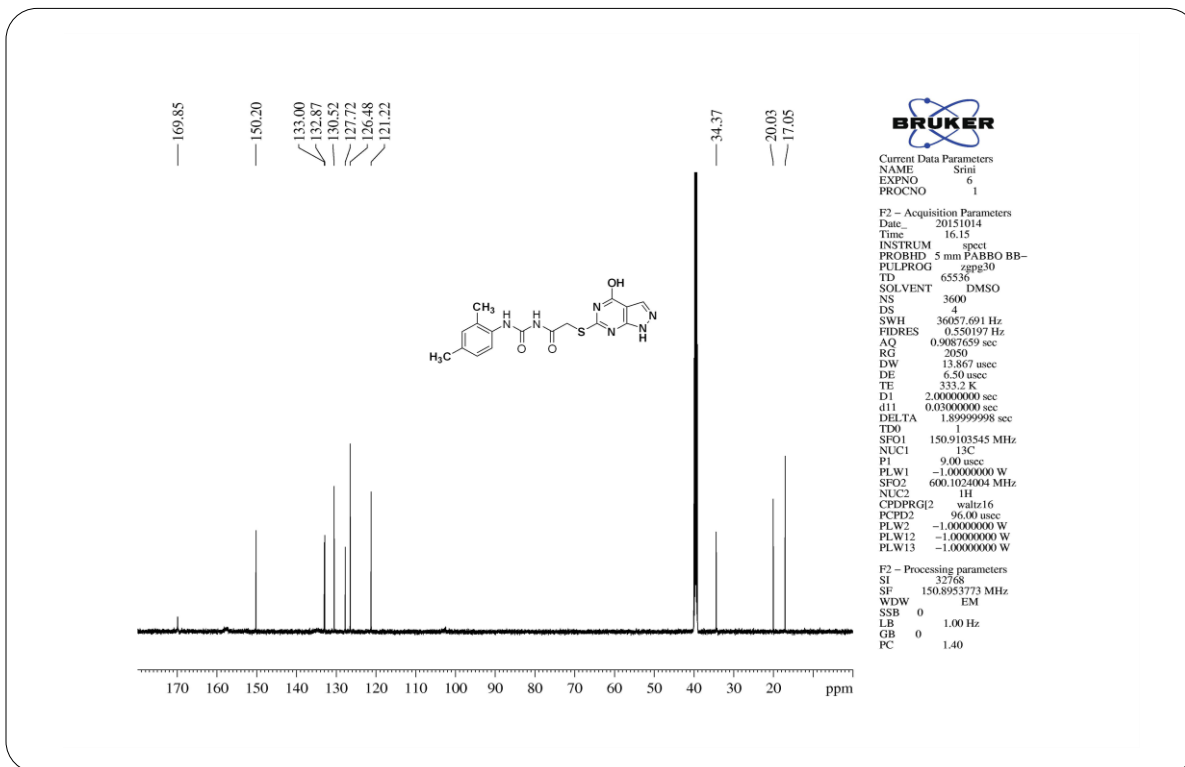
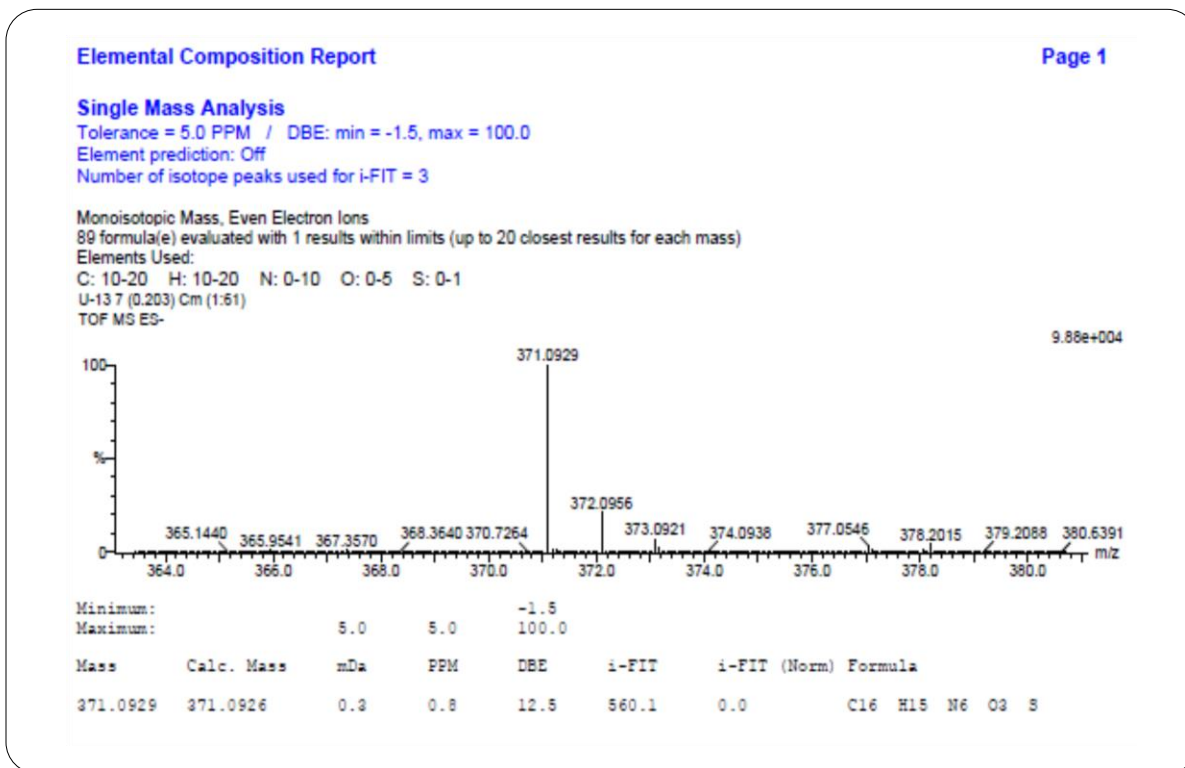
Design, synthesis and biological evaluation of novel pyrazolo[3,4-*d*]pyrimidine analogues as anticancer agents

Department of Pharmaceutical Chemistry, College of Health Sciences, University of KwaZulu-Natal, Durban 4000, South Africa.

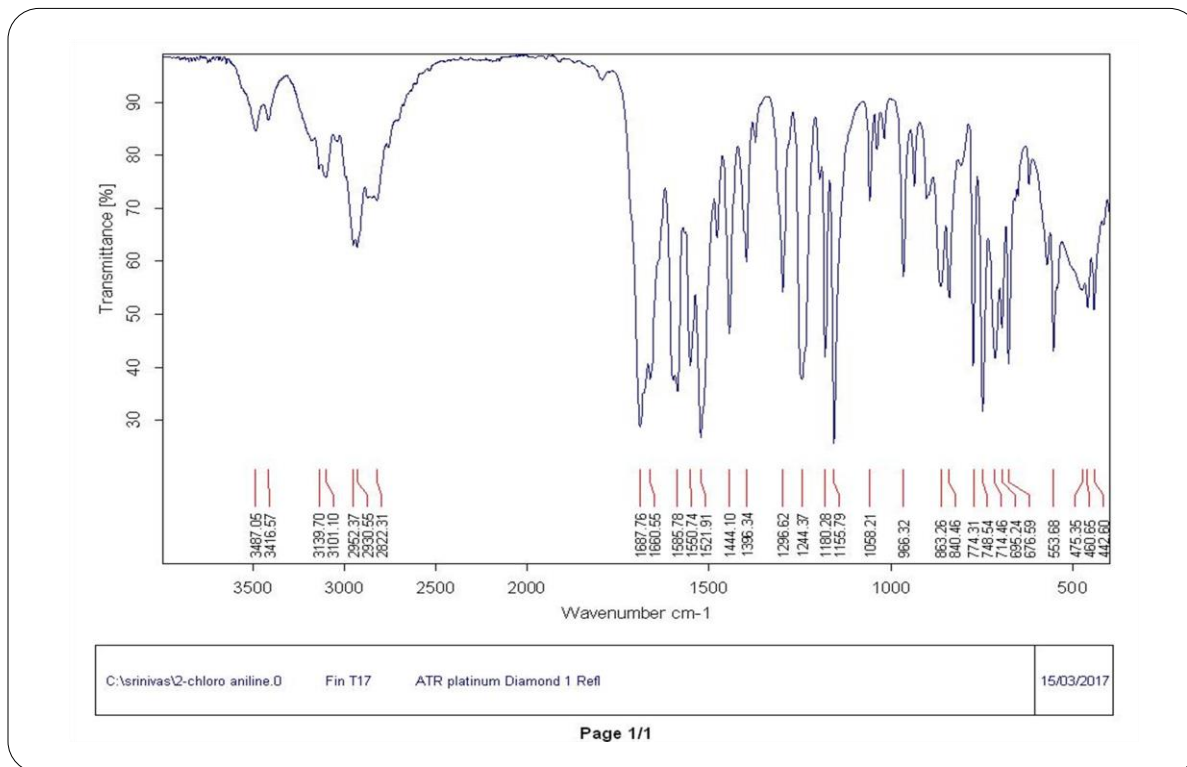


IR Spectrum of Compound 9a

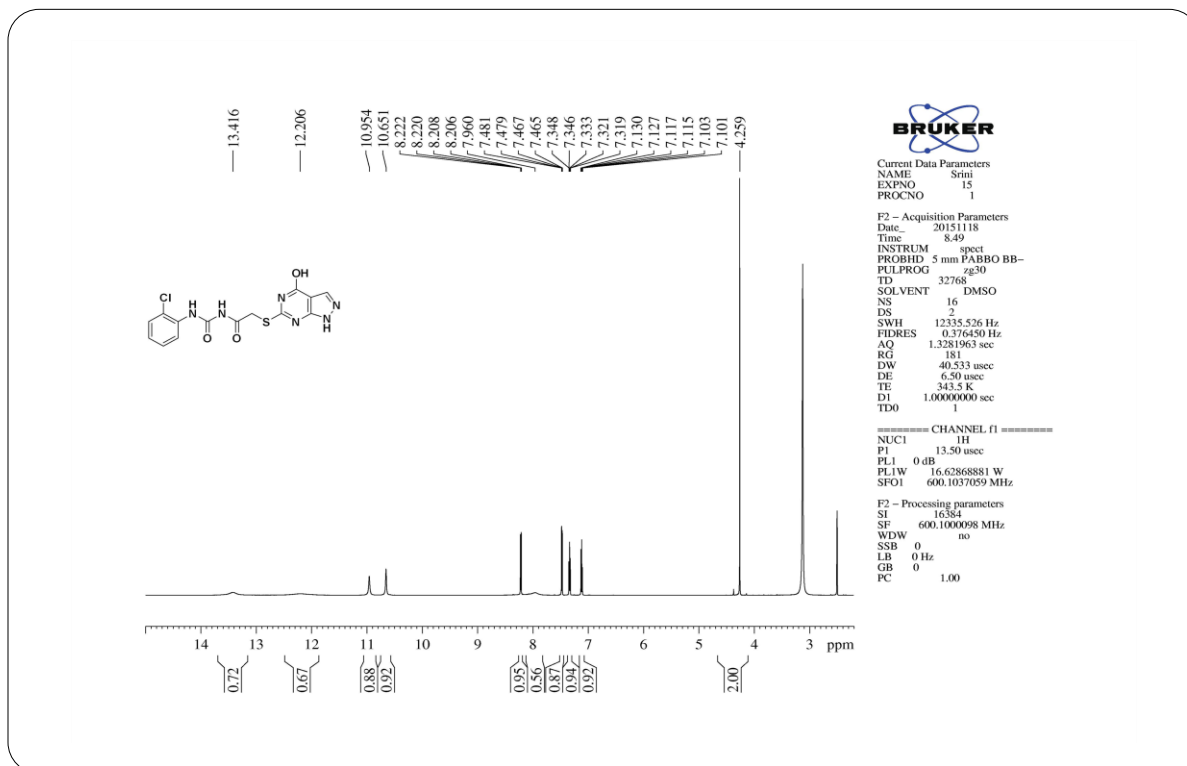
¹H NMR Spectrum of Compound 9a

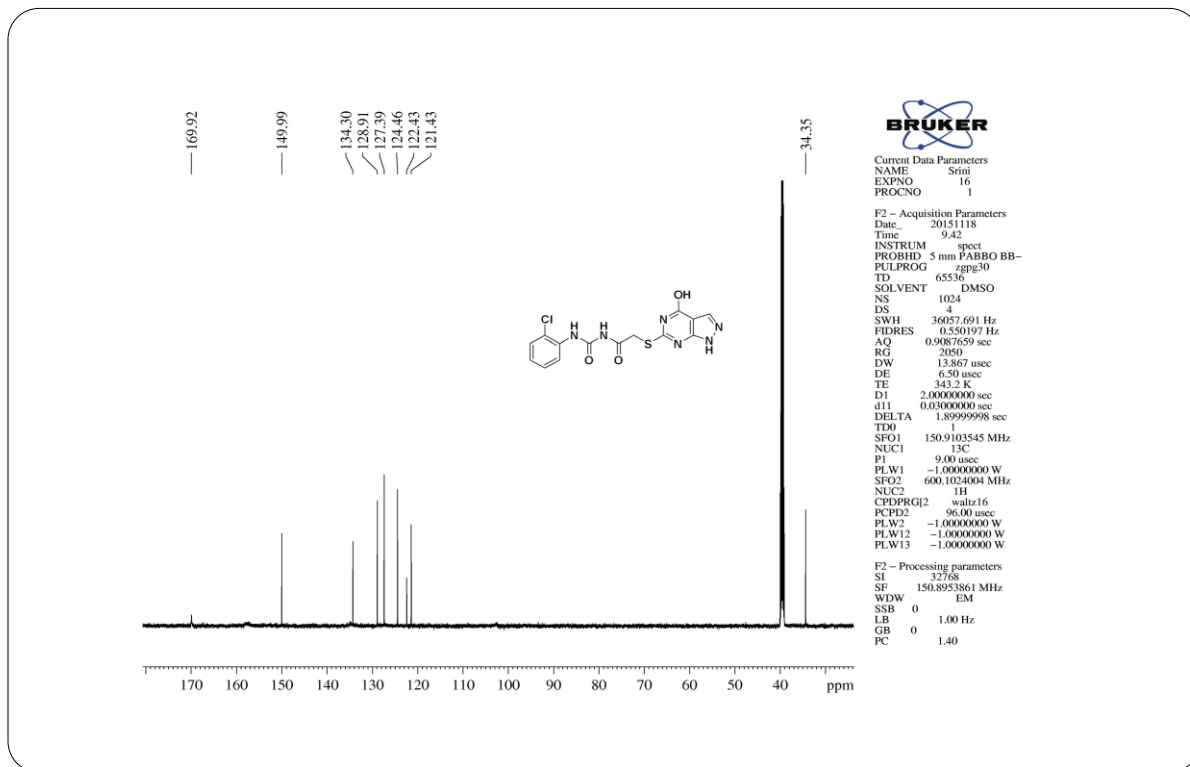
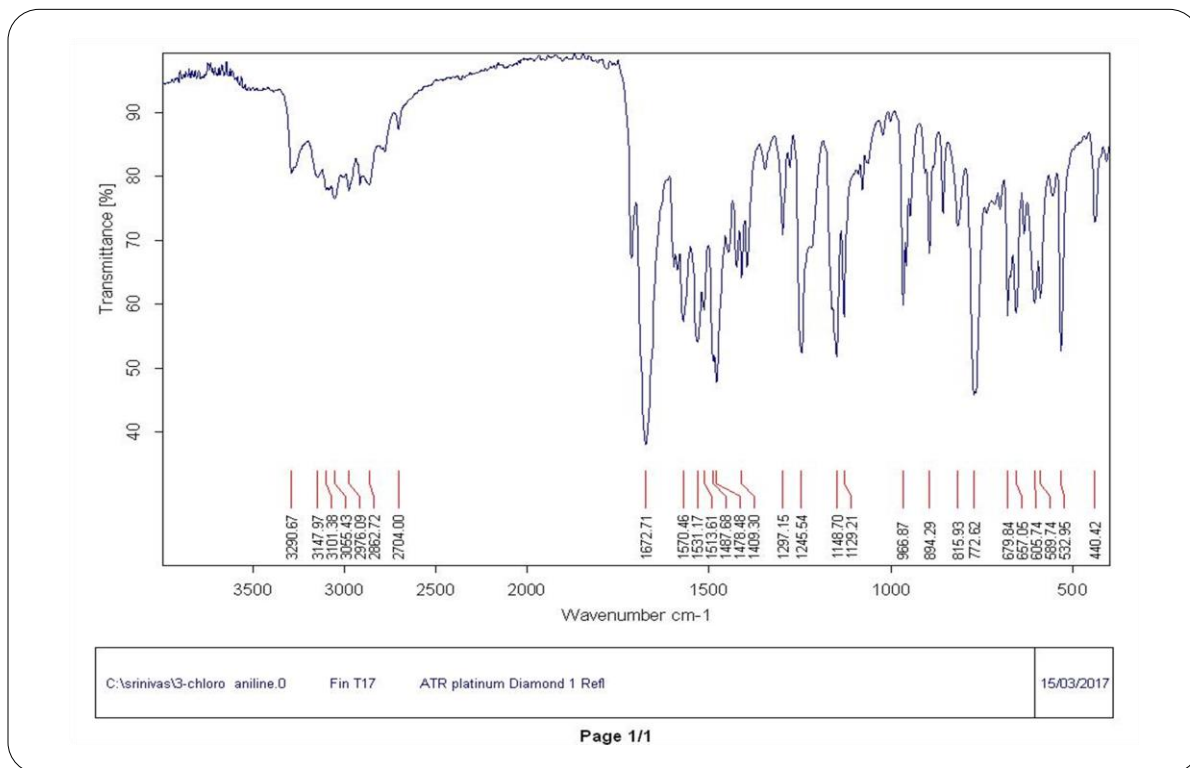
¹³C NMR Spectrum of Compound 9a

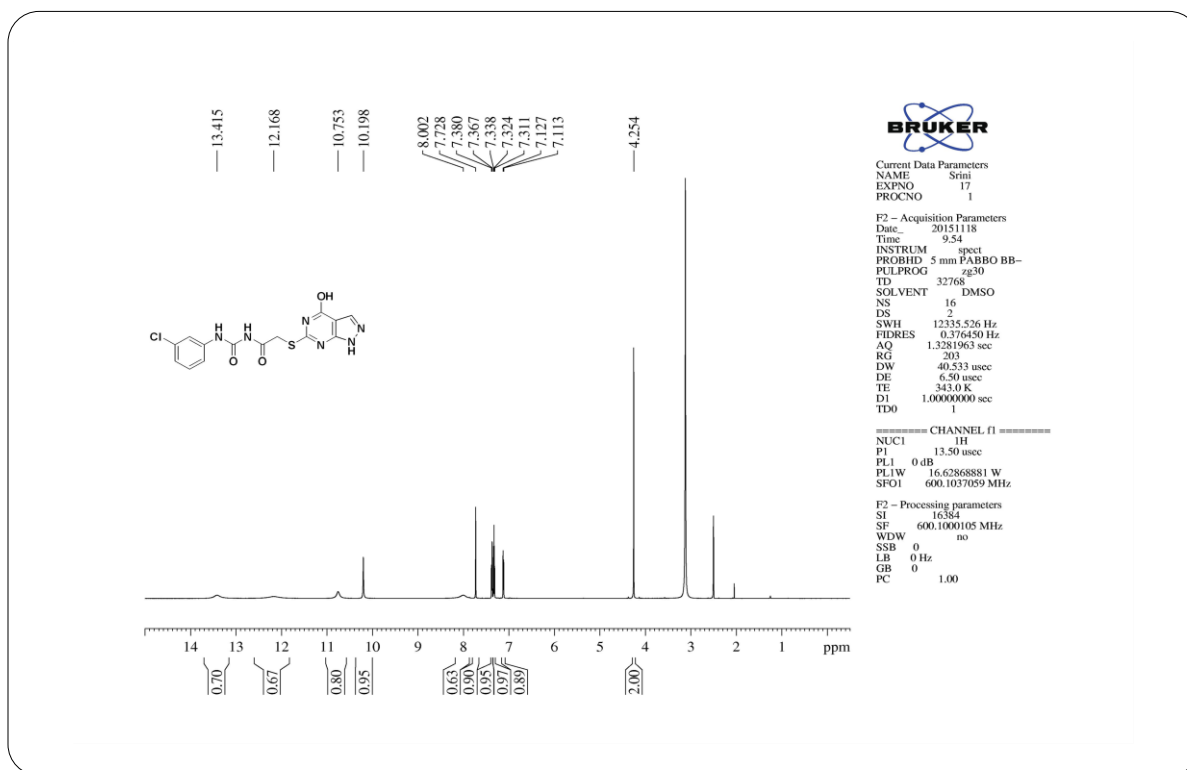
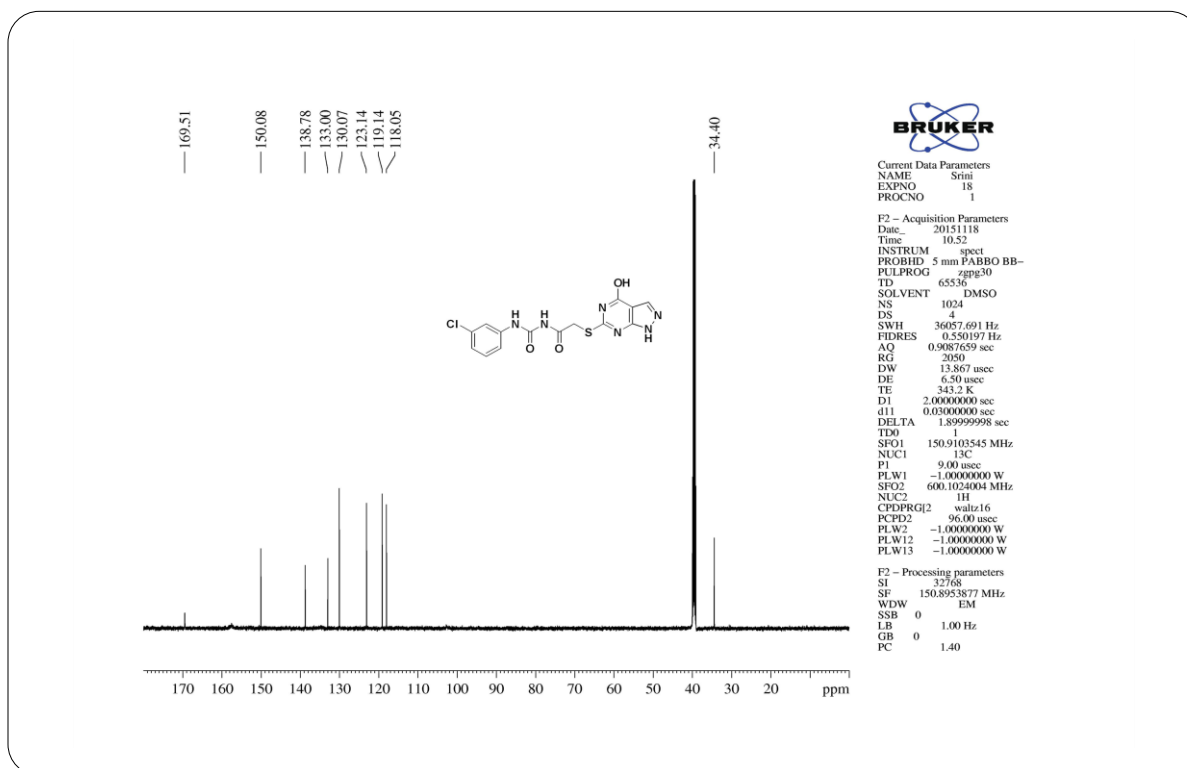
HRMS Spectrum of Compound 9a

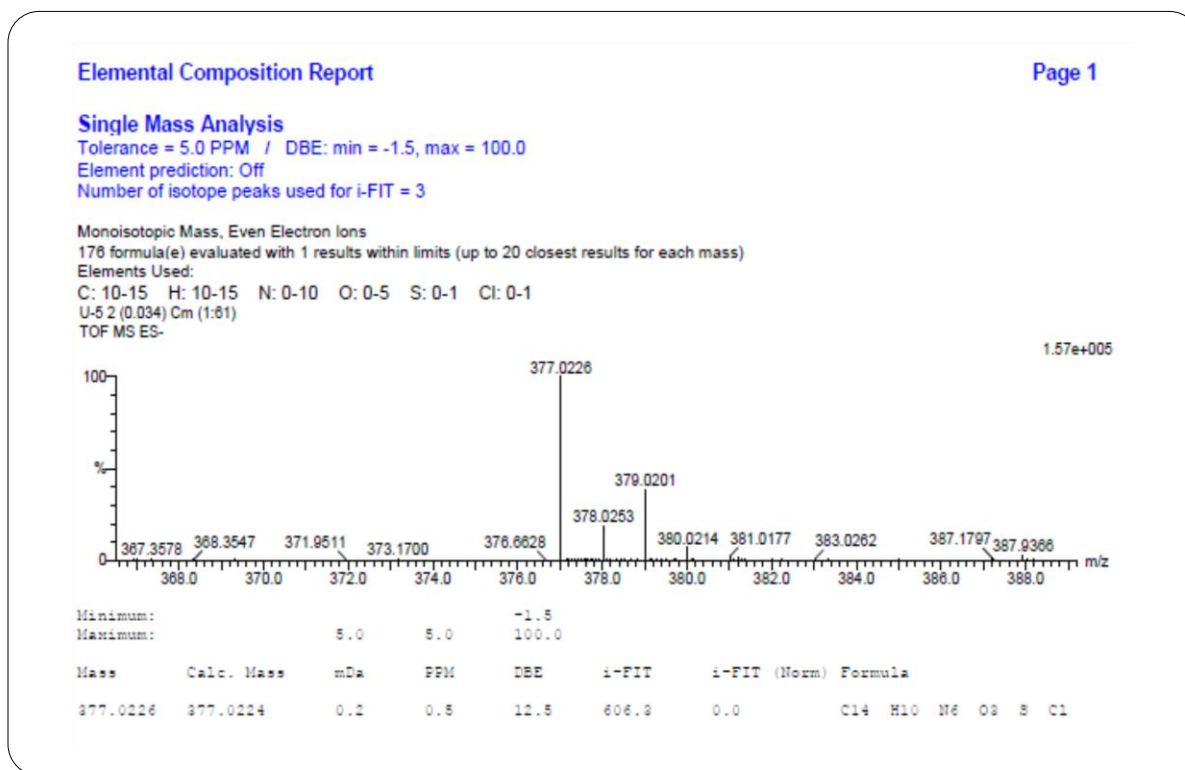


IR Spectrum of Compound 9b

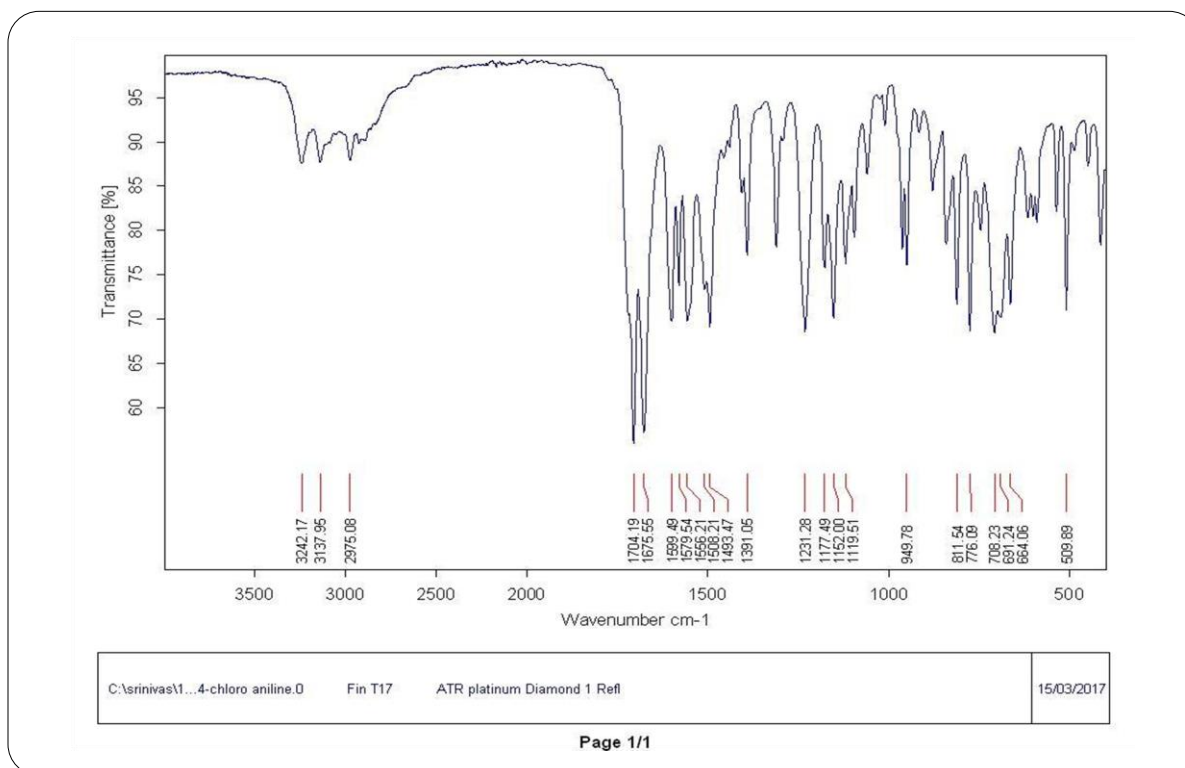
¹H MNR Spectrum of Compound 9b

**¹³C NMR Spectrum of Compound 9b****IR Spectrum of Compound 9c**

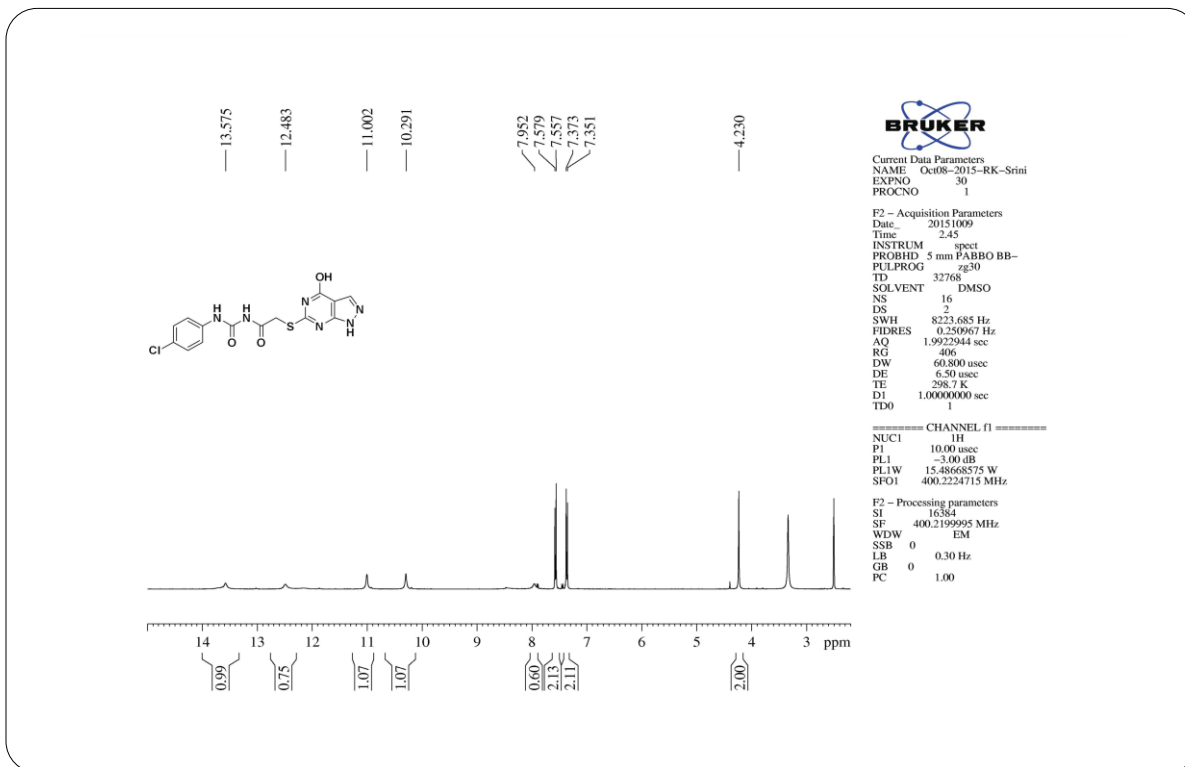
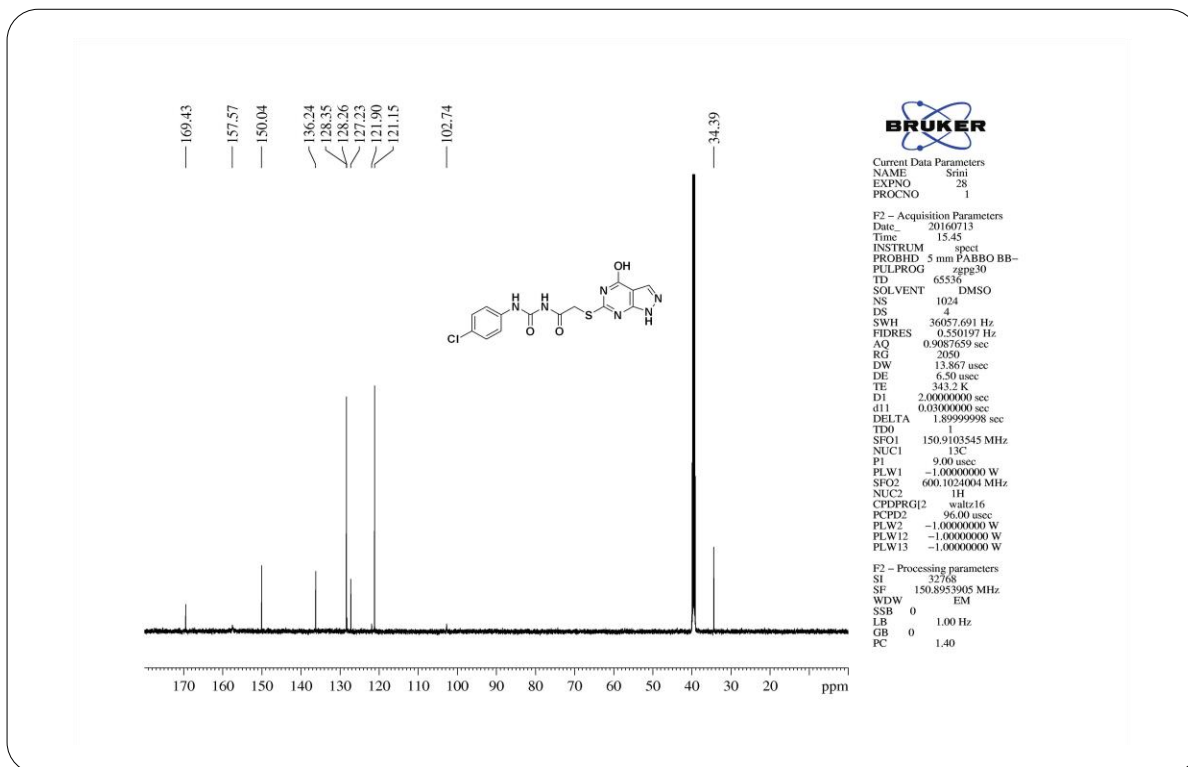
**¹H NMR Spectrum of Compound 9c****¹³C NMR Spectrum of Compound 9c**

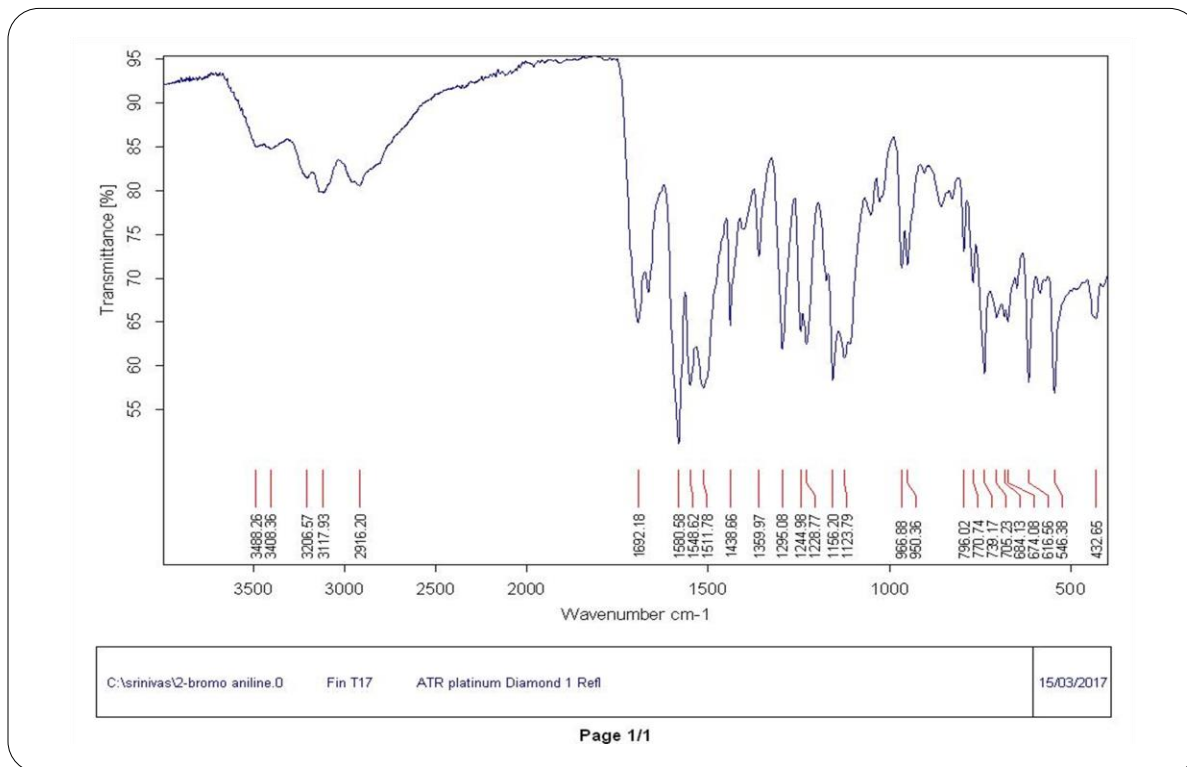


HRMS Spectrum of Compound 9c

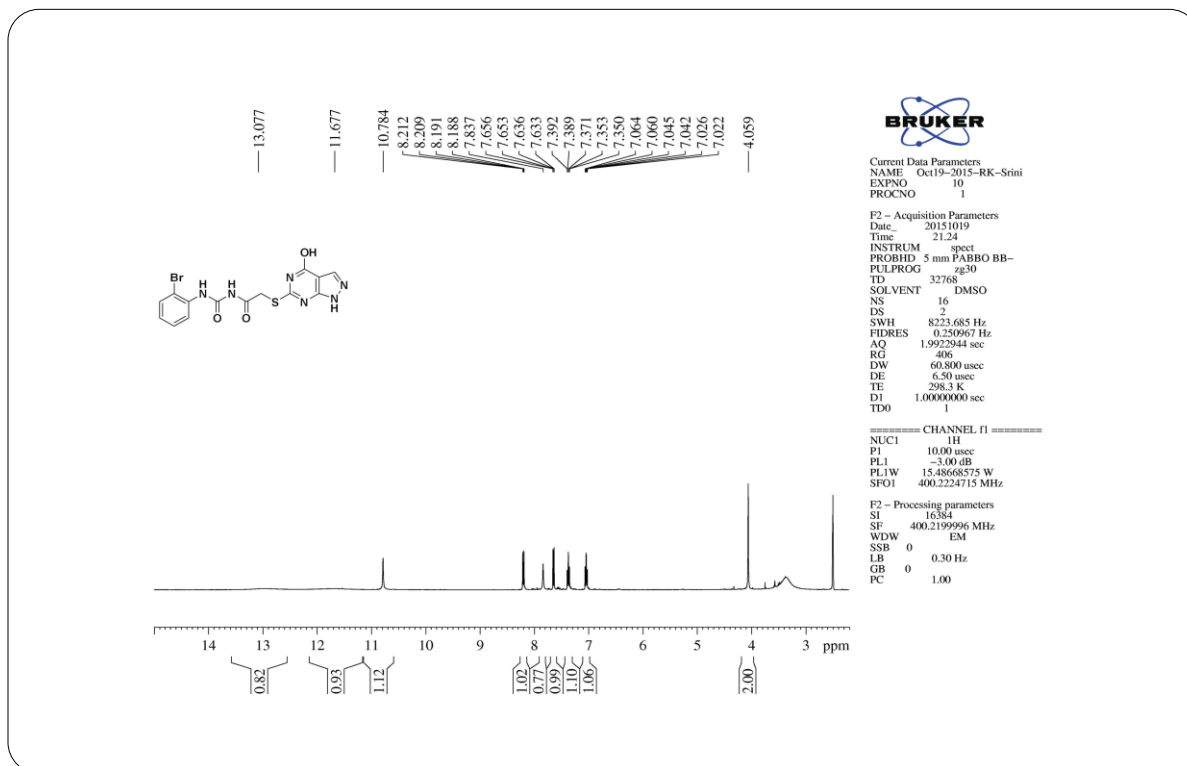


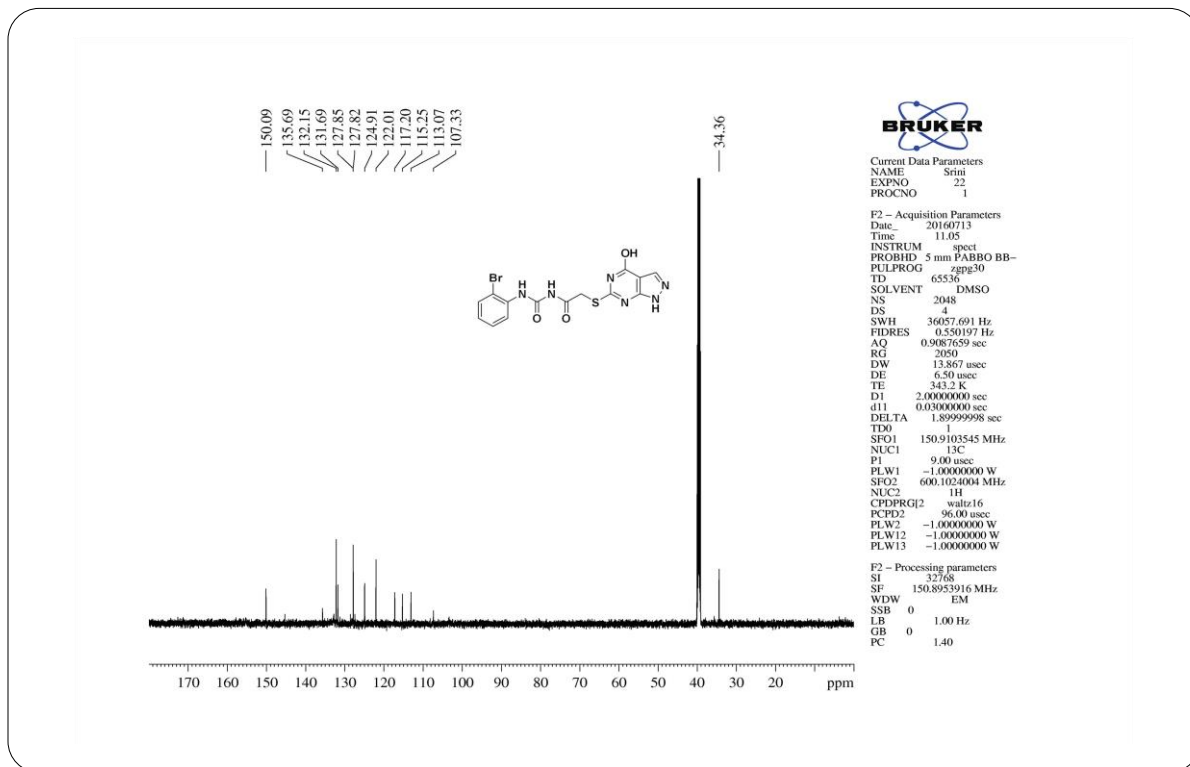
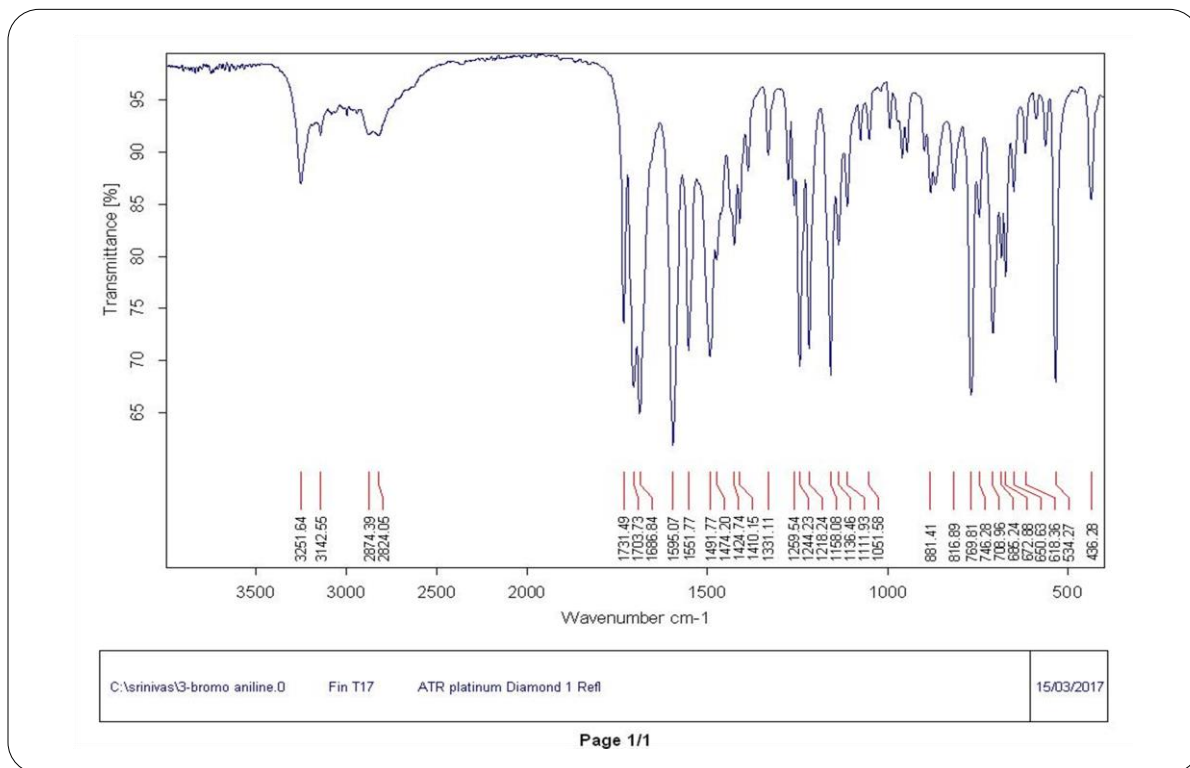
IR Spectrum of Compound 9d

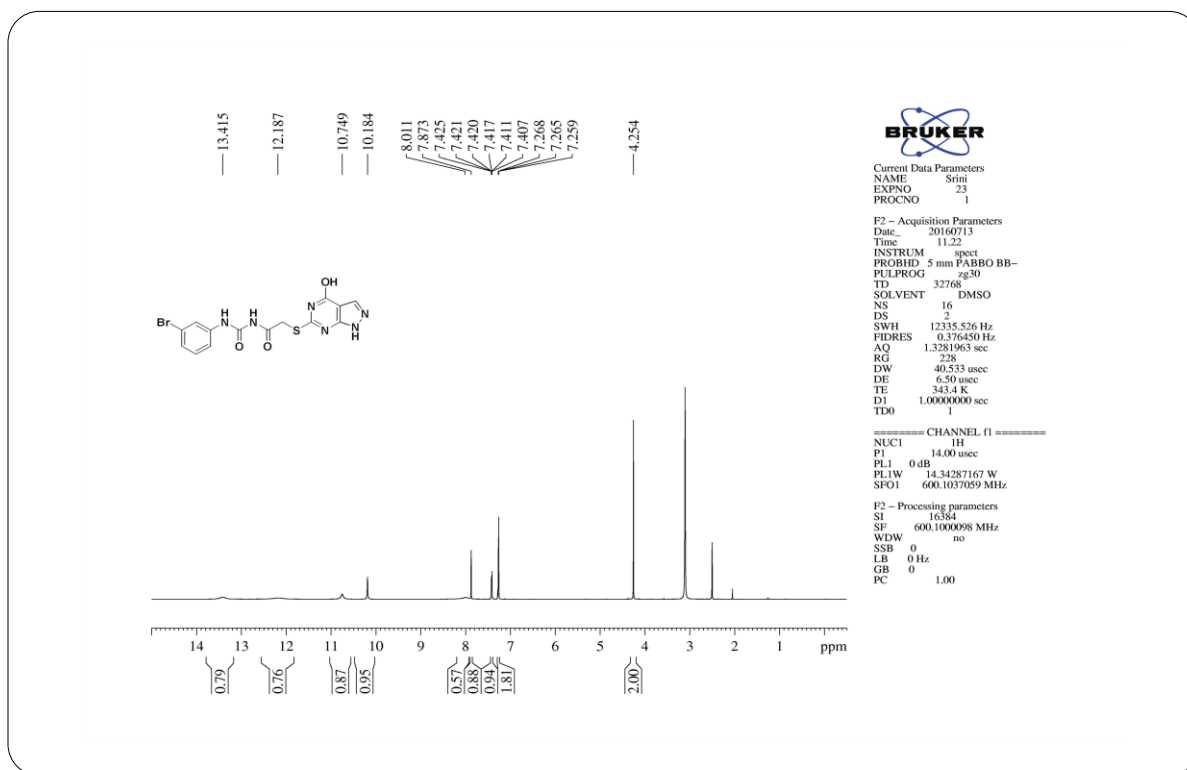
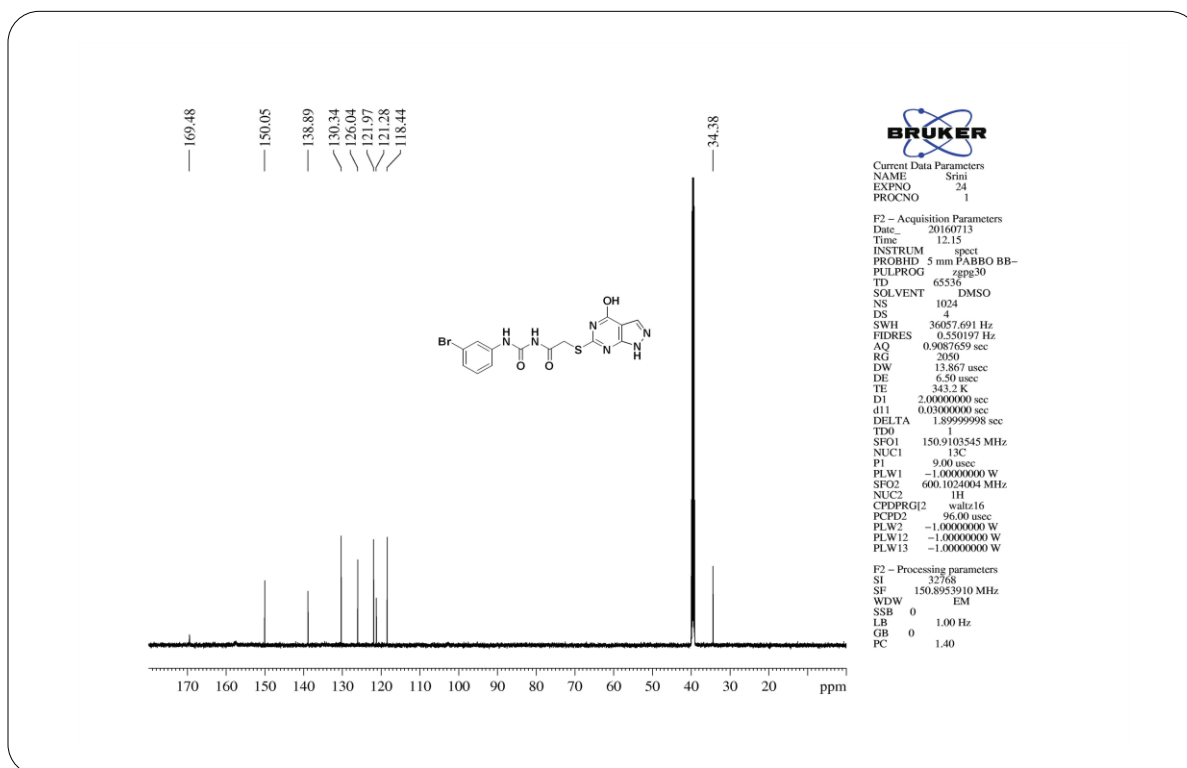
¹H NMR Spectrum of Compound 9d¹³C NMR Spectrum of Compound 9d

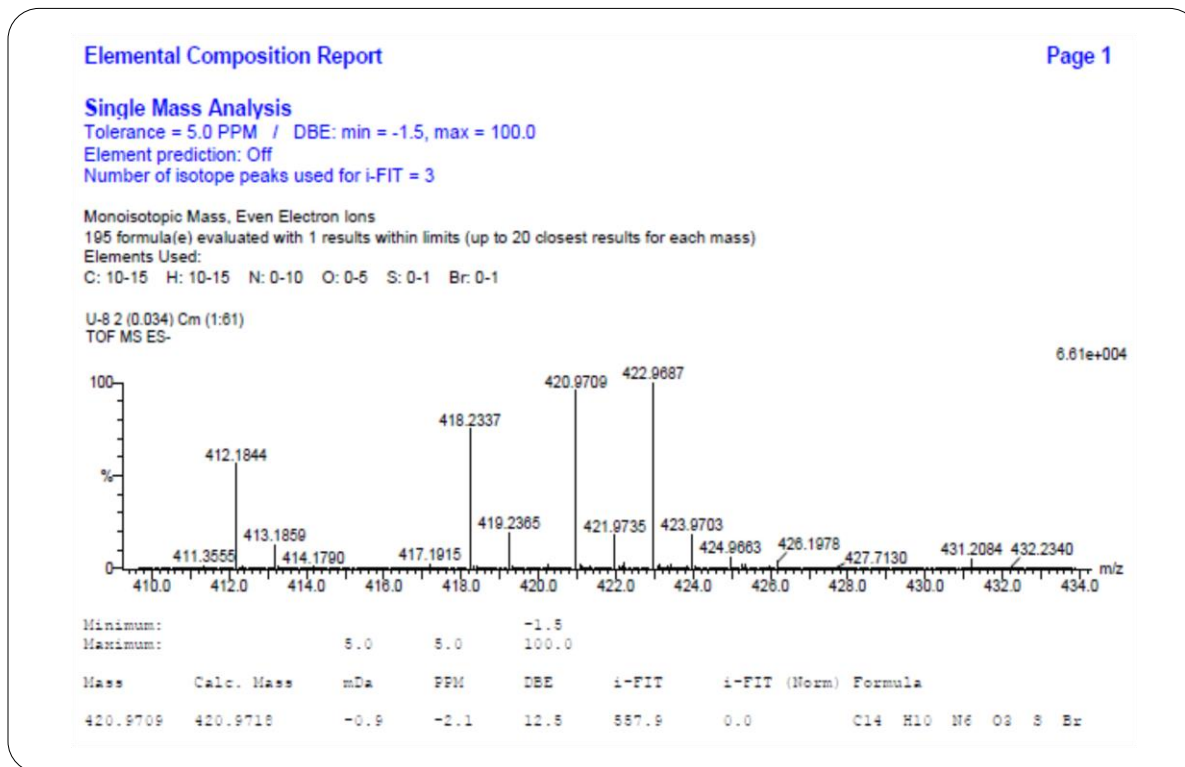


IR Spectrum of Compound 9e

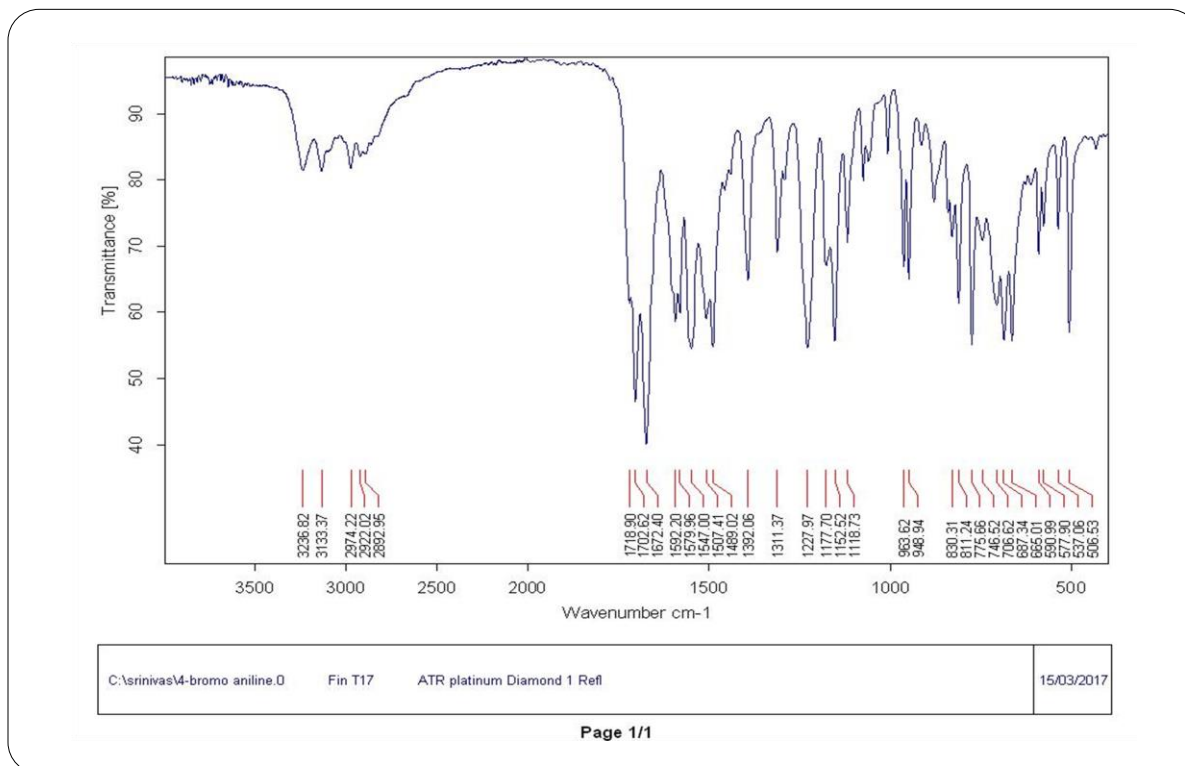
¹H NMR Spectrum of Compound 9e

**¹³C NMR Spectrum of Compound 9e****IR Spectrum of Compound 9f**

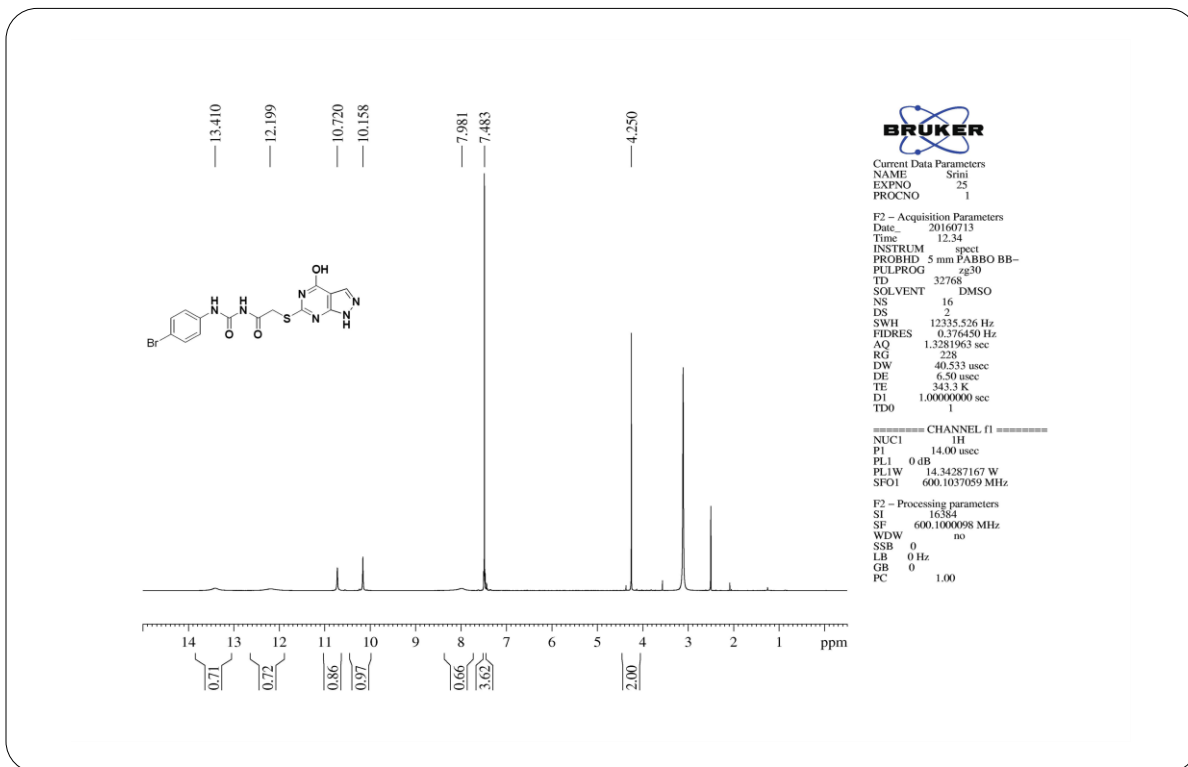
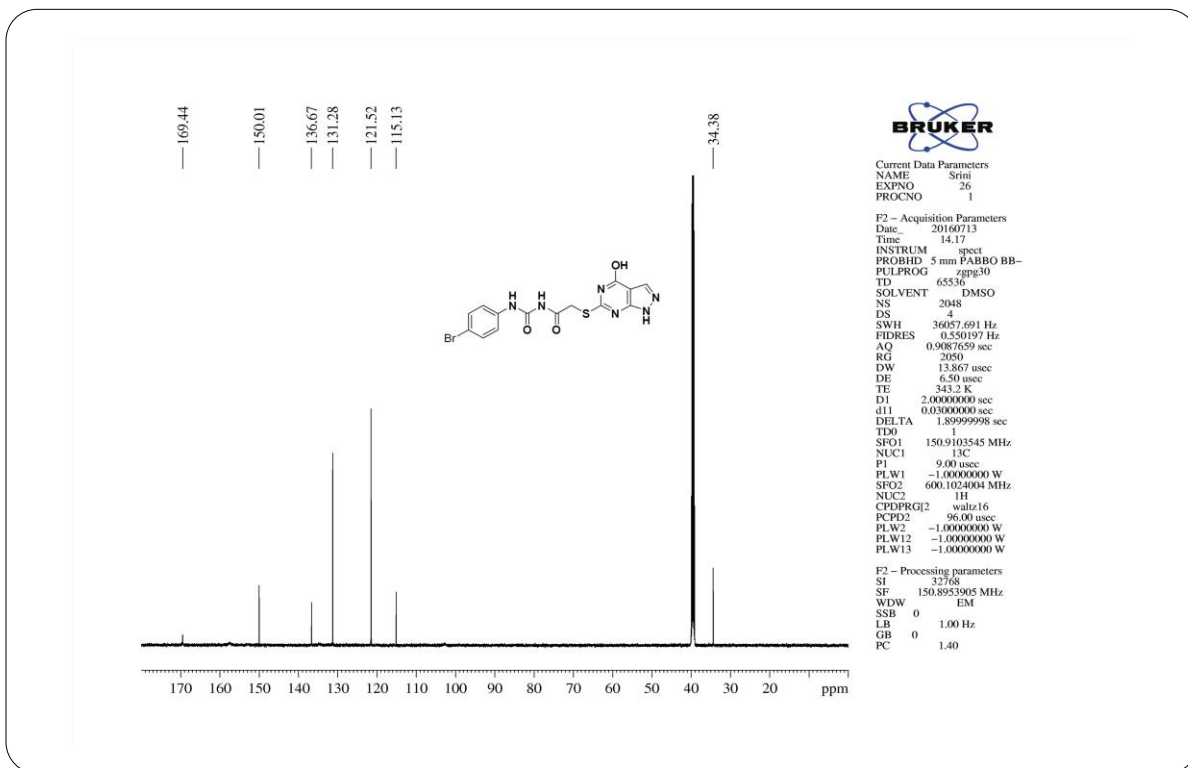
¹H NMR Spectrum of Compound 9f¹³C NMR Spectrum of Compound 9f

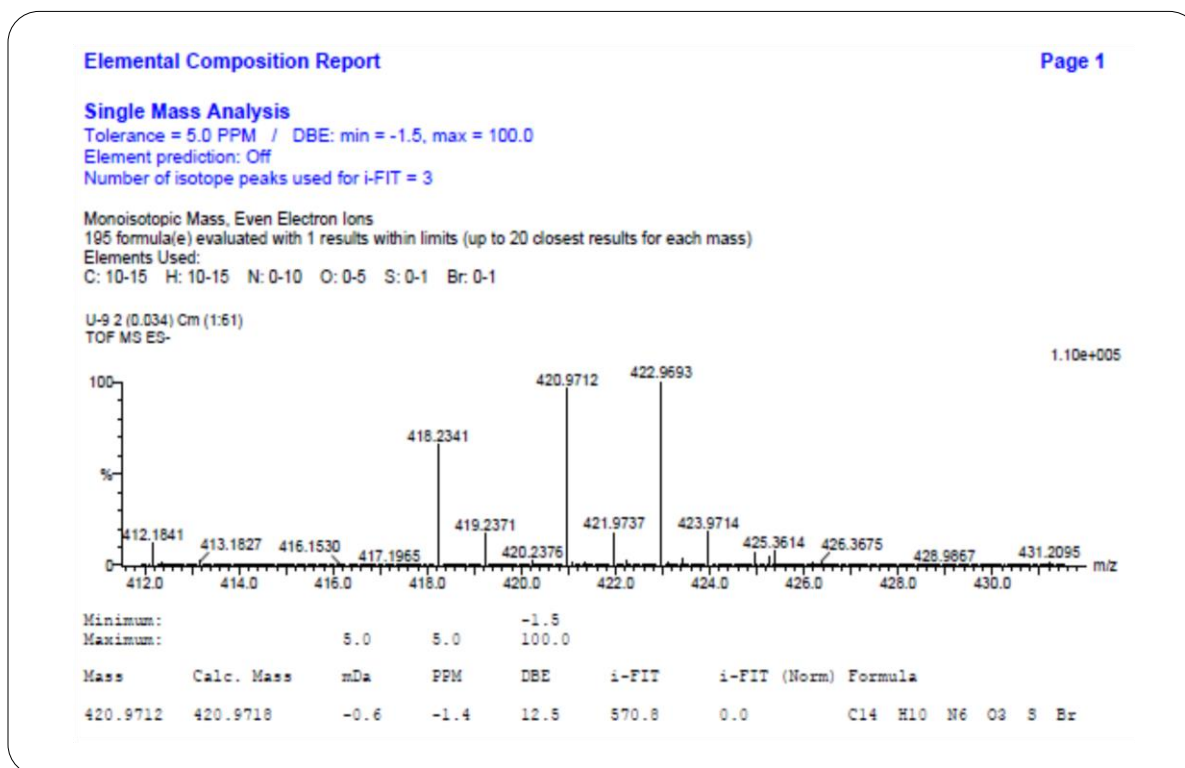


HRMS Spectrum of Compound 9f

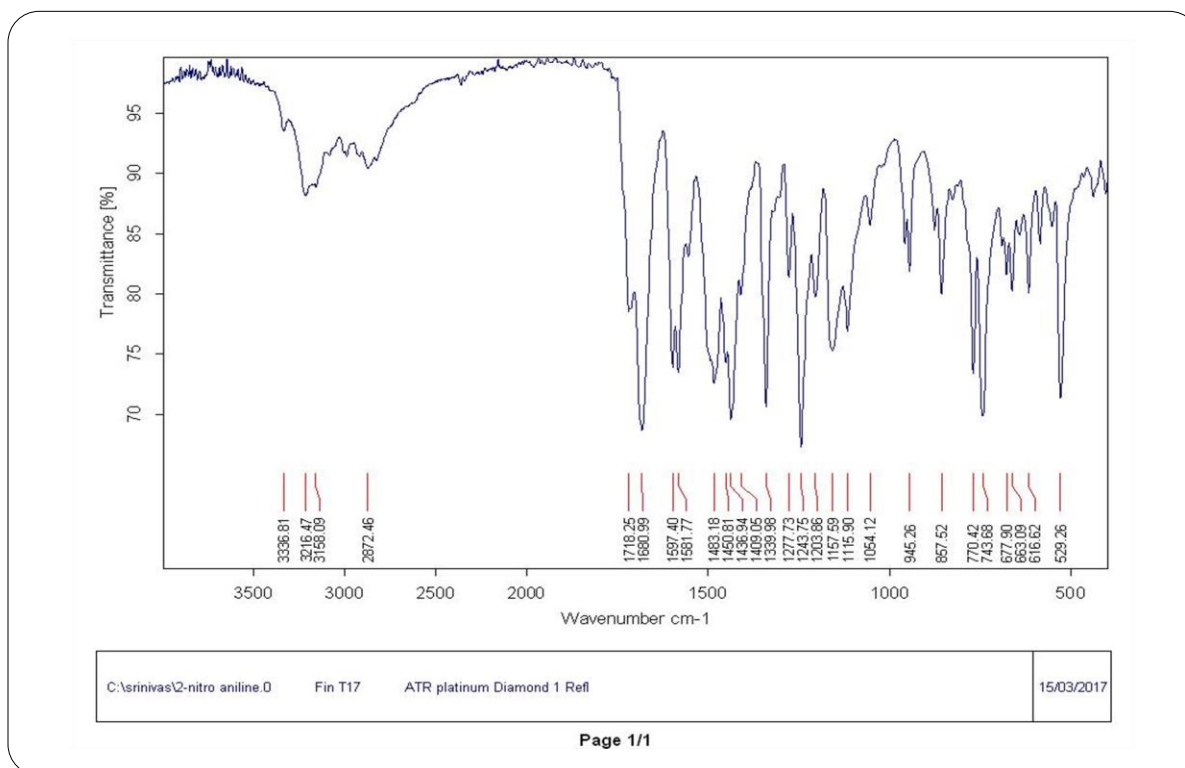


IR Spectrum of Compound 9g

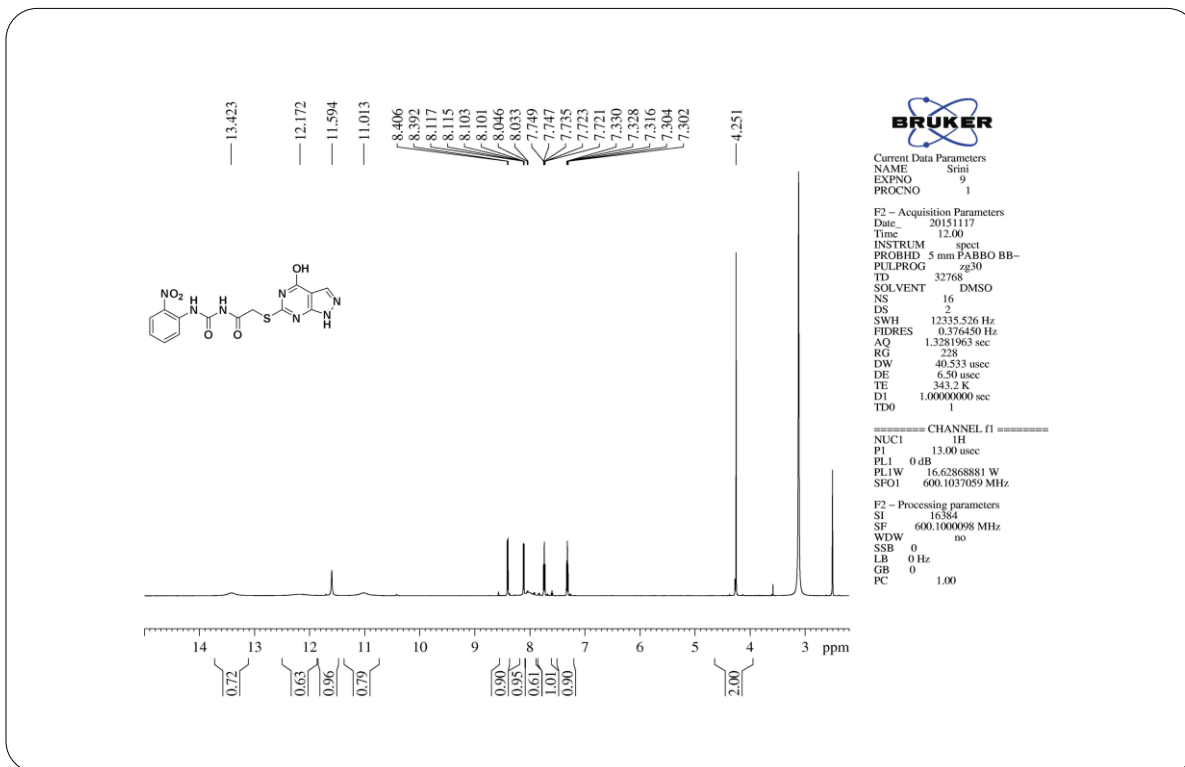
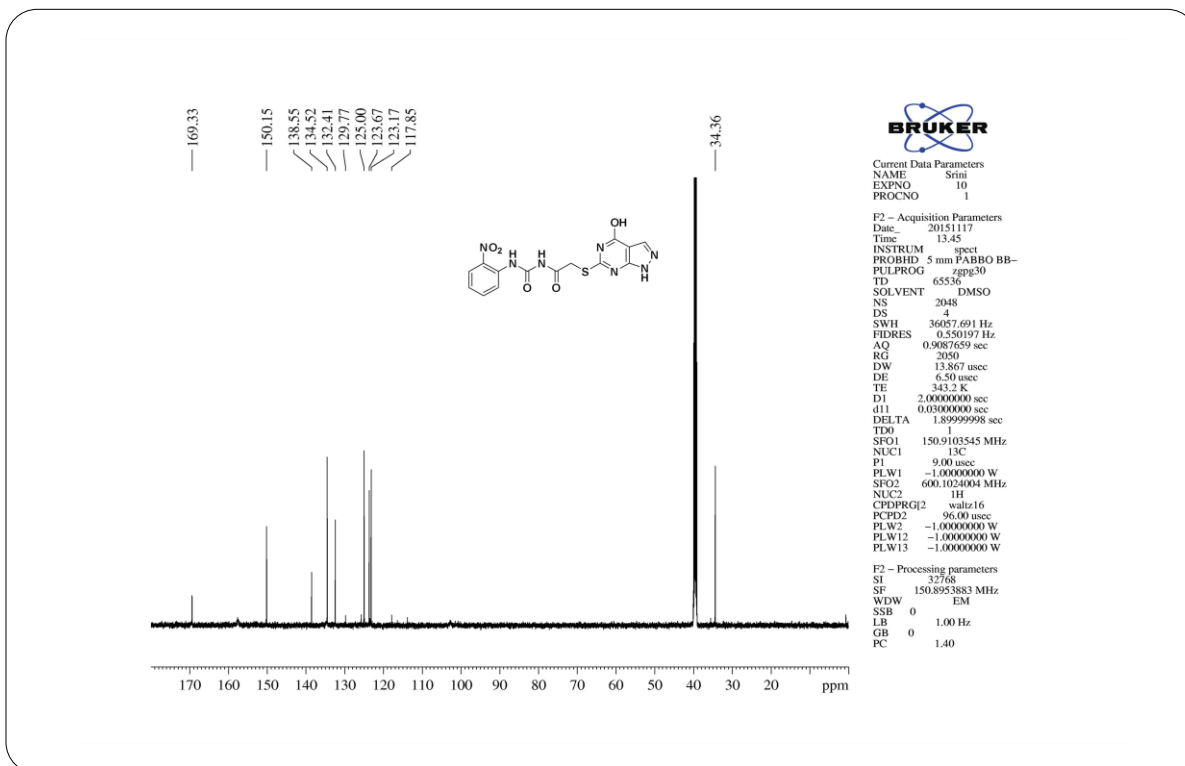
**¹H NMR Spectrum of Compound 9g****¹³C NMR Spectrum of Compound 9g**



HRMS Spectrum of Compound 9g



IR Spectrum of Compound 9h

**¹H NMR Spectrum of Compound 9h****¹³C NMR Spectrum of Compound 9h**

Elemental Composition Report

Page 1

Single Mass Analysis

Tolerance = 5.0 PPM / DBE: min = -1.5, max = 100.0

Element prediction: Off

Number of isotope peaks used for i-FIT = 3

Monoisotopic Mass, Even Electron Ions

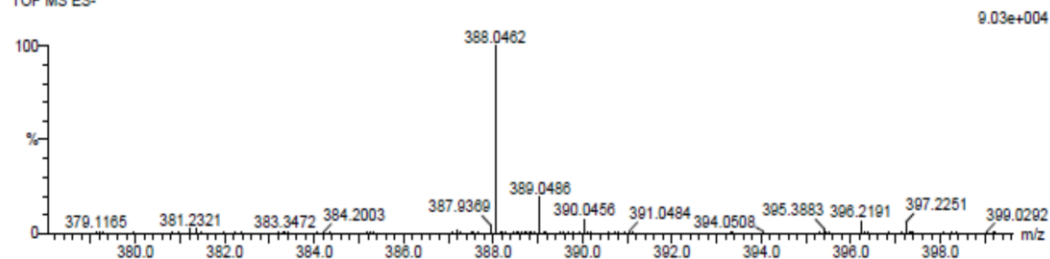
99 formula(e) evaluated with 1 results within limits (up to 20 closest results for each mass)

Elements Used:

C: 10-15 H: 10-15 N: 0-10 O: 0-5 S: 0-1

U-1.61 (2.024) Cm (1.61)

TOF MS ES-

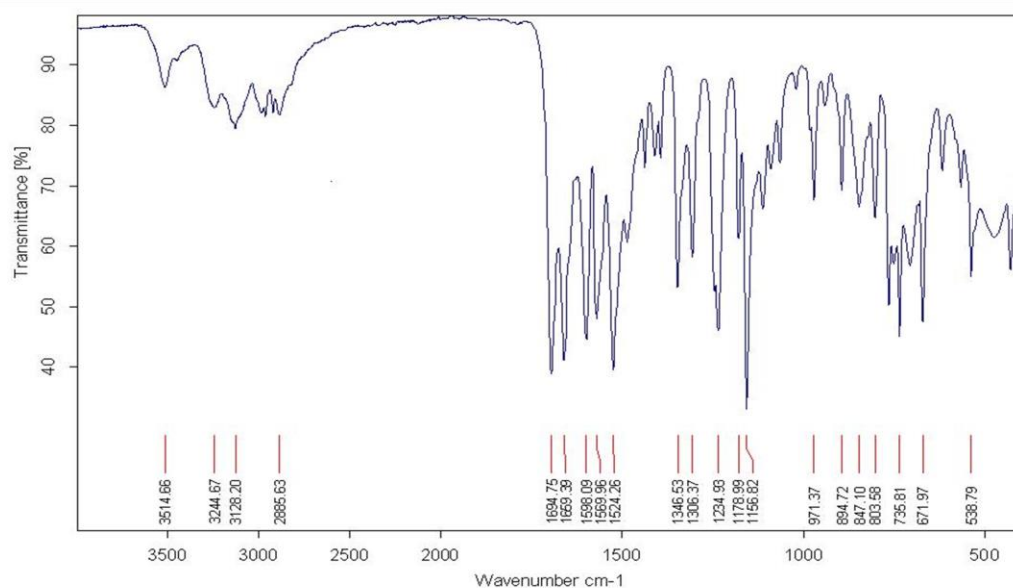


Minimum:

Maximum: 5.0 5.0 -1.5 100.0

Mass	Calc. Mass	mDa	PPM	DBE	i-FIT	i-FIT (Norm)	Formula
388.0462	388.0464	-0.2	-0.5	19.5	527.1	0.0	C14 H10 N7 O5 S

HRMS Spectrum of Compound 9h

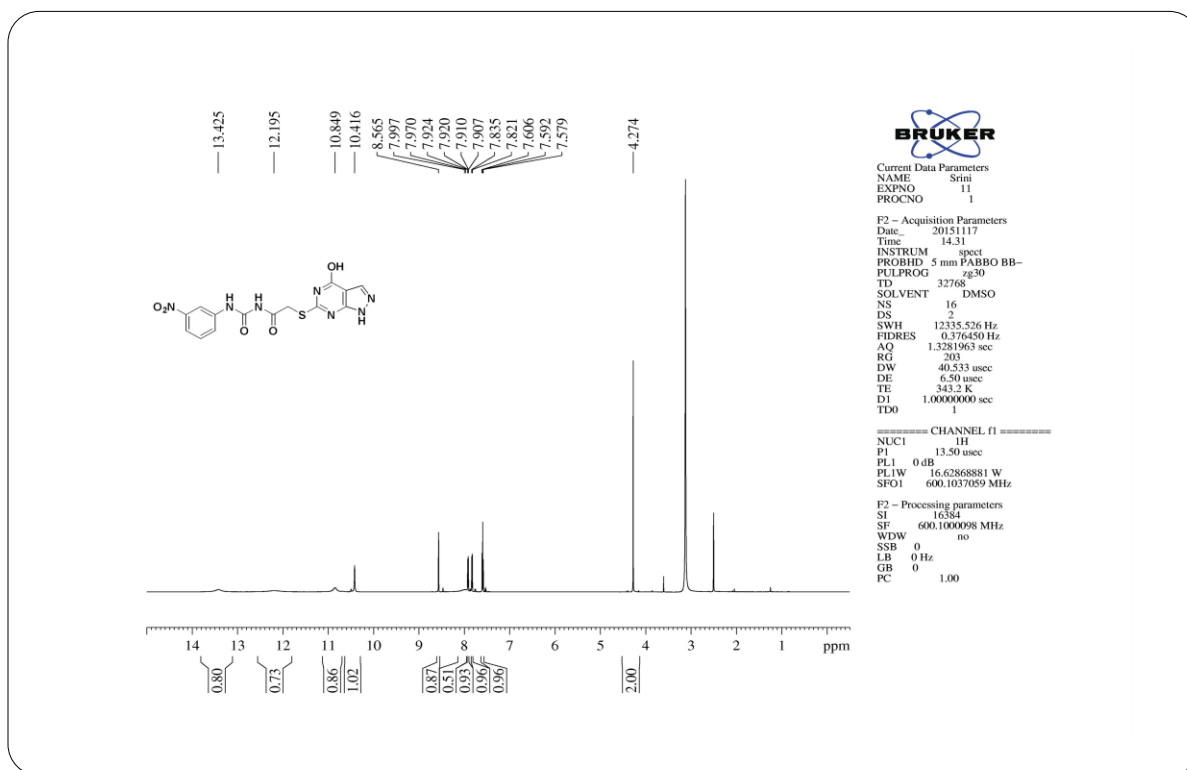
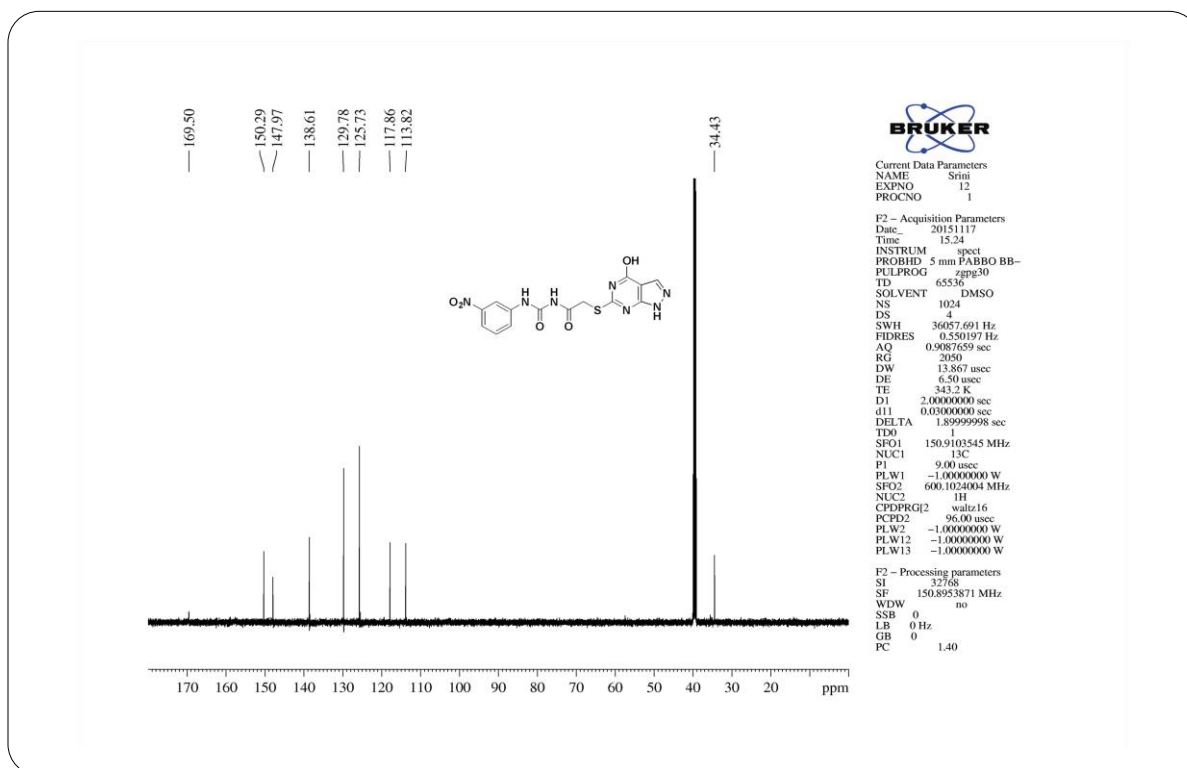


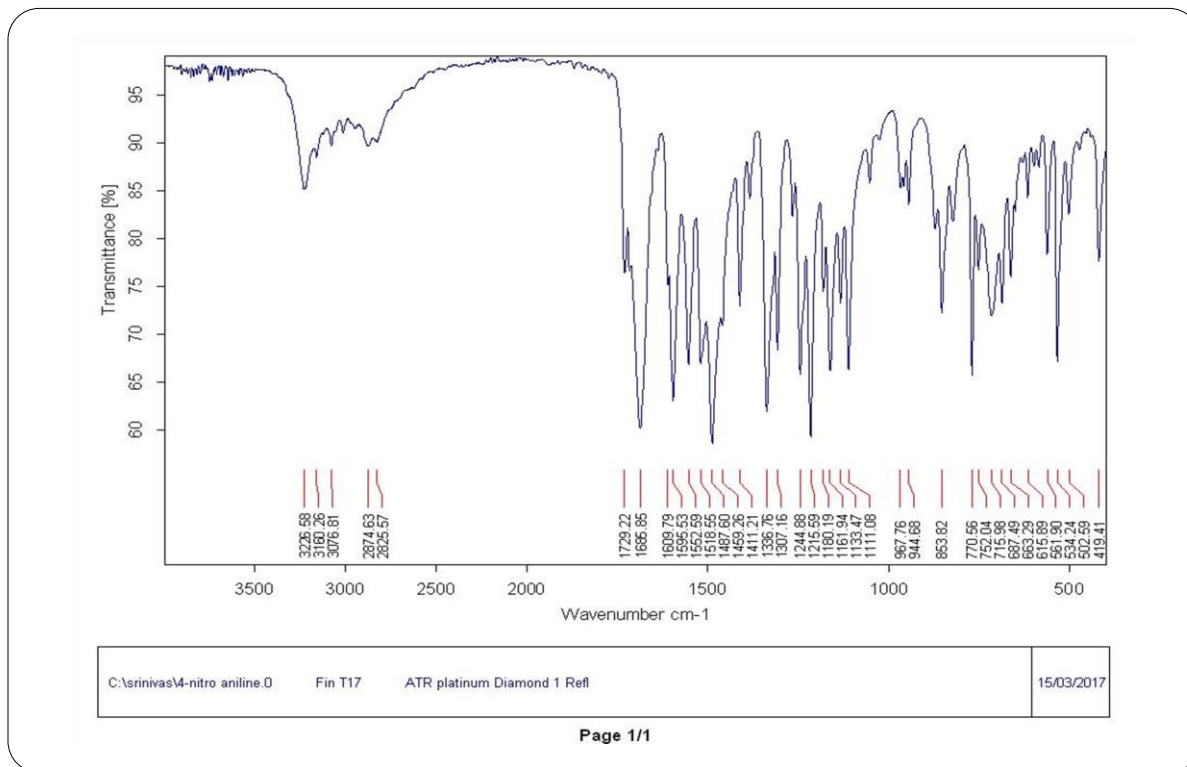
1,3-NITRO ANILINE.D Fin T17 ATR platinum Diamond 1 Refl

10/03/2017

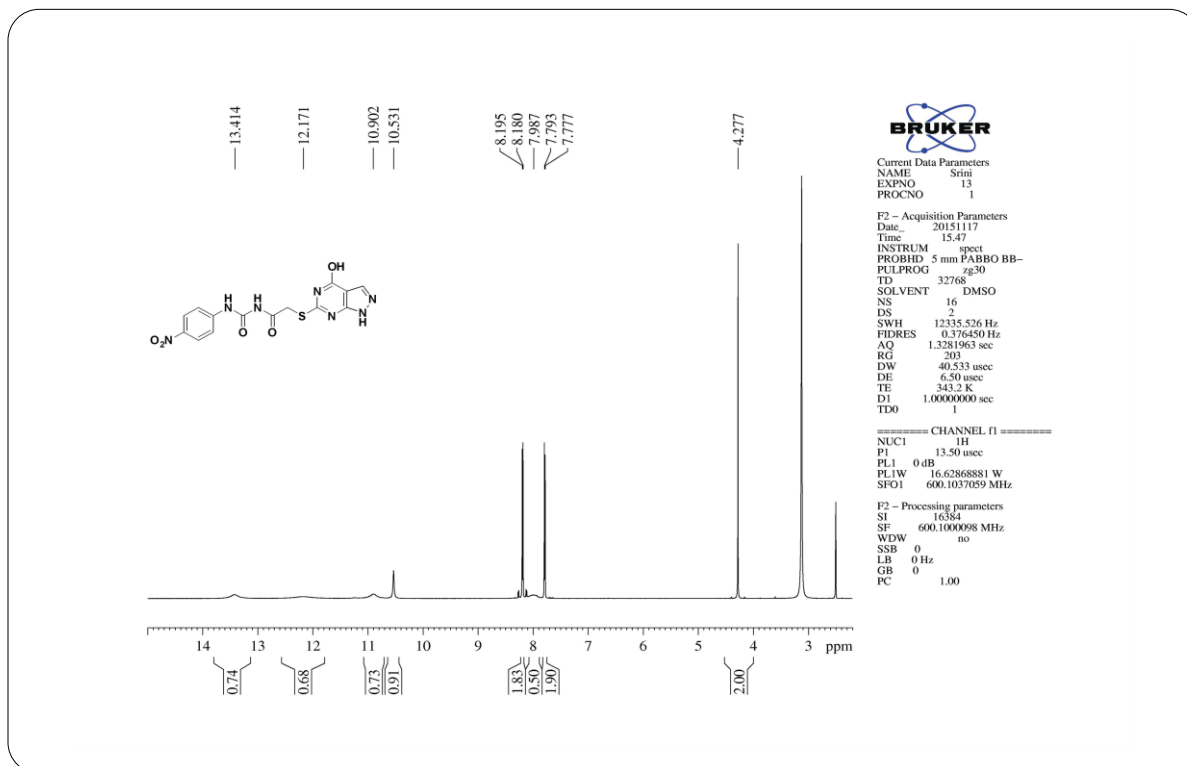
Page 1/1

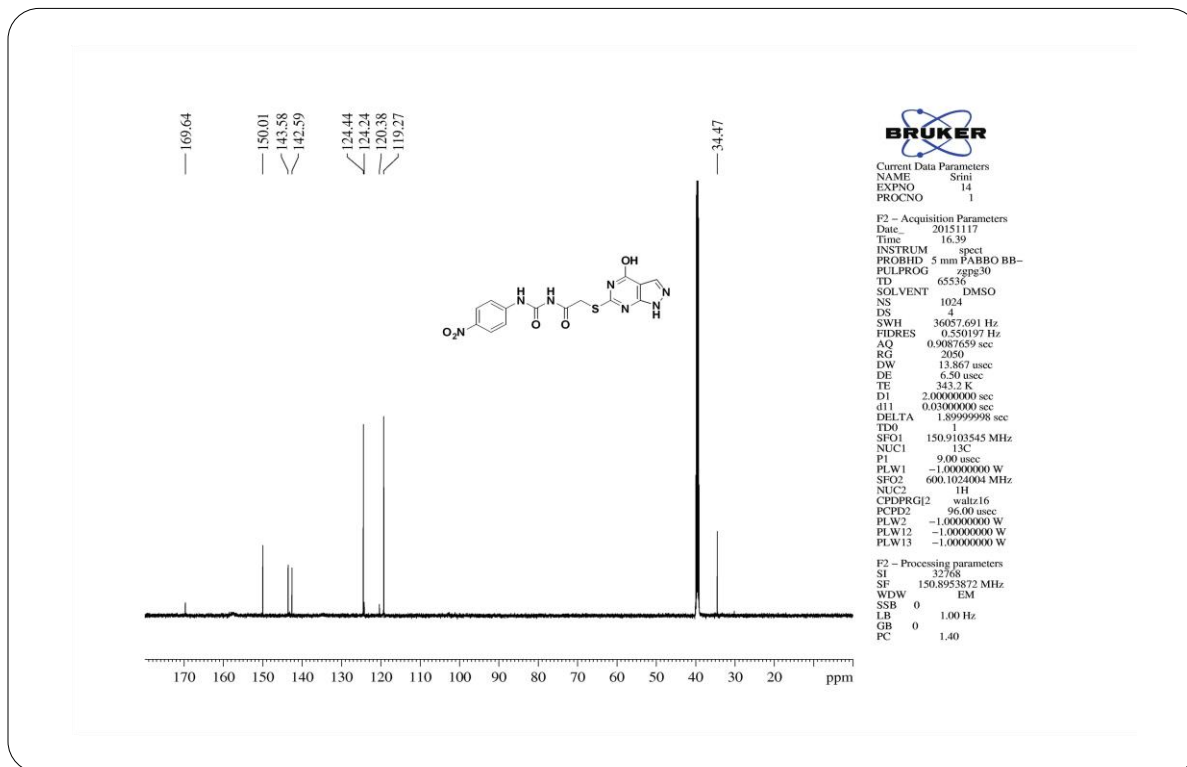
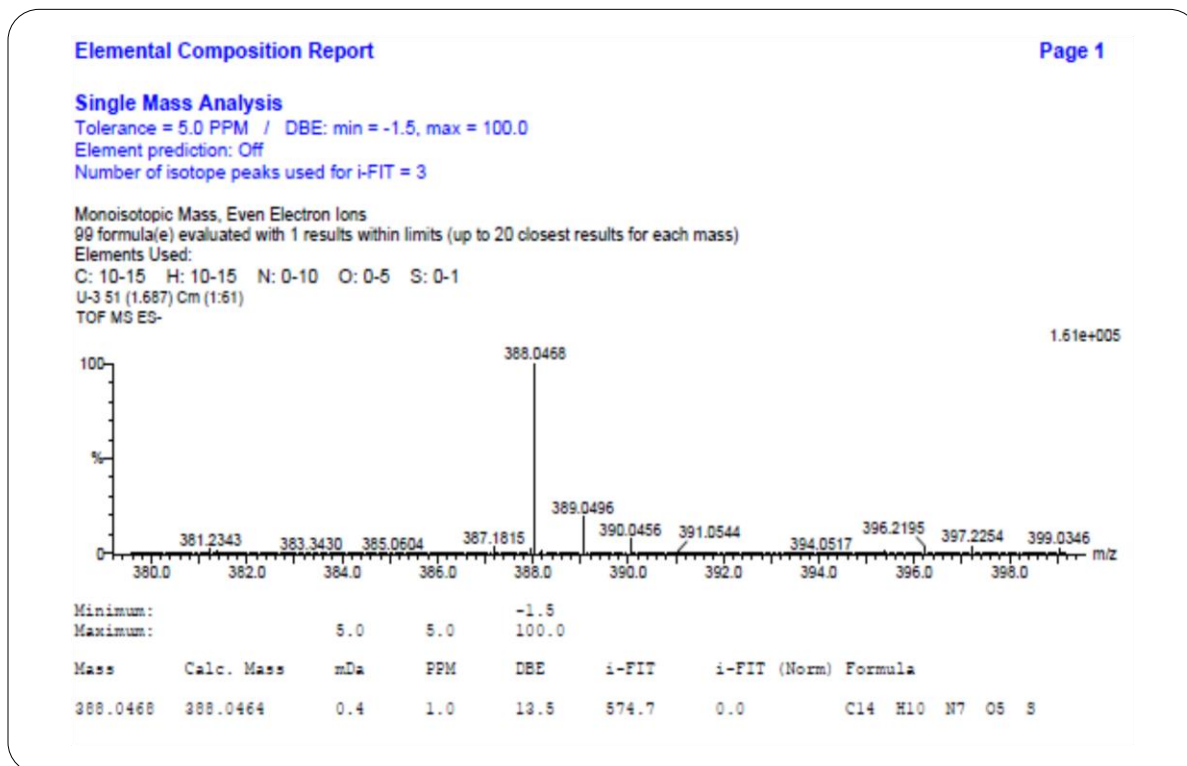
IR Spectrum of Compound 9i

**¹H NMR Spectrum of Compound 9i****¹³C NMR Spectrum of Compound 9i**

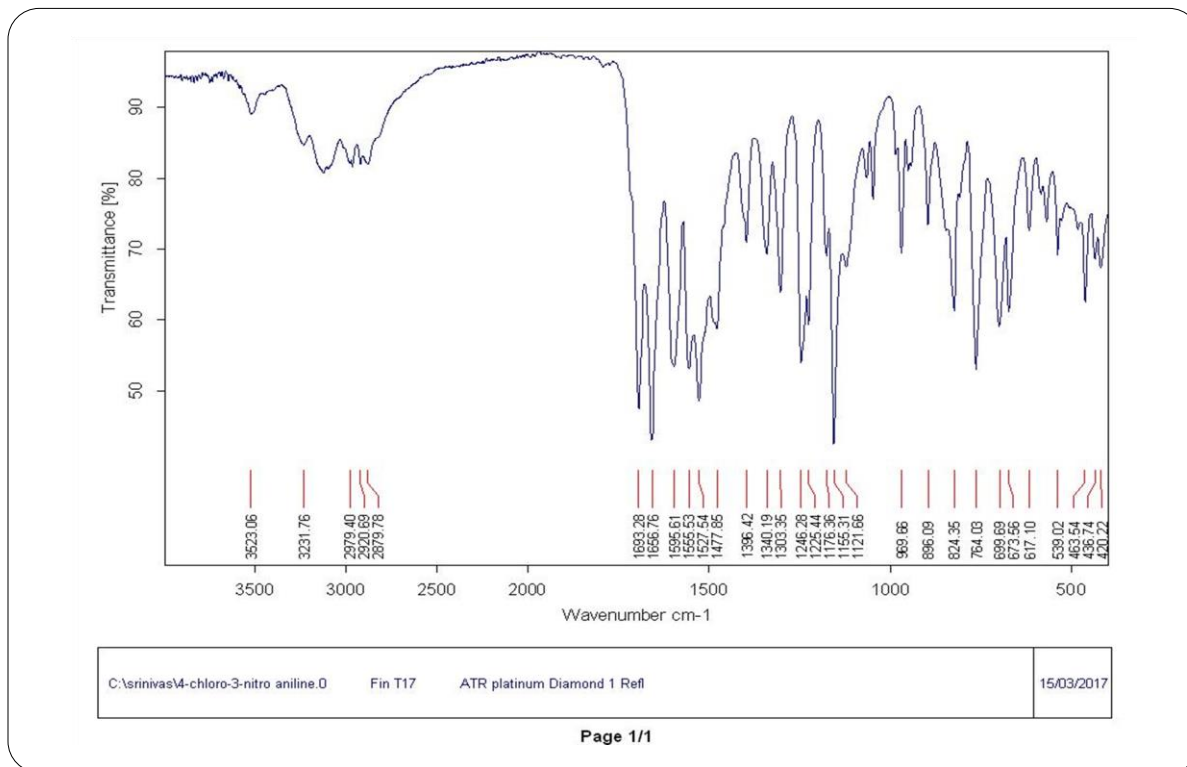


IR Spectrum of Compound 9j

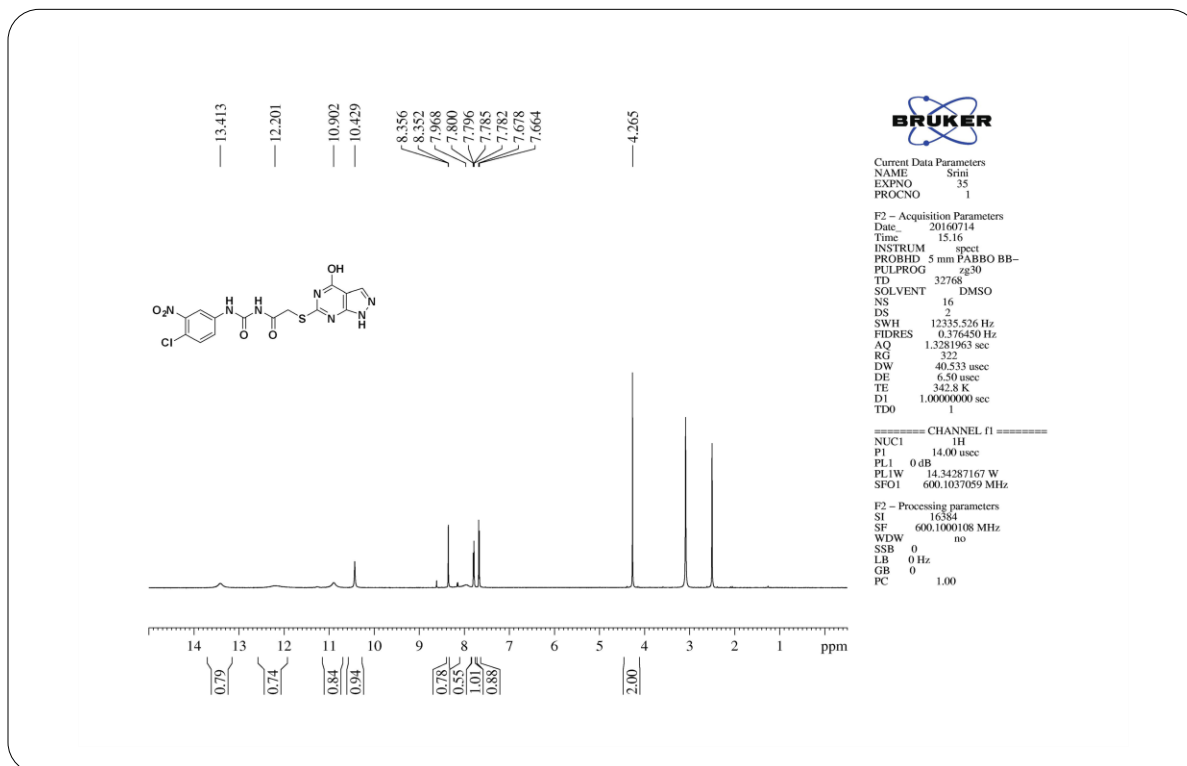
¹H NMR Spectrum of Compound 9j

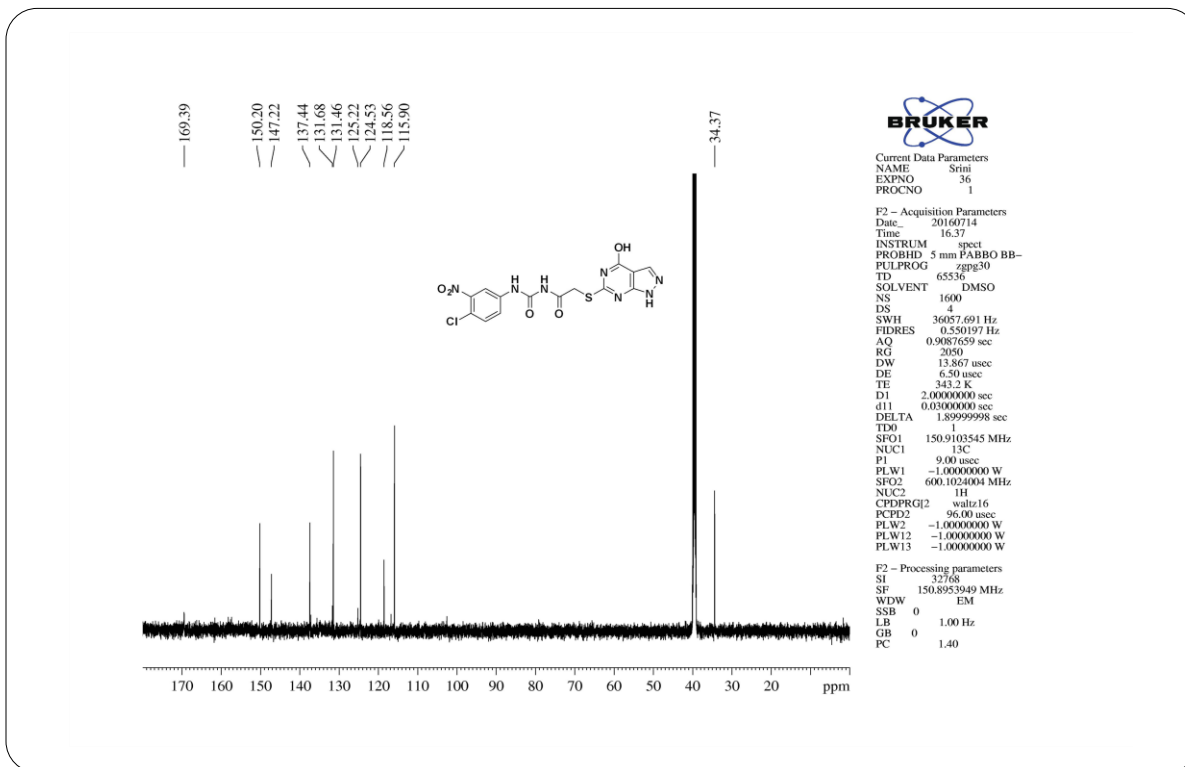
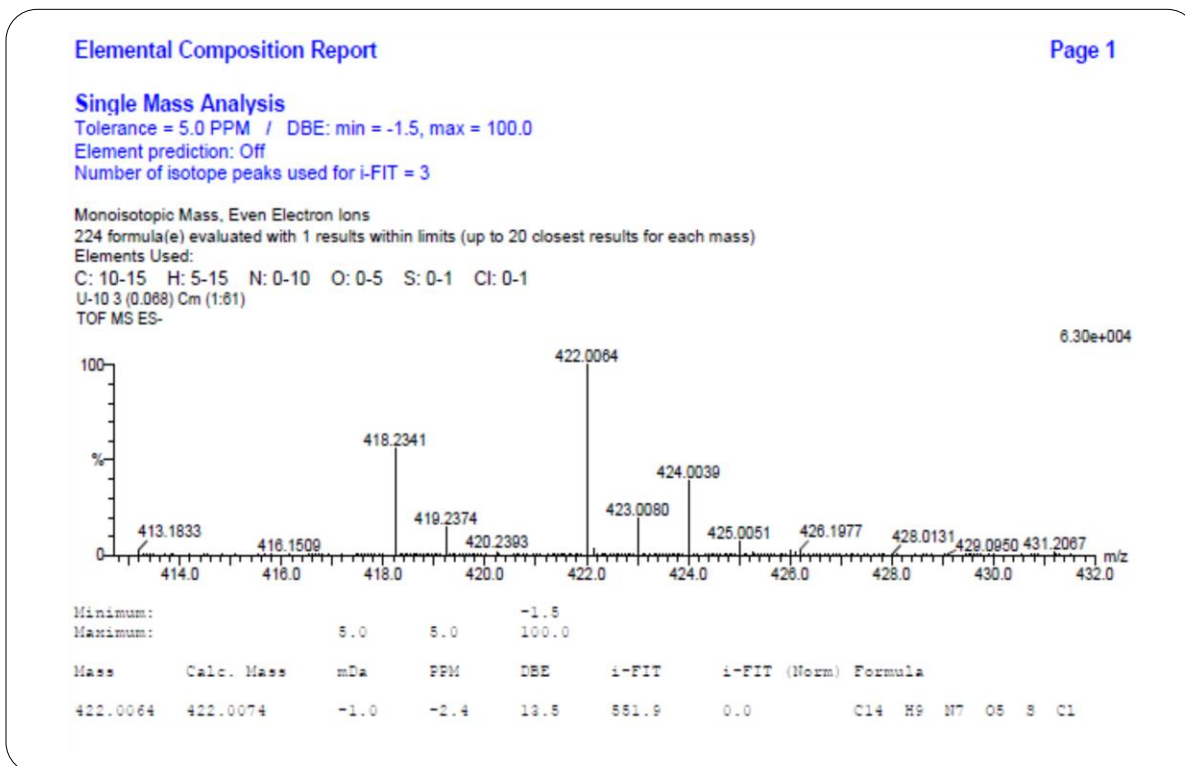
¹³C NMR Spectrum of Compound 9j

HRMS Spectrum of Compound 9j

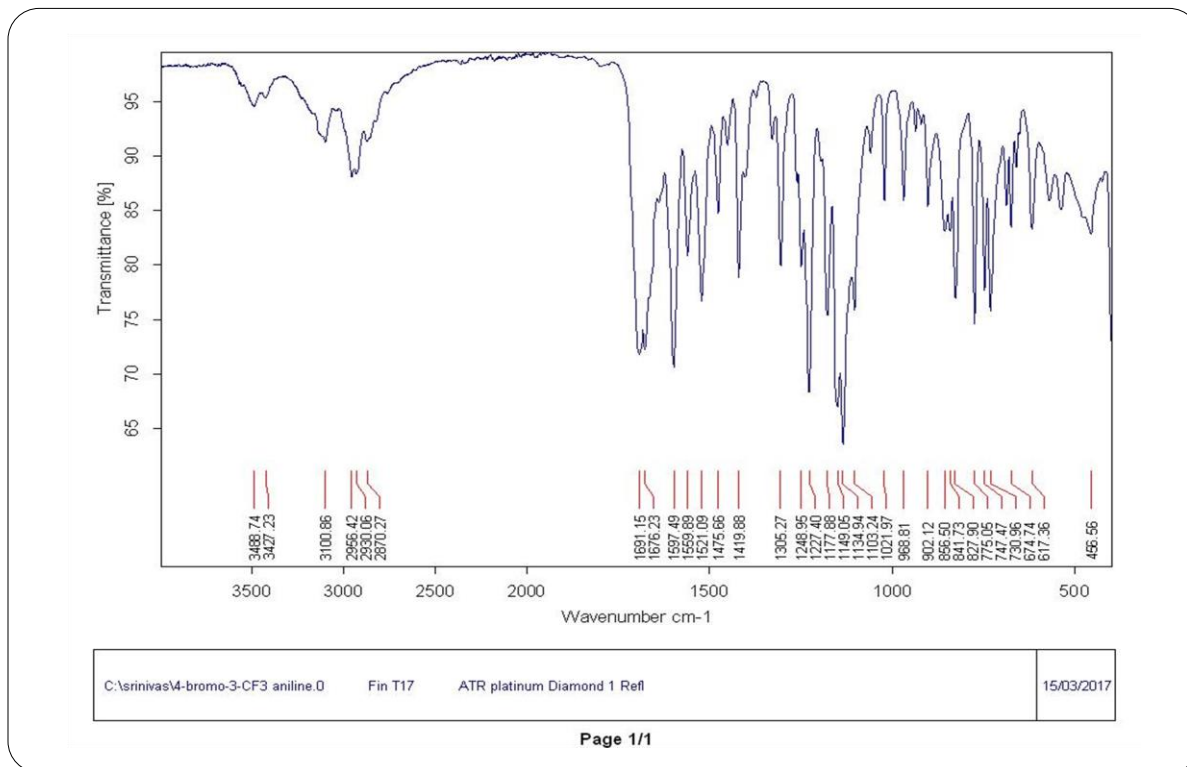


IR Spectrum of Compound 9k

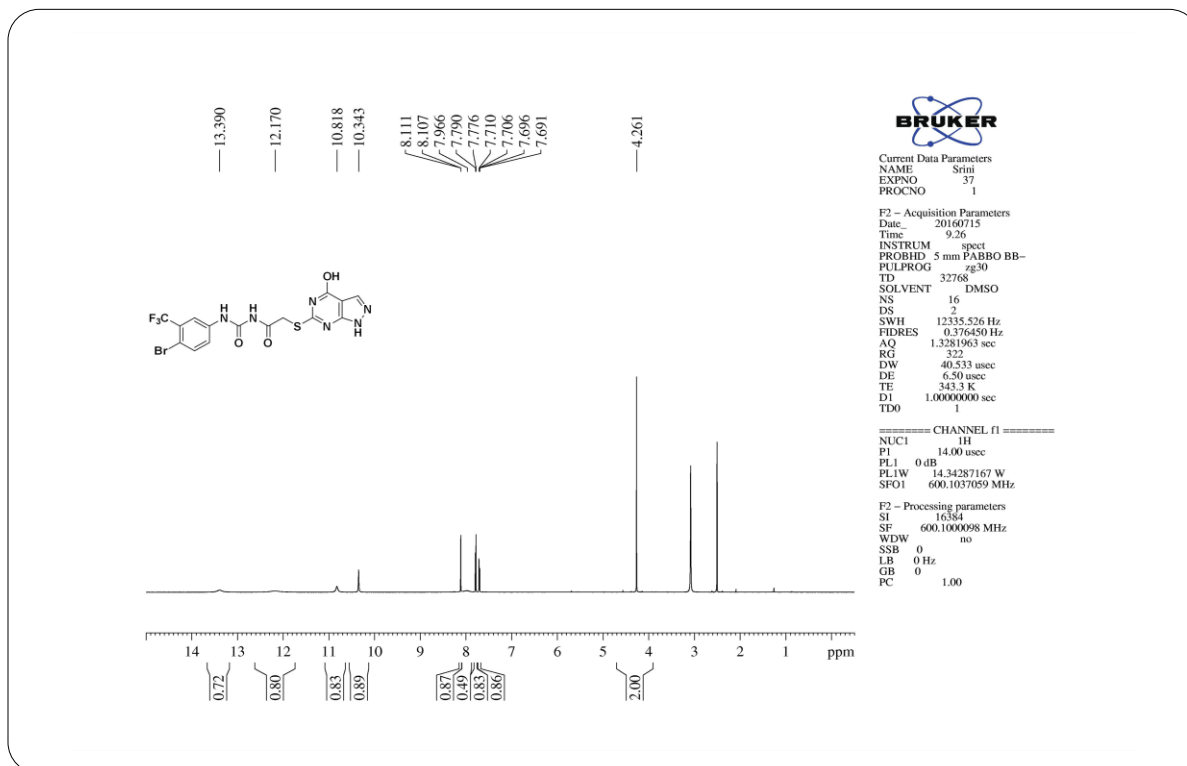
¹H NMR Spectrum of Compound 9k

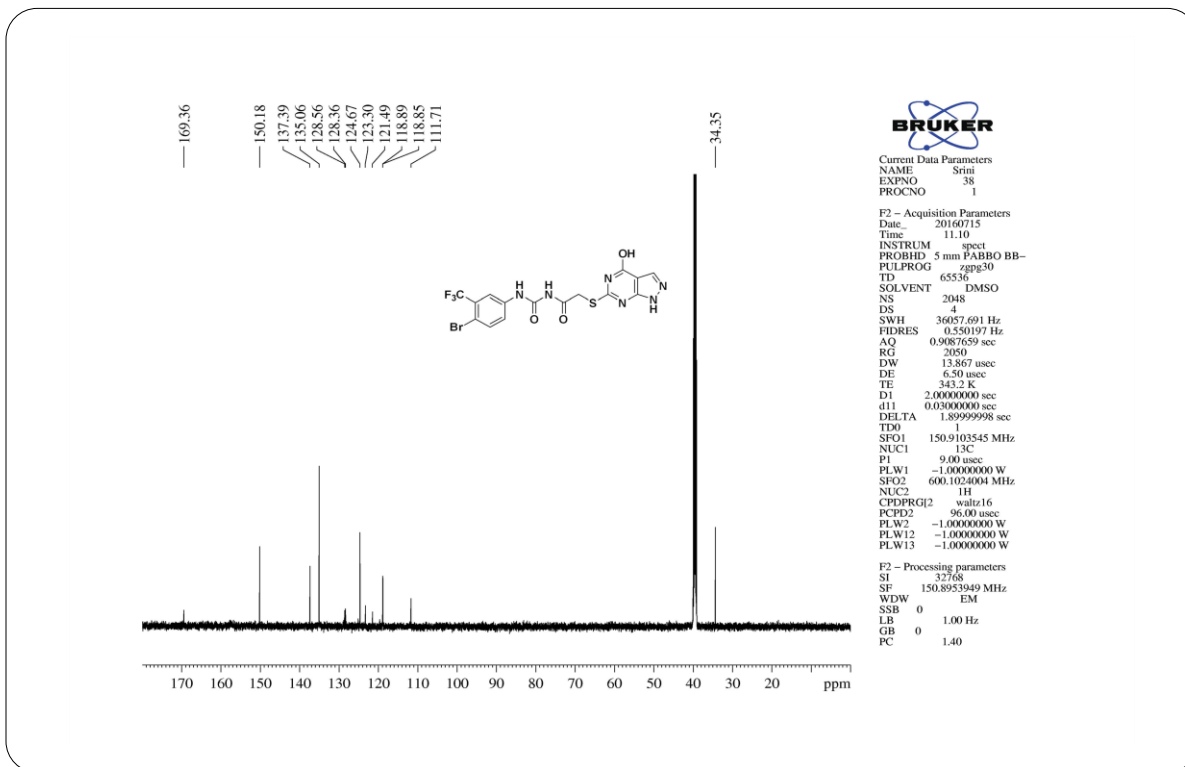
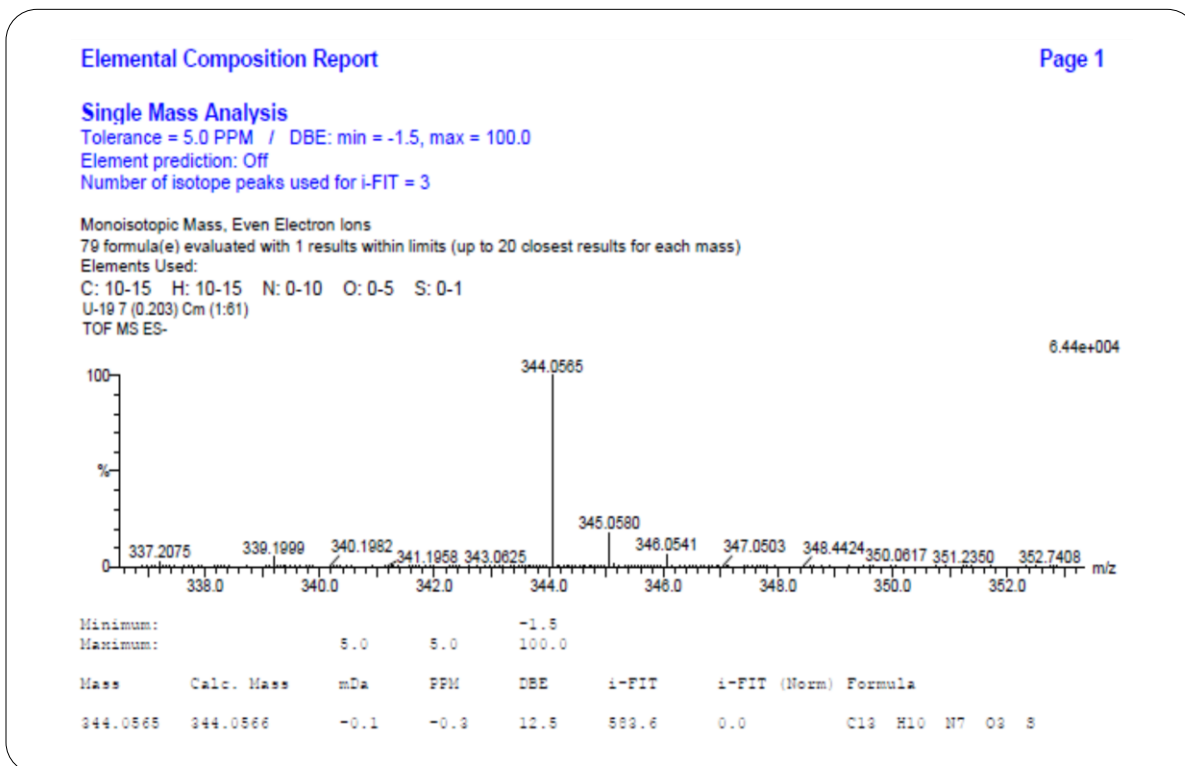
¹³C NMR Spectrum of Compound 9k

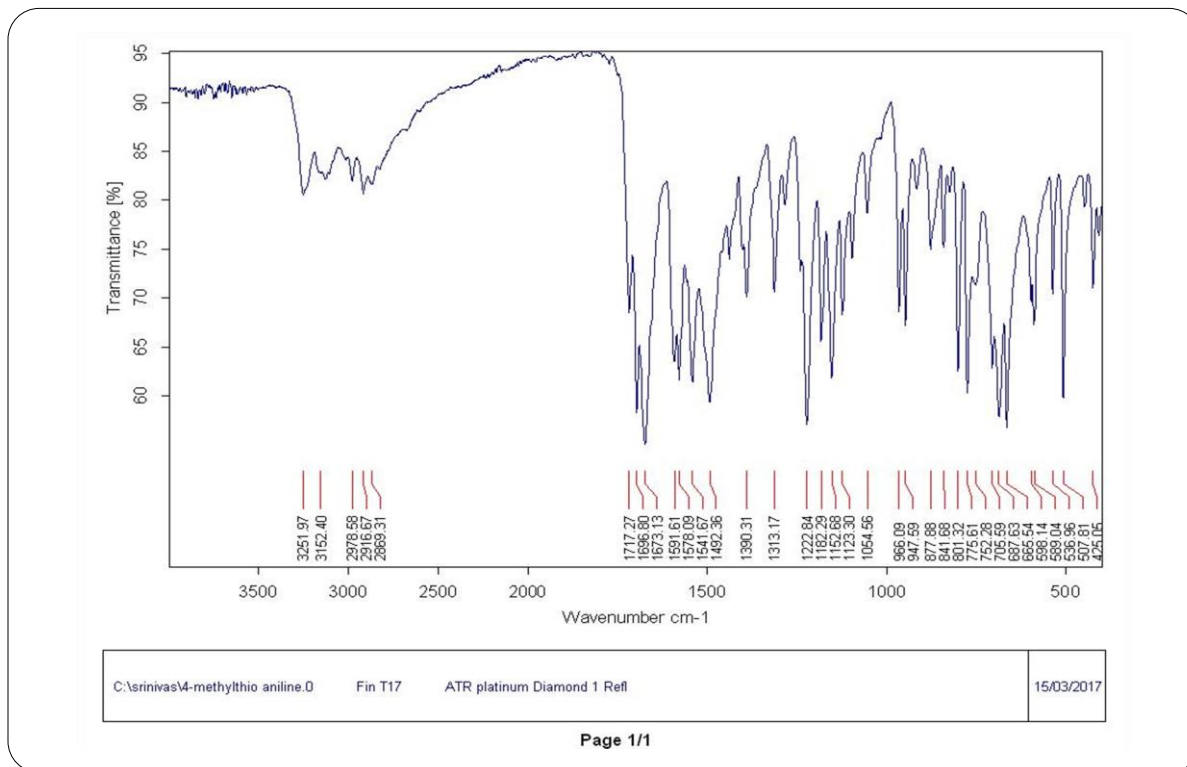
HRMS Spectrum of Compound 9k



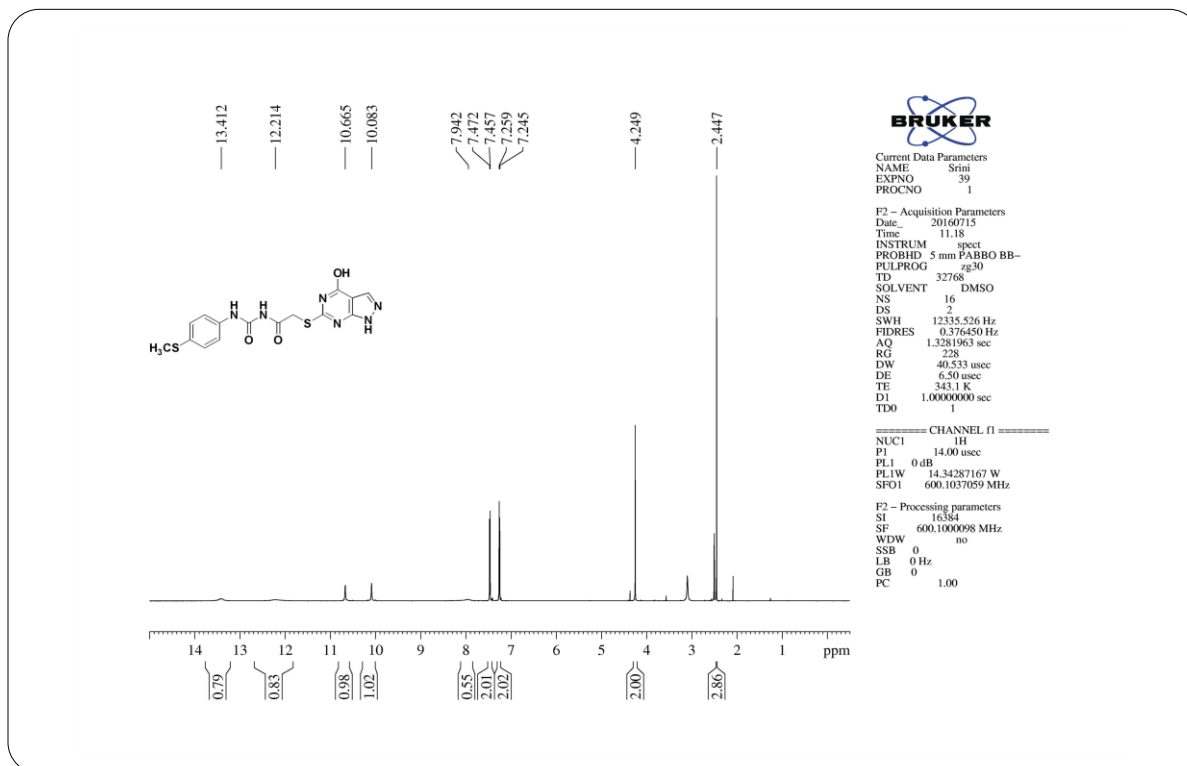
IR Spectrum of Compound 9l

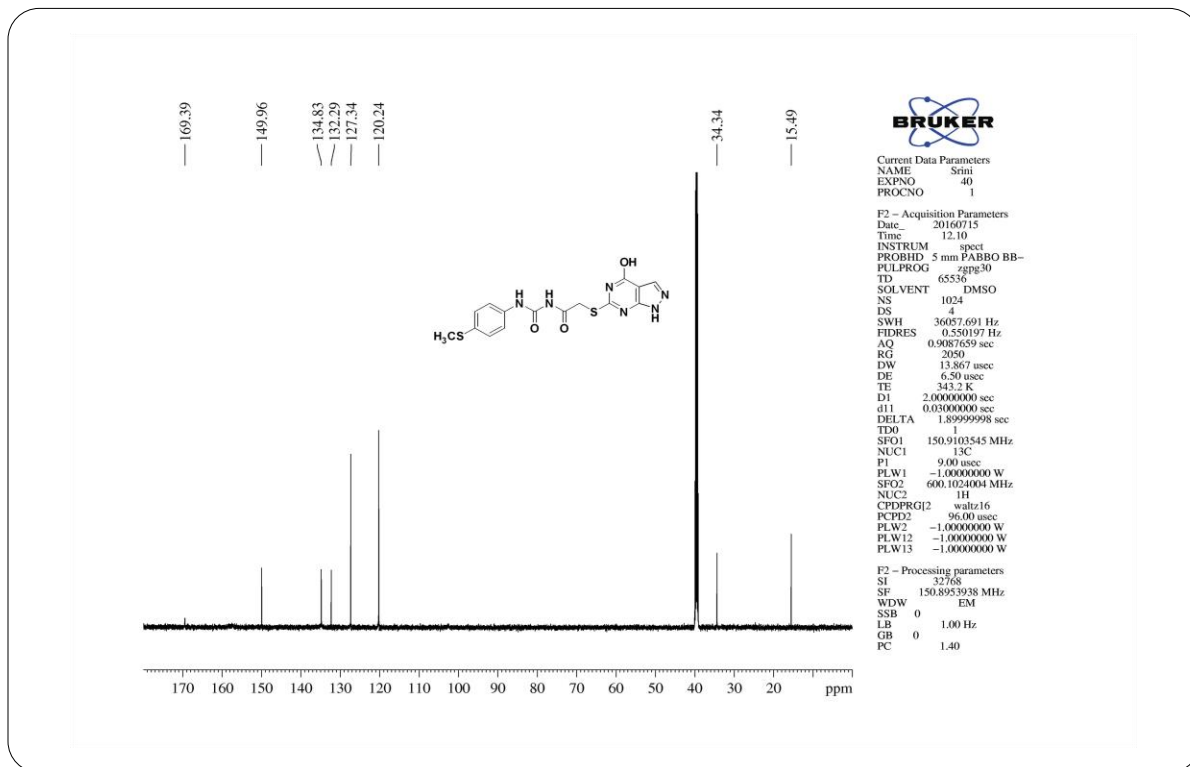
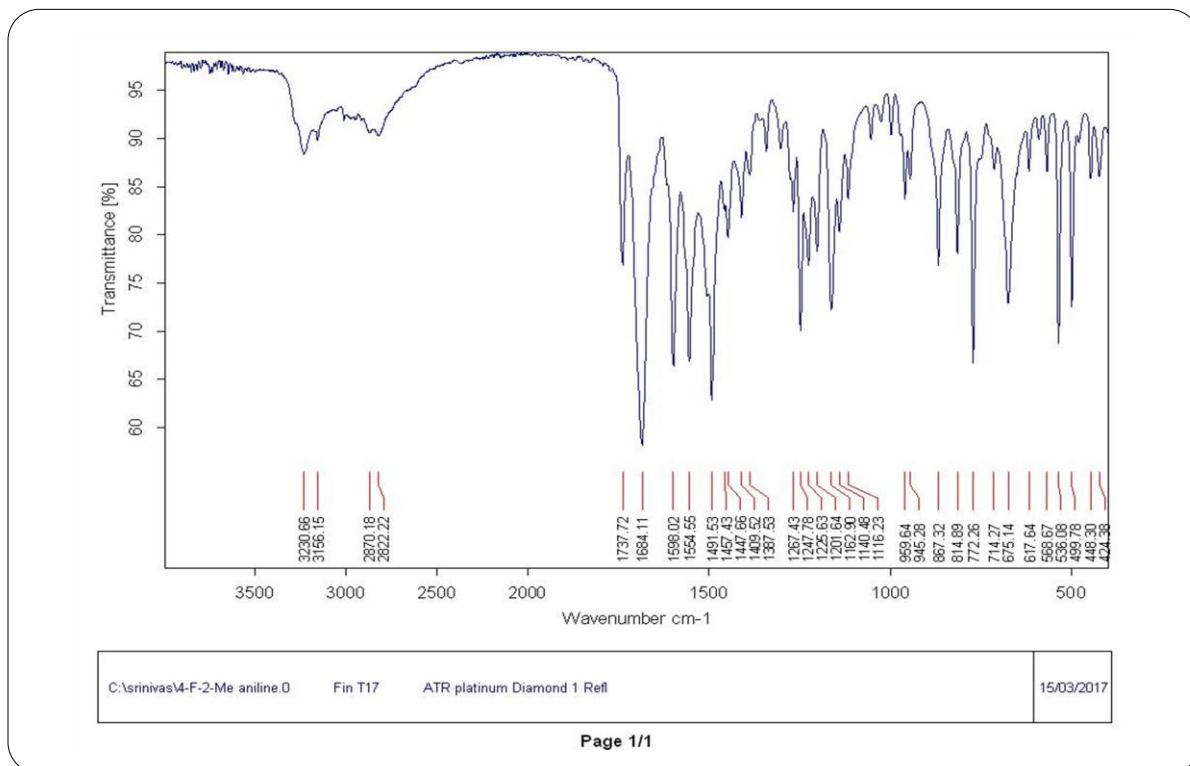
¹H NMR Spectrum of Compound 9l

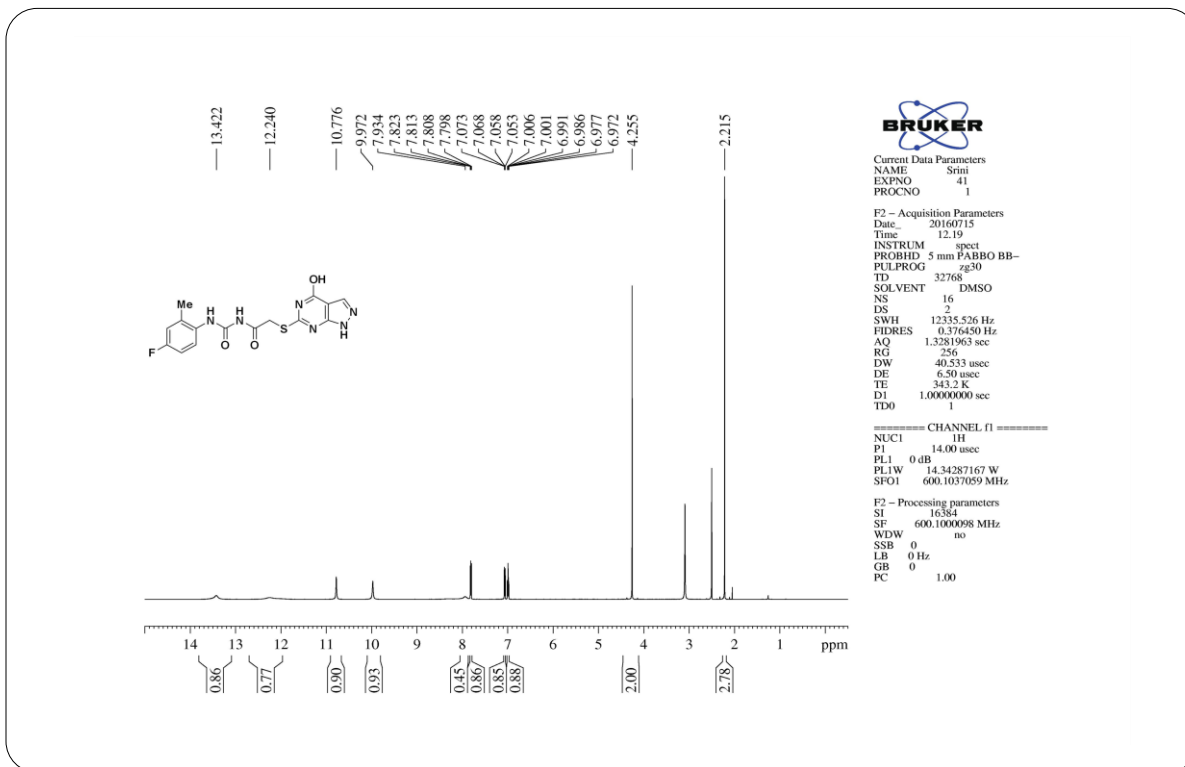
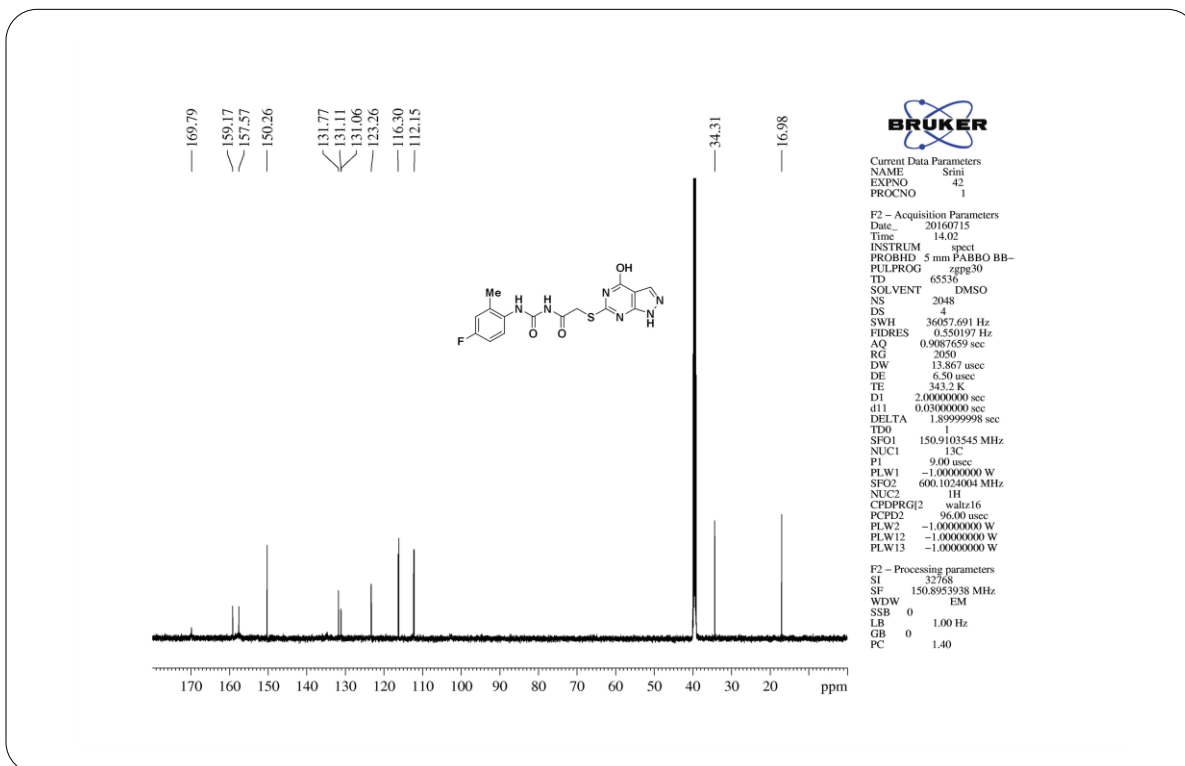
**¹³C NMR Spectrum of Compound 9l****HRMS Spectrum of Compound 9l**



IR Spectrum of Compound 9m

¹H NMR Spectrum of Compound 9m

**¹³C NMR Spectrum of Compound 9m****IR Spectrum of Compound 9n**

**¹H NMR Spectrum of Compound 9n****¹³C NMR Spectrum of Compound 9n**

Elemental Composition Report

Page 1

Single Mass Analysis

Tolerance = 5.0 PPM / DBE: min = -1.5, max = 100.0

Element prediction: Off

Number of isotope peaks used for i-FIT = 3

Monoisotopic Mass, Even Electron Ions

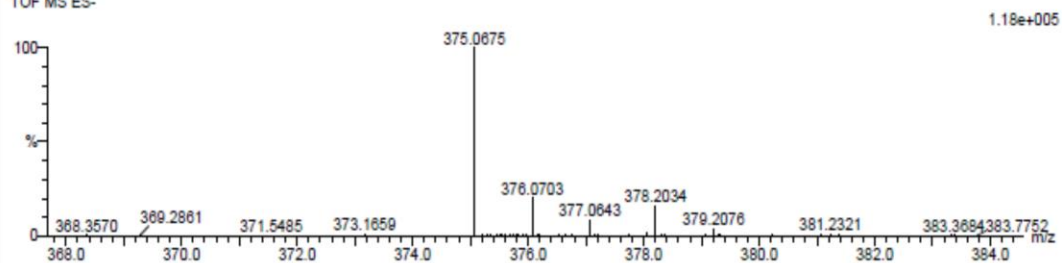
180 formula(e) evaluated with 1 results within limits (up to 20 closest results for each mass)

Elements Used:

C: 10-15 H: 10-15 N: 0-10 O: 0-5 F: 0-1 S: 0-1

U-12.48 (1.588) Cm (1.81)

TOF MS ES-

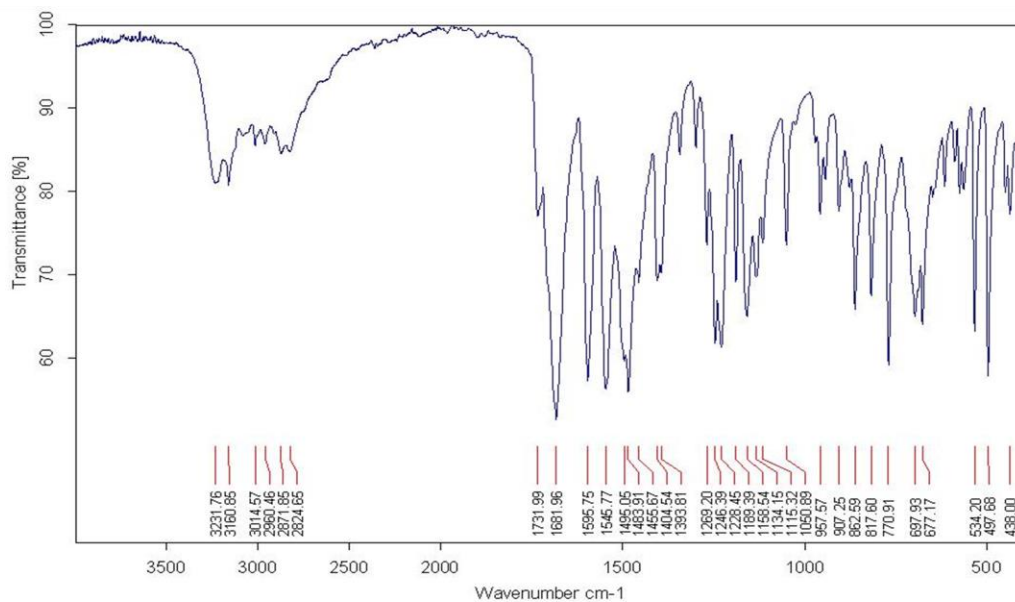


Minimum:

Maximum: 5.0 5.0 -1.5 100.0

Mass	Calc. Mass	mDa	PPM	DBE	i-FIT	i-FIT (Norm)	Formula
375.0675	375.0676	-0.1	-0.3	12.5	590.6	0.0	C15 H12 N6 O3 F 8

HRMS Spectrum of Compound 9n

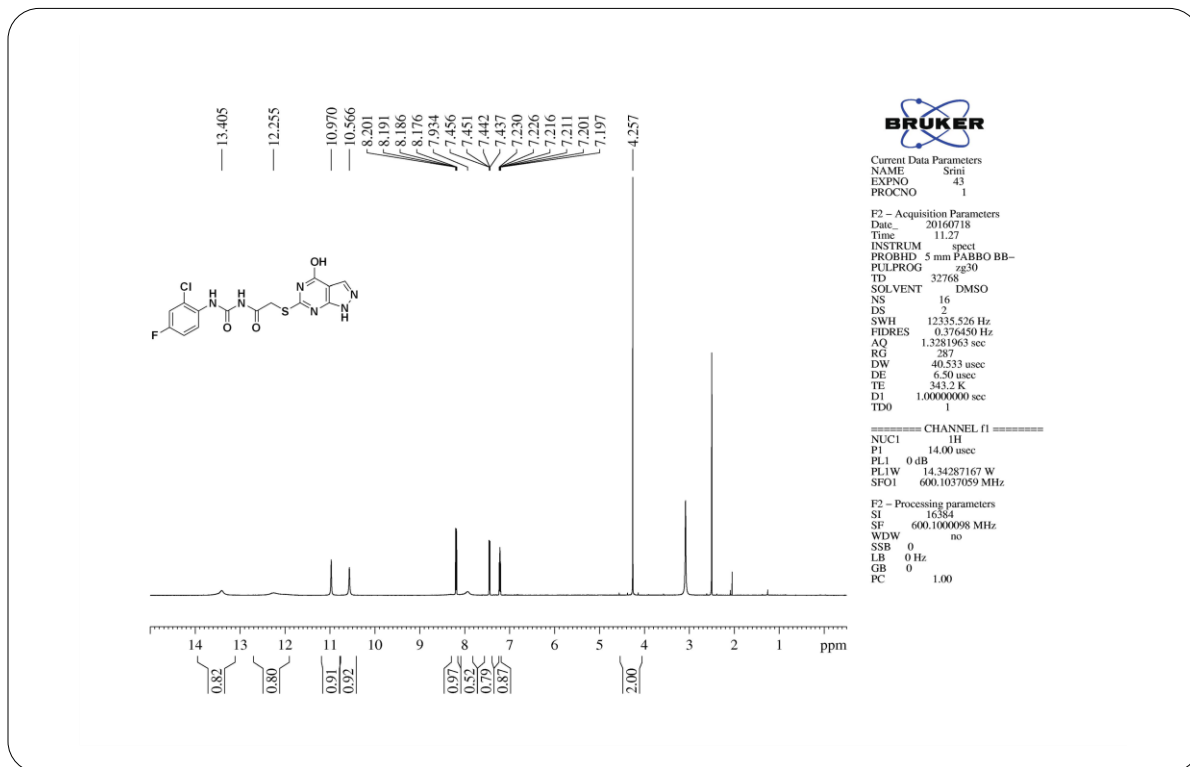
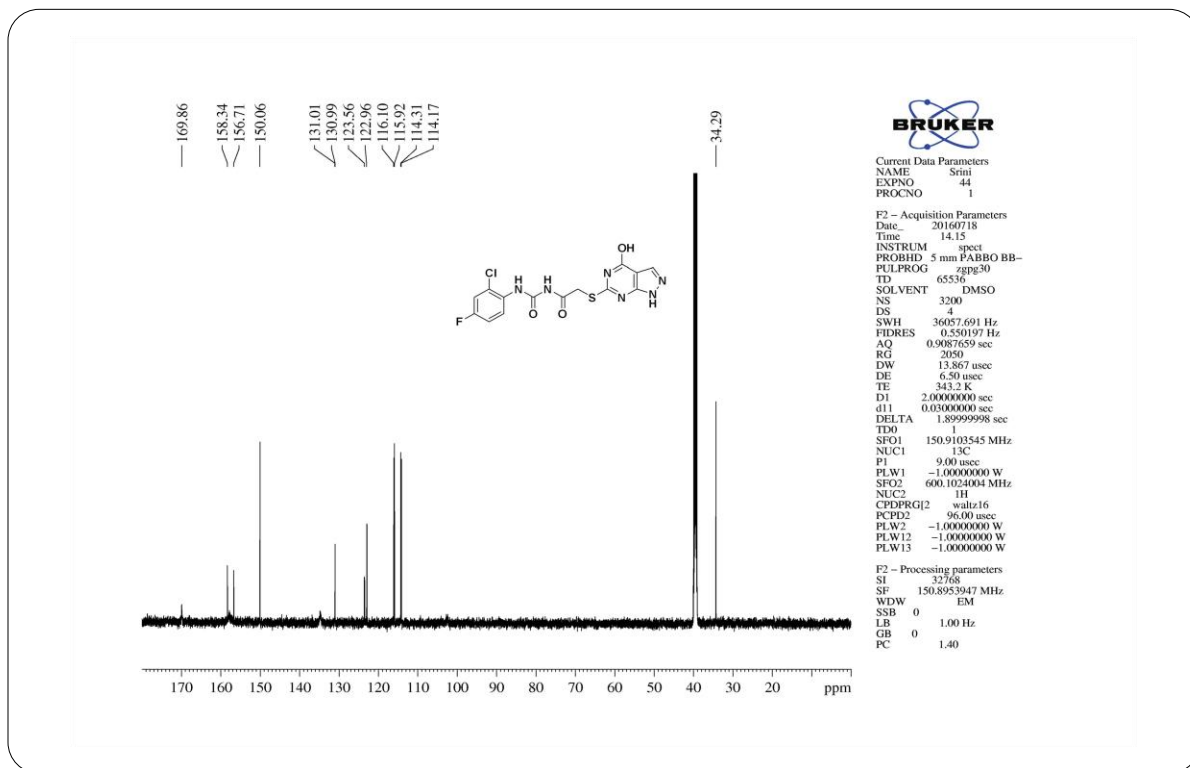


C:\srinivas\2-chloro-4-fluoro aniline.D Fin T17 ATR platinum Diamond 1 Refl

15/03/2017

Page 1/1

IR Spectrum of Compound 9o

**¹H NMR Spectrum of Compound 9o****¹³C NMR Spectrum of Compound 9o**

Elemental Composition Report

Page 1

Single Mass Analysis

Tolerance = 5.0 PPM / DBE: min = -1.5, max = 100.0

Element prediction: Off

Number of isotope peaks used for i-FIT = 3

Monoisotopic Mass, Even Electron Ions

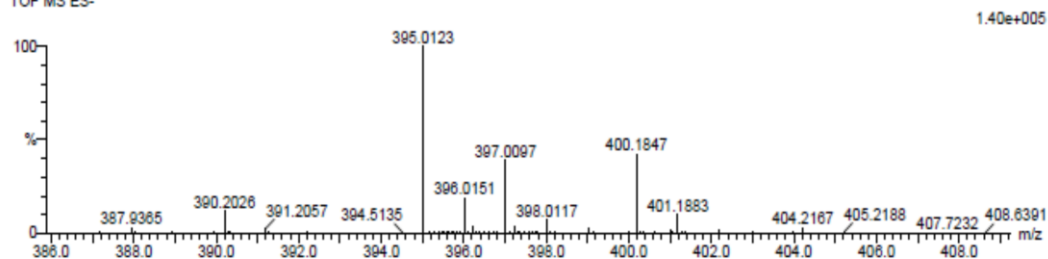
416 formula(e) evaluated with 1 results within limits (up to 20 closest results for each mass)

Elements Used:

C: 10-15 H: 5-15 N: 0-10 O: 0-5 F: 0-1 S: 0-1 Cl: 0-1

U-14.56 (1.855) Cm (1.61)

TOF MS ES-

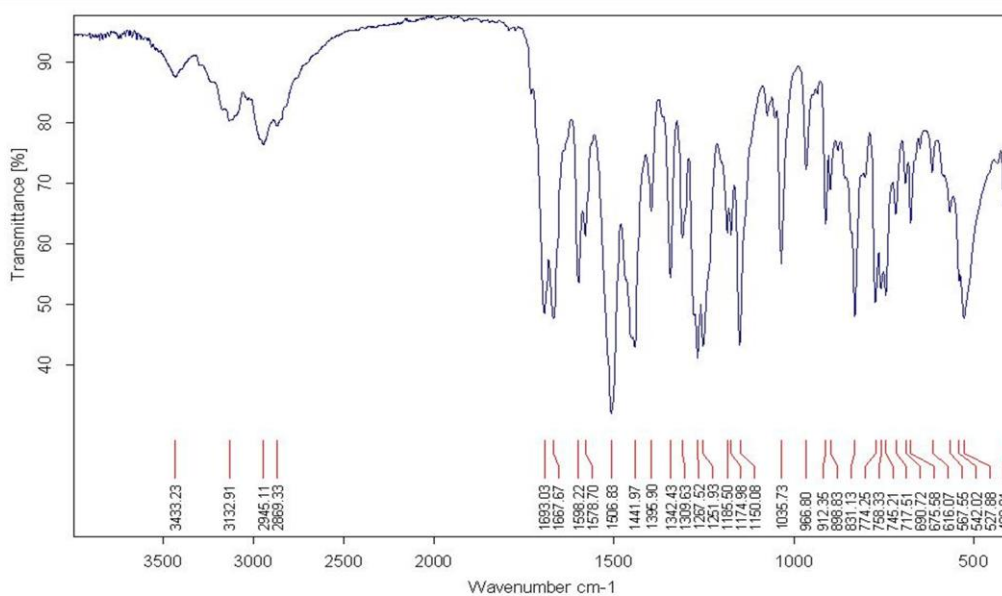


Minimum:

Maximum: 5.0 5.0 -1.5

Mass	Calc. Mass	mDa	PPM	DBE	i-FIT	i-FIT (Norm)	Formula
395.0123	395.0129	-0.6	-1.5	12.5	547.9	0.0	C14 H9 N6 O8 F 8 Cl

HRMS Spectrum of Compound 9o



C:\srinivas\4-methoxy-2-nitro aniline.D

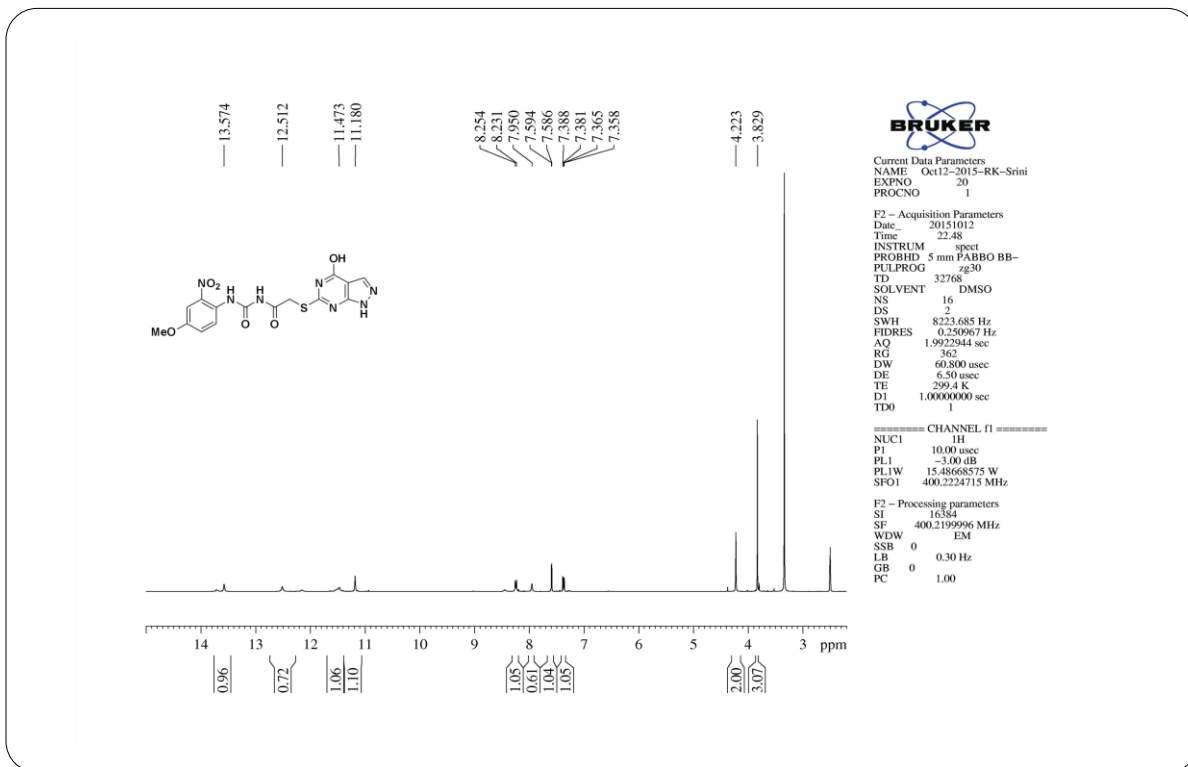
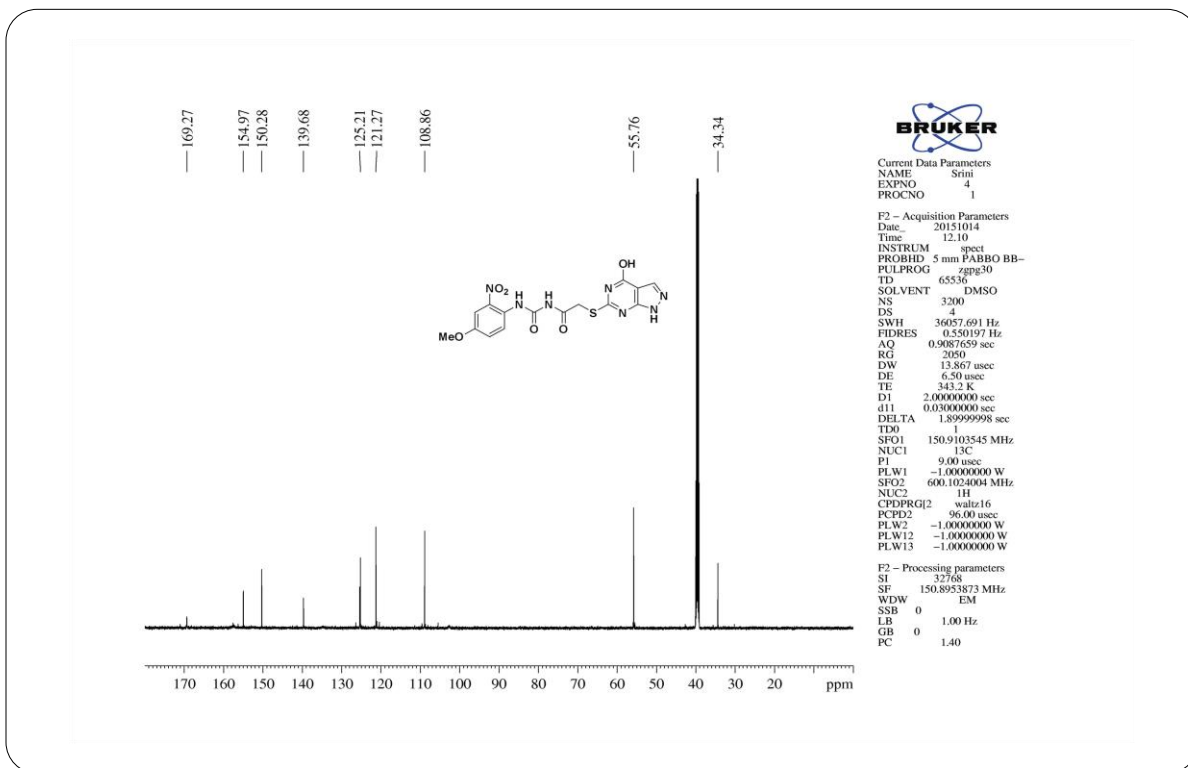
Fin T17

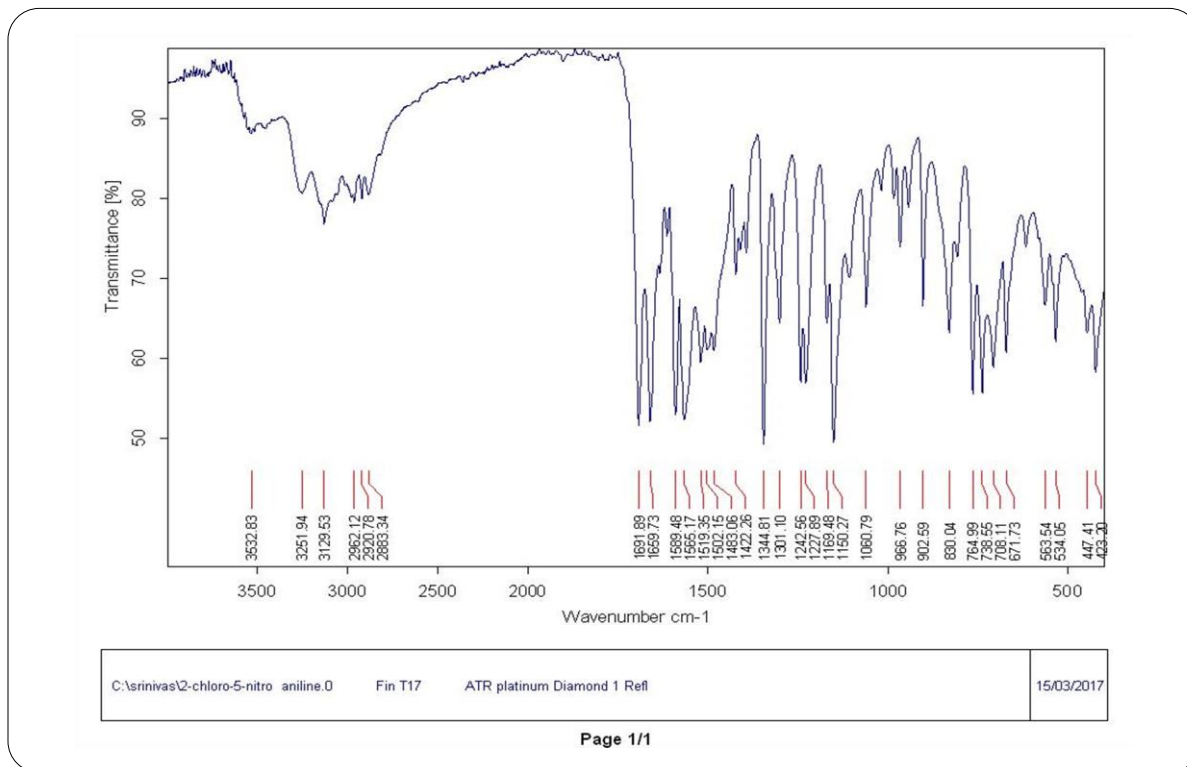
ATR platinum Diamond 1 Refl

15/03/2017

Page 1/1

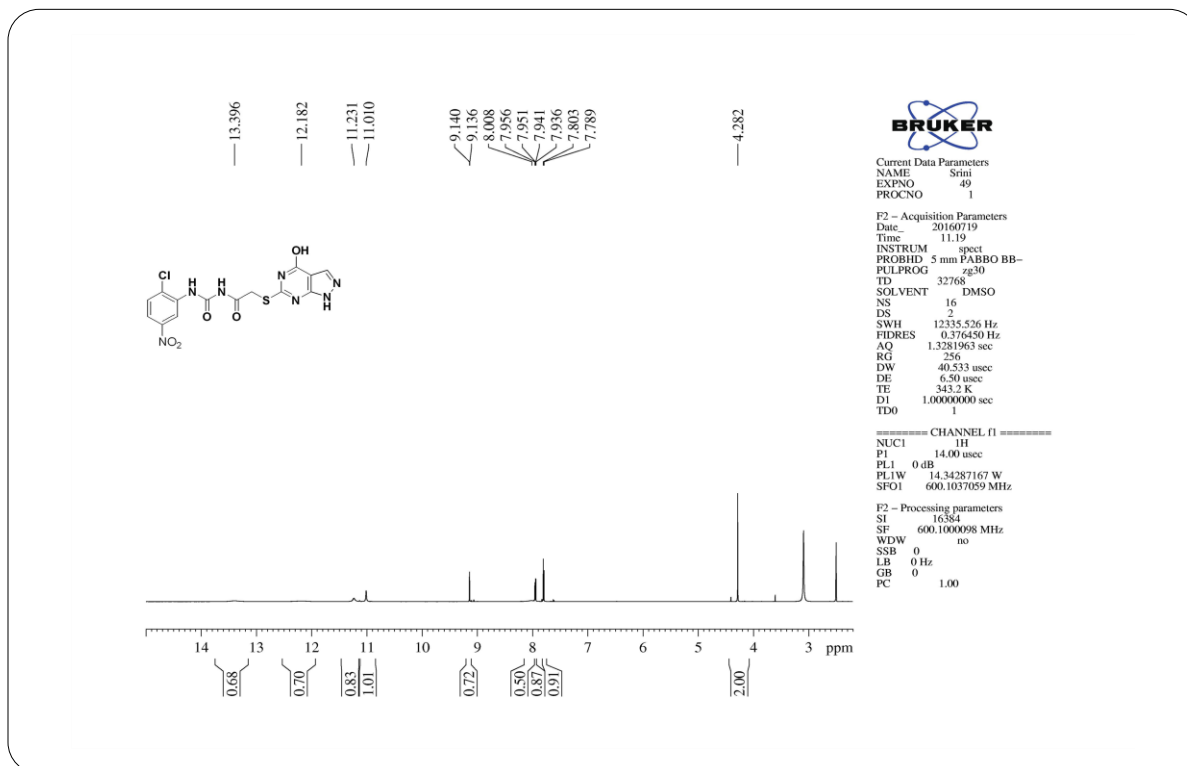
IR Spectrum of Compound 9p

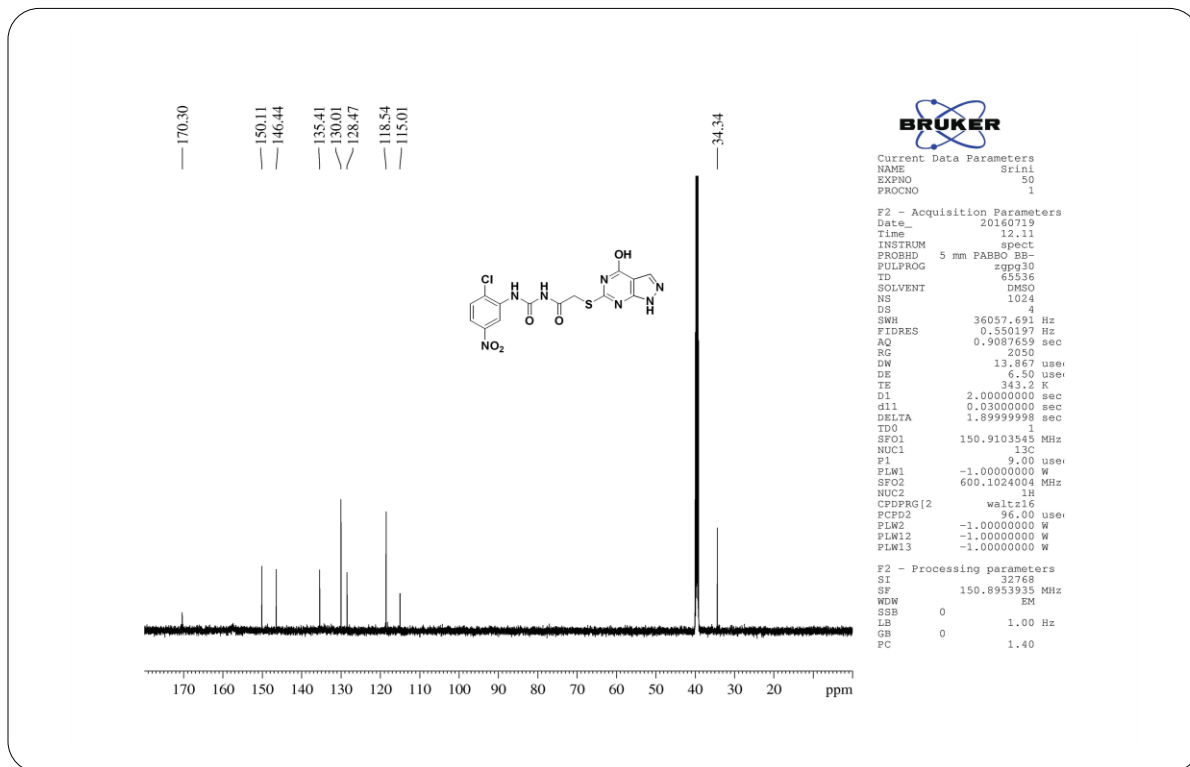
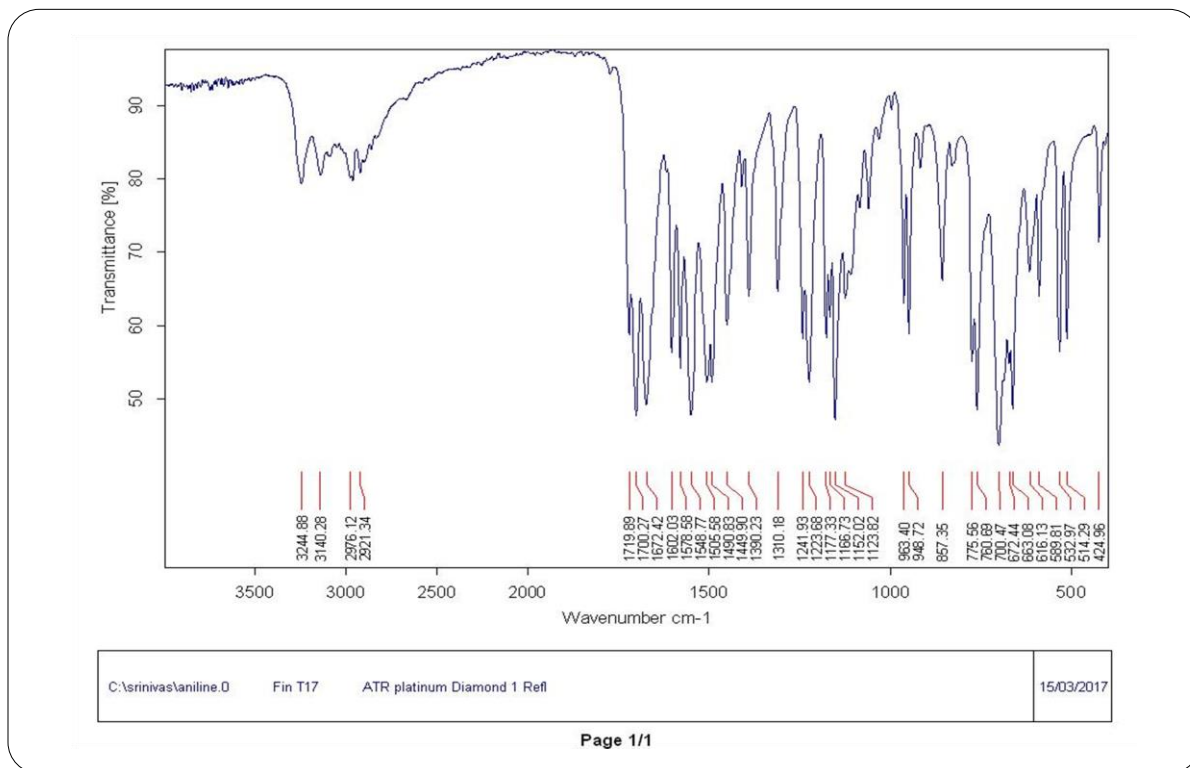
**¹H NMR Spectrum of Compound 9p****¹³C NMR Spectrum of Compound 20**

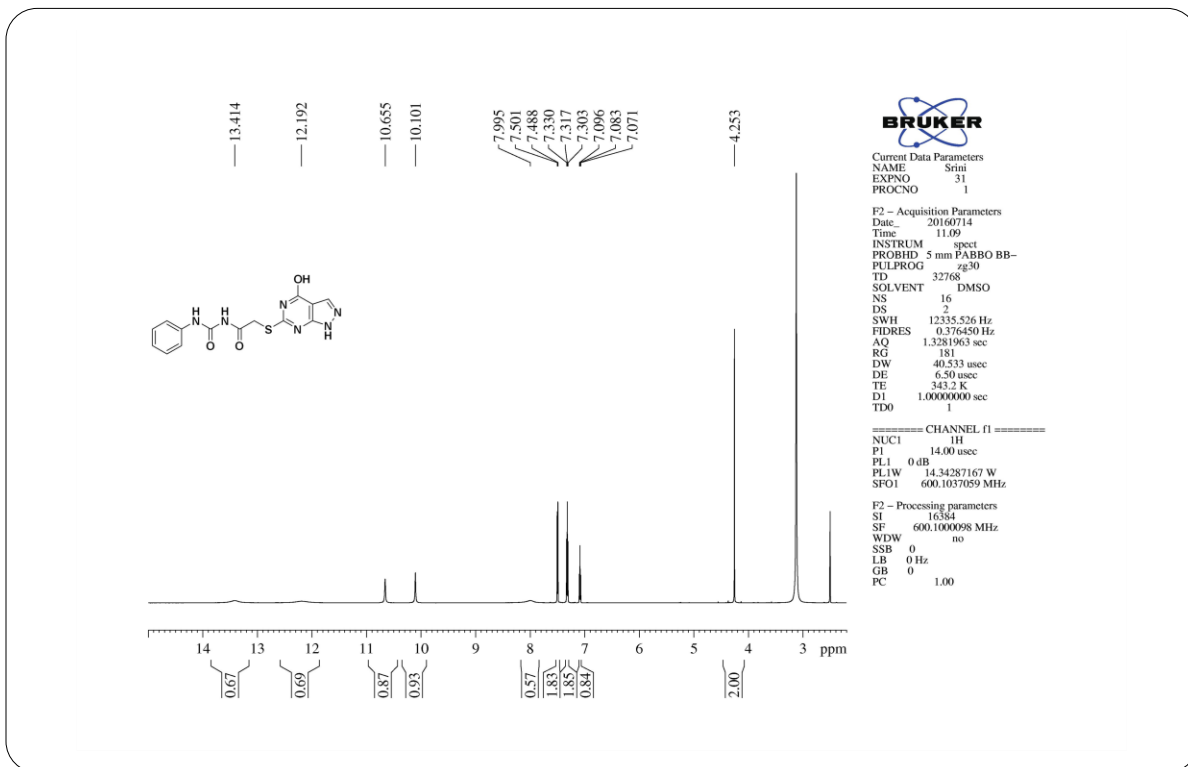
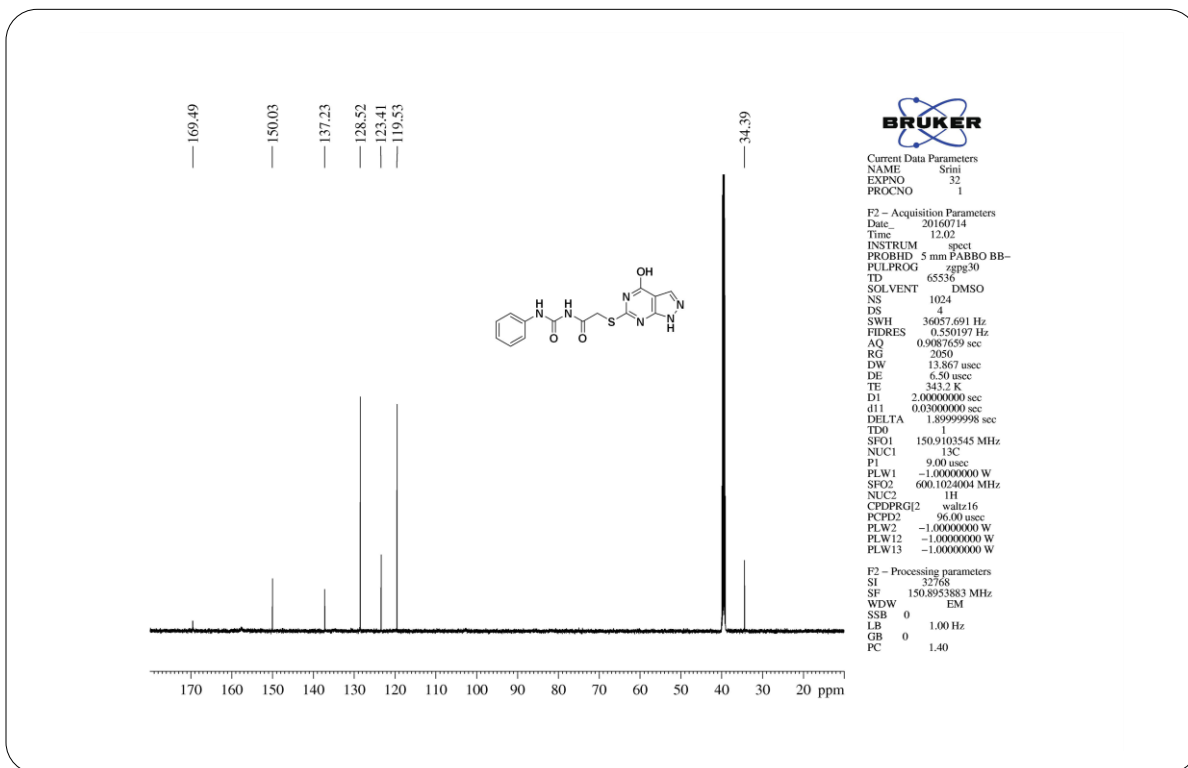


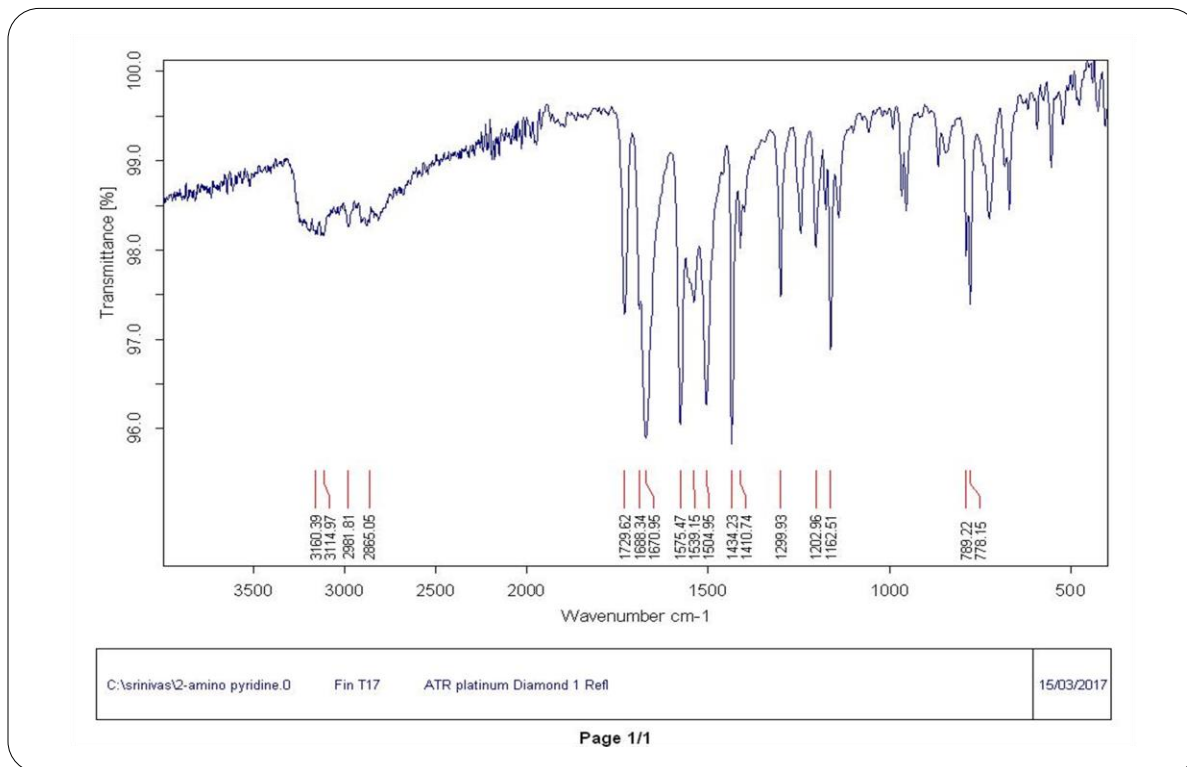
Page 1/1

IR Spectrum of Compound 9q

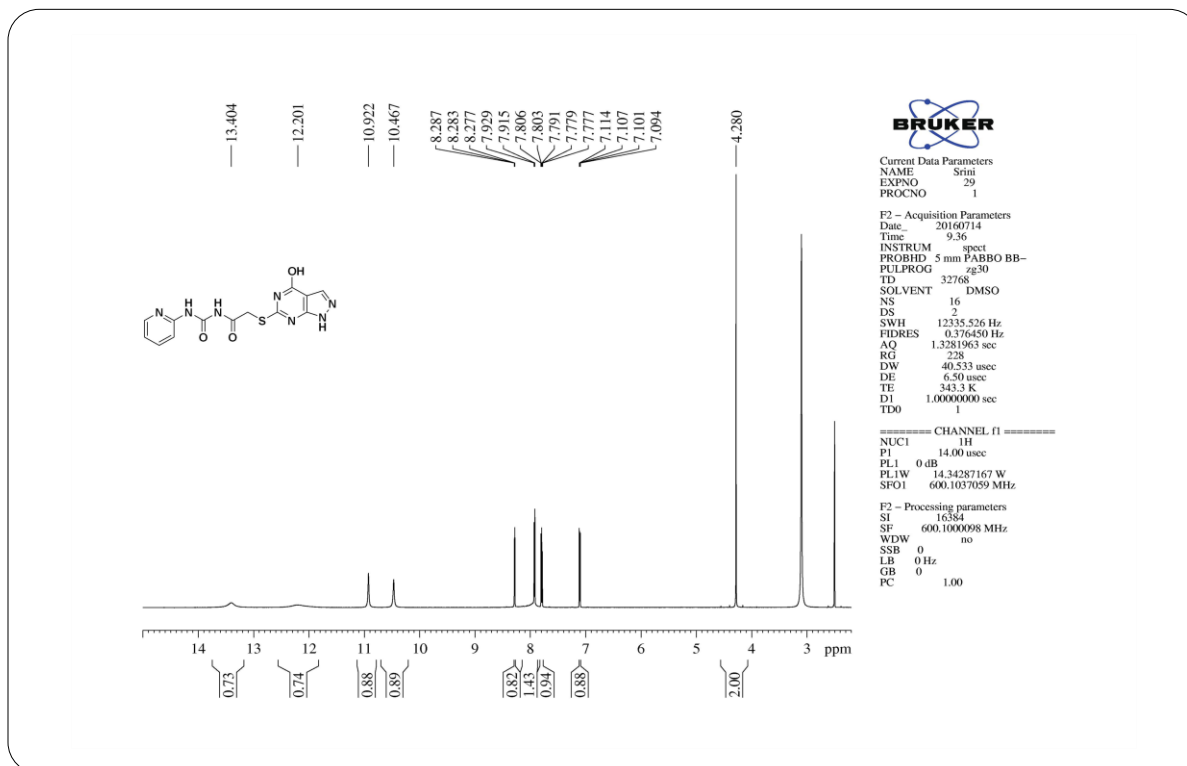
¹H NMR Spectrum of Compound 9q

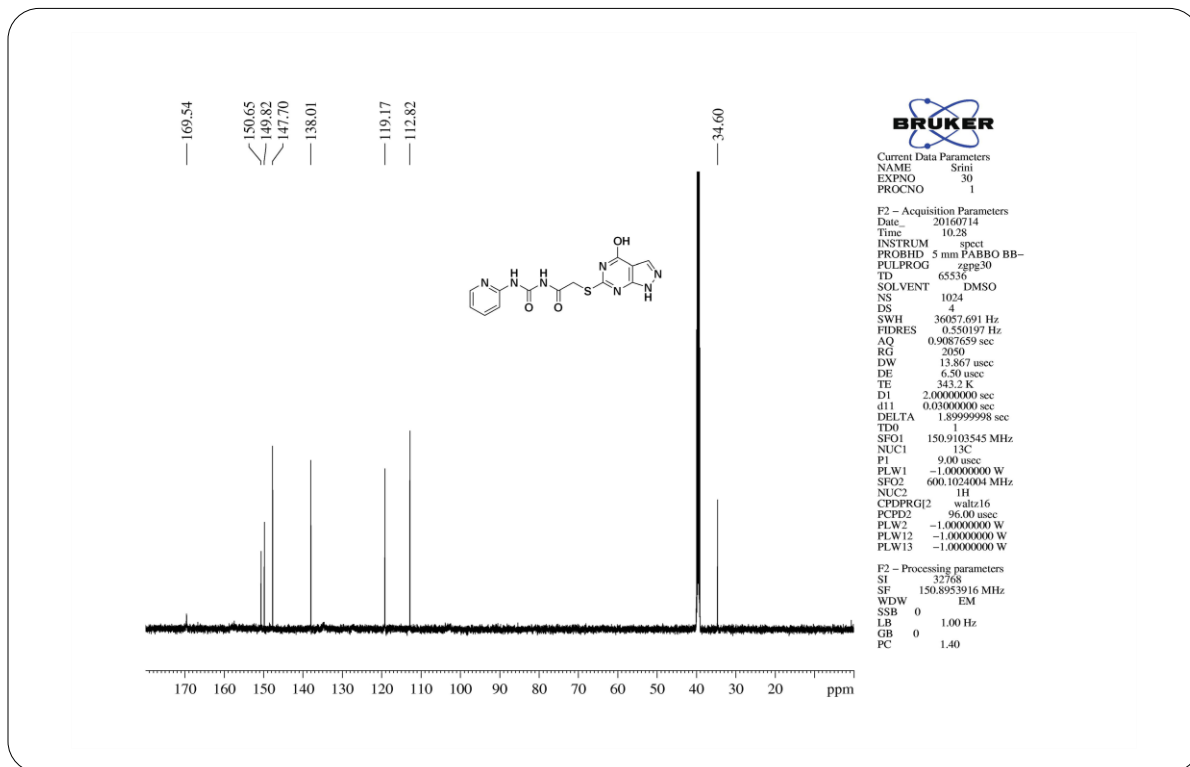
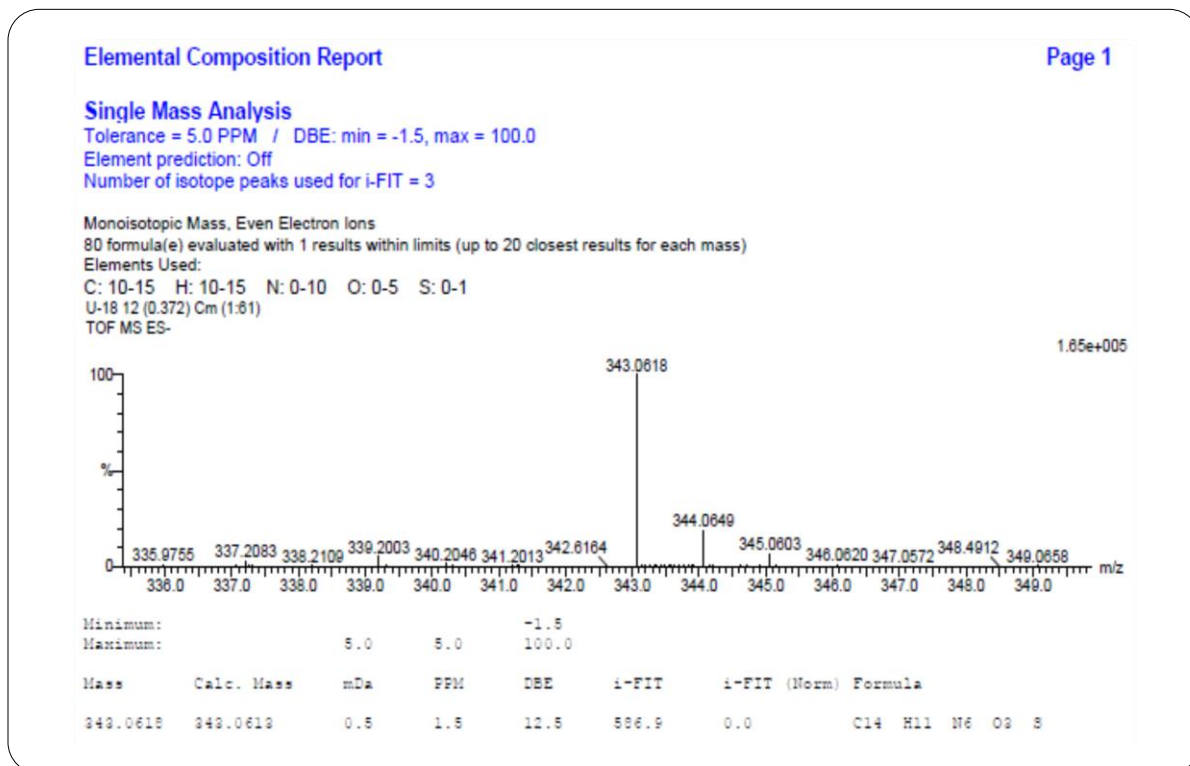
**¹³C NMR Spectrum of Compound 9q****IR Spectrum of Compound 9r**

**¹H NMR Spectrum of Compound 9r****¹³C NMR Spectrum of Compound 9r**



IR Spectrum of Compound 9s

¹H NMR Spectrum of Compound 9s

¹³C NMR Spectrum of Compound 9s

HRMS Spectrum of Compound 9s